



HAL
open science

Nanoréacteurs pour la catalyse en milieux aqueux

Christophe Deraedt

► **To cite this version:**

Christophe Deraedt. Nanoréacteurs pour la catalyse en milieux aqueux. Chimie organique. Université de Bordeaux, 2014. Français. NNT : 2014BORD0430 . tel-01242720

HAL Id: tel-01242720

<https://theses.hal.science/tel-01242720>

Submitted on 14 Dec 2015

HAL is a multi-disciplinary open access archive for the deposit and dissemination of scientific research documents, whether they are published or not. The documents may come from teaching and research institutions in France or abroad, or from public or private research centers.

L'archive ouverte pluridisciplinaire **HAL**, est destinée au dépôt et à la diffusion de documents scientifiques de niveau recherche, publiés ou non, émanant des établissements d'enseignement et de recherche français ou étrangers, des laboratoires publics ou privés.

THÈSE PRÉSENTÉE
POUR OBTENIR LE GRADE DE
DOCTEUR DE
L'UNIVERSITÉ DE BORDEAUX

ÉCOLE DOCTORALE DES SCIENCES CHIMIQUES DE BORDEAUX

SPÉCIALITÉ : CHIMIE ORGANIQUE

Par Christophe DERAEDT

Nanoréacteurs pour la catalyse en milieux aqueux

Sous la direction de : Prof. Didier ASTRUC

Soutenue le 19 décembre 2014 devant la commission d'examen

Membres du jury :

M. HAMON Jean-René	Directeur de Recherche au CNRS (Rennes 1)	Rapporteur
M. SAUVAGE, Jean-Pierre	Directeur de Recherche au CNRS (Strasbourg)	Rapporteur
Mme. CSIBA-DALKO Maria	Directeur de Recherche à l'Oréal	Examineur
M. FOUQUET, Eric	Professeur à l'Université de bordeaux	Président
M. SAILLARD Jean-Yves	Professeur à l'Université Rennes 1	Examineur
M. SALMON Lionel	Chargé de Recherche au CNRS (Toulouse)	Examineur
M. RUIZ Jaime	Ingénieur contractuel à l'Université de bordeaux	Invité
M. ASTRUC Didier	Professeur à l'université de bordeaux, IUF	Directeur de thèse

Titre : Nanoréacteurs pour la catalyse en milieux aqueux

Résumé: Cette thèse concerne l'élaboration par réaction "click" CuAAC de nouveaux nanomatériaux présentant diverses applications, en particulier en catalyse. Ces macromolécules (dendrimères, dendrimères supportés sur oxide et polymères) comprenant des cycles 1,2,3-triazoles ont été utilisés pour stabiliser des nanoparticules essentiellement de palladium actives en catalyse de couplage C-C, réduction du 4-nitrophenol et oxydation des alcools dans des solvants aqueux. L'utilisation de ces nanoparticules à l'échelle du ppm traduit leur efficacité et l'aspect écologique visé avec ce projet. L'intégration d'unités triazolylbiferrocéniques au sein de ces polymères a permis d'étendre la gamme d'applications de ces matériaux aux sondes électrochimiques, réduction d'ions métalliques en nanoparticules, composés poly-électrolytes, poly-électrochromes, à valence mixte. L'imprégnation de nanoparticules de palladium stabilisées par des dendrimères sur support magnétique a permis d'augmenter la robustesse des catalyseurs ainsi que leur recyclabilité par aimantation.

Mots clés : catalyse, nanoréacteur, dendrimère, nanoparticule, chimie verte

Title : Nanoreactors for catalysis in aqueous media

Abstract: This thesis concerns the synthesis by "click" CuAAC reactions of new nanomaterials that have various applications, in particular in catalysis. These macromolecules are dendrimers, supported dendrimers and polymers that contain 1,2,3-triazole rings and were used in the stabilization of essentially palladium nanoparticles (PdNPs). These PdNPs are extremely active in the catalysis in green solvents of C-C coupling, reduction of 4-nitrophenol and selective oxidation of alcohols. The use of these nanoparticle catalysts at the ppm level shows their efficiency and their ecological aspect. The integration of biferrocene units in the polymers allowed expanding their applications to electrochemical sensors, reductants of metallic ions to nanoparticles, polyelectrolytes, polyelectrochromic, and mixed-valent complexes. The impregnation of PdNPs stabilized by dendrimers on magnetic support led to the increase of the catalyst robustness and recyclability using a magnet.

Keywords : catalysis, nanoreactor, dendrimer, nanoparticle, green chemistry

Unité de recherche

Institut des Sciences Moléculaires (ISM, UMR CNRS 5255), Université de Bordeaux,
351 Cours de la libération, 33405 Talence Cedex

*Ce n'est pas que je suis plus intelligent, c'est que je
reste plus longtemps avec les problèmes*

(Albert Einstein)

*On ne fait jamais attention à ce qui a été fait; on ne
voit que ce qui reste à faire.*

(Marie Curie)

*Le week-end refroidit les idées, mais l'homme reste
le même.*

(Jaime Ruiz)

Remerciements

Ce travail a été effectué dans le groupe de recherche « Nanosciences et Catalyse » à l'Institut des Sciences Moléculaires (ISM) Université de bordeaux, sous la direction scientifique du Professeur Didier Astruc.



Je souhaite tout d'abord remercier l'équipe pédagogique de l'Université de Bordeaux (ex Bordeaux 1) qui m'a donné l'envie de poursuivre mes études jusqu'en Doctorat. Par la même occasion, je remercie le ministère de la recherche et de la technologie qui m'a financé durant mes trois années de Doctorat.



Je remercie le Professeur Didier Astruc pour son soutien en Licence 3, en Master 1 et en Master 2, pour m'avoir accueilli dans son groupe de recherche et pour m'avoir donné l'opportunité de développer des travaux de recherche autour de la catalyse en milieux aqueux et des nanoréacteurs. L'enthousiasme avec lequel le Professeur Didier Astruc a dirigé cette thèse, ainsi que les nombreux conseils et idées qu'il m'a apportés, m'ont permis d'avancer et de progresser tout au long de ma thèse. La fréquence hebdomadaire de nos réunions de groupe, l'intervention orale lors de plusieurs congrès ainsi que la rédaction de nos propres articles scientifiques "imposés" par le Professeur m'ont aidé à améliorer mon anglais oral et écrit. Pour finir, les galettes-parties chez le Professeur resteront à jamais dans ma mémoire.



J'adresse mes sincères remerciements à M. Jean-Pierre Sauvage et M. Jean-René Hamon, Directeurs de Recherche au CNRS pour avoir accepté d'être rapporteur de ce manuscrit.

J'exprime toute ma reconnaissance à Mme. Maria Csiba-Dalko, Directeur du Département Chimie à l'Oréal, M. Eric Fouquet, Professeur à l'Université de bordeaux, M. Jean-Yves Saillard, Professeur à l'Université de Rennes 1 et M. Lionel Salmon, Chargé de Recherche au CNRS, qui m'ont fait l'honneur de bien vouloir participer à mon jury de thèse.



J'exprime toute ma gratitude à M. Jaime Ruiz pour son courage et son aide précieuse depuis que je le connais. Sur le plan scientifique, professionnel, ou humain, ses conseils et discours m'ont forgé pour ma vie post-doctorat. Sa présence au laboratoire, son encadrement méticuleux des nouveaux entrants, sa joie de vivre, son déhanché chilien sur la music d'Amérique du sud, a aidé au maintien du laboratoire dans une atmosphère joyeuse, ce qui pour moi est essentielle pour garder le sourire malgré les mauvaises passes. Rendez-vous autour d'une bonne moussaka.



Je remercie toutes les personnes ayant participé à ces travaux de thèses: M. Lionel Salmon (images MET), Mme. Laetitia Etienne (ICP-OES), Mme. Christine Labrugère (XPS), Stéphanie (DRX), Paulette (ATG, DSC, seringues), Nico (SEC), Mell. Mélanie Bousquet (SEC), toute l'équipe du CESAMO (Noël, Jean-Michel, Claire,

Patricia, Pierre...). Sans toutes ces personnes, mes travaux de thèse n'auraient pas pu avancer aussi vite.



Passer une thèse est bien évidemment très enrichissant d'un point de vue scientifique mais aussi d'un point de vue relations humaines. Je remercie toutes les personnes avec lesquelles j'ai "vécu" pendant ces dernières années: tous les membres "non chimistes" de l'ISM (Bernadette, Vicky, Abdel, Sophie, Annie, les deux Karine, Fred, Georges, Fabrice, Pascale, mon Titi, Michel...), qui ont toujours tout fait pour nous aider d'une manière ou d'une autre (problème informatique, déchets solvants, financement pour partir en congrès), tous les membres chimistes (Dominique, Pascale, Chlotilde, Murielle, Damien ainsi que tous les permanents et étudiants de l'ISM que j'ai côtoyé).



Mes collègues et amis de la "Team" Landais/Fouquet sont à remercier tout particulièrement, car j'ai passé beaucoup de temps ces trois dernières années avec eux. Je remercie Clément pour son scandalisme à chaque soirée, Benjamin pour sa discrétion et ses cours de natation, Jojo pour ses goûts musicaux me laissant perplexe, Paul et Alex pour leur finesse et leur culture en choses inutiles très développée, Jessica pour son dévergondage de fin de thèse, Thomas (que l'on oublie tout le temps) pour sa sensibilité à fleur de peau, "Hugo" pour sa "grandeur" d'esprit, Simon et Haitham pour cette si belle compagnie à Toulouse, ainsi que tous les anciens; le grand manouche Antho, Tom, Sibylle, Marie, Jérôme, Luma, Sandy, Jürgen, Eric et F-X.



Mes meilleures pensées vont à tous les membres du groupe « Nanosciences et catalyse » avec qui j'ai passé d'excellents moments. Je souhaite tout le bonheur du monde à mes amis chinois Pengxiang, Lily, Dong, Li Na, Yanlan, Changlong, Xiang et Haibin que je reverrai un jour ou l'autre. Je souhaite la plus grande réussite à Martin et Virginie, les stagiaires que j'ai eu la chance d'encadrer. Je souhaite aussi une bonne chance à Sylvain pour son potentiel retour à Bordeaux. Le "Hot boy" du labo, Roberto qui a été d'une compagnie incroyable, je lui souhaite bonne chance pour la fin de son post-doc. Pour finir j'embrasse de tout mon cœur la grecque (Amalia) et la remercie pour tous ces moments passés ensemble et pour cette relation fluctueuse/évolutive dont la description pourrait constituer un manuscrit de thèse entier.



Mes dernières pensées vont à mes proches, ceux qui ont su me soutenir et me supporter ces trois dernières années. À commencer par mes parents, ma sœur (et Diune) qui comptent le plus pour moi, et qui ont toujours été là. Mes grands parents, mes tantes et oncles et cousins (trop nombreux pour être nommé) qui, bien évidemment, suivaient de près le déroulement de ma thèse. Je remercie mes meilleurs amis : Rémi, Matt, Arnaud, Jérémy, Clem, Meu/flo, Raph, Axel, Xav, Gatin, Alex, Yo, Wolf, Andres, Manouch, Red's, Bapt, Poullette, et Loulou pour m'avoir écouté me plaindre et pour avoir toujours trouvé le temps pour me divertir pendant mes moments libres.

Plan

Nanoréacteurs pour la catalyse en milieu aqueux

Introduction générale.....	P1
Partie 1. Dendrimères amphiphiles pour la stabilisation de nanoparticules actives en catalyse.....	P6
1. Introduction.....	P7
2. “Click” dendrimer-stabilized palladium nanoparticles as a green catalyst down to parts per million for efficient C-C Cross-Coupling reactions and reduction of 4-nitrophenol, <i>Adv. Synth. Catal.</i> 2014 , 356, 2525-2538.....	P8
3. “Click” dendrimers as efficient nanoreactors in aqueous solvent: Pd nanoparticle stabilization for sub-ppm Pd catalysis of Suzuki–Miyaura reactions of aryl bromides, <i>Chem. Commun.</i> 2013 , 49, 8169-8181.....	P22
4. Palladium nanoparticles stabilized by glycodendrimers and their application in catalysis, <i>Eur. J. Inorg. Chem.</i> 2014 , 4369-4375.....	P25
5. Gold nanoparticles stabilized by glycodendrimers: synthesis and application to the catalytic reduction of 4-nitrophenol, <i>Eur. J. Inorg. Chem.</i> 2014 , 2671-2677.....	P32
Partie 2. Polymères hydrophiles stabilisateurs de nanoparticules de palladium actives en catalyse.....	P40
1. Introduction.....	P41
2. Efficient click-polymer-stabilized palladium nanoparticle catalysts for Suzuki-Miyaura reactions of bromoarenes and reduction of 4-Nitrophenol in aqueous solvents, <i>Adv. Synth. Catal.</i> 2013 , 355, 2992-3001.....	P42
3. “Homeopathic” Palladium Nanoparticle Catalysis of Cross Carbon–Carbon Coupling Reactions, <i>Acc. Chem. Res.</i> 2014 , 47, 494-503.....	P52
Partie 3. Polymères triazolylbiferrocéniques: synthèse, réseaux et applications.....	P63
1. Introduction.....	P64
2. Multi-function redox polymers: electrochrome, polyelectrolyte, sensor, electrode modifier, nanoparticle stabilizer and catalyst template, <i>Angew. Chem., Int. Ed.</i> 2014 , 53, 8445-8449.....	P65
3. Mixed-valent intertwined polymer units containing biferrocenium chloride side chains form nanosnakes that encapsulate gold nanoparticles, <i>J. Am. Chem. Soc.</i> 2014 , 136, 13995-13999.....	P70

4. Catalytically-active palladium nanoparticles stabilized by triazolylbiferrocene containing polymers, *submitted to J. Inorg. Organomet. Polym. Matter.*P74

Partie 4. Nanoréacteurs dendritiques pour la catalyse par des ppm de Cu de la réaction “click” CuAAC dans l’eau.....P92

1. Introduction.....P93
2. Revue: Nanoreactors for catalysis (un-submitted yet)P94
3. Recyclable catalytic dendrimer nanoreactor for part-per-million Cu^I catalysis of “click” chemistry in water, *J. Am. Chem. Soc.* **2014**, *136*, 12092-12098.....P119

Partie 5. Hétérogénéisation sur supports magnétiques de catalyseurs nanoparticulaires de palladium stabilisés par des dendrimères.....P127

1. Introduction.....P128
2. Robust, efficient and recyclable catalyst by impregnation of dendritically preformed Pd nanoparticles on magnetic support, *ChemCatChem.* **2014**, accepted.....P129
3. Efficient and magnetically recoverable “click” PEGylated γ -Fe₂O₃-Pd nanoparticle catalysts for Suzuki-Miyaura, Sonogashira, and Heck reactions with positive dendritic effects, *Chem. Eur. J.* **2014**, accepted.....P136

Partie 6. NaBH₄ réducteur de précurseurs Pd^{II} et Au^{III} et stabilisateur de nanoparticules extrêmement actives en catalyse.....P150

1. Introduction.....P151
2. Sodium borohydride stabilizes very active gold nanoparticle catalysts, *Chem. Commun.* **2014**, *50*, 14194-14196.....P152

Annexes.....P156

Liste de publications.....P204

Conclusions et perspectives.....P208

Introduction générale

La chimie du XXI^{ème} siècle doit être verte, c'est à dire respectueuse de notre environnement. Cette nécessité incite les chimistes de synthèse à reconsidérer leurs stratégies.⁽¹⁾ La chimie verte est régie par douze principes: la prévention des déchets, l'économie d'atomes, l'emploi et la production de produits non ou peu toxiques, la minimisation de la toxicité pendant la fonctionnalisation, la diminution de la quantité de solvants ou leur suppression, l'économie d'énergie (température et pression se rapprochant de l'ambiante), l'introduction de matières premières renouvelables, la réduction du nombre de produits et d'étapes, la préférence pour la catalyse aux réactions nécessitant des réactifs stœchiométriques, la facile dégradation des produits, la prévention d'agents polluants avec des analyses en temps réel et la sécurité pour la prévention des accidents.⁽²⁾ C'est pourquoi l'utilisation de catalyseurs, de molécules organiques, nanoparticules et de nano-objets rendant une réaction plus rapide, plus sélective, plus efficace, moins dangereuse et moins énergétique devient un domaine de recherche privilégié des laboratoires. C'est dans cet état d'esprit que nous nous sommes dirigé tout au long de ce doctorat, en combinant la catalyse inorganique ou organométallique⁽³⁾ avec celle utilisant des nanoparticules.⁽⁴⁾

Durant le stage de Licence 3, l'occasion avait été donnée de travailler avec le Dr. Abdou Diallo sur la synthèse d'un dendrimère 27-TEG **1**, Fig. 1, composé d'un cœur hydrophobe et d'une périphérie hydrophile constituée de 27 chaînes tri(éthylène glycol) (TEG) permettant d'accélérer considérablement les réactions de métathèse (métathèse croisée, métathèse à fermeture de cycle, et métathèse des énynes) dans l'eau en présence du catalyseur de Grubbs de seconde génération.⁽⁵⁾ Cet additif dendritique permettait la solubilisation des substrats hydrophobes et du catalyseur au ruthénium dans l'eau, accélérant ainsi les réactions. Deux ans plus tard, la poursuite de l'exploration de ce concept de nanoréacteur dendritique a été choisie lors du stage de Master 2 et du doctorat.

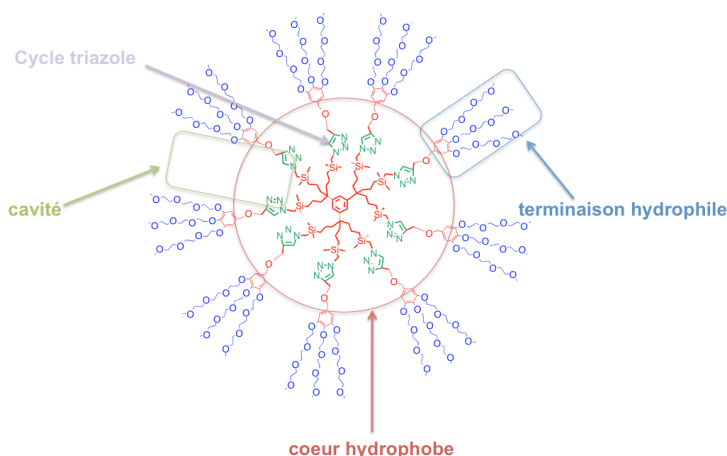


Figure 1. Dendrimère 27-TEG **1** utilisé tout au long de la thèse

Ce dendrimère **1** est à la fois soluble dans les solvants organiques et dans l'eau, grâce aux terminaisons TEG. La présence de cycles 1,2,3-triazoles et de cavités hydrophobes au sein du dendrimère lui confère les propriétés d'un nanoréacteur micellaire. Les atomes d'azote du cycle triazole sont de bons ligands des métaux de transition et seront utilisés dans cette thèse pour coordiner Pd(II) et Au(III) et pour stabiliser les nanoparticules de ces métaux dans lesquels le degré d'oxydation est formellement nul.

La stabilisation de nanoparticules par des macromolécules telles que, entre autres, les polymères⁽⁶⁾ et des dendrimères PAMAM⁽⁷⁾ est connue depuis longtemps, mais elle n'avait pas été optimisée en catalyse. Nous avons tenté d'utiliser le dendrimère **1** pour une fonction parallèle avec des catalyseurs moléculaires ou nanoparticulaires en employant des quantités de catalyseurs extrêmement faibles en milieux aqueux. La première partie de la thèse concernera la stabilisation de nanoparticules de palladium (PdNPs) par le dendrimère **1** grâce aux 9 groupes 1,2,3-triazoles qui le compose et à sa topologie. Le palladium étant un métal de transition très utilisé pour la catalyse de multiples réactions de synthèse organique et spécifiquement dans les réactions de couplages C-C ou C-N, ces nanoparticules ont été testées en catalyse (Suzuki-Miyaura, Heck, Sonogashira, hydrogénation)⁽⁶⁾ dans des conditions de chimie verte. L'utilisation de PdNPs à l'échelle du ppm a permis de mettre en exergue leur très grande et remarquable efficacité. La comparaison avec des nanoparticules stabilisées par d'autres dendrimères a aussi pu être effectuée grâce à la comparaison avec les résultats de la littérature et aussi à des collaborations au sein de notre groupe de recherche avec les Drs Na Li et Sylvain Gatard.

Ces études comparatives ont montré l'intérêt de la topologie spécifique du dendrimère **1**. La présence des cycles 1,2,3-triazoles combinée à celle de polyéthylène glycol (PEG) étant essentielle pour la stabilisation de PdNPs actives, cela nous a conduit à développer d'autres matériaux tels que des polymères hydrosolubles synthétisés par polycondensation (réaction de cycloaddition de type Huisgen catalysée par le cuivre (I), CuAAC).⁽⁸⁾ Ainsi, dans une deuxième partie, nous utiliserons cette stratégie de synthèse ainsi que des polymères triazolyle-PEG comme stabilisateurs de PdNPs actives en catalyse. L'intérêt de cette méthode de polymérisation réside dans la possibilité de synthétiser facilement et rapidement des co-polymères alternés (A-B-A-B...), ce qui a permis d'obtenir aussi des propriétés additionnelles.

La troisième partie consiste en la synthèse de polymères à multiples applications, synthétisés par la même méthode de polymérisation que celle développée dans la partie précédente. En polymérisant une unité di-azido PEG avec une unité di-éthynyl biferrocène, nous avons obtenu des matériaux hydrosolubles présentant diverses propriétés : polyélectrolytes, polyélectrochromes, réducteur de l'or (III) avec stabilisation de nanoparticules d'or (AuNPs), stabilisateur de PdNPs, catalyseurs, matériaux à valence mixe, sonde électrochimique. Dans cette même partie, ces nanomatériaux aux multiples propriétés seront comparés à d'autres métallopolymères synthétisés par Amalia Rapakousiou à l'occasion d'une collaboration au sein de notre groupe de recherche. L'intérêt majeur de la synthèse de ces polymères, présentée dans les deuxième et troisième parties, réside dans la rapidité et la simplicité de leur obtention. Néanmoins, ces polymères ne présentent pas de cavités hydrophobes conférant au dendrimère la propriété de nanoréacteur qui sera développée dans la quatrième partie.

Comme dit précédemment, la présence du dendrimère **1** accélère considérablement la réaction de métathèse dans l'eau grâce à sa propriété de micelle moléculaire. De la même façon, nous nous sommes engagé dans la recherche de l'accélération, à l'aide de ce dendrimère **1** (en quantité catalytique), de la réaction "click" catalysée au cuivre (I) dans l'eau. La présence du catalyseur cuivreux hydrophobe au sein du dendrimère a pu être mise en évidence par différentes techniques de Résonance Magnétique Nucléaire du proton (RMN ^1H), mettant en exergue ce rôle de nanoréacteur dendritique de **1**. Dans cette partie, nous discuterons aussi l'utilisation des 1,2,3-triazoles du dendrimère comme ligands activateurs du cuivre (I) contribuant à la mise en œuvre de ce nouveau catalyseur dendritique. Celui-ci présente une activité catalytique inégalée pour la réaction "click" CuAAC dans l'eau. Cette quatrième partie correspond à des études ayant débutées durant le stage de master 2 et achevées seulement en fin de thèse.

La cinquième partie concerne l'hétérogénéisation de PdNPs stabilisées par des dendrimères TEG (PdNPs développées dans la première partie) sur support magnétique (nanoparticule de Fe_2O_3 (cœur)/silice (coquille)). L'intérêt de ces nouveaux catalyseurs réside dans leur stabilité, leur isolation à l'état solide, leur utilisation simple et leur recyclabilité à l'aide d'un champ magnétique externe.

Actuellement, la synthèse de nanoparticules est devenue simple et requiert systématiquement la présence d'un réducteur et d'un stabilisateur (ligand, polymère, dendrimère, matériaux inorganique...). Or, dans la sixième partie nous démontrerons comment, lorsque NaBH_4 est utilisé en excès en tant que réducteur, il peut en même temps jouer le rôle de stabilisateur. Les nanoparticules ainsi formées sont dépourvues de ligands encombrants et seront par conséquent utilisées en tant que catalyseurs extrêmement actifs.

Ces six parties sont présentées par ordre chronologique des résultats positifs des recherches et traduisent aussi la démarche scientifique durant ces trois ans et demi au sein du groupe Nanosciences et Catalyse.

En annexes seront présentés des travaux sortant un tant soit peu de l'axe principal de la thèse. D'abord des études effectués avec un stagiaire de master 2, Martin D'Halluin autour de la catalyse de métathèse et de ses catalyseurs, puis des travaux commun de notre groupe sur l'influence stéréoélectronique des ligands stabilisateurs lors de la catalyse par les AuNPs de la réduction du para-nitrophénol.

Références

1. a) Astruc, D. La métathèse: de Chauvin à la chimie verte, *L'actualité chimique*. **2004**, n° 273, pp 3-11.
2. Anastas, P. T.; Warner, J. C. *Green Chemistry: Theory and Practice*, Oxford University Press, New York, **1998**.
3. Astruc D. *Chimie Organométallique et Catalyse*. EDP Sciences, Les Ullis, **2013**.
4. *Nanoparticles and Catalysis*, Rédacteur: Astruc D. Wiley-VCH, Weinheim, **2008**.
5. Diallo, A. K. ; Boisselier, E. ; Liang, L.; Ruiz, J.; Astruc, D. Dendrimer-induced molecular catalysis in water: the example of olefin metathesis, *Chem. Eur. J.* **2010**, *16*, 11832-11835.

6. a) Reetz, M. T.; Helbig, W.; Quaiser, S. A. in *Active metals: preparation, characterizations, applications*, ed. A. Fürstner, VCH, Weinheim, **1996**; b) Beletskaya, I. P.; Cheprakov, A. V. The Heck reaction as a sharpening stone of palladium catalysis. *Chem. Rev.* **2000**, *100*, 3009–3066; c) de Vries, J. G. *Dalton Trans.* **2006**, 421–429; d) Yin, L.; Liesbsher, J. Carbon-carbon coupling reactions catalyzed by heterogeneous palladium. *Chem. Rev.* **2007**, *107*, 133-173.
7. a) Zhao, M.; Crooks, R. M. Homogeneous hydrogenation catalysis with monodisperse, dendrimer-encapsulated Pd and Pt nanoparticles. *Angew. Chem., Int. Ed.* **1999**, *38*, 364-366; b) Myers, V. S.; Weier, M. G.; Carino, E. V.; Yancey, D. F.; Pande, S.; Crooks, R. M. Dendrimer-encapsulated nanoparticles: New synthetic and characterization methods and catalytic applications. *Chem. Sci.* **2011**, *2*, 1632-1646.
8. a) Rostovtsev, V. V.; Green, L. G.; Fokin, V. V.; Sharpless, K. B. A stepwise Huisgen cycloaddition process: copper (I)-catalyzed regioselective “ligation” of azides and terminal alkynes. *Angew. Chem., Int. Ed.* **2002**, *41*, 2596–2599; b) Tornøe, C. W.; Christensen, C.; Meldal, M. Peptidotriazoles on solid phase: [1,2,3]-triazoles by regiospecific copper (I)-catalyzed 1,3-dipolar cycloadditions of terminal alkynes to azides. *J. Org. Chem.* **2002**, *67*, 3057–3064.

**Partie 1. Dendrimères
amphiphiles pour la stabilisation
de nanoparticules actives en
catalyse.**

Partie 1. Dendrimères amphiphiles pour la stabilisation de nanoparticules actives en catalyse.

Au sein du laboratoire du Prof. Didier Astruc, il a été prouvé que les cycles 1,2,3-triazoles résultant d'une réaction CuAAC "click" pouvaient quantitativement lier des ions métalliques (ex: Pd(II)). Ainsi les dendrimères et les polymères triazolyles développés au laboratoire ont permis la stabilisation de nanoparticules de palladium (PdNPs) actives en catalyse.⁽¹⁾ Le problème majeur était que cette catalyse avait seulement été effleurée et qu'aucune étude catalytique (autre que la catalyse d'hydrogénation des alcènes et le couplage Suzuki-Miyaura du iodobenzène) n'avait été étudiée en profondeur. L'un des travaux principaux effectué au cours de cette thèse concerne la stabilisation de PdNPs par des dendrimères triazolyles à terminaisons triéthylène glycol (TEG). Deux générations (G0 et G1) de dendrimère TEG ont été synthétisés puis utilisés pour stabiliser des PdNPs dans l'eau. Ces nanoparticules se trouvent en solution aqueuse et résultent de la réduction chimique de K_2PdCl_4 par $NaBH_4$. Les analyses de microscopie électronique en transmission (MET) ont montré que la taille des PdNPs stabilisées par G0 (dendrimère **1** dans l'introduction générale) était plus petite que celle de PdNPs stabilisées par G1 ($1,4 \pm 0,7$ nm contre $2,7 \pm 1$ nm). Ces PdNPs ont été utilisées en catalyse lors de couplages C-C (Suzuki-Miyaura, Sonogashira et Heck) dans un mélange $H_2O/EtOH$ (1/1) et lors de la réduction du 4-nitrophenol (4-NP) en 4-aminophenol (4-AP) dans l'eau. Les résultats ont révélé que les PdNPs stabilisées par G0 étaient plus efficaces et que le couplage de Suzuki-Miyaura d'aromatiques bromés était quantitatif en présence de seulement 0,00003 % molaire de Pd (0,3 ppm) entraînant ainsi une contamination négligeable en Pd des produits issus du couplage. Cette quantité de palladium, minime permettant de catalyser la réaction a conduit à la dénomination de catalyse homéopathique par Beletskaya et De Vries.⁽²⁾ Les résultats obtenus au cours des autres réactions catalytiques sont aussi remarquables et révèlent l'efficacité de ces PdNPs. La petite taille des PdNPs serait liée à la méthode de synthèse imposant une concentration en sels de Pd(II) spécifique avant réduction en NPs ; il en est de même pour l'activité catalytique. Bien que ceci n'ait été prouvé qu'avec les dendrimères à terminaison TEG, durant la dernière année de thèse, nous avons collaboré avec le docteur Sylvain Gatard sur la stabilisation de NPs par des glyco-dendrimères. En reprenant notre méthode de synthèse de PdNPs, la taille des nanoparticules précédemment publiées⁽³⁾ est passée de 14 ± 3 nm à $2,3 \pm 0,4$ nm comme prévu. Cependant, l'activité catalytique (pour la réaction de Suzuki-Miyaura) de ces PdNPs est loin d'être aussi bonne que celle obtenue avec des dendrimères à terminaisons TEG, ce qui met en évidence le rôle des TEG.

Références:

- 1) a) Diallo, A. K.; Ornelas, C.; Salmon, L.; Ruiz, J.; Astruc, D. "Homeopathic" catalytic activity and atom-leaching mechanism in Miyaura-Suzuki reactions under ambient conditions with precise dendrimer-stabilized Pd nanoparticles, *Angew. Chem. Int. Ed.* **2007**, *46*, 8644–8648; b) Ornelas, C.; Diallo, A. K.; Ruiz, J.; Astruc, D. "Click" polymer-supported palladium nanoparticles as highly efficient catalysts for olefin hydrogenation and Suzuki coupling reactions under ambient conditions, *Adv. Synth. Catal.* **2009**, *351*, 2147-2154.
- 2) a) Beletskaya, I. P.; Cheprakov, A. V. The Heck reaction as a sharpening stone of palladium catalysis, *Chem. Rev.* **2000**, *100*, 3009–3066; b) Reetz, M.; de Vries, J. G. Ligand-free Heck reactions utilising low Pd-loading, *Chem. Commun.* **2004**, 1559–1563.
- 3) Gatard, S.; Liang, L.; Salmon, L.; Ruiz, J.; Astruc, D.; Bouquillon, S. Water-soluble glycodendrimers: synthesis and stabilization of catalytically active Pd and Pt nanoparticles, *Tetrahedron Lett.* **2011**, *52*, 1842–1846.

“Click” Dendrimer-Stabilized Palladium Nanoparticles as a Green Catalyst Down to Parts per Million for Efficient C–C Cross-Coupling Reactions and Reduction of 4-Nitrophenol

Christophe Deraedt,^a Lionel Salmon,^b and Didier Astruc^{a,*}

^a ISM, UMR CNRS 5255, Univ. Bordeaux, 351 Cours de la Libération, 33405 Talence Cedex, France
E-mail: d.astruc@ism.u-bordeaux1.fr

^b LCC, CNRS, 205 Route de Narbonne, 31077 Toulouse Cedex, France

Received: February 10, 2014; Published online: June 20, 2014

This article is dedicated to our distinguished colleague and friend Professor Marius Andruh on the occasion of his 60th birthday.



Supporting information for this article is available on the WWW under <http://dx.doi.org/10.1002/adsc.201400153>.

Abstract: The concept of the nanoreactor valuably contributes to catalytic applications of supramolecular chemistry. Therewith molecular engineering may lead to organic transformations that minimize the amount of metal catalyst to reach the efficiency of enzymatic catalysis. The design of the dendritic nanoreactor proposed here involves hydrophilic triethylene glycol (TEG) termini for solubilization in water and water/ethanol mixed solvents combined with a hydrophobic dendritic interior containing 1,2,3-triazole ligands that provide smooth stabilization of very small (1 to 2 nm) palladium nanoparticles (PdNPs). The PdNPs stabilized in such nanoreactors are extraordinarily active in water/ethanol (1/1) for the catalysis of various carbon-carbon cou-

pling reactions (Suzuki–Miyaura, Heck and Sonogashira) of aryl halides down to sub-ppm levels for the Suzuki–Miyaura coupling of aryl iodides and aryl bromides. The reduction of 4-nitrophenol to 4-aminophenol in water also gives very impressive results. The difference of reactivity between the two distinct dendrimers with, respectively, 27 (G0) and 81 (G1) TEG termini is assigned to the difference of PdNP core size, the smaller G0 PdNP core being more reactive than the G1 PdNP core (1.4 vs. 2.7 nm), which is also in agreement with the leaching mechanism.

Keywords: C–C coupling; dendrimers; green chemistry; nanoreactors; palladium nanoparticles (PdNPs)

Introduction

Nanoparticle catalysis has been shown to be a valuable approach to green processes, because it does not involve polluting ligands.^[1] In particular, palladium nanoparticles (PdNPs) are one of the most remarkable examples of efficient catalysts for the formation of carbon-carbon bonds.^[2] Dendrimers such as PAMAM and PPI are good catalytic supports that are widely used for active metal nanoparticle stabilization. Crooks' group has pioneered catalysis by PAMAM-encapsulated PdNPs^[3] and these PdNPs as well as various other polymer- and inorganic substrate-stabilized PdNPs are good catalysts for carbon-carbon bond formation reactions.^[1,4] Aryl cross-coupling reactions (Suzuki–Miyaura,^[5] Sonogashira,^[6] and Heck^[1b,6c,7] reactions) have indeed become powerful synthetic methods for preparing biaryl compounds,

such as, *inter alia*, natural products, pharmaceuticals and polymers. These cross-coupling reactions also allow a high degree of tolerance for a variety of functional groups. Another important issue is the use of minimum amounts of catalysts, because metal contamination tolerated in organic products does not exceed a few ppm. Along this line only few authors have reported PdNPs that can be active with 10⁻³ Pd mol%.^[2,5f,i,j,8] In this context, the stabilization of active PdNPs by “click” dendrimers terminated by triethylene glycol groups has been proposed. These PdNPs seem to be sufficiently stabilized by the triazolyl groups to avoid aggregation and are at the same time labile enough to catalyze the Suzuki–Miyaura reaction of various bromoarenes in an aqueous solvent. The advantage of PEG termini is that PdNPs can be synthesized in water by reduction of K₂PdCl₄ using NaBH₄,^[8f] which leads to a better activity than that

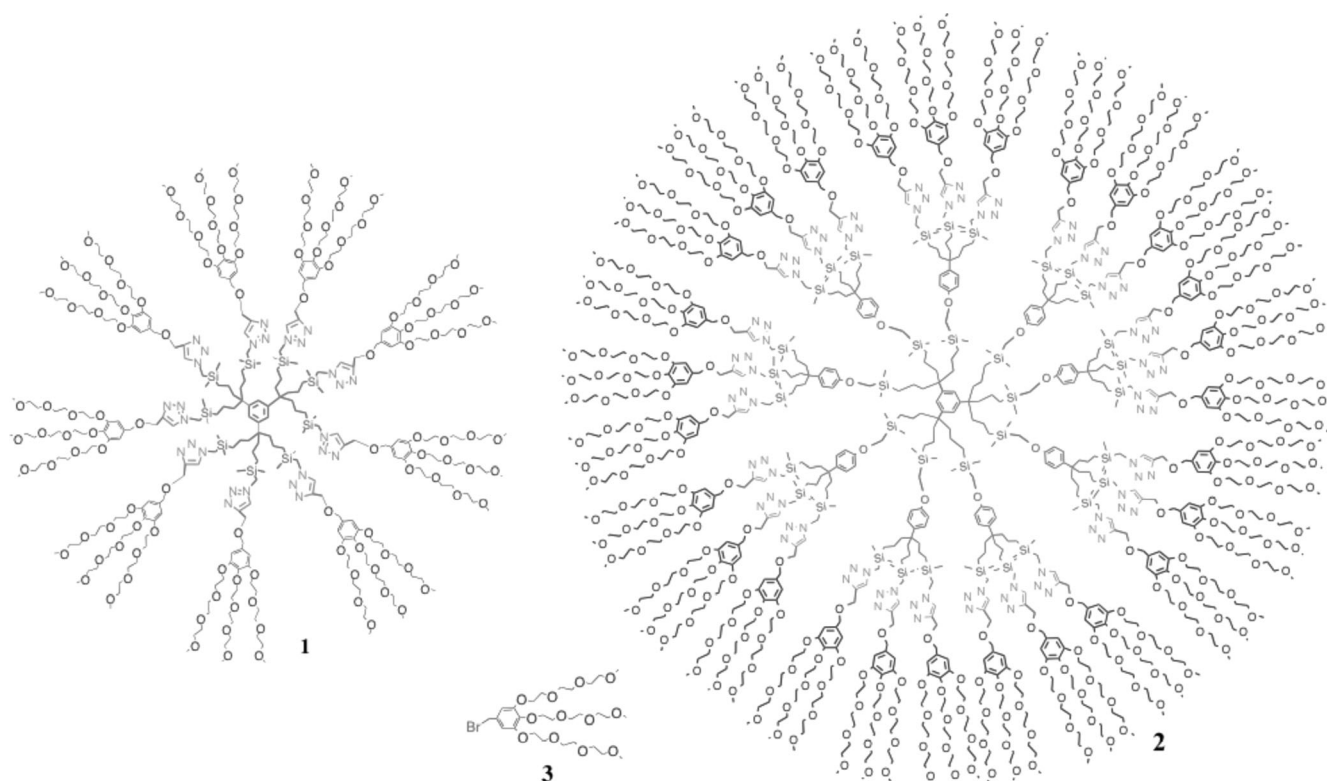


Figure 1. G0-27 TEG **1** dendrimer, G1-81 TEG **2** dendrimer and dendron TEG **3**.

previously observed upon dendrimer stabilization of PdNPs.^[8a]

We now report the optimized synthesis and full characterization of “click” dendrimer-stabilized PdNPs and their activity in very low amounts for cross carbon-carbon coupling reactions (Miyaura–Suzuki, Sonogashira and Heck) in “green” media such as water/ethanol (1/1) and for the reduction of 4-nitrophenol to 4-aminophenol in the presence of NaBH₄ in water. The latter reaction is also useful because 4-aminophenol is a potential industrial intermediate in the manufacture of many analgesic and antipyretic drugs, anticorrosion lubricants, and hair dyeing agents.^[9]

Results and Discussion

Synthesis and Characterization of the PdNP Catalysts

The water-soluble “click” dendrimers of 0th (G0) and 1st generation (G1), compounds **1** and **2** respectively, have been previously synthesized^[8f,10] and are represented in Figure 1. They contain 9 (G0) and 27 (G1) 1,2,3-triazolyl groups linking the dendritic core to Percec-type dendrons^[11] and, respectively, 27 and 81 triethylene glycol (TEG) termini. The dendrimer-Pd(II) complexes are synthesized in water by adding to the dendrimer one equiv. K₂PdCl₄ per dendritic tri-

azole group (the optimized stoichiometry towards further PdNP catalysis). The nature of the Pd(II) complexation sites in the dendrimer has been examined by UV-vis. spectroscopy, when K₂PdCl₄ is added to it. In the UV-vis. spectrum of K₂PdCl₄ alone, two characteristic bands are present at 208 nm and at 235 nm. When the UV-vis. spectra are recorded with the G0-TEG dendrimer **1** as a blank, a new band clearly appears at 217 nm upon mixing the aqueous solution of K₂PdCl₄ with that of **1** (after stirring for 5 min) (Figure 2). On the other hand, when Pd(II) is in the presence of the terminal TEG dendron **3** (no dendrimer core and no triazole ring, Figure 1), no band appears. The band observed at 217 nm when K₂PdCl₄ is added to the dendrimer in water has been assigned to a ligand-to-metal charge-transfer (LMCT) transition of Pd(II). It is associated to the complexation of the metal ions to the interior triazole of **1**. In Crooks' reports, a band at 225 nm has already been associated to the complexation of Pd(II) to the interior tertiary amine of the PAMAM dendrimer.^[3a,c] The UV-vis. spectrum of the mixture of K₂PdCl₄ and **3** does not correspond to the UV-vis. spectrum of the mixture of K₂PdCl₄ with **1**. In particular, no band is observed at 217 nm in the mixture of K₂PdCl₄ with **3**. These experiments show the intradendritic complexation of Pd(II) at the triazole sites of **1**, and they also indicate that there is no strong Pd(II) complexation of the terminal TEG groups. The importance of the triazolyl

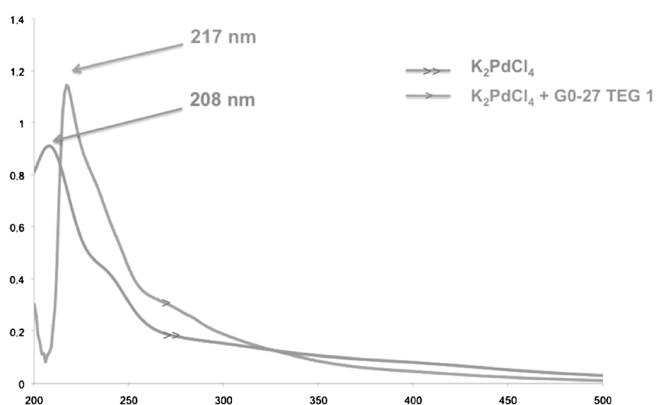
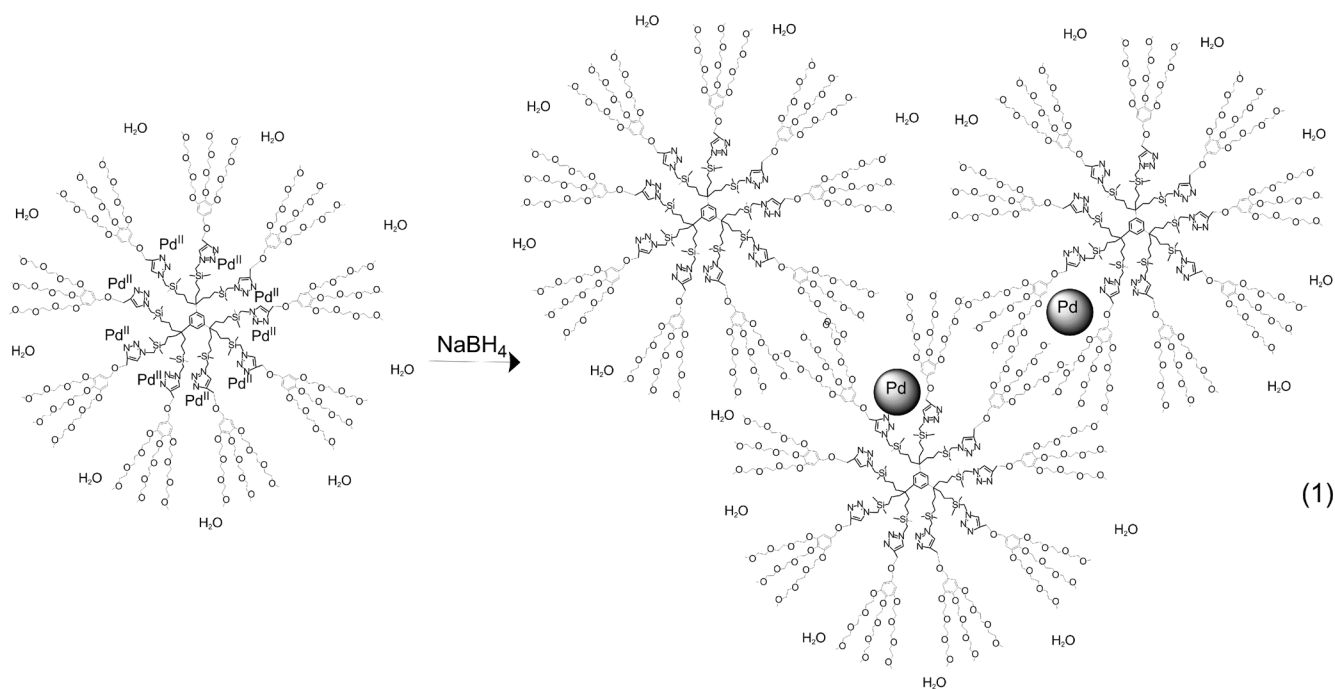


Figure 2. UV-vis spectrum of K_2PdCl_4 alone (one strong absorption band is observed at 208 nm) and UV-vis spectrum of Pd(II) complexed with the interior triazolyl groups of **1** (new absorption band at 217 nm). The UV-vis spectrum of complexed Pd(II) has been recorded with a solution of **1** alone as blank.

group in the stabilization of NPs has also been shown in former works during the synthesis/stabilization of AuNPs by various polyethylene glycol (PEG)-terminated dendrimers. When a dendrimer does not contain triazole groups, the AuNPs that are formed are very large (around 20 nm), whereas with a dendrimer containing triazole groups, smaller AuNPs are formed (around 4 nm).^[12a] This clear distinction demonstrates the key role of triazole groups in the dendrimer for the stabilization of small (active) PdNPs. In the 1H NMR spectrum, a shift of the triazolyl proton is observed upon adding 1, 5, and 9 equivalents of K_2PdCl_4 per G0 dendrimer **1** (7.85 ppm, 7.93 ppm,

7.96 ppm), and the peak becomes broader when Pd(II) is added, which confirms the presence of an interaction between the triazole group and Pd(II).

The reduction of Pd(II) (1 equiv. per triazolyl group) to Pd(0) is carried out in water using 10 equiv. $NaBH_4$ per Pd [Eq. (1)] in the case of PdNP stabilized by several equiv. of **1**). Dialysis is carried out in order to remove excess $NaBH_4$ and eventually purify the PdNPs from any Pd derivatives. It is not indispensable, however, because the results in catalysis are similar with and without dialysis. It is known that $NaBH_4$ inhibits catalytic activity by formation of borides at the particle surface,^[8a] but this is not the case in aqueous media, because the borohydride is then fully hydrolyzed. When dialysis is applied during 1 day, ICP-OES analysis indicates that the Pd loading in the PdNPs is 96% of starting Pd.^[8f] This result shows that 96% of the starting Pd is converted to PdNPs and they are stabilized by dendrimers. The polydispersities of these PdNPs shown by DLS are good, and the TEM and HRTEM images reveal that the PdNPs are very small, 1.4 ± 0.7 nm in **1** and 2.7 ± 1.0 nm in **2**, that is, of optimal size for their use in catalysis (Figure 3). The average number of Pd atoms in the G0-TEG-dendrimer **1** PdNPs is around 100 (with a large proportion on edges and corners) and that for G1-TEG **2** PdNPs is around 1000. Thus, although there are only 9 Pd(II) per G0-TEG dendrimer **1** and 27 Pd(II) per G1-TEG dendrimer **2**, the number of Pd atoms in the dendrimer-stabilized PdNPs is considerably larger than the number of Pd(II) ion precursors in each dendrimer. This means that the large majority of the dendrimer molecules do not contain a PdNP, and there is

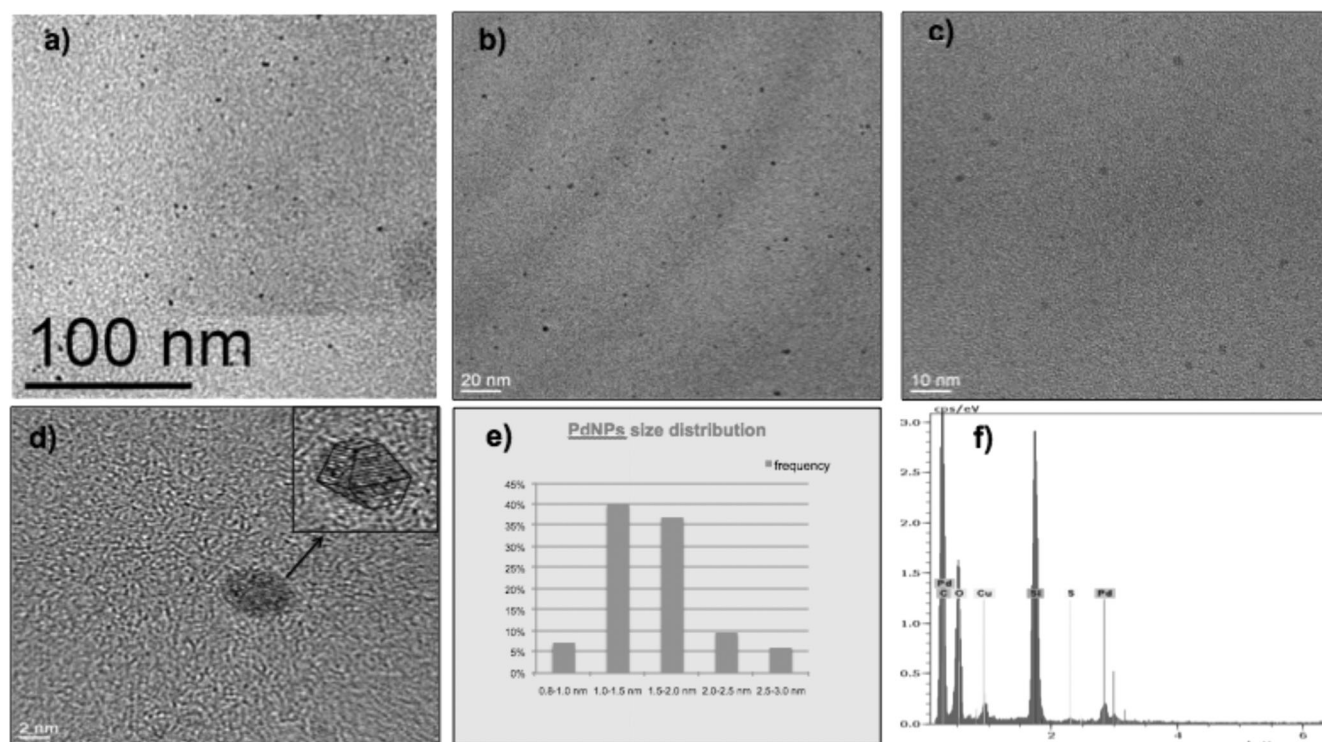


Figure 3. TEM HR-TEM of PdNPs stabilized by **1**. **a)** TEM of PdNPs stabilized by **1**. **b)** and **c)** HR-TEM of PdNPs stabilized by **1** with, respectively, 20 nm and 10 nm bar scales. **d)** PdNPs stabilized by **1** with a 2 nm bar scale, a truncated bipyramid is observed. **e)** PdNPs distribution (624 PdNPs). **f)** EDX of this system, indicating the presence of Pd in NP observed by HR-TEM.

thus an interdendritic contribution to the strong PdNP stabilization, specifically with **1** that has a relatively small size. That several dendrimers (11 small G0-TEG dendrimer molecules **1**) are necessary to stabilize a single PdNP is a situation that is in sharp contrast with the one previously encountered with ferrocenyl-terminated click dendrimers for which the number of Pd atoms in the PdNP matched that of Pd(II) precursors in each dendrimer.^[8a] This contrast is due to the TEG termini of the present “click” dendrimer family. The hydrodynamic diameters of the TEG dendrimers determined by DOSY NMR and DLS are 5.5 ± 0.2 nm and 9 nm, respectively, for **1** and 13.2 ± 0.2 nm and 16 nm, respectively, for **2**. The actual size is best reflected by the DOSY NMR values, and it is expected that the DLS values take into account the water solvation around the dendrimers that increases the apparent dendrimer size. These DLS values are much larger than what is expected for a single dendrimer, which means that a number of dendrimers aggregate in water to form a supramolecular assembly of dendrimers. The aggregation of TEG dendrimers is facilitated by TEG-terminated dendrimers that interpenetrate one another because of the supramolecular forces attracting the TEG tethers among one another. What is remarkable is that, when the PdNPs are formed, the DLS size value considerably increases for G0 from 9 to 31 whereas it only in-

creases from 16 nm to 18 nm for G1 (Figure 4). This strongly argues in favor of a full encapsulation of the stabilized PdNPs for the large dendrimer G1 that undergoes a modest size change upon PdNP formation and, on the opposite side, for an assembly of small dendrimers G0 stabilizing a PdNP. Note that the PdNPs stabilized by the TEG dendrimers are stable under air for several months without any sign of aggregation and that the size determined by TEM and the catalytic activity (*vide infra*) remain the same after such prolonged periods of time. It turns out that such an assembly of TEG dendrimers is ideal for the stabilization of a single PdNP. Thus, although dendrimer-stabilized NPs have been reported earlier,^[6,8b,a,12] one is dealing here with a new type of stabilization of PdNPs by dendrimers that is specifically due to the combination between 1,2,3-triazole and TEG at the dendrimer periphery. The other interests of TEG moieties are the biocompatibility and the compatibility with both hydrophobic substrates and hydrophilic media.

Catalytic Experiments

The catalytic activity of the PdNPs has been investigated for three different C–C cross-coupling reactions: the Suzuki–Miyaura, Sonogashira and Heck

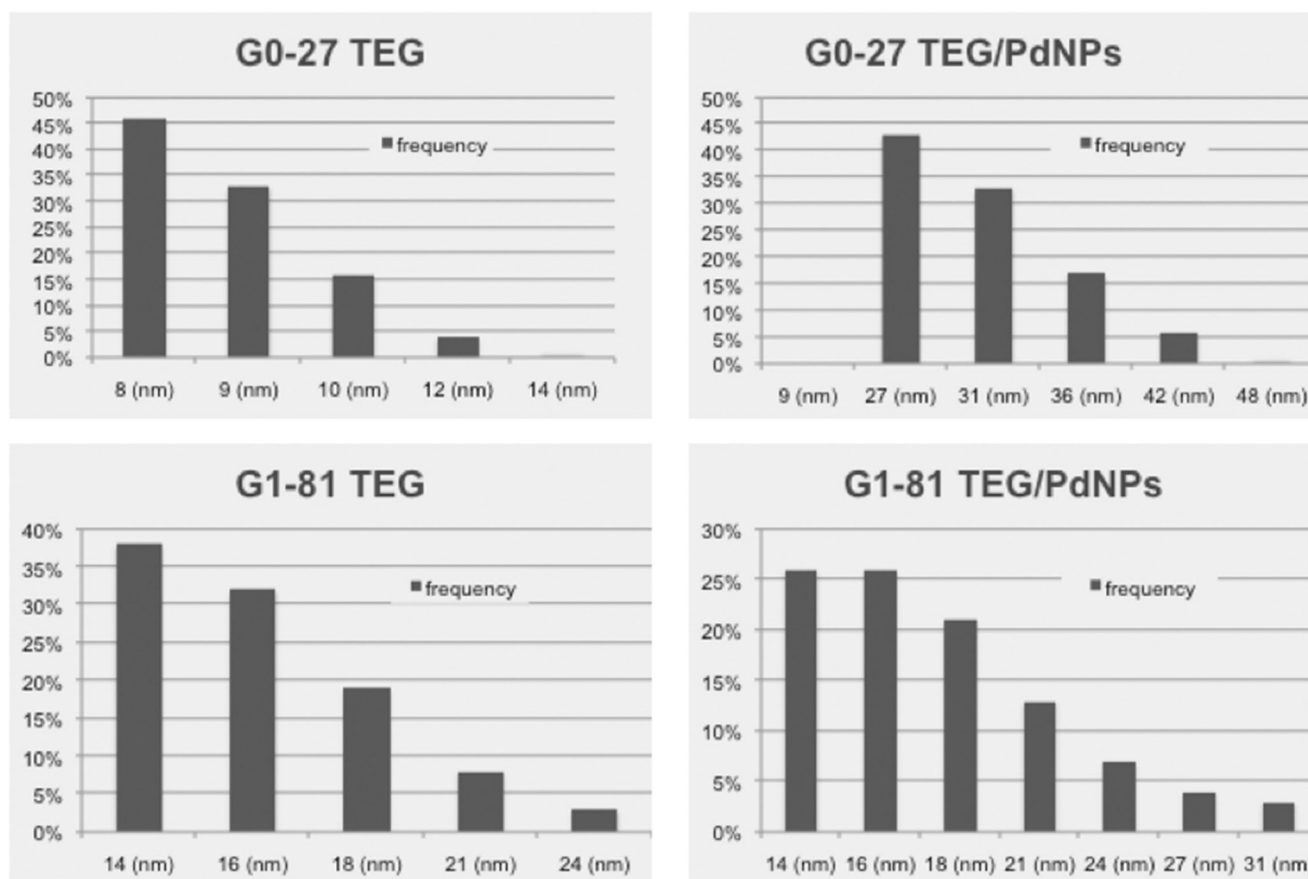
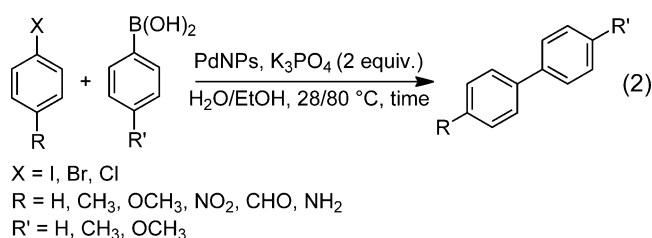


Figure 4. Dynamic light scattering (DLS) of dendrimers alone and dendrimer assemblies in the presence of PdNPs. **a)** DLS distribution of G0-27 TEG, **1**, alone. The average DLS size is 9 nm. **b)** DLS distribution of G0-27 TEG, **1**, with PdNPs. The average DLS size is 31 nm, no assemblage has been observed before 27 nm. **c)** DLS distribution of G1-81 TEG, **2**, alone. The average DLS size is 16 nm. **d)** DLS distribution of G1-81 TEG, **2**, with PdNPs. The average DLS size is 18 nm.

cross-coupling reactions and for the reduction of 4-nitrophenol to 4-aminophenol.

The Suzuki–Miyaura reactions were conducted in H₂O/EtOH (1/1), a green solvent, (as the two other C–C cross-coupling reactions) with three boronic acids and iodo-, bromo- and chloroarenes [Eq. (2)].



In the case of the reaction of iodobenzene with various boronic acids, the Suzuki–Miyaura reaction worked well even with a very small quantity of Pd (PdNPs stabilized by **1**), down to 3×10^{-5} mol%, that is, 0.3 ppm Pd in 80% yield (turnover number TON =

2.7×10^6 ; turnover frequency TOF = $2.8 \times 10^4 \text{ h}^{-1}$, entry 6). The effect of electron-releasing groups on phenylboronic acid and iodobenzene was examined, and the results are gathered in Table 1. The G0-PdNPs are still active after 96 h of reaction at 28 °C. Homocoupling between two iodobenzene molecules, that is, Ullmann-type coupling, is also catalyzed by the G0-PdNP, and at 28 °C it does not occur in the absence of PdNPs. With 0.1 mol% of these efficient PdNPs, the homocoupling yield is 20% in 24 h under the conditions of the reactions in Table 1, but lower amounts of G0-PdNPs give 0% yield of biphenyl, the homocoupling product, whereas a quantitative Suzuki–Miyaura coupling yield is obtained (with 1 ppm of Pd, for example). In the absence of iodoarene, no biphenyl is produced either in the presence of phenylboronic acid with 0.1% G0-PdNPs. This shows that the G0-PdNP-catalyzed cross-coupling reaction of iodobenzene occurs with complete selectivity. The reactions were also performed in air under the same conditions as those of entry 3 for comparison, and the yield was 98%, which is similar to that obtained

Table 1. Isolated yields and TONs for the catalysis by G0 PdNPs of the Suzuki–Miyaura coupling reactions between iodoarenes [p -RC₆H₄I] and arylboronic acids [p -R'C₆H₄B(OH)₂].^[a]

R	R'	Entry	Pd [%]	Time [h]	Yield ^[d] [%]	TON	
H	H	1 ^[b]	0.1	6	86	860	
		2 ^[b]	0.1	12	99	990	
		3	0.01	12	99	9900	
		4	0.001	15	99	99000	
		5	0.0001	96	92	920000	
		6 ^[b]	0.00003	120	80	2700000	
	OMe	7	0.1	12	99	990	
		8	0.01	15	96	9600	
		9	0.001	84	99	99000	
		10	0.0001	84	33	330000	
		CH ₃	11	0.1	12	99	990
			12	0.01	15	96	9600
			13	0.001	84	82	82000
			14	0.0001	84	66	640000
CH ₃ O	H	15 ^[b]	0.1	15	99	990	
		16	0.01	15	92	9200	
		17 ^[b]	0.001	84	14	14000	
		18 ^[c]	0.001	12	99	99000	
		19 ^[b]	0.1	15	80	800	
I	H	20 ^[b]	0.1	24	99	990	
		21 ^[b]	0.01	24	43	4300	

^[a] Each reaction is conducted with 0.1 mmol iodoarene p -RC₆H₄I, 0.15 mmol of arylboronic acid p -RC₆H₄B(OH)₂, 0.2 mmol of K₃PO₄ in EtOH/H₂O 1 mL/1 mL at 28 °C.

^[b] Each reaction is conducted with 1 mmol iodoarene p -RC₆H₄I, 1.5 mmol of arylboronic acid p -RC₆H₄B(OH)₂, 2 mmol of K₃PO₄ in EtOH/H₂O 10 mL/10 mL at 28 °C.

^[c] Standard conditions, but at 80 °C instead of 2 °C.

^[d] Isolated yield.

under nitrogen. This means that the catalytic G0-PdNPs are not sensitive to air during the Suzuki–Miyaura reactions at 28 °C during 12 h. The water solution of PdNPs can also be re-used. For instance, with 0.1 mol% Pd, the PdNPs can be recycled more than four times without decrease of reactivity, the yield remaining at 98% for the reaction between iodobenzene and phenyl boronic acid for 15 h at 28 °C. TEM analyses show that the PdNPs are larger after the reaction (8 ± 1 nm) than before ($1.4 \text{ nm} \pm 0.7 \text{ nm}$) but their sizes examined by TEM no longer increase after further catalytic runs. The catalytic activity with recycled PdNPs is the same with iodobenzene for G0-27 TEG under these conditions. At low PdNP concentration (1–5 ppm) with bromoarenes when the G0 PdNP size increased as indicated above, the catalytic activity decreased (*vide infra*). When the PdNPs are in very low amount, the recycling is very difficult to carry out. Another advantage of this system is that it

is very simple to recycle the dendrimer alone without any decomposition, its recovery being quantitative.

The G0-PdNP catalyst is extremely active and efficient for the Suzuki–Miyaura coupling reactions of bromoarenes. At 80 °C, the reaction between 1,4-bromonitrobenzene and phenylboronic acid with only 0.3 ppm of Pd reaches a TON of 2.7×10^6 after 2.5 days ($\text{TOF} = 4.5 \times 10^4 \text{ h}^{-1}$, entry 39). With only 1 ppm of Pd from the G0-PdNP catalyst, the cross-coupling of phenylboronic acid with bromobenzene is quantitative ($\text{TON} = 0.99 \times 10^6$; $\text{TOF} = 1.65 \times 10^4 \text{ h}^{-1}$, entry 25), and the yield is 63% for 1,4-bromoanisole ($\text{TON} = 0.63 \times 10^6$; $\text{TOF} = 1.05 \times 10^4 \text{ h}^{-1}$, entry 30). These reactions are not observed in the absence of catalyst with any studied substrate. The results of the Suzuki–Miyaura reactions of bromoarenes are gathered in Table 2. In conclusion for bromoarenes, the TONs are very impressive at 80 °C, sometimes even larger than 10^6 . Interestingly, catalysis of cross-cou-

Table 2. Isolated yields and TONs for the catalysis by G0 PdNPs of the Suzuki–Miyaura reactions between bromoarenes [p -RC₆H₄Br] and phenylboronic acid.^[a]

R	Entry	Pd [%]	Time [h]	Yield ^[e] [%]	TON	
H	22	0.1	15	99	990	
	23 ^[c]	0.1	96	66	660	
	24	0.01	24	99	9900	
	25 ^[b,d]	0.0001	60	99	990000	
	26	0.1	15	94	940	
CH ₃ O	27	0.01	24	99	9900	
	28	0.001	24	60	60000	
	29	0.001	48	99	99000	
	30	0.0001	60	63	630000	
	NH ₂	31	0.1	15	96	960
		32	0.01	24	31	3100
		33	0.01	48	40	4000
	NO ₂	34	0.1	15	99	990
		35 ^[c]	0.1	240	80	800
		36	0.001	24	87	87000
37		0.001	36	98	98000	
38 ^[d]		0.0001	60	91	910000	
39 ^[b]		0.00003	60	82	2700000	
40		0.1	24	99	990	
CH ₃	41	0.001	48	99	99000	
	42	0.0001	48	46	460000	
CHO	43	0.1	24	99	990	
	44	0.01	24	80	8000	
	45	0.001	24	20	20000	

^[a] Each reaction is conducted with 1 mmol bromoarene, [p -RC₆H₄Br] in 0.05 M as final concentration, 1.5 mmol of phenylboronic acid and 2 equiv. K₃PO₄ in EtOH/H₂O (10 mL/10 mL) at 80 °C.

^[b] Same conditions but in EtOH/H₂O (5 mL/5 mL), C[RC₆H₄Br] = 0.1 M.

^[c] Standard conditions but at 28 °C instead of 80 °C.

^[d] The reaction is also conducted on a larger scale (10 g of p -RC₆H₄Br), leading to similar isolated yields.

^[e] Isolated yield.

Table 3. Comparison of Suzuki–Miyaura reactions of bromoarenes catalyzed by various PdNP catalysts from the literature [Eq. (3)].^[a]

R ^[ref]	Catalyst	Temp. [°C]	TON	TOF [h ⁻¹]
4-H ^[13a]	PSSA-co-MA-Pd(0)	100	99	5940
4-OMe ^[13b]	Pd-SDS	100	38	456
4-OMe ^[8e]	Pd-PVP (MTPs)	100	1680	1680
4-Me ^[13c]	Pd-PEG	25	90	45
4-NO ₂ ^[13d]	Pd-1/FSG	100	990	123
4-OMe ^[6a]	Fe ₃ O ₄ -Pd	50	144	12
4-OMe ^[13e]	pEVPBr-Pd	90	340	38
4-OMe ^[13f]	Pd-PS	100	50	10
4-COMe ^[13g]	HAP-Pd(0)	100	139	23
4-OMe ^[13h]	PdCl ₂ (py) ₂ @SHS	60	4681	14050
4-COMe ^[5j]	Pd/IL	120	970	970
4-OMe ^[5l]	Pd-MEPI	100	24250	8083
4-COMe ^[5f]	Pd-salt	90	4250	1062
4-OMe ^[13i]	Pd@PNIPAM	90	300	30
4-Me ^[13j]	Pd _x ([PW ₁₁ O ₃₉] ⁷⁻) _y	80	89	7
4-OMe ^[13k]	Pd-block-co-poly	90	310	31
4-COMe ^[8c]	Pd-G3-p3	80	85000	2125
4-OMe ^[8c]	Pd-G3-p3	80	82	10
4-H ^[4l]	Pd@CNPCs	50	982	327
4-Me ^[13l]	PS-PdONPs	80	59	59
4-Me ^[4n]	Pd-TiO ₂	80	115	29
4-OMe ^[13m]	Pd@PMO-IL	75	475	95
4-NH ₂ ^[13n]	Pd-XH-15-SBA	90	96	7
4-OMe ^[13o]	Pd ²⁺ -G0	80	386	99
4-Me ^[13p]	Pd ⁽⁰⁾ /Al ₂ O ₃ -ZrO ₂	60	45	12
4-OMe ^[5i]	Pd(OAc) ₂ /L	100	19600	2800
4-OMe ^[13q]	Pd(OAc) ₂ /CNC-pincer	100	1000	500
4-H ^[5g]	Pd/Y Zeolite	100	13 × 10 ⁶	8.7 × 10 ⁶

^[a] The reactions have been conducted with various catalysts at various temperatures in aqueous solvents (the comparison is limited to representative PdNP catalysts that are used in aqueous solvents).

pling between bromobenzene and phenylboronic acid at 80 °C at relatively high concentrations such as 0.1 mol% Pd is relatively slow, that is, the yield is 20% after 2 h, 50% after 6 h, and 15 h are required for completion (entry 22). Thus diluting the catalyst 1000 times to the ppm level leads to only a period of time four times longer to reach completion (entry 25). This in favor of the leaching mechanism along with capture of the reactive leached atoms by the mother PdNP, an inhibition phenomenon that increases as the catalyst concentration increases.

Recycling experiments using the G0-PdNPs for which the TEM shows a size of 8 nm after the first run give a 78% yield of coupling between bromoanisole and phenylboronic acid at 80 °C (2.5 days) when 5 ppm Pd of the G0-PdNPs are used, which shows that the activity has decreased compared to the initial run, due to the increased size. Concerning the G1-PdNP catalyst, reactions under the same conditions as in Table 2, (80 °C, 2.5 days) between bromoarenes and phenylboronic acid using 1 ppm Pd give yields of 20% with bromobenzene, 27% with bromoanisole and 39% with 1,4-bromonitrobenzene.

The catalytic efficiency of G1-PdNPs is lower than that of the G0-PdNPs, which is taken into account by the fact that the G1-PdNPs are larger than the G0-PdNPs. This also is in accord with a leaching mechanism. Thus PdNPs stabilized by **2** will not be used for the other reactions.

With chloroarenes, the results with G0-PdNPs are less impressive than with the other haloarenes, because high temperatures (> 100 °C) are required to activate chloroarenes under these conditions, and at such temperatures these PdNPs aggregate more rapidly than activation of the reactions. For instance, in the case of 1,4-chloronitrobenzene, 0.1% Pd from G0-PdNPs at 90 °C for 2.5 days using KOH gives a 55% yield. Bromoarenes are often less expensive than chloroarenes, however, which is never the case for iodoarenes.

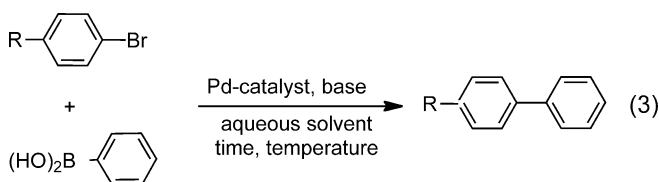
Some recent literature results are summarized in Table 3. These results concern the activity of PdNPs systems (various stabilizers) in the Suzuki–Miyaura cross-coupling reactions.

The G0-27 TEG-PdNPs catalyst is, to the best of our knowledge, one of the most active catalysts

Table 4. Comparison between various dendrimers for the stabilization of PdNPs.

Dendrimer	PdNP size	Solvent used for the synthesis	Storage	Air stable	Iodobenzene TON, TOF	Bromobenzene TON, TOF
G0-9 Fc	2.8 nm	CHCl ₃ /MeOH	no	no	540000, 1042 h⁻¹	265, 15 h⁻¹
*G1-27 Fc	1.3 nm	CHCl ₃ /MeOH	no	no	5200, 363 h⁻¹	–
G0-9 biFc	–	–	–	–	–	–
G1-27 biFc	<i>in situ</i>	CHCl ₃ /MeOH	no	no	5300, 221 h⁻¹	–
G0-9 SO ₃ ⁻	2.3 nm	H ₂ O	no	no	9200, 1533 h⁻¹	10000, 8700 h⁻¹
G1-27 SO ₃ ⁻	2.8 nm	H ₂ O	no	no	9400, 1567 h⁻¹	–
G0-27 TEG 1	1.4 nm	H ₂ O	yes	yes	2700000, 28000 h⁻¹	990000, 16000 h⁻¹

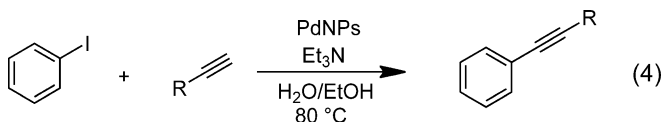
known for Suzuki–Miyaura coupling of bromoarenes [Eq. (3)]. The Suzuki–Miyaura reaction of bromoarenes should be of interest for industrial applications (multi-gram scale reactions have been carried out without decreases of yield and TONs). The use of a very low amount of catalyst will lead to lower costs and lower toxicity.



PdNPs stabilized by dendrimers have been previously reported with various triazolyl termini. First PdNPs were stabilized by dendrimer-containing triazolylferrocenes (Fc)^[8a] (G0-9 Fc, G1-27 Fc) or biferrocenes^[12f] (G0-9 biFc, G1-27 biFc). These dendrimers were not soluble in water, thus only PdNPs synthesized in the mixed solvent CHCl₃/MeOH were appropriate. The solution of PdNPs had to be kept under N₂ and fresh PdNPs used for catalysis. Concerning PdNPs stabilized by dendrimers containing triazolyl-sulfonated termini,^[8b] the PdNPs synthesis is the same as that used for the synthesis of PdNPs stabilized by G0-27 TEG and G1-81 TEG, thus the comparison is more suitable. Table 4 shows a comparison of all the PdNPs stabilized by the present dendrimers. The Suzuki–Miyaura cross-coupling reactions with PdNPs that are stabilized by ferrocenyl- and biferrocenyl-terminated dendrimers are not as favorable, and these reactions are carried out in CHCl₃/MeOH. Moreover, the PdNPs are less stable than in this present case. PdNPs stabilized by G1-27 Fc have sizes that are similar to those of PdNPs stabilized by G0-27 TEG, but the activity is completely different; no activity is observed with bromobenzene. Significant comparisons with G0-9 SO₃⁻ and G1-27 SO₃⁻ indicate that the PdNPs are a little larger than PdNPs stabilized by the TEG dendrimers, which shows the important role of the TEG termini of the dendrimers **1** and **2**. The ac-

tivity in the Suzuki–Miyaura reaction is also lower with the PdNPs stabilized by the sulfonated dendrimers. The stabilities of the PdNPs stabilized by **1** and **2** are far better than those observed earlier, with a possible storage of the present catalyst without strain for months.

The copper-free Sonogashira coupling is more difficult to carry out with PdNPs than the Suzuki–Miyaura reaction and has been investigated in the present study between iodobenzene and various terminal alkynes [Eq. (4)].



The reactions have been carried out in the same mixture of solvents as for the Suzuki–Miyaura reactions but the base Et₃N proved to be more efficient than KOH, K₂CO₃ or K₃PO₄. The results are reported in Table 5.

Remarkably, the Sonogashira coupling between iodobenzene and aromatic alkynes works without

Table 5. Sonogashira coupling between iodobenzene and different alkynes catalyzed by G0-27 TEG-PdNPs.^[a]

R [Eq. (4)]	Entry	Pd [%]	Time [h]	Yield ^[c] [%]	TON, TOF [h ⁻¹]
C ₆ H ₅	46 ^[b]	0.1	24	93	930, 38.75
C ₆ H ₅	47	0.01	24	90	9000, 375
<i>p</i> -Br-C ₆ H ₄	48	0.01	24	71	7100, 296
<i>p</i> -NH ₂ -C ₆ H ₄	49	0.01	24	75	7500, 312.5
<i>p</i> -NH ₂ -C ₆ H ₄	50	0.01	36	93	9300, 258.3
C ₅ H ₄ N ^[d]	51	0.01	36	79	7900, 219.4
<i>p</i> -CH ₃ -C ₆ H ₄	52	0.01	24	90	9000, 375

^[a] Each reaction is conducted with 1 mmol iodobenzene, 1.2 mmol of alkyne and 3 equiv. Et₃N in EtOH/H₂O (1 mL/1 mL) at 80 °C.

^[b] Same conditions but with 10/10 mL EtOH/H₂O.

^[c] Isolated yield.

^[d] Substrate = 3-ethynylpyridine.

Table 6. Examples of active PdNP catalysts in Sonogashira coupling between iodobenzene and phenylacetylene.

Catalyst ^[ref.]	Pd [mol%]	Solvent	Temp. [°C]	TON, TOF [h ⁻¹]
Pd/Pectin ^[14a]	0.28	DMF	100	325, 433
Pd/SiO ₂ @Fe ₂ O ₃ ^[14b]	1	DMF	100	95, 15.8
Pd/NH ₂ -SiO ₂ ^[14c]	0.05	DMF	110	1960, 980
Pd-C _{binaphthyl} ^[14d]	1	MeOH	90	91, 4.1
Pd/carbene ^[14e]	4	DMF/H ₂ O	90	23.5, 7.8
Pd/MOF-5 ^[14f]	2.8	MeOH	80	35, 11.6
Pd/PRGO ^[14g]	0.5	H ₂ O/EtOH	180 (<i>μw</i>)	184, 1104
PS-PdONPs ^[13i]	1.5	H ₂ O	80	66, 11

copper co-catalyst even with a low amount of Pd (i.e., 0.01% mol) leading to TONs up to 9300 and TOFs up to 375 h⁻¹ (entry 47). These results are not as impressive as those obtained for the Suzuki–Miyaura reaction (the reaction does not work with bromobenzene instead of the iodobenzene nor with aliphatic alkynes instead of aromatic alkynes), but in the context of using as little metal as possible, they are of great interest. Let us compare the reaction between iodobenzene and phenylacetylene in the presence of PdNPs in various solvents with literature data (Table 6). The results obtained with the present PdNP catalyst are comparable with those obtained with other systems. The solvent used is safer than in most cases, and the temperature is modest. Even if the time of reaction is longer, the small amount of catalyst used in the present study is a serious advantage in the perspective of "green" chemistry.

Table 7. Heck reaction between iodobenzene and styrene or methyl acrylate.^[a]

R	Entry	Pd [%]	Time [h]	Yield ^[f] [%]	TON, TOF [h ⁻¹]
C ₆ H ₅	53	0.1	14	73	730, 52
C ₆ H ₅	54	0.1	24	82	820, 34
C ₆ H ₅	55	0.1	24	50 ^[b]	500, 20.8
C ₆ H ₅	56	0.1	24	66 ^[c]	660, 27.5
C ₆ H ₅	57	0.1	24	8 ^[d]	80, 3.3
C ₆ H ₅	58	0.3	24	90	300, 12.5
C ₆ H ₅	59	0.01	24	8 ^[b]	800, 33
CH ₃ OC(O) ^[e]	60	0.1	14	42	420, 30
CH ₃ OC(O) ^[e]	61	0.1	14	0 ^[g]	0, 0
CH ₃ OC(O)	62	0.1	24	98	980, 40.8
CH ₃ OC(O)	63	0.01	48	20	2000, 41.6

^[a] Each reaction has been conducted with 1 mmol iodobenzene, 1.5 mmol alkene and 3 equiv. KOH in EtOH/H₂O: 1/1 at 105 °C.

^[b] Reaction conducted with K₃PO₄ (3 equiv.) as a base.

^[c] Reaction conducted with K₂CO₃ (3 equiv.) as a base.

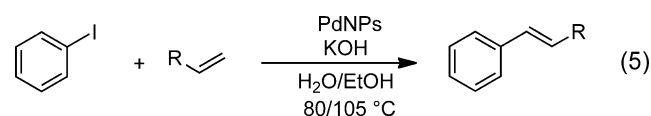
^[d] Reaction conducted with Et₃N (3 equiv.) as a base.

^[e] The reaction has been conducted at 80 °C.

^[f] Isolated yield.

^[g] Yield for the reaction in H₂O alone as solvent).

The Heck reaction between iodobenzene and styrene or methyl acrylate has been examined under the same conditions as the Suzuki–Miyaura and the Sonogashira reactions, that is, at 80 °C or 105 °C in H₂O/EtOH: 1/1 essentially with 0.1% Pd [Eq. (5)], and the results are gathered in Table 7.



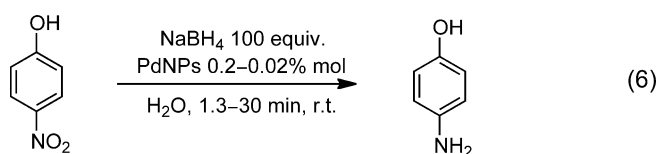
The reaction works well between iodobenzene and styrene, the best results being obtained using KOH as the base.

The reaction with methyl acrylate and iodobenzene leads to the corresponding phenylacrylic acid due to *in situ* saponification. Some destruction of the PdNPs and formation of Pd black precipitate are observed upon excessive heating. Moreover the reaction is not observed when bromobenzene is used instead of iodobenzene. With 0.01% PdNPs the yield is very low for this reaction (8%, entry 57; 20%, entry 63) due to complete precipitation of the PdNPs to Pd black. In water only as the solvent, the Heck reaction does not work with 0.1% Pd.

Seminal studies from the groups of Reetz,^[2a] Beletskaya,^[2b] and de Vries^[2c,4d,e] led to the designation of "homeopathic" palladium catalysis for Heck and Suzuki–Miyaura reactions with aryl iodides and, in some cases, aryl bromides, and industrial large-scale applications have been developed with the term "homeopathic" indicating the use of extremely low amounts of catalyst.^[2c]

The present results for the Heck reaction are not as impressive in comparison with the "homeopathic" studies of Beletskaya, Reetz, and de Vries (and others) but the term "homeopathic" could be assigned to the present results on the Suzuki–Miyaura and Sonogashira reactions.

The reduction of 4-nitrophenol (4-NP) to 4-aminophenol (4-AP) is another very quick and simple reaction that is catalyzed by these PdNPs stabilized by G0-27 TEG **1** [Eq. (6)].



4-AP is a potential industrial intermediate in manufacturing many analgesic and antipyretic drugs, anti-corrosion lubricants, and hair dyeing agents, thus efficient PdNP catalysis of 4-NP reduction is of great value. The high efficiency in the C–C cross-coupling reactions and the dependence of the rate of this catalysis on the nanoparticle size were encouraging factors to probe this reaction. A convenient aspect is the possibility of monitoring the progress of the reaction by UV-vis spectroscopy. Indeed, a typical peak at 400 nm is directly related to 4-NP (corresponding to 4-nitrophenate appearing in the presence of NaBH₄) and at 300 nm to the 4-AP. The disappearance of the yellow color of the solution is a sign of the reaction progress. The reduction of 4-NP has been carried out in the presence of excess of NaBH₄ (100 equiv.) as a “safe” source of H₂ and 0.2% mol of PdNPs in water. The progress of the reaction is connected to the concentration of 4-NP in water solution (Figure 5). When the solution is diluted (4 times) in order to conduct a kinetic monitoring of the reaction, it shows that it is complete in 400 seconds. The apparent rate constant k_{app} is directly obtained from the curve of $-\ln(C_t/C_0)$ vs. time by linear fit, $k_{app} = 0.004 \text{ s}^{-1}$.

In the absence of catalyst the reaction does not progress and the yellow color of the solution is retained after 1 hour. When only 10 equiv. of NaBH₄

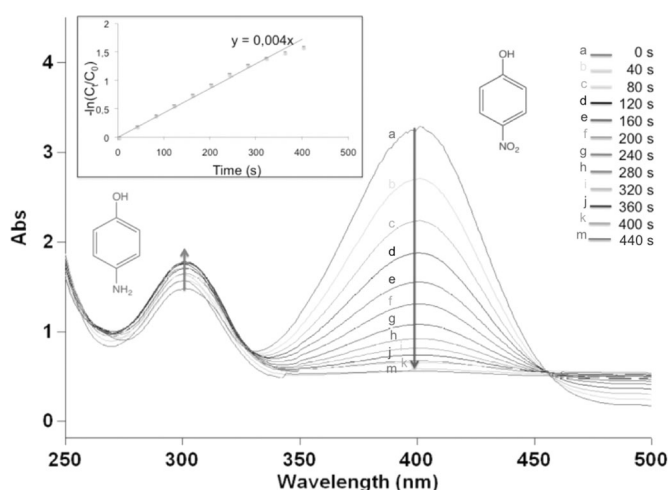


Figure 5. Kinetic study of 4-nitrophenol ($[4\text{-NP}] = 1.25 \times 10^{-3} \text{ M}$) reduction by NaBH₄ in the presence of 0.2% mol of PdNP stabilized by G0-27 TEG using UV-vis. spectroscopy at 400 nm and plot of $-\ln(C_t/C_0)$ vs. time (s) for its disappearance (left corner). (The solution of the reaction has been directly used for the kinetic study.)

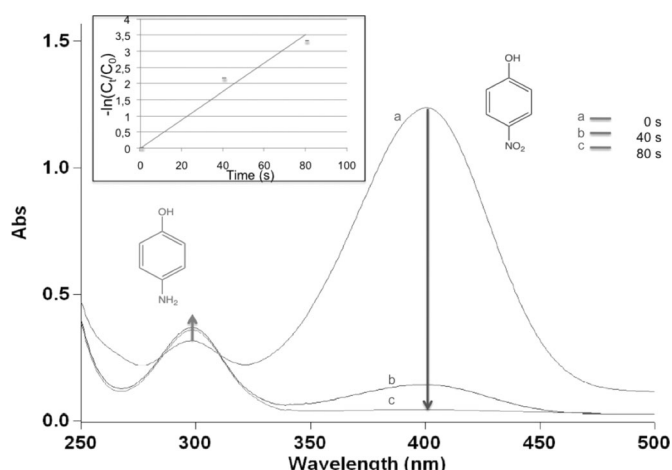


Figure 6. Kinetic study of the 4-nitrophenol ($[4\text{-NP}] = 5.0 \times 10^{-3} \text{ M}$) reduction by NaBH₄ in the presence of 0.2% mol of PdNP stabilized by G0-27 TEG, using UV-vis. spectroscopy at 400 nm and plot of $-\ln(C_t/C_0)$ vs. time (s) for its disappearance (left corner). (The solution of the reaction is diluted 4 times before recording each run).

are used, the reaction is complete in 30 min. When 4 times less water is used for the same quantity of substrate, the reduction is complete in 80 seconds, $k_{app} = 0.044 \text{ s}^{-1}$ (calculated with only 3 results because of the high reaction rate); see Figure 6 (moreover with 0.02% of PdNPs, the reaction is complete in 300 s). The reduction of 4-NP to 4-AP is successful at room temperature in water with a low amount of catalyst (0.2 mol% and 0.02 mol%).

The k_{app} obtained during our study is among the best ones ever obtained, and the TOFs are impressive, as it was in the case for the Suzuki–Miyaura coupling. The comparative Table 8 concerns Pd catalyst systems.

Let us also compare with the investigation of another metal nanoparticle catalyst, gold nanoparticles (AuNPs, Table 9). A large variety of PdNPs and

Table 8. Some examples of PdNP systems used in the reduction of 4-NP.

Catalyst ^[ref.]	Pd [mol%]	NaBH ₄ [equiv.]	k_{app} [s ⁻¹]	TOF [h ⁻¹]
CNT/PiHP/Pd ^[15a]	4	80	5×10^{-3}	300
Fe ₃ O ₄ /Pd ^[15b]	10	139	3.3×10^{-2}	300
PEDOT-PSS/Pd ^[15c]	77	excess	6.58×10^{-2}	13
SPB/Pd ^[15d]	0.36	100	4.41×10^{-3}	819
Microgels/Pd ^[15e]	2.1	100	1.5×10^{-3}	139
PPy/TiO ₂ ^[15f]	2.6	11	1.22×10^{-2}	326
SBA-15 ^[15g]	100	1000	1.2×10^{-2}	6
@Pd/CeO ₂ ^[15h]	0.56	83	8×10^{-3}	1068
G0-27 TEG	0.2	100	4.0×10^{-3}	4500
G0-27 TEG	0.2	100	4.4×10^{-2}	22500

Table 9. Some examples of AuNP systems used in 4-NP reduction.

Catalyst support ^[ref.]	Au [mol%]	NaBH ₄ [equiv.]	k_{app} [s ⁻¹]	TOF [h ⁻¹]
GO ^[16a]	2.6	23	1.9×10^{-1}	126
4,4-bpy ^[16b]	5	100	7.2×10^{-4}	19
PDDA/NCC ^[16c]	2.7	100	5.1×10^{-3}	212
Boehmite ^[16d]	270	100	1.7×10^{-3}	0.69
PANI ^[16e]	1.7	4.4	1.2×10^{-2}	570
GO/SiO ₂ ^[16f]	1.6	200	1.7×10^{-2}	1028
SNTs ^[16g]	27	42	1.1×10^{-2}	46
PNIPAP-b-P4 VP ^[16h]	20	33	1.5×10^{-3}	16
PDMAEMA-PS ^[16i]	700	57	3.2×10^{-3}	1
Poly(DVP-co-AA) ^[16j]	0.37	37	6.0×10^{-3}	222
Chitosan ^[16k]	17	3	1.2×10^{-2}	50
CSNF ^[16l]	0.66	100	5.9×10^{-3}	563
PMMA ^[16m]	6.6	1500	7.2×10^{-3}	89
DMF ^[16n]	1	2000	3.0×10^{-3}	83
SiO ₂ ^[16o]	10.6	29	1.0×10^{-3}	14
PAMAM ^[16p]	1	17	2.0×10^{-3}	196
EGCG-CF ^[16q]	100	1320	2.4×10^{-3}	2
Biomass ^[16r]	5	66	4.6×10^{-4}	20
TWEEN/GO ^[16s]	62.5	23	4.2×10^{-3}	7
HPEI-IBAm ^[16t]	9.5	100	–	120
Graphene ^[16u]	43.4	71	3.2×10^{-3}	12
hydrogel ZnO ^[16v]	333	3000	2.4×10^{-3}	3
α CD ^[16w]	16.6	42	4.7×10^{-3}	34
Peptide ^[16x]	200	246	1.3×10^{-3}	7
PC/PEI/PAA ^[16y]	26.3	160	7.0×10^{-3}	33
MPFs ^[16z]	5	200	3.0×10^{-3}	80
SiO ₂ @Au/CeO ₂ ^[15h]	5	83	1.3×10^{-2}	240

AuNPs stabilized by various supports (polymers, dendrimers, inorganic materials, organic materials and bio-molecules) has been used in the catalytic reduction of 4-NP. All the characteristic of these systems and their catalytic activities are indexed in Table 8 and Table 9.

This comparison shows the high efficiency of our system for this reaction. Even if the k_{app} is not the biggest (although it is nearly so), the amount of catalyst is the lowest and the TOF the largest disclosed one so far.

Conclusions

The TEGylated click dendrimer assemblies represent a new type of nanoreactors for PdNPs that provide stability and catalytic activity during several months without the strain of inert atmosphere. The TEG termini of the dendrimer tethers are responsible for this high degree of intradendritic PdNP stabilization, because they interact interdentritically to form large assemblies. The intradendritic PdNPs are loosely liganded by the 1,2,3-triazoles, which present an excellent compromise between stabilization and lability for an

optimized catalytic activity. The catalytic activity of these PdNPs is exceptionally high with both iodoarene and bromoarene families, reaching TONs that are equal to or larger than 10^6 for both families in the Suzuki–Miyaura reactions. The catalyst **1**-PdNPs is so far, to the best of our knowledge, the most active one for the Suzuki–Miyaura reaction in terms of TONs for bromoarenes. The activity for the Sonogashira coupling is also very remarkable, because the Pd catalyst is copper-free and only 0.01% mol of Pd is used for this coupling, which is rarely used for this reaction (Table 5). The Heck coupling with these PdNPs gives positive results, but because of the instability of the PdNPs at high temperature ($>100^\circ\text{C}$), 0.1 mol% is used for this coupling, and no reaction is observed with less catalyst. The last reaction investigated during this work is the reduction of 4-nitrophenol. As it was in the case of the Suzuki–Miyaura coupling, the results are very impressive and never reached by other systems (Table 8 and Table 9). The amount of Pd is quite low (down to 0.02 mol%) and the TOFs are very high. All these reasons and especially the fact that very low amounts of Pd (down 0.3 ppm) are used, are in agreement with the principles of green chemistry.

It is suggested that the reason for this exceptional catalytic activity of the dendritic nanoreactor **1** is the loose intradendritic stabilization of PdNPs by the triazole ligands combined with the interdentritic assembly provided by the TEG termini that better protects the PdNPs than a single dendrimer. The small size of the PdNPs stabilized by **1** (1.4 ± 0.7 nm), with a truncated bipyramid shape, provides a higher proportion of reactive Pd atoms on the edges and summits than is the case for larger NPs. As a consequence, extremely high TONs are reached, because the catalytic activity is retained at extremely high substrate/catalyst ratios, which is compatible with a leaching mechanism with absence (or rarity) of quenching of the catalytically active species (presumably atoms) at high dilution. At relatively high PdNP concentration, the formation of Pd black that destroys the Pd precatalyst in conventional PdNP catalytic systems is suppressed here by the dendritic stabilization. Finally, these water-soluble dendrimers themselves are very stable and easy to recover whenever needed, and they are re-used many times without signs of decomposition.

Experimental Section

General Data

All the solvents (THF, EtOH, Et₃N) and chemicals were used as received. ¹H NMR spectra were recorded at 25°C with a Bruker AC 200 or 300 (200 or 300 MHz) spectrometer. All the chemical shifts are reported in parts per million

(δ , ppm) with reference to Me₄Si (TMS) for the ¹H spectra. The UV-vis. absorption spectra were measured with Perkin-Elmer Lambda 19 UV-vis. The DLS measurements were made using a Malvern Zetasizer 3000 HSA instrument at 258 °C at an angle of 90°.

Preparation of the PdNPs for Catalysis

Dendrimer **1** (2.59 mg, 3.6×10^{-4} mmol) was dissolved in 1.1 mL of water in a Schlenk flask, and an orange solution of K₂PdCl₄ (3.2×10^{-3} mmol in 1.1 mL water) was added to the solution of the dendrimer. 30 mL of water were then added, and the solution was stirred for 5 min. The concentration of Pd(II) is 0.1 mM. A 1 mL aqueous solution containing 3.2×10^{-2} mmol of NaBH₄ was added dropwise, provoking the formation of a brown/black color (see the Supporting Information) corresponding to the reduction of Pd(II) to Pd(0) and PdNP formation. Then, dialysis was conducted for 1 day in order to remove excess NaBH₄ and eventually purify the PdNPs from any Pd derivatives. Thereafter, ICP-OES analysis indicated that the Pd loading in the PdNPs solution is 96% of starting Pd. This solution was directly used for catalysis. 10 mL of this solution were used when 0.1 mol% Pd per mol substrate is needed for a reaction between 1 mmol of haloarene and 1.5 mmol of boronic acid, and 10 μ L of this solution were used when 1 ppm Pd per mol substrate was needed (in the case of the Suzuki-Miyaura reaction).

General Procedure for Suzuki-Miyaura Catalysis

In a Schlenk flask containing tribasic potassium phosphate (2 equiv.), phenylboronic acid (1.5 equiv.), aryl halide (1 equiv.) and 10 mL of EtOH were successively added. Then the solution containing the dendrimer-stabilized PdNPs was added followed by addition of water in order to respect a volume ratio of H₂O/EtOH of 1/1 (when only water was used, the reaction did not work as well, because of the hydrophobicity of the substrates). The suspension was allowed to stir under N₂ or air (no yield difference). After the reaction time (see Table 1 and Table 2), the reaction mixture was extracted twice with Et₂O (all the reactants and final products are soluble in Et₂O), the organic phase was dried over Na₂SO₄, and the solvent was removed under vacuum. In parallel, the reaction was checked using TLC in only petroleum ether as eluent in nearly all the cases and ¹H NMR. Purification by flash chromatography column was conducted with silica gel as stationary phase and petroleum ether as mobile phase. Another procedure of purification consists in cooling the Schlenk flask at the end of the reaction. The product precipitated, and a simple filtration allowed collection of the product that was then washed with a cold solution of H₂O/EtOH. After each reaction, the Schlenk flask was washed with a solution of aqua regia (3 volumes of hydrochloric acid for 1 volume of nitric acid) in order to remove traces of Pd.

General Procedure for Sonogashira Catalysis

In a Schlenk flask containing triethylamine (3 equiv.), the alkyne (1.2 equiv.), iodobenzene (1 equiv.) and 1 mL of EtOH (volume ratio of H₂O/EtOH of 1/1) were successively added. Then the solution containing the dendrimer-stabi-

lized PdNPs was added (1 mL). The suspension was allowed to stir under N₂ or air (no yield difference). After the reaction time (see Table 5), the reaction mixture was extracted twice with Et₂O (or CH₂Cl₂), the organic phase was dried over Na₂SO₄, and the solvent was removed under vacuum. In parallel, the reaction was checked using TLC in only petroleum ether as eluent and ¹H NMR. Purification by flash chromatography column was conducted with silica gel as stationary phase. After each reaction, the Schlenk flask was washed with a solution of aqua regia (3 volumes of hydrochloric acid for 1 volume of nitric acid) in order to remove traces of Pd.

General Procedure for Heck Catalysis

In a Schlenk flask containing the base (3 equiv.), the alkene (1.2 equiv.), iodobenzene (1 equiv.) and 10 mL of EtOH (volume ratio of H₂O/EtOH of 1/1) were successively added. Then the solution containing the dendrimer-stabilized PdNPs was added (10 mL). The suspension was allowed to stir under N₂ or air (no yield difference). After the reaction time (see Table 7), the reaction mixture was extracted twice with Et₂O (or CH₂Cl₂), the organic phase was dried over Na₂SO₄, and the solvent was removed under vacuum. In parallel, the reaction was checked using TLC in only petroleum ether as eluent in the 2 cases, and ¹H NMR. Purification by flash chromatography column was conducted with silica gel as stationary phase. After each reaction, the Schlenk flask was washed with a solution of aqua regia (3 volumes of hydrochloric acid for 1 volume of nitric acid) in order to remove traces of Pd.

General Procedure for the Reduction of 4-Nitrophenol

In a beaker, 7 mg of 4-nitrophenol (5.03×10^{-5} mol) were mixed with 195 mg of NaBH₄ (5.13×10^{-3} mol) in 20 mL of water. 1 mL of the PdNPs was added (0.2% mol), and the reaction was complete in 80 seconds. 0.5 mL of the total solution was diluted with 1.5 mL of water before the reaction started in order to follow its course by UV-vis. This diluted reaction mixture went to completion in 400 seconds.

PdNP Recycling Procedure

The recycling procedure was carried out 4 times for the Suzuki-Miyaura coupling between iodobenzene (1 mmol) and phenylboronic acid (1.5 mmol). The standard cross-coupling procedure was followed using 0.1% mol PdNPs (10 mL). 1 mL of the PdNP solution was kept before the reaction in order to measure the PdNP size by TEM. After the reaction, the products were extracted twice from the H₂O/EtOH solvent using Et₂O (the dendrimer **1** is not soluble in Et₂O, thus it remains in the aqueous phase with PdNPs). The organic solvent was dried, evaporated, and purification on a column was carried out. 1 mL of the 10 mL aqueous phase was retained for TEM analysis. The remaining solution (containing **1** and PdNPs recycled) was introduced into the following reaction mixture in which all the compounds (1 mmol halide, 1.5 mmol boronic acid, 2 mmol K₃PO₄, 9 mL EtOH) except Pd, have been introduced. This procedure was repeated three more times.

Alternatively, the PdNPs were recycled as follows. In order to investigate the efficiency of the re-used PdNPs, a classic Suzuki–Miyaura reaction was launched between iodobenzene and phenylboronic acid. When the reaction was finished, the solution contained biphenyl, the excess of phenylboronic acid, the base, H₂O/EtOH (10/10 mL) and PdNPs with a size of 8 nm. The preceding solution (100 µL) corresponding to 5 ppm of PdNPs for 1 mmol of substrate was used to catalyze a Suzuki–Miyaura reaction between bromoarenes and phenylboronic acid. The dendrimers alone **1** and **2** were easily quantitatively separated and recycled.

Acknowledgements

Helpful discussions with Dr Jaime Ruiz (Univ. Bordeaux) and financial support from the Univ. Bordeaux and Univ. Toulouse III, the CNRS and the Ministère de l'Enseignement Supérieur et de la Recherche (PhD grant to CD) are gratefully acknowledged.

References

- [1] a) *Nanotechnology in Catalysis, Vols. 1 and 2*, (Eds.: B. Zhou, S. Hermans, G. A. Somorjai), in: *Nanostructure Science and Technology*, Springer, Heidelberg, Berlin, **2003**; b) *Nanoparticles and Catalysis*, (Ed.: D. Astruc) Wiley-VCH, Weinheim, **2008**; c) *Modern Surface Organometallic Chemistry*, (Eds.: J.-M. Basset, R. Psaro, D. Roberto, R. Ugo), Wiley-VCH, Weinheim, **2009**; d) L. M. Bronstein, Z. B. Shifrina, *Chem. Rev.* **2011**, *111*, 5301–5344; e) *Nanomaterials in Catalysis*, (Eds.: P. Serp, K. Philippot), Wiley-VCH, Weinheim, **2013**.
- [2] a) M. T. Reetz, W. Helbig, S. A. Quaiser, in: *Active metals: preparation, characterizations, applications*, (Ed.: A. Fürstner), Wiley-VCH, Weinheim, **1996**, p 279; b) I. P. Beletskaya, A. V. Cheprakov, *Chem. Rev.* **2000**, *100*, 3009–3066; c) J. G. de Vries, *Dalton Trans.* **2006**, 421–429.
- [3] a) M. Zhao, R. M. Crooks, *Angew. Chem.* **1999**, *111*, 375–377; *Angew. Chem. Int. Ed.* **1999**, *38*, 364–366; b) R. M. Crooks, M. Zhao, L. Sun, V. Chechik, L. K. Yeung, *Acc. Chem. Res.* **2001**, *34*, 181–190; c) R. W. J. Scott, H. C. Ye, R. R. Henriquez, R. M. Crooks, *Chem. Mater.* **2003**, *15*, 3873–3878; d) R. W. J. Scott, O. M. Wilson, R. M. Crooks, *Phys. Chem. B* **2005**, *109*, 692–704; e) V. S. Myers, M. W. Weier, E. V. Carino, D. F. Yancey, S. Pande, R. M. Crooks, *Chem. Sci.* **2011**, *2*, 1632–1646.
- [4] a) R. T. Reetz, E. Westermann, *Angew. Chem.* **2000**, *112*, 170–173; *Angew. Chem. Int. Ed.* **2000**, *39*, 165–168; b) H. Bönemann, R. Richards, *Eur. J. Inorg. Chem.* **2001**, *10*, 2455–2480; c) Y. Li, M. A. El-Sayed, *J. Phys. Chem. B* **2001**, *105*, 8938–8943; d) A. H. M. de Vries, J. M. C. A. Mulders, J. H. M. Mommers, H. J. W. Hendericks, J. G. de Vries, *Org. Lett.* **2003**, *5*, 3285–3288; e) A. H. M. de Vries, J. G. de Vries, *Eur. J. Org. Chem.* **2003**, *5*, 799–811; f) M. T. Reetz, J. G. de Vries, *Chem. Commun.* **2004**, *14*, 1559–1563; g) X. Tao, Y. Zhao, D. A. Sheng, *Synlett* **2004**, *2*, 359–361; h) D. Astruc, F. Lu, J. Ruiz, *Angew. Chem.* **2005**, *117*, 8062–8083; *Angew. Chem. Int. Ed.* **2005**, *44*, 7852–7872; i) D. Astruc, K. Heuze, S. Gatard, D. Méry, S. Nlate, L. Plault, *Adv. Synth. Catal.* **2005**, *347*, 329–338; j) N. T. S. Phan, M. van der Sluys, C. J. Jones, *Adv. Synth. Catal.* **2006**, *348*, 609–669; k) *Metal-catalyzed Cross-coupling Reactions*, (Eds.: F. Diederich, P. Stang), Wiley-VCH, Weinheim, **2008**; l) R. P. Beletskaya, A. N. Kashin, I. A. Khotina, A. R. Khokhlov, *Synlett* **2008**, 1547–1552; m) D. Astruc, *Tetrahedron: Asymmetry* **2010**, *21*, 1041–1054; n) B. Sreedhar, D. Yada, P. S. Reddy, *Adv. Synth. Catal.* **2011**, *353*, 2823–2836; o) P. Zhang, Z. Weng, J. Guo, C. Wang, *Chem. Mater.* **2011**, *23*, 5243–5249; p) M. Pagliaro, V. Pandarus, R. Ciriminna, F. Béland, P. Demma Carà, *ChemCatChem* **2012**, *4*, 432–445; q) T. V. Magdesieva, O. M. Nikitina, O. A. Levitskaya, V. A. Zinov'yevab, I. Bezverkhyc, E. V. Zolotukhinab, M. A. Vorotyntsev, *J. Mol. Catal. A* **2012**, *353–354*, 50–57; r) Z. Guan, J. Hu, Y. Gu, H. Zhang, G. Li, T. Li, *Green Chem.* **2012**, *14*, 1964–1970.
- [5] a) N. Miyaura, A. Suzuki, *Chem. Rev.* **1995**, *95*, 2457–2483; b) J. Hassan, M. Sévignon, C. Gozzi, E. Schulz, M. Lemaire, *Chem. Rev.* **2002**, *102*, 1359–1469; c) S. Kotha, K. Lahiri, D. Kashinath, *Tetrahedron* **2002**, *58*, 9633–9695; d) A. Suzuki, in: *Modern Arene Chemistry*, (Ed.: D. Astruc), Wiley-VCH: Weinheim, **2002**, 53; e) F. Bellina, A. Carpita, R. Rossi, *Synthesis* **2004**, 2419–2440. f) For instance, activated bromoarenes such as 4-bromoacetophenone were coupled with phenylboronic acid using 0.02% Pd(OAc)₂, K₂CO₃, NMP/H₂O: 19/1, 90 °C in 95% yield and the Pd loading could be decreased to 25 ppm. Under these conditions in toluene, bromobenzene gave a 50% yield using 0.05% Pd catalyst. The mechanism involved PdNP catalysts or precatalysts formed *in situ* at 90 °C. A. Alimardanov, L. Schmieder-van de Vondervoort, A. H. M. de Vries, J. G. de Vries, *Adv. Synth. Catal.* **2004**, *346*, 1812–1817; g) K. Okumara, T. Tomiyama, S. Okuda, H. Yoshida, M. Niwa, *J. Catal.* **2010**, *273*, 156–166; h) I. Favier, D. Madec, E. Teuma, M. Gómez, *Curr. Org. Chem.* **2011**, *15*, 3127–3174; i) C. Zhou, J. Wang, L. Li, R. Wang, M. A. Hong, *Green Chem.* **2011**, *13*, 2100–2106; j) Y. M. A. Yamada, S. M. Sarkar, Y. Uozumi, *J. Am. Chem. Soc.* **2012**, *134*, 3190–3198.
- [6] a) P. D. Stevens, F. G. Li, J. D. Fan, M. Yen, Y. Gao, *Chem. Commun.* **2005**, 4435–4437; b) R. Chinchilla, C. Najera, *Chem. Rev.* **2007**, *107*, 874–922; c) D. Astruc, *Inorg. Chem.* **2007**, *46*, 1884–1894; d) R. Chinchilla, C. Najera, *Chem. Soc. Rev.* **2011**, *40*, 5084–5121.
- [7] a) W. Cabri, I. Candiani, *Acc. Chem. Res.* **1995**, *28*, 2–7; b) N. J. Whitcombe, K. K. Hii, S. E. Gibson, *Tetrahedron* **2001**, *57*, 7449–7476; c) V. Farina, *Adv. Synth. Catal.* **2004**, *346*, 1553–1582.
- [8] a) A. K. Diallo, C. Ornelas, L. Salmon, J. Ruiz, D. Astruc, *Angew. Chem.* **2007**, *119*, 8798–8802; *Angew. Chem. Int. Ed.* **2007**, *46*, 8644–8648; b) C. Ornelas, J. Ruiz, L. Salmon, D. Astruc, *Adv. Synth. Catal.* **2008**, *350*, 837–845; c) S. Ogasawara, S. Kato, *J. Am. Chem. Soc.* **2010**, *132*, 4608–4613; d) P. M. Uberman, L. M. Pérez, G. I. Lacconi, S. E. Martín, *J. Mol. Catal. A: Chem.* **2012**, *363–364*, 245–253; e) A. B. Patil, D. S. Patil, B. M. Bhanage, *J. Mol. Catal. A: Chem.* **2012**, *365*, 146–153; f) C. Deraedt, L. Salmon, L. Etienne, J.

- Ruiz, D. Astruc, *Chem. Commun.* **2013**, *49*, 8169–8171; g) C. Deraedt, L. Salmon, J. Ruiz, D. Astruc, *Adv. Synth. Catal.* **2013**, *355*, 2992–3001; h) C. Gao, H. Zhou, S. Wei, Y. Zhao, J. You, G. Gao, *Chem. Commun.* **2013**, *49*, 1127–1129.
- [9] P. Zhang, C. Shao, Z. Zhang, M. Zhang, J. Mu, Z. Guo, Y. Liu, *Nanoscale* **2011**, *3*, 3357–3363.
- [10] A. K. Diallo, E. Boisselier, L. Liang, J. Ruiz, D. Astruc, *Chem. Eur. J.* **2010**, *16*, 11832–11835.
- [11] V. Percec, C. Mitchell, W.-D. Cho, S. Uchida, M. Glodde, G. Ungar, X. Zeng, Y. Liu, V. S. K. Balagurusamy, *J. Am. Chem. Soc.* **2004**, *126*, 6078–6094.
- [12] a) E. Boisselier, A. K. Diallo, L. Salmon, C. Ornelas, J. Ruiz, D. Astruc, *J. Am. Chem. Soc.* **2010**, *132*, 2729–2742; b) D. Astruc, *Nat. Chem.* **2012**, *4*, 255–267; c) M. Bernechea, E. De Jesús, C. Lopez-Mardomingo, P. Terberos, *Inorg. Chem.* **2009**, *48*, 4491–4496; d) E. H. Rahim, F. S. Kamounah, J. Frederiksen, J. B. Christensen, *Nano Lett.* **2001**, *1*, 499–501; e) I. Nakamura, Y. Yamanoi, T. Imaoka, K. Yamamoto, H. Nishihara, *Angew. Chem.* **2011**, *123*, 5952–5955; *Angew. Chem. Int. Ed.* **2011**, *50*, 5830–5833; f) R. Djeda, A. Rapakoussiou, L. Liang, N. Guidolin, J. Ruiz, D. Astruc, *Angew. Chem.* **2010**, *122*, 8328–8332; *Angew. Chem. Int. Ed.* **2010**, *49*, 8152–8156.
- [13] a) Ö. Metin, F. Durap, M. Aydemir, S. Özkar, *J. Mol. Catal. A: Chem.* **2011**, *337*, 39–44; b) D. Saha, K. Chattopadhyay, B. C. Ranu, *Tetrahedron Lett.* **2009**, *50*, 1003–1006; c) S. Sawoo, D. Srimani, P. Dutta, R. Lahiri, A. Sarkar, *Tetrahedron* **2009**, *65*, 4367–4374; d) L. Wang, C. Cai, *J. Mol. Catal. A: Chem.* **2009**, *306*, 97–101; e) L. Z. Ren, L. J. Meng, *Express Polym. Lett.* **2008**, *2*, 251–255; f) S. E. Lyubimov, A. A. Vasilev, A. A. Korlyukov, M. M. Ilyin, S. A. Pisarev, V. V. Matveev, A. E. Chalykh, S. G. Zlotin, V. A. Davankov, *React. Funct. Polym.* **2009**, *69*, 755–758; g) N. Jamwal, M. Gupta, S. Paul, *Green Chem.* **2008**, *10*, 999–1003; h) Z. Guan, J. Hu, Y. Gu, H. Zhang, H. Li, T. Li, *Green Chem.* **2012**, *14*, 1964–1970; i) G. Wei, W. Zhang, F. Wen, Y. Wang, M. Zhang, *J. Phys. Chem. C* **2008**, *112*, 10827–10832; j) V. Kogan, Z. Aizenshtat, R. Popovitz-Biro, R. Neumann, *Org. Lett.* **2002**, *4*, 3529–3532; k) X. Jiang, G. Wei, X. Zhang, W. Zhang, P. Zheng, F. Wen, L. Shi, *J. Mol. Catal. A: Chem.* **2007**, *277*, 102–106; l) A. Ohtaka, T. Teratani, R. Fujii, K. Ikeshita, T. Kawashima, K. Tatsumi, O. Shimomura, R. Nomura, *J. Org. Chem.* **2011**, *76*, 4052–4060; m) B. Karimi, D. Elhamifar, J. H. Clark, A. J. Hunt, *Chem. Eur. J.* **2010**, *16*, 8047–8053; n) C. M. Crudden, M. Sateesh, R. Lewis, *J. Am. Chem. Soc.* **2005**, *127*, 10045–10050; o) G. M. Scheuermann, L. Rumi, P. Steurer, W. Bannwarth, R. Mülhaupt, *J. Am. Chem. Soc.* **2009**, *131*, 8262–8270; p) A. Gniewek, J. Ziolkowski, A. Trzeciak, M. Zawadzki, H. Grabowska, J. Wrzyszczyk, *J. Catal.* **2008**, *254*, 121–130; q) F. Churrua, R. SanMartin, B. Inés, I. Tellitu, E. Dominguez, *Adv. Synth. Catal.* **2006**, *348*, 1836–1840.
- [14] a) A. Khazaei, S. Rahmati, S. Saednia, *Catal. Commun.* **2013**, *37*, 9–13; b) P. Li, L. Wang, L. Zhang, G.-W. Wang, *Adv. Synth. Catal.* **2012**, *354*, 1307–1318; c) P. Veerakumar, M. Velayudham, K.-L. Lu, S. Rajagopal, *Appl. Catal. A: General* **2013**, *455*, 247–260; d) D. Ganapathy, G. Sekar, *Catal. Commun.* **2013**, *39*, 50–54; e) A. John, S. Modak, M. Madasu, M. Katari, P. Ghosh, *Polyhedron* **2013**, *32*, 20–29; f) S. Gao, N. Zhao, M. Shu, S. Che, *Appl. Catal. A: General* **2010**, *388*, 196–201; g) S. Moussa, A. R. Siamaki, B. F. Gupton, M. S. El-Shall, *ACS Catal.* **2012**, *2*, 145–154.
- [15] a) H. Li, L. Han, J. Cooper-White, I. Kim, *Green Chem.* **2012**, *14*, 586–591; b) K. Jiang, H. X. Zhang, Y. Y. Yang, R. Mothes, H. Lang, W. B. Cai, *Chem. Commun.* **2011**, *47*, 11924–11926; c) S. Harish, J. Mathiyarasu, K. L. N. Phani, V. Yegnaraman, *Catal. Lett.* **2009**, *128*, 197–202; d) Y. Mei, Y. Lu, F. Polzer, M. Ballauff, M. Drechsler, *Chem. Mater.* **2007**, *19*, 1062; e) X. Lu, X. Bian, G. Nie, C. Zhang, C. Wang, Y. Wei, *J. Mater. Chem.* **2012**, *22*, 12723–12730; f) J. Morere, M. J. Tenorio, M. J. Torralvo, C. Pando, J. A. R. Renuncio, A. Cabanas, *J. Supercrit. Fluids* **2011**, *56*, 213–222; g) R. Bhandari, M. R. Knecht, *ACS Catal.* **2011**, *1*, 89–98; h) B. Liu, S. Yun, Q. Wang, W. Hu, P. Jing, Y. Liu, W. Jia, Y. Liu, L. Liu, J. Zhang, *Chem. Commun.* **2013**, *49*, 3757–3759.
- [16] a) D. Jana, A. Dandapat, G. De, *Langmuir* **2010**, *26*, 12177–12184; b) J. Han, L. Li, R. Guo, *Macromolecules* **2010**, *43*, 10636–10644; c) C. Zhu, L. Han, P. Hu, S. Dong, *Nanoscale* **2012**, *4*, 1641–1646; d) Z. Zhang, C. Shao, P. Zou, P. Zhang, M. Zhang, M. Mu, Z. Guo, X. Li, C. Wang, Y. Liu, *Chem. Commun.* **2011**, *47*, 3906–3908; e) Y. Wang, G. Wei, W. Zhang, X. Jiang, P. Zheng, L. Shi, A. Dong, *J. Mol. Catal. A: Chem.* **2007**, *266*, 233–238; f) M. Zhang, L. Liu, C. Wu, G. Fu, H. Zhao, B. He, *Polymer* **2007**, *48*, 1989–1997; g) W. Liu, X. Yang, W. Huang, *J. Colloid Interface Sci.* **2006**, *304*, 160–165; h) Y. C. Chang, D. H. Chen, *J. Hazard. Mater.* **2009**, *165*, 664–669; i) H. Koga, E. Tokunaga, M. Hidaka, Y. Umemura, T. Saito, A. Isogai, T. Kitaoka, *Chem. Commun.* **2010**, *46*, 8567–8569; j) K. Kuroda, T. Ishida, M. Haruta, *J. Mol. Catal. A: Chem.* **2009**, *298*, 7–11; k) H. Yamamoto, H. Yano, H. Kouchi, Y. Obora, R. Arakawa, H. Kawasaki, *Nanoscale* **2012**, *4*, 4148–4154; l) S.-H. Wu, C.-T. Tseng, Y.-S. Lin, C.-H. Lin, Y. Hung, C.-Y. Mou, *J. Mater. Chem.* **2011**, *21*, 789–794; m) H. Wu, Z. Liu, X. Wang, B. Zhao, J. Zhang, C. Li, *J. Colloid Interface Sci.* **2006**, *302*, 142–148; n) H. Wu, X. Huang, M. Gao, X. Liao, B. Shi, *Green Chem.* **2011**, *13*, 651–658; o) K. B. Narayanan, N. Sakthivel, *J. Hazard. Mater.* **2011**, *189*, 519–525; p) W. Lu, R. Ning, X. Qin, Y. Zhang, G. Chang, S. Liu, Y. Luo, X. Sun, *J. Hazard. Mater.* **2011**, *197*, 320–326; q) X.-Y. Liu, F. Cheng, Y. Liu, H.-J. Liu, Y. Chen, *J. Mater. Chem.* **2010**, *20*, 360–368; r) J. Li, C.-Y. Liu, Y. Liu, *J. Mater. Chem.* **2012**, *22*, 8426–8430; s) H. Koga, T. Kitaoka, *Chem. Eng. J.* **2011**, *168*, 420–425; t) T. Huang, F. Meng, L. Qi, *J. Phys. Chem. C* **2009**, *113*, 13636–13642; u) R. Bhandari, M. R. Knecht, *Catal. Sci. Technol.* **2012**, *2*, 1360–1366; v) B. Ballarin, M. C. Cassani, D. Tonelli, E. Boanini, S. Albonetti, M. Blosi, M. Gazzano, *J. Phys. Chem. C* **2010**, *114*, 9693–9701; w) Y. Zhu, J. Shen, K. Zhou, C. Chen, X. Yang, C. Li, *J. Phys. Chem. C* **2011**, *115*, 1614–1619; x) Y. Xia, Z. Shi, Y. Lu, *Polymer* **2010**, *51*, 1328–1335; y) H. Wei, Y. Lu, *Chem. Asian J.* **2012**, *7*, 680–683; z) H. Yang, K. Nagai, T. Abe, H. Homma, T. Norimatsu, R. Ramaraj, *ACS Appl. Mater. Inter.* **2009**, *1*, 1860–1864.

COMMUNICATION

“Click” dendrimers as efficient nanoreactors in aqueous solvent: Pd nanoparticle stabilization for sub-ppm Pd catalysis of Suzuki–Miyaura reactions of aryl bromides†

Cite this: *Chem. Commun.*, 2013, **49**, 8169

Received 8th July 2013,
Accepted 19th July 2013

DOI: 10.1039/c3cc45132a

www.rsc.org/chemcomm

Christophe Deraedt,^a Lionel Salmon,^b Laetitia Etienne,^c Jaime Ruiz^a and Didier Astruc^{*a}

Palladium nanoparticles (PdNPs) with a size of 1.4 nm are stabilized by dendritic nanoreactors containing 1,2,3-triazole ligands with hydrophilic triethylene glycol (TEG) termini. These PdNPs are stable for months under air and are extremely active for the Suzuki–Miyaura reactions of aryl bromides down to sub-ppm levels.

The concept of nanoreactors arose in the early 1970's with Breslow's seminal work on artificial enzymes based on transition-metal complex derivatives of cyclodextrins,¹ and has more recently been elegantly pursued with appropriately designed supramolecular containers.² Crook's group has pioneered catalysis by PAMAM-encapsulated Pd nanoparticles (PdNPs),³ and these PdNPs as well as various other polymer- and inorganic substrate-stabilized PdNPs are good catalysts for Suzuki–Miyaura reactions of aryl iodides and activated bromides with Pd catalyst amounts of the order of 10^{-1} – 10^{-2} mol%.⁴ Such reactions are useful, especially with aryl bromides, because they are usually inexpensive and often cheaper than aryl chlorides. The Suzuki–Miyaura⁵ cross-coupling reaction has indeed become one of the most powerful synthetic methods for preparing biaryl compounds, such as natural products, pharmaceuticals, polymers, *etc.* Another important issue is the use of minimum amounts of catalysts, because metal contamination tolerated in organic products does not overtake a few ppm. Along this line only very few authors have reported PdNPs that can be active with 10^{-3} Pd mol%.⁶ Among them, we have already noted that click ferrocenyl dendrimers^{6b} can catalyze this reaction of aryl iodides with quite good TONs, but very low TOFs.

We now report that when such dendrimers are terminated by triethyleneglycol groups, the PdNPs are stabilized, retain their catalytic activity for months and present an extraordinary activity even in air, for the first time down to the sub-ppm level of Pd, as pre-catalysts for the Suzuki–Miyaura reactions of aryl bromides in 50% EtOH–water, a “green” solvent. Moreover, these dendrimers are easily recycled. Such

reactions can also be conducted on multi-gram scales with the same very high TONs and optimized efficiency, which is promising in view of industrial applications. The water-soluble click dendrimers **1** and **2** have been synthesized and are represented in Fig. 1. They contain, respectively, 9 (for G0) and 27 (for G1) 1,2,3-triazolyl groups linking the dendritic core to Percec-type dendrons⁷ and, respectively, 27 and 81 TEG termini. The dendrimer **1** is already known,⁸ whereas the new dendrimer **2** has now been synthesized *via* “click” chemistry (see ESI† elemental analysis: calcd for $C_{1125}H_{1947}N_{81}O_{360}Si_{36}$: C 57.79, H 8.39, N 4.85, found C 57.78, H 8.32, N 4.82%). Inductively coupled plasma optical emission spectroscopy (ICP-OES) analysis confirms the indication of elemental analyses according to which Cu ions used for click syntheses of these dendrimers have been totally removed (<0.1 ppm, the ICP-OES detection limit).

PdNPs are stabilized in water by **1** and **2** after reduction of Pd^{II} to Pd⁰. Firstly, the dendrimer–Pd^{II} complexes are synthesized in water by adding one equiv. of K_2PdCl_4 per dendritic triazole group (the optimized stoichiometry for further PdNP catalysis) to the dendrimer. The nature of the Pd^{II} complexation sites in the dendrimer has been examined by UV-vis spectroscopy. An absorption band is observed at 217 nm when K_2PdCl_4 is added to the dendrimer in water (Fig. 2), which is assigned to a ligand-to-metal charge transfer (LMCT) transition of Pd^{II}. Here, it is associated with the complexation of the metal ions to the interior triazoles of **1** (ESI†). Previously, a band at 225 nm has already been associated with the complexation of Pd^{II} to the intradendritic tertiary amine of the PAMAM dendrimer.^{3a,c}

Then reduction of Pd^{II} (1 equiv. per triazolyl group) to Pd⁰ is carried out in aqueous solution using 10 equiv. of $NaBH_4$ per Pd (see the color change in the ESI†). Finally, dialysis is conducted for 1 day in order to remove excess $NaBH_4$ and eventually purify the PdNPs from any Pd derivatives. Thereafter, ICP-OES analysis indicates that the Pd loading in the PdNPs is 96% of starting Pd. It is known that $NaBH_4$ inhibits catalytic activity by the formation of borides at the particle surface,^{6c} but this is not the case in aqueous media, because the borohydride is then fully hydrolyzed. Catalysis results (*vide infra*) are the same with and without dialysis, however, thus dialysis is not indispensable in view of catalysis experiments. So, after reduction of Pd^{II} in PdNPs, the water solution of PdNPs is ready for catalysis experiments.

^a ISM, UMR CNRS 5255, Univ. Bordeaux, 351 Cours de la Libération, 33405 Talence Cedex, France

^b LCC, CNRS, 205 Route de Narbonne, 31077 Toulouse Cedex, France

^c ICMCB, UPR CNRS No. 9048, 87 avenue, Pey-Berland, 33608 Pessac Cedex, France

† Electronic supplementary information (ESI) available: Experimental details and characterization data. See DOI: 10.1039/c3cc45132a

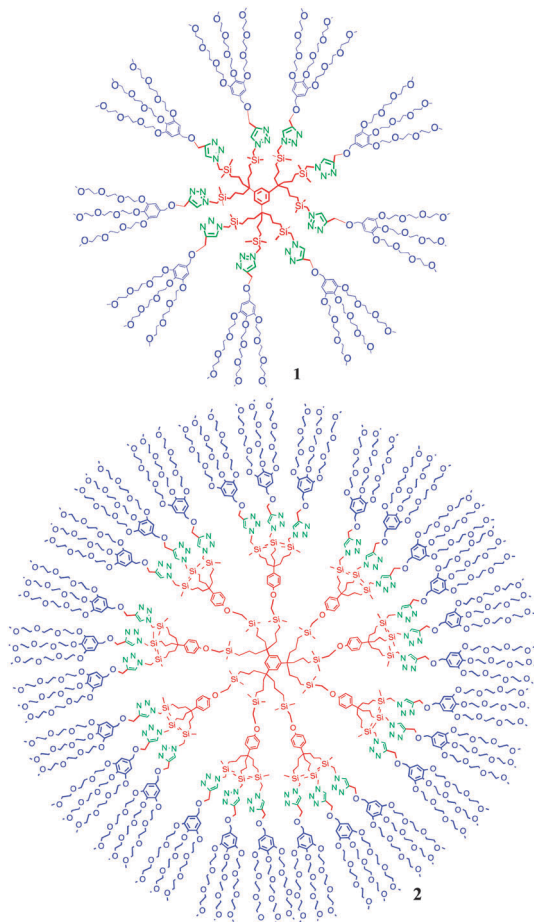


Fig. 1 Dendrimer G0-27 TEG **1** (top) and dendrimer G1-TEG **2** (bottom).

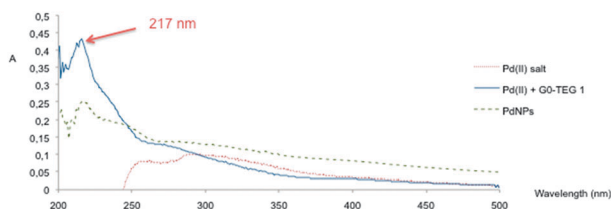


Fig. 2 UV-vis spectra of Pd(II) salt, **1**-Pd^{II} complex and PdNPs stabilized by **1**. The three spectra have been recorded using **1** as a blank.

The polydispersities of these PdNPs shown by DLS are good, and TEM and HRTEM (ESI[†]) reveal that the PdNPs are very small, 1.4 ± 0.7 nm in **1** (Fig. 3 and ESI[†] truncated bipyramid, 100 atoms per NP) and 2.7 ± 1 nm in **2** (ESI[†] Fig. S4), thus of optimal size for their use in catalysis. The hydrodynamic diameters of the TEG dendrimers determined by DOSY NMR and DLS are 5.5 ± 0.2 nm⁸ and 9 nm, respectively, for **1** and 13.2 ± 0.2 nm and 16 nm, respectively, for **2** (ESI[†]). The actual size is best reflected by the DOSY NMR values, and it is expected that the DLS values take into account the water solvation around the dendrimers that increases the apparent dendrimer size. These DLS values are much larger than what is expected for a single dendrimer, which means that a number of dendrimers aggregate in water to form a supramolecular assembly of dendrimers. The aggregation of TEG dendrimers is facilitated by the amphiphilic nature of the TEG termini so that the TEG-terminated dendrimers

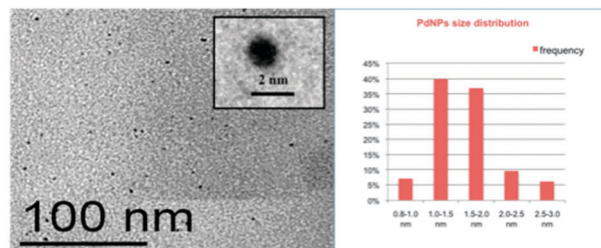
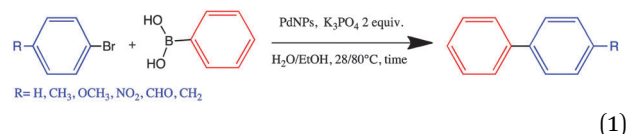


Fig. 3 TEM of PdNPs stabilized by G0-27 TEG **1** (left) and the distribution on 138 PdNPs (right). The average PdNP size is 1.4 ± 0.7 nm.

interpenetrate one another because of the supramolecular forces attracting the TEG tethers among one another. What is remarkable is that, when the PdNPs are formed, the DLS size value considerably increases for G0 from 9 nm to 31 nm, whereas it only increases from 16 nm to 18 nm for G1 (see ESI[†] Fig. S7). This strongly argues for the full encapsulation of the stabilized PdNPs for the large dendrimer G1 that undergoes a modest size change upon PdNP formation and, in contrast, for an assembly of small dendrimers **1** (11×1 /PdNP) stabilizing a PdNP. Note that the PdNPs stabilized by the TEG dendrimers are stable under air conditions for several months without any sign of aggregation and that the size determined by TEM and the catalytic activity (*vide infra*) remain the same after such prolonged periods of time (see ESI[†] Fig. S3).

The Suzuki–Miyaura reactions were conducted in H₂O–EtOH (1/1) with iodo-, bromo- and chloroarenes (eqn (1)).



(1)

As the Suzuki–Miyaura coupling works very well at 28 °C with iodoarenes even with less than 1 ppm of Pd,[†] we decided to focus on bromoarenes.

The G0-PdNP catalyst is extremely active and efficient for the Suzuki–Miyaura coupling reactions of bromoarenes even at 28 °C. At 80 °C, the reaction between 1,4-bromonitrobenzene and phenylboronic acid with only 0.3 ppm of Pd reaches a TON of 2.7×10^6 after 2.5 days (TOF = 4.5×10^4 h⁻¹). With only 1 ppm of Pd in the G0-PdNP catalyst, the cross-coupling with phenylboronic acid is quantitative with bromobenzene: TON = 0.99×10^6 ; TOF = 1.65×10^4 h⁻¹, and the yield is 63% for 1,4-bromoanisole (TON = 0.63×10^6 ; TOF = 1.05×10^4 h⁻¹).

The results of the Suzuki–Miyaura reactions of bromoarenes are gathered in Table 1. In conclusion, for bromoarenes, the TONs are very impressive at 80 °C, sometimes even larger than 10^6 . Concerning the G1-PdNP catalyst, reactions under the same conditions as in Table 1 (80 °C, 2.5 days) between bromoarenes and phenylboronic acid using 1 ppm Pd give yields of 20% with bromobenzene, 27% with bromoanisole and 39% with 1,4-bromonitrobenzene. The catalytic efficiency of G1-PdNPs is lower than that of the G0-PdNPs, which is taken into account by the fact that PdNPs prepared in G1-81 TEG **2** are larger than those in G0-27 TEG **1**. This also is in accord with the leaching mechanism.^{4c} With chloroarenes, the results with G0 are less impressive than with the other halogenoarenes, because high temperatures (>100 °C) are required to activate chloroarenes

Table 1 Isolated yields and TONs for the catalysis by G0 PdNPs of the Suzuki–Miyaura reactions between bromoarenes [*p*-RC₆H₄Br] and phenylboronic acid

R	Entry	Pd (%)	Time (h)	Yield (%)	TON
H	1	0.1	15	99	990
	2 ^b	0.1	96	66	660
	3	0.01	24	99	9900
	4 ^{a,c}	0.0001	60	99	990 000
CH ₃ O	5	0.1	15	94	940
	6	0.01	24	99	9900
	7	0.001	24	60	60 000
	8	0.001	48	99	99 000
	9	0.0001	60	63	630 000
NH ₂	10	0.1	15	96	960
	11	0.01	24	31	3100
	12	0.01	48	40	4000
NO ₂	13	0.1	15	99	990
	14 ^b	0.1	240	80	800
	15	0.001	24	87	87 000
	16	0.001	36	98	98 000
	17 ^c	0.0001	60	91	910 000
	18 ^a	0.00003	60	82	2 700 000
CH ₃	19	0.1	24	99	990
	20	0.001	48	99	99 000
	21	0.0001	48	46	460 000
CHO	22	0.1	24	99	990
	23	0.01	24	80	8000
	24	0.001	24	20	20 000

Each reaction is conducted with 1 mmol bromoarene, [*p*-RC₆H₄Br] in 0.05 M as final concentration, 1.5 mmol of phenylboronic acid and 2 equiv. of K₃PO₄ in EtOH–H₂O (10 mL/10 mL) at 80 °C. ^a Same conditions but in EtOH–H₂O (5 mL/5 mL), C[RC₆H₄Br] = 0.1 M. ^b Standard conditions but at 28 °C instead of 80 °C. ^c The reaction is also conducted on a larger scale (10 g of *p*-RC₆H₄Br), leading to similar isolated yields.

under these conditions, and at such temperatures these PdNPs aggregate more rapidly than the activation reactions.

In conclusion, the TEGylated click dendrimer assemblies represent a new type of nanoreactors for PdNPs that provide stability and catalytic activity during several months without the strain of an inert atmosphere. The TEG termini of the dendrimer tethers are responsible for this high degree of intradendritic PdNP stabilization, because they interact interdentritically to form large assemblies. The intradendritic PdNPs are loosely liganded by the 1,2,3-triazoles, which present an excellent compromise between stabilization and lability for an optimized catalytic activity. The catalytic activity of these PdNPs is exceptionally high with bromoarenes, reaching TONs that are equal to or larger than 10⁶, which was never reached with PdNPs stabilized with ferrocene^{6c} or sulfonated^{6d} dendrimer's termini, which enhances the role of the TEG termini (see ESI,† Table S4). The catalyst 1-PdNPs is the most active for the Suzuki–Miyaura reaction in aqueous solvent, in terms of TONs for bromoarenes^{4–6} (see ESI,† Table S3), with longstanding catalytic activity on multi-gram scales of substrates. We suggest that the reasons for this exceptional catalytic activity of the dendritic nanoreactor **1** are (i) the loose intradendritic stabilization of PdNPs by the triazole ligands combined with the inter-dendritic assembly provided by the TEG termini, which better protects the PdNPs than a single dendrimer, (ii) the leaching mechanism,^{4c} which generates very active Pd atoms in solution that are less easily quenched by the

mother PdNPs because of the protection by the nanoreactor, and (iii) the leaching, which is easier for small PdNPs (1.4 ± 0.7 nm, truncated bipyramid, high proportion of reactive Pd atoms on the edges and summits) than for larger ones. As a consequence, extremely high TONs are reached, because the catalytic activity is retained at extremely high substrate/catalyst ratios. Finally, these water-soluble dendrimers are very stable and easy to recover⁸ whenever needed when they are used in substantial quantity, and they can indefinitely be re-used.

Notes and references

† In the case of iodobenzene, the Suzuki–Miyaura reaction worked well at 28 °C even with a very small quantity of Pd (PdNPs stabilized by G0-27 TEG), down to 3 × 10⁻⁵ mol%, i.e. 0.3 ppm Pd in 80% yield (TON = 2.7 × 10⁶; TOF = 2.8 × 10⁴ h⁻¹).

- R. Breslow and L. E. Overman, *J. Am. Chem. Soc.*, 1970, **92**, 1075.
- (a) J. Kang and J. Rebek, *Nature*, 1997, **385**, 50; (b) M. Yoshizawa, M. Tamura and M. Fujita, *Science*, 2006, **312**, 251; (c) M. D. Pluth, R. G. Bergman and K. N. Raymond, *Science*, 2007, **316**, 85; (d) J. A. A. W. Eleman, J. J. L. M. Cornelissen, M. C. Feiters, A. E. Rowman and R. J. M. Nolte, in *Supramolecular Catalysis*, ed. P. W. N. M. van Leeuwen, Wiley-VCH, Weinheim, 2008, ch. 6.
- (a) M. Zhao and R. M. Crooks, *Angew. Chem., Int. Ed.*, 1999, **38**, 364; (b) R. M. Crooks, M. Zhao, L. Sun, V. Chechik and L. K. Yeung, *Acc. Chem. Res.*, 2001, **34**, 181; (c) R. W. J. Scott, H. C. Ye, R. R. Henriquez and R. M. Crooks, *Chem. Mater.*, 2003, **15**, 3873; (d) R. W. J. Scott, O. M. Wilson and R. M. Crooks, *J. Phys. Chem. B*, 2005, **109**, 692; (e) M. V. Gomez, J. Guerra, A. H. Velders and R. M. Crooks, *J. Am. Chem. Soc.*, 2009, **131**, 15564; (f) M. Bernechea, E. De Jesús, C. Lopez-Mardomingo and P. Terreros, *Inorg. Chem.*, 2009, **48**, 4491; (g) V. S. Myers, M. G. Weier, E. V. Carino, D. F. Yancey, S. Pande and R. M. Crooks, *Chem. Sci.*, 2011, **2**, 1632.
- (a) L. M. Bronstein and Z. B. Shifrina, *Chem. Rev.*, 2011, **111**, 5301; (b) M. T. Reetz, W. Helbig and S. A. Quaiser, in *Active metals: preparation, characterizations, applications*, ed. A. Fürstner, VCH, Weinheim, 1996, p. 279; (c) J. G. de Vries, *Dalton Trans.*, 2006, 421; (d) M. T. Reetz and J. V. de Vries, *Chem. Commun.*, 2004, 1559; (e) A. H. M. de Vries and J. G. de Vries, *Eur. J. Org. Chem.*, 2003, 799; (f) N. T. S. Phan, M. van der Sluis and C. J. Jones, *Adv. Synth. Catal.*, 2006, **348**, 609; (g) D. Astruc, F. Lu and J. Ruiz, *Angew. Chem., Int. Ed.*, 2005, **44**, 7852; (h) Y. Li and M. A. El-Sayed, *J. Phys. Chem. B*, 2001, **105**, 8938; (i) R. P. Beletskaya, A. N. Kashin, I. A. Khotina and A. R. Khokhlov, *Synlett*, 2008, 1547; (j) B. Sreedhar, D. Yada and P. S. Reddy, *Adv. Synth. Catal.*, 2011, **353**, 2823; (k) Z. Guan, J. Hu, Y. Gu, H. Zhang, G. Li and T. Li, *Green Chem.*, 2012, **14**, 1964; (l) P. Zhang, Z. Weng, J. Guo and C. Wang, *Chem. Mater.*, 2011, **23**, 5243.
- Reviews on Suzuki–Miyaura reactions catalyzed by nanoparticles: (a) N. Miyaura and A. Suzuki, *Chem. Rev.*, 1995, **95**, 2457; (b) j. Hassan, M. Sévignon, C. Gozzi, E. Schulz and M. Lemaire, *Chem. Rev.*, 2002, **12**, 1359; (c) F. Bellina, A. Carpita and R. Rossi, *Synthesis*, 2004, 2419; (d) I. Beletskaya and A. V. Cheprakov, *J. Organomet. Chem.*, 2004, **689**, 4055; (e) A. Suzuki, *Chem. Commun.*, 2005, 4759; (f) M. Lamblin, L. Nassar-Hardy, J. C. Hierso, E. Fouquet and F.-X. Felpin, *Adv. Synth. Catal.*, 2010, **352**, 33; (g) I. Favier, D. Macec, E. Teuma and M. Gomez, *Curr. Org. Chem.*, 2011, **15**, 3127.
- (a) A. Alimardanov, L. Schmieder-van de Vondervoort, A. H. M. de Vries and J. G. de Vries, *Adv. Synth. Catal.*, 2004, **346**, 1812; (b) F. Churrua, R. SanMartin, B. Inés, I. Tellitu and E. Dominguez, *Adv. Synth. Catal.*, 2006, **348**, 1836; (c) A. K. Diallo, C. Ornelas, L. Salmon, J. Ruiz and D. Astruc, *Angew. Chem., Int. Ed.*, 2007, **46**, 8644; (d) C. Ornelas, J. Ruiz, L. Salmon and D. Astruc, *Adv. Synth. Catal.*, 2008, **350**, 837; (e) B. Inés, R. SanMartin, M. J. Moure and E. Dominguez, *Adv. Synth. Catal.*, 2009, **351**, 2124; (f) S. Ogasawara and S. Kato, *J. Am. Chem. Soc.*, 2010, **132**, 4608; (g) C. Zhou, J. Wang, L. Li, R. Wang and M. A. Hong, *Green Chem.*, 2011, **13**, 2100; (h) Y. M. A. Yamada, S. M. Sarkar and Y. Uozumi, *J. Am. Chem. Soc.*, 2012, **134**, 3190; (i) A. B. Patil, D. S. Patil and B. M. Bhanage, *J. Mol. Catal. A: Chem.*, 2012, **365**, 146; (j) P. M. Uberman, L. M. Pérez, G. I. Lacconi and S. E. Martín, *J. Mol. Catal. A: Chem.*, 2012, **363–364**, 245; (k) C. Gao, H. Zhou, S. Wei, Y. Zhao, J. You and G. Gao, *Chem. Commun.*, 2013, **49**, 1127.
- V. Percec, C. Mitchell, W.-D. Cho, S. Uchida, M. Glodde, G. Ungar, X. Zeng, Y. Liu and V. S. K. Balagurusamy, *J. Am. Chem. Soc.*, 2004, **126**, 6078.
- A. K. Diallo, E. Boisselier, L. Liang, J. Ruiz and D. Astruc, *Chem.–Eur. J.*, 2010, **16**, 11832.

DOI:10.1002/ejic.201402457

Palladium Nanoparticles Stabilized by Glycodendrimers and Their Application in Catalysis

Sylvain Gatard,^{*[a,b]} Lionel Salmon,^[c] Christophe Deraedt,^[a] Jaime Ruiz,^[a] Didier Astruc,^{*[a]} and Sandrine Bouquillon^{*[b]}

Keywords: Nanoparticles / Dendrimers / Glycodendrimers / Heterogenous catalysis / Palladium / Reduction

Palladium nanoparticles stabilized by glycodendrimers (PdDSNs) in water were prepared by coordination of Pd^{II} to intradendritic triazole ligands upon reaction of K₂PdCl₄ with the dendrimer in water followed by aqueous NaBH₄ reduction to Pd⁰. TEM images show that the PdDSNs are small (average diameter: 2.3 nm) and relatively monodisperse owing to a low concentration of metal precursor. The catalytic activity of these PdDSNs was evaluated for the reduction of 4-nitrophenol (4-NP) to 4-aminophenol (4-AP) by NaBH₄

(only 0.2 mol-% of Pd per mol substrate is used) and for the Miyaura–Suzuki C–C coupling with various substituted aryl bromides (only 0.01 mol-% of Pd per mol substrate is used). Comparisons of the catalytic activities of these PdDSNs with those of larger PdDSNs (diameter: 14 nm) reveal that smaller NPs catalyze faster 4-NP reduction than their larger counterparts but lack any notable surface dependency for Suzuki–Miyaura catalysis.

Introduction

The development of small monodisperse nanoparticles (NPs) is crucial to a number of applications in optics, magnetism, electronics, and especially in catalysis.^[1] Indeed, in catalysis many reactions proceed at the surface of the NPs, and the nanosize therefore benefits from the high surface-area-to-volume ratio.^[2] Among organic macromolecules, dendrimers^[3] offer a specific topology that allows smooth intradendritic coordination controlling the size of the NPs and preventing agglomeration. The groups of Crooks, Tomalia and Esumi pioneered the use of PAMAM and PPI-based commercial dendrimers as templating agents for various transition metal NPs, and Crooks' group developed seminal catalysis by dendrimer-encapsulated late transition-metal NPs including PdNPs.^[4] Palladium is a metal of choice for catalysis,^[5] and PdNPs stabilized by dendrimers have proven to be very powerful catalysts for generating carbon–carbon bonds (Suzuki–Miyaura, Stille, Heck, Sonogashira, etc.), for reduction of nitroarenes to aminoarenes and for hydrogenation reactions.^[6,7]

Moreover, dendritic stabilizers offer an assortment of possible ending groups at their surface from which to

choose; these may affect NP stabilization, solubility, toxicity and protection.^[8] For our part, we have been interested for several years in the application of regional agro-resources, particularly pentose for the decoration of dendrimers.^[9] The use of carbohydrates as reducing and stabilizing agents for metal NPs offers a number of key advantages for further applications such as reduced toxicity, cheap and abundant building blocks, biological recognition with proteins to form lectins, chiral surfaces, and water solubility.^[10] Among these stabilizing agents of metal NPs, glycodendrimers,^[11] are of interest as exemplified in the literature. Indeed, a few groups have reported the formation of metal NPs stabilized by glycodendrimers without any external reductant.^[12] Most of the cited examples examined dendrimers decorated by hexoses. However, the chemistry of pentose decorating dendrimers for metal NPs stabilization remains quite unexplored.^[9]

Recently, we reported the synthesis of pentose-terminated dendrimers displaying great stability for up to several months. These dendrimers were used to stabilize PtNPs, PdNPs and AuNPs through their 1,2,3-triazolyl linkages. The roles of this linkage have been evident during formation of metal NPs and include aiding in the sequestration of metal ions within the dendrimer before their reduction to zero-valent metals.^[9b,9c] However, TEM studies showed that PdDSNs obtained in this way did not have a good monodispersity and displayed an average diameter of 14 ± 3 nm. This led us to improve the synthesis of these PdDSNs. We now find that, upon decreasing the concentration of metal precursor during the synthesis of the NPs, it is possible to form smaller and relatively more monodisperse PdDSNs.

[a] ISM, UMR CNRS 5255, Univ. Bordeaux, 33405 Talence Cedex, France
E-mail: d.astruc@ism.u-bordeaux1.fr
astruc.didier.free.fr

[b] ICMR, UMR CNRS 7312, Univ. Reims Champagne-Ardenne, BP 1039, 51687 Reims Cedex, France
E-mail: sylvain.gatard@univ-reims.fr
sandrine.bouquillon@univ-reims.fr

[c] LCC, CNRS & Université de Toulouse (UPS, INP), 31077 Toulouse, France

Supporting information for this article is available on the WWW under <http://dx.doi.org/10.1002/ejic.201402457>.

The new results relevant to the synthesis of glycodendrimers-stabilized PdDSNs are significant, because it is shown that the concentration of precursor metal used during the synthesis modulates the size of the NPs generated. This observation has been previously disclosed during the preparation of gold NPs using TritonX-100 inverse microemulsion.^[13] Moreover, these new PdDSNs are successfully used in the reduction of the aqueous pollutant 4-nitrophenol (4-NP) to 4-aminophenol (4-AP) and in the Suzuki–Miyaura reaction in aqueous media with very low concentrations of Pd. The Suzuki–Miyaura coupling^[14] and the reduction of 4-NP^[15] have been widely reported in the literature and serve here as model reactions enabling us to probe the catalytic potential of PdDSNs under study.

Results and Discussion

Synthesis and Characterization of Pentose-Terminated Dendrimer-Stabilized PdNPs

The preparation of water-soluble glycodendrimers containing nine pentose units at the periphery was described previously using click methodology from the nona-azide dendritic core.^[9] PdDSNs were prepared by complexation of Pd^{II} using K₂PdCl₄ in water over the course of 20 min under N₂. This reaction time was selected to provide enough time for Pd^{II} to be encapsulated upon coordination to the nine intradendritic triazole ligands inside the nona-pentose hydrophilic dendrimer. The stoichiometry corresponded to the same number as that of the triazole rings in the glycodendrimer. Compared to a previous publication,^[9b] the concentration of Pd^{II} was decreased from 1.8×10^{-3} M to 1.4×10^{-4} M. An aqueous solution of NaBH₄

(10 equiv. per Pd) was then added dropwise to reduce the Pd^{II} to Pd⁰ (Scheme 1). The use of NaBH₄ to reduce Pd^{II} ions is justified by the absence of reducing power of these glycodendrimers; this lack of glycodendrimer reducing potential is attributed to the absence of free hemiacetals in the peripheral sugars.^[9c] It is notable that PdNPs stabilized by the pentose-terminated dendrimers, after their preparation under nitrogen, were found to be stable to air for several weeks without any sign of aggregation.

Transmission electron microscopy (TEM) (Figure 1) indicated that a less concentrated Pd^{II} solution allowed us to obtain PdDSNs with a smaller average particle diameter of 2.3 ± 0.4 nm (over 75 counted NPs) and that were more monodisperse than previously synthesized PdDSNs (14 ± 3 nm).^[9b]

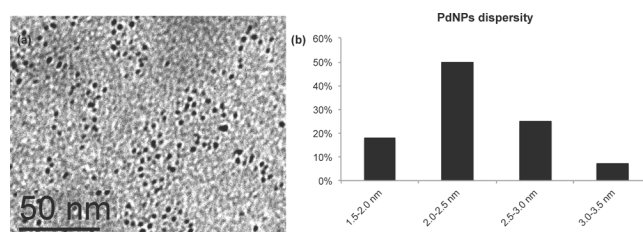
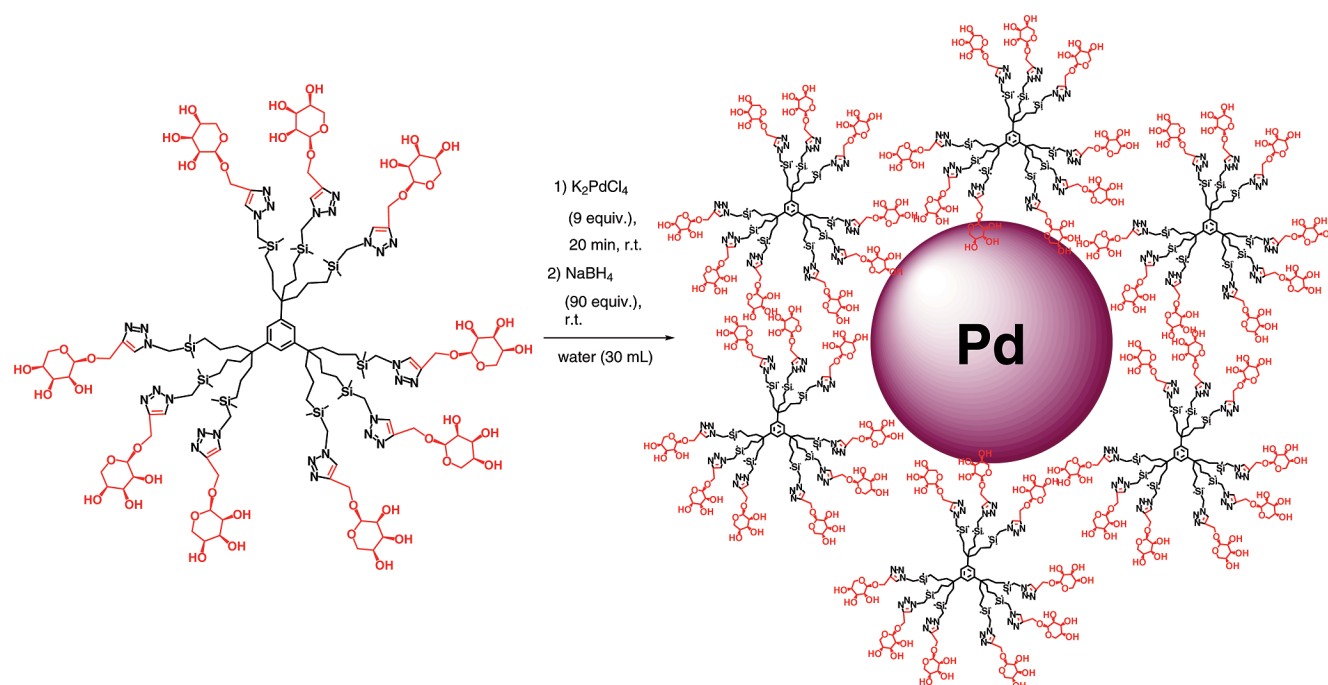


Figure 1. (a) TEM analysis of the PdDSNsA stabilized by the glycodendrimers; (b) size distribution histogram of the PdDSNsA stabilized by the glycodendrimers.

For the remainder of this work, the nanoparticles prepared in this manuscript will be noted as PdDSNsA ($D = 2.3 \pm 0.4$ nm) and those synthesized in the previous work^[9b] will be indicated as PdDSNsB ($D = 14 \pm 3$ nm).



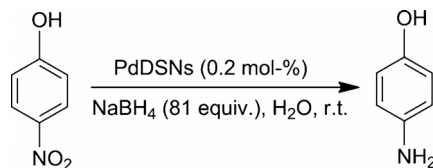
Scheme 1. Preparation of monometallic Pd DSNs stabilized by glycodendrimers.

Catalysis of 4-NP Reduction

The catalytic activities of PdDSNsA and PdDSNsB were first compared in reduction reactions of 4-NP to 4-AP. In the literature, a few groups have already described the activity of PdDSNs stabilized by commercial dendrimers PAMAM and PPI (generations 2, 3 and 4) as catalysts in the reduction of 4-NP to 4-AP.^[6c,7g,7i]

The reactions were conducted in water; the concentrations of sodium borohydride (here 81 equiv. of NaBH₄ per mol 4-NP, optimized conditions from previous work with AuDSNs^[9c]) and 4-NP (2.5 × 10⁻⁴ M, 1 equiv.) were kept constant for all the following reactions presented in this work.

The reduction of 4-NP was monitored by UV/Vis spectroscopy in a spectrophotometric cell at 25 °C (Scheme 2), and the disappearance of the strong absorption band at λ_{max} = 405 nm corresponding to 4-nitrophenolate ions (yellow color) and the concomitant formation of 4-AP (colorless) at λ_{max} = 300 nm were followed.



Scheme 2. Reduction of 4-NP to 4-AP in water and in presence of excess NaBH₄ using glycodendrimer-stabilized PdDSNs as catalyst.

Without PdNPs, and only in the presence of the glycodendrimer (5.8 × 10⁻⁸ M), no reduction of 4-NP was observed after 20 min. Both types of PdDSNs (PdDSNsA and

PdDSNsB) stabilized by glycodendrimers were found to be catalytically active at effecting reduction of 4-NP in water in the presence of NaBH₄. The same concentration of palladium in solution was used for both experiments (5.0 × 10⁻⁷ M, only 0.2 mol-% of Pd was used).

Figure 2 displays the typical evolution of the UV/Vis spectra for both systems [(a) PdDSNsA and (b) PdDSNsB]. It is worth noting that a short induction time was observed for the reaction with PdDSNsB from 0–180 seconds, which might be attributed to a *restructuration of the metal surface by nitrophenol* in the event of a Langmuir–Hinshelwood (LH) mechanism, as proposed by Ballauff and co-workers.^[16]

The plots of -ln(C_t/C₀) (C_t = concentration at the time t, C₀ = concentration at t = 0 second) as a function of time (in seconds) show a typical pseudo-first order dependence as it is usually observed for the reduction of 4-NP and allow determination of the apparent rate constant (k_{app}). As reported earlier,^[9c] the [4-NP] used in these experiences led to UV/Vis. spectra in which absorbance are greater than 2. In accord with the Beer–Lambert law these results were deemed irrelevant. Consequently, these data were not used to build up the kinetic plots. For PdDSNsA, the UV/Vis spectrum at 41 s was taken as the initial spectrum [see Figure 3 (a)] and for PdDSNsB [see Figure 3 (b)], at 900 s.

In the presence of 0.2 mol-% of PdDSNsA, with a 4-NP concentration of 2.5 × 10⁻⁴ M, the reaction was almost completed in about 400 seconds, corresponding to a k_{app} value of 4 × 10⁻³ s⁻¹. When the same reaction was performed in the presence of PdDSNsB, the reaction was much slower, displaying a k_{app} value of 1.1 × 10⁻³ s⁻¹. To explain

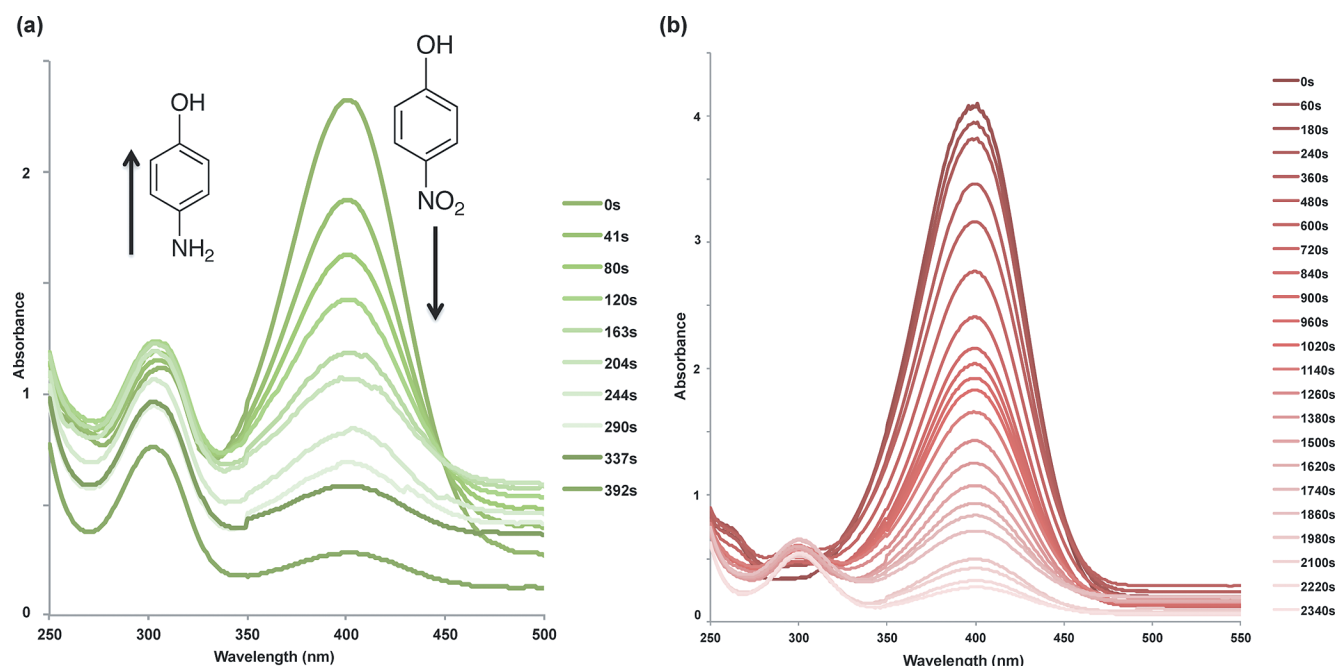


Figure 2. (a) Successive spectra monitoring the reduction of 4-NP (2.5 × 10⁻⁴ M) in the presence of PdDSNsA (0.2 mol-%) stabilized by glycodendrimers. (b) Successive spectra monitoring the reduction of 4-NP (2.5 × 10⁻⁴ M) in the presence of PdDSNsB (0.2 mol-%) stabilized by glycodendrimers. In both experiments, the optical measurements were disrupted by the presence of H₂ bubbles during the course of the reaction, and led to the shift of the spectra and the loss of the isosbestic points.^[15b]

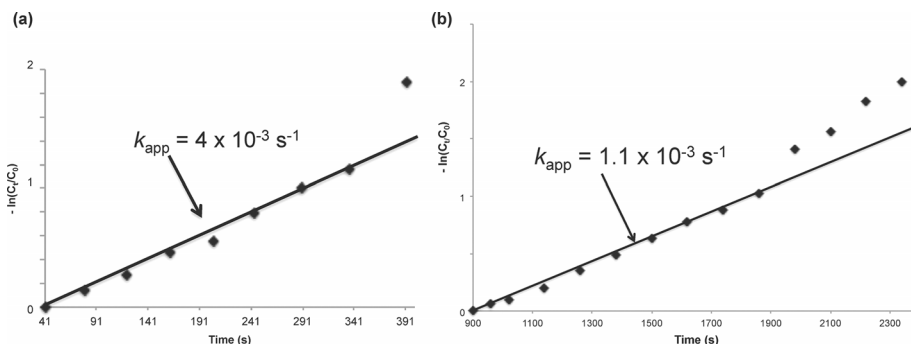


Figure 3. (a) Plot of $-\ln(C_t/C_0)$ as a function of time for the reduction of 4-NP (2.5×10^{-4} M) in the presence of PdDSNsA (0.2 mol-%) stabilized by glycodendrimers. (b) Plot of $-\ln(C_t/C_0)$ as a function of time for the reduction of 4-NP (2.5×10^{-4} M) in the presence of PdDSNsB (0.2 mol-%) stabilized by glycodendrimers.

these results, since it is well established that the mechanism of 4-NP reduction involves rate-limiting transformations on the NP metal surface,^[15,16] it is important to link the catalytic activity of each type of NP to the total surface area available for catalysis in solution. The total surface area of PdDSNsA in solution was determined to be $1.2 \times 10^{-2} \text{ m}^2 \text{ L}^{-1}$, whereas the total surface of PdDSNsB was found to be $2 \times 10^{-3} \text{ m}^2 \text{ L}^{-1}$ (Supporting Information). These results show that the reaction with smaller NPs (PdDSNsA) seems faster. This is most likely attributable to a surface area that is six times larger than in the PdDSNsB case, considering that both reactions contain the same number of palladium atoms in solution (5×10^{-7} M).

The catalytic efficiency of the PdDSNsA surface was then compared to the catalytic efficiency of PdDSNs of the same size that are stabilized by PPI dendrimers of low and comparable generation at their surface (8 branches) described by Esumi and co-workers.^[6c] This choice was justified by the fact that the catalytic efficiency of a considered system also depends on the dendrimer generation used (steric or filtering effect at the periphery of the dendrimer).^[6c,7g] To evaluate this catalytic efficiency, the rate constant (k_1) normalized to the surface (S) was estimated using the Equation (1) using the hypothesized LH mechanistic model (see Table 1):^[15b,17]

$$\frac{d[4\text{-NP}]}{dt} = -k_{\text{app}} [4\text{-NP}] = -k_1 S [4\text{-NP}] \quad (1)$$

Table 1. Catalytic activity of the PdDSNsA in the reduction of 4-NP: comparison with Esumi's G2 PPI dendrimer-stabilized PdNPs (see Supporting Information for a more detailed table and an explanation of calculations).

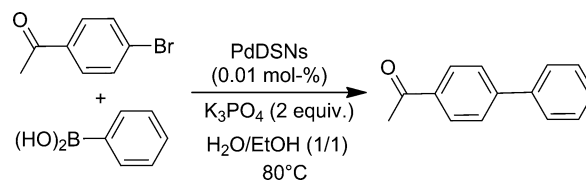
PdNPs	$D^{[a]}$ [nm]	$S^{[b]}$ [$\text{m}^2 \text{ L}^{-1}$]	k_{app} [s^{-1}]	k_1 [$\text{L s}^{-1} \text{ m}^{-2}$]
PdDSNsA	2.3 ± 0.4	1.2×10^{-2}	4×10^{-3}	0.33
PdNPs-G2-PPI	2.0 ± 0.5	5.4×10^{-1}	0.2165	0.40

[a] D is the average particle diameter of one single nanoparticle determined by TEM. [b] S is the total surface of PdDSNs in solution.

The k_1 values for PdDSNsA ($0.33 \text{ L s}^{-1} \text{ m}^{-2}$) and PdDSNs stabilized by PPI dendrimers ($0.40 \text{ L s}^{-1} \text{ m}^{-2}$) are quite similar probably due to the fact that both types of PdDSNs are stabilized by neutral ligands, that form only weak coordination bonds with the PdNP surface. The comparable generation of dendrimers for both scenarios also is likely responsible for the similar k_1 values noted. In applying the LH mechanistic model (hypothetical), ligand displacement by the substrate (surface restructuring) and the filtering effect at the periphery of the dendrimers are likely key factors in the reduction of 4-NP.^[6c,7g,15]

Catalysis of the Suzuki–Miyaura Reaction of Bromoarenes

The catalytic activities of the PdDSNsA and PdDSNsB were also investigated in Suzuki–Miyaura cross carbon–carbon coupling reactions. The coupling reactions were carried out using phenylboronic acid (1.5 equiv.) and 4'-bromoacetophenone (1 equiv.) in the presence of catalytic amounts (only 0.01 mol-% of Pd per mol substrate used) of PdDSNsA and PdDSNsB stabilized by glycodendrimers. The reaction mixture in water/ethanol (1:1) was heated at 80 °C in the presence of K_3PO_4 (2 equiv.) (Scheme 3).^[7i] All results are summarized below in Table 2.



Scheme 3. Suzuki–Miyaura coupling of 4'-bromoacetophenone with phenylboronic acid catalyzed by glycodendrimer-stabilized PdDSNs.

For comparison purposes, the reaction was performed without PdNPs; in such cases, no coupling product was obtained (Table 2, Entry 1). In the presence of 0.01 mol-% of PdDSNsA after 2 h at 80 °C, the reaction afforded a 77% yield of 4'-bromoacetophenone and phenylboronic acid coupled product (Table 2, Entry 2, TON = 7860; TOF = 3930 h^{-1}). Increasing the reaction time to 18 h led to a sub-

Table 2. Suzuki–Miyaura coupling of 4'-bromoacetophenone with phenylboronic acid at 80 °C.

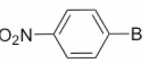
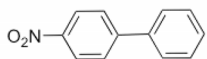
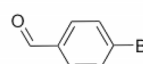
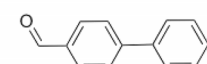
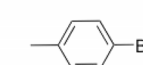
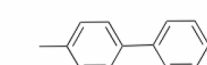
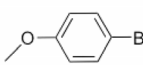
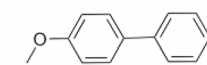
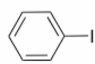
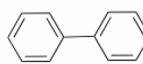
Entry	mol-% Pd	Time [h]	Yield ^[c] [%]	TON ^[d]	TOF ^[e] [h ⁻¹]
1	0	2	0	0	0
2 ^[a]	0.01	2	77	7860	3930
3 ^[a]	0.01	18	96	9800	544
4 ^[b]	0.01	18	95	9540	530

[a] Catalyzed by PdDSNsA. [b] Catalyzed by PdDSNsB. [c] Isolated after flash chromatography. [d] TON is the turnover number. [e] TOF is the turnover frequency.

stantially improved yield of 96% (Table 2, Entry 3, TON = 9800; TOF = 544 h⁻¹). The same reaction performed with PdDSNsB instead of PdDSNsA afforded the same product in practically the same yield (95%) (Table 2, Entry 4, TON = 9540; TOF = 530 h⁻¹) indicating what appears to be a lack of surface dependency for Suzuki–Miyaura catalysis.

To broaden the scope of these reaction conditions, the reaction was conducted using various aryl bromides bearing an assortment of electron-donating or -withdrawing groups with phenylboronic acid (1.5 equiv.) in the presence of PdDSNsA (0.01 mol-%) and K₃PO₄ (2 equiv.) in a 1:1 mixture of H₂O/EtOH (Table 3). After 18 h at 80 °C, all substrates were coupled with phenylboronic acid with yields ranging from 84 to 96%. Additionally, the same conditions applied to the reaction of iodobenzene with phenylboronic acid gave the desired coupling product with a yield of 89%.

Table 3. Suzuki–Miyaura reaction of various aryl bromides and iodobenzene with phenylboronic acid as catalyzed by glycodendrimer-stabilized PdDSNsA (0.01 mol-%) stabilized after 18 h at 80 °C.

Entry	Substrat	Product	Yield ^[a] (%)
1			86
2			96
3			84
4			84
5			89

[a] Isolated after flash chromatography.

Conclusions

The use of a low concentration of the palladium precursor K₂PdCl₄ led to the preparation of smaller and more monodisperse PdDSNs stabilized by water-soluble triazolyl glycodendrimers; this was achieved upon stoichiometric coordination of Pd^{II} to the intradendritic triazole ligands. These small PdDSNs were found to be catalytically active

in the reduction of 4-NP to 4-AP by NaBH₄ and showed levels of activity similar to comparable systems reported by Esumi and co-workers. Moreover, the reaction proceeded faster with small PdDSNs than with larger ones that had been previously prepared. This difference in activity is explained by the larger overall active surface presented by the smaller PdDSNs relative to their larger predecessors. These observations are in agreement with the mechanism proposed by Ballauf involving a rate-limiting organization at the NP surface. These PdDSNs were also tested in the Suzuki–Miyaura C–C coupling with various substituted aryl bromides and proved to be efficient catalysts. In these cases, the comparison of catalytic activities of PdDSNs of different sizes showed that they are similar. Whereas the reduction of 4-NP appears to operate at the NP surface, Suzuki–Miyaura catalysis indicates a lack of surface dependency. This study shows that glycodendrimers are of general interest for the stabilization of catalytically efficient homogeneous PdNPs of various sizes in the context of sustainable development.

Experimental Section

General: All reagents were used as received. The glycodendrimer was synthesized as described in the literature.^[9b] The PdDSN size was determined by TEM using a JEOL JEM 1400 (120 kV) microscope. TEM samples were prepared by deposition of the nanoparticle suspension (10 μL) on a carbon-coated microscopy copper grid. The infrared (IR) spectra were recorded with an ATI Mattson Genesis series FT-IR spectrophotometer. UV/Vis absorption spectra were measured with a Perkin–Elmer Lambda 19 UV/Vis spectrometer.

Procedure for the Preparation of PdDSNsA: Glycodendrimer (1.4 mL of a 3.1 × 10⁻⁴ M aqueous solution) was added to deionized water (25.8 mL), followed by the addition of freshly prepared K₂PdCl₄ (1.3 mL of 3.1 × 10⁻³ M aqueous solution) under nitrogen. The resulting mixture was then stirred for 20 min and NaBH₄ (1.5 mL of a 2.6 × 10⁻² M) was added dropwise, provoking the formation of a pink-brown color corresponding to the reduction of Pd^{II} to Pd⁰ and PdNPs formation.

General Procedure for the Reduction of 4-NP: 4-NP (1 equiv.) was mixed with NaBH₄ (81 equiv.) in water (200 mL) under air, then the solution containing the freshly prepared PdDSNs, was added. After adding NaBH₄, the color of the solution changed from light yellow to dark yellow due to the formation of the 4-nitrophenolate anion. Then, this solution loses its dark yellow colour with the time after addition of PdDSNs. The reaction was monitored by UV/Vis spectroscopy.

General Procedure for the Suzuki–Miyaura Reaction: Into a Schlenk flask containing tribasic potassium phosphate (2 equiv.) are successively added phenylboronic acid (1.5 equiv.), aryl halide (1 equiv.) and EtOH (5 mL). Then the solution containing the glycodendrimer-stabilized PdDSNs is added followed by addition of water in order to achieve a volume ratio of H₂O/EtOH: 1:1. Note: when only water is used, the reaction does not work as well due to substrate hydrophobicity. The suspension is then allowed to stir under air at 80 °C after which time (see Tables 2 and 3 for exact data), the reaction mixture is extracted three times with CH₂Cl₂ (all the reactants and final products are soluble in CH₂Cl₂). The combined organic phase is then dried with Na₂SO₄, solids are fil-

tered, and the volatile solvent removed under vacuum. In parallel, the reaction is routinely checked using TLC (Petroleum ether in nearly all cases) and by ^1H NMR spectroscopy.

Supporting Information (see footnote on the first page of this article): Table S1 (a more detailed version of Table 1) and an explanation of calculations.

Acknowledgments

Financial support from the Centre National de la Recherche Scientifique (CNRS) (support to S. G.), the Universities Bordeaux I, Toulouse III and Reims Champagne-Ardenne), the CPER 2007-2013 framework Pentoraffinerie (State Region Project Contract) and the European Regional Development Fund (ERDF) are gratefully acknowledged.

- [1] a) M. T. Reetz, W. Helbig, S. A. Quaiser, in: *Active Metals: Preparation, Characterizations, Applications* (Ed.: A. Fürstner), Wiley-VCH, Weinheim, Germany, **1996**, p. 279; b) I. P. Beletskaya, A. V. Cheprakov, *Chem. Rev.* **2000**, *100*, 3009–3066; c) H. Bönemann, R. Richards, *Eur. J. Inorg. Chem.* **2001**, *10*, 2455–2480; d) V. Rotello, *Nanoparticles Building Block for Nanotechnology*, Kluwer Academic Publishers, New York, USA, **2004**; e) D. Astruc, F. Lu, J. Ruiz, *Angew. Chem. Int. Ed.* **2005**, *44*, 7852–7872; *Angew. Chem.* **2005**, *117*, 8062; f) J. G. de Vries, *Dalton Trans.* **2006**, 421–429; g) G. Schmid, *Nanoparticles: From Theory to Application*, 2nd completely revised and updated edition, Wiley-VCH, Weinheim, Germany, **2010**; h) L. M. Bronstein, Z. B. Shifrina, *Chem. Rev.* **2011**, *111*, 5301–5344; i) P. Serp, K. Philippot, *Nanomaterials in Catalysis*, Wiley-VCH, Weinheim, Germany, **2013**.
- [2] a) H. Ohde, C. M. Wai, H. Kim, J. Kim, M. Ohde, *J. Am. Chem. Soc.* **2002**, *124*, 4540–4541; b) R. Narayanan, M. A. El-Sayed, *J. Am. Chem. Soc.* **2003**, *125*, 8340–8347; c) D. Astruc, *Inorg. Chem.* **2007**, *46*, 1884–1894; d) H. M. Lu, X. K. Meng, *J. Phys. Chem. C* **2010**, *114*, 1534–1538.
- [3] a) D. A. Tomalia, A. M. Naylor, W. A. Goddard III, *Angew. Chem. Int. Ed. Engl.* **1990**, *29*, 138–175; *Angew. Chem.* **1990**, *102*, 119; b) G. R. Newkome, C. N. Moorefield, *Aldrichim. Acta* **1992**, *25*, 31; c) G. R. Newkome, *Pure Appl. Chem.* **1998**, *70*, 2337; d) A. W. Bosman, H. M. Janssen, E. W. Meijer, *Chem. Rev.* **1999**, *99*, 1665–1688; e) S. Hecht, J. M. J. Fréchet, *Angew. Chem. Int. Ed.* **2001**, *40*, 74–91; *Angew. Chem.* **2001**, *113*, 76; f) C. Ornelas, J. Ruiz, C. Belin, D. Astruc, *J. Am. Chem. Soc.* **2009**, *131*, 590–601; g) D. Astruc, E. Boisselier, C. Ornelas, *Chem. Rev.* **2010**, *110*, 1857–1959; h) G. R. Newkome, C. Shreiner, *Chem. Rev.* **2010**, *110*, 6338–6442; i) A.-M. Caminade, C.-O. Turrin, R. Laurent, A. Ouali, B. Delavaux-Nicot, *Dendrimers: Towards Catalytic, Material and Biomedical Uses*, Wiley, Chichester, UK, **2011**; j) *Designing Dendrimers* (Eds.: S. Camapagna, P. Ceroni, F. Puntoriero), John Wiley & Sons, Hoboken, NJ, USA, **2012**.
- [4] a) M. Zhao, L. Sun, R. M. Crooks, *J. Am. Chem. Soc.* **1998**, *120*, 4877–4878; b) K. Esumi, A. Suzuki, N. Aihara, K. Usui, K. Torigoe, *Langmuir* **1998**, *14*, 3157–3159; c) L. Balogh, D. A. Tomalia, *J. Am. Chem. Soc.* **1998**, *120*, 7355–7356.
- [5] a) D. Astruc, K. Heuze, S. Gatard, D. Méry, S. Nlate, L. Plault, *Adv. Synth. Catal.* **2005**, *347*, 329–338; b) D. Astruc, *Organometallic Chemistry and Catalysis*, Springer, Heidelberg, Germany, **2007**, chapter 21; c) B. Cornils, W. A. Herrmann, *Applied Homogeneous Catalysis with Organometallic Compounds: A Comprehensive Handbook in Three Volumes*, 2nd completely revised and enlarged edition, Wiley-VCH, Weinheim, Germany, **2008**; d) *Modern Surface Organometallic Chemistry* (Eds.: J.-M. Basset, R. Psaro, D. Roberto, R. Ugo), Wiley-VCH, Weinheim, Germany, **2009**; e) W. K. Chow, O. Y. Yuen, P. Y. Choy, C. M. So, C. P. Lau, W. T. Wong, F. Y. Kwong, *RSC Adv.* **2013**, *3*, 12518–12539; f) R. Chinchilla, C. Nájera, *Chem. Rev.* **2014**, *114*, 1783–1826.
- [6] a) Y. Li, M. A. El-Sayed, *J. Phys. Chem. B* **2001**, *105*, 8938–8943; b) M. Pittelkow, K. Moth-Poulsen, U. Boas, J. B. Christensen, *Langmuir* **2003**, *19*, 7682–7684; c) K. Esumi, R. Isono, T. Yoshimura, *Langmuir* **2004**, *20*, 237–243; d) L. Wu, B.-L. Li, Y.-Y. Huang, H.-F. Zhou, Y.-M. He, Q.-H. Fan, *Org. Lett.* **2006**, *8*, 3605–3608; e) A. K. Diallo, C. Ornelas, L. Salmon, J. Ruiz, D. Astruc, *Angew. Chem. Int. Ed.* **2007**, *46*, 8644–8648; *Angew. Chem.* **2007**, *119*, 8798; f) C. Ornelas, L. Salmon, J. Ruiz, D. Astruc, *Chem. Commun.* **2007**, 4946–4948; g) T. Mizugaki, M. Murata, S. Fukubayashi, T. Mitsudome, K. Jit-sukawa, K. Kaneda, *Chem. Commun.* **2008**, *2*, 241–243; h) E. Badetti, A.-M. Caminade, J.-P. Majoral, M. Moreno-Manas, R. M. Sebastian, *Langmuir* **2008**, *24*, 2090–2101; i) C. Ornelas, J. Ruiz, L. Salmon, D. Astruc, *Chem. Eur. J.* **2008**, *14*, 50–64.
- [7] a) F. Lu, J. Ruiz, D. Astruc, *Tetrahedron Lett.* **2004**, *45*, 9443–9445; b) C. Ornelas, J. Ruiz, L. Salmon, D. Astruc, *Adv. Synth. Catal.* **2008**, *350*, 837–845; c) L. Wu, Z.-W. Li, F. Zhang, Y.-M. He, Q.-H. Fan, *Adv. Synth. Catal.* **2008**, *350*, 846–862; d) G. Ou, L. Xu, B. He, Y. Yuan, *Chem. Commun.* **2008**, *35*, 4210–4212; e) K. Ratheesh, K. Venugopal, K. R. Gopidas, *Tetrahedron Lett.* **2011**, *52*, 3102–3105; f) Y. Xu, Z. Zhang, J. Zheng, Q. Du, Y. Li, *Appl. Organomet. Chem.* **2013**, *27*, 13–18; g) J. A. Johnson, J. J. Makis, K. A. Marvin, S. E. Rodenbusch, K. J. Stevenson, *J. Phys. Chem. C* **2013**, *117*, 22644–22651; h) C. Gaebler, J. Jeschke, G. Nurgazina, S. Dietrich, D. Schaarschmidt, C. Georgi, M. Schlesinger, M. Mehring, H. Lang, *Catal. Lett.* **2013**, *143*, 317–323; i) C. Deraedt, L. Salmon, D. Astruc, *Adv. Synth. Catal.* DOI: 10.1002/adsc.201400153.
- [8] a) R. M. Crooks, M. Zhao, L. Sun, Y. Chechik, L. K. Yeung, *Acc. Chem. Res.* **2001**, *34*, 181–190; b) R. W. J. Scott, O. M. Wilson, R. M. Crooks, *J. Phys. Chem. B* **2005**, *109*, 692–704; c) V. S. Myers, M. W. Weier, E. V. Carino, D. F. Yancey, S. Pande, R. M. Crooks, *Chem. Sci.* **2011**, *2*, 1632–1646.
- [9] a) J. Camponovo, C. Hadad, J. Ruiz, E. Cloutet, S. Gatard, J. Muzart, S. Bouquillon, D. Astruc, *J. Org. Chem.* **2009**, *74*, 5071–5074; b) S. Galard, L. Liang, L. Salmon, J. Ruiz, D. Astruc, S. Bouquillon, *Tetrahedron Lett.* **2011**, *52*, 1842–1846; c) S. Gatard, L. Salmon, C. Deraedt, D. Astruc, S. Bouquillon, *Eur. J. Inorg. Chem.* DOI: 10.1002/ejic.201402067.
- [10] For recent examples of nanoparticles stabilized by carbohydrates, see: a) J. E. Camp, J. J. Dunsford, E. P. Cannons, W. J. Restorick, A. Gadzhieva, M. W. Fay, R. J. Smith, *ACS Sustainable Chem. Eng.* **2014**, *2*, 500–505; b) M. Rezayat, R. K. Blundell, J. E. Camp, D. A. Walsh, W. Thielemans, *ACS Sustainable Chem. Eng.* **2014**, *2*, 1241–1250; c) Á. Molnár, A. Papp, *Catal. Sci. Technol.* **2014**, *4*, 295; d) X. Wu, C. Lu, Z. Zhou, G. Yuan, R. Xiong, X. Zhang, *Environ. Sci.: Nano* **2014**, *1*, 71–79.
- [11] a) A. Schmitzer, E. Perez, I. Rico-Lattes, A. Lattes, S. Rosca, *Langmuir* **1999**, *15*, 4397–4403; b) A. Schmitzer, S. Franceschi, E. Perez, I. Rico-Lattes, A. Lattes, L. Thion, M. Erard, C. Vidal, *J. Am. Chem. Soc.* **2001**, *123*, 5956–5961; c) M. Touaiba, A. Wellens, C. S. Tze, Q. Wang, S. Sirois, J. Bouckaert, R. Roy, *ChemMedChem* **2007**, *2*, 1190–1201; d) Y. M. Chabre, R. Roy, *Curr. Top. Med. Chem.* **2008**, *8*, 1237–1285; e) P. Rajakumar, R. Anandhan, V. Kalpana, *Synlett* **2009**, *9*, 1417–1422; f) C. Hadad, J.-P. Majoral, J. Muzart, A.-M. Caminade, S. Bouquillon, *Tetrahedron Lett.* **2009**, *50*, 1902–1905; g) R. Kikkeri, X. Liu, A. Adibekian, Y.-H. Tsai, P. H. Seeberger, *Chem. Commun.* **2010**, *46*, 2197–2199; h) J. G. Fernandez-Bolanos, I. Maya, A. Oliete, *Carbohydr. Chem.* **2012**, *38*, 303–337; i) M. Gingras, Y. M. Chabre, M. Roy, R. Roy, *Chem. Soc. Rev.* **2013**, *42*, 4823–4841; j) R. Roy, T. C. Shiao, K. Rittenhouse-Olson, *Braz. J. Pharm. Sci.* **2013**, *49*, 85–108; k) K. Hatano, K. Matsuoka, D. Terunuma, *Chem. Soc. Rev.* **2013**, *42*, 4574–4598; l) Y. M. Chabre, R. Roy, *Chem. Soc. Rev.* **2013**, *42*, 4657–4708.
- [12] a) K. Esumi, T. Hosoya, A. Suzuki, K. Torigoe, *Langmuir* **2000**, *16*, 2978–2980; b) A. Köth, J. Koetz, D. Appelhans, B. Voit, *Colloid Polym. Sci.* **2008**, *286*, 1317–1327; c) T. Pietsch,

- D. Appelhans, N. Gindy, B. Voit, A. Fahmi, *Colloids Surf. A* **2009**, *341*, 93–102.
- [13] T. Ahmad, I. A. Wani, J. Ahmed, O. A. Al-Hartomy, *Appl. Nanosci.* **2014**, *4*, 491–498.
- [14] a) N. Miyaoura, T. Yanagi, A. Suzuki, *Synth. Commun.* **1981**, *11*, 513; b) N. Miyaoura, A. Suzuki, *Chem. Rev.* **1995**, *95*, 2457; c) L. Ackermann, *Historical development of cross-coupling reactions*, in: *Modern Arylation Methods*, Wiley-VCH, Weinheim, Germany, **2009**, p. 1–24; d) D. Astruc, *Tetrahedron: Asymmetry* **2010**, *21*, 1041–1054; e) A. Fihri, M. Bouhrara, B. Nekoueishahraki, J.-M. Basset, V. Polshettiwar, *Chem. Soc. Rev.* **2011**, *40*, 5181–5203; f) C. C. C. J. Seechurn, M. O. Kitching, T. J. Colacot, V. Sniekus, *Angew. Chem. Int. Ed.* **2012**, *51*, 5062–5085; g) C. Deraedt, D. Astruc, *Acc. Chem. Res.* **2014**, *47*, 494–503.
- [15] a) K. Kuroda, T. Ishida, M. Haruta, *J. Mol. Catal. A* **2009**, *298*, 7–11; b) S. Wunder, F. Polzer, Y. Lu, Y. Mei, M. Ballauff, *J. Phys. Chem. C* **2010**, *114*, 8814–8820; c) P. Hervés, M. Pérez-Lorenzo, L. M. Liz-Marzán, J. Dzubiella, Y. Lu, M. Ballauff, *Chem. Soc. Rev.* **2012**, *41*, 5577–5587; d) J. Li, C.-Y. Liu, Y. Liu, *J. Mater. Chem.* **2012**, *22*, 8426–8430; e) H. Woo, K. H. Park, *Catal. Commun.* **2014**, *46*, 133–137; f) J. Zhang, G. Chen, D. Guay, M. Chaker, D. Ma, *Nanoscale* **2014**, *6*, 2125–2130; g) P. Deka, R. C. Deka, P. Bharali, *New J. Chem.* **2014**, *38*, 1789–1793; h) Q. Geng, J. Du, *RSC Adv.* **2014**, *4*, 16425–16428; i) Y. Chi, J. Tu, M. Wang, X. Li, Z. Zhao, *J. Colloid Interface Sci.* **2014**, *423*, 54–59.
- [16] a) S. Wunder, Y. Lu, M. Albrecht, M. Ballauff, *ACS Catal.* **2011**, *1*, 908–916; b) X. Zhou, W. Xu, G. Liu, D. Panda, P. Chen, *J. Am. Chem. Soc.* **2010**, *132*, 138–146.
- [17] a) Y. Mei, Y. Lu, F. Polzer, M. Ballauff, *Chem. Mater.* **2007**, *19*, 1062–1069; b) S. Panigrahi, S. Basu, S. Praharaj, S. Pande, S. Jana, A. Pal, *J. Phys. Chem. C* **2007**, *111*, 4596–4605.

Received: May 22, 2014

Published Online: July 30, 2014

DOI:10.1002/ejic.201402067

Gold Nanoparticles Stabilized by Glycodendrimers: Synthesis and Application to the Catalytic Reduction of 4-Nitrophenol

Sylvain Gatard,^{*[a,b]} Lionel Salmon,^[c] Christophe Deraedt,^[a] Jaime Ruiz,^[a] Didier Astruc,^{*[a]} and Sandrine Bouquillon^{*[b]}

Keywords: Nanoparticles / Dendrimers / Gold / Reduction

Air-stable gold nanoparticles stabilized by glycodendrimers (AuDSNs) in water were prepared in the presence of a reducing agent, NaBH₄. A UV/Vis spectroscopy study demonstrates that no spontaneous reduction of Au³⁺ ions occurs in the presence of glycodendrimers. The AuDSNs were characterized by UV/Vis spectroscopy and transmission electron microscopy (TEM). TEM images show that the AuDSNs were

very small (average diameter: 2.6 nm). The catalytic activity of these AuDSNs was evaluated for the reduction of 4-nitrophenol (4-NP) to 4-aminophenol (4-AP) by NaBH₄ monitored by UV/Vis spectroscopy. Studies of the reduction reaction reveal that the rate constant depends on the concentration of 4-NP.

Introduction

Recent advances in the development of nanoparticles (NPs) have led to potential applications in several areas of nanosciences including photophysics, biological sensing, medicine, and catalysis.^[1] The growing interest in NPs might be explained by the improvement of their methods of preparation: the use of organic additives such as dendrimers allows one to control the size of the NPs by preventing agglomeration, increase the stability, and influence the solubility in organic and aqueous media of the formed NPs.^[2] Dendrimers^[3] offer advantages over other stabilizers in that they have well-defined, compartmentalized structures in the nanometer-sized range, narrow polydispersity, and globular morphology (applicable to higher-generation dendrimers), which enable them to entrap and stabilize NPs, especially if they contain heteroatoms in their interiors. The most common pathway to dendrimer-encapsulated nanoparticles is the reduction of transition-metal ions within the dendrimers.^[2] In addition to these aspects (solubility, stabilization,

protection), the dendrimers confer specific functionalities on the NPs for potential applications. In catalysis, NPs stabilized by dendrimers present advantages of both homogeneous and heterogeneous catalysts: (i) the size and the solubility of the NPs is controlled by the architecture of the dendrimer, (ii) the accessibility to the NP is determined by the surface of the dendrimer, and (iii) the recyclability often is facile. In this context, and as a continuation of our study on dendrimer-stabilized metal NPs,^[4] we wish to disclose the facile “click” preparation of air-stable glycodendrimer-stabilized Au nanoparticles (DSNs) that contain 1,2,3-triazolyl linkages, the role of which has been evidenced in the formation of gold nanoparticles (AuNPs) templated by dendrimers and polymers.^[5] Then, the reduction of 4-nitrophenol (4-NP) to 4-aminophenol (4-AP) was selected as a model reaction^[6,7] to evaluate the catalytic potential of these new DSNs. Nitrophenols are among the most toxic and hazardous micropollutants, thus their degradation is really challenging for environmental purposes.^[8]

AuNPs have found potential applications in various fields (catalysis, optics, electronics, biology, medicine) owing to their unique spectroscopic and chemical properties.^[9] In the field of catalysis, AuNPs have witnessed a burst of interest since the discovery by Haruta and co-workers of their low-temperature catalyst properties in the oxidation reaction of carbon monoxide by dioxygen.^[10] In the literature, a number of works have dealt with the contribution of AuNPs stabilized by dendrimers in various redox reactions including oxidation of alcohols,^[11] and reduction of nitrobenzene^[12] and 4-NP.^[13] Mainly AuNPs stabilized by commercial poly(amido amine) (PAMAM) and poly(propyleneimine) (PPI) dendrimers are described in these works.

[a] ISM, UMR CNRS 5255, Université de Bordeaux, 33405 Talence Cedex, France
E-mail: d.astruc@ism.u-bordeaux1.fr
<http://astruc.didier.free.fr>

[b] ICMR, UMR CNRS 7312, Université de Reims Champagne-Ardenne, BP 1039, 51687 Reims Cedex, France
E-mail: sandrine.bouquillon@univ-reims.fr
sylvain.gatard@univ-reims.fr
<http://www.univ-reims.fr/site/laboratoire-labellise/icmr/presentation,9938,17756.html>

[c] LCC, CNRS & Université de Toulouse (UPS, INP), 31077 Toulouse, France

Supporting information for this article is available on the WWW under <http://dx.doi.org/10.1002/ejic.201402067>.

However, our interest is in the intradendritic 1,2,3-triazole ligands formed by “click” functionalization of dendrimers that coordinate transition-metal cations undergoing further reduction to catalytically very active metal NPs. The use of amphiphilic glycodendrimers for AuNP stabilization addresses important problems, such as aqueous catalysis and biological recognition.^[14] In these fields, the presence of carbohydrates at the periphery of the dendrimers confers to AuNPs key properties such as reduced toxicity, water solubility, chiral surface for asymmetric induction,^[15] and capacity to form supramolecular interactions with proteins such as lectins that are useful in nanomedicine.^[14g] Although glycodendrimers are a rich area^[16] and the use of dendrimers decorated by C6 sugars in enantioselective catalysis has already been described,^[16a,16b] to the best of our knowledge the literature on pentoses decorating dendrimers remains scarce.^[4,16g,16h] From an ecological and economic perspective, pentoses are abundant, renewable, and low-cost molecules from agricultural resources.^[17] The use of pentoses to decorate dendrimers is therefore part of a sustainable development strategy and might contribute to lower their price. Therefore, readily available pentose-decorated dendrimers are utilized in the present article to generate “click” dendrimer-stabilized AuNPs that show remarkable catalytic activity.

Results and Discussion

The dendritic core used for pentose dendrimer synthesis results from the classic mild CpFe⁺-induced (Cp = cyclopentadienyl) nona-allylation of mesitylene followed by visible-light photo-decomplexation, hydrosilylation of the double bonds with chloromethyldimethylsilane, and nucleophilic chloride substitution by azide.^[18] The Cu^I-catalyzed click reaction yielding the nona-pentose hydrophilic den-

drimer has been reported,^[4] and this dendrimer is now used for Au^{III} complexation. The most common pathway to DSNs is the reduction of such transition-metal ions within the dendrimers. Therefore, the water-soluble glycodendrimer containing 9 terminal modified xylose branches and HAuCl₄ (9 equiv.) were mixed together in water for 20 min under air, to provide enough time for Au³⁺ ions to be encapsulated into the dendrimer interior. The stoichiometry corresponds to the number of triazole rings in the glycodendrimer, as in previous studies.^[4,5] Then, an aqueous solution of NaBH₄ was added dropwise to reduce the Au³⁺ ions to zerovalent Au (Scheme 1).

As demonstrated by the optical extinction spectrum (Figure 1), the formation of AuDSNs stabilized by the glycodendrimers was instantaneous, and a pink-brown solution was obtained. The optical extinction spectrum of the AuDSNs shows a broad band at around $\lambda = 520$ nm corresponding to the plasmon band of AuNPs.^[9] As reported earlier in the literature and because of the low generation

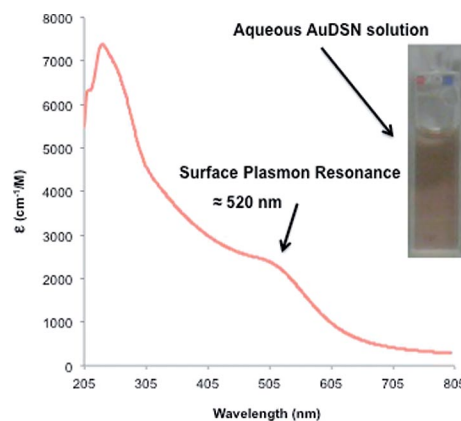
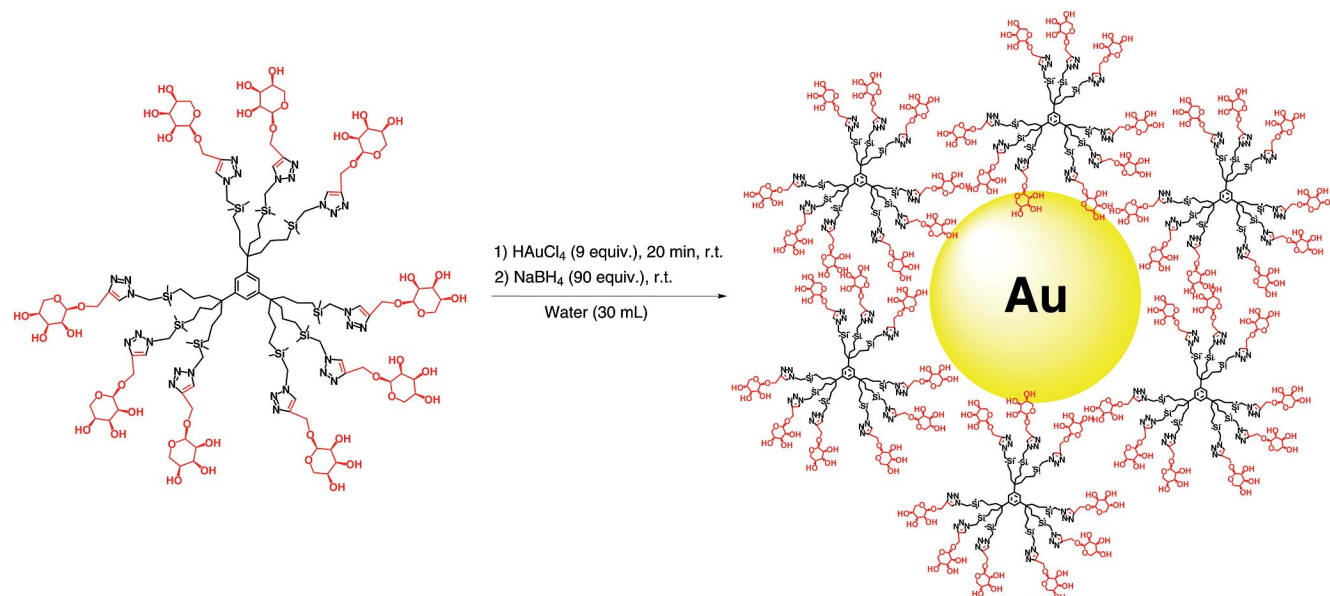


Figure 1. Optical extinction spectrum of AuDSNs in solution in water recorded with glycodendrimer in water as the blank.



Scheme 1. Preparation of monometallic AuDSNs stabilized by glycodendrimers.

of the glycodendrimer that is used, the AuNPs are stabilized by several small dendrimers at the surface (DSNs).^[2e,2f,5a]

A few groups have reported the formation of AuNPs stabilized by dendrimers without any external reductant.^[5b,14d–14f] In particular, Esumi and co-workers pointed out the role of hydroxy groups of peripheral sugar balls of poly(amidoamine)dendrimers reducing Au³⁺ ions and yielding AuNPs after 90 min with the observation of a plasmon band at 520 nm.^[14d] These hydroxy groups were oxidized to carbonyl groups, which was confirmed by the comparison of FTIR spectra of gold particles/sugar balls and the apparition of a new band near 1732 cm⁻¹ corresponding to carbonyl groups. These results led us to study the reducing power of our glycodendrimers through various analytical techniques such as UV/Vis, FTIR, and fluorescence spectroscopy.

A dilute aqueous solution containing a mixture of the glycodendrimer and HAuCl₄ was followed by UV/Vis spectroscopy, over a period of 24 hours (Figure 2). In the aqueous solution before adding the glycodendrimer, HAuCl₄ shows a strong absorption band at $\lambda = 217$ nm and a shoulder at 290 nm owing to ligand-to-metal charge transfer (LMCT) between the metal and chloro ligands.^[2d] 40 min after adding the glycodendrimer, the shoulder at 290 nm increased but no growing Au plasmon shoulder appeared with time in this spectrum (even after 24 h, Figure 2, c), contrary to other reports with other glycodendrimers.^[14d–14f]

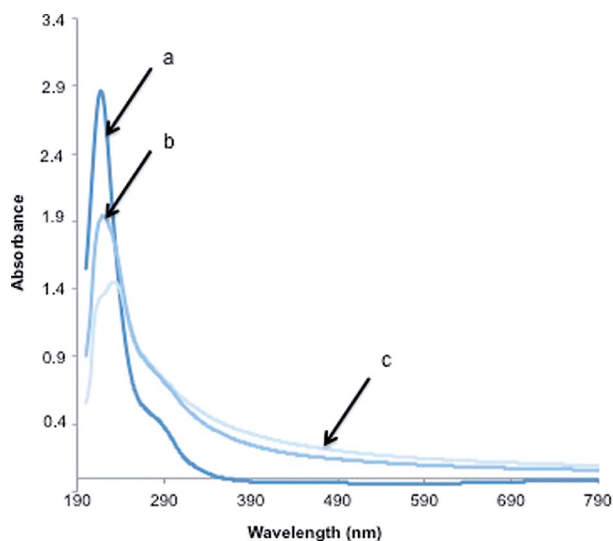
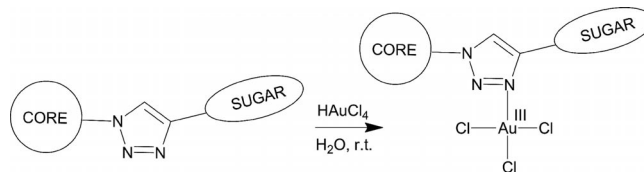


Figure 2. UV/Vis spectra: (a) HAuCl₄ in water; (b) HAuCl₄ and the glycodendrimer after 40 min; (c) HAuCl₄ and the glycodendrimer after 24 h. UV/Vis spectra presented in (b) and (c) were recorded with glycodendrimer in water as the blank.

The increase in absorbance at $\lambda = 290$ nm may be explained by the complexation of Au^{III} to the triazole rings. Complexation of Au^{III} to the 1,2,3-triazolyl ring in water at room temperature (Scheme 2) has already been suggested by Bortoluzzi and co-workers^[19] and by us.^[5b]



Scheme 2. Schematic representation of the complexation of Au^{III} to the 1,2,3-triazolyl ring.

FTIR spectra of solutions containing AuCl₄⁻ (9 equiv.) / glycodendrimer (1 equiv.) in water after 1 and 20 h of stirring showed the absence of carbonyl groups. The fluorescence spectrum was also recorded after 24 h (excitation at 510 nm, from a xenon arc source), but no signal indicating the formation of Au⁰ particles was detected. All these results are consistent with a lack of reduction of Au³⁺ ions to Au⁰ at room temperature in water after 24 h in the presence of the glycodendrimers used in this study. The absence of reducing power of these glycodendrimers might be attributed to the absence of free hemiacetal functions in the peripheral sugars.

The TEM analysis of the AuDSNs stabilized by the glycodendrimers is shown in Figure 3. The particles have an average size of (2.6 ± 0.4) nm (over 100 counted NPs), which corresponds to 541 Au atoms per NP, calculated by using the equation $n = 4\pi r^3 / 3V_g$, in which n is the number of Au atoms, r is the radius of the Au nanoparticle determined by TEM, and V_g is the volume of one Au atom (17 Å³).^[20]

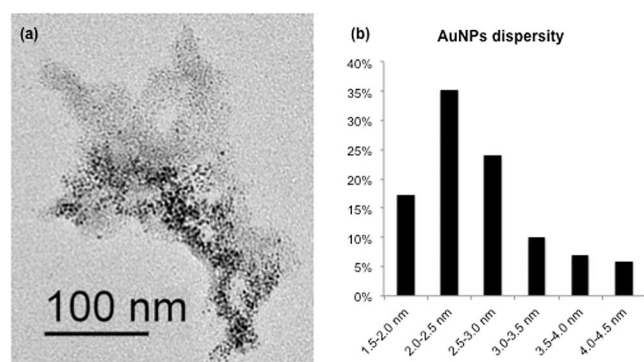
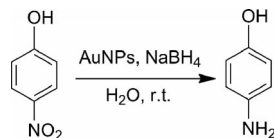


Figure 3. (a) TEM analysis of AuDSNs stabilized by the glycodendrimers; (b) Size distribution of AuNPs stabilized by the glycodendrimers.

The most efficient NPs in catalysis have small sizes (<10 nm). Indeed, when the particle size decreases, the proportion of the number of atoms on the surface, corners, and edges, which are expected to be the catalytically active ones, increases.^[1b,1d] Therefore, it appeared interesting to check the catalytic activity of these very small AuDSNs, and the reduction of 4-NP to 4-AP was chosen. Various groups have already reported the reduction of 4-NP catalyzed by Au dendrimer-stabilized nanoparticles, mainly with commercial PAMAM and PPI dendrimers.^[21]

The reduction of 4-NP (1 equiv.) to 4-AP in water in the presence of NaBH₄, using AuDSNs stabilized by glycodendrimers as catalyst was monitored in a spectrophotometric

cell in water at 25 °C by the disappearance of the strong absorption band at $\lambda_{\text{max}} = 405 \text{ nm}$ ($\epsilon = 18450 \text{ cm}^{-1} \text{ M}^{-1}$). The appearance of this band corresponds to the instantaneous formation of 4-nitrophenolate in the presence of NaBH_4 . The formation of 4-AP is characterized by the increase of an absorption band at 300 nm (Scheme 3).



Scheme 3. Reduction of 4-NP to 4-AP in water in the presence of NaBH_4 using glycodendrimer-stabilized AuNPs as catalyst.

Figure 4a shows the successive UV/Vis spectra corresponding to the reduction of 4-NP using 10 mol-% of AuNPs and 100 equiv. of NaBH_4 , and Figure 4 (b), the plot of $-\ln(C_t/C_0)$ ($C_t =$ concentration at time t , $C_0 =$ concentration at $t = 0$) as a function of time (in seconds), which allows the rate constant (k) to be determined. As previous studies showed, there is an induction time, t_0 , that corresponds, in the assumption of a Langmuir–Hinshelwood mechanism, to "an activation or restructuring of the metal surface by nitrophenol"^[22] before the reduction actually starts. Then, the reaction follows pseudo-first order as usually accepted.^[21] The rate constant k was calculated to be $2.4 \times 10^{-3} \text{ s}^{-1}$.

Table 1 shows a comparison of the average diameter and the rate constants obtained in the reduction of 4-NP, between the AuDSNs synthesized in the present study and AuDSNs stabilized by PAMAM- NH_2 and PPI dendrimers (2nd generation) reported in the literature.^[21a] For all the data in Table 1, AuDSNs are stabilized by dendrimers of low, comparable generation at their surface. G2-PAMAM- NH_2 and G2-PPI dendrimers have 8 branches at the surface and the present glycodendrimer has 9 branches. From Table 1 it appears that the AuDSNs prepared in the present

study have comparable catalytic activity and diameter to those reported with PPI and PAMAM dendrimers.

Table 1. Comparison with selected results from the literature obtained with AuNPs stabilized by dendrimers.

Dendritic system	Average diameter [nm]	Mol-% AuNPs	[4-NP] [10^{-4} M]	NaBH_4 [equiv.]	k [10^{-3} s^{-1}]
G0-Glyco	2.6	10	1	100	2.4
G2-PAMAM- NH_2 ^[21a]	3.7	10	1	100	1.74
G2-PPI ^[21a]	3.6	10	1	100	1.23

To optimize this reaction and to deepen our understanding of our catalytic system we varied the molar percentage of AuDSNs (mol-%) and the concentration of 4-NP ([4-NP]) and kept constant the amount of NaBH_4 at 81 equiv. instead of 100 equiv. All the results are summarized in Table 2 (see Figures S1–S3 in the Supporting Information for details).

Table 2. Reduction of 4-NP to 4-AP with AuDSNs using NaBH_4 (81 equiv.).

Entry	Mol-% AuNPs	[4-NP] [10^{-4} M]	k [10^{-3} s^{-1}]
1	0.2	6.2	6.5
2 ^[a]	0.2	6.2	— ^[b]
3 ^[c]	0	6.2	— ^[b]
4	0.2	2.5	1.3
5	0.5	1.5	1.1
6	2	1.5	1.8

[a] The reduction of 4-NP was conducted in the presence of 0.2 mol-% Au taken from a freshly prepared solution containing AuNPs, following the procedure described in the Experimental Section but without glycodendrimer. [b] Not determined because too slow. [c] The reduction of 4-NP was conducted in the presence of the same concentration of glycodendrimer as used for entry 1 but without Au.

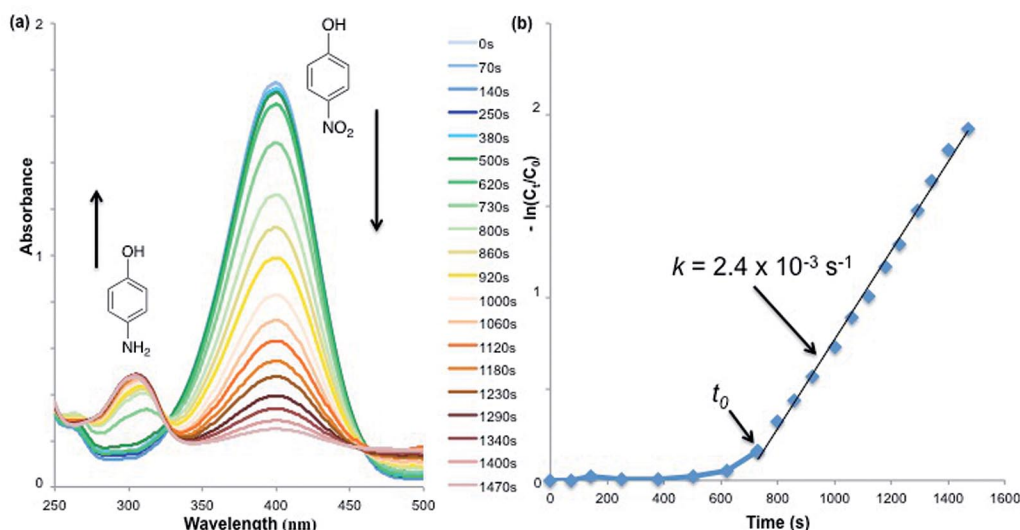


Figure 4. (a) Successive spectra monitoring the reduction of 4-NP ($1 \times 10^{-4} \text{ M}$) in the presence of AuDSNs (10 mol-%) stabilized by glycodendrimers. (b) Plot of $-\ln(C_t/C_0)$ as a function of time (s).

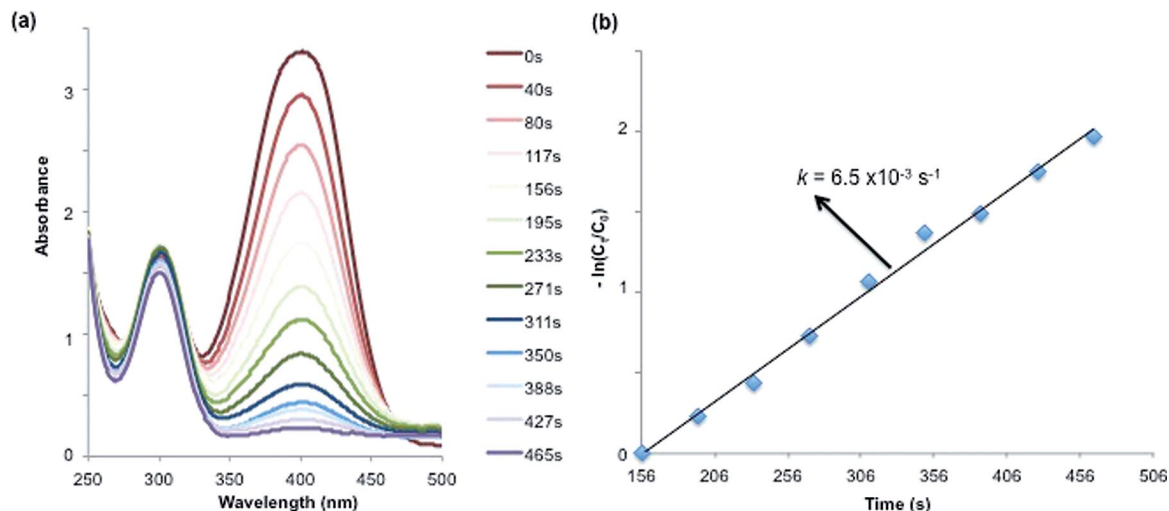


Figure 5. (a) Successive spectra monitoring the reduction of 4-NP (6.2×10^{-4} M) in the presence of AuDSNs (0.2 mol-%) stabilized by glycodendrimers. (b) Plot of $-\ln(C_t/C_0)$ as a function of time (s).

In the presence of 0.2 mol-% of metal, with a concentration of 6.2×10^{-4} M 4-NP, the reaction was almost completed in 465 s, which corresponds to a k value of $6.5 \times 10^{-3} \text{ s}^{-1}$ (Table 2, entry 1, Figure 5). The [4-NP] used in this experiment led to starting UV/Vis spectra (from 0 to 117 s) in which absorbances are greater than 2. With respect to the Beer–Lambert law, it was considered that these results were not relevant, and therefore they were not used to build up the kinetic plots. The UV/Vis spectrum at 156 s was treated as the initial spectrum for this reduction.

The same reaction performed in the absence of the glycodendrimer, with AuNPs formed only with NaBH_4 , led after 20 min to UV/Vis spectra in which absorbances are still greater than 2 for the absorption band of 4-nitrophenolate at $\lambda = 405$ nm (Table 2, entry 2, for example, after 24 min, the absorbance at 405 nm is 3.60). This result shows the advantage of using AuNPs stabilized by glycodendrimers containing 1,2,3-triazolyl linkages for the reduction of 4-NP. Since Schmitzer and co-workers showed that glycodendrimers without AuNPs catalyze the reduction of cyclohexylphenyl ketone to alcohol,^[16b] we carried out the reduction of 4-NP (6.2×10^{-4} M) only in the presence of the glycodendrimer (Table 2, entry 3). After 20 min, no reduction of the 4-NP was observed. When the concentration of 4-NP was decreased to 2.5×10^{-4} M, the reaction was completed after 1219 s with a k value of $1.3 \times 10^{-3} \text{ s}^{-1}$ (Table 2, entry 4). Increasing the quantity of catalyst from 0.5 to 2 mol-% led to an increase of the reaction rate (Table 2, entry 5 and 6), as expected. However, the variation of this parameter seems to have less effect on the reaction rate than the concentration of 4-NP.

Conclusion

The decoration of dendrimers with pentose allows them to be solubilized in water at low cost, to combine them with

metal ions such as Au^{III} and further to metallic nanoparticles, and to enable them to catalyze reactions that need to be carried out in water. In the course of our study on the preparation of these AuDSNs, we have discarded the idea that Au^{3+} might be spontaneously reduced to Au^0 in presence of the glycodendrimers. These DSNs are catalytically active in the reduction of 4-NP to 4-AP by NaBH_4 and show similar catalytic activity and diameter with previously comparable AuDSNs synthesized with PAMAM and PPI dendrimers. These results show the advantage of the triazole linkages in water-soluble glycodendrimers for the mild AuNP stabilization and their good catalytic activity.

Experimental Section

General Data: All chemicals were used as received. Glycodendrimer was synthesized as described in the literature.^[4] Particle size was determined by TEM by using a JEOL JEM 1400 (120 kV) microscope. TEM samples were prepared by deposition of the nanoparticle suspension (10 μL) on a carbon-coated microscopy copper grid. The IR spectra were recorded on an ATI Mattson Genesis series FTIR spectrophotometer. UV/Vis absorption spectra were measured with a Perkin–Elmer Lambda 19 UV/Vis spectrometer.

Procedure for the Preparation of AuNPs: A 3.1×10^{-4} M aqueous solution of glycodendrimer (1.4 mL) was added to deionized water (25.6 mL), followed by the addition of a freshly prepared 2.6×10^{-3} M aqueous solution of HAuCl_4 (1.5 mL). The resulting mixture was then stirred for 20 min under air and a 2.6×10^{-2} M NaBH_4 aqueous solution (1.5 mL) was added dropwise, provoking the formation of a pink-brown color corresponding to the reduction of Au^{3+} ions to Au^0 and AuNPs formation. The UV/Vis spectrum of AuNPs (Figure 1) was recorded with a blank solution of glycodendrimer (1.45×10^{-5} M) in water.

Investigation of the Interaction Between the Glycodendrimer and the Au^{III} Salt: The following aqueous solutions were prepared: (A)

HAuCl₄ (1.37 × 10⁻⁴ M), (B) HAuCl₄ (1.37 × 10⁻⁴ M) + glycodendrimer (1.53 × 10⁻⁵ M) and (C) glycodendrimer (1.53 × 10⁻⁵ M). The UV/Vis spectrum of solution A is presented in Figure 2 (a). The evolution of solution B was monitored by UV/Vis spectroscopy over a period of 24 h; UV/Vis spectra were recorded after 40 min and after 24 h using solution C as a blank and these spectra are presented in Figure 2 (b and c).

General Procedure for the Reduction of 4-NP: 4-NP (1 equiv.) was mixed with NaBH₄ (81 equiv.) in water under air, then the solution containing the freshly prepared AuNPs was added. After adding NaBH₄, the solution changed from light yellow to dark yellow owing to the formation of the 4-nitrophenolate ion. Then, this solution loses its dark yellow color with time after addition of AuNPs. The reaction was monitored by UV/Vis spectroscopy.

Supporting Information (see footnote on the first page of this article): UV/Vis spectra of the reduction of 4-nitrophenol by AuNPs stabilized by glycodendrimers and the corresponding plots of $-\ln(C/C_0)$ as a function of the time can be found in the Supporting Information.

Acknowledgments

Financial support from the Centre National de la Recherche Scientifique (CNRS) (grant to S. G.), the University of Bordeaux I, the University of Toulouse III, the University of Reims Champagne-Ardenne, the CPER 2007–2013 framework (Pentoraffinerie program), and the European Regional Development Fund (ERDF) are gratefully acknowledged.

- [1] a) V. Rotello, *Nanoparticles: Building Blocks for Nanotechnology*, Kluwer Academic Publishers, New York, USA, **2004**; b) D. Astruc, *Nanoparticles and Catalysis*, Wiley-VCH, Weinheim, Germany, **2008**; c) G. Schmid, *Nanoparticles: From Theory to Application*, 2nd edition, Wiley-VCH, Weinheim, Germany, **2010**; d) P. Serp, K. Philippot, *Nanomaterials in Catalysis*, Wiley-VCH, Weinheim, Germany, **2013**.
- [2] a) M. Zhao, L. Sun, R. M. Crooks, *J. Am. Chem. Soc.* **1998**, *120*, 4877–4878; b) K. Esumi, A. Suzuki, N. Aihara, K. Usui, K. Torigoe, *Langmuir* **1998**, *14*, 3157–3159; c) L. Balogh, D. A. Tomalia, *J. Am. Chem. Soc.* **1998**, *120*, 7355–7356; d) K. Esumi, A. Suzuki, A. Yamahira, K. Torigoe, *Langmuir* **2000**, *16*, 2604–2608; e) R. M. Crooks, M. Zhao, L. Sun, V. Chechik, L. K. Yeung, *Acc. Chem. Res.* **2001**, *34*, 181–190; f) R. W. J. Scott, O. M. Wilson, R. M. Crooks, *J. Phys. Chem. B* **2005**, *109*, 692–704.
- [3] a) D. A. Tomalia, A. M. Naylor, W. A. III Goddard, *Angew. Chem. Int. Ed. Engl.* **1990**, *29*, 138–175; *Angew. Chem.* **1990**, *102*, 119; b) A. W. Bosman, H. M. Janssen, E. W. Meijer, *Chem. Rev.* **1999**, *99*, 1665–1688; c) S. Hecht, J. M. J. Fréchet, *Angew. Chem. Int. Ed.* **2001**, *40*, 74–91; *Angew. Chem.* **2001**, *113*, 76; d) D. Astruc, K. Heuze, S. Gatard, D. Méry, S. Nlate, L. Plault, *Adv. Synth. Catal.* **2005**, *347*, 329–338; e) D. Astruc, E. Boisselier, C. Ornelas, *Chem. Rev.* **2010**, *110*, 1857–1959; f) G. R. Newkome, C. Shreiner, *Chem. Rev.* **2010**, *110*, 6338–6442; g) A.-M. Caminade, C.-O. Turrin, R. Laurent, A. Ouali, B. Delavaux-Nicot, *Dendrimers: Towards Catalytic, Material and Biomedical Uses*, Wiley, Chichester, UK, **2011**.
- [4] S. Gatard, L. Liang, L. Salmon, J. Ruiz, D. Astruc, S. Bouquillon, *Tetrahedron Lett.* **2011**, *52*, 1842–1846.
- [5] a) C. Ornelas, J. Ruiz, L. Salmon, D. Astruc, *Adv. Synth. Catal.* **2008**, *350*, 837–845; b) E. Boisselier, A. K. Diallo, L. Salmon, C. Ornelas, J. Ruiz, D. Astruc, *J. Am. Chem. Soc.* **2010**, *132*, 2729–2742; c) D. Astruc, L. Liang, A. Rapakousiou, J. Ruiz, *Acc. Chem. Res.* **2012**, *45*, 630–640.
- [6] a) K. Kuroda, T. Ishida, M. Haruta, *J. Mol. Catal. A* **2009**, *298*, 7–11; b) S. Wunder, F. Polzer, Y. Lu, M. Ballauf, *J. Phys. Chem. C* **2010**, *114*, 8814–8820; c) A. Gangula, R. Podila, R. M. L. Karanam, C. Janardhana, A. M. Rao, *Langmuir* **2011**, *27*, 15268–15274; d) S.-N. Wang, M.-C. Zhang, W. Q. Zhang, *ACS Catal.* **2011**, *1*, 207–211; e) P. Hervés, M. Pérez-Lorenzo, L. M. Liz-Marzán, J. Dzubiella, Y. Lu, M. Ballauf, *Chem. Soc. Rev.* **2012**, *41*, 5577–5587.
- [7] a) J. Li, C.-Y. Liu, Y. Liu, *J. Mater. Chem.* **2012**, *22*, 8426–8430; b) J. Zhang, D. Han, H. Zhang, M. Chaker, Y. Zhao, D. Ma, *Chem. Commun.* **2012**, *48*, 11510–11512; c) X.-K. Kong, Z.-Y. Sun, M. Chen, C.-L. Chen, Q.-W. Chen, *Energy Environ. Sci.* **2013**, *6*, 3260–3266; d) N. C. Antonels, R. Meijboom, *Langmuir* **2013**, *29*, 13433–13442; e) A. Shivhare, S. J. Ambrose, H. Zhang, R. W. Purves, R. W. J. Scott, *Chem. Commun.* **2013**, *49*, 276–278.
- [8] Z. V. Feng, J. L. Lyon, J. S. Croley, R. M. Crooks, D. A. V. Bout, K. J. Stevenson, *J. Chem. Educ.* **2009**, *86*, 368–372.
- [9] a) M.-C. Daniel, D. Astruc, *Chem. Rev.* **2004**, *104*, 293–346; b) S. Eustis, M. A. El-Sayed, *Chem. Soc. Rev.* **2006**, *35*, 209–217; c) M. E. Stewart, C. R. Anderton, L. B. Thompson, J. Maria, S. K. Gray, J. A. Rogers, R. G. Nuzzo, *Chem. Rev.* **2008**, *108*, 494–521; d) A. Llevot, D. Astruc, *Chem. Soc. Rev.* **2012**, *41*, 242–257; e) C. Louis, O. Pluchery, *Gold Nanoparticles for Physics, Chemistry, Biology*, Imperial College, London, **2012**; f) N. Li, P. Zhao, D. Astruc, *Angew. Chem. Int. Ed.* **2014**, *53*, 1756–1789.
- [10] M. Haruta, T. Kobayashi, H. Sano, N. Yamada, *Chem. Lett.* **1987**, 405–408.
- [11] T. Endo, T. Yoshimura, K. Esumi, *J. Colloid Interface Sci.* **2005**, *286*, 602–609.
- [12] W. Zhang, L. Li, Y. Du, X. Wang, P. Yang, *Catal. Lett.* **2009**, *127*, 429–436.
- [13] E. Murugan, R. Rangasamy, I. Pakrudheen, *Sci. Adv. Mater.* **2012**, *4*, 1103–1110.
- [14] a) H. Wu, Z. Liu, X. Wang, B. Zhao, J. Zhang, C. Li, *J. Colloid Interface Sci.* **2006**, *302*, 142–148; b) E. Murugan, R. Rangasamy, *J. Polym. Sci., Part A* **2010**, *48*, 2525–2532; c) L. Li, Z. Zheng, M. Cao, R. Cao, *Microporous Mesoporous Mater.* **2010**, *136*, 42–49; d) K. Esumi, T. Hosoya, A. Suzuki, K. Torigoe, *Langmuir* **2000**, *16*, 2978–2980; e) A. Köth, J. Koetz, D. Appelhans, B. Voit, *Colloid Polym. Sci.* **2008**, *286*, 1317–1327; f) T. Pietsch, D. Appelhans, N. Gindy, B. Voit, A. Fahmi, *Colloids Surf. A* **2009**, *341*, 93–102; g) A. Bogdan, R. Roy, M. Morin, *RSC Adv.* **2012**, *2*, 985–991.
- [15] N. Malik, R. Wiwattanapatapee, R. Klopsch, K. Lorenz, H. Frey, J. W. Weener, E. W. Meijer, W. Paulus, R. Duncan, *J. Controlled Release* **2000**, *65*, 133–148.
- [16] a) A. Schmitzer, E. Perez, I. Rico-Lattes, A. Lattes, S. Rosca, *Langmuir* **1999**, *15*, 4397–4403; b) A. Schmitzer, S. Franceschi, E. Perez, I. Rico-Lattes, A. Lattes, L. Thion, M. Erard, C. Vidal, *J. Am. Chem. Soc.* **2001**, *123*, 5956–5961; c) R. A. Roy, *Trends Glycosci. Glycotechnol.* **2003**, *85*, 291–310; d) M. Touaiba, A. Wellens, C. S. Tze, Q. Wang, S. Sirois, J. Bouckaert, R. Roy, *ChemMedChem* **2007**, *2*, 1190–1201; e) Y. M. Chabre, R. Roy, *Curr. Top. Med. Chem.* **2008**, *8*, 1237–1285; f) P. Rajakumar, R. Anandhan, V. Kalpana, *Synlett* **2009**, *9*, 1417–1422; g) J. Camponovo, C. Hadad, J. Ruiz, E. Cloutet, S. Gatard, J. Muzart, S. Bouquillon, D. Astruc, *J. Org. Chem.* **2009**, *74*, 5071–5074; h) C. Hadad, J.-P. Majoral, J. Muzart, A.-M. Caminade, S. Bouquillon, *Tetrahedron Lett.* **2009**, *50*, 1902–1905; i) R. Kikkeri, X. Liu, A. Adibekian, Y.-H. Tsai, P. H. Seeberger, *Chem. Commun.* **2010**, *46*, 2197–2199; j) M. Gingras, Y. M. Chabre, M. Roy, R. Roy, *Chem. Soc. Rev.* **2013**, *42*, 4823–4841.
- [17] F. W. Lichtenhaler, S. Peters, *C. R. Chim.* **2004**, *7*, 65–90.
- [18] C. Ornelas, J. Ruiz, C. Belin, D. Astruc, *J. Am. Chem. Soc.* **2009**, *131*, 590–601.

- [19] M. Bortoluzzi, A. Scrivanti, A. Reolon, E. Amadio, V. Bertolasi, *Inorg. Chem. Commun.* **2013**, 33, 82–85.
- [20] a) D. V. Leff, P. C. Ohara, J. R. Heath, W. M. Gelbart, *J. Phys. Chem.* **1995**, 99, 7036–7041; b) R. W. J. Scott, O. M. Wilson, S.-K. Oh, E. A. Kenik, R. M. Crooks, *J. Am. Chem. Soc.* **2004**, 126, 15583–15591.
- [21] a) K. Esumi, K. Miyamoto, T. Yoshimura, *J. Colloid Interface Sci.* **2002**, 254, 402–405; b) K. Hayakawa, T. Yoshimura, K. Esumi, *Langmuir* **2003**, 19, 5517–5521; c) M. Nemanashi, R. Meijboom, *J. Colloid Interface Sci.* **2013**, 389, 260–267.
- [22] a) S. Wunder, Y. Lu, M. Albrecht, M. Ballauf, *ACS Catal.* **2011**, 1, 908–916; b) X. Zhou, W. Xu, G. Liu, D. Panda, P. Chen, *J. Am. Chem. Soc.* **2010**, 132, 138–146.

Received: February 17, 2014
Published Online: May 2, 2014

**Partie 2. Polymères hydrophiles
stabilisateurs de nanoparticules de
palladium actives en catalyse.**

Partie 2. Polymères hydrophiles stabilisateurs de nanoparticules de palladium actives en catalyse.

Les études développées au cours de la première partie ont montré l'importance des cycles 1,2,3-triazoles (trz) dans la stabilisation des PdNPs mais aussi l'importance de chainons TEG pour une catalyse efficace (synergie). L'idée survenue par la suite était de synthétiser une molécule pouvant mimer le rôle du dendrimer TEG mais en évitant les 9 étapes de synthèses qui, bien que simples, demandent du temps et un coût non négligeable. Catia Ornelas, dans notre groupe avait montré l'avantage en terme de stabilisant des PdNPs, de l'utilisation d'un polymère résultant de la polymérisation radicalaire du chlorométhylstyrène en présence de l'amorceur AIBN. Le groupement azido substituant ensuite le groupement chloré, permettait une post-fonctionnalisation du polymère par réaction "click" CuAAC.⁽¹⁾ Nous avons élaboré un polymère contenant des cycles 1,2,3-triazoles (résultat d'une réaction "click") et de parties PEG en réalisant la polycondensation entre unités di-azido PEG et di-alcyne PEG par CuAAC, méthode de synthèse alliant simplicité, rapidité et économie sachant qu'une seule étape de synthèse est nécessaire pour l'obtention de ce nouveau polymère (80% de rendement à partir de produits commerciaux). La même méthode de synthèse de PdNPs, utilisée avec les dendrimères, a été employée ici mais en présence de ce nouveau polymère PEG-trz. En revanche, du fait de la proximité entre les cycles 1,2,3-triazoles et de la topologie non dendritique, une stœchiométrie 10/1 trz/Pd s'est avérée nécessaire pour une bonne stabilisation de PdNPs (taille révélée par MET: $1,6 \pm 0,3$ nm). L'étude catalytique de ces PdNPs a exhalé une activité quasi-similaire au dendrimer TEG comme attendu, plaçant ce catalyseur comme l'un des plus actifs pour la réaction de Suzuki-Miyaura (pour les aromatiques bromés) et pour la réduction du 4-NP en 4-AP. Cette partie se termine par un « Account » sur la catalyse homéopathique récapitulant les découvertes de catalyses de formation de liaisons C-C au niveau du ppm en Pd.

Références:

1) Ornelas, C.; Diallo, A. K.; Ruiz, J.; Astruc, D. "Click" polymer-supported palladium nanoparticles as highly efficient catalysts for olefin hydrogenation and Suzuki coupling reactions under ambient conditions, *Adv. Synth. Catal.* **2009**, *351*, 2147-2154.

Efficient Click-Polymer-Stabilized Palladium Nanoparticle Catalysts for Suzuki–Miyaura Reactions of Bromoarenes and Reduction of 4-Nitrophenol in Aqueous Solvents

Christophe Deraedt,^a Lionel Salmon,^b Jaime Ruiz,^a and Didier Astruc^{a,*}

^a ISM, UMR CNRS 5255, Univ. Bordeaux, 351 Cours de la Libération, 33405 Talence Cedex, France
E-mail: d.astruc@ism.u-bordeaux1.fr

^b LCC, CNRS & University of Toulouse, 205 Route de Narbonne, 31077 Toulouse Cedex, France

Received: July 19, 2013; Revised: September 10, 2013; Published online: October 9, 2013



Supporting information for this article is available on the WWW under <http://dx.doi.org/10.1002/adsc.201300633>.

Abstract: Palladium nanoparticles (size = 1.6 ± 0.3 nm) stabilized by a polyethylene glycol containing triazolyl rings, synthesized by click reaction in water, are efficient catalysts for the Suzuki–Miyaura coupling of bromoarenes in aqueous ethanol and the borohydride reduction of 4-nitrophenol in water. Turnover numbers (TONs) reach 99,000 and turn-

over frequencies (TOFs) are up to $198,000 \text{ h}^{-1}$ for the C–C cross coupling reactions in water/ethanol.

Keywords: bromoarenes; catalysis; click chemistry; green chemistry; 4-nitrophenol; palladium nanoparticles; polymers; Suzuki–Miyaura reaction

Introduction

Palladium is the most frequently used transition metal in catalysis,^[1] especially in the cross-coupling reactions for carbon-carbon bond formation,^[2] among which the Suzuki–Miyaura^[3] reaction is the most useful one. Metal nanoparticles (NPs) have appeared as a very promising solution towards efficient catalysis under mild, environmentally benign conditions because of their large surface-to-volume ratio and specific surface reactivities.^[4] The advantage of the NPs, compared to organometallic catalysts, is that one does not need to use large amounts of catalyst (generally less than 1 mol%),^[2a,b,4,5] and ligands (that are often expensive and sometimes toxic) are not required, which is also important for the treatment of the reactions, ligands often being difficult to separate from the final products.

PdNPs with a dimension of less than 10 nm have exhibited high catalytic activities toward different types of reactions.^[2a,b,4,5] They are often stabilized by polymers (PVP, PS, PEG, copolymers), dendrimers,^[6] cyclodextrins (CDs),^[7] inorganic materials,^[8] or ionic liquids.^[8c,9] For instance, among recent works,^[10] Nomura's group conducted quantitative Suzuki–Miyaura reactions with various substrates in water at 80 °C with PdNPs (1.5 mol% Pd) stabilized by a PS polymer.^[10b] Reddy's group carried out Suzuki–Miyaura reactions with various bromoarenes at room

temperature, with an amount of catalyst of 0.8–1 mol% Pd, the PdNPs being supported on TiO₂.^[10c] Beletskaya's group proposed the term homeopathic Pd catalysis for Heck reactions using PdNP precatalysts.^[2a] De Vries used the “homeopathic” concept to investigate the mechanism of high-temperature Heck reactions using low PdNP loading.^[10a] Hong's group also used PdNPs stabilized by a bidentate ionic ligand in 0.001 mol% Pd for the Suzuki–Miyaura coupling of activated aryl bromides, the reactions being carried out in only water at 120 °C for a few hours.^[10d]

Here we wish to examine the stabilization and catalytic efficiency of PdNPs produced upon NaBH₄ reduction of the water-soluble Pd(II) precursor K₂PdCl₄ in the presence specific ethylene glycol oligomer **3** and polymer **5** formed by “click” reactions, i.e., containing 1,2,3-triazolyl (trz) linkages. We are also interested in comparing these properties with those of the known water-soluble arene-centered “click” dendrimer C₆H₃-1,3,5[C{(CH₂)₃SiMe₂CH₂-trz-CH₂OCH₂C₆H₂-2,3,4-((OCH₂CH₂)₃OCH₃)₃}₃]₃, **6**, that contains 9 trz linkages and 27 TEG termini (TEG = triethylene glycol). Triazolyl rings that were introduced by “click” functionalization in the oligomer, polymer and dendrimer with TEG termini provide the stabilization of the PdNPs after reduction of Pd(II) by NaBH₄. The PdNPs stabilized by **6** present a very good activity in the Suzuki–Miyaura reaction of various bromoarenes.^[10e,f] Bromoarenes are indeed

very important aromatic substrates, because they are often cheaper than their chloroarene analogues, and therefore they are now subjected to further study.

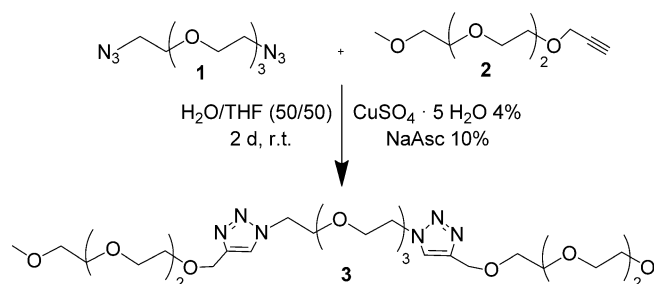
The catalytic activity of PdNPs stabilized by **3** and **5** in the Suzuki–Miyaura coupling of bromoarenes in an aqueous solvent, H₂O:ethanol=1:1 and the reduction of 4-nitrophenol to 4-aminophenol by sodium borohydride in water have now been examined. 4-Aminophenol is a potential industrial intermediate in the manufacture of many analgesic and antipyretic drugs, anticorrosion lubricants, and hair drying agents. Therefore efficient catalysts for the borohydride reduction of 4-nitrophenol to 4-aminophenol are called for.

Results and Discussion

Synthesis of the PEG-Bis-triazolyl Oligomer **3** and Triazolyl-PEG Polymer **5**

New PEG oligomers and polymers have been designed with 1,2,3-triazole rings in their branches in order to provide the mild stabilization of PdNPs by the synergistic combination of triazoles that bind the PdNP surface and PEG that contribute by their steric effect. Click chemistry offers a simple and practical possibility for the synthesis of such oligomers and polymers. The PEG-bis-triazolyl-PEG **3** was synthesized upon clicking tetraethylene glycol bisazide **1** with 2,5,8,11-tetraoxatetradec-13-yne **2** in H₂O/THF (50/50) with 4 mol% of CuSO₄·5H₂O as catalyst and 10 mol% sodium ascorbate as reductant of Cu(II) to Cu(I). This reaction leads to **3** in 90% yield (Scheme 1).

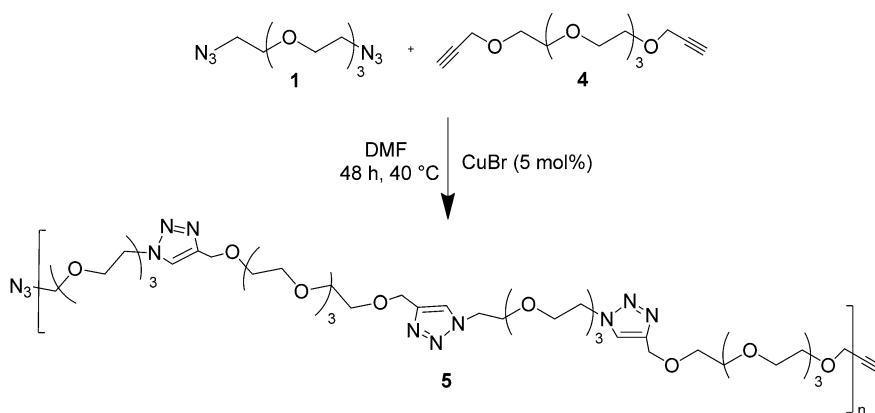
The compound **3** has been characterized by ¹H NMR, ¹³C NMR, heterogeneous single quantum coherence (HSQC), electrospray ionization (ESI) mass spectroscopy, and elemental analysis (see the Supporting Information).



Scheme 1. Synthesis of the PEG-bis-triazolyl oligomer **3** by “click” reaction between tetraethylene glycol bisazide **1** and 2,5,8,11-tetraoxatetradec-13-yne **2**.

“Click” chemistry was also used for the synthesis of the polymer triazolyl-PEG **5**. The reaction between equimolar amounts of the commercial products tetraethylene glycol bisazide **1** and 4,7,10,13,16-pentaoxa-nonadeca-1,18-diyne **4** in DMF and in the presence of 5 mol% CuBr as catalyst leads to the polymer triazolyl-PEG **5** in 80% yield (Scheme 2). The final polymer has been characterized by ¹H NMR, ¹³C NMR, IR, MALDI TOF mass spectroscopy, size exclusion chromatography (SEC) and dynamic light scattering (DLS, see the Supporting Information).

The SEC analysis provides the polydispersity of the polymer, PDI=1.3, for this uncontrolled polymerization. The molecular weight, 5 × 10⁴ g mol⁻¹, is determined by SEC using polystyrene as a reference, which corresponds to 97 dimeric units, i.e., 194 triazolyl rings. The mass spectrum shows the presence of small oligomers with 18 triazolyl rings (molecular weight = 4626 g mol⁻¹), but polymers with higher molecular weights cannot be observed due to saturation of the detector with the small oligomers. In ¹H NMR, the peak at 2.4 ppm corresponding to the alkyne proton of the starting material is not observed, which allows the conclusion that all the monomeric dialkyne has reacted with the monomeric diazide, but does not



Scheme 2. Synthesis of the triazolyl-PEG polymer **5** by “click” reaction between tetraethylene glycol bisazide **1** and 4,7,10,13,16-pentaoxa-nonadeca-1,18-diyne **4**.

permit any conclusion concerning the number of units.

The polymer **5** and the oligomer **3** are both soluble in water as expected and desired for the synthesis of PdNPs in water.

PdNP Stabilization

The palladium-polymer complex is prepared in water upon mixing aqueous solutions of the polymer and of K_2PdCl_4 at 20 °C. In previous works with dendrimers containing triazolyl TEG (**6**)^[10e] and sulfonated termini,^[6c] the stoichiometry between the triazolyl group and the Pd(II) complex was 1:1, and this stoichiometry was explained by the dendritic protection of the interior triazole ligands. In the case of the polymer, the best conditions for the stabilization of PdNPs are a stoichiometry between triazolyl group and Pd(II) around 10:1. In aqueous K_2PdCl_4 , a solution of the polymer (or oligomer) is added in this stoichiometry. After five minutes of stirring of Pd(II)/triazole reaction, a solution of sodium borohydride is rapidly added in order to form PdNPs upon reduction of Pd(II) to Pd(0) (see the Experimental Section). The light-yellow solution of Pd(II) instantaneously became orange/brown (see Figure 1), which indicated the quick formation of PdNPs. A fast reduction of Pd(II) to PdNPs is preferred to the dropwise addition leading to a slower reduction, because a high reduction rate results in smaller PdNPs than a slow reduction rate. It is well known that the catalytic activity is improved by reducing the PdNP size within the range of a few nm.^[14e]

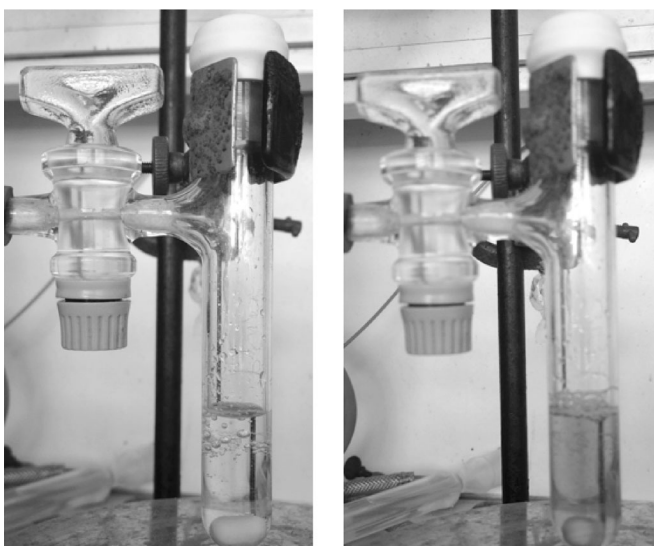
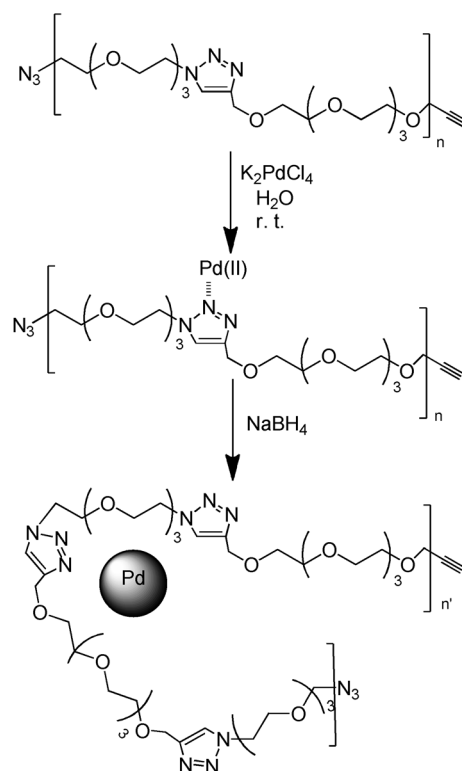


Figure 1. During the PdNP synthesis, the reduction of Pd(II) to PdNPs by $NaBH_4$ is visible by the change of a light (yellow) solution (*left*), to a darker (orange/brown) solution (*right*).

TEM analyses (Figure 2) have been conducted on the PdNPs, showing a diameter of 2.0 ± 0.5 nm upon stabilization by **3** and 1.6 ± 0.3 nm upon stabilization by **5**. The bright-grey colour around PdNPs in the TEM pictures shows the stabilizing oligomer or polymer that appears to surround several PdNPs.

The DLS experiments show that the hydrodynamic diameter of the polymer in the absence of PdNPs is in the range 45–55 nm, which corresponds to an agglomerate of **5** in water. When the PdNPs are stabilized by **5**, the hydrodynamic diameter remains unchanged. There is an excess of polymer vs. the PdNPs in the synthesis, and it appears in the TEM images that an agglomeration of polymers surrounds the PdNPs. A parallel experiment has been carried out with the same conditions of PdNP synthesis but with the replacement of the new polymer **5** by commercial PEG 2000, and in that case the PdNPs agglomerated several hours after the Pd(II) reduction to Pd(0). Concerning the PdNPs stabilized by the polymer **5**, no trace of Pd aggregation is observed several days after the synthesis. This comparison shows the essential role of the triazole ligands in the PdNP stabilization by **5** (Scheme 3).

On the other hand, when PdNPs are stabilized by the oligomer **3**, some black Pd formation is observed



Scheme 3. Principle of PdNP stabilization. Pd(II) is added to the polymer triazolyl-PEG **5** and is coordinated by nitrogen atoms of the triazolyl ring. Pd(II) is then reduced to Pd(0) forming PdNPs that are stabilized by the overall polymer frameworks including crucial triazole-PdNP interactions.

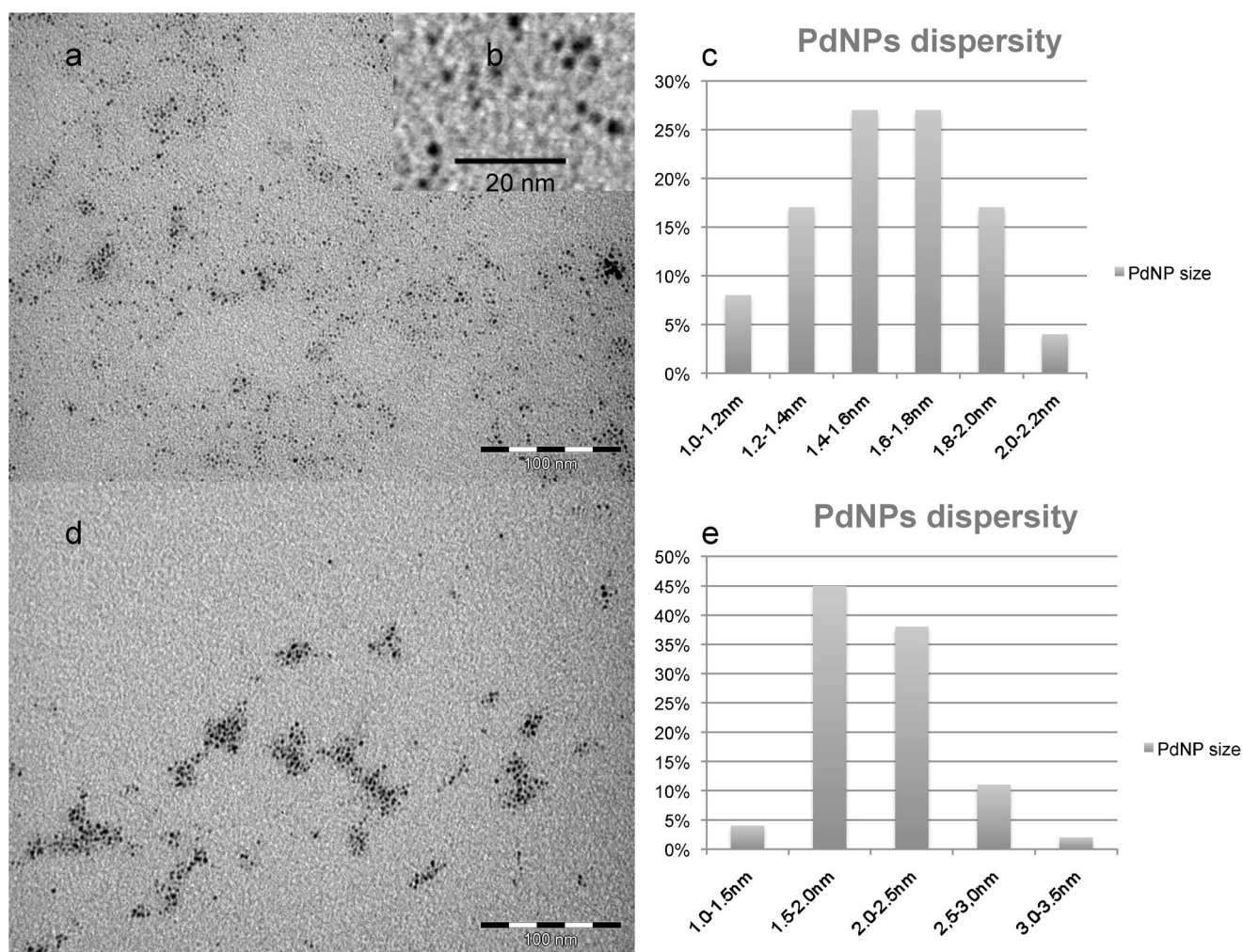
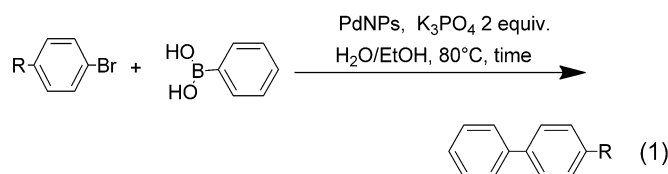


Figure 2. TEM pictures of the PdNPs. (a) TEM analysis of PdNPs stabilized by **5**; (b) zoom on several PdNPs; (c) distribution of 1100 PdNPs; average diameter value: 1.6 ± 0.3 nm. (d) TEM analysis of PdNPs stabilized by **3**; (e) distribution of 1250 PdNPs; average diameter value: 2.0 ± 0.5 nm.

after 2–3 days, indicating the decisive role of the bulk of the molecular framework of the polymer **5**.

Catalytic Studies

In order to check the catalytic activity of PdNPs, the Suzuki–Miyaura coupling has been investigated. The Suzuki–Miyaura cross coupling reactions of various bromoarenes [Eq. (1)] have been carried out in the environmentally friendly mixture water:ethanol (1:1) in the presence of K_3PO_4 , with as little palladium as possible. All the results are summarized in Table 1. The most remarkable result is that obtained in the Miyaura–Suzuki reaction of 4-bromoacetophenone and phenylboronic acid that is quantitative with 1 ppm of catalyst during 16 h at 80 °C. Under these or analogous conditions, the TONs vary between 10^3 and 10^6 with various bromoarenes. Of course, the catalysis



R = H, CH₃, OCH₃, NO₂, CHO, Br, COCH₃

also works very well with iodoarenes, because they are more easily activated, as it is well known.^[11]

The Suzuki–Miyaura reaction works very well with activated (electron-withdrawing substituents) as well as deactivated (electron-donating substituents) bromoarenes with 0.001 mol% of Pd (i.e., 10 ppm). What is very remarkable is the TON up to 99,000 for the reaction with the 4-bromoacetophenone (entry 13),

Table 1. Suzuki–Miyaura of various bromoarenes catalyzed by PdNPs stabilized by **5**.^[a]

Entry	R	Time [h]	Pd [mol%]	Yield ^[c] [%]	TON; TOF [h ⁻¹]
1	4-OMe	12	0.1	99	990; 82.5
2	4-OMe	12	0.01	99	9900; 825
3	4-OMe	20	0.002	98	49,000; 2450
4	4-OMe	20	0.001	80	80,000; 4000
5	H	23	0.002	99	49,500; 2152
6 ^[a]	H	23	0.001	99	99,000; 4304
7	4-Me	20	0.002	99	49,500; 2475
8	4-Me	24	0.001	72	72,000; 3000
9 ^[a]	4-NO ₂	2.5	0.001	99	99,000; 39,600
10	4-CHO	24	0.01	90	9000; 375
11	4-Br	14	0.002	96	48,000; 3429
12	4-Br	18	0.001	98	98000; 5444
13 ^[b]	4-COMe	0.5	0.001	99	99,000; 198,000

^[a] All the reactions have been carried out in 10 mL of H₂O/EtOH (1/1) with 1 mmol of bromoarene, 1.5 mmol of phenylboronic acid, 2 mmol of K₃PO₄ at 80 °C.

^[b] The reaction has been also conducted on a multi-gram scale (*n*=15 mmol), and the yield remained the same.

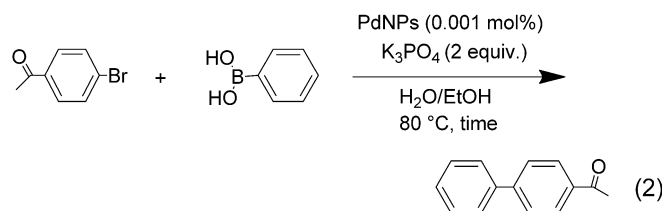
^[c] Isolated yields.

and that the reaction is finished in 30 min, which corresponds to a TOF=198,000 h⁻¹ that was never obtained before this study with bromoarenes. The reactions with deactivated arenes such as 1,4-bromoanisole (entry 4) or 1,4-bromotoluene (entry 8) lead to a TON of 80,000 and 72,000, respectively, in a relatively short time too. The reaction with activated bromoarenes such as 1,4-bromonitrobenzene or 1,4-dibromobenzene leads to a quantitative yield for both substrates in a relatively short time (2 h and 14 h, respectively). These results are expected because the oxidative addition on the Pd species is faster when bromoarenes are functionalized with electron-withdrawing groups that weaken the carbon-halogen bond.

These results show the excellent catalytic activity of PdNPs stabilized by the polymer **5** due to ideal stabilization for catalysis by the triazolyl groups (as with dendrimer **6** containing triazolyl TEG termini^[10e]). Catalysis with PdNPs stabilized by the oligomer **3** is also efficient down to 0.002 mol% of Pd (quite the same as PdNPs stabilized by the polymer **5**), but then with less than 0.002 mol% the activity is almost non-existent due to the lack of sufficient stabilization.

We attempted to conduct Suzuki–Miyaura reactions with PdNPs stabilized by the commercial PEG 2000, under the same conditions as those indicated in Table 1 (entry 3, for example), and no C–C coupling was observed.

Suzuki–Miyaura Reaction between 4-Bromoacetophenone and Phenylboronic Acid in EtOH:H₂O = 1:1 [Eq. (2)]



Kinetic Study of the Reaction

The kinetic study (Figure 3) shows that the reaction between 4-bromoacetophenone and phenylboronic acid is complete in 30 min and that after 10 min the isolated yield is already 72%.

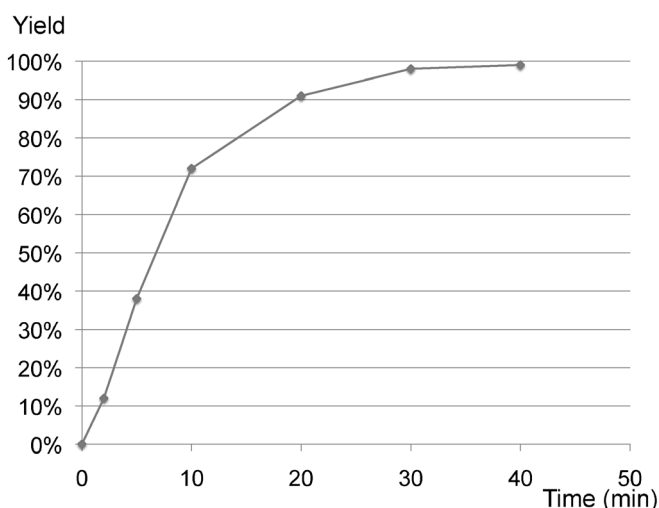


Figure 3. Kinetic study of the Suzuki–Miyaura reaction between 4-bromoacetophenone and phenylboronic acid. The reaction reaches a quantitative yield in 30 min.

Concentration Study

A study of the influence of the concentration has been conducted in order to optimize the reaction conditions (Table 2). It shows that a total volume of the solvent mixture in the range 5–10 mL is necessary for optimized reactions.

The results show that the reaction with 10 ppm Pd (PdNPs) is nearly quantitative with several bromoarenes; therefore the minimal quantity of catalyst necessary for the reaction with the most reactive substrate, 4-bromoacetophenone, has been investigated (Table 3).

The series of TONs data obtained here in Suzuki–Miyaura reactions with various bromoarenes are very

Table 2. Influence of the volume of the solvent mixture EtOH/H₂O: 1/1 on the yield of the Suzuki–Miyaura reactions between 4-bromoacetophenone and phenylboronic acid.^[a]

Total volume [mL]	Yield of the reaction [%]
0.2	48
2	90
5	99
10	99
20	60
40	50

^[a] The reactions have been carried with 0.001 mol% PdNPs at 80 °C during 1 h.

Table 3. Influence of the PdNPs loading on the TONs and TOFs of the Suzuki–Miyaura reactions between 4-bromoacetophenone and phenylboronic acid.^[a]

Entry	Time [h]	Pd [mol%]	Yield [%]	TON; TOF [h ⁻¹]
13	0.5	0.001	99	99,000; 198,000
14	2	0.0005	99	198,000; 99,000
15	16	0.0001	99	990,000; 61,875
16	24	0.00005	–	–

^[a] All the reactions have been carried out in 10 mL of H₂O/EtOH (1/1) with 1 mmol of 4-bromoacetophenone, 1.5 mmol of phenylboronic acid and 2 mmol of K₃PO₄ at 80 °C.

good in comparison with literature results reported in Table 4, and the TOFs obtained here are superior to those obtained with PdNPs stabilized by dendrimer **6** (Table 5).

In Table 4, the literature data found for Miyaura–Suzuki cross-coupling reactions of bromoarenes in aqueous solutions are summarized, indicating that the PdNP catalysts reported here are among the very best ones reported so far.

Interestingly, the PdNPs stabilized by polymer **5** provide lower TONs, but better TOFs than those with dendrimer **6**. The better TONs obtained with the dendrimer **6** than with the polymer **5** are taken into account by a better protection by encapsulation of the PdNPs in the dendrimer,^[10c] whereas the better TOFs obtained with the polymer result from freer access of the substrates to the PdNP surface. See the comparative findings between PdNP stabilized by the dendrimer **6** and PdNP stabilized by **5** (Table 5).

The advantage of this system in comparison with dendrimer **6** is that the polymer needs only one simple synthetic step, and that PdNPs stabilized by the polymer **5** are almost as active for the Suzuki–Miyaura coupling as the dendrimer **6** but with the particular feature of a faster reaction (higher TOFs).

Table 4. Comparison of literature results obtained with PdNP catalysts in aqueous medium for the Miyaura–Suzuki reactions of bromoarenes.

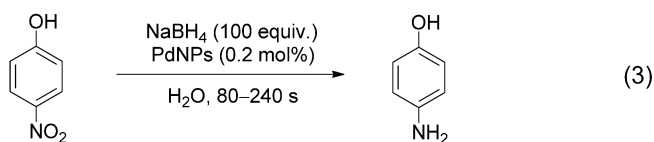
R ^[ref.]	Catalyst	Temp. [°C]	TON	TOF [h ⁻¹]
4-COMe ^[12a]	PSSA-co-MA-Pd(0)	100	99	1980
4-OMe ^[12b]	Pd-SDS	100	38	456
4-OMe ^[12c]	Pd-PVP (MTPs)	100	1680	1680
4-COMe ^[12d]	Pd-PEG	25	98	49
4-COMe ^[12e]	Pd-1/FSG	100	950	119
4-OMe ^[12f]	Fe ₃ O ₄ -Pd	50	144	12
4-OMe ^[12g]	pEVPBr-Pd	90	340	38
4-OMe ^[12h]	Pd-PS	100	50	10
4-COMe ^[12i]	HAP-Pd(0)	100	156	39
4-OMe ^[12j]	PdCl ₂ (py) ₂ @SHS	60	4681	14050
4-COMe ^[10d]	Pd/IL	120	970	970
4-OMe ^[12k]	Pd-MEPI	100	24250	8083
4-COMe ^[10c]	Pd-salt	90	4250	1062
4-OMe ^[12l]	Pd@PNIPAM	90	300	30
4-COMe ^[4c]	Pdx- ([PW ₁₁ O ₃₉] ⁷⁻) _y	80	92	8
4-OMe ^[12m]	Pd-block-co-poly	90	310	31
4-COMe ^[12n]	Pd-G3-p3	80	85000	2125
4-COMe ^[12o]	Pd@CNPCs	50	990	3960
4-COMe ^[12p]	Pd-PPy/PS	80	230	77
4-COMe ^[10a]	PS-PdONPs	80	66	66
4-Me ^[10b]	Pd-TiO ₂	80	115	29
4-OMe ^[12q]	Pd@PMO-IL	75	475	95
4-NH ₂ ^[12r]	Pd-XH-15-SBA	90	96	7
4-OMe ^[12s]	Pd ²⁺ -G0	80	386	99
4-Me ^[12t]	Pd(0)/Al ₂ O ₃ -ZrO ₂	60	45	12
4-OMe ^[12u]	Pd(OAc) ₂ /L	100	19600	2800

Table 5. Comparison between the properties of the PdNPs stabilized by dendrimer **6** properties and those of the PdNPs stabilized by **5**.

Support: Properties	Dendrimer 6	Polymer 5
Size PdNP	1.4 ± 0.7 nm	1.6 ± 0.3 nm
TON (Suzuki–Miyaura)	2.7 × 10 ⁶	9.9 × 10 ⁵
TOF (Suzuki–Miyaura)	4.5 × 10 ⁴ h ⁻¹	1.98 × 10 ⁵ h ⁻¹
Storage	Several months	Several weeks
Air stable	yes	yes
Easy synthesis of the support	yes	yes
Synthesis of the support	8 steps	1 step

Reduction of 4-Nitrophenol to 4-Aminophenol

The high efficiency of PdNPs described above in the Suzuki–Miyaura-catalyzed C–C coupling and the fact that the rate of this catalysis clearly depends on the size of the nanoparticles led to the idea that such catalysts might also be efficient for nitrophenol reduction. This reaction is very fast and simple, with the advantage of the possibility of monitoring by UV-vis.



spectroscopy. Indeed, a typical peak at 400 nm is directly linked to 4-nitrophenol (corresponding to 4-nitrophenolate that instantaneously appears in the presence of NaBH_4) and at 300 nm to 4-aminophenol. The disappearance of the yellow colour in the solution shows the reaction progress. The reduction of 4-nitrophenol has been carried out in the presence of an excess of NaBH_4 (100 equiv.) and 0.2 mol% of PdNPs/**5** in water in the presence of catalytic amounts of Pd from the above PdNPs.

The reaction is completed in 240 seconds, which corresponds to a K_{app} value of $6.0 \times 10^{-3} \text{ s}^{-1}$ (Figure 4). When the reduction of 4-nitrophenol is carried out in a concentration that is increased four times, the K_{app} value is nearly ten times higher ($K_{\text{app}} = 5.5 \times 10^{-2} \text{ s}^{-1}$), and the reaction is completed in less than 80 seconds. The reaction rate constant K_{app} is calculated using the rate equation $-\ln(C_t/C_0) = K_{\text{app}} \cdot t$ (the catalyst exhibits a pseudo-first order kinetics).

The results obtained with the catalyst **5** are among the best results ever recorded (here only Pd catalysts have been compared in Table 6, but Au catalysts are less impressive too) in terms of high TOF values, low amounts of catalyst and similar to the literature in term of rate constant K_{app} .

Concluding Remarks

The polymer **5** has been synthesized by a “click” reaction between commercial PEG diazide and PEG diyne and shown to be a very good stabilizer of PdNPs of 1.6 nm diameter in comparison with PEG 2000 that leads to PdNP aggregation. The combination of triazolyl rings and PEG offers a compro-

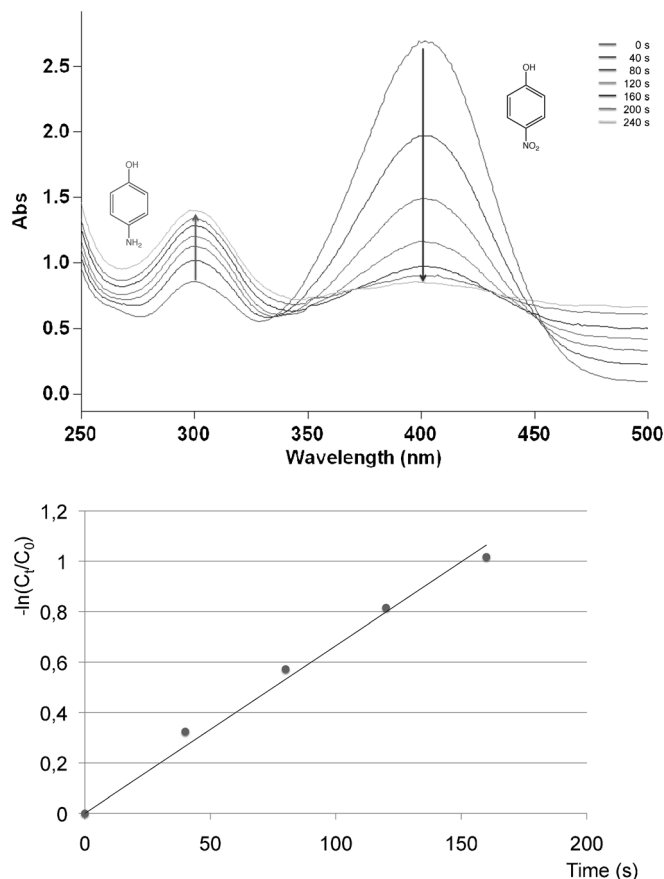


Figure 4. Kinetic study of the 4-nitrophenol reduction by NaBH_4 using UV-vis. spectroscopy at 400 nm (top) and plot of $-\ln(C_t/C_0)$ vs. time (s) for its disappearance (bottom).

mise for an excellent activity in the Suzuki–Miyaura reaction of bromoarenes in $\text{EtOH}:\text{H}_2\text{O} = 1:1$ with a very low amount of catalyst confirming results with the triazolyl-TEG dendrimer **6**. The use of only 1 ppm Pd leads to a quasi-quantitative reaction with 4-bromoacetophenone (entry 15, Table 3 TON: 990,000), and by increasing the amount of catalyst, this reaction is complete in 30 min. The results obtained in the reduction of 4-nitrophenol are also ex-

Table 6. Comparison of literature results obtained with PdNP catalysts for the reduction of 4-nitrophenol in water.

Catalyst/support	Pd [mol%]	Size Pd [nm]	NaBH_4 [equiv.]	K_{app} [s^{-1}]	TOF [h^{-1}]
CNT/PiHP ^[14a]	4	2.7	80	5×10^{-3}	300
Fe_3O_4 ^[14b]	10	16.9 ± 1.3	139	3.3×10^{-2}	300
PEDOT-PSS ^[14c]	77	< 9	excess	6.6×10^{-2}	13
SPB ^[14d]	0.36	2.4 ± 0.5	100	4.41×10^{-3}	819
Microgels ^[14e]	2.1	3.8 ± 0.6	100	1.5×10^{-3}	139
PPy/ TiO_2 ^[14f]	2.6	2.0	11	1.22×10^{-2}	326
SBA-15 ^[14g]	100	~8	1000	1.2×10^{-2}	6
CeO_2 ^[14h]	0.56	3–5	83	8×10^{-3}	1 068
5	0.2	1.6	100	6×10^{-3}	7 500
5	0.2	1.6	100	5.5×10^{-2}	22 500

cellent. Macromolecules such as dendrimer **6** or polymer **5** are outstanding for a compromise between stabilization and catalytic activity of PdNPs, whereas small molecules such as the oligomer **3** are not sufficiently efficient stabilizers to provide active PdNPs. This is due to the fact that PdNPs can take shelter in the holes of the dendrimer or can be enveloped by several polymer molecules **5**. The comparison between the triazole-containing dendrimer **6** and polymer **5** interestingly shows that the polymer provides higher TOF values because of freer access than the dendrimer, whereas the higher protection in the dendrimer interior offers higher TONs than with the polymer due to the better PdNP protection.

The extremely low amount of Pd catalyst and the biocompatibility of the PEG polymers opens an access to biological applications without the need for treatment of the product in order to remove the metal. The multi-gram scale reaction reported here is also very useful for potential industrial applications of the Miyaura–Suzuki reactions of bromoarenes, especially given their modest cost among the halogenoarenes.

Experimental Section

General Data

All the solvents (THF, EtOH, DMF, CH₂Cl₂, Et₂O) and chemicals were used as received. ¹H and ¹³C NMR spectra were recorded at 25 °C with a Bruker AC 200, 300 or 400 (200, 300 or 400 MHz) spectrometer. All the chemical shifts are reported in parts per million (δ, ppm) with reference to Me₄Si (TMS) for the ¹H NMR spectra. The infrared (IR) spectra were recorded on an ATI Mattson Genesis series FT-IR spectrophotometer. Size exclusion chromatography (SEC) of the polymer **5** was performed using a JASCO HPLC pump type 880-PU, TOSHAAS TSK gel columns (G4000, G3000, G2000 with pore sizes of 20,75, and 200 Å respectively, connected in series), a Varian (series RI-3) refractive index detector, with DMF as the mobile phase and calibrated with polystyrene standard. MALDI-TOF mass spectra were recorded with a PerSeptive Biosystems Voyager Elite (Framingham, MA) time-of-flight mass spectrometer. This instrument is equipped with a nitrogen laser (337 nm), a delayed extraction, and a reflector. It was operated at an accelerating potential of 20 kV in both linear and reflection modes. The mass spectra shown represent an average over 256 consecutive laser shots (3 Hz repetition rate). Peptides were used to calibrate the mass scale using the two points calibration software 3.07.1 from PerSeptive Biosystems. Mentioned *m/z* values correspond to monoisotopic masses. Elemental analysis (EA) results were obtained with a Thermo Flash 2000 EA; the sample is introduced in a tin container for CHS analysis.

Synthesis of the PEG-bis-triazolyl Oligomer **3**

Bisazide **1** (0.122 g, 0.5 mmol) and **2** (0.202 g, 1 mmol, 2 equiv.) were dissolved in 2 mL THF in a Schlenk tube. CuSO₄·5H₂O was added (0.0048 g, 0.02 mmol, 0.04 equiv.) after dissolving in 1 mL of water, followed by the dropwise addition of a freshly prepared solution of sodium ascorbate (0.0124 g, 0.1 mmol, 0.1 equiv.) in order to set a 1:1 THF:water ratio. The reaction mixture was stirred for 2 days at 25 °C under N₂. After removing THF under vacuum, CH₂Cl₂ (100 mL) and an aqueous ammonia solution (2.0 M, 50 mL) were successively added. The mixture was allowed to stir for 10 min in order to remove all the Cu(II) trapped inside the trimer as [Cu(NH₃)₂(H₂O)₂] [SO₄]. The organic phase was washed twice with water. The organic phase was dried with sodium sulfate, and the solvent is removed under vacuum to afford **3**; yield: 0.290 g (90%). The product was fully characterized by ¹H NMR, ¹³C NMR, HSQC, ESI, EA (see the Supporting Information).

Synthesis of Triazolyl-PEG Polymer **5**

Bisazide **1**^[13] (0.244 g, 1 mmol) and **4**^[13] (0.270 g, 1 mmol, 1 equiv.) were dissolved in 1 mL DMF in a Schlenk tube. CuBr was added in the vessel (0.0102 g, 0.05 equiv.). The reaction mixture was stirred for 2 days at 40 °C under N₂. The solution was then added to 200 mL of Et₂O in order to precipitate the polymer formed. The precipitate was filtered, and CH₂Cl₂ (100 mL) and an aqueous ammonia solution (2.0 M, 50 mL) were successively added. The mixture was allowed to stir for 10 min in order to remove all the Cu(II) trapped inside the polymer as [Cu(NH₃)₂(H₂O)₂] [SO₄]. The organic phase was washed twice with water, then this operation was repeated once more to ensure the complete removal of copper ions. The organic phase was dried with sodium sulfate, and the solvent was removed under vacuum to afford **5**; yield: 0.410 g (80%). The product has been fully characterized by ¹H NMR, ¹³C NMR, IR, MALDI TOF, DLS, SEC (see the Supporting Information).

Preparation of the PdNPs for Catalysis

a): 1.62 × 10⁻² mmol of polymer triazolyl PEG **5** (dimer MW = 514 g·mol⁻¹, 0.8368 mg) were dissolved in 0.3 mL of water in a Schlenk flask, and an orange solution of K₂PdCl₄ (3.2 × 10⁻⁵ mmol in 0.11 mL water) was added to the solution of **5**. Then 2.8 mL of water were added, and the solution was stirred for 5 min at 20 °C. 0.1 mL of an aqueous solution containing 3.2 × 10⁻⁴ mmol of NaBH₄ was added dropwise, provoking the formation of a brown/black colour corresponding to the reduction of Pd(II) to Pd(0) and PdNP formation [Figure S13 in the Supporting Information shows the full reduction of Pd(II) in Pd(0)]. The use of NaBH₄ is essential in order to obtain small, active PdNPs for efficient catalysis. When PdNPs are formed *in situ* (without NaBH₄) during the Suzuki–Miyaura reaction, the catalytic activity of the PdNPs is much lower. The same reaction as entry 13 was carried out with PdNPs formed *in situ*, and 22 h were needed for a quantitative reaction instead of 2 h with PdNPs reduced by NaBH₄.

b): 1.3 × 10⁻³ mmol of oligomer PEG **3** (MW = 648 g·mol⁻¹, 0.8368 mg) were dissolved in 0.3 mL of water in a Schlenk flask, and an orange solution of K₂PdCl₄ (3.2 ×

10^{-5} mmol in 0.11 mL water) was added to the solution of **5**. Then 2.8 mL of water were added, and the solution was stirred for 5 min at 20 °C. 0.1 mL of an aqueous solution containing 3.2×10^{-4} mmol of NaBH_4 was added dropwise, provoking the formation of a brown/black colour that corresponds to the reduction of Pd(II) to Pd(0) and PdNP formation.

The stoichiometry, 10 triazolyl groups per Pd(II), is necessary in order to avoid PdNPs aggregation. When the stoichiometries 1:1, 2:1, and 5:1 are used, PdNPs precipitate after several hours due to aggregation.

General Procedure for the Suzuki–Miyaura Catalysis

In a Schlenk flask containing tribasic potassium phosphate (2 equiv.), phenylboronic acid (1.5 equiv.), the aryl halide (1 equiv.) and 5 mL of EtOH (volume ratio of $\text{H}_2\text{O}:\text{EtOH} = 1:1$) were successively added. Then the solution containing the PdNPs was added. The suspension was allowed to stir under N_2 or air. After the reaction time (see Table 1), the reaction mixture was extracted twice with diethyl ether (Et_2O ; all the reactants and final products are soluble in Et_2O), the organic phase was dried over Na_2SO_4 , and the solvent was removed under vacuum.

In parallel, the reaction was checked using TLC in only petroleum ether as eluent in nearly all the cases, and ^1H NMR. Purification by flash chromatography column was conducted with silica gel as stationary phase and petroleum ether as mobile phase. Another purification procedure consists in cooling the Schlenk flask at the end of the reaction. The product precipitates, and a simple filtration allows one to obtain the product that is then washed with a cold solution of $\text{H}_2\text{O}/\text{EtOH}$ (this is not the case of all the bromoarenes). With 1 ppm of catalyst, the reuse of the catalyst shows a very slow reaction, which indicates that after 24 h hours at 80 °C the catalyst is deactivated in solution. The aqueous phase obtained after filtration cannot be reused, because the polymer-stabilized catalyst is not stable for a long time.

After each reaction, the Schlenk flask was washed with a solution of aqua regia (3 volumes of hydrochloric acid for 1 volume of nitric acid) in order to remove traces of Pd. All the reactions have been carried out with 1 mmol of bromoarene. Three other reactions with 15 mmol of bromoarenes have been conducted in order to check the efficiency of the system on a multigram scale. The yields obtained with 15 mmol of bromobenzene, 1,4-nitrobenzene or 4-bromoacetophenone are the same as that obtained with 1 mmol.

General Procedure for the Reduction of 4-Nitrophenol

In a beaker, 7 mg of 4-nitrophenol (5.03×10^{-5} mol) were mixed with 195 mg of NaBH_4 (5.13×10^{-3} mol) in 20 mL water, 1 mL of PdNPs was added to the reaction mixture (0.2 mol%), and the reaction was completed in 80 seconds. Alternatively, 0.5 mL of the total solution was diluted with 1.5 mL of water before the reaction started in order to follow the reaction by UV-vis. spectroscopy. This reaction was complete in 240 seconds.

Purification by Flash Chromatography of the Coupling Products of the Suzuki–Miyaura Reactions

Biphenyl (white powder): reaction between bromobenzene and phenylboronic acid was followed by simple flash chromatography with petroleum ether as mobile phase and silica as stationary phase; yield: 152 mg (99%) when 1 mmol of bromoarene is used.

4-Methylbiphenyl (colourless crystals): reaction between 4-bromotoluene and phenylboronic acid was followed by simple flash chromatography with petroleum ether as mobile phase and silica as stationary phase; yield: 166 mg (99%) when 1 mmol of bromoarene is used.

4-Methoxybiphenyl (white powder): reaction between bromoanisole and phenylboronic acid was followed by flash chromatography with petroleum ether as mobile phase and silica as stationary phase at the beginning and then 95% petroleum ether/5% diethyl ether; yield: 183 mg (99%) when 1 mmol of bromoarene is used.

4-Nitrobiphenyl (yellow crystals): reaction between 1,4-bromonitrobenzene and phenylboronic acid is followed by flash chromatography with 95% petroleum ether/5% dichloromethane as mobile phase and silica as stationary phase; yield: 197 mg (99%) when 1 mmol of bromoarene is used.

4-Biphenylcarboxaldehyde (light yellow crystals): reaction between bromobenzaldehyde and phenylboronic acid was followed by flash chromatography with 95% petroleum ether/5% dichloromethane as mobile phase and silica as stationary phase; yield: 164 mg (90%) when 1 mmol of bromoarene is used.

p-Terphenyl (white powder): reaction between 1,4-dibromobenzene and phenylboronic acid was followed by simple flash chromatography with petroleum ether as mobile phase and silica as stationary phase; yield: 226 mg (908%) when 1 mmol of bromoarene is used.

4-Acetylbiphenyl (white powder): reaction between 4-bromoacetophenone and phenylboronic acid was followed by flash chromatography with 95% petroleum ether/5% diethyl ether as mobile phase and silica as stationary phase; yield: 195 mg (99%) when 1 mmol of bromoarene is used.

Acknowledgements

The staff of the CESAMO department of the Univ. Bordeaux (elemental analyses and mass spectra), Paul Coupillaud, LCPO, Univ. Bordeaux (SEC analyses) and financial support from the Univ. Bordeaux 1 and Toulouse 3, the CNRS and the Ministère de l'Enseignement Supérieur et de la Recherche (PhD grant to CD) are gratefully acknowledged.

References

- [1] a) B. Cornils, W. A. Herrmann, (Eds.), *Applied Homogeneous Catalysis with Organometallic Compounds*, 2nd edn., Wiley-VCH, Weinheim, **2008**; b) D. Astruc, *Organometallic Chemistry and Catalysis*, Springer, Heidelberg, **2007**, Chap. 21.

- [2] a) I. P. Beletskaya, A. V. Cheprakov, *Chem. Rev.* **2000**, *100*, 3009–3066; b) N. T. S. Phan, M. Van Der Sluys, C. W. Jones, *Adv. Synth. Catal.* **2006**, *348*, 609–679; c) F. Diederich, P. Stang, *Metal-catalyzed Cross-coupling Reactions*, John Wiley & Sons, New York, **2008**; d) M. Pagliaro, V. Pandarus, R. Ciriminna, F. Béland, P. Demma Carà, *ChemCatChem* **2012**, *4*, 432–445.
- [3] a) N. Miyaura, A. Suzuki, *Chem. Rev.* **1995**, *95*, 2457–2483; b) J. Hassan, M. Sévignon, C. Gozzi, E. Schulz, M. Lemaire, *Chem. Rev.* **2002**, *102*, 1359–1470; c) F. Bellina, A. Carpita, R. Rossi, *Synthesis* **2004**, 2419–2440; d) I. Favier, D. Madec, E. Teuma, M. Gomez, *Curr. Org. Chem.* **2011**, *15*, 3127–3174.
- [4] a) H. Bönemann, R. M. Richards, *Eur. J. Inorg. Chem.* **2001**, 2455–2480; b) A. Roucoux, J. Schulz, H. Patin, *Chem. Rev.* **2002**, *102*, 3757–3778; c) M. Moreno-Mañas, R. Pleixats, *Acc. Chem. Res.* **2003**, *36*, 638–643; d) D. Astruc, F. Lu, J. Ruiz, *Angew. Chem.* **2005**, *117*, 8062–8083; *Angew. Chem. Int. Ed.* **2005**, *44*, 7852–7872; e) *Nanoparticles and Catalysis*, (Ed.: D. Astruc), Wiley-VCH, Weinheim, **2008**.
- [5] a) J. G. de Vries, *Dalton Trans.* **2006**, 421–429; b) V. S. Myers, M. G. Weir, E. V. Carino, D. F. Yancey, S. Pande, R. M. Crooks, *Chem. Sci.* **2011**, *2*, 1632–1646.
- [6] a) R. M. Crooks, M. Zhao, L. Sun, V. Chechik, L. K. Yeung, *Acc. Chem. Res.* **2001**, *34*, 181–190; b) D. Astruc, K. Heuzé, S. Gatard, D. Méry, S. Nlate, L. Plault, *Adv. Synth. Catal.* **2005**, *347*, 329–338; c) C. Ornelas, J. Ruiz, L. Salmon, D. Astruc, *Adv. Synth. Catal.* **2008**, *350*, 837–845.
- [7] L. Liang, A. K. Diallo, L. Salmon, J. Ruiz, D. Astruc, *Eur. J. Inorg. Chem.* **2012**, *2012*, 2950–2958.
- [8] a) M. Shakeri, C. Tai, E. Göthelid, S. Oscarsson, J.-E. Bäckvall, *Chem. Eur. J.* **2011**, *17*, 13269–13273; b) B. Karimi, D. Elhamifar, J. H. Clark, A. J. Hunt, *Org. Biomol. Chem.* **2011**, *9*, 7420–7426; c) Y. Wang, A. V. Biradar, T. Asefa, *ChemSusChem* **2012**, *5*, 132–139.
- [9] a) K. Qiao, R. Sugimura, Q. Bao, D. Tomida, C. Yokoyama, *Catal. Commun.* **2008**, *9*, 2470–2474; b) X. Yang, Z. Fei, D. Zhao, W. H. Ang, Y. Li, P. J. Dyson, *Inorg. Chem.* **2008**, *47*, 3292–3297.
- [10] a) A. Alimardanov, L. Schmieder-van de Vondervoort, A. M. de Vries, J. de Vries, *Adv. Synth. Catal.* **2004**, *346*, 1812–1817; b) A. Ohtaka, T. Teratani, R. Fujii, K. Ikehita, T. Kawashima, K. Tatsumi, O. Shimomura, R. Nomura, *J. Org. Chem.* **2011**, *76*, 4052–4060; c) B. Sreedhar, D. Yada, P. S. Reddy, *Adv. Synth. Catal.* **2011**, *353*, 2823–2836; d) C. Zhou, J. Wang, L. Li, R. Wang, M. Hong, *Green Chem.* **2011**, *13*, 2100–2106; e) C. Draedt, L. Salmon, J. Ruiz, D. Astruc, *Chem. Commun.* **2013**, *49*, 8169–8171; f) for the synthesis of the triazolyl TEG dendrimer **6**, see: A. K. Diallo, E. Boisselier, L. Liang, J. Ruiz, D. Astruc, *Chem. Eur. J.* **2010**, *16*, 11832–11835.
- [11] The reaction between the idobenzene and phenylboronic acid under the same conditions as bromoarenes, is finished in less than 5 min with 5 and 10 ppm of PdNPs and in less than 30 min with 1 ppm of PdNPs.
- [12] a) Ö. Metin, F. Durap, M. Aydemir, S. Özkar, *J. Mol. Catal. A: Chem.* **2011**, *337*, 39–44; b) D. Saha, K. Chattopadhyay, B. C. Ranu, *Tetrahedron Lett.* **2009**, *50*, 1003–1006; c) A. B. Patil, D. S. Patil, B. M. Bhanage, *J. Mol. Catal. A: Chem.* **2012**, *365*, 146–153; d) S. Sawoo, D. Srimani, P. Dutta, R. Lahiri, A. Sarkar, *Tetrahedron* **2009**, *65*, 4367–4374; e) L. Wang, C. Cai, *J. Mol. Catal. A: Chem.* **2009**, *306*, 97–101; f) P. D. Stevens, G. Li, J. Fan, M. Yen, Y. Gao, *Chem. Commun.* **2005**, 4435–4437; g) L. Z. Ren, *Express Polym. Lett.* **2008**, *2*, 251–255; h) S. E. Lyubimov, A. A. Vasil'ev, A. A. Korlyukov, M. M. Ilyin, S. A. Pisarev, V. V. Matveev, A. E. Chalykh, S. G. Zlotin, V. A. Davankov, *React. Funct. Polym.* **2009**, *69*, 755–758; i) N. Jamwal, M. Gupta, S. Paul, *Green Chem.* **2008**, *10*, 999–1003; j) Z. Guan, J. Hu, Y. Gu, H. Zhang, G. Li, T. Li, *Green Chem.* **2012**, *14*, 1964–1970; k) Y. M. A. Yamada, S. M. Sarkar, Y. Uozumi, *J. Am. Chem. Soc.* **2012**, *134*, 3190–3198; l) G. Wei, W. Zhang, F. Wen, Y. Wang, M. Zhang, *J. Phys. Chem. C* **2008**, *112*, 10827–10832; m) X. Jiang, G. Wei, X. Zhang, W. Zhang, P. Zheng, F. Wen, L. Shi, *J. Mol. Catal. A: Chem.* **2007**, *277*, 102–106; n) S. Ogasawara, S. Kato, *J. Am. Chem. Soc.* **2010**, *132*, 4608–4613; o) P. Zhang, Z. Weng, J. Guo, C. Wang, *Chem. Mater.* **2011**, *23*, 5243–5249; p) S. Fujii, S. Matsuzawa, Y. Nakamura, A. Ohtaka, T. Teratani, K. Akamatsu, T. Tsuruoka, H. Nawafune, *Langmuir* **2010**, *26*, 6230–6239; q) B. Karimi, D. Elhamifar, J. H. Clark, A. J. Hunt, *Chem. Eur. J.* **2010**, *16*, 8047–8053; r) C. M. Crudden, M. Saateesh, R. Lewis, *J. Am. Chem. Soc.* **2005**, *127*, 10045–10050; s) G. M. Scheuermann, L. Rumi, P. Steurer, W. Bannwarth, R. Mülhaupt, *J. Am. Chem. Soc.* **2009**, *131*, 8262–8270; t) A. Gniewek, J. Ziolkowski, A. Trzeciak, M. Zawadzki, H. Grabowska, J. Wrzyszczyk, *J. Catal.* **2008**, *254*, 121–130; u) C. Gao, H. Zhou, S. Wei, Y. Zhao, J. You, G. Gao, *Chem. Commun.* **2013**, *49*, 1127–1129.
- [13] L. A. Canalle, S. S. van Berkel, L. T. de Haan, J. C. M. van Hest, *Adv. Funct. Mater.* **2009**, *19*, 3464–3470.
- [14] a) H. Li, L. Han, J. Cooper-White, I. Kim, *Green Chem.* **2012**, *14*, 586–591; b) K. Jiang, H. X. Zhang, Y. Y. Yang, R. Mothes, H. Lang, W. B. Cai, *Chem. Commun.* **2011**, *47*, 11924–11926; c) S. Harish, J. Mathiyarasu, K. L. N. Phani, V. Yegnaraman, *Catal. Lett.* **2009**, *128*, 197–202; d) Y. Mei, Y. Lu, F. Polzer, M. Ballauff, M. Drechsler, *Chem. Mater.* **2007**, *19*, 1062–1069; e) X. Lu, X. Bian, G. Nie, C. Zhang, C. Wang, Y. Wei, *J. Mater. Chem.* **2012**, *22*, 12723–12730; f) J. Morere, M. J. Tenorio, M. J. Torralvo, C. Pando, J. A. R. Renuncio, A. Cabanas, *J. Supercrit. Fluids* **2011**, *56*, 213–222; g) R. Bhandari, M. R. Knecht, *ACS Catal.* **2011**, *1*, 89–98; h) B. Liu, S. Yu, Q. Wang, W. Hu, P. Jing, Y. Liu, W. Jia, Y. Liu, L. Liua, J. Zhang, *Chem. Commun.* **2013**, *49*, 3757–3759.

“Homeopathic” Palladium Nanoparticle Catalysis of Cross Carbon–Carbon Coupling Reactions

CHRISTOPHE DERAEDT AND DIDIER ASTRUC*

ISM, UMR CNRS 5255, Université Bordeaux, 33405 Talence Cedex, France

RECEIVED ON JULY 25, 2013

CONSPECTUS

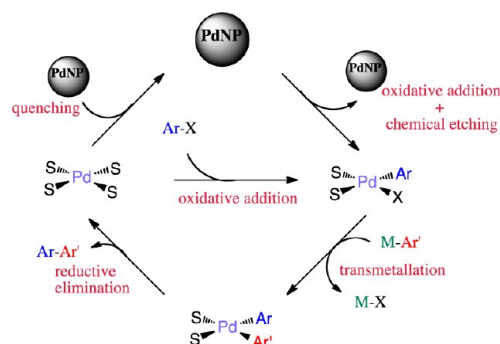
Catalysis by palladium derivatives is now one of the most important tools in organic synthesis. Whether researchers design palladium nanoparticles (NPs) or nanoparticles occur as palladium complexes decompose, these structures can serve as central precatalysts in common carbon–carbon bond formation. Palladium NPs are also valuable alternatives to molecular catalysts because they do not require costly and toxic ligands.

In this Account, we review the role of “homeopathic” palladium catalysts in carbon–carbon coupling reactions. Seminal studies from the groups of Beletskaya, Reetz, and de Vries showed that palladium NPs can catalyze Heck and Suzuki–Miyaura reactions with aryl iodides and, in some cases, aryl bromides at part per million levels. As a result, researchers coined the term “homeopathic” palladium catalysis. Industry has developed large-scale applications of these transformations.

In addition, chemists have used Crooks' concept of dendrimer encapsulation to set up efficient nanofilters for Suzuki–Miyaura and selective Heck catalysis, although these transformations required high PdNP loading. With arene-centered, ferrocenyl-terminated dendrimers containing triazolyl ligands in the tethers, we designed several generations of dendrimers to compare their catalytic efficiencies, varied the numbers of Pd atoms in the PdNPs, and examined encapsulation vs stabilization. The catalytic efficiencies achieved “homeopathic” (TON = 540 000) behavior no matter the PdNP size and stabilization type. The TON increased with decreasing the Pd/substrate ratio, which suggested a leaching mechanism.

Recently, we showed that water-soluble arene-centered dendrimers with tri(ethylene glycol) (TEG) tethers stabilized PdNPs involving supramolecular dendritic assemblies because of the interpenetration of the TEG branches. Such PdNPs are stable and retain their “homeopathic” catalytic activities for Suzuki–Miyaura reactions for months. (TONs can reach 2.7×10^6 at 80 °C for aryl bromides and similar values for aryl iodides at 28 °C.) Sonogashira reactions catalyzed by these PdNPs are quantitative with only 0.01% Pd/mol substrate. Kato's group has reported remarkable catalytic efficiencies for mesoporous catalysts formed by polyamidoamine (PAMAM) dendrimer polymerizations. These and other mesoporous structures could allow for catalyst recycling, with efficiencies approaching the “homeopathic” behavior.

In recent examples of Suzuki–Miyaura reactions of aryl chlorides, chemists achieved truly “homeopathic” catalysis when a surfactant such as a tetra-*n*-butylammonium halide or an imidazolium salt was used in stoichiometric quantities with substrate. These results suggest that the reactive halide anion of the salt attacks the neutral Pd species to form a palladate. In the case of aryl chlorides, the reaction may occur through the difficult, rate-limiting oxidative-addition step.

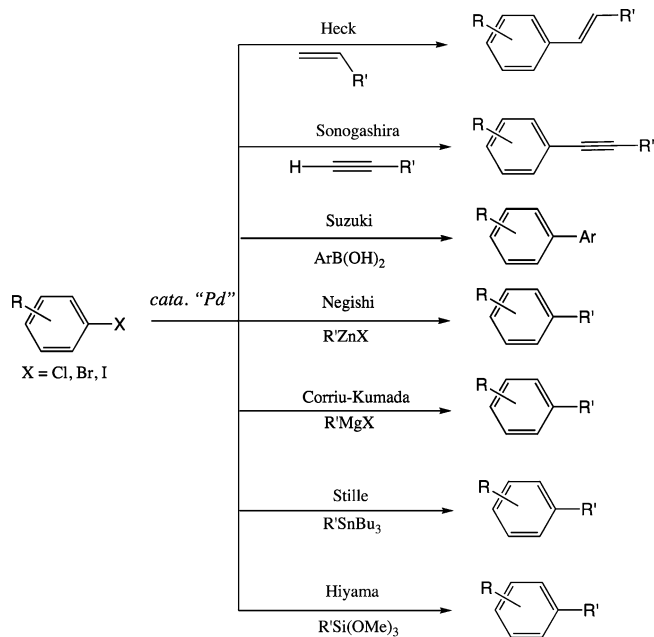


Introduction

Palladium-catalyzed cross carbon–carbon coupling reactions that include Heck, Suzuki–Miyaura, Sonogashira, Negishi, Stille, Hiyama, and Kumada–Corriu reactions (Scheme 1) are among the most useful organic reactions.^{1–5}

Although molecular palladium catalysts containing various tertiary phosphines^{1–5} or singlet *N*-heterocyclic

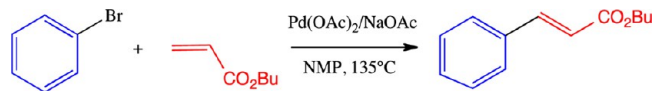
carbene ligands⁶ have long proven to be efficient and very popular, these ligands are toxic, expensive, or both, and therefore continuous investigations are pursuing the search of “green”, so-called “ligandless”, palladium precatalysts for applications to large-scale industrial processes.² Along this line, palladium nanoparticles (PdNPs) have appeared as a valuable alternative with several benefits relevant to

SCHEME 1. Main Palladium Catalyzed Cross Carbon–Carbon Coupling Reactions


"green" chemistry. PdNPs generated by reduction of palladium salts were shown in the 1990s by pioneering studies of the groups of Bönnerman⁷ and Reetz⁸ to be active catalysts of Heck and Suzuki–Miyaura reactions. In parallel, it was found that Pd⁰ or Pd^{II} complexes that were intended to behave as molecular catalysts were in fact thermally decomposed to PdNPs, which were the actual catalysts or precatalysts under the catalytic reaction conditions of high-temperature Heck reactions (usually between 120 and 160 °C).^{9,10} One of the most critical cases was that of palladacycles that were shown by Beller and Herrmann to be excellent C–C cross-coupling catalysts and initially believed to involve Pd^{IV} palladacycle intermediates in the catalytic cycles^{11,12} until it was realized, in particular following studies by Hartwig's group, that PdNPs were the actual precatalysts resulting from palladacycle decomposition.^{9,10,13} Indeed, seminal reports by Takahashi,¹⁴ Mizoroki,¹⁵ and Heck¹⁶ already in the early 1970s used the "ligandless" complexes Pd(dba) (dba = dibenzylideneacetone), PdCl₂ in the presence of sodium acetate, and Pd(OAc)₂, respectively, as sources of PdNPs.

The "Homeopathic" Mechanism of PdNP-Catalyzed Heck Reaction

One of the key advantages of PdNPs is that they are catalytically active in much lower amounts than molecular Pd catalysts. Indeed, the use of very low PdNP catalyst

SCHEME 2. Heck Reaction between Bromobenzene and Butyl Acrylate in NMP with a Homeopathic Amount of Pd(OAc)₂


amounts led to the term "homeopathic" doses. Beletskaya reported that 5 ppm Pd/mol iodobenzoic acid catalyzed Heck heterocoupling,² Reetz's group reported that 9 ppm Pd/substrate catalyzed Heck bromobenzene coupling to styrene,⁹ and de Vries' group showed that homeopathic amounts of Pd catalysts were efficient to carry out Heck reactions of a variety of aryl bromides in *N*-methylpyrrolidone (NMP) at 135 °C (Scheme 2).¹⁰

Sometimes, the PdNP amount was so low that reactions first appeared as proceeding in their absence,¹⁷ before the authors realized that they were occurring with "homeopathic" quantities of PdNPs.^{10,18}

The past decade has provided a large body of literature data whereby cross-coupling reactions are catalyzed by designed PdNPs in catalytic amounts on the order of 0.01 to 0.1 mol % and sometimes lower.^{19–23} Mechanistically, it has been proposed by de Vries (Figure 1) that for the Heck reaction oxidative addition of an aryl iodide onto the PdNP surface is followed by detachment (chemical etching) of metal atoms from the surface followed by highly efficient turnover in solution of the "ligandless" atoms that are possibly negatively charged as a result of attack by halide anions.²⁴

The fact that palladate Pd⁰ species are better activators than neutral Pd⁰ species had been proposed by Tchoubar²⁴ and demonstrated electrochemically in the case of Pd–phosphine catalysts by Amatore and Jutand.²⁵ de Vries' group discovered by ES-MS experiments that anionic Pd⁰ species such as PhPdCl₂[–] were indeed present in the catalytic reaction medium when NaCl was used as an additive.^{26,27} Thus, the roles of the anions are multiple and complex in the "homeopathic" mechanism (*vide infra*).

These reactive atoms in some form are quenched by the mother PdNP in sufficiently concentrated solutions, whereas upon dilution less frequent quenching due to higher distance between the two species results in increasing efficiency. Indeed, in all ligand-free Heck reactions on aryl bromides, the turnover frequency increases with decreasing catalyst concentration, which confirms the "homeopathic" designation. A "dead-end" point is the formation of Pd black (Scheme 3) resulting from agglomeration of the mother PdNPs depending on its stabilization, concentration

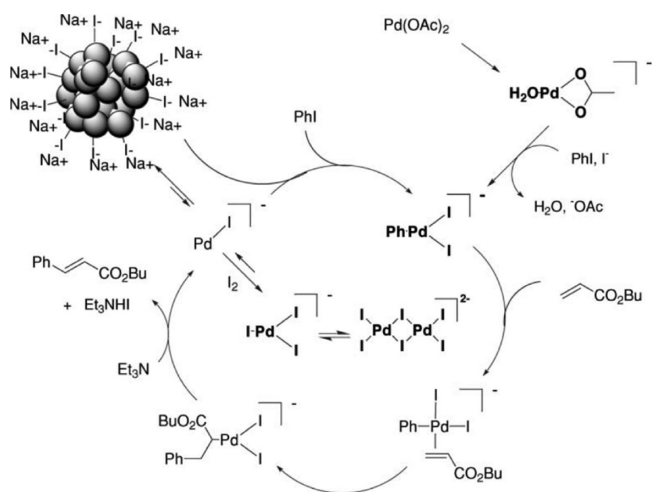
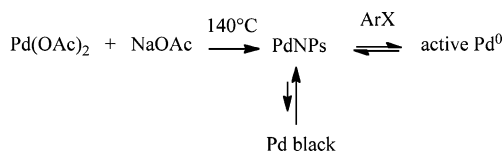


FIGURE 1. Mechanistic proposal for ligand-free Heck reactions of aryl iodide by de Vries (intermediates in bold have been observed by ES–MS or by EXAFS). Reprinted with permission from ref 10 (de Vries). Copyright 2006 Royal Society of Chemistry.

SCHEME 3. High-Temperature Generation of PdNPs from a Pd Precursor Complex with Formation of Pd Black (Heck Reaction Conditions)



(less or no Pd black forms with diluted PdNPs), and reaction temperature.^{9,10}

The Pd doses used are all the lower because only surface PdNP atoms are reactive, whereas the interior PdNP atoms do not participate in the catalysis; thus the actual % Pd atoms used per substrate is lower than the nominal ones.

Industrial Applications and Extension to Other Cross C–C Coupling Reactions

The method is of industrial interest, because the Heck reaction is of considerable use for applications, and various syntheses have been scaled up to kilogram size to prepare drug intermediates.^{28,29} In these seminal examples, the catalytic systems are homogeneous, but various heterogeneous PdNP systems with solid support have also been greatly developed, although the PdNP amount is not so low.^{21,26,27} The above indications are characteristic of the Heck reaction, but the de Vries' group also reported "homeopathic" ligand-free PdNP catalysis of Suzuki–Miyaura and Negishi reactions. For instance, with the Suzuki reaction, the best results were obtained using the Pd(OAc)₂ catalyst precursor in toluene with K₂CO₃ as the base (25 ppm Pd/mol bromoacetophenone and phenylboronic acid substrates),

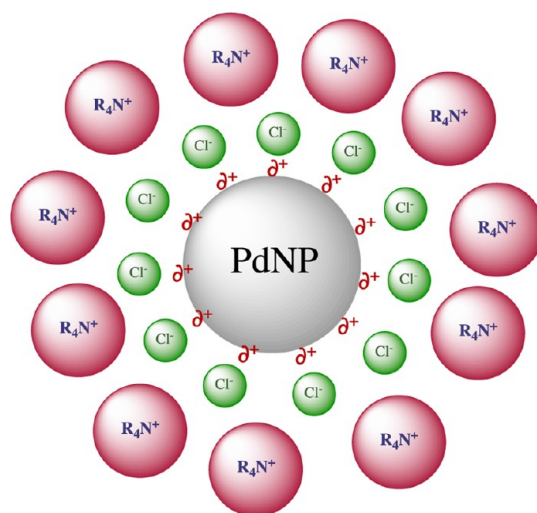


FIGURE 2. "Electrosteric" (that is electrostatic and steric) stabilization of Pd nanoparticles obtained by reduction of PdCl₂ in the presence of a tetra-*n*-alkylammonium salt. The halide anions provide electrostatic stabilization, and the tetra-*n*-butylammonium cations provide steric stabilization.

although aryl chlorides were poorly reactive; for Negishi coupling, a 75% yield was obtained upon reaction between ethyl 4-bromobenzoate and PhZnBr at 50 °C in DMF catalyzed by 0.02% Pd(OAc)₂.³⁰ Altogether, the application of PdNP catalysis to organic chemistry is considerable and has been recently reviewed.^{31–33} Finally, the principles developed here with PdNPs are rather general and have also been applied to other late transition metal NPs for catalysis, although not yet with "homeopathic" doses,^{34–36} detailed analysis being beyond the scope of this Account.

Stabilization of the Pd Nanoparticles

At high temperatures required for productive Heck reactions, it was shown that PdNPs are stabilized by the presence of polar solvents such as propylene carbonate, tetra-*n*-alkylammonium salts, or ionic liquids (imidazolium salts or else).^{9,19–21} Since the first report by Grätzel of ammonium salt-stabilized transition-metal nanoparticles (with PtNPs),³⁷ it has been shown that the first layer surrounding the NP core was that of the anions (Figure 2),³⁸ and stabilization was improved upon increasing the anion size.³⁹

Altogether, two components, steric and ionic (electrostatic), are essential to stabilize transition-metal NPs for catalytic use as shown, for instance, by the extensive use of such surfactants in high-temperature Heck reactions.^{28,29,40–42} The nature of the organic stabilizer is important for the determination and design of the PdNP size, but the nature and addition rate of the reductant of Pd^{II} to Pd⁰ also is decisive in order to reach the ideal size between 1 and 2 nm

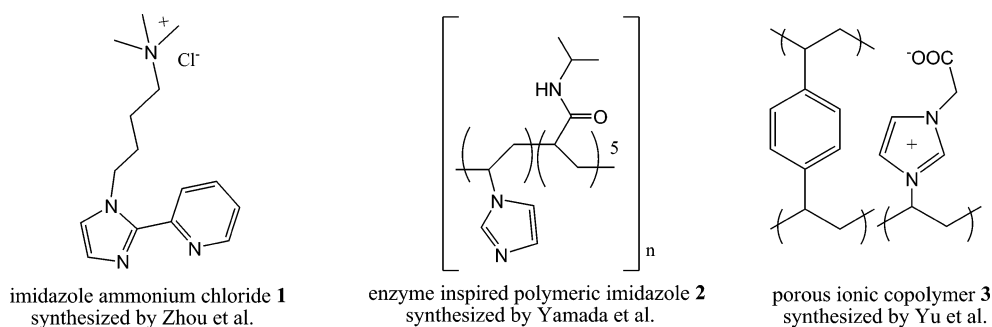
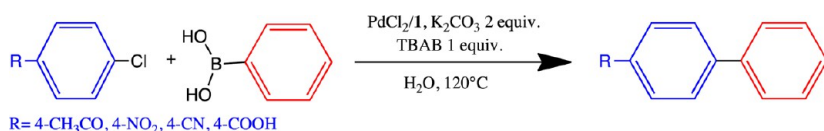


FIGURE 3. Examples of supports and ligands used for the stabilization of PdNPs active in C–C coupling with a parts per million scale of Pd in the presence of stoichiometric amounts of salt.^{46,48,49}

SCHEME 4. Suzuki–Miyaura Reaction of Various Chloroarenes in Water in the Presence of 1 equiv of TBAB and between 100 and 10 ppm of PdNP Stabilized by Ligand **1**



that provides the optimal proportion of surface Pd atoms while preserving the PdNP nature. Fast reduction of Pd^{II} leads to the formation of such small NPs if the organic stabilizer is efficient. According to Marcus theory, a strong driving force, that is, a large difference of potentials between the standard reduction potential of the metal ion precursor and that of the reductant, results in fast reduction, but experience shows that in this concern the rate of reductant addition (most often NaBH₄ but various other reductants are also used^{35,43}) is crucial. Sometimes, no reductant is necessary at the high temperatures required by Heck reactions, because at such temperatures the anion of the Pd^{II} salt serves at the reductant of Pd^{II} to Pd⁰. Even alkylthiolate ligands, however, provide excellent stability and reactivity of PdNPs in minute amounts for Suzuki–Miyaura coupling of aryl halides under ambient conditions in toluene despite the absence of ionic stabilizer, and no poisoning occurs.⁴⁴ However, the most successful organic stabilizers in terms of stability and catalytic efficiency of PdNPs at the level of a few parts per million of Pd atoms per mol substrate (or sometimes even less) for Heck or Suzuki–Miyaura cross coupling of aryl halides are those containing a large ammonium or imidazolium cation (Figure 3).^{28,29,45–50}

The amount of such salts in homogeneous catalytic reaction conditions was always very high, usually as high as that of the substrates and base, and the reaction mixture also contained a nitrogen ligand (eventually bonded to the cationic surfactant), whereas the PdNP amount was "homeopathic".^{48,49} Under these conditions, the Heck and

Suzuki–Miyaura cross coupling reactions of aryl chloride can occur efficiently in water (or in aqueous solvent) at high temperatures (Scheme 4).

The halide anion of these salts not only serves as the first protecting layer of the PdNP. Also, the fact that aryl chlorides are activated in their presence in huge excess indicates that their coordination to reactive Pd atoms that produces palladate species is crucial for the difficult oxidative addition of these aryl halides (Scheme 5). This factor and de Vries' detection of palladates strongly argue in favor of the intermediacy of these palladate species in the catalytic activation mechanism.

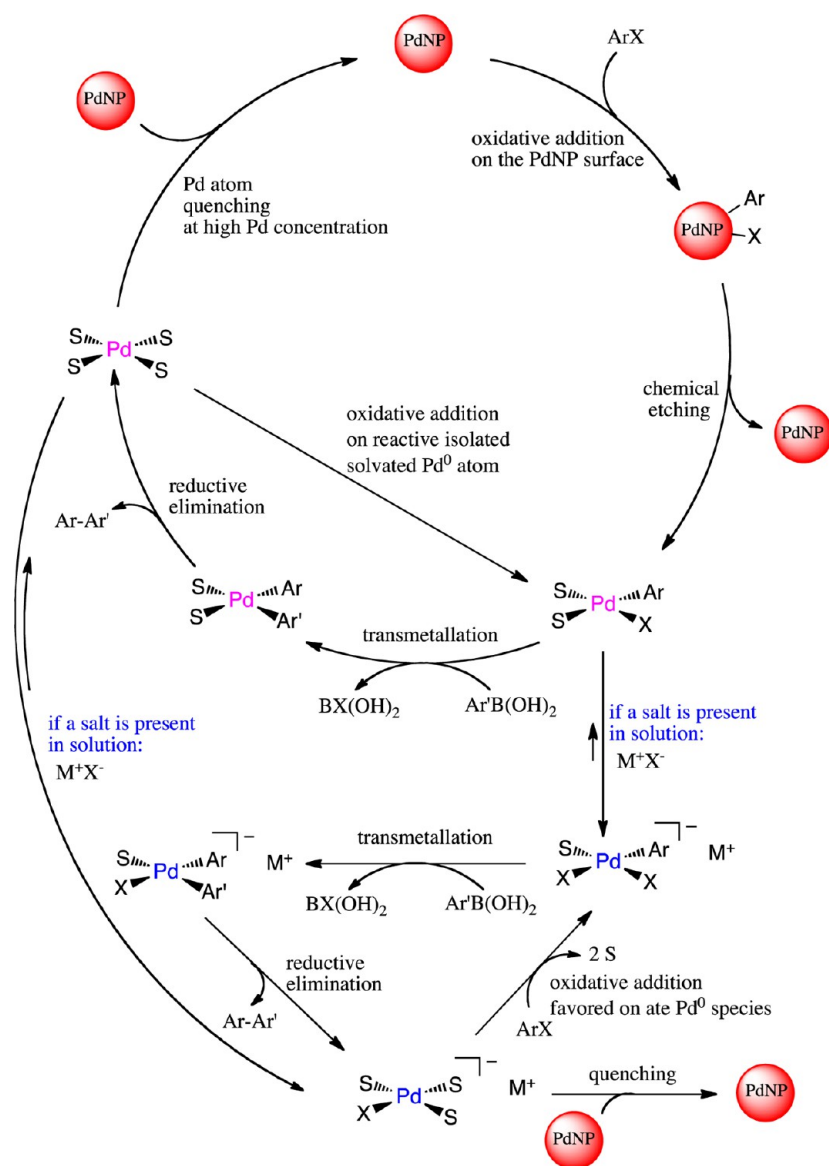
Heterogeneous supports (sometimes binding the ammonium or imidazolium salt) are also valuable alternatives to high salt concentrations.^{45–47}

Catalysis by Dendrimer-Encapsulated and Stabilized Pd Nanoparticles

In 1999, Crooks' group pioneered catalysis by PdNPs and PtNPs encapsulated in Tomalia's commercial polyamidoamine (PAMAM) dendrimers (Scheme 6).⁵¹

These studies followed catalysis by NPs stabilized by polymers such as NMP studied in particular by Toshima's group in the 1990s.⁵² These two types of macromolecules have in common their large size, their neutrality, and the presence of functional groups stabilizing NPs by coordination. The dendrimers have the advantage of a spherical topology and precise molecular definition with size control upon progressive increase of the generation number, G_n,

SCHEME 5. Homeopathic Mechanism for the Suzuki–Miyaura Reaction Inspired from the de Vries Mechanism^a



^aS = solvent molecule; X = halide. The quantity of salt (typically a tetra-*n*-butylammonium halide in which the halide is reactive) is very high in aryl chloride-activating system favoring palladate formation and thus the rate-limiting oxidative addition step.

SCHEME 6. Crook's Synthesis of a Nanoparticle inside a PAMAM Dendrimer^a



^aReprinted with permission from ref 53. Copyright 2011 Royal Society of Chemistry.

and according to Crooks they serve as substrate nanofilters for encapsulated NPs whereby the filtering efficiency increases along with Gn.^{53,54} In the early 2000s, several

groups investigated the Heck and Suzuki reaction catalyzed by PdNPs encapsulated in PAMAM and polypropyleneimine (PPI) dendrimers.^{53–60} The latter PdNPs provided 100% selectivity in Heck reaction between iodobenzene and *n*-butyl acrylate at 363 K.⁴⁸ With Gn-PAMAM dendrimer PdNPs, G2 yielded a more reactive catalyst than G4, but G4 provided a more stable catalyst.⁵⁵ For catalysis of the Stille reaction, the size of PAMAM-dendrimer-encapsulated PdNPs was shown to increase, which may be an indication of leaching during catalysis,⁶¹ and this point was debated using G6-PAMAM-encapsulated PdNPs whereby leaching was only observed in the presence of N₂ or air but not H₂.⁶²

Heterogeneous PAMAM dendrimer templates that are polymerized with an acrylate are a valuable microporous host for excellent PdNP catalysis reported by Kato et al.

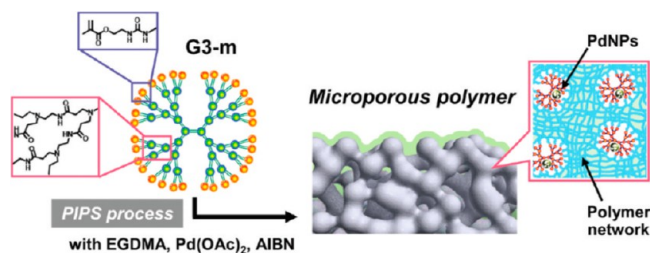


FIGURE 4. Schematic outline of the preparation of microporous network polymers that contain PdNPs. Reprinted with permission from ref 45. Copyright 2010 American Chemical Society.

(Figure 4). This group recently conducted Suzuki–Miyaura cross coupling of bromoacetophenone with phenyl boronic acid with TONs reaching 8.5×10^4 . In addition, this catalyst could be recycled more than 8 times with >90% yield even until the last run. ICP-MS analysis indicated a loss of only 0.27% Pd in solution showing the absence of leaching or recombination of leached Pd atoms as in the "homeopathic" mechanism.⁴⁵

Homeopathic C–C Cross Coupling by "Click" Dendrimer-Stabilized Pd Nanoparticles

Whereas commercial PAMAM and PPI dendrimers usually required relatively high Pd loading, the design of "click" ferrocenyl dendrimers⁶³ allowed evaluation of the coordination

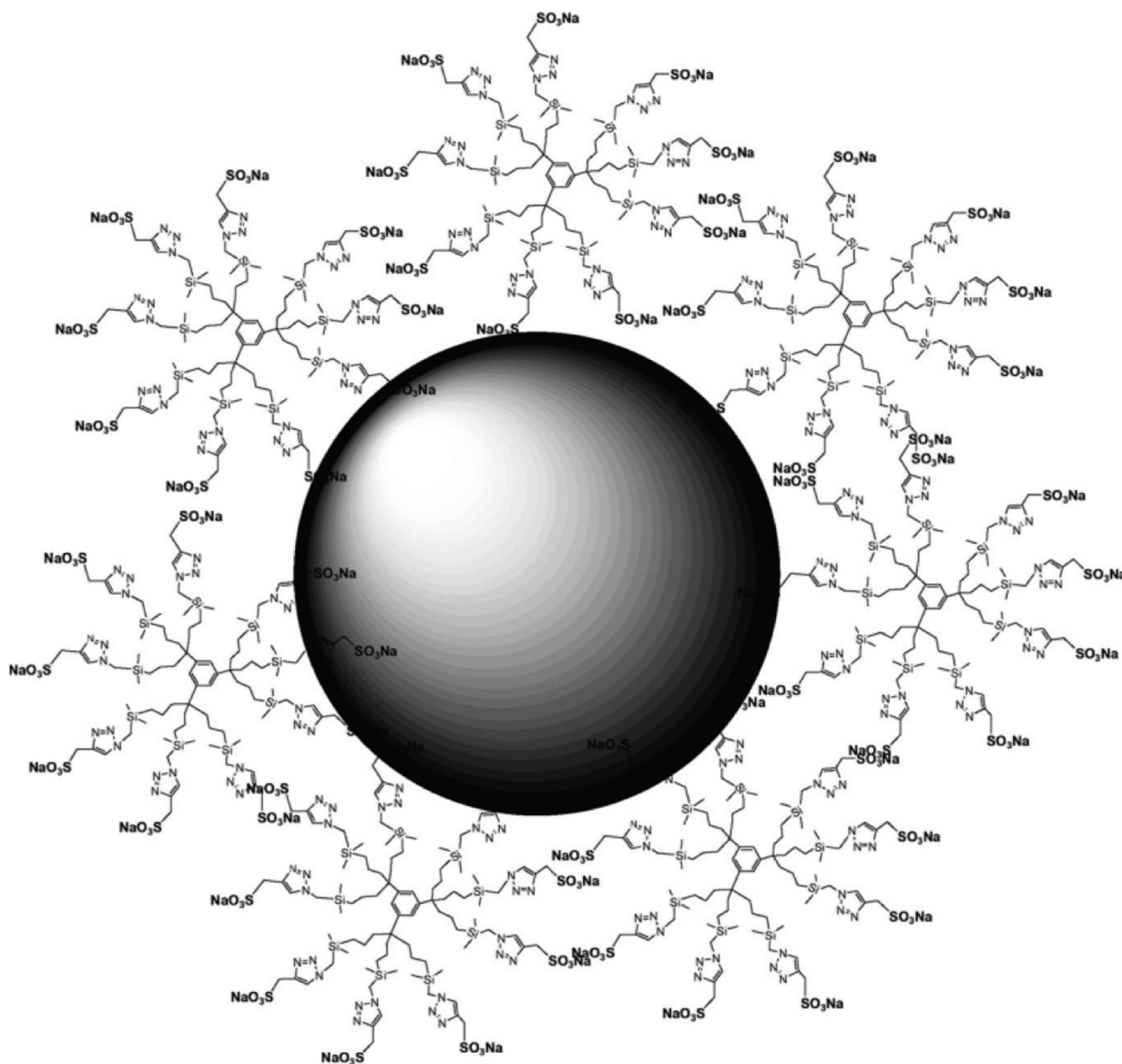


FIGURE 5. PdNP stabilized by several G0 arene-centered dendrimers with sulfonate termini.⁶⁷

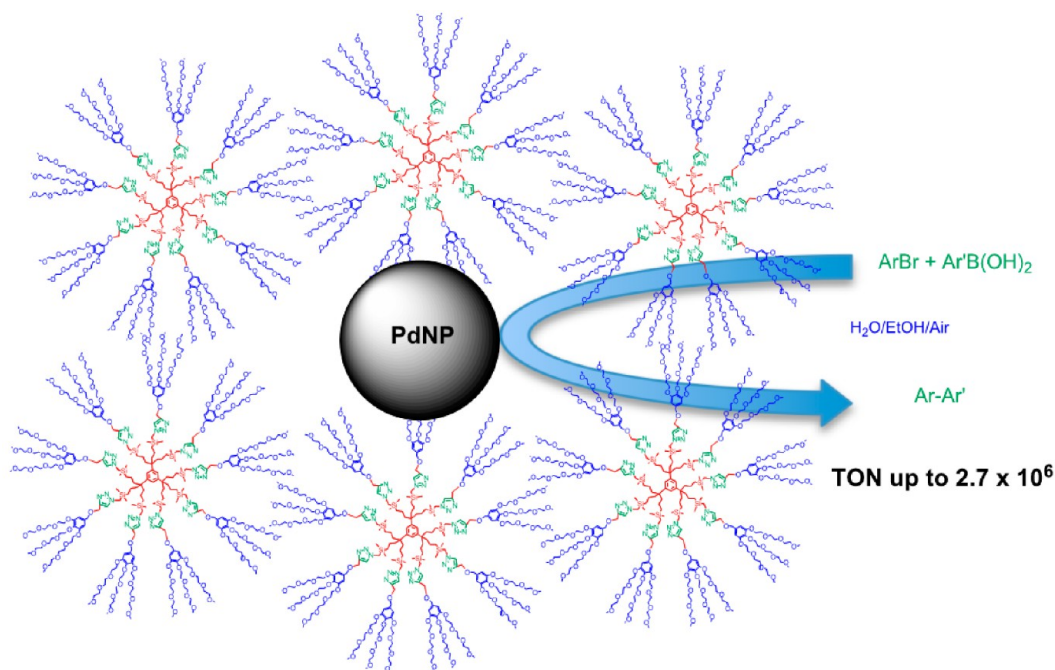


FIGURE 6. Stabilization of a PdNP by a supramolecular assembly of several G0 27-TEG dendrimers after reduction of Pd^{II} by NaBH₄. The Suzuki–Miyaura reaction of various bromoarenes has been carried out in H₂O/EtOH media with Pd amount between 10 ppm to 0.3 ppm. Turnover numbers reached 2.7×10^6 .⁷¹

of metal cations including Pd^{II} upon redox recognition of these cations using a ferrocenyl group attached to triazolyl dendrimer branch termini.⁶⁴ Indeed, the electrochemical titration indicated a 1:1 Pd^{II}/triazole branch stoichiometry. After reduction of Pd^{II} to Pd⁰, the forecasted number of Pd atoms encapsulated inside the “click” dendrimers could be verified by TEM for the G1 and G2 dendrimers containing, respectively, 27 and 81 ferrocenyltriazole termini, resulting in encapsulated PdNPs that were 1.3 ± 0.2 nm and 1.6 ± 0.3 nm, respectively. With the G0 dendrimer containing 9 ferrocenyl triazole termini, the PdNPs were larger (2.8 nm), because they were surrounded by several dendrimers rather than being encapsulated inside a single dendrimer. Whereas hydrogenation of diene to monoene was all the faster because the PdNPs were smaller as expected for a surface mechanism,⁶⁵ C–C coupling between iodobenzene and phenylboronic acid in toluene was independent of the PdNP size and of whether the PdNP was encapsulated inside a large G1 or G2 dendrimer or stabilized by small G0 dendrimers. Catalysis was all the more efficient as the PdNP concentration was lower, and at high PdNP concentration, the yield was not quantitative, which was taken into account by atom quenching by the PdNP in analogy to the high-temperature Heck “homeopathic” mechanism. With 1 ppm Pd, a TON of 540 000 was obtained at room temperature, although the reaction was slow.⁶⁶ When the terminal “click”

dendrimer groups were sulfonates, they were water-soluble and stabilized PdNPs (but did not encapsulate them, Figure 5), and the Suzuki–Miyaura coupling of iodobenzene with phenylboronic acid was conducted in aqueous solvents resulting in TONs up to almost 10000 (almost quantitative) under ambient conditions with TOFs up to 1500 mol PhI (mol Pd)^{−1} h^{−1},⁶⁷ these values being higher than with the comparable “click” sulfonate polymer.⁶⁸

The next series of “click” dendrimers were designed to contain both triazolyl linkages and tri(ethylene glycol) (TEG) termini in Percec-type tripodal dendrons.⁶⁹ These new water-soluble dendritic nanoreactors were efficient in both molecular⁷⁰ and PdNP catalysis.⁷¹ The G0 dendrimer contains 27 TEG termini and 9 triazole linkers, whereas the G1 dendrimer contains 81 TEG termini and 27 triazole linkers. Addition of Pd^{II} ions as K₂PdCl₄ in water was shown by UV–vis spectroscopy to coordinate efficiently only to the triazole ligands according to a 1:1 Pd/triazole stoichiometry. Reduction to PdNPs yielded a large supramolecular assembly that required several dendrimers to stabilize a single truncated bipyramid PdNP of 1.4 ± 0.7 nm core size containing approximately 100 Pd atoms. On the other hand, the dendrimer size of G1 hardly increases upon PdNP encapsulation. The dendrimer-stabilized PdNPs are stable in air and water and retain their catalytic activity for months, the G0-stabilized PdNPs being the most active catalyst.

TABLE 1. Selected Examples of Extremely Active PdNP Catalysts Discussed in the Text^a

catalyst	PdNP (nm)	R	solvent	temp (°C)	Pd loading, TON
Pd(OAc) ₂		H	DMF/H ₂ O, HMPA/H ₂ O	85	5 ppm, ² 200000
Pd(OAc) ₂		H	NMP/H ₂ O (19/1)	90	0.9 ppm, ⁹ 94444
Pd(OAc) ₂ + n-Bu ₄ NBr		S	NMP/H ₂ O	90	50 ppm, ³⁰ 16600
		N	DMF	50	200 ppm, 4050
Pd/C	2.4	H	NMP	140	50 ppm, ²⁹ 18000
Pd(OAc) ₂ /G3-P3	2.0	S	H ₂ O	80	10 ppm, ⁴⁵ 85000
Pd(OAc) ₂ / 3 + TBAB	2.0–5.0	S	H ₂ O	100	10 ppm, ⁴⁶ 95000
K ₂ PdCl ₄ , PVP	10	S	H ₂ O/EtOH (3/1)	90	8 ppm, ⁴⁷ 117500
(NH ₄) ₂ PdCl ₄ / 2 + TBAF	4.9	S	H ₂ O	100	0.28 ppm, ⁴⁸ 3570000 (ArI) 66 ppm, 14848 (ArCl)
PdCl ₂ / 1	3.0	S	H ₂ O	120	10 ppm, ⁴⁹ 100000 (ArBr)
PdCl ₂ / 1 + TBAB	3.0	S	H ₂ O	120	10 ppm, ⁴⁹ 66000 (ArCl)
H ₂ PdCl ₄ /SBA-15 + TBAB	6.4	S	H ₂ O	80	6 ppm, ⁵⁰ 121666
K ₂ PdCl/PPPI		H	Et ₃ N	90	(3–5) × 10 ⁴ ppm, ⁵⁴ low
K ₂ PdCl ₄ /G4-OH		H	DMA	140	25 ppm, ⁵⁶ 36800
K ₂ PdCl ₄ /G4-OH	1.4	S	H ₂ O/EtOH (6/4)	80	1.5 × 10 ⁴ ppm, ⁵⁷ low
K ₂ PdCl ₄ /G4-OH	3.2	S	EtOH	78	550 ppm, ⁵⁸ 1771
K ₂ PdCl ₄ /G4-OH	1.6	St	H ₂ O	40	3 × 10 ³ ppm, ⁶¹ low
Pd(OAc) ₂ /G0-9Fc	2.8	S	CHCl ₃ /MeOH (2/1)	rt	1 ppm ⁶⁵ 540000 (ArI)
K ₂ PdCl ₄ / G0-9SO ₃ ⁻	2.3	S	H ₂ O/EtOH (1/1)	rt	100 ppm, ⁶⁷ 9200 (ArI)
K ₂ PdCl ₄ / G1-27SO ₃ ⁻	2.8	S	H ₂ O/EtOH (1/1)	rt	100 ppm, ⁶⁷ 9400 (ArI)
K ₂ PdCl ₄ / G0-27TEG	1.4	S	H ₂ O/EtOH (1/1)	80	0.3 ppm, ⁷¹ 2700000 (ArBr)
K ₂ PdCl ₄ / G1-81TEG	2.7	S	H ₂ O/EtOH (1/1)	80	1 ppm, ⁷¹ 390000 (ArBr)

^aCatalyst, Pd source/stabilizer + additive; R, reaction (S, Suzuki; H, Heck; St, Stille; and N, Negishi). G4-OH, 4th generation PAMAM dendrimer with OH termini. PPPI, perfluorinated polyether-derivatized poly(propylene) imine. G0-9Fc: zeroth-generation dendrimer with 9 ferrocene termini; G0-9SO₃⁻ and G1-27SO₃⁻, zeroth- and first-generation dendrimers with, respectively, 9 and 27 sulfonated termini; G0-27TEG and G1-81TEG, zeroth- and first-generation dendrimers with, respectively, 27 and 81 tri(ethylene glycol) termini.

These PdNPs catalyze Suzuki–Miyaura coupling of inactivated bromoarenes with phenylboronic acids at 80 °C with TONs that reach or overtake 1 million and that of iodoarenes also at the sub-part per million level at 28 °C.⁷¹ It appears that the TEG tethers, in addition to bringing biocompatibility,⁷² allow interpenetration of a set of dendrimers to create large assemblies favoring PdNP stabilization (Figure 6). Comparatively, "click" polymers containing TEG tethers are also extremely active but less stable, lacking the nanocontainer property of the related "click" dendrimers.⁷³ For Heck or Suzuki–Miyaura coupling of chloroarenes, the results are less impressive, because these PdNPs decompose above 100 °C, and classic surfactants used in large quantities remain superior for "homeopathic" catalysis. Note, however, that the "click" TEG dendrimers are fully recycled and also used in very small quantities contrary to surfactants.

The "click" TEG dendrimer-stabilized PdNPs also efficiently catalyze *inter alia* the more demanding Sonogashira reactions at 100 °C, and the amount of Pd vs substrate that is required reaches 0.01%, that is, higher than "homeopathic" quantities. Nevertheless, the "ligand-free" nature of the PdNP precatalyst is of interest in terms of "green" chemistry despite the lack of mechanistic information.

In Table 1, we compare the "homeopathic" catalysis for a variety of carbon–carbon bond formation reactions catalyzed by PdNPs. The data show the advantage of recyclable

dendrimers that stabilize highly active PdNP precatalyst in Miyaura–Suzuki reactions.

Conclusion and Prospects

The "ligand-free" Pd-catalyzed Heck reaction was a considerable breakthrough from both standpoints of saving costly or toxic ligands and requiring so-called "homeopathic" quantities of PdNP catalysts; moreover, it provided the occasion of a novel mechanistic insight into NP catalysis. The "homeopathic" nomenclature should not be taken here strictly as in the traditional meaning of infinite dilution, but the analogy only involves (i) activity at extremely low, sometimes sub-part per million Pd concentration and (ii) catalytic activity increasing with dilution (until a certain point) because the mother PdNP quenches the active Pd atoms, a process disfavored upon dilution. Consequently, industrial applications resulted from this new generation of catalysts. Recently, the principle of "homeopathic" catalysis by PdNPs could be extended to room-temperature Suzuki–Miyaura catalysis in aqueous solvents using preformed PdNPs that were precisely designed in terms of size and shape using dendrimers that permitted the optimization of the PdNP stability and efficiency. There are also an increasing number of recent reports on homeopathic PdNP catalysis using stoichiometric amounts of cationic (ammonium or imidazolium) stabilizers that allow chloroarene Heck and Suzuki–Miyaura coupling in water. The requirement of

these salts containing reactive anions in large excess facilitates the formation of palladate species that are better candidates than neutral Pd species for the difficult oxidative addition of aryl chlorides.

Alternatively, sophisticated microporous solid supports that are eventually functionalized with cationic PdNP stabilizers also lead to excellent catalysis results in terms of catalytic Heck and Suzuki–Miyaura reactions sometimes using almost "homeopathic" PdNP amounts.⁷⁴

The forthcoming challenges leading to improved simultaneous stabilization and catalytic efficiency of Pd catalyst now involve (i) "homeopathic" PdNP catalysis requiring as little salt as possible in aqueous solvents, (ii) activation of chloroarenes with "homeopathic" dendrimer-stabilized PdNPs, (iii) continuous improvements of recyclable "homeopathic" heterogeneous catalysts, and (iv) extension of the "homeopathic" PdNP catalysis beyond the Heck and Suzuki–Miyaura reactions to other PdNP-catalyzed cross coupling reactions for which the PdNP is still relatively high as reported in known studies.^{35,74}

Fruitful discussions with Drs. Catia Ornelas, Abdou Diallo, and Jaime Ruiz (Univ. Bordeaux) and Dr. Lionel Salmon (LCC, Toulouse) and financial support from the University Bordeaux 1, the Centre National de la Recherche Scientifique (CNRS), the Institut Universitaire de France (IUF), the Ministry of Research (Ph.D. grant to C.D.), the Agence Nationale pour la Recherche (ANR), and l'Oréal (Research and Development) are gratefully acknowledged.

BIOGRAPHICAL INFORMATION

Christophe Deraedt received his master degree of nanosciences and life chemistry in 2011 at the University Bordeaux 1. He presently is in his second year of Ph.D. program in the research group "Nanosciences and catalysis" of Prof. Didier Astruc, working on the synthesis and uses of "green" nanoreactors for catalysis of reactions including carbon–carbon bond formation and transformation.

Didier Astruc is Professor of Chemistry at the University of Bordeaux and Member of the Institut Universitaire de France. He did his Ph.D. research in Rennes with R. Dabard and postdoctoral work at MIT with R. R. Schrock. His present interests are in dendrimers and nanoparticles and their applications in catalysis, molecular materials science, and nanomedicine.

FOOTNOTES

*Corresponding author. E-mail: d.astruc@ism.u-bordeaux1.fr. The authors declare no competing financial interest.

REFERENCES

- Bräse, S.; de Meijere, A. In *Metal-Catalyzed Cross-Coupling Reactions*; Diederich, F., Stang, P. J., Eds.; Wiley-VCH: Weinheim, Germany, 1998; pp 99–166.
- Beletskaya, I. P.; Cheprakov, A. V. The Heck Reaction as a Sharpening Stone of Palladium Catalysis. *Chem. Rev.* **2000**, *100*, 3009–3066.

- Metal-Catalyzed Cross-Coupling Reactions*; de Meijere, A., Diederich, F., Eds.; Wiley-VCH: Weinheim, Germany, 2004.
- Ackermann, L. Historical development of cross-coupling reactions. In *Modern Arylation Methods*; Ackermann, L. Ed.; Wiley-VCH: Weinheim, Germany, 2009; pp 1–24.
- Seechurn, C. C. C. J.; Kitching, M. O.; Colacot, T. J.; Sniekus, V. Palladium-Catalyzed Cross Coupling: A Historical Contextual Perspective to the 2010 Nobel Prize. *Angew. Chem., Int. Ed.* **2012**, *51*, 5062–5085.
- Herrmann, W. A. N-Heterocyclic Carbenes: A New Concept in Organometallic Catalysis. *Angew. Chem., Int. Ed.* **2002**, *41*, 1290–1309.
- Bonnemann, H.; Brioux, W.; Brinkmann, R.; Dinjux, E.; Joussem, T.; Korall, B. Formation of Colloidal Transition-Metals in Organic Phases and Their Application in Catalysis. *Angew. Chem., Int. Ed. Engl.* **1991**, *30*, 1312–1314.
- Reetz, M. T.; Lohmer, G. Propylene Carbonate Stabilized Nanostructured Palladium Clusters as Catalysts in Heck Reactions. *Chem. Commun.* **1996**, 1921–1922.
- Reetz, M.; de Vries, J. G. Ligand-free Heck Reactions Utilising Low Pd-Loading. *Chem. Commun.* **2004**, 1559–1563.
- de Vries, J. G. A Unifying Mechanism for All High-Temperature Heck reactions. The Role of Palladium Colloids and Anionic Species. *Dalton Trans.* **2006**, 421–429.
- Herrmann, W. A.; Broßmer, C.; Öfele, K.; Reisinger, C.-P.; Priemeier, T.; Beller, M.; Fischer, H. Palladacycles as Structurally Defined Catalysts for the Heck Olefination of Chloro- and Bromoarenes. *Angew. Chem., Int. Ed. Engl.* **1995**, *34*, 1844–1847.
- Louie, J.; Hartwig, J. F. A Route to Pd-0 from Pd-II Metallacycles in Amination and Cross-Coupling Chemistry. *Angew. Chem., Int. Ed. Engl.* **1996**, *35*, 2359–2361.
- Nowotny, M.; Hanefeld, U.; van Koningsveld, H.; Maschmeyer, T. Cyclopalladated Imine Catalysts in Heck Arylation: Search for the Catalytic Species. *Chem. Commun.* **2000**, 1877–1878.
- Takahashi, Y.; Ito, T.; Sakai, S.; Ishii, Y. A Novel Palladium(0) Complex - Bis-(Dibenzylideneacetone)Palladium(0). *J. Chem. Soc. D* **1970**, 1065–1066.
- Mizoroki, T.; Mori, K.; Ozaki, A. Arylation of Olefin with Aryl Iodide Catalyzed by Palladium. *Bull. Chem. Soc. Jpn.* **1971**, *44*, 581–584.
- Heck, R. F.; Nolley, J. P., Jr. Palladium-Catalyzed Vinylic Hydrogen Substitution Reactions with Aryl, Benzyl, and Styryl Halides. *J. Org. Chem.* **1972**, *37*, 2320–2322.
- Leadbeater, N. E.; Marco, M. Transition-Metal-Free Suzuki-Type Coupling Reactions. *Angew. Chem., Int. Ed.* **2003**, *42*, 1407–1409.
- Arvela, R. K.; Leadbeater, N. E.; Sangi, M. S.; Williams, V. A.; Granados, P.; Singer, R. D. A Reassessment of the Transition-Metal Free Suzuki-Type Coupling Methodology. *J. Org. Chem.* **2005**, *70*, 161–168.
- Liu, Y.; Wang, S. S.; Liu, W.; Wan, Q. X.; Wu, H. H.; Gao, G. H. Transition-Metal Catalyzed Carbon-Carbon Couplings Mediated with Functionalized Ionic Liquids, Supported-Ionic Liquid Phase, or Ionic Liquid Media. *Curr. Org. Chem.* **2009**, *13*, 1322–1346.
- Dupont, J.; Scholten, J. D. On the Structural and Surface Properties of Transition-Metal Nanoparticles in Ionic Liquids. *Chem. Soc. Rev.* **2010**, *39*, 1780–1804.
- Yin, L. X.; Liebscher, J. Carbon-Carbon Coupling Reactions Catalyzed by Heterogeneous Palladium Catalysts. *Chem. Rev.* **2007**, *107*, 133–173.
- Phan, N. T. S.; Van Der Sluys, M.; Jones, C. W. On the Nature of the Active Species in Palladium Catalyzed Mizoroki-Heck and Suzuki-Miyaura Couplings - Homogeneous or Heterogeneous Catalysis, a Critical Review. *Adv. Synth. Catal.* **2006**, *348*, 609–679.
- Astruc, D. Palladium Nanoparticles as Efficient Green Homogeneous and Heterogeneous Carbon-Carbon Coupling Precatalysts: A Unifying View. *Inorg. Chem.* **2007**, *46*, 1884–1894.
- Loupy, A.; Tchoubar, B. *Salt Effects in Organic and Organometallic Chemistry*; VCH: Weinheim, Germany, 1992.
- Amatore, C.; Jutand, A. Anionic Pd⁰ and Pd^{II} Intermediates in Palladium-Catalyzed Heck and Cross-Coupling Reactions. *Acc. Chem. Res.* **2000**, *33*, 314–321.
- de Vries, A. H. M.; Mulders, J. M. C. A.; Mommers, J. H. M.; Henderickx, H. J. W.; de Vries, J. G. Homeopathic Ligand-Free Palladium as a Catalyst in the Heck Reaction. A Comparison with a Palladacycle. *Org. Lett.* **2003**, *5*, 3285–3288.
- Suzuki, A. In *Modern Arene Chemistry*; Astruc, D., Ed. Wiley-VCH: Weinheim, Germany, 2002; pp 53–106.
- Tucker, C. E.; de Vries, J. G. Homogeneous Catalysis for the Production of Fine Chemicals. Palladium- and Nickel-Catalyzed Aromatic Carbon–Carbon Bond Formation. *Top. Catal.* **2002**, *19*, 111–118.
- Köhler, K.; Heidenreich, R. G.; Krauter, J. G. E.; Pietsch, J. Highly Active Palladium/Activated Carbon Catalysts for Heck Reactions: Correlation of Activity, Catalyst Properties, and Pd Leaching. *Chem.—Eur. J.* **2002**, *3*, 622–631.
- Alimardanov, A.; Schmieder-van de Vondervort, L.; de Vries, A. M. H.; de Vries, J. G. Use of "Homeopathic" Ligand-Free Palladium as Catalyst for Aryl-Aryl Coupling Reactions. *Adv. Syn. Catal.* **2004**, *346*, 1812–1817.
- Durand, J.; Teuma, E.; Gómez, M. An Overview of Palladium Nanocatalysts: Surface and Molecular Reactivity. *Eur. J. Inorg. Chem.* **2008**, 3577–3586.
- Favier, I.; Madec, D.; Teuma, E.; Gómez, M. Palladium Nanoparticles Applied in Organic Synthesis As Catalytic Precursors. *Curr. Org. Chem.* **2011**, *15*, 3127–3174.

- 33 Balanta, A.; Godard, C.; Claver, C. Pd Nanoparticles for C-C Coupling Reactions. *Chem. Soc. Rev.* **2011**, *40*, 4973–4985.
- 34 Lu, F.; Ruiz, J.; Astruc, D. Nanoparticle Catalysis. *Angew. Chem., Int. Ed.* **2005**, *44*, 7852–7872.
- 35 *Nanoparticles and Catalysis*; Astruc, D., Ed.; Wiley-VCH: Weinheim, Germany, 2008.
- 36 *Nanomaterials in Catalysis*; Sep, P., Philippot, K., Eds.; Wiley-VCH: Weinheim, Germany, 2013.
- 37 Kiwi, J.; Grätzel, M. Protection, Size Factors and Reaction Dynamics of Colloidal Redox Catalysts Mediating Light Induced Hydrogen Evolution from Water. *J. Am. Chem. Soc.* **1979**, *101*, 7214–7217.
- 38 Deng, Z.; Irish, D. E. SERS Investigation of the Adsorption and Decomposition of Tetramethylammonium Ions on Silver Electrode Surfaces in Aqueous Media. *J. Phys. Chem.* **1994**, *98*, 11169–11177.
- 39 Özkar, S.; Finke, R. G. Nanocluster Formation and Stabilization Fundamental Studies: Ranking Commonly Employed Anionic Stabilizers via the Development, Then Application, of Five Comparative Criteria. *J. Am. Chem. Soc.* **2002**, *124*, 5796–5810.
- 40 Jeffery, T. Palladium-Catalysed Vinylation of Organic Halides under Solid–Liquid Phase Transfer Conditions. *Chem. Commun.* **1984**, 1287–1289.
- 41 de Vries, A. H. M.; Parlevliet, F. J.; Schmieder-van de Vodervoort, L.; Mommers, J. H. M.; Henderickx, H. J. W.; Walet, M. A. N.; de Vries, J. G. A Practical Recycle of a Ligand-Free Palladium Catalyst for Heck Reactions. *Adv. Syn. Catal.* **2002**, *344*, 996–1002.
- 42 Roucoux, A. Stabilized Noble Metal Nanoparticles: An Unavoidable Family of Catalysts for Arene Derivative Hydrogenation. *Top. Organomet. Chem.* **2005**, *16*, 261–279.
- 43 Boisselier, E.; Diallo, A. K.; Salmon, L.; Omelas, C.; Ruiz, J.; Astruc, D. Encapsulation and Stabilization of Gold Nanoparticles with "Click" Polyethyleneglycol Dendrimers. *J. Am. Chem. Soc.* **2010**, *132*, 2729–2742.
- 44 Lu, F.; Ruiz, J.; Astruc, D. Palladium-dodecanethiolate nanoparticles as stable and recyclable catalysts for the Suzuki-Miyaura reaction of aryl halides under ambient conditions. *Tetrahedron Lett.* **2004**, 9443–9445.
- 45 Ogasawara, S.; Kato, S. Pd Nanoparticles Captured in Microporous Polymers: A Tailor-Made Catalyst for Heterogeneous Carbon Cross Coupling Reactions. *J. Am. Chem. Soc.* **2010**, *132*, 4608–4613.
- 46 Yu, Y.; Hu, T.; Chen, X.; Xu, K.; Zhang, J.; Huang, J. Pd nanoparticles on a porous ionic copolymer and recyclable catalyst for Suzuki-Miyaura under air and water. *Chem. Commun.* **2011**, *47*, 3592–3594.
- 47 Uberman, P. M.; Pérez, L. A.; Lacconi, G. I.; Martín, S. E. PVP-stabilized Pd nanoparticles electrochemically obtained as effective catalysts in aqueous medium Suzuki-Miyaura reaction. *J. Mol. Catal. A: Chem.* **2012**, *363–364*, 245–253.
- 48 Yamada, Y. M. A.; Sarkar, S. M.; Uozulmi, Y. Self-Assembled Poly(imidazole-Pd): Highly Active, Reusable Catalyst at Parts per Million to Parts per Billion Levels. *J. Am. Chem. Soc.* **2012**, *134*, 3190–3198.
- 49 Zhou, C.; Wang, J.; Li, L.; Wang, R.; Hong, M. A Palladium Chelating Complex of Ionic Water-Soluble Nitrogen-Containing Ligand: The Efficient Precatalyst for Suzuki–Miyaura Reaction in Water. *Green Chem.* **2011**, *13*, 2100–2106.
- 50 Zhi, J.; Song, D.; Li, Z.; Lei, X.; Hu, A. Pd Nanoparticles in Carbon Thin Film-Lined SBA-15 Nanoreactors: Efficient Heterogeneous Catalysts for Suzuki-Miyaura Cross Coupling Reaction in Aqueous Media. *Chem. Commun.* **2011**, *47*, 10707–10709.
- 51 Crooks, R. M.; Zhao, M.; Chechik, V.; Yeung, L. K. Dendrimer-Encapsulated Metal Nanoparticles: Synthesis, Characterization, and Applications to Catalysis. *Acc. Chem. Res.* **2001**, *34*, 181–190.
- 52 Toshima, N.; Yonezawa, T. Bimetallic Nanoparticles- Novel Materials for Chemical and Physical Applications. *New J. Chem.* **1998**, *22*, 1179–1201.
- 53 Meyers, V. S.; Weier, M. G.; Carino, E. V.; Yancey, D. F.; Pande, S.; Crooks, R. M. Dendrimer-Encapsulated Nanoparticles: New Synthetic and Characterization Methods and Catalytic Applications. *Chem. Sci.* **2011**, *2*, 1632–1646.
- 54 Yeung, L. K.; Crooks, R. M. Heck Heterocoupling within a Dendritic Nanoreactor. *Nano Lett.* **2001**, *1*, 14–17.
- 55 Yeung, L. K.; Lee, C. T.; Johnston, K. P.; Crooks, R. M. Catalysis in Supercritical CO₂ Using Dendrimer-Encapsulated Pd Nanoparticles. *Chem. Commun.* **2001**, 2290–2291.
- 56 Rahim, E. H.; Kamounah, F. S.; Fredericksen, J.; Christensen, J. B. Heck Reactions Catalyzed by PAMAM Dendrimer-Encapsulated Pd⁰ Nanoparticles. *Nano Lett.* **2001**, *1*, 499–501.
- 57 Li, Y.; El-Sayed, M. A. The Effect of Stabilizers on the Catalytic Activity and Stability of Pd Colloidal Nanoparticles in the Suzuki Reaction in Aqueous solution. *J. Phys. Chem. B* **2001**, *105*, 8938–8943.
- 58 Pittelkow, M.; Moth-Poulsen, K.; Boas, U.; Christensen, J. B. PAMAM Dendrimer-Stabilized Pd(0) Nanoparticles as Catalyst for the Suzuki Reaction. *Langmuir* **2003**, *19*, 7682–7684.
- 59 Ooe, M.; Murata, M.; Mizugati, T.; Ebitani, K.; Kaneda, K. Supramolecular Catalysts by Encapsulating Pd Complexes within Dendrimers. *J. Am. Chem. Soc.* **2004**, *124*, 1604–1605.
- 60 Lemo, J.; Heuzé, K.; Astruc, D. Synthesis and Catalytic Activity of DAB-Dendrimer Encapsulated Pd Nanoparticles for the Suzuki Coupling Reaction. *Inorg. Chim. Acta* **2006**, *359*, 4909–4911.
- 61 Bernechea, M.; de Jesús, E.; Lopez-Mardomingo, C. Dendrimer-Encapsulated Pd Nanoparticles versus Pd Acetate as Catalyst Precursors in the Stille Reaction in Water. *Inorg. Chem.* **2009**, *48*, 4491–4496.
- 62 Carino, E. V.; Knecht, M. R.; Crooks, R. M. Quantitative Analysis of the Stability of Pd Dendrimer-Encapsulated Nanoparticles. *Langmuir* **2009**, *25*, 10279–10284.
- 63 Omelas, C.; Ruiz, J.; Cloutet, E.; Alves, S.; Astruc, D. Click Assembly of 1,2,3-Triazole-Linked Dendrimers Including Ferrocenyl Dendrimers that Sense Both Oxo-anions and Metal Cations. *Angew. Chem., Int. Ed.* **2007**, *46*, 872–877.
- 64 Omelas, C.; Salmon, L.; Ruiz, J.; Astruc, D. Catalytically Efficient Palladium Nanoparticles Stabilized by Click Ferrocenyl Dendrimers. *Chem. Commun.* **2007**, 4946–4948.
- 65 Diallo, A. K.; Omelas, C.; Salmon, L.; Ruiz, J.; Astruc, D. Homeopathic Catalytic Activity and Atom-Leaching Mechanism in the Miyaura-Suzuki Reactions under Ambient Conditions Using Precise "Click" Dendrimer-Stabilized Pd Nanoparticles. *Angew. Chem., Int. Ed.* **2007**, *46*, 8644–8648.
- 66 Omelas, C.; Salmon, L.; Ruiz, J.; Astruc, D. "Click" Dendrimers: Synthesis, Redox Sensing of Pd(OAc)₂, and Remarkable Catalytic Hydrogenation Activity of Precise Pd Nanoparticles Stabilized by 1,2,3-Triazole-Containing Dendrimers. *Chem.—Eur. J.* **2008**, *14*, 50–64.
- 67 Omelas, C.; Ruiz, J.; Salmon, L.; Astruc, D. Sulfonated "Click" Dendrimer-Stabilized Palladium Nanoparticles as Highly Efficient Catalysts for Olefin Hydrogenation and Suzuki Coupling Reactions Under Ambient Conditions in Aqueous Media. *Adv. Syn. Catal.* **2008**, *350*, 837–845.
- 68 Omelas, C.; Diallo, A. K.; Ruiz, J.; Astruc, D. "Click" Polymer-Supported Palladium Nanoparticles As Highly Efficient Catalysts for Olefin Hydrogenation and Suzuki Coupling Reaction under Ambient Conditions. *Adv. Synth. Catal.* **2009**, *351*, 2147–2154.
- 69 Percec, V.; Johansson, G.; Ungar, G.; Zhou, J. Fluorophobic Effect Induces the Self-Assembly of Semifluorinated Tapered Monodendrons Containing Crown Ethers into Supramolecular Columnar Dendrimers Which Exhibit a Homeotropic Hexagonal Columnar Liquid Crystalline Phase. *J. Am. Chem. Soc.* **1996**, *118*, 9855–9866.
- 70 Diallo, A. K.; Boisselier, E.; Liang, L.; Ruiz, J.; Astruc, D. Dendrimer-Induced Molecular Catalysis in Water: The Example of Olefin Metathesis. *Chem.—Eur. J.* **2010**, *16*, 11832–11835.
- 71 Deraedt, C.; Salmon, L.; Ruiz, J.; Astruc, D. "Click" Dendrimers As Efficient Nanoreactors in Aqueous Solvent: Pd Nanoparticles Stabilization for Sub-ppm Pd Catalysis of Suzuki-Miyaura Reactions of Aryl Bromides. *Chem. Commun.* **2013**, *49*, 8169–8171.
- 72 Llevot, A.; Astruc, D. Application of Gold Nanoparticles to the Diagnostic and Therapy of Cancer. *Chem. Soc. Rev.* **2012**, *41*, 242–257.
- 73 Deraedt, C.; Salmon, L.; Ruiz, J.; Astruc, D. Efficient Click-Polymer-Stabilized Palladium Nanoparticle Catalysts for Suzuki-Miyaura Reactions of Bromoarenes and Reduction of 4-Nitrophenol in Aqueous Solvents. *Adv. Synth. Catal.* **2013**, *355*, 2992–3001.
- 74 Bronstein, L. M.; Shifrina, Z. B. Dendrimers as Encapsulating, Stabilizing, or Directing Agents for Inorganic Nanoparticles. *Chem. Rev.* **2011**, *111*, 5301–5344.

**Partie 3. Polymères
triazolylbiferrocéniques: synthèse,
réseaux et applications.**

Partie 3. Polymères triazolylbiférocéniques : synthèse, réseaux et applications.

La polycondensation par CuAAC ayant fait ses preuves lors de la synthèse du polymère PEG-trz l'idée suivante était d'effectuer la même synthèse de polymère, mais en présence de deux monomères différents de manière à étendre l'utilité du polymère. Le biférocène possède des propriétés électrochimiques remarquables impliquant trois différents degrés red/ox (Fe(II)/Fe(II), Fe(II)/Fe(III), et Fe(III)/Fe(III)), ce qui conduit à diverses applications (composé électrolytique, composé à valence mixe, composé électrochromique, sonde électrochimique...).⁽¹⁾ La première étape de ce projet consistait à synthétiser le diéthynyl biférocène, un composé connu nécessitant 4 étapes de synthèse dont un couplage d'Ullmann (qui échoua à plusieurs reprises).⁽²⁾ Parallèlement la synthèse du di-azido PEG₄₀₀ a été effectuée. Nous avons décidé d'utiliser le PEG₄₀₀ au lieu d'un simple TEG (comme dans le cas de la partie 2) pour augmenter les chances d'hydrosolubilité. Cependant, le co-polymère résultant de la polycondensation entre le diéthynyl biférocène et le di-azido PEG₄₀₀ n'était pas soluble dans l'eau, ce qui nous a conduit à effectuer la synthèse d'un autre co-polymère, cette fois hydrosoluble, comportant une unité PEG₁₀₀₀. Ces polymères ont été dessinés et utilisés pour stabiliser des PdNPs très actives encore une fois en catalyse de Suzuki-Miyaura, mais aussi employés en électrochimie pour la reconnaissance de cations (étude effectuée par Amalia Rapakousiou), et dans la synthèse de polymères à valence mixe/polymères électrochromiques (étude réalisée par le Dr. Yanlan Wang). Le potentiel d'oxydo-réduction du couple Au(III)/Au(0) étant supérieur à celui du couple Fe(III)/Fe(II) d'un des ferrocènes composant le biférocène, ces polymères PEG-trz-biFc ont servi à réduire Au(III) et stabiliser les AuNPs qui se sont avérées actives en catalyse de réduction du 4-NP en 4-AP.

Cette même méthode de réduction de Au(III) en AuNPs a parallèlement été utilisée lors d'une collaboration avec Amalia Rapakousiou au cours de laquelle la comparaison entre différents types de polymères biférocéniques (poly-styrène-biférocène, poly-norbornène-biférocène et poly PEG-trz-biférocène) a donné des résultats remarquables. Lorsque l'unité biFc se trouve en ramification, la formation d'architectures polymériques en forme de filaments contenant des AuNPs (nanoserpent = image du serpent gobant des AuNPs) au cours du temps est observée par MET. En présence de polymère biFc ne contenant pas de ramification, aucune architecture de ce type n'est visualisée. Ce comportement inhabituel est attribué à la topologie du polymère ainsi qu'à la présence de l'unité biFc ionique oxydée en Fe(III)/Fe(II) par Au(III). Ces différents polymères biFc ont aussi pu être comparés pour d'autres applications (catalyse, reconnaissance électrochimique, etc.).

Références:

1) a) Djeda, R.; Rapakousiou, A.; Liang, L.; Guidolin, N.; Ruiz, J.; Astruc, D. Click syntheses of 1,2,3-triazolylbiferrocenyl dendrimers and the selective roles of the inner and outer ferrocenyl groups in the redox recognition of ATP²⁻ and Pd²⁺. *Angew. Chem. Int. Ed.* **2010**, *49*, 8152–8156; b) Dong, T.-Y.; Chang, S.-W.; Lin, S.-F.; Lin, M.-C.; Wen, Y.-S.; Lee, L. Toward the development of molecular wires: A terpyridine spacer containing polyferrocenylalkyne linkages, *Organometallics* **2006**, *25*, 2018-2024.

Multifunctional Redox Polymers: Electrochrome, Polyelectrolyte, Sensor, Electrode Modifier, Nanoparticle Stabilizer, and Catalyst Template**

Christophe Deraedt, Amalia Rapakousiou, Yanlan Wang, Lionel Salmon, Melanie Bousquet, and Didier Astruc*

Dedicated to Alan H. Cowley on the occasion of his 80th birthday

Abstract: Simple “click” polycondensation metallopolymers of redox-robust bis(ethynyl)biferrocene (biFc) and di(azido) poly(ethylene glycol) (PEG400 and PEG1000) were designed for multiple functions including improvement of water solubility and biocompatibility, the introduction of mixed valency and sensing capabilities, and as nanoparticle stabilizers for catalysis.

The development of sustainable and biocompatible nanomaterials that have a variety of functions is highly desirable.^[1] Here we propose a significant step toward this goal by using biferrocene units to construct water-soluble polymers, which can be used for a variety of applications including sensing and catalysis. Nowadays, a variety of ferrocene-based polymers are known, which exhibit very useful electrochromic properties. For example, orange ferrocene polymers that turn blue upon oxidation to ferricenium were synthesized by ring-opening polymerization of ferrocenophanes by Manners and co-workers.^[2] To strengthen the electron-deficient ferricenium groups in polymers, we have now synthesized biferrocene^[3,4] polymers in which the electron-releasing ferrocene units stabilize the adjacent ferricenium units to produce robust blue-green mixed-valence biferrocenium polymers. In addition to the electrochromic properties, these new metallopolymers have been constructed with poly(ethylene glycol) (PEG) chains that not only introduce water solubility and biocompatibility to the nanomaterials but also provide

reasonable dimensions to make use of the enhanced permeability and retention (EPR) effect to achieve accumulation in cancer cells.^[5] The PEG chains and biferrocene (BiFc) units have been assembled by the copper-catalyzed alkyne–azide 1,3-cycloaddition (CuAAC) reaction (“click” chemistry),^[6,7] generating 1,2,3-triazole (trz) linkages. Indeed, these heterocyclic nitrogen ligands are known to sense and stabilize transition-metal ions such as Pd^{II} and Au^{III}, which in turn are precursors for useful metal nanoparticles (NPs) if the polymer can protectively encapsulate and stabilize them.^[8] Small Pd NPs and Au NPs are efficient catalysts for a variety of reactions, and their stabilization through the triazole-containing polymer would be a fast and efficient way to provide templated catalysts. Depending on the Au^{III} to Au⁰ reduction mode, the size of the Au NPs might be tuned for various applications in catalysis or biomedicine, in which the PEG coating provides additional benefits. Another interesting property of the biferrocene polymers is that the parent unit itself reduces Au^{III} to the polymer-stabilized Au NPs.

The synthesis of the copolymers PEG-trz-biFc **4** [poly(PEG₄₀₀-biFc)] and **5** [poly(PEG₁₀₀₀-biFc)] was achieved by the simple CuAAC “click” reaction between bis-azido-poly(ethylene glycol) with molecular weights of 400 or 1000 g mol⁻¹ (PEG₄₀₀ and PEG₁₀₀₀; **1** and **2**, respectively)^[9] and 1,1'-biethynyl-biFc **3**.^[10] The biferrocene unit provides the electrochemical properties (recognition ability, polyelectrolytic and polyelectrochromic features) while the PEG chains of variable length introduce tunable solubility into the polymer. The 1,2,3-triazole ring constructed by “click” chemistry stabilizes active palladium nanoparticles for catalysis of the Suzuki–Miyaura^[11] reaction, which was performed with as little as 2 to 20 ppm of Pd. Additionally, gold nanoparticles were used to efficiently catalyze the reduction of 4-nitrophenol.

The “click” polymerization (polycondensation) between **1** or **2** and diethyne **3** is carried out at 40 °C over 2 days in THF/H₂O (3:2) using the Sharpless–Fokin catalyst consisting of CuSO₄, H₂O (5 equiv), and sodium ascorbate (NaAsc; Scheme 1). After removal of the copper ions the polymers are precipitated from Et₂O providing **4** as a red-orange air-stable film and **5** as a paste in 78 % and 58 % yield, respectively (see the Supporting Information, SI).

These neutral metallopolymers have been fully characterized by NMR, UV/Vis, and IR spectroscopy, matrix-assisted laser desorption/ionization time-of-flight (MALDI-TOF) mass spectrometry, elemental analysis (EA), cyclic

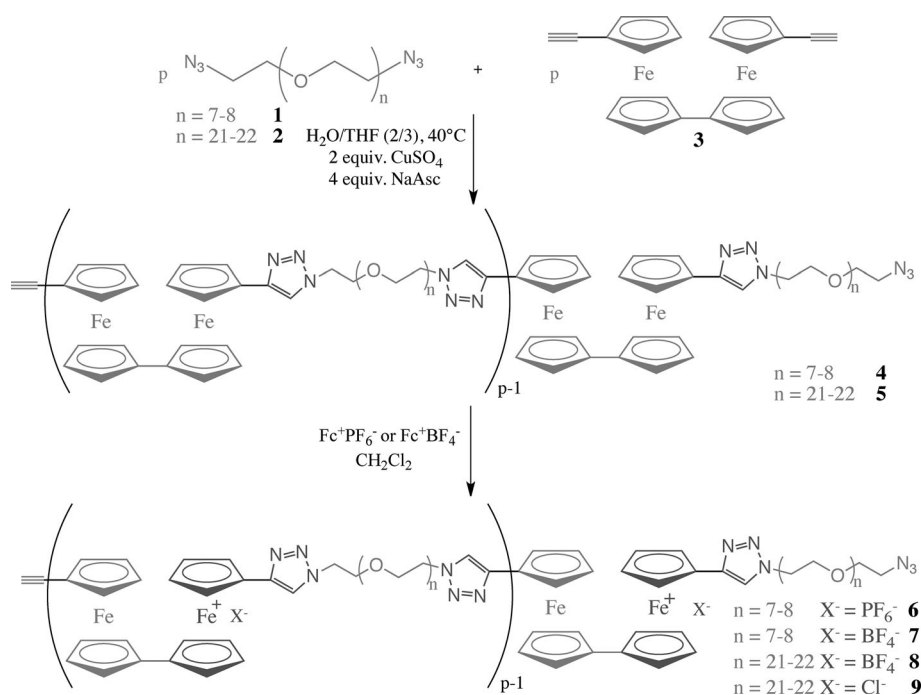
[*] C. Deraedt, A. Rapakousiou, Y. Wang, Prof. D. Astruc
ISM, UMR CNRS N°5255, Univ. Bordeaux
33405 Talence, cedex (France)
E-mail: d.astruc@ism.u-bordeaux.fr
Homepage: <http://astruc.didier.free.fr>

M. Bousquet
Laboratoire de Chimie des Polymères Organiques
UMR CNRS N° 5629, Univ. Bordeaux
33607 Pessac, cedex (France)

Dr. L. Salmon
Laboratoire de Chimie de Coordination UPR CNRS N°8241
31077 Toulouse cedex (France)

[**] Helpful discussions with Dr. J. Ruiz (Univ. Bordeaux) and financial support from the Univ. Bordeaux and Toulouse III, the CNRS, and the Ministère de l'Enseignement Supérieur et de la Recherche (Ph.D. grant to C.D.) are gratefully acknowledged.

Supporting information for this article is available on the WWW under <http://dx.doi.org/10.1002/anie.201403062>.



Scheme 1. Synthesis of the PEG-biFc polymers **4** and **5** and the mixed-valence polymers **6–9**.

voltammetry (CV), and size-exclusion chromatography (SEC) (SI). Mass spectrometry shows that **4** is composed of at least eight co-units, which corresponds to 15 trz rings. No higher polymer has been observed by mass spectrometry presumably due to saturation of the detector with small oligomers. The polydispersity of PEG₁₀₀₀ prevents the observation of **5** by mass spectrometry. No chain terminus (CH₂-N₃ or -C≡CH) has been observed in the NMR spectra of either polymer. The polymeric nature of **4** and **5** was also confirmed by IR spectroscopy (no vibrations corresponding to azide and alkyne groups were found) and by CV measurements (estimation for **4**: 62 ± 12 co-units; **5**: 131 ± 20 co-units; SI). The dispersity of the polymers was measured by SEC analyses (**4**: D = 1.24 and **5**: D = 1.27) and is particularly low for a polycondensation process, which makes it possible to exclude the formation of macrocycles. If any macrocycles would be formed in small quantities, they would be removed during the precipitation from ether.^[12]

The polymers exhibit a variety of interesting features. First of all, the synthesis is very simple, because only one step is needed from known products, and the CuAAC reaction conveniently yields products, which are easy to purify. Secondly, the use of PEG units introduces biocompatibility, while at the same time the easy availability and simple synthesis from the starting materials **1** and **2** is maintained. Additionally, the use of linear PEG minimizes steric bulk around the trz-biFc-trz units. Thirdly, the “click” chemistry provides triazolyl groups, which are important for the binding of metals and the stabilization of metal NPs. The crucial role of the trz rings in the catalysis by metal NPs is exemplified below.^[13] Finally, the presence of biFc units results in multiple stable redox states, which is the most interesting feature of polymers **4** and **5**. These polymers have multifaceted supra-

molecular properties: because of their redox properties and as stable and isolable mixed-valence compounds, they can act as molecular electron storage systems. Cyclic voltammetry involving the bis(trz-Fc) units has been applied to sense ions with potential applications such as the fabrication of modified electrodes. The solubilization properties of the two polymers with distinct PEG lengths are complementary; indeed **4** is soluble only in CH₂Cl₂, CHCl₃, DMF, whereas due to the long PEG chain, **5** is soluble in many more solvents including THF, MeOH, EtOH, and H₂O.

The cyclic voltammograms of **4** and **5** measured with a Pt electrode in CH₂Cl₂ using 0.1 M [nBu₄N][PF₆] as the supporting electrolyte and decamethylferrocene, [Cp*₂Fe] (Cp* = η⁵-C₅Me₅), as the internal reference show two reversible waves at 0.440 and 0.785 V vs.

[Cp*₂Fe]⁺⁰ (Figure 1 a) and 0.420 and 0.800 V vs. [Cp*₂Fe]⁺⁰ (SI), respectively. The presence of only two reversible waves, like in biferrocene itself, implies that the two Fc moieties of one biFc unit are dependent on each other, whereas each biFc unit is independent of other biFc units. One interesting

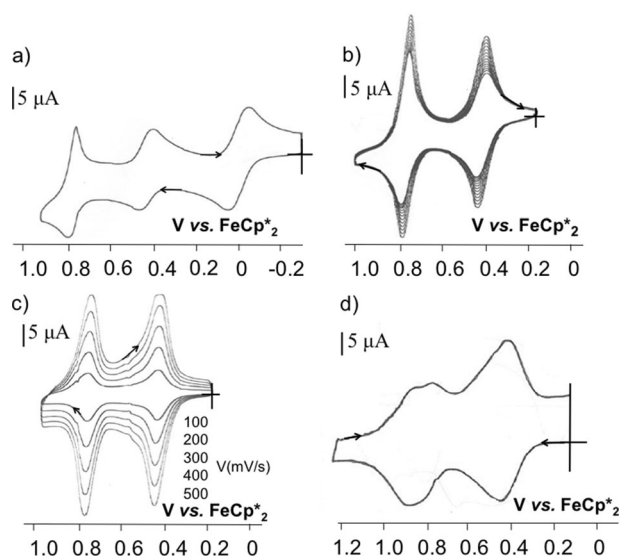


Figure 1. a) Cyclic voltammogram of **4** in CH₂Cl₂; reference electrode: Ag; working and counter electrodes: Pt; scan rate: 0.2 V s⁻¹; supporting electrolyte: [nBu₄N][PF₆]. Two reversible waves are present, one at 0.440 V and a second at 0.785 V. b) Progressive adsorption of **4** upon scanning around the biFc area. c) The modified Pt electrode at various scan rates in a CH₂Cl₂ solution, which only contains the supporting electrolyte. d) Splitting of the second oxidation wave upon addition of Pd(OAc)₂ to **4** (1 equiv of Pd^{II} per BiFc unit).

feature of **4** is its progressive adsorption on the electrode, as can be seen from the cyclic voltammogram (Figure 1 b). This allows the facile formation of robust metallopolymer-modified electrodes upon scanning back and forth around the biFc potential zone (Figure 1 c). Variation of the intensity with the scan rate during the electrode modification provides a linear function as it would be expected for a correctly modified electrode (SI). The adsorption of **5** on the electrode is weaker than that of **4** owing to the better solubility of **5** and its ferricenium form. The CV behavior of **4** allows its use and that of the corresponding modified electrode for ion recognition. After addition of Pd(OAc)₂ to a solution of **4**, a splitting of 70 mV of the second biFc oxidation wave is observed, reflecting the coordination of Pd^{II} to the nitrogen atoms of the trz ligand. This modifies the electron density of the Fc centers (Figure 1 d). The complexation of Pd(OAc)₂ by trz can also be monitored by ¹H NMR spectroscopy in CDCl₃/MeOH (this solvent mixture was also used in the Pd NP catalysis, see below). The ¹H NMR signal of the acetate is shifted upon addition of **4**. This shift is observed until 1 equiv Pd(OAc)₂ per triazolyl ring has been added (SI). The 1:1 stoichiometry of Pd^{II}/trz ligand proves to be important in catalysis (see below), when Pd NPs resulting from the reduction of trz-coordinated Pd^{II} species are used.

The proximity of the Fc moieties in the BiFc units implies another application, which is the synthesis of stable mixed-valence polymers affording electrochromic and polyelectrolyte materials. The mixed-valence polymers **6** and **7** were quantitatively synthesized by stoichiometric exergonic reactions of **4** in CH₂Cl₂ with [Cp₂Fe][PF₆]₂ and [Cp₂Fe][BF₄]₂, respectively, because the redox potential of [Cp₂Fe]⁺⁰ is higher than the first oxidation potential of the biFc⁺⁰ units. An additional driving force for these reactions is the precipitation of the mixed-valence polymers **6** and **7** from CH₂Cl₂. The acetonitrile-soluble polymers **6** and **7** are blue-green, whereas the starting material **4** is orange. Likewise, the mixed-valence polymer **8** was synthesized from **5** in the presence of 1 equiv [Cp₂Fe][BF₄]₂ per biFc unit and fully characterized (SI). The mixed-valence polyelectrolytes **6** and **7** are insoluble in water, whereas **8** is water-soluble. The three polymers were characterized by UV/Vis, FTIR, near-IR, and Mössbauer spectroscopy. The FTIR spectrum of **6** inconveniently contains a band of PF₆⁻ at 841 cm⁻¹, but both the ferrocenyl and the ferricenium groups of the BF₄⁻ polymeric salts **7** and **8** are detected at 818 cm⁻¹ (ν_{Fc}) (compare to 819 cm⁻¹ in **4**) and 832 cm⁻¹ (ν_{Fc*}), respectively (SI), indicating a localized mixed valency even at high IR frequency (10¹³ s⁻¹), which was already observed for the parent biferricenium. Further proof of this class II mixed valency is the presence of absorption bands in the near-infrared range corresponding to a transition from the ground state to the intervalence charge-transfer (IVCT) state (SI). The recorded Mössbauer spectrum of **6** (Figure 2) at zero field and 78 K further confirms the localized class II mixed valency with the presence of both the ferrocenyl and the ferricenium groups, which was expected since this spectroscopic method covers lower frequencies (10⁷ s⁻¹) than IR. Finally in the UV/Vis spectra the λ_{max} of **6–8** (ca. 600 nm) was strongly shifted relative to the λ_{max} of **4** and **5** (ca. 456 nm) (SI).

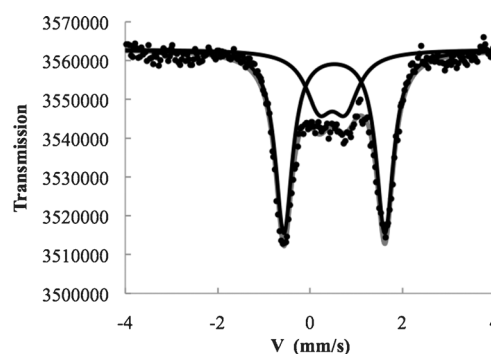


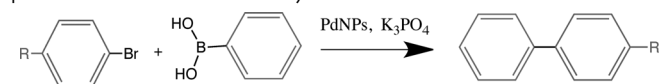
Figure 2. Mössbauer spectrum of **6** at zero field and 78 K showing the localized class II mixed valency at 10⁷ s⁻¹ with both ferrocenyl (doublet I.S. = 0.536 mm s⁻¹ vs. Fe; Q.S. = 2.192 mm s⁻¹) and ferricenium groups (doublet I.S. = 0.490 mm s⁻¹ vs. Fe; Q.S. = 0.571 mm s⁻¹).

The presence of triazole units in the polymer chains allows the coordination of 1 equiv Pd^{II} or Au^{III} ions per heterocycle ligand (see above and SI) and further reduction leads to the formation of polymer-stabilized Pd NPs and Au NPs, respectively. These nanomaterials were shown to be active catalysts for various reactions. In addition, it was shown that the longer PEG chains in **5** (PEG₁₀₀₀) result in the solubilization of these stabilized NPs in water.

The Suzuki–Miyaura reaction has been conducted in the presence of Pd NPs stabilized by **4** and **5**. Polymer **4** is mixed with Pd(OAc)₂ (1 equiv per triazole unit) in CHCl₃/MeOH (2/1) and stirred for 5 min. Then NaBH₄ (10 equiv per Pd^{II}) is added to the solution, leading to the formation of black Pd NPs. These stable Pd NPs at a loading of 0.25 mol % Pd are efficient in the Suzuki–Miyaura cross-coupling reaction of various bromoarenes with phenylboronic acid (Table 1) in CHCl₃/MeOH (2:1) at 90 °C for 16 h. The water-soluble Pd NPs stabilized by **5** are prepared by mixing aqueous solutions of **5** and K₂PdCl₄ at 20 °C and stirring for 5 min (1/1 Pd/triazole stoichiometry) followed by the quick addition of a NaBH₄ solution (10 equiv per Pd^{II}). The yellow solution of Pd^{II}-**5** instantaneously turned orange-brown (SI), confirming the formation of Pd NPs. Transmission electron microscopy (TEM) reveals that the size of Pd NPs stabilized by **5** is (2.3 ± 0.6) nm after they had been stored for one month, which is ideal for efficient catalysis (Figure 3).

The Suzuki–Miyaura reaction has also been performed with this catalyst system, using the “greener” solvent mixture EtOH/H₂O (1:1) at 80 °C for 24 h with only 20 ppm of Pd (Pd NPs). The results are summarized in Table 1 and demonstrate the high activity of **5**-PdNPs. A loading of only 20 ppm Pd is sufficient to obtain good yields using both activated as well as deactivated bromoarenes. Moreover, the amount of Pd can be further reduced. In the case of the coupling of 4-bromoacetophenone and phenylboronic acid at 80 °C only 2 ppm of Pd was necessary to achieve a reaction yield of 82 % after 36 h (TON = 410 000, TOF = 11 400 h⁻¹). The use of such a low amount of catalyst is very rare in the Suzuki–Miyaura reaction, further underlining the interesting properties of the nanomaterial described here. A comparative table (SI) positions **5**-PdNPs as one of the best catalysts known for the Suzuki–Miyaura reaction.

Table 1: Results of the Suzuki–Miyaura reaction of bromoarenes in the presence of Pd NPs stabilized by **4** and **5**.



Bromoarene	Conditions ^[a]	Conv. [%] ^[b]	Yield [%] ^[c]	TON [h ⁻¹]	TOF [h ⁻¹]
R =					
H	A (PdNP-4)	100	99	396	24.8
CH ₃	A (PdNP-4)	100	97	388	24.3
OCH ₃	A (PdNP-4)	98	97	388	24.3
NO ₂	A (PdNP-4)	100	99	396	24.8
CHO	A (PdNP-4)	100	99	396	24.8
COCH ₃	A (PdNP-4)	100	99	396	24.8
H	B (PdNP-5)	100	90	45 000	1875
CH ₃	B (PdNP-5)	100	80	40 000	1667
OCH ₃	B (PdNP-5)	100	78	39 000	1625
NO ₂	B (PdNP-5)	100	91	45 500	1896
CHO	B (PdNP-5)	100	91	45 500	1896
COCH ₃	B (PdNP-5)	100	99	49 500	2062

[a] Conditions A: the reactions were carried out with 1 mmol of bromoarene, 1.5 mmol of phenylboronic acid, 2 mmol of K₃PO₄, and 0.25 mol % of Pd NPs stabilized by **4** in 3 mL of CHCl₃/MeOH (2:1) for 16 h at 90 °C. Conditions B: the reactions were carried out with 1 mmol of bromoarene, 1.5 mmol of phenylboronic acid, 2 mmol of K₃PO₄, and 0.002 mol % of Pd NPs stabilized by **5** in 6 mL of EtOH/H₂O (1:1) for 24 h at 80 °C. [b] The conversion was determined by ¹H NMR analysis. [c] Yield of isolated product.

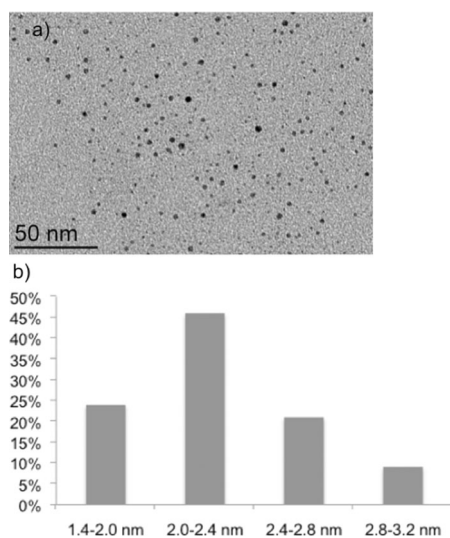


Figure 3. a) TEM image of Pd NPs stabilized by **5**. b) Size distribution of the Pd NPs present in the TEM picture (average size of 103 Pd NPs: (2.3 ± 0.6) nm).

Polymer **5** is oxidized to the mixed-valence water-soluble polyelectrolyte **9** when 1 equiv HAuCl₄ is added per 3 equiv biferrocene unit according to the redox stoichiometry, thereby forming Au⁰ atoms that give polymer-stabilized Au NPs. Due to the plasmon absorption, which is detected by UV/Vis spectroscopy at 534 nm (SI) the Au NPs solution presents a purple coloration. TEM analysis shows that these Au NPs have an average size of around (12 ± 2) nm

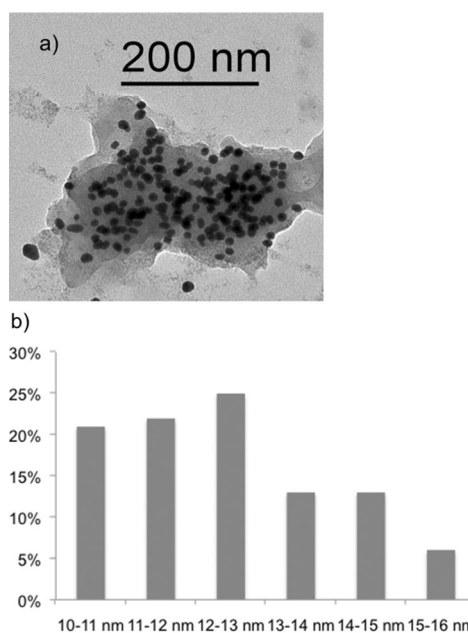


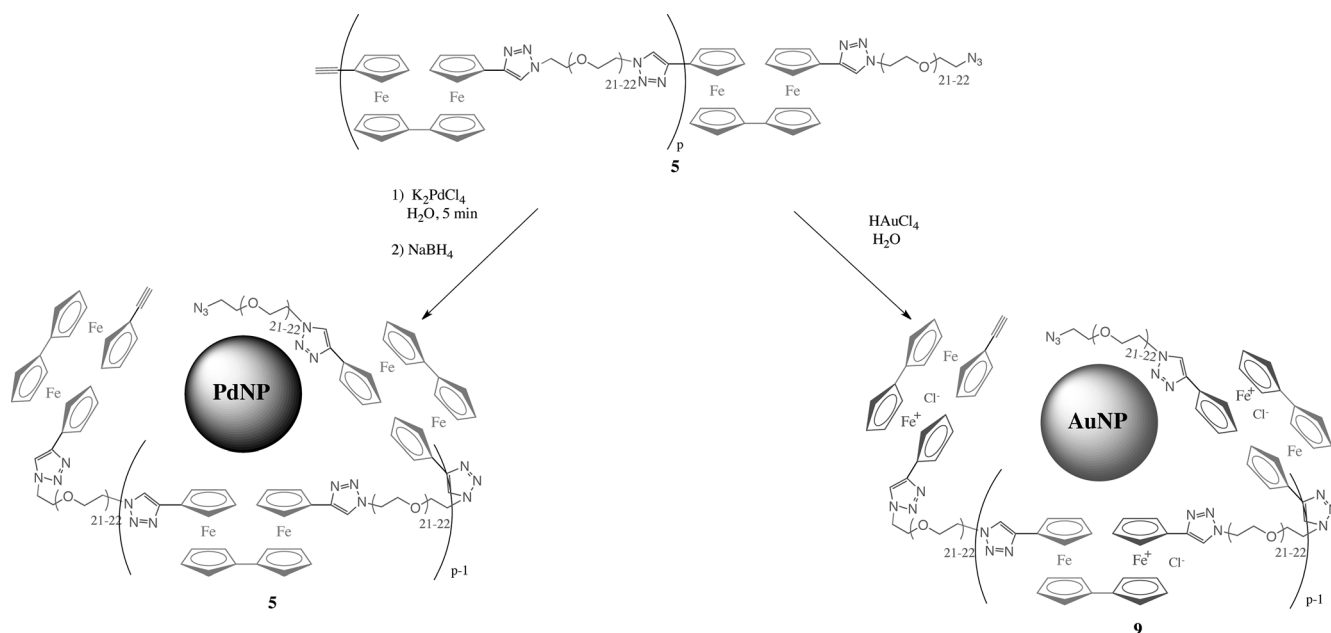
Figure 4. a) TEM image of Au NPs synthesized by reduction of Au^{III} with **5**. b) Size distribution of the Au NPs present in the TEM picture (average size of 98 Au NPs: (12 ± 2) nm).

(Figure 4). Scheme 2 shows the reduction and stabilization of both **5**-PdNPs and **5**-AuNPs. The Au NPs (0.6–1.2 mol %) were used to catalyze the reduction of 4-nitrophenol to 4-aminophenol by an excess of NaBH₄; 4-aminophenol is a potential industrial intermediate in the production of many analgesic and antipyretic drugs, anticorrosion lubricants, and hair dyeing agents.^[14] When 1.2 mol % of Au NPs is used, the reaction is complete within 350 seconds, which corresponds to a k_{app} value of $6.0 \times 10^{-3} \text{ s}^{-1}$. The reaction rate constant k_{app} is calculated using the rate equation $-\ln(C_t/C_0) = k_{app}t$ (the catalyst exhibits pseudo-first-order kinetics; SI).

In conclusion, the two copolymers **4** and **5** synthesized by “click” polycondensation show multifunctional properties as polyelectrolytes and electrochromes, redox sensors for transition-metal cations, electrode modifiers, and excellent templates for the synthesis of efficient Pd and Au nanoparticle catalysts. The biferrocene unit provides a more stable ferricenium form than the parent ferricenium, which makes the polymers ideal as class II mixed-valence polyelectrolytes and electrochromes. The proximity of the triazole ring to the biFc units facilitates redox sensing as well as the understanding of the stoichiometry of metal cation complexation. The stabilization and solubilization of Pd NPs and Au NPs by easily available polymers yield extremely efficient catalysts for current organic reactions.

Received: March 6, 2014
Published online: May 28, 2014

Keywords: biferrocenes · click chemistry · heterogeneous catalysis · nanoparticles · polymers



Scheme 2. Synthesis of Pd NPs (left) and Au NPs (right).

- [1] a) J.-M. Lehn, *Science* **2002**, 295, 2400–2403; b) J. C. Love, L. A. Estroff, J. K. Kriebel, R. G. Nuzzo, G. M. Whitesides, *Chem. Rev.* **2005**, 105, 1103–1169; c) M. R. Langille, M. L. Personick, C. A. Mirkin, *Angew. Chem.* **2013**, 125, 14158–14189; *Angew. Chem. Int. Ed.* **2013**, 52, 13910–13930; d) D. Astruc, *Nat. Chem.* **2012**, 4, 255–267.
- [2] a) E. M. Leitao, T. Jurca, I. Manners, *Nat. Chem.* **2013**, 5, 817–829; b) R. Rulkens, A.-J. Lough, I. Manners, S. R. Lovelace, C. Grant, W. E. Geiger, *J. Am. Chem. Soc.* **1996**, 118, 12683–12695.
- [3] a) D. O. Cowan, F. Kaufman, *J. Am. Chem. Soc.* **1970**, 92, 219–220; b) T. Yamamoto, T. Morikita, T. Maruyama, *Macromolecules* **1997**, 30, 5390–5396.
- [4] a) Y. Men, K. Kubo, M. Kurihara, H. Nishihara, *Phys. Chem. Chem. Phys.* **2001**, 3, 3427–3430; b) M. Yamada, H. Nishihara, *Chem. Commun.* **2002**, 2578–2579; c) M. Yamada, H. Nishihara, *Eur. Phys. J. D* **2003**, 24, 257–260; d) C. A. Nijhuis, K. A. Dolatowska, B. Jan Ravoo, J. Huskens, D. N. Reinhoudt, *Chem. Eur. J.* **2007**, 13, 69–80; e) R. Djeda, A. Rapakousiou, L. Liang, N. Guidolin, J. Ruiz, D. Astruc, *Angew. Chem.* **2010**, 122, 8328–8332; *Angew. Chem. Int. Ed.* **2010**, 49, 8152–8156.
- [5] a) I. Brigger, C. Dubernet, P. Couvreur, *Adv. Drug Delivery Rev.* **2002**, 54, 631–651; b) A. Llevot, D. Astruc, *Chem. Soc. Rev.* **2012**, 41, 242–257.
- [6] a) V. V. Rostovtsev, L. G. Green, V. V. Fokin, K. B. Sharpless, *Angew. Chem.* **2002**, 114, 2708–2711; *Angew. Chem. Int. Ed.* **2002**, 41, 2596–2599; b) C. W. Tornøe, C. Christensen, M. Meldal, *J. Org. Chem.* **2002**, 67, 3057–3064.
- [7] a) For CuAAC “click” polymer assemblies, see: G. W. Goodall, W. Hayes, *Chem. Soc. Rev.* **2006**, 35, 280–312; b) M. Malkoch, R. Vestberg, N. Gupta, L. Mespouille, P. Dubois, A. F. Mason, J. L. Hedrick, Q. Liao, C. W. Frank, K. Kingsbury, C. J. Hawker, *Chem. Commun.* **2006**, 2774–2776; c) J. E. Moses, A. D. Moorhouse, *Chem. Soc. Rev.* **2007**, 36, 1249–1262; d) P. L. Golas, K. Matyjaszewski, *Chem. Soc. Rev.* **2010**, 39, 1338–1354; e) L. Liang, D. Astruc, *Coord. Chem. Rev.* **2011**, 255, 2933–2945; f) F. Herbst, S. Seiffert, W. H. Binder, *Polym. Chem.* **2012**, 3, 3084–3092; g) M. H. Samiullah, D. Reichert, T. Zinkevich, J. Kressler, *Macromolecules* **2013**, 46, 6922–6935.
- [8] a) C. Ornelas, J. Ruiz, E. Cloutet, S. Alves, D. Astruc, *Angew. Chem.* **2007**, 119, 890–895; *Angew. Chem. Int. Ed.* **2007**, 46, 872–877; b) A. K. Diallo, C. Ornelas, L. Salmon, J. Ruiz, D. Astruc, *Angew. Chem.* **2007**, 119, 8798–8802; *Angew. Chem. Int. Ed.* **2007**, 46, 8644–8648; c) E. Boisselier, A. K. Diallo, L. Salmon, C. Ornelas, J. Ruiz, D. Astruc, *J. Am. Chem. Soc.* **2010**, 132, 2729–2742.
- [9] PEG derivatives **1** and **2** were synthesized from PEG₄₀₀ and PEG₁₀₀₀: L. A. Canalle, S. S. van Berkel, L. T. de Haan, J. C. M. van Hest, *Adv. Funct. Mater.* **2009**, 19, 3464–3470.
- [10] Diethynyl biFc **3** was synthesized from ferrocene: T.-Y. Dong, S.-W. Chang, S.-F. Lin, M.-C. Lin, Y.-S. Wen, L. Lee, *Organometallics* **2006**, 25, 2018–2024.
- [11] a) N. Miyaura, A. Suzuki, *Chem. Rev.* **1995**, 95, 2457–2483; b) J. Hassan, M. Sévignon, C. Gozzi, E. Schulz, M. Lemaire, *Chem. Rev.* **2002**, 102, 1359–1469; c) F. Bellina, A. Carpita, R. Rossi, *Synthesis* **2004**, 2419–2440; d) I. Beletskaya, A. V. Cheprakov, *J. Organomet. Chem.* **2004**, 689, 4055–4082; e) D. Astruc, F. Lu, J. Ruiz, *Angew. Chem.* **2005**, 117, 8062–8083; *Angew. Chem. Int. Ed.* **2005**, 44, 7852–7872; f) D. Astruc, K. Heuzé, S. Gatard, D. Méry, S. Nlate, L. Plault, *Adv. Synth. Catal.* **2005**, 347, 329–338; g) I. Favier, D. Madec, E. Teuma, M. Gomez, *Curr. Org. Chem.* **2011**, 15, 3127–3174; h) *Nanomaterials in Catalysis* (Eds.: P. Serp, K. Philippot), Wiley-VCH, Weinheim, **2013**.
- [12] B. P. Mudraboyina, M. M. Obadia, R. Sood, A. Serghei, E. Drockenmüller, *Chem. Mater.* **2014**, 26, 1720–1726.
- [13] a) C. Deraedt, L. Salmon, J. Ruiz, D. Astruc, *Adv. Synth. Catal.* **2013**, 355, 2992–3001; b) C. Deraedt, D. Astruc, *Acc. Chem. Res.* **2014**, 47, 494–503.
- [14] a) K. Kuroda, M. Haruta, *J. Mol. Catal. A* **2009**, 298, 7–11; b) S. Wunder, Y. Lu, M. Albrecht, M. Ballauf, *ACS Catal.* **2011**, 1, 908–916; c) J. P. Zhang, C. Shao, Z. Zhang, M. Zhang, J. Mu, Z. Guo, Y. Liu, *Nanoscale* **2011**, 3, 3357–3363; d) P. Hervés, M. Pérez-Lorenzo, L. M. Liz-Marzán, J. Dzubiella, M. Ballauf, *Chem. Soc. Rev.* **2012**, 41, 5577–5587; e) A. Shihvare, S. J. Ambrose, H. Zhang, R. W. Purves, R. W. Scott, *Chem. Commun.* **2013**, 49, 276–278.

Mixed-Valent Click Intertwined Polymer Units Containing Biferrocenium Chloride Side Chains Form Nanosnakes that Encapsulate Gold Nanoparticles

Amalia Rapakousiou,[†] Christophe Deraedt,[†] Haibin Gu,[†] Lionel Salmon,[‡] Colette Belin,[†] Jaime Ruiz,[†] and Didier Astruc^{*,†}

[†]ISM, UMR CNRS 5255, Univ. Bordeaux, 351 Cours de la Libération, 33405 Talence Cedex, France

[‡]Laboratoire de Chimie de Coordination, UPR CNRS 8241, 205 Route de Narbonne, 31077 Toulouse Cedex 04, France

S Supporting Information

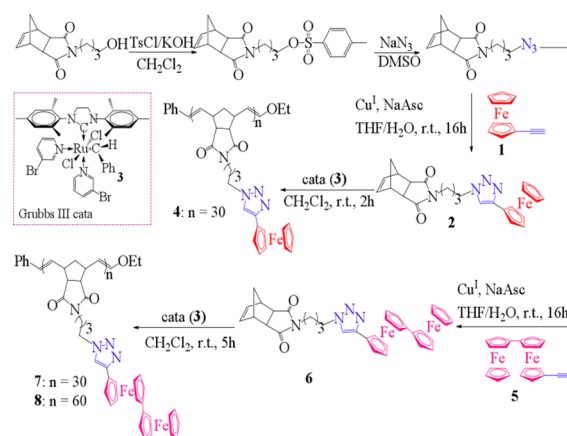
ABSTRACT: Polymers containing triazolylbiferrocene are synthesized by ROMP or radical chain reactions and react with HAuCl₄ to provide class-2 mixed-valent triazolylbiferrocenium polyelectrolyte networks (observed *inter alia* by TEM and AFM) that encapsulate gold nanoparticles (AuNPs). With triazolylbiferrocenium in the side polymer chain, the intertwined polymer networks form nanosnakes, unlike with triazolylbiferrocene in the main polymer chain. By contrast, simple ferrocene-containing polymers do not form such a ferricenium network upon reaction with Au^{III}, but only small AuNPs, showing that the triazolyl ligand, the cationic charge, and the biferrocenium structure are coresponsible for such network formations.

Gold nanoparticles (AuNPs) have attracted considerable interest because of their applications in optics, nano-electronics, nanomedicine, and catalysis depending on their size, shape and stabilizer.¹ Therefore, the way into which specific macromolecules direct such NP formation and assembly including size, shape, and organized network is of paramount importance toward nanoscience applications.² Ferrocene-containing macromolecules³ may be biocompatible candidates for AuNP stabilization owing to the suitably matching redox potentials of ferrocenes and Au^{III} precursors⁴ and the antitumoral properties of various ferrocene derivatives,⁵ although such a strategy has not yet been envisaged. An engineered approach to biferrocene polymer-mediated stabilization and encapsulation of AuNPs is presented here together with the intriguing properties of these new nanomaterials.

A simple way to construct ferrocene polymers is to branch ferrocene to polymerizable monomers by click Cu(I)-catalyzed Azide Alkyne Cycloaddition (CuAAC) reaction using commercial ethynylferrocene **1**.⁶ A ferrocenyl-containing poly-(norbornene) polymer **4** was synthesized using the ring-opening metathesis polymerization (ROMP) of monomer **2** using the third-generation Grubbs catalyst **3**.⁷ The reaction of **4** with HAuCl₄ leads to a triazolylferricenium polymer, but this product rapidly decomposes due to the instability of the ferricenium group under these conditions. Therefore, we subsequently addressed the possibility of using biferrocene, because the mixed-valent biferrocenium cation⁸ is much more robust than

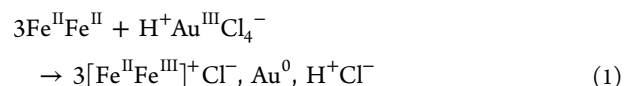
ferricenium (Scheme 1). Thus, low-dispersity biferrocene analogues **7** and **8** of **6** were synthesized identically with **30**

Scheme 1. Synthesis of Biferrocene Polymers **7** and **8** Involving ROMP Initiated by the Ru Metathesis Catalyst “Grubbs III”



and 60 triazolylbiferrocene units, respectively. These polymers were characterized by ¹H and ¹³C NMR including HSQC 2D, HMBC 2D, and NOESY 2D NMR (Supporting Information (SI)) and cyclic voltammetry showing only the two chemically and electrochemically reversible waves of the biferrocenyl units at 0.42 and 0.75 V⁸ due to the absence of intramolecular electronic interaction among the multiple biferrocenyl units.

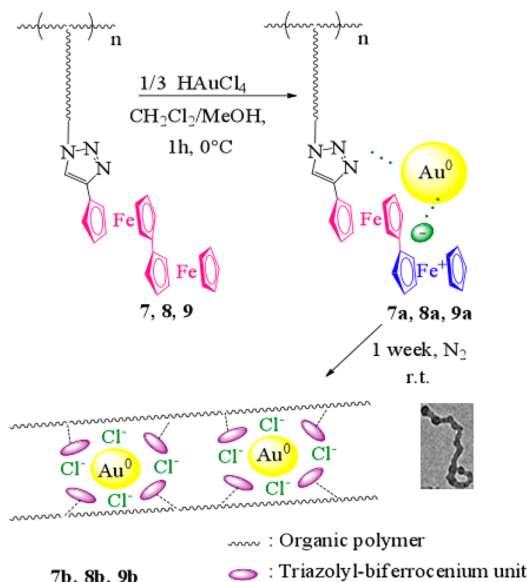
The reactions of these biferrocene polymers with HAuCl₄ in dichloromethane–methanol provided the formation of Au⁰NP-containing nanostructures **7a** and **8a** that were stabilized by the green mixed-valent triazolylbiferrocenium polymer **7⁺**,Cl⁻ or **8⁺**,Cl⁻ (Scheme 2) according to the stoichiometry of eq 1:



IR spectroscopy of **7a** and **8a** shows the presence of both Fe^{II} (ferrocene C–H bending, 813 cm⁻¹) and Fe^{III} (ferricenium C–

Received: August 2, 2014

Published: September 25, 2014

Scheme 2. Formation of Biferrocenium Chloride Polymer-Encapsulated AuNPs upon Reaction of 7, 8, or 9 with H₂AuCl₄


H bending, 834 cm^{-1}), near-infrared spectroscopy shows the presence of the intervalent charge-transfer band at $\lambda_{\text{max}} = 1558$ nm, characteristic of class-II mixed valency,⁹ and CV shows the same waves as the precursor polymers 7 and 8 (SI).

Incubation for 1 week progressively led to the formation of polymer nanosnakes 7b and 8b (Scheme 2). After only 3 days, the nanosnakes are not yet formed, but their nanostructuration appears in progress by TEM (SI, p S74). Finally, the isolated nanosnakes shown in Figure 2a presents a thickness of 8.7 nm \pm 1.5 nm, a length of 210 \pm 15 nm, and encapsulated 11 spherical AuNPs of 13.5 \pm 1.5 nm size observed by transmission electron microscopy (TEM) with inter-AuNP distances of 5.2 \pm 3 nm. The formation of polymer nanosnakes is taken into account by the electrostatic repulsion between the cationic biferrocenium units that is characteristic of polyelectrolytes.¹⁰

At this point, it was necessary to investigate the relationship between the polymer structure and the morphology of the AuNPs that are formed upon reaction with H₂AuCl₄. Lengthening the polymer by increasing the number of biferrocene units from 30 in 7 to 60 units in 8 did not provoke a significant morphology change.

The polymer framework was modified otherwise by designing another monosubstituted polymer 9 containing biferrocenyl units in the side chain. The CuAAC “click” reaction with ethynylbiferrocene 5 and a polystyrene core with an azido terminus catalyzed by [Cu^Itren(benzyl)₆], 10,¹¹ provided the triazolylbiferrocene polymer 9 (Figure 1).

Upon treatment of 9 (containing approximately 30 biferrocene units; see SI, pp S48, S53, and S56) with H₂AuCl₄ followed by incubation for 1 week under the same conditions as those with 7 and 8, the isolated biferrocenium-containing

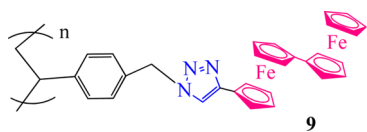


Figure 1. Polystyrene-derived polymer containing the biferrocene units in the side chain synthesized by “click” CuAAC reaction.

polymer nanosnake 9b presented in TEM a length of 269 \pm 10 nm, a thickness of 8.5 \pm 2 nm and contained 14 AuNPs of 14.5 \pm 1.5 nm size with inter-AuNP distances of 13.5 \pm 1.5 nm (Figure 2b). Thus, the similarity of nanosnakes 7b, 8b, and 9b that

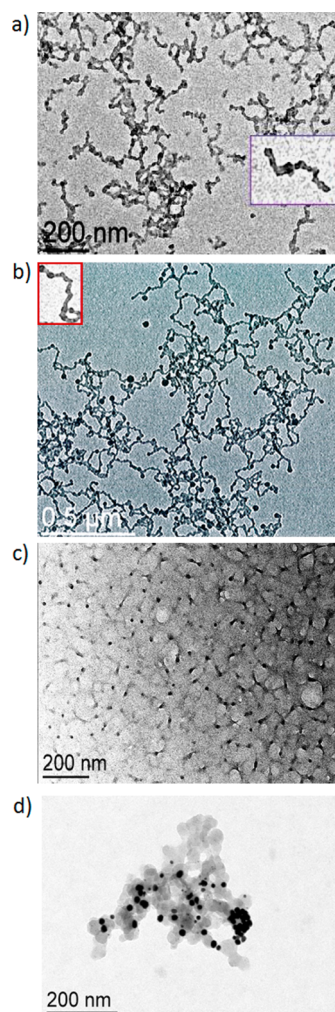


Figure 2. TEM of (a) 8b, (b) 9b, (c) 13b, and (d) 9c.

encapsulate spherical AuNPs obtained with the two very distinct types of polymerization and distinct polymer length showed that the nanosnake formation does not significantly depend on these parameters. Reduction of 9b by NaBH₄ to its neutral biferrocenyl form 9c leads to flocculation, and TEM (Figure 2d) shows AuNPs of the same size as in the case of 9b, but the network is destroyed due to the absence of electrostatic contribution to the AuNPs stabilization.

Another drastic structural modification is the incorporation of the biferrocenyl unit in the main polymer chain instead of the side chain. Thus, such a disubstituted biferrocene-diyl polymer 13 was prepared by CuAAC polycondensation of bis(azido) triethylene glycol 11 with bis(ethynyl)biferrocene 12 (Scheme 3).^{4b}

Reactions of these polymers with H₂AuCl₄ were carried out analogously and also provided AuNPs that are stabilized and encapsulated by mixed-valent biferrocenium chloride polymers 13a (Scheme 4). Incubation showed that the polymer containing bis(triazolylbiferrocenium) in the main chain led to a well-organized non-nanosnake network 13b (TEM, Figure 2c). It can be concluded that the nanomaterial containing biferrocenium

In conclusion, it has been shown that the first metallopolymers containing biferrocene in the side chain synthesized with various structures by ROMP with the Grubbs-III metathesis catalyst or radical chain form, upon oxidation with HAuCl_4 in dichloromethane–methanol followed by one-week incubation, class-II mixed-valent biferrocenium chloride nanosnake polymers that encapsulate AuNPs. With biferrocene in the main polymer chain, a non-nanosnake network that encapsulates AuNPs also forms, but only small AuNPs without a polymer network are observed by TEM when polyferrocene without a triazolyl substituent synthesized by ROMP is oxidized by HAuCl_4 . This shows that the combination of the triazole ligand and the positive charge of the biferrocenium polymer are responsible for the AuNP encapsulation. The nanosnake formation by intertwining polymers is specific to electrolyte metallopolymers with triazolylbiferrocenium in the side chain. This nanoengineering strategy involving structural and electrostatic parameter variations shows that AuNP wrapping and encapsulation by metallopolymers can control networks eventually forming nanosnakes. Applications are forecasted for the control and visualization of polymers and nanostructures.

■ ASSOCIATED CONTENT

■ Supporting Information

Experimental methods, 1D and 2D (^1H) and (^{13}C) NMR spectroscopy, infrared, UV–vis, and mass spectra, SEC, DLS, cyclic voltammograms, TEM and AFM data. This material is available free of charge via the Internet at <http://pubs.acs.org>.

■ AUTHOR INFORMATION

Corresponding Author

didier.astruc@u-bordeaux.fr

Notes

The authors declare no competing financial interest.

■ ACKNOWLEDGMENTS

Helpful assistance and discussions with Claire Mouche (mass spectrometry, CESAMO) and Noël Pinaud (2D NMR spectroscopy, CESAMO, University of Bordeaux) and financial support from the University of Bordeaux, the Centre National de la Recherche Scientifique (CNRS), and L'Oréal are gratefully acknowledged.

■ REFERENCES

- (1) (a) Haruta, M.; Date, M. *Appl. Catal., A* **2001**, *222*, 227. (b) Cao, Y. W. C.; Jin, R.; Mirkin, C. A. *Science* **2002**, *297*, 1536–1540. (c) Daniel, M.-C.; Astruc, D. *Chem. Rev.* **2004**, *104*, 293–346. (d) Myroshnychenko, V.; Rodriguez-Fernandez, J.; Pastoriza-Santos, I.; Funston, A. M.; Novo, C.; Mulvaney, P.; Liz-Marzan, L. M.; de Abajo, F. J. G. *Chem. Soc. Rev.* **2008**, 1792–1805. (e) Xia, Y.; Xiong, B.; Lim, S. E. *Angew. Chem., Int. Ed.* **2009**, *48*, 60–103. (f) Lal, S.; Clare, S. E.; Halas, N. J. *Acc. Chem. Res.* **2008**, *41*, 1842–1851. (g) Corma, A.; Leyva-Perez, A.; Maria Sabater, J. *Chem. Rev.* **2011**, *111*, 1657. (h) Dimitratos, N.; Lopez-Sanchez, J. A.; Hutchings, G. J. *Chem. Sci.* **2012**, *3*, 20–44. (i) Herves, P.; Perez-Lorenzo, M.; Liz-Marzan, L. M.; Dzubiel, J.; Lu, Y.; Ballauff, M. *Chem. Soc. Rev.* **2012**, *41*, 5577–5587. (j) Li, N.; Zhao, P.; Astruc, D. *Angew. Chem., Int. Ed.* **2014**, *52*, 1756–1789.
- (2) (a) Sau, T. K.; Murphy, C. J. *Langmuir* **2005**, *21*, 2923–2929. (b) DeVries, G. A.; Brunnbauer, M.; Hu, Y.; Jackson, A. M.; Long, B.; Neltner, B. T.; Yzun, O.; Wunsch, B. H.; Stellaci, F. *Science* **2007**, *315*, 358–361. (c) Wang, X. J.; Li, G. P.; Chen, T.; Yang, M. X.; Zhang, Z.; Wu, T.; Chen, H. Y. *Nano Lett.* **2008**, *8*, 2643–2647. (d) Chen, G.; Wang, Y.; Tan, L. H.; Yang, M.; Tan, L. S.; Chen, Y.; Chen, H. *J. Am. Chem. Soc.* **2009**, *131*, 4218–4219. (e) Shen, X.; Chen, L.; Li, D.; Zhu,

L.; Wang, H.; Liu, C.; Wang, Y.; Xiong, Q.; Chen, H. *ACS Nano* **2011**, *5*, 8426–8433. (f) Buck, M. R.; Bondi, J. F.; Schaak, R. E. *Nat. Chem.* **2012**, *4*, 37–44. (g) Buck, M. R.; Schaak, R. E. *Angew. Chem., Int. Ed.* **2013**, *52*, 6154–6178. (h) Wang, Y.; Salmon, L.; Ruiz, J.; Astruc, D. *Nat. Commun.* **2014**, *5*, number 3489. (i) Wang, H.; Song, X.; Liu, C.; He, J.; Chong, W. H.; Chen, H. *ACS Nano* **2014**, *8*, 8063–8073.

- (3) (a) Manners, I. *Science* **2001**, *294*, 1664–1666. (b) Hudson, R. D. *J. Organomet. Chem.* **2001**, *637–639*, 47–69. (c) Wang, X.; Guérin, G.; Wang, H.; Wang, Y.; Manners, I.; Winnik, M. A. *Science* **2007**, *317*, 644–647. (d) Boisselier, E.; Diallo, A. K.; Salmon, L.; Ornelas, C.; Ruiz, J.; Astruc, D. *J. Am. Chem. Soc.* **2010**, *132*, 2729–2742. (e) Astruc, D. *Nat. Chem.* **2012**, *4*, 255–267. (f) Abd-El-Aziz, A. S.; Agatemor, C.; Etkin, N. *Macromol Rapid Commun.* **2014**, *35*, 513–559. (g) Deraedt, C.; Rapakousiou, A.; Wang, Y.; Salmon, L.; Bousquet, M.; Astruc, D. *Angew. Chem., Int. Ed.* **2014**, *53*, 8445–8449.

- (4) Ag nanoparticles have been encapsulated inside block copolymers: (a) Wang, X. S.; Wang, H.; Coombs, N.; Winnik, M. A.; Manners, I. *J. Am. Chem. Soc.* **2005**, *127*, 8924–8925. (b) Wang, H.; Wang, X.; Winnik, M. A.; Manners, I. *J. Am. Chem. Soc.* **2008**, *130*, 12921–12930.

- (5) (a) Ornelas, C. *New J. Chem.* **2011**, *35*, 1973–1985. (b) Graga, S. S.; Silva, A. M. S. *Organometallics* **2013**, *32*, 5626–5639. (c) Jaouen, G.; Top, S. In *Advanced in Organometallic Chemistry and Catalysis*; Pombeiro, A. J. L., Ed.; Wiley: Hoboken, NJ, USA, 2014; pp 563–580.

- (6) (a) Ornelas, C.; Ruiz, J.; Cloutet, E.; Alves, S.; Astruc, D. *Angew. Chem., Int. Ed.* **2007**, *46*, 872–877. (b) Astruc, D.; Liang, L.; Rapakousiou, A.; Ruiz, J. *Acc. Chem. Res.* **2012**, *45*, 630–640.

- (7) (a) Vougioukalakis, G. C.; Georgios, C.; Grubbs, R. H. *Chem. Rev.* **2010**, *110*, 1746–1787. (b) Gu, H.; Rapakousiou, A.; Ruiz, J.; Astruc, D. *Organometallics* **2014**, *33*, 4323–4335.

- (8) (a) Levanda, C.; Cowan, D. O.; Bechgaard, K. *J. Am. Chem. Soc.* **1975**, *97*, 1980–1981. (b) Dong, T. Y.; Lee, T. Y.; Lee, S. H.; Lee, G. H.; Peng, S. M. *Organometallics* **1994**, *13*, 2337–2348. (c) Yamada, M.; Nishihara, H. *Chem. Phys. Chem.* **2004**, *5*, 555–559. (d) Nijhuis, C. A.; Dolatowska, K. A.; Jan Ravoo, B.; Huskens, J.; Reinhoudt, D. N. *Chem.—Eur. J.* **2007**, *13*, 69–80. (e) Djeda, R.; Rapakousiou, A.; Liang, L.; Guidolin, N.; Ruiz, J.; Astruc, D. *Angew. Chem., Int. Ed.* **2010**, *49*, 8152–8156.

- (9) (a) Robin, M. B.; Melvin, B.; Day, P. *Adv. Inorg. Chem. Radiochem.* **1967**, *10*, 247–422. (b) Allen, G. C.; Hush, N. S. *Prog. Inorg. Chem.* **1967**, *8*, 357–389. (c) Richardson, D. E.; Taube, H. *Coord. Chem. Rev.* **1984**, *60*, 107–129.

- (10) (a) Decher, G. *Science* **1997**, *277*, 1232–1237. (b) Paul, C. F. J.; Antonietti, M. *Adv. Mater.* **2003**, *15*, 673–683. (c) Jiang, H.; Taranekekar, P.; Reynolds, J. R.; Shanze, K. S. *Angew. Chem., Int. Ed.* **2009**, *48*, 4300–4316. (d) Lu, J.; Yan, F.; Texter, J. *Prog. Polym. Sci.* **2009**, *34*, 431–448. (e) Couture, G.; Alaeddine, A.; Boschet, F.; Ameduri, B. *Prog. Polym. Sci.* **2011**, *36*, 1521–1557.

- (11) Liang, L.; Ruiz, J.; Astruc, D. *Adv. Synth. Catal.* **2011**, *353*, 3434–3450.

Catalytically-active Palladium Nanoparticles Stabilized by Triazolylbiferrocenyl-containing Polymers

Christophe Deraedt,^[a] Amalia Rapakousiou,^[a] Lionel Salmon,^[b] Jaime Ruiz,^[a]
Didier Astruc^[a]*

^[a] ISM, UMR CNRS 5255, Univ. Bordeaux, 351 Cours de la Libération, 33405 Talence Cedex, France.

^[b] LCC, CNRS, 205 Route de Narbonne, 31077 Toulouse Cedex, France.

Dedicated to the memory of Professor Eberhard W. Neuse

Abstract

Four different triazolylbiferrocenyl-containing polymers are used for the stabilization of palladium nanoparticles (PdNPs) upon reducing triazole-coordinated Pd(II) both in organic solvents and in water. The resulting PdNPs are active in the Suzuki-Miyaura coupling of bromoaromatics even with down to only 20 ppm of Pd. The comparison between the four different polymer-stabilized PdNPs allows concluding that a flexible polyethylene glycol moiety in the linear triazolylbiferrocenyl polymer permits a better stabilization of the PdNPs than polymers containing triazolylbiferrocenyl side chains with a rigid styrene or succinimide moieties.

Keywords

Palladium; nanoparticle, catalysis; polymer; biferrocene; click

Introduction

Catalytically active metallic nanoparticles (MNPs) that result from the reduction of ionic metals M^{n+} to zero-valent metals M^0 must be stabilized by nanosystems in order to avoid aggregation.^[1] Macromolecules such as polymers^[2] and dendrimers^[3] have for a long time fulfilled the role of MNP stabilizers. Following the pioneer work by Crooks' group in which the stabilization of various MNPs by PAMAM dendrimers

and their catalytic activity has been reported,^[3] our group has developed the stabilization of catalytically-active PdNPs by various 1,2,3-triazolyl-containing dendrimers^[4] that were assembled by “CuAAC” click chemistry.^[5] Thereafter, related work has been conducted in which 1,2,3-triazolyl-containing polymers replaced clicked dendrimers for a catalytic purpose bringing the advantage of lower synthesis cost and time.^[6] Poly-azidomethylstyrene has been functionalized first by three different ethynyl-containing molecules (phenyl acetylene, ethynyl ferrocene and the sodium propargyl sulfonate) and then used for the stabilization of small PdNPs (from 1.0 to 2.8 nm). While these PdNPs were active in the alkene hydrogenation catalysis, no quantitative reaction was observed in the Suzuki-Miyaura reaction of carbon-carbon coupling between iodobenzene and phenyl boronic acid.^[6a] Then, polymers that were synthesized by “click” CuAAC polycondensation between a di-azido-poly ethylene glycol (PEG) unit and a di-alkyne-PEG unit were used in the stabilization of PdNPs. This latter family of linear water-soluble polymers stabilized PdNPs (1.6 ± 0.3 nm) that were very active in the Suzuki-Miyaura coupling between bromo-aromatics and phenyl boronic acid even with only 0.0001 % mol of Pd at 80°C in a H₂O/EtOH mixture.^[6b] Now, we are comparing various linear polymers with similar functional groups in the stabilization of PdNPs as catalyst for the Suzuki-Miyaura C-C coupling reaction, in order to delineate the factors that lead to the optimization of the efficiency of this type of catalyst.

Biferrocene has been used in the organometallic field for its electrochemical properties.^[7] Indeed the three main oxidation states of biferrocene (Fe(II)/Fe(II), Fe(III)/Fe(II) and (Fe(III)/Fe(III)) have been applied using the incorporation of biferrocene into metallomacromolecules for various applications (mixed-valency, polyelectrochromes, polyelectrolyte).^[8] Another interest of this molecule is that its monoethynyl and diethynyl derivatives have been successfully synthesized and isolated⁹ contrary to diethynylferrocenes that are not stable. Thus biferrocene has been incorporated into three different polymers by one or two successive “click” CuAAC reactions.^[8e,f] In these polymers, the biferrocenyl or biferrocene-diyl units are located in the lateral chain of two polymers (poly-styrene and poly-norbornene) and in the linear chain of the last kind of polymer synthesized by CuAAC polycondensation. Here these three metallopolymers are used and compared in the stabilization of PdNPs for catalytic application.

Result and discussion

Since the CuAAC “click” reaction is used to synthesize polymers, these macromolecules contain the crucial 1,2,3 triazole that has already been shown in earlier works by cyclic voltammetry and ^1H NMR to quantitatively coordinate to Pd(II) ions.^[10] Poly(styrene-1,2,3 triazolylbiferrocene) **1** and poly(norbornene-1,2,3 triazolylbiferrocene) **2** were previously synthesized by free-radical polymerization with AIBN as initiator and ROMP polymerization with Grubbs 3rd generation catalyst respectively (Figure 1).^[8f] While the synthesis time is comparable between these two polymerization ways, the controllable size of the polymer by ROMP living polymerization is a serious advantage. These two polymers of a relatively similar length, containing biferrocenyl moieties in the lateral chain, were used in the stabilization of PdNPs. These PdNPs were employed in C-C cross coupling reactions in order to compare the effect of the aromatic ring of **1** with that of the succinimide moieties of **2**.

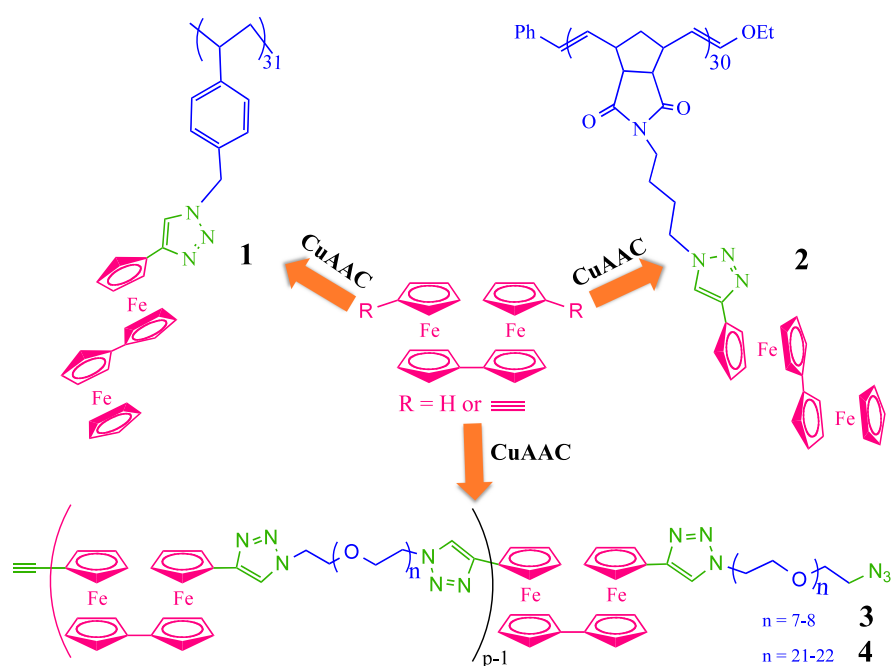


Figure 1. Routes to polymers **1**, **2**, **3** and **4** from ethynyl biferrocene or from diethynyl biferrocene via CuAAC click reaction.

The poly-(PEG₄₀₀-1,2,3-triazolyl biferrocene) **3** and the poly-(PEG₁₀₀₀-1,2,3-triazolyl biferrocene) co-polymer **4** were also previously synthesized by CuAAC polycondensation. The control of the length is quite hazardous for these later polymers, but the dispersity of the two polymers remains very low for a polycondensation process ($D = 1.24$ and $D = 1.27$ revealed by size-exclusion chromatography).^[8e] The advantage of this polycondensation method is that very few steps were required from diethynyl biferrocene to obtain polymers **3** and **4** in comparison with polymers **1** and **2**.

Polymers **1**, **2**, **3** and **4** were used in the synthesis of PdNPs. As only polymer **4** is water soluble, the synthesis of PdNPs were performed in organic solvents. The precursor Pd(OAc)₂, was used as the Pd(II) source, and NaBH₄ was used as the reducing agent of Pd(II) to Pd(0) nanoparticles.^[10] The reduction of Pd(II) with NaBH₄ is supposed to provide triazole-coordinated nanoparticles that are small (in the 1.4 to 3-nm range) in comparison with those obtained using MeOH or heat. As Pd(OAc)₂ is in the form of a trimeric species, MeOH must be used in order to destroy these clusters producing monomeric species that are able to bind the 1,2,3-triazole rings.^[11] As the polymers are not soluble in MeOH alone, CHCl₃ that is a good solubilising solvent with a higher boiling point than that of CH₂Cl₂ was also used in the PdNPs synthesis. Thus the PdNPs synthesis that was previously developed with hydrophobic dendrimers and polymers was followed.^[10] Briefly, nine equivalents of Pd(OAc)₂ in CHCl₃ [$\text{[Pd(OAc)}_2\text{]} = 4.4 \text{ mmol.L}^{-1}$] were added to the hydrophobic polymer (**1**, **2** or **3**) in CHCl₃ ($\text{[polymer]} = 1.3 \text{ mmol.L}^{-1}$), then MeOH was introduced in order to obtain a final concentration [$\text{[Pd(OAc)}_2\text{]} = 0.89 \text{ mmol.L}^{-1}$] and a ratio of CHCl₃/MeOH = 2/1. Then, ten equivalents per Pd(II) of NaBH₄ were added^[12] at r.t. to the solution leading to an instantaneous change of colour from yellow to brown/black characteristic of PdNPs (Figure 2).

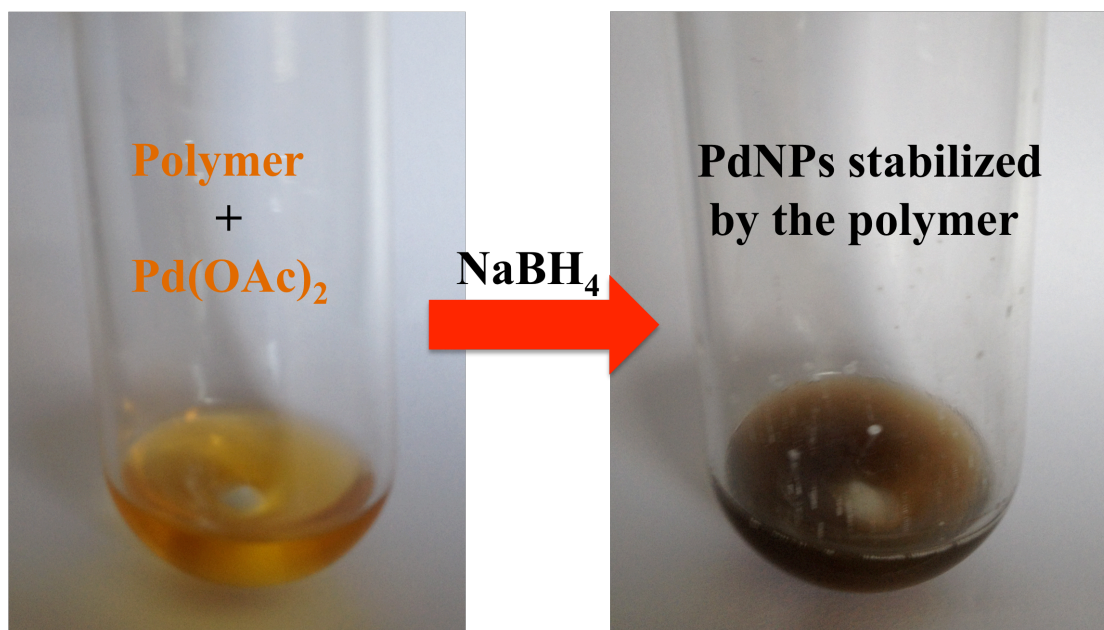


Figure 2. Reduction of Pd(II) to PdNPs with NaBH₄ in the presence of polymer **1** (as example).

The PdNPs that were obtained in this way were sufficiently stable to be analyzed by TEM and this analysis revealed that the size of PdNPs stabilized by **1**, **2** and **3** were 1.4 ± 0.6 nm, 1.4 ± 0.5 nm and 3.0 ± 0.8 nm respectively. After 1 hour a little bit of a precipitate was observed in the solution of the PdNPs stabilized by **2**, allowing to conclude on the positive π -effect on the PdNPs stabilization by the styrenyl moiety of **1**.

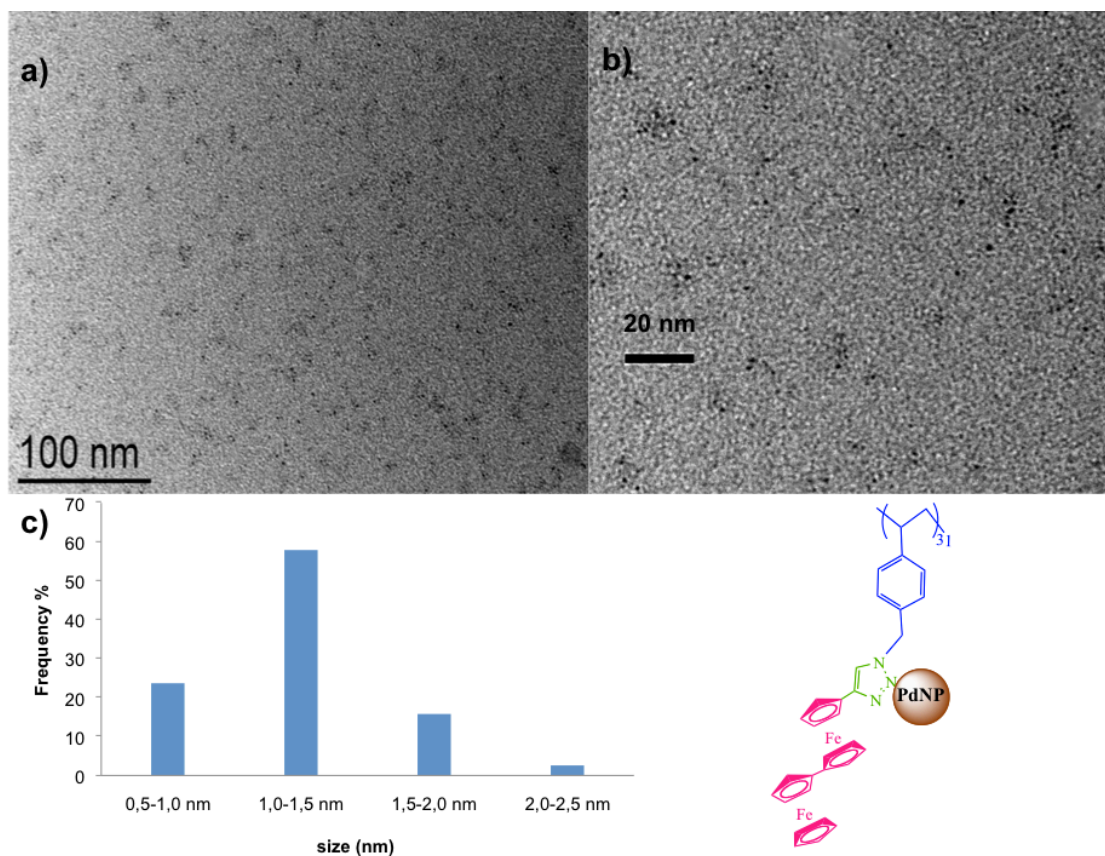


Figure 3. (a) and (b) TEM images of PdNPs stabilized by **1**, with different zoom, (c) PdNPs size distribution (average size 1.4 ± 0.6 nm).

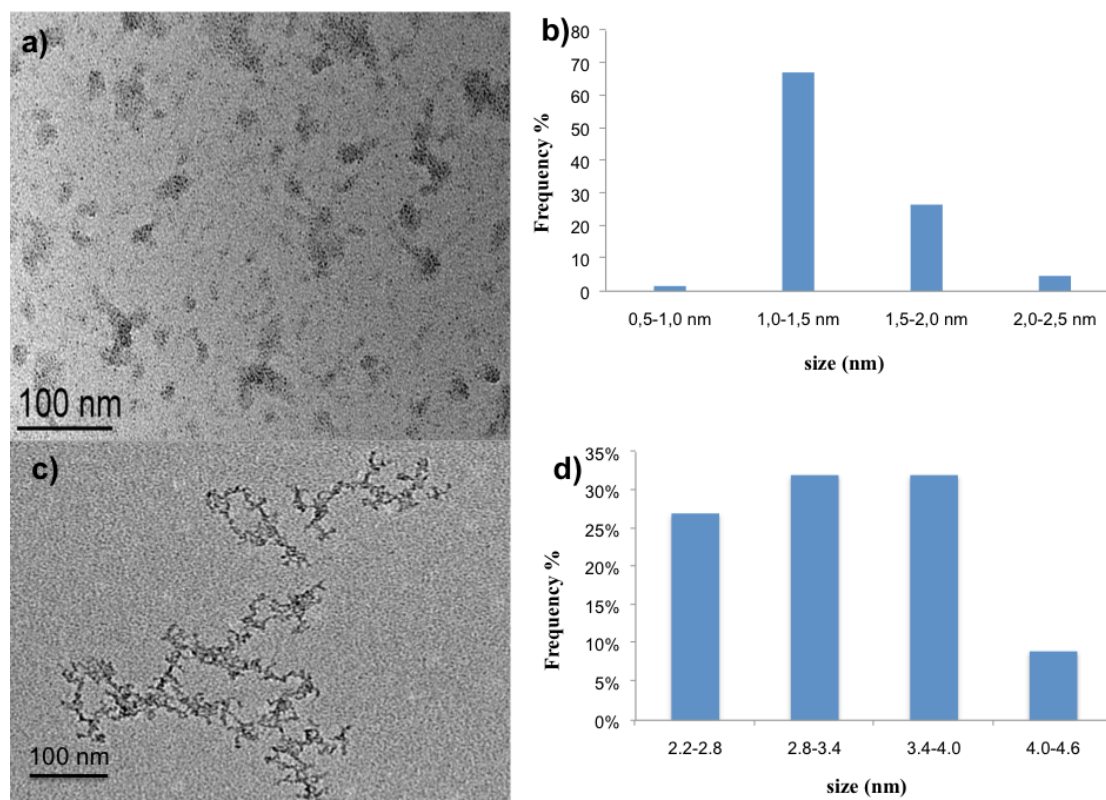


Figure 4. (a),(b) TEM image of PdNPs stabilized by **2** and the distribution of PdNPs (average size 1.4 ± 0.5 nm). (c), (d) TEM image of PdNPs stabilized by **3** and the distribution of PdNPs (average size 3.0 ± 0.8 nm).

Interestingly, the grey part around the PdNPs in the TEM images (figures 3 and 4) is attributed to the biferrocene polymer, showing its encapsulating role in the stabilization process.

The catalytic efficiency of these PdNPs was tested for the Suzuki-Miyaura C-C cross coupling reactions. This reaction has become one of the most well known and powerful Pd⁰ reactions allowing the synthesis of biaryl compounds, such as natural products, pharmaceuticals and polymers.^[13] This reaction has been developed both in industry and academic areas for three main reasons. First, the scope of the protocol can be extended to many functional groups due to the mild reaction conditions, which makes this reaction an attractive one for the total synthesis of complex drug molecules. Second, boron compounds are readily available, stable, and considered to

be non toxic or of low toxicity. Third, the reaction works well with a wide range of substrates. These stable PdNPs in the proportion of 0.25% mol of Pd⁰ are efficient in the Suzuki-Miyaura cross-coupling reaction of various bromoarenes with phenylboronic acid (equation 1, table 1) at 90°C during 16h in CHCl₃/MeOH (2/1).

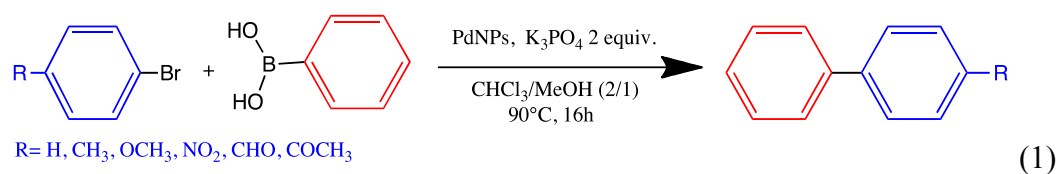


Table 1. Suzuki-Miyaura coupling with PdNPs stabilized by **1**, **2** or **3**.^[a]

entry	R	Poly.	Conv. (%)	Yield (%)	TON	TOF (h ⁻¹)
1	H	1	100	95	380	23.8
2	H	2	20	18	72	4.5
3	H	3	100	99	396	24.8
4	CH ₃	1	61	60	264	10.2
5	CH ₃	2	15	10	40	3.1
6	CH ₃	3	100	97	388	24.3
7	OCH ₃	1	15	15	60	3.8
8	OCH ₃	2	13	10	40	3.1
9	OCH ₃	3	98	97	388	24.3
10	NO ₂	1	92	91	364	22.8
11	NO ₂	2	66	64	256	10
12	NO ₂	3	100 ^[b]	99	396	24.8
13	CHO	1	74	70	280	17.5
14	CHO	2	42	40	160	10
15	CHO	3	100	99	396	24.8
16	COCH ₃	1	100	99	396	24.8
17	COCH ₃	2	89	88	252	22
18	COCH ₃	3	100	99	396	24.8

[a] The reactions were carried out with 1 mmol of bromoarene, 1.5 mmol of phenyl boronic acid, 2 mmol of K₃PO₄, 0.25 mol % of PdNPs stabilized by **1**, **2** or **3**, in 3 mL of CHCl₃/MeOH (2/1) during 16h at 90°C. [b] the same reaction was carried out with Pd(OAc)₂ + **3** without pre-reduction with NaBH₄, and a 96% of conversion was observed.

The three different PdNPs synthesized from polymers **1**, **2** and **3** were compared under the same conditions for six different bromoarenes. The activity of PdNPs/**1** in the Suzuki-Miyaura coupling is relatively good, especially for activated bromo arenes (entries 10 and 16) and for the neutral bromobenzene (entry 1), whereas only activated 4-bromoacetophenone shows a quite quantitative reaction with PdNPs/**2** (entry 17). As the size of PdNPs/**1** and PdNPs/**2** are equal, the activity was attributed to the stability of these PdNPs at high temperature. On the other hand, the Suzuki-Miyaura reaction carried out with PdNPs/**3** was successful with activated bromoarenes (entries 12, 15, and 18) as well as deactivated bromoarenes (entries 6, and 9). Again the activity is not directly linked to the size of the PdNPs, which in this case was larger than the PdNPs stabilized by **1** or by **2**. The excellent efficiency of these PdNPs is certainly due to their good stability at high temperature and is related to the flexible PEG₄₀₀ co-units and/or to the presence of 1,2,3-triazole in the main linear chain (not in the lateral chain). As PEG₄₀₀ is composed of lot of oxygen atoms, the great stability of PdNPs/**3** could be also linked to these numerous electron-rich atoms.

As mentioned above, the co-polymer **4** is the only polymer in the series studied here that is soluble in water allowing the synthesis of PdNPs in water, which is ideal from an ecological point of view. Thus another PdNPs synthesis was conducted in this case. As Pd(OAc)₂ is not soluble in water, K₂PdCl₄ served as the Pd(II) source. After mixing the polymer **4** in water, 1 equivalent of Pd(II) per 1,2,3-triazole was added under N₂ at r.t. leading to a concentration [Pd(II)] = 0.1 mmol.L⁻¹, then 10 equivalents of NaBH₄ in water per Pd(II) (29 mmol.L⁻¹) was quickly added, leading to an instantaneous change of colour from yellow to golden brown, which is characteristic of PdNP formation. The same [Pd(II)] addition as in the first synthesis described above was not followed in this case, because it would lead to a direct precipitation of PdNPs, thus a more diluted solution was employed. TEM reveals that the size of the PdNPs is 2.3 ± 0.6 nm.

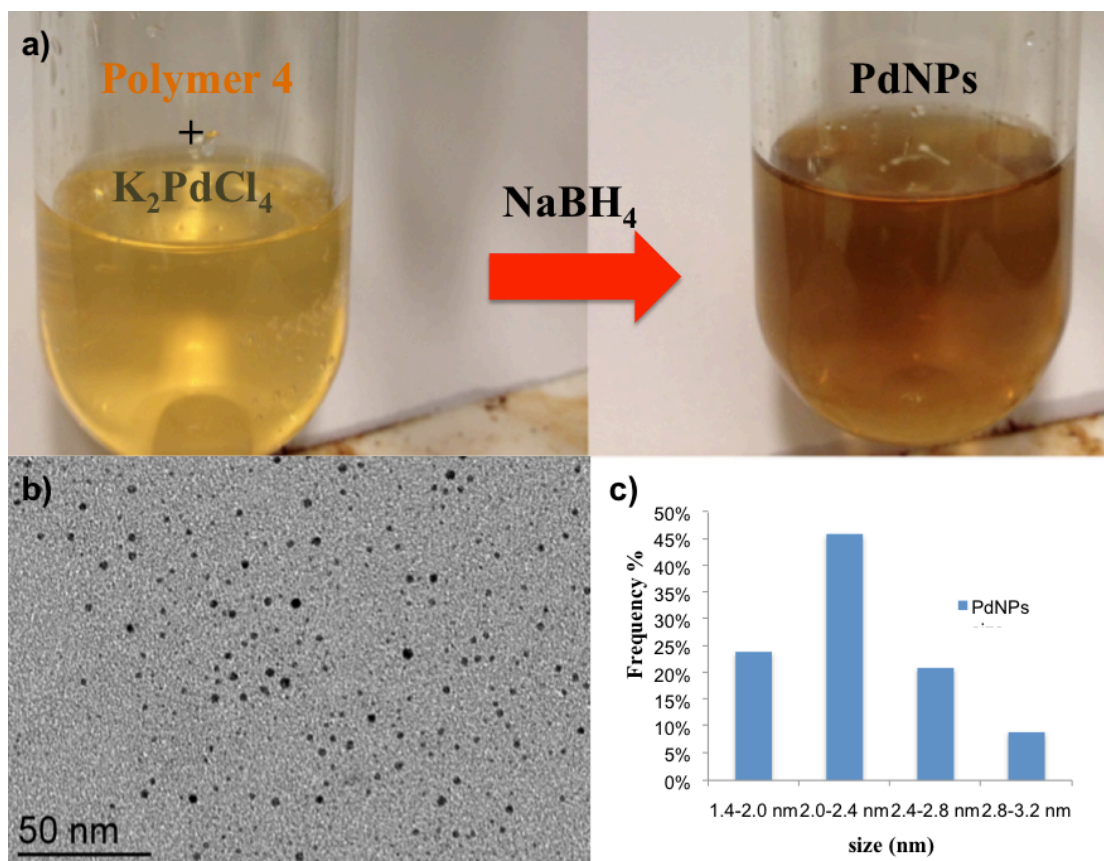


Figure 5. (a) Reduction of Pd(II) to PdNPs with NaBH₄ in the presence of polymer 4. (b), (c) TEM image and size distribution of PdNPs stabilized by 4.

The Suzuki-Miyaura reaction has also been performed with this system, but now in the greener solvent mixture EtOH/H₂O (1/1) at 80°C during 24h with only 20 ppm of Pd (PdNPs) (equation 1 and table 2).

The results summarized in Table 2 are impressive, because the amount of PdNPs/4 used was only 20 ppm of Pd⁰ and the reactions proceeded in good yields with both activated and deactivated bromoarenes. Additionally, the amount of Pd was further reduced. In the case of the coupling between 4-bromoacetophenone and phenyl boronic acid at 80°C, when only 2 ppm of Pd was used, the reaction yield was 82% after 36 hours (TON = 410 000, TOF = 11 400 h⁻¹, entry 25). A low amount of PdNP catalyst used here is very rare in the Suzuki-Miyaura reaction (see reference 6b for a comparative table). At the high catalyst concentration (0.25 mol%), Pd^{II} is also an efficient catalyst (see Table 1), but at such very catalyst concentration as 20 ppm, only pre-reduced Pd catalyst to PdNP is efficient, as already shown previously.^[14] In fact, it is well-known that at 80°C, Pd^{II} is reduced in situ to PdNP.^[10]

Table 2. Suzuki-Miyaura coupling with PdNPs stabilized by **4**.^[a]

Entry ^[14]	R	polymer	Conv. (%)	Yield (%)	TON	TOF (h ⁻¹)
19	H	4	100	90	45 000	1 875
20	CH ₃	4	100	80	40 000	1 667
21	OCH ₃	4	100	78	39 000	1 625
22	NO ₂	4	100	91	45 500	1 896
23	CHO	4	100	91	45 500	1 896
24	COCH ₃	4	100	99	49 500	2 062
25 ^[b]	COCH ₃	4	85	82	410 000	11 400

[a] The reactions were carried out with 1 mmol of bromoarene, 1.5 mmol of phenyl boronic acid, 2 mmol of K₃PO₄, 0.002 mol % of PdNPs stabilized by **4** in 6 mL of EtOH/H₂O (1/1) during 24h at 80°C; [b] same conditions, but with only 0.0002 mol % of PdNPs stabilized by **4**.

Conclusion

Two different syntheses of PdNPs have been presented in organic solvent and in water. The PdNPs synthesis method reserved to water-soluble polymers provides a higher PdNP activity. Through this work, it has been shown that the 1,2,3-triazole rings were responsible for the controlled size of the PdNPs (1.4 nm for PdNPs/**1** and PdNPs/**2** and a little bit more for PdNPs/**3** and PdNPs/**4**) but that other moieties of the polymer play a role in the stabilization at higher temperature, and thus also in the catalytic activity. The polymer (**1**) containing aromatic rings provided a better stabilization of the PdNPs than the polymer (**2**) lacking π -donor groups, whereas the polymers **3** and **4** containing PEG units offered the greatest stability thanks to the oxygen atoms and the flexibility of the chain. PdNPs/**4** present the highest activity leading to TON = 410 000 and TOF = 11 400 h⁻¹.

Experimental section

General data: All the solvents (EtOH, CHCl₃, MeOH, Et₂O) and chemicals (Pd(OAc)₂, K₂PdCl₄, NaBH₄) were used as received.

Synthesis of PdNPs/1: A solution of **1** (2.96 mg, monomer Mw = 553 g. mol⁻¹) in chloroform (4 mL) was introduced into a Schlenk flask under nitrogen. A solution of Pd(OAc)₂ (1.2 mg, 5.28 x 10⁻³ mmol, 1 equiv. per triazole) in chloroform (2.4 mL) was added. Chloroform (1.6 mL) and methanol (3 mL) were added in order to obtain a solution 1.64 x 10⁻³ M in Pd, 2:1 (CHCl₃/MeOH). The solution was stirred for 5 min, NaBH₄ (2 mg, 5.87x10⁻² mmol, 10 equiv. per Pd) in 1 mL of MeOH was added, and the yellow solution turned black indicating the formation of PdNPs.

Synthesis of PdNPs/2: A solution of **2** (3.50 mg, monomer: Mw = 654 g. mol⁻¹) in chloroform (4 mL) was introduced into a Schlenk flask under nitrogen. A solution of Pd(OAc)₂ (1.2 mg, 5.28 x 10⁻³ mmol, 1 equiv. per triazole) in chloroform (2.4 mL) was added. Chloroform (1.6 mL) and methanol (3 mL) were added in order to obtain a solution 1.64 x 10⁻³ M in Pd, 2:1 (CHCl₃/MeOH). The solution was stirred for 5 min, NaBH₄ (2 mg, 5.87x10⁻² mmol, 10 equiv. per Pd) in 1 mL of MeOH was added, and the yellow solution turned to black indicating the formation of PdNPs.

Synthesis of PdNPs/3: A solution of **3** (1.76 mg, dimer: Mw = 668 g. mol⁻¹) in chloroform (2 mL) was introduced into a Schlenk flask under nitrogen. A solution of Pd(OAc)₂ (1.2 mg, 5.28 x 10⁻³ mmol, 1 equiv. per triazole) in chloroform (1.2 mL) was added. Chloroform (0.8 mL) and methanol (2 mL) were added in order to obtain a solution 8.82 x 10⁻⁴ M in Pd, 2:1 (CHCl₃/MeOH). The solution was stirred for 5 min, NaBH₄ (2 mg, 5.87x10⁻² mmol, 10 equiv. per Pd) was added, and the yellow solution turned black indicating the formation of PdNPs.

Synthesis of PdNPs/4: A solution of **4** (2.48 mg, dimer: Mw = 1 470 g. mol⁻¹) in H₂O (2 mL) was introduced into a Schlenk flask under nitrogen. A solution of K₂PdCl₄ (1.1 mg, 3.37 x 10⁻³ mmol, 1 equiv. per triazole) in H₂O (1.1 mL) was added. H₂O (28.9 mL) was added in order to obtain a solution 1.0 x 10⁻⁴ M in Pd. This solution was stirred for 5 min, NaBH₄ (1.1 mg, 3.37 x 10⁻² mmol, 10 equiv per Pd) was added,

and the yellow solution turned golden brown indicating the nanoparticle formation.

General procedure for the catalytic Suzuki-Miyaura reaction in CHCl₃/MeOH:

In a Schlenk flask containing tribasic potassium phosphate (2 mmol, 2 equiv.), phenylboronic acid (1.5 mmol, 1.5 equiv.), aryl halide (1 mmol 1 equiv.) and PdNPs (stabilized by **1**, **2** or **3**) were successively added. The mixture solvent CHCl₃/MeOH (2/1) was also added in order to obtain a total volume of 6 mL. The reaction mixture was stirred during 16h at 90°C under N₂. Then H₂O (15 mL), and CH₂Cl₂ (15 min) were added, and the organic phase was kept. The water phase was washed with 15 mL of CH₂Cl₂, and both organic phases were gathered, dried over Na₂SO₄, and the solvent was removed under vacuum. In parallel, the reaction was checked using TLC in petroleum ether as eluent in nearly all the cases (see below), and ¹H NMR. Purification by flash chromatography column was conducted with silica gel as stationary phase and petroleum ether as mobile phase (see below). After each reaction, the Schlenk flask was washed with a solution of aqua regia (3 volumes of hydrochloric acid for 1 volume of nitric acid) in order to remove the traces of Pd.

General procedure for the catalytic Suzuki-Miyaura reaction in H₂O/EtOH: In a Schlenk flask containing tribasic potassium phosphate (2 mmol, 2 equiv.), phenylboronic acid (1.5 mmol, 1.5 equiv.), aryl halide (1 mmol 1 equiv.) and 10 mL of EtOH (volume ratio of H₂O/EtOH: 1/1) were successively added. Then the solution containing PdNPs/**4** was added in the appropriated amount. The suspension was allowed to stir under N₂ or air (no yield difference) at 80°C. After the reaction time (24h, 36h), the reaction mixture was extracted twice with diethyl ether (Et₂O, all the reactants and final products were soluble in Et₂O), the organic phase was dried over Na₂SO₄, and the solvent was removed under vacuum. In parallel, the reaction was checked using TLC in petroleum ether as eluent in nearly all the cases (see below), and ¹H NMR. Purification by flash chromatography column was conducted with silica gel as stationary phase and petroleum ether as mobile phase (see below). After each reaction, the Schlenk flask was washed with a solution of aqua regia (3 volumes of hydrochloric acid for 1 volume of nitric acid) in order to remove traces of Pd.

Purification procedure:

Biphenyl: bromobenzene and phenyl boronic acid: simple flash chromatography with petroleum ether as mobile phase and silica as stationary phase.

4-methylbiphenyl: Reaction between bromotoluene and phenyl boronic acid: simple flash chromatography with petroleum ether as mobile phase and silica as stationary phase.

4-methoxybiphenyl: Reaction between bromoanisole and phenyl boronic acid: flash chromatography with petroleum ether as mobile phase and silica as stationary phase at the beginning and then 95% petroleum ether/5% diethyl ether.

4-nitrobiphenyl: Reaction between 1,4-bromonitrobenzene and phenyl boronic acid: flash chromatography with 95% petroleum ether/ 5% dichloromethane as mobile phase and silica as stationary phase.

4-biphenylcarboxaldehyde: Reaction between bromobenzaldehyde and phenyl boronic acid: flash chromatography with 95% petroleum ether/5% dichloromethane as mobile phase and silica as stationary phase.

4-acetylbiphenyl: Reaction between 4-bromoacetophenone and phenyl boronic acid: flash chromatography with 95% petroleum ether/5% diethyl ether as mobile phase and silica as stationary phase.

Acknowledgement

Financial support from the Univ. Bordeaux and Toulouse III, the CNRS and the Ministère de l'Enseignement Supérieur et de la Recherche (PhD grant to CD) are gratefully acknowledged.

References

- [1] a) M. T. Reetz, W. Helbig, S. A. Quaiser, in *Active metals: preparation, characterizations, applications*, (Ed.: A. Fürstner), Wiley-VCH, Weinheim, p. 279 (1996); b) H. Bönnemann, W. Brijoux In *Active Metals: Preparation, Characterization, Applications* (Ed.: A. Fürstner) VCH, Weinheim, p.339

- (1996); c) I. P. Beletskaya, A. V. Cheprakov, A. V. Chem.Rev. **100**, 3009 (2000); d) H. Bönemann, R. Richards, Eur J. Inorg. Chem. **10**, 2455 (2001); e) *Nanotechnology in Catalysis, Vol.1 and 2 (Nanostructure Science and Technology)*, (Eds.: B. Zhou, S. Hermans, G. A. Somorjai), (2003); f) A. H. M. de Vries, J. M. C. A. Mulders, J. H. M. Mommers, H. J. W. Hendericks, J. G. de Vries, Org. Lett. **5**, 3285 (2003); g) A. H. M. de Vries, J. G. de Vries, Eur. J. Org. Chem. **5**, 799 (2003); h) M. T. Reetz, J. G. de Vries, Chem. Commun. **14**, 1559 (2004); i) X. Tao, Y. Zhao, D. A. Sheng, Synlett. **2**, 359 (2004); j) D. Astruc, F. Lu, J Ruiz, Angew. Chem., Int. Ed. **44**, 7852 (2005); k) J. G. de Vries, Dalton Trans. 421 (2006); l) N. T. S. Phan, M. van der Sluys, C. J. Jones, Adv. Synth. Catal. **348**, 609 (2006); m) *Metal-catalyzed Cross-coupling Reactions* (Eds.: F. Diederich, P. Stang), Wiley-VCH, Weinheim, (2008); n) R. P. Beletskaya, A. N. Kashin, I. A. Khotina, A. R. Khokhlov, Synlett. **10**, 1547 (2008); o) *Nanoparticles and Catalysis* (Ed.: D. Astruc) Wiley-VCH, Weinheim, (2008); p) *Modern Surface Organometallic Chemistry*, (Eds.: J.-M. Basset, R. Psaro, D. Roberto, R. Ugo), Wiley-VCH, Weinheim, (2009); q) L. M. Bronstein, Z. B. Shifrina, Chem. Rev. **111**, 5301 (2011); r) B. Sreedhar, D. Yada, P. S. Reddy, Adv. Synth. Catal. **353**, 2823 (2011); s) *Nanomaterials in Catalysis*; (Eds.: P. Serp, K. Philippot), Wiley-VCH, Weinheim, (2013).
- [2] a) N. Toshima, in *Fine Particle Advances and Technology: from Micro- to New Particles* (Ed.: E. Pelizzetti) Kluwer, Dordrecht, p. 371 (1996); b) R. P. Andres, J.-D. Bielefeld, J.-I. Henderson, D.-B. Janes, V.-R. Kolagunta, V.-P. Kukink, . Mahoney, R. G. Osifchin, R. Reifengerger, Science **273**, 1690 (1996); c) N. Toshima, T. Yonezawa, New J. Chem. **22**, 1179 (1998); d) T. Yonezawa, N. Toshima, In *Advanced Functional Molecules and Polymers, Vol 2* (Ed.: H. S. Nalwa) *Accelerated Development*, Chap. 3, p. 65 (2001); e) A. B. R. Mayer Polym. Adv. Technol. **12**, 96 (2001); f) J.-H. He, I. Ichinose, T. Knitake, A. Nakao, Y. Shiraishi, N. Toshima, J. Am. Chem. Soc. **56**, 11034 (2003); g) R. Naryanan, M. A. El Sayed, J. Am. Chem. Soc. **125**, 8340 (2003); h) B. P. S. Chauhan, J. S. Rathore, T. Bando, J. Am. Chem. Soc. **126**, 8493 (2004).
- [3] a) M. Zhao, R. M. Crooks, Angew. Chem. Int. Ed. **38**, 364 (1999); b) R. M. Crooks, M. Zhao, L. Sun, V. Chechik, L. K. Yeung, Acc. Chem. Res. **34**, 181

- (2001); c) D. Astruc, *Tetrahedron Asymmetry* **21**, 1041 (2010); d) V. S. Myers, M. G. Weier, E. V. Carino, D. F. Yancey, S. Pande, R. M. Crooks, *Chem. Sci.* **2**, 1632 (2011).
- [4] a) A. K. Diallo, C. Ornelas, L. Salmon, J. Ruiz, D. Astruc, *Angew. Chem., Int. Ed.* **46**, 8644 (2007); b) C. Ornelas, J. Ruiz, L. Salmon, D. Astruc, *Adv. Synth. Catal.* **350**, 837 (2008); c) E. Boisselier, A. Diallo, L. Salmon, C. Ornelas, J. Ruiz, D. Astruc, *J. Am. Chem. Soc.* **132**, 2729 (2010); d) C. Deraedt, L. Salmon, L. Etienne, J. Ruiz, D. Astruc, *Chem. Commun.* **49**, 8169 (2013).
- [5] a) V. V. Rostovtsev, L. G. Green, V. V. Fokin, K. B. Sharpless, *Angew. Chem., Int. Ed.* **41**, 2596 (2002); b) C. W. Tornøe, C. Christensen, M. Meldal, *J. Org. Chem.* **67**, 3057 (2002); c) M. Meldal, C. W. Tornøe, *Chem. Rev.* **108**, 2952 (2008); d) G. Franc, A. Kakkar, *Chem. Commun.* 5267 (2008); e) W. H. Binder, R. Zirbs, *In Encyclopedia of Polymer Science and Technology*, Wiley, New York, pp. 1-45 (2009); f) B. Sumerlin, A. P. Vogt, *Macromolecules* **43**, 1 (2010); g) J. E. Hein, V. V. Fokin, *Chem. Soc. Rev.* **39**, 1302 (2010); h) L. Liang, D. Astruc, *Coord. Chem. Rev.* **255**, 2933 (2011).
- [6] a) C. Ornelas, A. K. Diallo, J. Ruiz, D. Astruc, *Adv. Synth. Catal.* **351**, 2147 (2009); b) C. Deraedt, L. Salmon, J. Ruiz, D. Astruc, *Adv. Synth. Catal.* **355**, 2992 (2013).
- [7] a) D. O. Cowan, F. Kaufman, *J. Am. Chem. Soc.* **92**, 219 (1970); b) W. H. Morrison Jr., S. Krogsrud, D. N. Hendrickson, *Inorg. Chem.* **12**, 1998 (1973); c) W. H. Morrison, D. N. Hendrickson, *Inorg. Chem.* **14**, 2331 (1975); d) C. Levanda, K. Bechgaard, D. O. Cowan, *J. Org. Chem.* **41**, 2700 (1976); e) M. J. Powers, T. J. Meyer, *J. Am. Chem. Soc.* **100**, 4393 (1978); f) N. Camire, U. T. Mueller-Westerhoff, W. E. Geiger, *J. Organomet. Chem.* **637–639**, 823 (2001).
- [8] a) T. Horikoshi, M. Itoh, M. Kurihara, K. Kubo, H. Nishihara, *J. Electroanal. Chem.* **473**, 113 (1999); b) H. Nishihara, *Adv. Inorg. Chem.* **53**, 41 (2002). c) M. Yamada, H. Nishihara, *Chem. Commun.* 2578 (2002); d) M. Yamada, T. Tadera, K. Kubo, H. Nishihara, *J. Phys. Chem. B* **107**, 3703 (2003); e) C. Deraedt, A. Rapakousiou, Y. Wang, L. Salmon, M. Bousquet, D. Astruc, *Angew. Chem. Int. Ed.* **53**, 8445 (2014); f) A. Rapakousiou, C. Deraedt, H. Gu, L. Salmon, C. Belin, J. Ruiz, D. Astruc, *J. Am. Chem. Soc.* **136**, 13995 (2014).

- [9] a) N. J. Long A. J. Martin, R. Vilar, A. J. P. White, D. J. Williams, M. Younus *Organometallics* **18**, 4261 (1999); b) T.-Y. Dong, S.-W. Chang, S.-F. Lin, M.-C. Lin, Y.-S. Wen, L. Lee, *Organometallics* **25**, 2018 (2006). c) R. Djeda, A. Rapakousiou, L. Liang, N. Guidolin, J. Ruiz, D. Astruc, *Angew. Chem., Int. Ed.* **49**, 8152 (2010).
- [10] a) C. Ornelas, J. Ruiz, E. Cloutet, S. Alves, D. Astruc, *Angew. Chem. Int. Ed.* **46**, 872 (2007); b) C. Ornelas, L. Salmon, J. Ruiz, D. Astruc, *Chem. Eur. J.* **14**, 50 (2008).
- [11] a) A. C. Skapski, M. L. Smart, *J. Chem. Soc. D* 658 (1970); b) F. A. Cotton, S. Han, *Re. Chim. Miner.* **20**, 496 (1983); c) W. Bauer, M. Prem, K. Polborn, K. Sünkel, W. Steglich, W. Beck, *Eur. J. Inorg. Chem.* 485 (1998); d) V. I. Bakhmutov, J. F. Berry, F. A. Cotton, S. Ibragimov, C. A. Murillo, *Dalton Trans.* 989 (2005).
- [12] 10 equivalents of NaBH₄ is required to reduce all the Pd(II) to Pd(0), this has been checked by XPS analysis in the following paper: D. Wang, C. Deraedt, L. Salmon, C. Labrugère, L. Etienne, J. Ruiz, D. Astruc, *Chem. Eur. J.* (2014). DOI: 10.1002/chem.201404590
- [13] a) S. Kotha, K. Lahiri, D. Kashinath, *Tetrahedron* **58**, 9633 (2002); b) F. Lu, J. Ruiz, D. Astruc, *Tetrahedron Lett.* 9443 (2004); c) K. C. Nicolaou, P. G. Bulger, D. Sarlah, *Angew. Chem., Int. Ed.* **44**, 4442 (2005); d) C. Torborg, M. Beller, *Adv. Synth. Catal.* **351**, 3027 (2009).
- [14] According to ref [6b], the pre-reduction of Pd(II) to PdNPs with NaBH₄ is necessary for efficient catalysis.

**Partie 4. Nanoréacteurs
dendritiques pour la catalyse par
des ppm de Cu de la réaction
“click” CuAAC dans l’eau.**

Partie 4. Nanoréacteurs dendritiques pour la catalyse par des ppm de Cu de la réaction “click” CuAAC dans l’eau.

Le dendrimère G0 1,2,3-triazole TEG, avant d’être utilisé pour stabiliser des PdNPs, avait servi de nanoréacteur pour les réactions de métathèse des oléfines dans l’eau. Il s’est avéré qu’en présence de 0,086% mol du dendrimère et d’un catalyseur au ruthénium (Grubbs 1^{ère} et 2^{nde} génération ou Grubbs-Hoveyda) la catalyse se faisait efficacement, tandis que sans dendrimère aucune réaction n’avait été observée dans les mêmes conditions opératoires.⁽¹⁾ Par la suite nous avons envisagé d’examiner et d’étendre ce comportement de nanoréacteur micellaire moléculaire pour d’autres réactions chimiques. La réaction “click” CuAAC étant considérablement utilisée dans la littérature et énormément au sein de notre groupe de recherche, cette réaction a été sélectionnée comme réaction test. Le Dr. Liyuang Liang, ex-thésarde du laboratoire, a montré l’efficacité d’un nouveau catalyseur, le complexe Cu(I)hexabenzyltren (en quantité 0,1 % mol), pour la réaction CuAAC dans des solvants organiques (pentane ou toluène) à température ambiante en 24h.⁽²⁾ Nous avons tenté d’effectuer cette même réaction dans des conditions plus douces (solvant = eau, temps < 24h, etc.) grâce à la présence du dendrimère. Nous nous sommes rendu compte qu’avec 1% mol de dendrimère la réaction “click” entre l’azoture de benzyle et le phényl acétylène était quasi-quantitative en 3 heures dans l’eau alors qu’en l’absence de dendrimère la réaction avait à peine débuté. Des études complémentaires ont permis d’étendre l’applicabilité de la réaction à d’autres substrats, de prouver la recyclabilité du nanoréacteur et surtout de localiser le catalyseur au sein du nanoréacteur. Dans une deuxième partie de ce travail, nous avons développé l’utilisation des cycles 1,2,3-triazoles composant le nanoréacteur pour ligander et activer et cuivre (I), ce qui a été démontré par RMN ¹H. Ce nouveau catalyseur dendritique présente un grand intérêt car il permet de réaliser la réaction CuAAC quantitativement avec seulement 5 ppm de cuivre pour la réaction témoin. Cette activité extrême est attribuée à la synergie entre l’effet micellaire du nanoréacteur dendritique et l’activation du cuivre (I) par les cycles 1,2,3-triazoles. L’applicabilité du système a été démontrée avec divers substrats ainsi qu’avec des composés d’intérêt biologique.

Avant de parler de ces travaux de recherche, cette partie commencera avec une revue sur les macromolécules (macrocycles, cages, capsules, molécule micellaires) comportant une cavité servant de nanoréacteur.

Références:

- 1) Diallo, A. K. ; Boisselier, E. ; Liang, L.; Ruiz, J.; Astruc, D. Dendrimer-induced molecular catalysis in water: the example of olefin metathesis, *Chem. Eur. J.* **2010**, *16*, 11832-11835.
- 2) Liang, L.; Ruiz, J.; Astruc, D. The efficient copper(I) (hexabenzyl)tren catalyst and dendritic analogues for green “click” reactions between azides and alkynes in organic solvent and in water: positive dendritic effects and monometallic mechanism. *Adv. Syn. Catal.* **2011**, *353*, 3434–3450.

Nanoreactors for catalysis

Introduction

The 21st century chemistry must be green, that is to say respectful of the environment. This needs lead the researchers to drastically change their means of synthesis. According to Anastas,^[1] green chemistry could be driven by twelve principles, among which the use of catalysis instead of stoichiometric reactions is highly advised. Therefore inspiration comes from Nature. By using well-defined reaction environments such as those of enzymes (relatively simple systems) or cells (extremely complex assemblies), nature operates chemical conversions allowing the life to exist. Enzymes are nanometer-sized molecules with three-dimensional structures created by the folding and self-assembly of polymeric peptides through supramolecular interactions. They perform catalytic functions (abundant chemical biotransformations) usually accompanied by a variety of conformational states.^[2] The synthesis and the use of sophisticated molecules that mimics nature's agents is essential towards the discovery of new green systems able to carry out efficient catalysis. The direct use of enzymes could be the solution, but by taking into account the difficulty to precisely understand the relationships between the supramolecular structures and the catalytic features of the enzymes, the synthesis of new simpler molecules is required. These systems, called nanoreactors, are composed of a cavity and accommodate substrates allowing a catalytic reaction. Inside this nanoreactor, the reaction pathways is influenced allowing a reaction to occur more quickly and/or more selectively, but also the size and the morphology of the products can be influenced, for instance in the case of crystals. There are several characteristic properties in enzyme catalysis; (i) providing hydrophobic pockets, (ii) strong substrate binding therein, (iii) transition-state or intermediate stabilization, and (iv) weak product binding. In order to take these properties into account, supramolecular interactions including hydrogen bonding, electrostatic, Van Der Waals and π - π interactions, steric effects, shape complementarity, and hydrophilic/hydrophobic effects, can be engineered. As proposed by Pauling,^[3] the powerful catalytic action of enzymes involves specific tight binding to the transition state species. Because the reaction rate is proportional to the fraction of the reactant in the transition state complex, the enzyme increases the concentration of the reactive species. Many nanoreactors rely on this principle proposed 70 years ago involving the supramolecular interactions mentioned above. Recently, several excellent reviews were reported on enzyme mimics and artificial enzymes.^[4-6]

After recalling seminar reports of nanoreactors, emphasis will be placed on more recent nanoreactors for catalytic reactions. The first nanoreactors were macrocyclic^[7-12] molecules among which crown-ether, cyclodextrins, calixarenes, cyclophanes, cucurbituril and other macrocycles have proved to be very useful in catalytic reactions. Then the main nano-containers (bowl-shape, capsule and cages) composed of a confined cavity will be reviewed. These nano-containers are built via covalent bonds or electrostatic interactions but also via coordination chemistry between metallic ions and specific ligands. Finally, micellar^[13,14] nanoreactors such as micelles, vesicles and dendritic molecular micelles will be discussed. Only molecules having a cavity as microenvironment will be envisaged here, excluding inorganic materials such as inorganic nanoparticles or mesoporous materials. The aim is to

understand how to design the most efficient nanoreactors in order to improve catalysis.

Macrocycles

The synthesis and the use of macrocycles presenting a microenvironment at the cavity center is essential in order to isolate the substrate from the environment. The first, simple examples of nanoreactors were crown ethers and cryptands (tri-dimensional crown ether) invented by Lehn,^[15] Cram^[16] and Pederson^[17] who were awarded the 1987 Nobel Prize. Compared to simple molecular catalysis, the use of these nanoreactors required a first step of recognition corresponding to the binding of the substrates, followed by the enhanced chemical transformation, i.e. catalysis.

These structures are well known for the complexation of cations such as alkali metal cations Na⁺, K⁺ or transition metal cations for the recognition of small molecules or for the stabilization of instable molecules, and they also have been used in the catalytic field. In an early study, a crown-ether bearing side chains with thiols **1** was able to specifically cleave activated esters with marked rate enhancements and chiral discrimination between optically active substrate. The macrocycle **1** binds *p*-nitrophenyl (PNP) esters of amino acids and peptides thanks to its oxygen atoms, and reacts with the bound species, releasing *p*-nitrophenol (Figure 1). Different features were observed, with first the selectivity of the substrate inducing a rate enhancement in favor of dipeptide ester substrates, then high chiral recognition between enantiomeric dipeptide esters, and slow but definite catalytic turnover. Finally the presence of metallic cations inhibits the reaction because of the competition between the substrate and these cations during the recognition process.^[18] A series of aza-crown ethers with a carboxylic arm were synthesized and used in the deacylation of amino acid *p*-nitrophenyl ester to mimic aspartic proteinase. The systems have shown a selectivity in the encapsulation and deacylation.^[19] The cavity created by the macrocycle allows the insertion and activation of small molecules such as O₂ gas. The examples of monoaza-18-crown-6 ethers as efficient and a selective phase transfer catalysts of the asymmetric oxidation of aromatic ketones by molecular oxygen is noteworthy.^[20]

As crown-ether macrocycles, cryptands have been used for a long time for the recognition of cations that is more selective with stronger coordination than with macrocycles. In most cases, cryptands are associated to a metallic cation located in the cavity called metal-cryptate and used as homogeneous catalyst. It is of interest that the cavity is large, because it lets more space for organic molecules to approach the bonded metal inside the cavity. Cu(II) and Co(II) cryptates of **2** were probed for possible catalytic roles in the oxidation of organic substrates. Metal cryptates have been suggested to be effective as homogeneous catalysts because of their increased kinetic and thermodynamic stability. Transition metal catalyzed oxidation of organic substrates such as that of alkene to epoxyde with dioxygen is closely related to important biological processes like enzymatic oxygenation that serve for biomimetic modeling.^[21]

Cyclophanes are macrocycles composed of aromatic units with an aliphatic chain forming a bridge. The group of Diederich proposed rare examples of cyclophanes as nanoreactors. Thiazoliocyclophanes with aromatic binding substrates sites such as **4** were used in the oxidation of aromatic aldehydes to their corresponding methyl esters in the presence of an oxidizing agent, mimicking pyruvate oxidase. The high activity

was rationalized with the fact that substrates bind the macrocycle in the presence of a microenvironment. The activity is lower with the acyclic “thiazoliocyclophane” **5**).^[22,23]

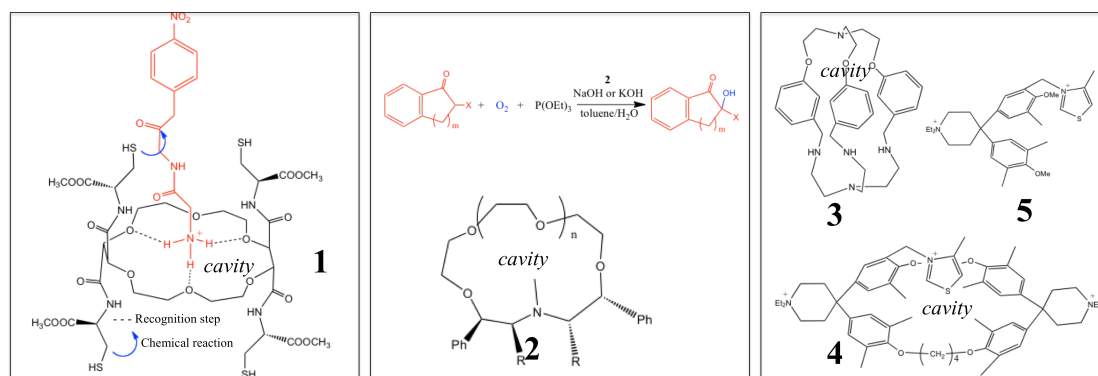


Figure 1. Various macrocycles used as nanoreactors

Cyclodextrins (CDs) are a family of natural macrocycles (see Figure 2). Composed of 6, 7 or 8 glucopyranose units (α , β or γ cyclodextrin respectively), these hydrophilic macrocycles form a hydrophobic cavity (4.5, 7.0, 8.5 Å respectively) able to encapsulate various hydrophobic substrates (adamantane and ferrocene are typical examples) in water. The hydroxyl groups composing each glucopyranose unit allow the easy functionalization of cyclodextrin. Moreover, the two rims of hydroxyl groups can either react with substrates themselves or be used to attach other catalytic and functional groups. Since the pioneering work of Breslow,^[24] Saengers^[25] or Tabushi^[26] a myriad of cyclodextrin systems has been developed as nanoreactors, mainly due to the availability of the macrocycle, which avoids syntheses. The first examples in which cyclodextrin appears show the acetylation of the glucopyranose hydroxyl group by hydrolysis of an ester increasing up to 5 900 000-fold in comparison with the reaction without CD, due to the position of the substrate in the cavity orienting the ester toward the hydroxyl group.^[27] The preliminary studies developed by Breslow et al. show that the binding into a simple cyclodextrin **5** was enough to direct a selective aromatic substitution reaction, in which a chlorine atom is delivered to the bound substrate by one of the cyclodextrin hydroxyl group. The result of this chlorination (anisole **6** becomes 4-chloroanisole **7**) was better than with the enzyme catalyst (Figure 2). β -CD **5** was also used by Breslow’s group for increasing the rate of the Diels Alder reaction between cyclopentadiene **8** and a slim dienophile such as acrylonitrile **9**. No reaction (no final product **10**) was observed when α -CD was used because of a smaller cavity, enlighting the entrance of the substrate inside the cavity (Figure 2).^[28] Other unmodified CDs were used as nanoreactors. For example β -CD **5** was used as catalyst in the synthesis of quinoxalines in water. The presence of 1 equiv. of CD leads to 90% yield in 2 hours, whereas without CD only 25% yield was obtained after 48 hours. β -CD appears to be involved in activating the phenacyl bromide **11** by forming a host-guest complex and promotes the reaction (Figure 2).^[29] In the same way β -CD was used in a highly regioselective ring-opening reaction of oxiranes with phenoxides in water (Figure 2). Whereas no reaction was observed without β -CD, quantitative yields were obtained.^{30]} Oxidation of various alcohols and epoxides with *N*-bromosuccinimide (NBS) catalyzed by β -CD in water at room temperature (r.t.) has been developed by the group of Rao. The high

selectivity and yield was connected to the encapsulation of both the substrate and the oxidizing agent, no reaction being observed without CD (Figure 2).^[31] Wang et al. discovered that in the presence of other oxidizing agent such as NaClO at 50°C various alcohols were also oxidized to the corresponding aldehydes or ketones.^[32] Very recently, β -CD was used as nanoreactor for the CuAAC click reaction in water. In the presence of a catalytic amount of β -CD (2.5% mol), the click reaction between benzyl azide **12** and the phenyl acetylene **13** was quantitative in 15 min at r.t. with 5% mol of the Sharpless catalyst ($\text{CuSO}_4 \cdot 5\text{H}_2\text{O}/\text{NaAsc}$) whereas without CD only 40.5% of conversion was observed in 1 hour (Figure 2).^[33] Another example, reported by the group of Inoue, used γ -CD for enantiodifferentiating [4 + 4] photocyclodimerization of 2-anthracenecarboxylate **14** by UV (ee up to 32% at 25% and 40% at 0°C).^[34]

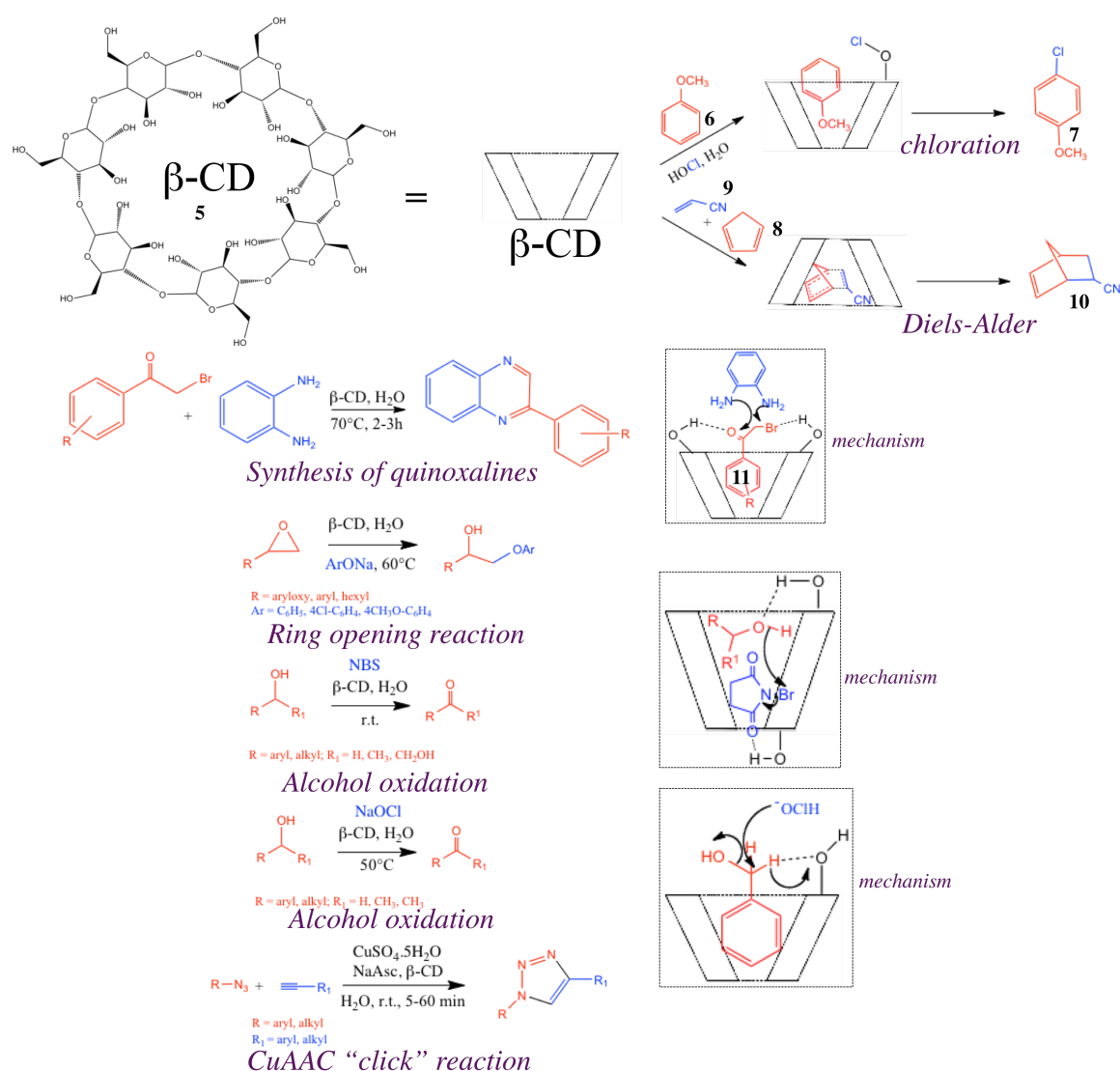


Figure 2. Several examples of catalysis in the presence of β -cyclodextrin nanoreactor.

As cyclodextrin is composed of several possible functionalized hydroxyl groups, various modified cyclodextrins have been synthesized. Bols et al. have developed a lot of different CDs and have observed that by changing two OH group of the upper rim of the β -CD by COOH **14** or by CH(OH)CN **15** the rate of the hydrolysis reaction of 4-nitrophenyl- β -CD-glucoside **16** into glucose **17** and 4-nitrophenol **18** was

enhanced 35-fold (against 18-fold with α -CD) and 1047 respectively, enlighting the tunable properties of CD.^[35] The same research group reported the enhanced reaction rate of the oxidation of both amines (1 068-fold) and benzyls alcohol (60 000 fold) via H_2O_2 with a two-ester-bridged modified cyclodextrin **19** playing the role of nanoreactor. The oxidation of benzyl alcohol **20** to benzaldehyde **21** is exemplified in Figure 3. When the cavity of the CD imprisons the substrate in the desire reactive position, the bridge brings the oxidizing agent closer.^[36] Dimeric, tetrameric and oligomeric CDs have been also synthesized for catalytic applications. Mao et al have synthesized two new CD dimers linked by a diphenyl group **22** or a 2,2'-bipyridine **23** group used in the hydrolysis of esters. One of the hydrophobic cavities of the dimer is assembled with a Zn^{2+} -triamine complex containing pendant side of 4-*tert*-butylbenzyl **24** to construct a supramolecular metallohydrolase model, in which hydroxyl species acting as active catalysis species are supramolecularly stabilized in solution. The other hydrophobic cavity of the dimer is used to capture the substrate containing a hydrophobic group, such as *p*-nitrophenyl acetate (pNA) **25** (Figure 3). In such a host-guest system, an original intermolecular reaction between ZnL and pNA is translated into a quasi-intramolecular reaction by the cooperative hydrophobic interaction between the two CD cavities and the catalyst/substrate.^[37] Two Ru-porphyrin-linked β -cyclodextrin units forming a supramolecular system **26** were synthesized by Woggon's group, and they selectively catalyze the cleavage of the central carotinoid **27** E-double bond in the presence of a co-oxidizing *tert*-butylhydroperoxide agent, mimicking carotene dioxygenases (Figure 3). No reaction was observed without the co-oxidizing agent, and binding of the starting material to the receptor is enhanced by an increase in planarity thanks to the porphyrin link. Binding of the desired product is three times lower than that of the substrate. The high regioselectivity of the system that leads to only traces of by-products was attributed to the specific binding of the substrate into the two CDs of the dimer and to the specific localization of the metallic catalyst positioned very close to the desired bond cleavage.^[38] The hydrosolubility coupled both with the hydrophobicity of the various cavities (α , β and γ) and the commercial availability of the cyclodextrins make this family among the most used nanoreactors.

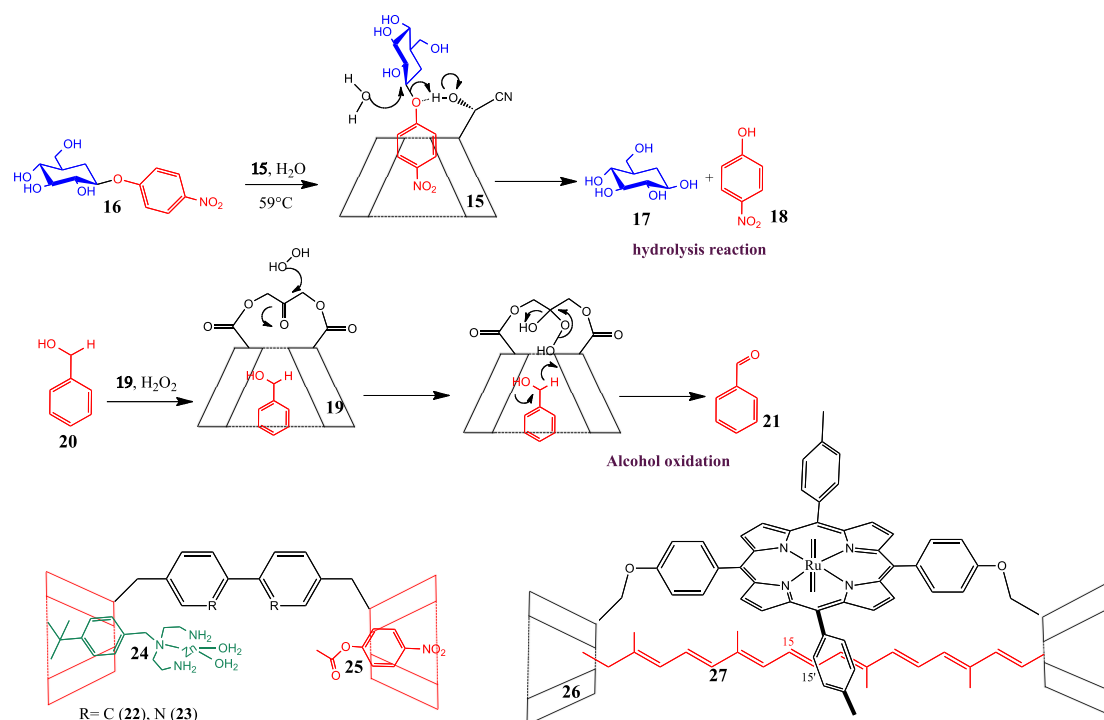


Figure 3. Modified cyclodextrins developed by Bols, Mao and Woggon.

Calixarenes are also considered as nanoreactors. Produced by hydroxyalkylation between a phenolic unit and an aldehyde, these macrocycles are generally composed of 4 (calix[4]arene), 5, 6, 7 or 8 aromatic units inducing a central cavity, a wide upper rim and a narrow lower rim. Lots of calixarenes encapsulating metals or covalently linked to them have been used in catalysis, and the review reported by Homden and Redshaw describes them very well. In a number of these processes, it has become clear that the ability of the calixarene frame to “hold” the metal center and the substrate at a certain distance from one another is critical to the success of the catalytic process, as is the ability of the calixarene to undergo phenol conformational change.^[39] Matt et al. have developed a series of calix[4]arenes bearing two phosphorus pendent groups, among which three enantiomeric pure calixarenes (**28**, **29**, **30**, Figure 4) were used as Pd ligand for the Pd-catalyzed alkylation of 1,3-diphenylprop-2-enyl acetate. The enantiomeric excess (ee) up to 67% in the quantitative reaction was linked to the steric bulk of the lower rim bearing the catalytic species. It appears likely that increasing the size difference between the two auxiliary groups should result in higher ee's. Chiral calixarenes in which the two phosphine arms occupy proximal instead of distal phenolic positions were found to be considerably less effective in catalysis of both allylic alkylation and hydrogenation when the calixarene is bearing a Rh catalyst.^[40] Reinhoudt et al. have for a long time worked on calixarene, and this group has reported the synthesis of mono-, di- and trinuclear Zn(II) or Cu(II) phosphatase mimics (Figure 4). The mono-nuclear Zn(II) calixarene **31**, presents a better activity in the transesterification of the RNA model substrate 2-hydroxypropyl-*p*-nitrophenyl phosphate (HPNP) than the non-calixarene mono-nuclear Zn(II) **32**, which means that the calixarene cavity is involved in the catalysis. Moreover the di and tri-nuclear Zn(II) calixarenes **33** and **34** bring an enhancement in the reaction rate of 23 000-fold and 24 000-fold respectively, i. e. around 50-fold the rate of the mono-nuclear Zn(II) calixarene catalyst over the non-catalyzed transesterification. This suggests a cooperative effect between several

glycoluril monomers linked by methylene bridges. Mock conducted seminal studies with cucurbit[6]uril **42** (cavity 5.8 Å) as nanoreactor in the early 1980's. The 1,3-cycloaddition between an ammonium-alkyne **43** and an ammonium-azide **44** leading selectively to the 1,4-isomer **45** in an aqueous acid formic solution at 40°C increased 55 000-fold compared to the reaction without nanoreactor leading to isomers 1,4- **45** and 1,5- **46**. The substrates enter in the nanoreactor thanks to hydrogen bonds between the ammonium moiety and the carbonyl of the glycoluril. As the cavity is not large enough to accommodate both substrates, they must be compressed together, resulting in additional kinetic acceleration beyond that expected solely by proper orientation of the substrates at their van der Waals distance. The nanoreactor preferentially binds the transition state as in the Pauling catalysis principle.^[44] In the last decade, cucurbit[7]uril **47** with a cavity of 7.3 Å and cucurbit[8]uril **48** with a cavity of 8.8 Å have been employed to catalyze various types of photocycloaddition reactions. Cucurbit[8]uril has been shown to control the stereoselectivity of the photodimerization of cinnamic acids in the solid state (Figure 5).^[45] The same nanoreactor effect was observed in the photodimerization of protonated azastilbenes **49** in water. When olefins yield products of geometric isomerisation **50**, cyclization **51**, and hydration **52**, in the presence of nanoreactor the predominant product is that of dimerization **53**, **54** (Figure 5). Such a change in product distribution is attributed to the localization of the olefins by the host cucurbit[8]uril. The nature of the single dimer that was formed is rationalized on the basis of the principles of “best fit” and “minimization of electrostatic repulsion”. The cucurbit[8]uril acts as a templating agent thanks to its ability to provide a reaction cavity that is tight and time independent, which compares to micelles (*vide infra*) as it is the case with cyclodextrins and calixarenes.^[46] Macartney et al. demonstrated that the [4+4] photodimerization of protonated 2-aminopyridine **55** within a 2:1 guest:host complex with cucurbit[7]uril is highly stereoselective, producing exclusively the *anti-trans*-DADAT²⁺ (4,8-diamino-3,7-diazatricyclo[4.2.2.2^{2,5}]dodeca-3,7,9,11-tetraene) isomer **56** and protecting the dimer from thermal rearomatization. Without the nanoreactor, the photochemical reaction produces the *anti-trans* **56** and *syn-trans* **57** photodimers in a 4:1 ratio (Figure 5). This is the first example of the use of cucurbit[7]uril.^[47] According to the same principle Sivaguru et al. very recently proposed the photodimerization of coumarins in water leading to *syn* dimers, whereas *trans* dimers are formed in the absence of nanoreactor.^[48]

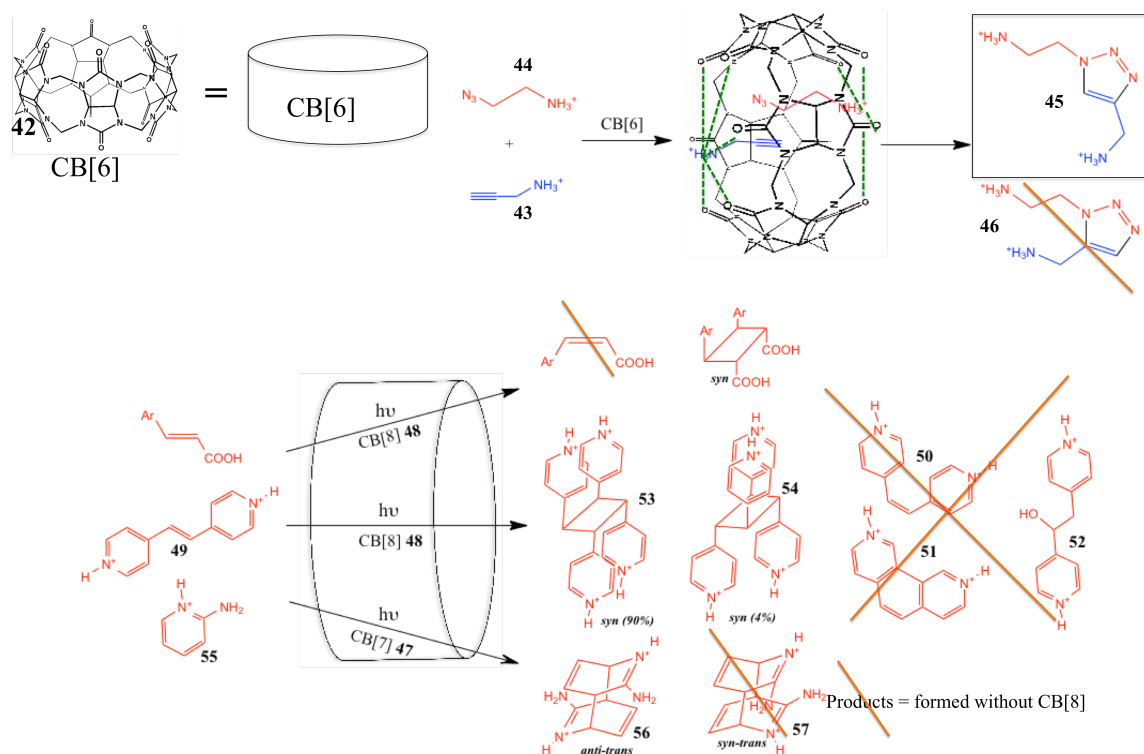


Figure 5. Huisgen type 1,3 cycloaddition and several photodimerization in presence of cucurbiturils.

Sai-feng et al. studied the use of cucurbit[8]uril as nanoreactor in the oxidation of various alcohol to corresponding aldehydes in the presence of *o*-iodoxybenzoic acid (IBX) as oxidizing agent in aqueous solvent. The catalytic tests revealed that the catalyst prefers aryl and allyl alcohols to alkyl alcohols, and the conversions of most aryl and allyl alcohols have been increased by 30–50% in the presence of the nanoreactor. The catalytic selectivity suggests that the IBX oxidation proceeds *via* a stabilized α -carbanion intermediate, and the supramolecular catalysis should be mechanistically related to the electron density and reactivity of the α -carbanion. By comparing the reaction in presence of the nanoreactors CB[6], CB[7], CB[8], α -CD, β -CD, γ -CD, a dependent size cavity was observed with better results observed in presence of the cucurbit[8]uril.^[49,50]

Sanders' group has synthesized sophisticated macrocycles (**58** and **59** Figure 6) that consist in three Zn-porphyrins units covalently linked via aromatic-alkyne rigid bond and accelerates very specific reactions of functional pyridines. The strategy used herewith involves convergent binding sites that are positioned in such a way that substrate molecules are held in close proximity. The trimer acts as an 'entropic trap' and accelerates reactions for which the transition-state geometry matches the relative orientation of bound ligands. For instance, it catalyzes the Diels-Alder reaction between pyridine-modified maleimide **60** and pyridyne-modified furane diene **61**. The presence of pyridine in each substrate is necessary to bind the Zn-porphyrins. The reaction is accelerated 200-fold in comparison with the reaction without the trimer, as the *exo*-adduct **62** is obtained in 65% yield, whereas no *endo*-adduct **63** was detected. By changing the length of the linkers, the *endo* product **63** is favoured (Figure 6). The final product also enters in the competition of complexation, thus the yield of the reaction is not so high.^[51,52] In the same way, the trimer accelerates by 16-fold the acyl transfer between an alcohol substrate and an amide substrate. The comparison

with acyclic porphyrin ligand shows that the pre-orientation of the two substrates by the trimeric species is essential.^[53]

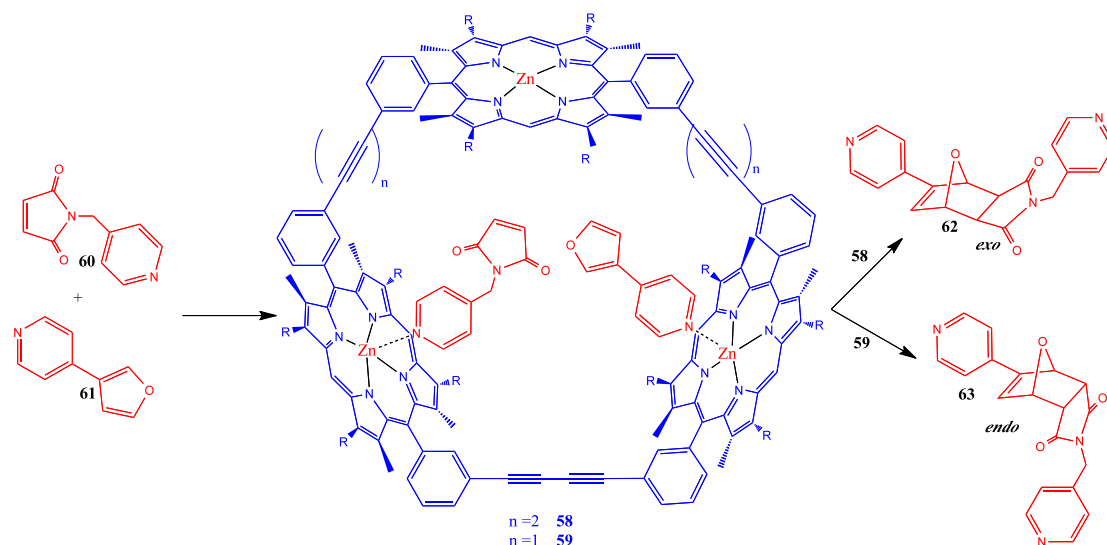


Figure 6. Sanders' macrocycles used in the Diels-Alder reaction.^[51,52]

Molecules containers

Cavitands are bowl-shaped container possessing a concave surface, generally deriving from calixarene decorated with “high walls”, and Rebek's group directed most of the researches using this family of containers. The Diels-Alder reaction was also studied with cavitands. By positioning a dienophilic maleimide group at the amido-rim of the cavitand using the encapsulation of a hydrophobic adamantate part, the hydrogen-bonding groups of the cavitand accelerate the cycloaddition between the maleimide **64** and 9-anthracenemethanol **65** (Figure 7). The reaction is accelerated 60-fold, the reaction rate being driven by the larger size of the final product **66** compared to the substrates and lower affinity constant than the substrates, which avoids inhibition of the reaction. Others studies show the presence of a hydrogen-bonding arm at the top of the cavitand **67**, which orientates the substrate inside the cavity. In this way, the rearrangement of suitable 1,5-epoxyalcohols to tetrahydrofuran derivatives (Figure 7) was performed with help of the hydrogen bonding of the acidic arm of the cavitand and the epoxyde group of the substrate inside the cavity that pre-organized the beginning of the rearrangement. The reaction rate was increased up to 300-fold.^[54] Another astute recent example reports the switchable catalysis with a light-responsive cavitand. The cavitand is composed of an azo-wall that is photo-isomerized between *trans* (with 448 nm light) and *cis* (with 365 nm light) configurations. In the *trans* resting state the cavitand presents a cavity accessible to guests; in the *cis* configuration a self-fulfilling introverted arrangement results. The *trans* cavitand promotes the piperidinium acetate-catalyzed Knoevenagel condensation between malononitrile and aromatic aldehydes by binding the catalyst inside its cavity. The reaction rate increased 3.5-fold in the presence of this nanoreactor. The catalyst is rejected when the host is photo-isomerized into the *cis*-cavitand, inducing a decreased reaction rate.^[55]

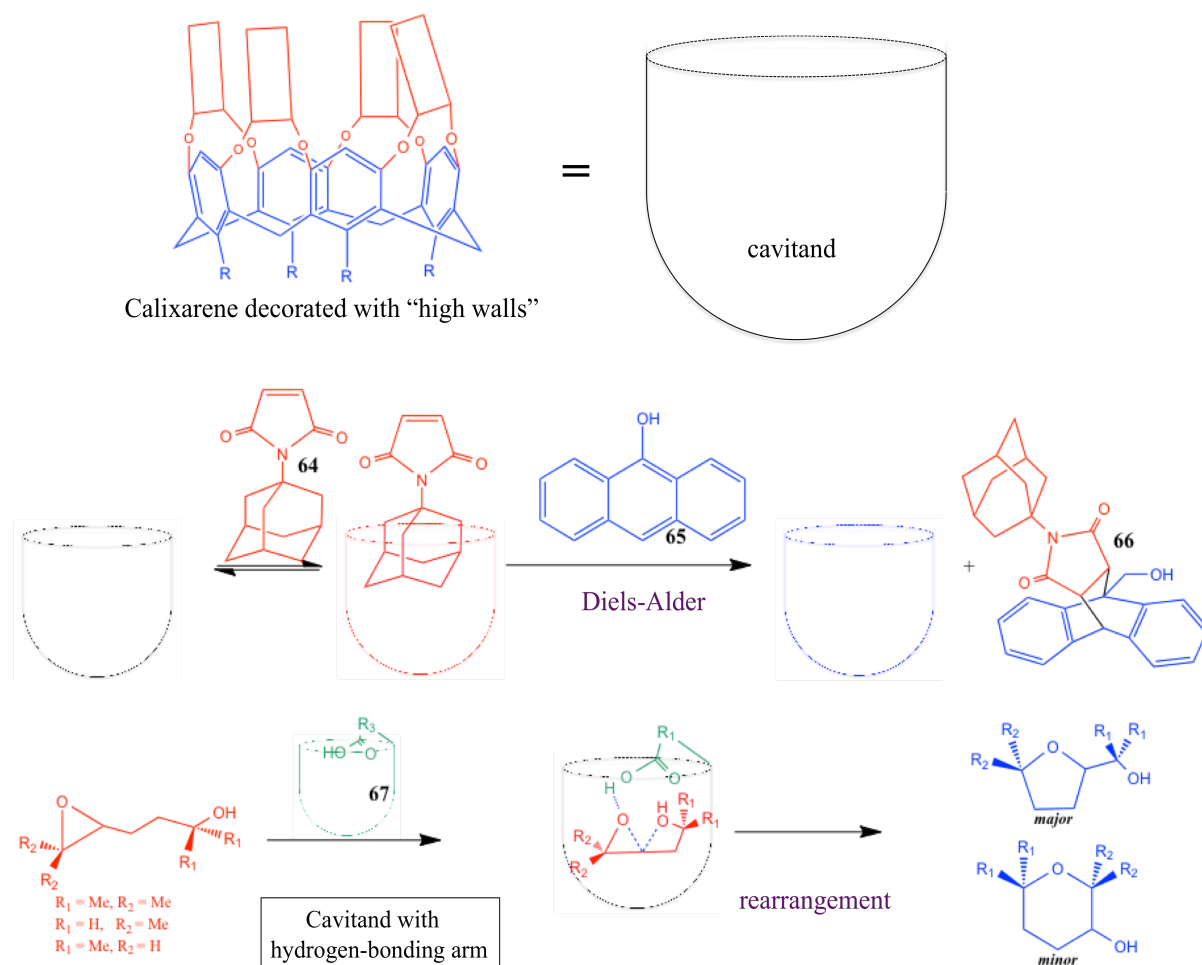


Figure 7. Rebeck's cavitands as nanoreactors.^[53,54]

Real molecule containers were synthesized via hydrogen bonding, covalent bonding or metal-ligand coordination. One of the first examples of nanoreactor that were self-assembled *via* hydrogen bonds was reported by Rebeck et al. A pseudo-spherical shell, called “soft-ball” **68** was assembled via 16 H-bonds between two glycoluril moieties in an organic solvent and used in the Diels-Alder reaction. The reaction between *p*-quinone **69** and cyclohexadiene **70** in *p*-xylene was studied at r.t., and substrates could enter inside the capsule using the π - π stacking interactions with the cavity of the capsule. A 200-fold acceleration of the reaction was observed in the presence of the capsule because the concentration of the substrates inside the capsule is increased, however the final product **71** presents a better affinity with the capsule, which inhibits the use of the nanoreactor in catalytic amount.^[56] This research group also simultaneously developed a cylinder-shaped capsule **72** composed of two self-complementary vase-shaped resorcinarenes. These two cavitands are substituted with four imide-functionalities on their upper rim and formed a seam of eight bifurcated hydrogen bonds, i.e. sixteen hydrogen bonds. This cylinder-shaped capsule allows the selective 1,3-cycloaddition to 1,4-triazole compound **75** between the phenylacetylene **73** and the phenylazide **74**. The capsule constrains the guests orientation edge-to-edge, influencing the selectivity of the reaction, as both 1,4 and 1,5 triazoles were obtained without capsule. However, the final product remains trapped, however, and therefore also inhibits the catalytic reaction.^[57]

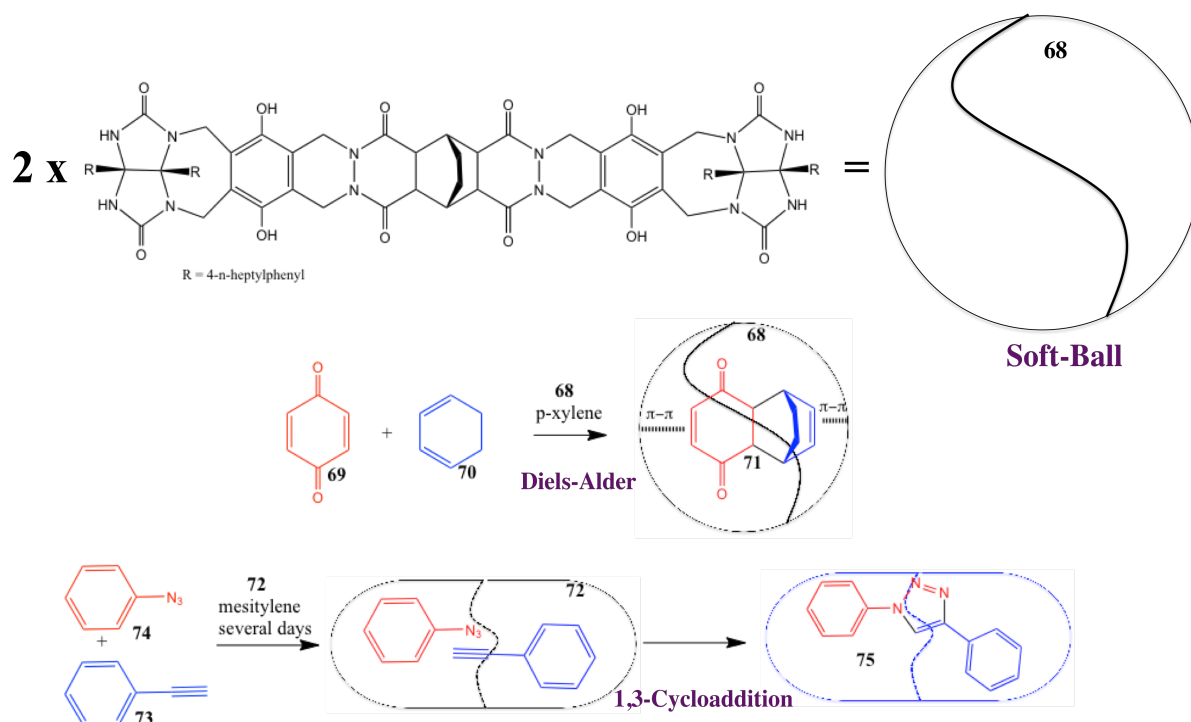


Figure 8. Self-assembled capsules developed by Rebek.^[56,57]

By using the hexameric resorcin[4]arene self-assembled cage that involves 60 hydrogen bonds and was reported by Atwood and MacGillivray,^[58] Reek et al. have encapsulated a gold-NHC catalyst that performed oxidation of alkyne leading to unusual products due to the steric requirements of the host's cavity.^[59] Nanoreactor self-assembly could also be assembled using a suitable guest. This is the case of the di-carcerand octaacid capsule developed by Gibb et al. that has actually only been used for the selective oxidation of olefins by singlet oxygen.^[60]

The group of Fujita and that of Bergman and Raymond are most active on coordination cages for enzyme-like catalysis. A decade ago, the latter group reported various tetrahedral assemblies of $[M_4L_6]^{12-}$ stoichiometry ($M = Ga^{3+}, Al^{3+}, Fe^{3+}$; $L =$ bis(bidentate) catecholamide) formed through the self-assembly of achiral components to yield exclusively a racemic mixture of homochiral $\Delta, \Delta, \Delta, \Delta$ - or $\Lambda, \Lambda, \Lambda, \Lambda$ -clusters with Δ or Λ configuration at each metal center (Figure 9). One such $[Ga_4L_6]^{12-}$ assembly utilizes a naphthalene based catecholamide ligand backbone. This highly negatively charged capsule **76** is soluble in polar solvents such as water, and the naphthalene-based ligand scaffold generates a hydrophobic cavity of approximately 0.5 nm^3 . This hydrophobic cavity allows the cage to encapsulate a variety of hydrophobic monocationic species or species containing double bonds or aromatic moiety thank to hydrophobic effect + π - π stacking interactions with naphthalene. The first example of catalysis with such a cage used an iridium complex that was encapsulated inside the cavity allowing the C-H bond activation of aldehydes (Figure 9).^[61] The same nanoreactor is also able to stabilize protonated substrates and consequently catalyzes the normally acidic hydrolysis of orthoformates in basic solution, with rate accelerations of up to 890-fold. The catalysis reaction obeys Michaelis-Menten kinetics and exhibits competitive inhibition, and the substrate scope displays size selectivity (as for the C-H bond activation of aldehydes), consistent with the constrained binding environment of the molecular host.^[62] Other

studies have proved the use of the cage in catalytic amount for the aza-Cope rearrangement (Figure 9). Thanks to the binding of the substrates in a reactive conformation, the host assembly accelerates the rates of rearrangement (up to 184 in the case of propargyl enammonium cations).^[63,64] The Nazarov cyclization of pentadienols to form cyclopentadienes was also studied in the presence of $[\text{Ga}_4\text{L}_6]^{12-}$ above with a rate increased up to 10^6 -fold. The final product must be a poor guest for the cavity in order to avoid inhibition of the reaction and therefore be trapped with maleimide via a Diels-Alder reaction (Figure 9). Very recently, kinetic analysis of the reaction, ^{18}O -exchange experiments, and computational studies demonstrated a mechanism in which encapsulation, protonation, and water loss from substrate are reversible, followed by irreversible electrocyclicization. Although electrocyclicization is rate determining in the uncatalyzed reaction, the barrier for water loss and for electrocyclicization are nearly equal in the cage-catalyzed reaction. Analysis of the proposed energies of the catalyzed and uncatalyzed reactions revealed that transition-state stabilization contributes significantly to the catalytic rate acceleration. This, in addition to the enhanced basicity caused by encapsulation in the cage, is responsible for the dramatic million-fold rate enhancement over the uncatalyzed reaction.^[65,66]

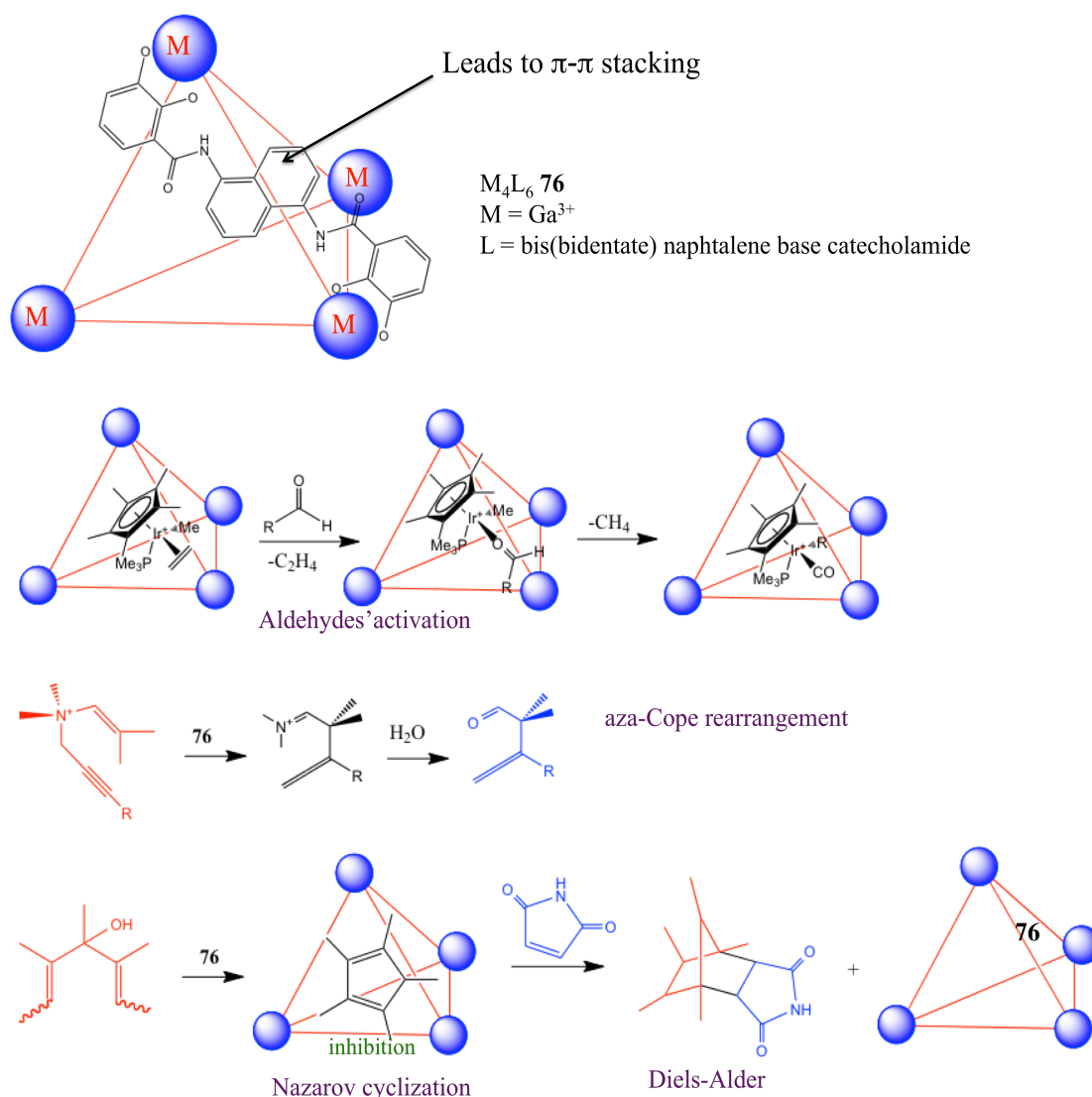


Figure 9. Raymond and Bergman's system

Very recently, these authors showed that such water-soluble host assemblies were capable of catalyzing the substitution reaction at a secondary benzylic carbon center to give products with overall stereochemical retention, while reaction of the same substrates in bulk solution gives products with stereochemical inversion.^[67]

Fujita's group has developed an octahedral cage M_6L_4 **77** assembled from *cis* end-capped Pd(II) ions and triazine-cored tridentate pyridine ligands. This coordinated cage was used as nanoreactor for diverse catalytic reactions (Wacker oxidation, Diels-Alder, photodimerisation and Knoevenagel condensation) and compared to the nanoreactor of a square-pyramidal bowl, half open cage **78** synthesized by the same research group (Figure 10). The Wacker oxidation of the styrene **79** to the acetophenone **80** with 10 % mol of a Pd catalyst yielded 82% in the presence of 10 % mol of the cage, whereas without cage only a 4% yield was obtained (Figure 10). Moreover due to the strong binding ability of the cage toward electron-rich aromatic compounds, the Wacker oxidation of various aromatics was particularly efficient for electron-rich substrates.^[68] The photodimerisation of olefins in water at 80°C during 10 min within the cage **77** or within the square-pyramidal bowl **78** was then studied. For example, the regioselectivity in the photodimerization of 2-methylnaphthoquinone **81** within the cage was very high (96% of the syn head-to-tail product **82**), but only moderate within the bowl (78% **82** head-to-tail). The reaction without nanoreactor gives the *anti* dimer **83** with a yield of 21% (Figure 10). Also in this case, the nanoreactors nicely accommodate the substrate in the cavity through aromatic interactions (π - π and CH- π).^[69,70] More recently the cage (1 % mol) has been used in the Knoevenagel condensation of aromatic aldehydes in water under neutral conditions. The addition of a nucleophile to the aldehyde to generate anionic intermediates seems to be facilitated by the cationic environment of the cavity. The products resulting from the condensation of an aromatic aldehyde with Meldrum's acid are ejected from the cage as a result of the host-guest size discrepancy (Figure 10). The reaction with the 2-naphthaldehyde **84** leads to 96% of the desire product **85** in the presence of the cage **77** (1% mol), only 17% even in the presence of the bowl **78** in stoichiometric amount and 2% without nanoreactor.^[71] The last well-representative example is the use of these two nanoreactors in the Diels-Alder reaction between the 9-hydroxymethylantracene **86** and the *N*-cyclohexylphthalimide **87** in water. Generally the reaction leads to the coupling product **88** bridging the central ring at the 9,10-position due to the high localization of π -electron density at that site. However, in the presence of the cage **77**, an unusual regioselectivity is observed: the Diels-Alder reaction occurs at the terminal ring (1,4-position, leading to product **89**). The cage increases the effective concentration and preorganization of the reactants, greatly reducing the entropic cost and supporting an increase in the naphthalene reactivity as a diene during the Diels-Alder reaction. This increase in reactivity was also proved via unreactive substrates such as naphthalene, that underwent the Diels-Alder reaction in the presence of the cage.^[72] The square-pyramidal bowl also plays an important role as nanoreactor. In the Diels-Alder reaction between 9-hydroxymethylantracene **86** and the *N*-cyclohexylphthalimide **87**, the anthracene stacks onto the triazine ligand of the bowl, gaining considerable stabilization via aromatic-aromatic or charge-transfer interactions. The Diels-alder reaction efficiently occurs yielding 99% of the central (9,10-position) adduct **88** with only 1% mol of the bowl, whereas in the same condition without the bowl only 3% of the final product was observed (Figure 1a). One of the driving forces of the reaction is that the final product is losing the aromatic stacking interaction with the bowl, which ejects the product from the bowl. The adduct obtained in this case at the 9,10-position

instead of 1,4-position in the presence of the cage was explained by the fact that no preorganization of the substrates inside the bowl, i.e. no strains imposed by a closed environment occurs because of the concave open space.^[73]

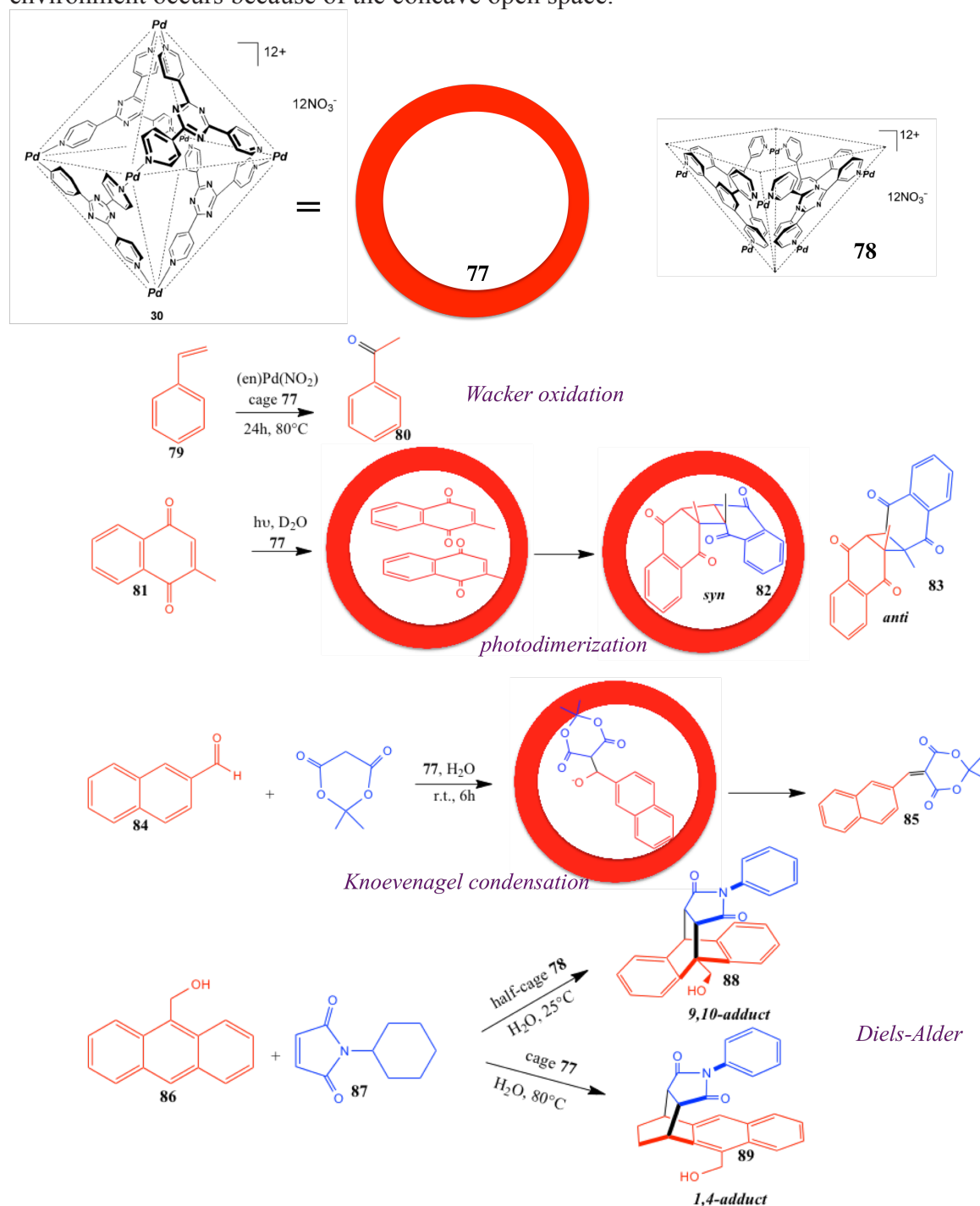


Figure 10. Fujita's capsules and their catalytic applications.^[68-73]

Recently, Mukherjee et al. have developed a water-soluble semi-cylindrical cage with a hydrophobic cavity formed via a two-component self-assembly of a $90^\circ Pd^{II}$ acceptor and a triimidazole donor. This nanoreactor was used in the Knoevenagel condensation and Diels-Alder reaction and compared to Fujita's systems. As it was the case with Fujita's bowl, the Diels-alder reaction between 9-hydroxymethylanthracene **86** and the N -cyclohexylamide **87** in water at r.t. with 10% mol of the new cage leads to the adduct **88** bridging the central ring at the 9,10-

position. This is due to the open space as with the Fujita's half cage **78** that did not impose a specific restricted conformation as contrary to the cage **77**. The entrance of the substrates inside the cage was also guided by hydrophobic interactions and π - π stacking interactions with the wall of the cage. The loss of aromaticity of the adduct at the end of the reaction allows the displacement of the reaction equilibrium, which explains well the nanoreactor effect involving 49% yield with the cage against 9% yield without the cage. By changing the cyclohexyl of the amide by a benzyl group, π - π stacking interactions are added inducing a better encapsulation of the dienophile substrate, which leads to a 89% yield instead of 11% yield in the absence of nanoreactor.^[74]

Micellar nanoreactors

Micelles are spherical aggregates of amphiphilic molecules. Generally, the amphiphilic molecules are composed of a hydrophilic head and a long hydrophobic tail, mimicking fatty acids. Block copolymers are not treated here. Direct micelles are formed in water whereas inverse micelles are observed in organic solvents. The micelle solubilizes both polar and nonpolar reactants from an aqueous phase thanks to the difference in polarity between the hydrophilic surface and the hydrophobic core. In that way, micelles allow the enhancement of a reaction by increasing the local concentration of the substrate or by stabilizing a transition state. The simplicity of synthesis of the amphiphilic molecules leads to the huge use of micelle in the catalytic field. Only most representative examples will be discussed here. As well-known examples, Kobayashi and co-workers studied a variety of acid-catalyzed reactions in water in the presence of various surfactants such as sodium dodecyl sulfate (SDS) **89**, a cationic surfactant cetyltrimethyl ammonium bromide (CTAB) **90** and a non-ionic surfactant Triton X-100 **91**. The example of the Aldol reaction between the benzaldehyde **92** and the benzene [(Z)-1-[(trimethylsilyl)oxy]-1-propen-1-yl] **93** in the presence of scandium tris(dodecylsulfate) (Sc(DS)₃) as catalyst (10% mol) was chosen. In water, at r.t., only the reaction in presence of SDS (20 mol %, 35nM) is giving 88% of the Aldol compound **94** in 4 hours but only 3% yield without surfactant or in presence of CTAB **90**, and in the presence of Triton X-100 **91** in 60 hours the reaction yield is 89%. The effectiveness of the anionic surfactant is attributed to a high local concentration of scandium cations on the surfaces of dispersed organic phases, which are surrounded by the surfactant molecules. The Lewis acid-surfactant combined catalyst was expected to act both as Lewis acid to activate the reactants and as surfactant to form a stable colloidal dispersion. This kind of catalyst was used in other carbon-carbon bond forming reactions such as allylations and Mannich-type conversions.^[75, 76] Otto and co-workers have performed Diels-Alder Lewis acid-catalyzed reactions in micellar media. Micelles such as SDS **89**, CTAB **90** and C₁₂E₇ **95** have shown no real effect on the Diels-Alder reaction, whereas micelles of Cu(DS)₂ copper dodecyl sulfate **96** induce rate enhancements up to a factor 1.8x10⁶ compared to the uncatalyzed reaction in acetonitrile. This nanoreactor effect results from efficient complexation of the dienophile to the catalytically active copper ions, both species being concentrated at the micellar surface. The micelle provides a confined environment that leads to a faster reaction. Moreover, the higher affinity of cyclopentadiene for Cu(DS)₂ **96** compared to SDS **89** and CTAB **90** micelles diminishes the inhibitory effect due to spatial separation of the dienophile and the diene as observed for SDS **89** and CTAB **90**.^[77] Another classic

use of surfactant is described through the well-known emulsion polymerization for instance by ring opening metathesis polymerization for the production of a variety of polymers under mild, practical, and environmentally friendly conditions.^[78] Following the success of the emulsion polymerization, ring closing metathesis (RCM) and cross metathesis (CM) under heterogeneous aqueous conditions were described. Davis and Sinou studied the activity of Grubbs 1st generation and related complexes towards RCM in water in the presence of surfactants, such as SDS **89**, SDSO₃Na **97**, CTAHSO₄ **98**, Brij 30 **99**, Tween40 **100**, HDAPS **101**, and DDAPS **102**. Although the RCM of diethyldiallylmalonate (25°C, 15–60 min) occurred in degassed water even in the absence of the surfactant, the addition of SDS **89** (5 mol%) improved conversion because of the formation of micelles.^[79] Lipshutz et al. have reported the use of Grubbs 2nd generation (2 mol %) for CM and ROM-CM (Ring Opening Methathesis) in water in the presence of a specific non-ionic surfactant PTS **103** derived from vitamin E (2.5 mol %), whereas other classic surfactants were less efficient.^[80] Lot of reactions has been studied in the presence of surfactants, and very recently Lipshutz' group has developed the use of specific surfactant TPGS-750-M **104** for the aerobic oxidation of aryl alkynes and arylsulfinate salts to β-ketosulfones^[81] and activated alcohols (to ketones or aldehydes),^[82] in water at r.t. The oxidation is taking place within the lipophilic core of the nanomicelles (53 nm) present in aqueous solution, moreover the nanomicelle solubilizes oxygen from air inside the hydrophobic core which increases the reaction rate. No similar good results were observed in the presence of classic surfactants.

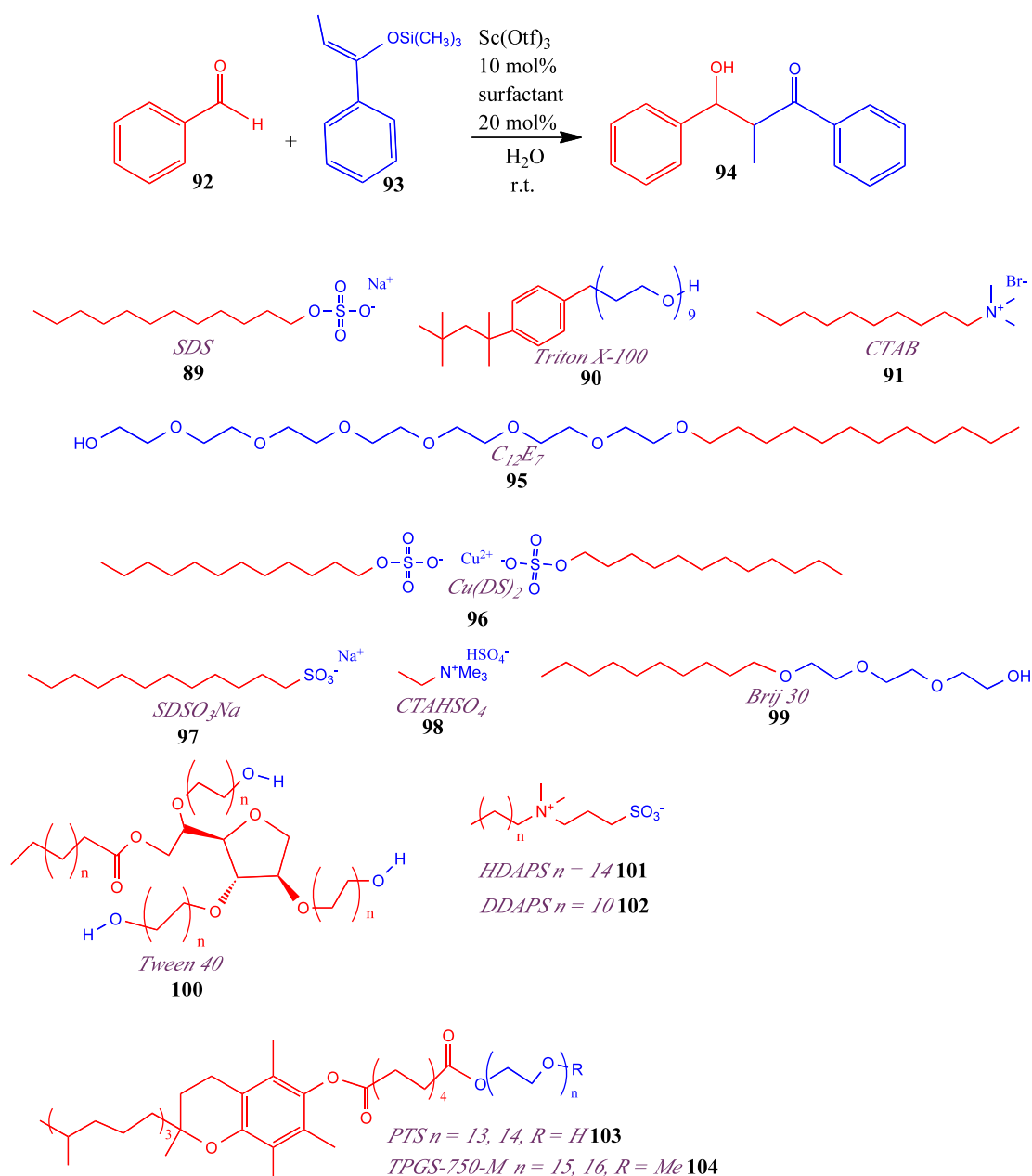


Figure 11. Surfactants as nanoreactors.

Usually, surfactants and amphiphilic block copolymers assemble at low concentration up to their critical micellar concentration MCM into micelles. Depending on the relative hydrophobicity and the relative composition/geometry of hydrophilic and hydrophobic moieties, spherical, prolate or oblate micelles are formed.^[83] On the other hand lipids usually form lamellar bilayer structures over the majority of their phase diagrams, and in dilute solutions they form vesicles. As for micelles, vesicles formed with polymers have superior stability and toughness than vesicles formed with lipids. Recently, Desset et al. demonstrated that 1-octyl-3-methylimidazolium **105** and other alkylimidazolium salts accelerated the hydroformylation of alkenes in aqueous-biphasic medium.^[84,85] van Leeuwen et al. prepared water-soluble analogues of Xantphos (**106**, **107**). **106** and **107**, alone as well as when coordinated to the Rh precursor, gave vesicles in water.^[86] By reacting **106** with $[\text{Rh}(\text{H})\text{CO}(\text{PPh}_3)_3]$, the complex **108** was synthesized and formed vesicles with an average diameter of 140 nm alone and of 500–600 nm in the presence of 1-octene, the substrate for the

hydroformylation experiments. When this reaction is performed at 343 K, ligands **106** and **107** are 6 times and 12 times more active, respectively, than the water-soluble diphosphine 2,7-bis(SO₃Na)Xantphos (**109**). At 393 K, when the vesicles are partly disrupted, the relative reaction rate decreased, **107** being only three times more active than **109**) Importantly, a high selectivity is maintained with ligands **106** and **107** (1 : b = 98 : 2) and during the recycling process neither emulsions nor transfer of the Rh metal into the organic phase is observed. Thus several runs with the same catalyst were performed without loss of activity and selectivity. In most cases, organic or polymeric vesicles and micelles are used for the stabilization of nanoparticles that are used as catalyst.^[87]

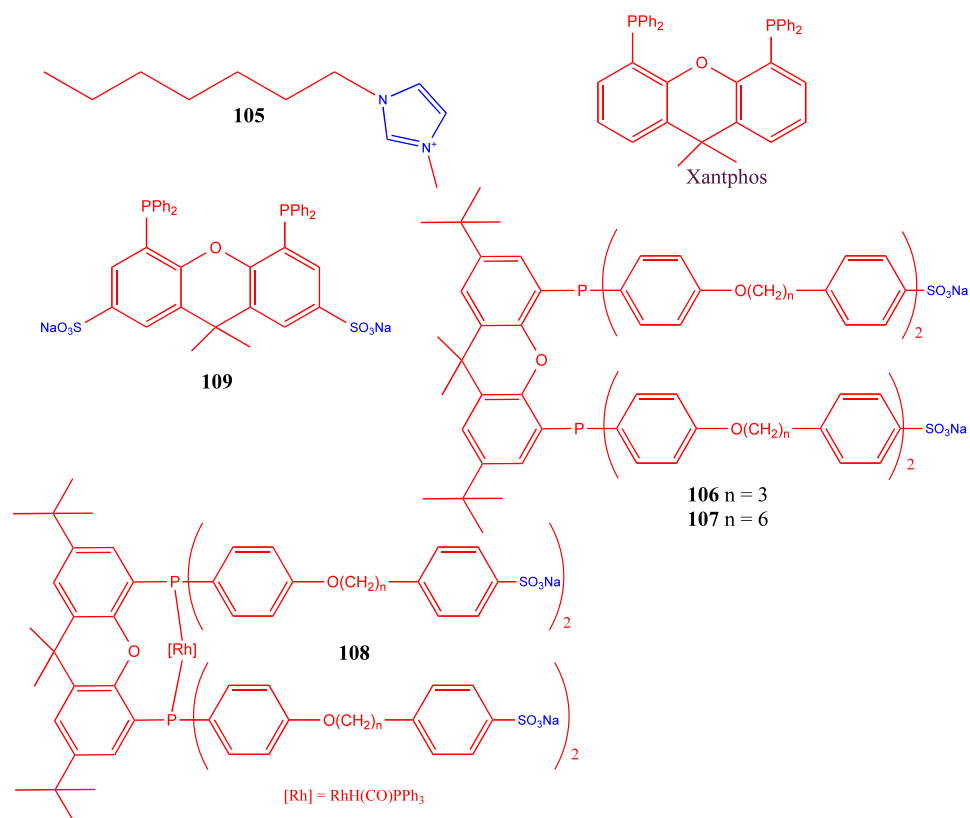


Figure 12. Other surfactants forming micelles or vesicles.

As the stability of the micelles and the vesicles actually depend on the environment, such as the concentration of the surfactants, the pH or the temperature of the solution, the synthesis of dendrimers and dendronized polymers was introduced as a valuable, molecularly well-defined alternative. Dendrimers are unimolecular micelles; they are macromolecules with the shape of a cauliflower. The dendrimers are composed of holes between their branches, which allow the encapsulation of various molecules. Dendrimers are flexible when they are small, but they adopt a globular shape by increasing in generation, eventually leading to more rigid macromolecules.

Four different kinds of dendritic catalysts can be designed, i.e. the catalytic species can be (i) covalently linked to the core of the dendrimer, (ii) covalently linked to the periphery of the dendrimer, (iii) coordinatively attached inside the dendrimer to amide or triazole group for example and (iv) encapsulated inside the dendrimer for example by hydrophobic interactions. Diederich's group also developed dendrophanes such as **110** (Figure 13) composed of a cyclophane moiety at the core and a dendritic

periphery, also with a catalytic thiazolium site. This dendritic macrocycle catalyzed the model reaction of oxidation of naphthalene-2-carbaldehyde thanks to π - π and/or hydrophobic interactions of the substrates with the nanoreactor allowing the dynamic entry into the cavity.^[88] Crooks' group is using hydroxyl-terminated poly(amidoamine) (PAMAM) dendrimers as nanofilters. After coordinating Pd^{II} to the amido groups inside the dendrimers of different generations, the Pd^{II} is chemically reduced into Pd⁰ nanoparticles (PdNPs). As the dendrimers G4-OH, G6-OH, and G8-OH are sufficiently large, the PdNP is encapsulated inside the dendrimer (DEN). While G4-OH(Pd₄₀) allows the hydrogenation of both small and big alkenes, only small alkenes were hydrogenated with G6-OH(Pd₄₀). On the contrary no hydrogenation reaction was observed for small and large substrates in the presence of G8-OH(Pd₄₀) (Figure 13). The different nanofilters provided selectivity in the hydrogenation catalysis.^[89,90]

The Astruc group synthesized an amphiphilic dendrimer **111** via "click" copper (I)-catalyzed azide alkyne cycloaddition (CuAAC) reaction between an arene-nona azido core and 9 tris-triethylene glycol dendrons. This dendrimer was very efficiently employed as nanoreactor for the metathesis reactions in water. In the presence of low amount of various commercial ruthenium metathesis catalysts, and in particular of only 0.083 mol % of the nanoreactor and 0.04-2mol % of Grubbs' 2nd generation catalyst, RCM, EYM (enynes metathesis) and CM were carried out efficiently. For example, the CM of 1,7-octadiene in water at room temperature with 0.1 mol % of catalyst and 0.083 mol % of the dendrimer yielded 86% in water, whereas no final product was obtained under these conditions without dendrimer. It is proposed that the dendrimer solubilizes the hydrophobic molecules at the hydrophobic core that allows gathering in the dendrimer interior the catalyst and the substrate.^[91,92] The very low amount of catalyst used, contrasting with relatively high amounts of metathesis catalyst usually used by chemists in organic solvents results from the protection inside the dendrimer of the Ru-methylene intermediate of metathesis reactions that is subjected to side reactions under ordinary conditions outside the dendrimer. Recently they stabilized PdNPs with various dendrimers containing these 1,2,3-triazole ligands resulting from their construction including such low-generation amphiphilic dendrimers.^[93-95] The combination between the 1,3-triazolyl rings coming from the CuAAC reaction and the triethylene glycol termini (dendrimer **111**) provided excellent stabilization of PdNPs in water and excellent catalytic activity of these PdNPs in aqueous media for carbon-carbon cross coupling reaction and for the reduction of 4-nitrophenol. Under these conditions, it has been demonstrated that the Suzuki-Miyaura coupling of bromoaromatics proceeded in H₂O/EtOH (1/1) at 80°C with only 0.3 ppm of Pd (TON up to 2 700 000).^[96-98]

In the same research group, this dendritic nanoreactor was used for a very efficient "click" CuAAC catalysis in only water. After showing by 600 MHz NMR in D₂O the encapsulation of the hydrophobic Cu(I) catalyst (hexabenzyltren-Cu(I)) **112** driven by hydrophobic effect inside the dendrimer, the "click" reaction was performed on several substrates at r.t. with 0.1 mol % of catalyst **112** and 1 mol % of dendrimer. As an example, the reaction between benzyl azide **113** and phenyl acetylene **73** yielded 91% of 1,4-triazole product **114** in three hours whereas without nanoreactor the reaction yield was below 5% (Figure 13). No change in the reaction yield was observed after 10 times recycling of the dendrimer.

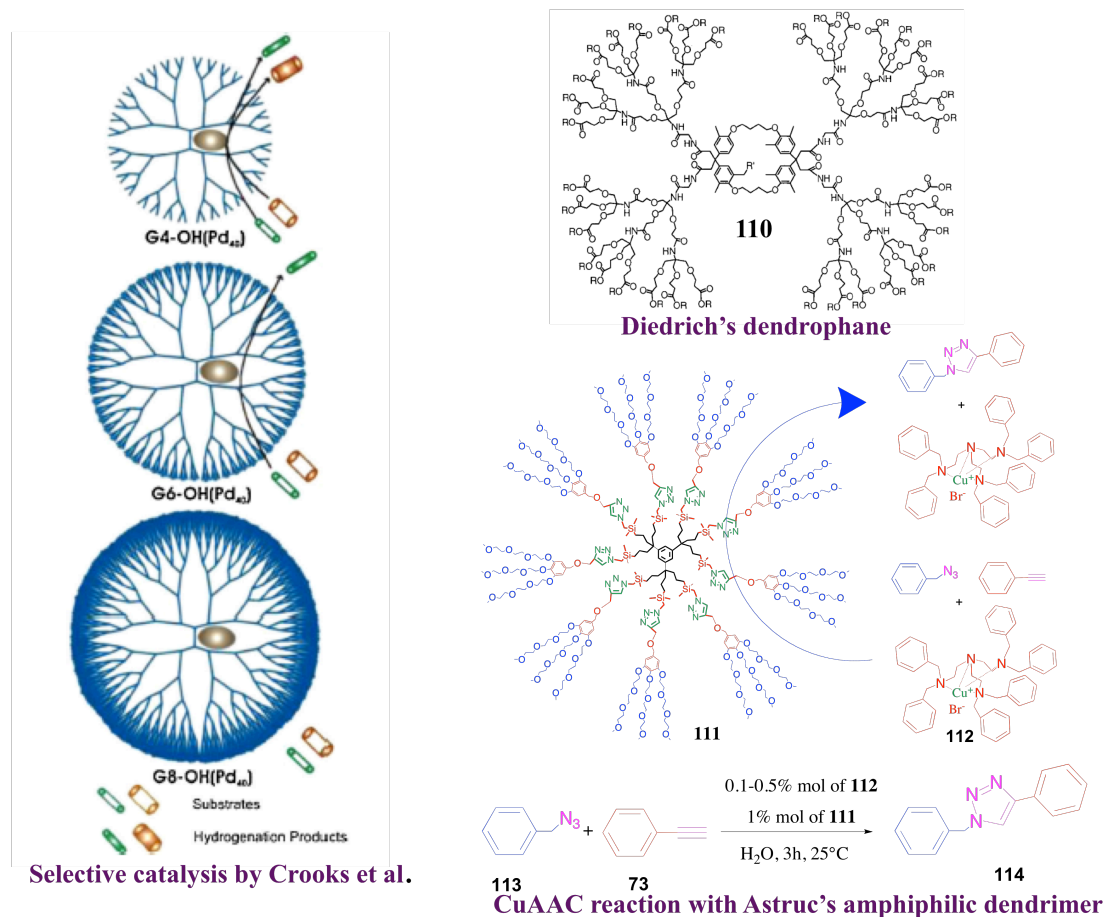


Figure 13. Dendrimer as nanoreactors for selective catalysis, efficient catalysis or catalysis in water.

Interestingly, by coupling the micellar effect of the dendrimer and ligand activation Cu(I), simply generated by reduction of $\text{CuSO}_4 \cdot 5\text{H}_2\text{O}$ by sodium ascorbate, by the intradendritic 1,3-triazole rings, the same click reaction between benzyl azide **113** and phenyl acetylene **73** in water at 30°C was quantitative with only 5 ppm of Cu(I) in 24 hours (TON up 510 000), Figure 14.^[99] This latter system is the most active one for the CuAAC “click” reaction. Yet, it is rather simple, and the dendrimer is recycled many times.

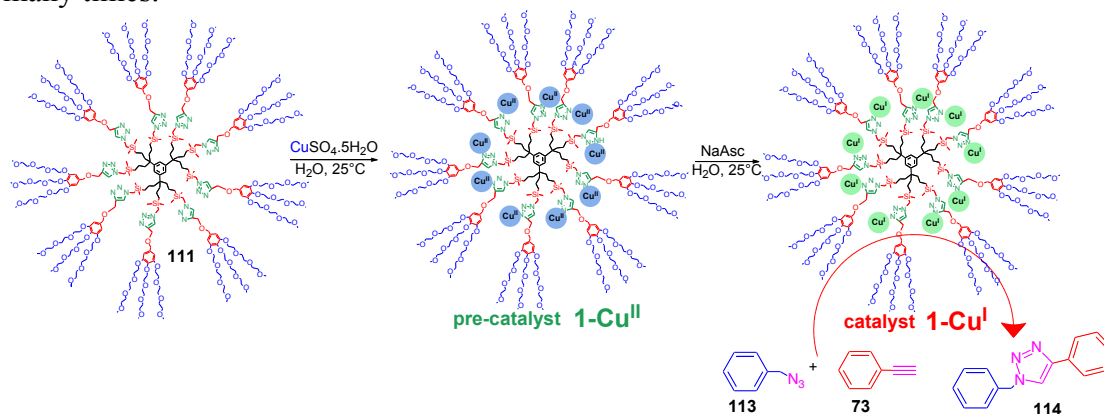


Figure 14. Cu(I) activated with dendrimer **111** as very efficient catalyst/nanoreactor for the CuAAC reaction.

Conclusion

It has been shown in this review that researchers have for several decades astutely used their skills in chemistry in order to engineer, synthesize and use macromolecules with cavities. From the first nanoreactors, the macrocycles and cryptates found their utility in catalysis using as a first recognition step of ionic part generally helping the orientation of a chemical reaction, to cyclodextrins, calixarenes or cucurbituril that bring a micro-environment in which real catalytic reaction can occur, these macrocycles accelerate reactions, or make them more selective. The use of more “sophisticated” systems such as nano-container takes an important place in this nanoreactor field essentially because of the universality of these systems. The cage of Fujita or the ones of Bergman and Raymond are possibly the most representative systems because they have proved their efficiency in several reactions that were essentially reviewed here. Micellar systems, such as unimicellar dendrimers are also good candidate for the place of a universal nanoreactor with several very efficient catalytic reactions that were developed very recently. It is important to notice that in all the cases reported here, a first recognition step was necessary in order to enter in the cavity, in order to shelter in a micro-environment, which will increase the local concentration of the substrates or will position the substrates in their “transition state” during a the chemical reaction, leading to an improvement of the reaction rate. This first step of recognition corresponds to hydrogen bonding, electrostatic interaction, Van Der Waals interaction, π - π interaction, steric effect, shape complementarity, or hydrophilic/hydrophobic effects. Improvement of several systems remains a challenge, because frequently the high affinity of the final product for the nanoreactor leads to inhibition of the reaction avoiding the catalytic use of the nanoreactor. Along this line, engineered dendritic molecular nanoreactors have shown remarkable efficiency for numerous key catalytic reactions, easy recycling and escape of products resulting from the dendritic tether flexibility.

References

1. P. T. Anastas, J. C. Warner, Green Chemistry: Theory and Practice, *Oxford University Press*: New York, **1998**, p.30.
2. A. D. Smith (Ed) (**1997**). *Oxford dictionary of biochemistry and molecular biology*. Oxford [Oxfordshire]: Oxford University Press
3. L. Pauling, *Chem. Eng. News* **1946**, *24*, 1375-1377.
4. M. J. Wiester, P. A. Ulmann, C. A. Mirkin, *Angew. Chem. Int. Ed.* **2011**, *50*, 114-137.
5. Z. Dong, Q. Luo, J. Liu, *Chem. Soc. Rev.* **2012**, *41*, 7890–7908.
6. M. Raynal, P. Ballester, A. Vidal-Ferran, P. W. N. M. Van Leeuwen, *Chem. Soc. Rev.* **2014**, *43*, 1734-1787.
7. E. M. M. Del Valle, *Process Biochem.* **2004**, *39*, 1033-1046.
8. B. Sarkar, P. Mukhopadhyay, P. K. Bharadwaj, *Coord. Chem. Rev.* **2003**, *236*, 1-13.
9. V. Böhmer, *Angew. Chem.; Int. Ed. Engl.* **1995**, *34*, 713-745.
10. C. D. Gutsche, (**1989**). *Calixarenes*. Cambridge: Royal Society of Chemistry
11. J. Lagona, P. Mukhopadhyay, S. Chakrabart, L. Isaacs, *Angew. Chem.; Int. Ed.* **2005**, *44*, 4844–4870.

12. J. W. Steed, J. L. Atwood, *supramolecular chemistry* 2nd Edition, (2009), Wiley.
13. M. Fischer, F. Vögtle, *Angew. Chem.; Int. Ed.* **1999**, *38*, 884-905.
14. M. Antonietti S. Förster, *Adv. Mater.* **2003**, *15*, 1323-1333.
15. J. M. Lehn, *Angew. Chem. Int. Ed. Engl.* **1988**, *27*, 89–112
16. D. J. Cram, *Angew. Chem. Int. Ed. Engl.* **1988**, *27*, 1009–1020.
17. C. J. Pederson, *Angew. Chem. Int. Ed. Engl.* **1988**, *27*, 1021–1027.
18. J.-M. Lehn, C. Sirlin, *J. Chem. Soc. Chem. Commun.* **1978**, 949-951.
19. L. Jiang, Z. L. Liu, Z. Liang, Y. H. Gao, *Bioorg. Med. Chem.* **2005**, *13*, 3673-3680.
20. E. F.J. de Vries, L. Ploeg, M. Colao, J. Brussee, A. van der Gen, *Tetrahedron: Asymmetry* **1995**, *6*, 1123-1132.
21. B. Sarkar, P. Mukhopadhyay, P. K. Bharadwaj, *Coord. Chem. Rev.* **2003**, *236*, 1-13.
22. P. Mattei, F. Diederich, *Helv. Chim. Acta.* **1997**, *80*, 1555-1588.
23. F. Diederich, H. D. Lutter, *J. Am. Chem. Soc.* **1989**, *111*, 8438-8446.
24. R. Breslow, *Acc. Chem. Res.* **1995**, *28*, 146-153.
25. W. Saenger, *Angew. Chem. Int. Ed. Engl.* **1980**, *19*, 344-362.
26. I. Tabushi, *Acc. Chem. Res.* **1982**, *15*, 66-72.
27. R. Breslow, G. Trainor, A. Ueno, *J. Am. Chem. Soc.* **1983**, *105*, 2739-2744.
28. D. Rideout, R. Breslow, *J. Am. Chem. Soc.* **1980**, *102*, 7812-7815.
29. B. Madhav, S. Narayana Murthy, V. Prakash Reddy, K. Rama Rao, Y. V. D. Nageswar, *Tetrahedron Letters* **2009**, *50*, 6025–6028.
30. K. Surendra, N. Srilakshmi Krishnaveni, Y. V. D. Nageswar, K. Rama Rao, *J. Org. Chem.* **2003**, *68*, 4994-4995.
31. N. Srilakshmi Krishnaveni, K. Surendra, K. Rama Rao, *Adv. Synth. Catal.* **2004**, *346*, 346-350.
32. H.-B. Ji, D.-P. Shi, M. Shao, Z. Li, L.-F. Wang, *Tetrahedron Letters* **2005**, *46*, 2517–2520.
33. J.-A. Shin, Y.-G. Lim, K.-H. Lee, *J. Org. Chem.* **2012**, *77*, 4117–4122.
34. A. Nakamura, Y. Inoue, *J. Am. Chem. Soc.* **2003**, *125*, 966-972.
35. L. G. Marinescu, M. Bols, *Angew. Chem. Int. Ed.* **2006**, *45*, 4590–4593.
36. J. Bjerre, C. Rousseau, L. Marinescu, M. Bols, *Appl. Microbiol. Biotechnol.* **2008**, *81*, 1–11.
37. Y.-H. Zhou, M. Zhao, H. Sun, Z.-W. Mao, L.-N. Ji, *J. Mol. Catal. A: Chemical* **2009**, *308*, 61–67.
38. R. R. French, P. Holzer, M. G. Leuenberger, W.-D. Woggon, *Angew. Chem. Int. Ed.* **2000**, *39*, 1267-1269.
39. D. M. Homden, C. Redshaw, *Chem. Rev.* **2008**, *108*, 5086–5130.
40. C. Dieleman, S. Steyer, C. Jeunesse, D. Matt, *J. Chem. Soc., Dalton Trans.* **2001**, 2508–2517.
41. P. Molenveld, J. F. J. Engbersen, D. N. Reinhoudt, *Chem. Soc. Rev.* **2000**, *29*, 75–86.
42. E. Karakhanov, T. Buchneva, A. Maximov, M. Zavertyaeva, *J. Mol. Catal. A: Chemical* **2002**, *184*, 11–17.
43. Z.-X. Xu, G.-K. Li, C.-F. Chen, Z.-T. Huang, *Tetrahedron* **2008**, *64*, 8668–8675.
44. W. L. Mock, N.-Y. Shih, *J. Org. Chem.* **1983**, *48*, 3619-3620.
45. M. Pattabiraman, A. Natarajan, L. S. Kaanumalle, V. Ramamurthy, *Org. Lett.* **2005**, *7*, 529-532.

46. M. V. S. N. Maddipatla, L. S. Kaanumalle, A. Natarajan, M. Pattabiraman, V. Ramamurthy, *Langmuir* **2007**, *23*, 7545-7554.
47. R. Wang, L. Yuan, D. H. Macartney, *J. Org. Chem.* **2006**, *71*, 1237-1239.
48. B. C. Pemberton, R. Raghunathan, S. Volla, J. Sivaguru, *Chem. Eur. J.* **2012**, *18*, 12178-12190.
49. Y.-Huan Wang, H. Cong, F.-F. Zhao, S.-F. Xue, Z. Tao, Q.-J. Zhu, G. Wei, *Catal. Commun.* **2011**, *12*, 1127-1130.
50. H. Cong, F.-F. Zhao, J.-X. Zhang, X. Zeng, Z. Tao, S.-F. Xue, Q.-J. Zhu, *Catal. Commun.* **2009**, *11*, 167-170.
51. C. J. Walter, H. L. Anderson, J. K. M. Sanders, *Chem. Soc., Chem. Commun.* **1993**, 458-460.
52. Z. Clyde-Watson, A. Vidal-Ferran, L. J. Twyman, C. J. Walter, D. W. J. McCallien, S. Fanni, N. Bampos, R. S. Wylie, J. K. M. Sanders, *New J. Chem.* **1998**, 493-502.
53. L. G. Mackay, R. S. Wylie, J. K. M. Sanders, *J. Am. Chem. Soc.* **1994**, *116*, 3141-3142.
54. R. J. Hooley, J. Rebek, Jr., *Chem. & Biol.* **2009**, *16*, 255-264.
55. O. B. Berryman, A. C. Sather, A. Lled, J. Rebek Jr., *Angew. Chem. Int. Ed.* **2011**, *50*, 9400-9403.
56. J. Kang, J.; Rebek, Jr., *Nature* **1997**, *385*, 50-52.
57. J. Chen, J. Rebek, Jr., *Org. Lett.* **2002**, *4*, 327-329.
58. L. R. MacGillivray, J. L. Atwood, *Nature* **1997**, *389*, 469-472.
59. A. Cavarzan, A. Scarso, P. Sgarbossa, G. Strukul, J. N. H. Reek, *J. Am. Chem. Soc.* **2011**, *133*, 2848-2851.
60. A. Natarajan, L. S. Kaanumalle, S. Jockusch, C. L. D. Gibb, B. C. Gibb, N. J. Turro, V. Ramamurthy, *J. Am. Chem. Soc.* **2007**, *129*, 4132-4133.
61. D. H. Leung, D. Fiedler, R. G. Bergman, K. N. Raymond, *Angew. Chem. Int. Ed.* **2004**, *43*, 963-963.
62. M. D. Pluth, R. G. Bergman, K. N. Raymond, *Science* **2007**, *316*, 85-88.
63. D. Fiedler, R. G. Bergman, K. N. Raymond, *Angew. Chem. Int. Ed.* **2004**, *43*, 6748-6751.
64. C. J. Hastings, D. Fiedler, R. G. Bergman, K. N. Raymond, *J. Am. Chem. Soc.* **2008**, *130*, 10977-10983.
65. C. J. Hastings, M. D. Pluth, R. G. Bergman, K. N. Raymond, *J. Am. Chem. Soc.* **2010**, *132*, 6938-6940.
66. C. J. Hastings, R. G. Bergman, K. N. Raymond, *Chem. Eur. J.* **2014**, *20*, 3966-3973.
67. C. Zhao, F. D. Toste, K. N. Raymond, R. G. Bergman, *J. Am. Chem. Soc.* **2014**, *136*, 14409-14412.
68. H. Ito, T. Kusukawa, M. Fujita, *Chem. Lett.* **2000**, 598-599.
69. M. Yoshizawa, Y. Takeyama, T. Kusukawa, M. Fujita, *Angew. Chem. Int. Ed.* **2002**, *41*, 1347-1349.
70. M. Yoshizawa, Y. Takeyama, T. Okano, M. Fujita, *J. Am. Chem. Soc.* **2003**, *125*, 3243-3247.
71. T. Murase, Y. Nishijima, M. Fujita, *J. Am. Chem. Soc.* **2012**, *134*, 162-164.
72. S. Horiuchi, T. Murase, M. Fujita, *Chem. Asian J.* **2011**, *6*, 1839-1847.
73. M. Yoshizawa, M. Tamura, M. Fujita, *Science*, **2006**, *312*, 251-254.
74. D. Samanta, S. Mukherjee, Y. P. Patil, P. S. Mukherjee, *Chem. Eur. J.* **2012**, *18*, 12322-12329.
75. S. Kobayashi, K. Manabe, *Acc. Chem. Res.* **2002**, *35*, 209-217.

76. K. Manabe, Y. Mori, T. Wakabayashi, S. Nagayama, S. Kobayashi, *J. Am. Chem. Soc.* **2000**, *122*, 7202-7207.
77. S. Otto, J. B. F. N. Engberts, J. C. T. Kwak, *J. Am. Chem. Soc.* **1998**, *120*, 9517-9525.
78. A.M. van Herk, *Chemistry and Technology of Emulsion Polymerization*, Wiley-VCH, Weinheim, **2005**.
79. K. J. Davis, D. Sinou, *J. Mol. Catal. A* **2002**, *177*, 173-178.
80. B. H. Lipshutz, G. T. Aguinaldo, S. Ghorai, K. Voigtritter, *Org. Lett.* **2008**, *10*, 1325-1328.
81. S. Handa, J. C. Fennewald, B. H. Lipshutz, *Angew. Chem. Int. Ed.* **2014**, *53*, 3432-3435.
82. B. H. Lipshutz, M. Hageman, J. C. Fennewald, R. Linstadt, E. Slack, K. Voigtritter, *Chem. Commun.* **2014**, *50*, 11378-11381.
83. J. N. Israelachvili, D. J. Mitchell, B. W. Ninham, *J. Chem. Soc., Faraday Trans. II* **1976**, *72*, 1525-1568.
84. R. Nguyen, L. Allouche, E. Buhler, N. Giuseppone, *Angew. Chem., Int. Ed.* **2009**, *48*, 1093-1096.
85. B. Wang, I. O. Sutherland, *Chem. Commun.* **1997**, 1495-1496.
86. M. S. Goedheijt, B. E. Hanson, J. N. H. Reek, P. C. J. Kamer, P. W. N. M. van Leeuwen, *J. Am. Chem. Soc.*, **2000**, *122*, 1650-1657.
87. M. P. Pileni, *J. Phys. Chem.* **1993**, *97*, 6961-6973.
88. T. Habicher, F. Diederich, V. Gramlich, *Helv. Chim. Acta*, **1999**, *82*, 1066-1095.
89. R. M. Crooks, M. Zhao, L. Sun, V. Chechik, L. K. Yeung, *Acc. Chem. Res.* **2001**, *34*, 181-190.
90. Y. Niu, L. K. Yeung, R. M. Crooks, *J. Am. Chem. Soc.* **2001**, *123*, 6840-6846.
91. A. K. Diallo, E. Boisselier, J. Ruiz, D. Astruc, *French Patent* 08/05548, **2008**
92. A. K. Diallo, E. Boisselier, L. Liang, J. Ruiz, D. Astruc, *Chem. Eur. J.* **2010**, *16*, 11832-11835.
93. C. Ornelas, J. Ruiz, E. Cloutet, S. Alves, D. Astruc *Angew. Chem., Int. Ed.* **2007**, *46*, 872-877.
94. A. K. Diallo, C. Ornelas, L. Salmon, J. Ruiz, D. Astruc, *Angew. Chem. Int. Ed. Engl.* **2007**, *46*, 8644-8648.
95. D. Astruc, C. Ornelas, J. Ruiz, *Acc. Chem. Res.*, **2008**, *41*, 841-856.
96. C. Deraedt, L. Salmon, L. Etienne, J. Ruiz, D. Astruc, *Chem. Commun.* **2013**, *49*, 8169-8171.
97. C. Deraedt, L. Salmon, D. Astruc, *Adv. Syn. Catal.* **2014**, *356*, 2525-2538.
98. C. Deraedt, D. Astruc *Acc. Chem. Res.* **2014**, *47*, 494-503.
99. C. Deraedt, N. Pinaud, D. Astruc, *J. Am. Chem. Soc.* **2014**, *136*, 12092-12098.

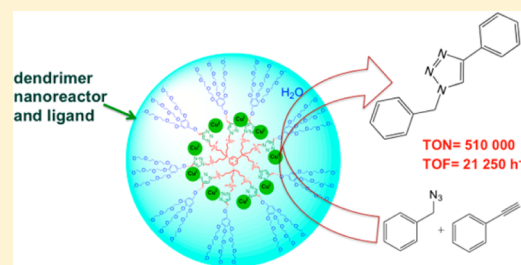
Recyclable Catalytic Dendrimer Nanoreactor for Part-Per-Million Cu^I Catalysis of “Click” Chemistry in Water

Christophe Deraedt, Noël Pinaud, and Didier Astruc*

ISM, Univ. Bordeaux, 351 Cours de la Libération, 33405 Talence, France

S Supporting Information

ABSTRACT: Upon catalyst and substrate encapsulation, an amphiphilic dendrimer containing 27 triethylene glycol termini and 9 intradendritic triazole rings serves as a catalytic nanoreactor by considerably accelerating the Cu^I-catalyzed alkyne–azide cycloaddition (CuAAC) “click” reactions of various substrates in water using the catalyst Cu(hexabenzyltren)Br (tren = triaminoethylamine). Moreover this recyclable nanoreactor with intradendritic triazole rings strongly also activates the simple Sharpless–Fokin catalyst CuSO₄ + sodium ascorbate in water under ambient conditions leading to exceptional TONs up to 510 000. This fully recyclable catalytic nanoreactor allows to considerably decrease the amount of this cheap copper catalyst down to industrially tolerable residues, and some biomedical and cosmetic applications are exemplified.



INTRODUCTION

Since Breslow’s concept of supramolecular nanoreactors with cyclodextrins,¹ nanoreactors are becoming increasingly investigated in catalysis as illustrated by Fujita’s capsule M₆L₄,² Rebek’s soft ball,³ cucurbit[6]uril,⁴ and biresorcinarenes,⁵ respectively, studied by Mock and Warmuth, porphyrin⁶ used by Reek and Van Leuwen, Sanders’ porphyrine macrocycle⁷ and Bergman and Raymond’s capsule.^{8,9} Surfactants and ionic liquids,¹⁰ copolymers that form micelles and polymersomes,¹¹ and dendrimers^{12–29} are useful for the encapsulation or stabilization of catalytically active nanoparticles.^{12–18} In particular, Newkome has proposed dendritic molecular micelles,^{19–21} and Crooks has used dendrimers as nanofilters for nanoparticle catalysis.^{12–14} Along this line, dendrimers have the potential to serve as molecular containers,^{22–24,29} and dendrimers with internal triazole rings on their tethers have been shown to facilitate the catalysis by Pd nanoparticles of C–C cross-coupling reactions.^{18,23–27,30}

It was then of interest to examine whether these dendritic nanoreactors are of general application in catalysis and, in particular, if they can also facilitate or activate catalysis by molecular catalysts. Therefore, we have now addressed their utility in the Cu^I-catalyzed Huisgen-type azide–alkyne 1,3-cycloaddition (CuAAC), the most common “click” reaction allowing to link together two organic, bioorganic, or other functional molecular fragments.^{31,32} The catalytically active Cu^I species is usually generated from CuSO₄ and sodium ascorbate in excess, a very convenient system that works well in aqueous solvents.³² Various genuine Cu^I catalysts that do not require a sacrificial reductant are also known, the advantage of liganded Cu^I, particularly with nitrogen ligands, being the rate acceleration, for instance with the efficient polytriazoles^{33,34} and tris(2-aminoethyl)amine derivatives (tren).^{35–38} The nitrogen ligands allow the use of Cu^I catalysts in amounts that are much reduced (most often of

the order of 1%) compared to the original, simple, and practical catalyst CuSO₄ + sodium ascorbate that is still the most commonly utilized catalyst but in much larger quantities that are often even stoichiometric or superior to stoichiometry.^{25–27} The large quantity of metal catalyst used in the CuAAC “click” reaction and its difficult complete removal presently remain the main problems, inhibiting the utilization of such “click” chemistry in electronics and biomedicine.

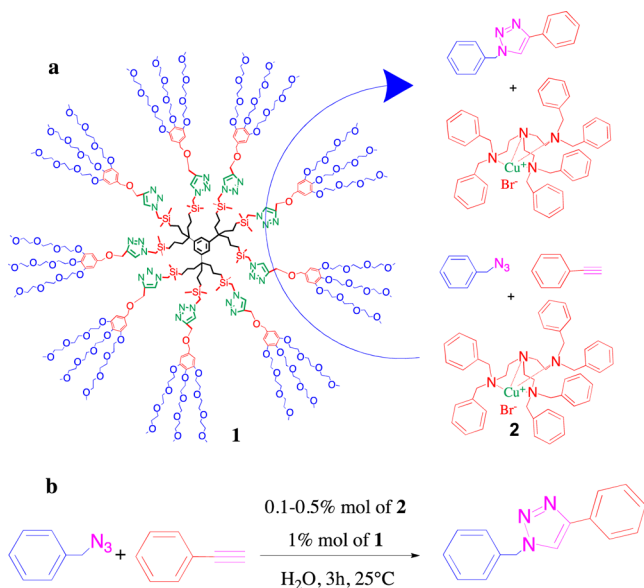
Now the use of the dendrimer **1** terminated by 27 triethylene glycol (TEG) termini³⁹ (Scheme 1a) is proposed as an amphiphilic micellar nanoreactor, stabilizer, and activator of CuAAC reactions in water leading to a considerable decrease of the required Cu^I catalyst for these reactions. The water-soluble dendrimer **1** is also fully recyclable and reusable many times without consumption or decomposition.

Two approaches are shown here to be extremely efficient for this purpose. First, the reactions of various substrates are catalyzed in water using the complex [hexabenzyltren-Cu]Br, **2**,³⁷ with the dendrimer **1** taking advantage of its molecular-micelle effect. In this strategy, it is possible to catalyze click reactions with down to only 0.1% of the Cu^I catalyst **2** and to localize this hydrophobic solid catalyst **2** inside the dendrimer in D₂O by 600 MHz ¹H NMR, bringing an enlightening support for the role of **1** as a nanoreactor. Second, now utilizing both advantages of micellar dendritic encapsulation and catalytic activation of “naked” Cu^I by intradendritic triazole ligands, the recyclable dendrimer **1** in very small quantities allows the use of only part-per-million Cu^I catalyst (CuSO₄ + sodium ascorbate) at 30 °C in only water, an exceptional efficacy of this convenient, simple, and commercial catalyst.

Received: June 18, 2014

Published: August 5, 2014

Scheme 1. CuAAC Reaction between Benzyl Azide and Phenyl Acetylene Catalyzed by the Cu^I Complex 2 in the Presence of Small Amounts of the Dendrimer 1 (a, b).



RESULTS AND DISCUSSION

Activation of Click Catalysis by Micellar Dendrimer Effect: the Dendrimer 1 As a Nanoreactor. The CuAAC reaction is first conducted in water during 3 h between the water-insoluble substrates benzyl azide and phenyl acetylene with various amounts of catalyst 2 in the presence of 1% mol of 1 (Scheme 1a,b and Table 1).

Table 1. CuAAC Reactions between Benzyl Azide and Phenyl Acetylene^a

entry	catalyst 2 (mol %)	dendrimer 1 (mol %)	yield (%) ^b
1	0.1	0	2
2	0.1	1	91 ^c
3	0.2	1	92
4	0.5	1	98

^aFrom Scheme 1b. All the reactions were carried out with 0.1 mmol of azide, 0.105 mmol of alkyne, 2 mL of water at 25 °C during 3 h. ^bIsolated yield. ^cThis reaction was repeated 10 times with the same recycled dendrimer 1, and after reusing 1 ten times, the yield remained 91%.

According to Table 1, the “click” reaction with 1% of 1 works well when the amount of catalyst 2 is in the range 0.1–0.5% mol (yields: 92–98%). When the same reaction is conducted without 1, the reaction does not work under these conditions, the yield being only 2% (entry 1).

The water/organic compatible TEG termini render the dendrimer 1 water-soluble, and the hydrophobic core allows solubilization in water of the hydrophobic catalyst 2 and the substrates. The results from Table 1 confirm that the hydrophobic substrates and catalyst 2 meet more easily in the hydrophobic core of 1 than outside 1 in water. Scheme 1a illustrates the schematic principle of the reaction. The insolubility of 1 in diethyl ether allows the complete extraction of the organic products from the reaction medium upon keeping 1 in the water phase. In this way, 1 was recycled more than ten times without change of structure during the catalysis (the experiment

of entry 2 was repeated 10 times, with the same recycled dendrimer 1 without change in reaction yield). The next-generation dendrimer 3³⁹ containing a hydrophobic core and 81 TEG termini (see structure in the Supporting Information Scheme S1) was also used in the test CuAAC reaction between benzyl azide and phenyl acetylene under the conditions indicated in Table 1 in order to check its behavior as a nanoreactor. The reaction performed in the presence of 3 was nearly quantitative (90%) after 3 h as in the presence of 1 (91%, entry 2), indicating that the micellar effect of 1 and 3 in the catalysis of CuAAC reactions was similar. Because the synthesis of 3 is longer than that of 1, the following studies of the “click” reactions were only conducted with the dendrimer 1.

The CuAAC reaction has been conducted using the nanoreactor 1 in water for seven other substrates in order to check the applicability and generality of the method for this reaction (eq 1 and Table 2)

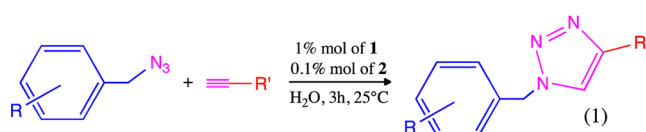
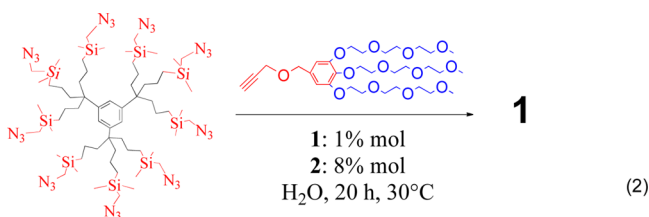


Table 2. CuAAC Reactions between Various Azides and Alkynes Using 0.1 Mol % of Catalyst 2 in the Presence of Catalytic Amounts of Dendrimer 1^a

Entry	Azide	Alkyne	Yield/conv. (%) ^b
5			89/97
6			93/100
7			93/100
8			90/97
9			95/100
10			91/98
11			90/97
12			96/100

^aSee eq 1. All the reactions are carried out with 0.1 mmol of azide, 0.105 mmol of alkyne, 1% mol of dendrimer 1, 0.1% mol of 2, and 2 mL of water at 25 °C, during 3 h. ^bIsolated yield/¹H NMR conversion.

The method that is proposed here is efficient for the “click” reaction of various substrates, leading to yields of around 90% or more for classic nonactivated substrates. Finally the catalyst 2 was used during the “autocatalytic” synthesis of the nanoreactor 1 itself. Remarkably, with only 8% mol of 2 per branch, the “click” reaction between the nona-core azide and the tris-TEGylated alkynyl dendron (eq 2) is completed in 570 min at 30 °C in the presence of only 1 mol % 1 per branch, leading to 1 in 81% isolated yield. If 1 is absent at the beginning of the reaction, the yield under these conditions is only 39% (in 1200 min), clearly showing the strong autocatalytic effect of very small amounts of 1 on its own formation. The kinetic study of the reaction (see Supporting Information, Figures S29



and S30) shows that after 90 min, the conversion of the starting material is already 45.8% in the presence of **1** against only 2% without **1** at the beginning of the reaction. In the absence of **1** at the beginning of the reaction, its synthesis using catalyst **2** requires 2 days to reach completion; thus, the presence of **1** at the beginning of the reaction clearly accelerates its synthesis.

¹H NMR Characterization of the Solubilization of the Hydrophobic Catalyst **2 in Water and Encapsulation in the Dendrimer **1**.** In order to provide further insight into the catalytic activation by the dendrimer **1**, ¹H NMR and DOSY NMR studies of **1** have been conducted.

The ¹H NMR study of **1** in D₂O shows a minute shift of the triazole proton (from 7.79 to 7.76 ppm) upon diluting **1** 32 times (from 2.8×10^{-3} to 8.7×10^{-5} M, Figure 1a). This

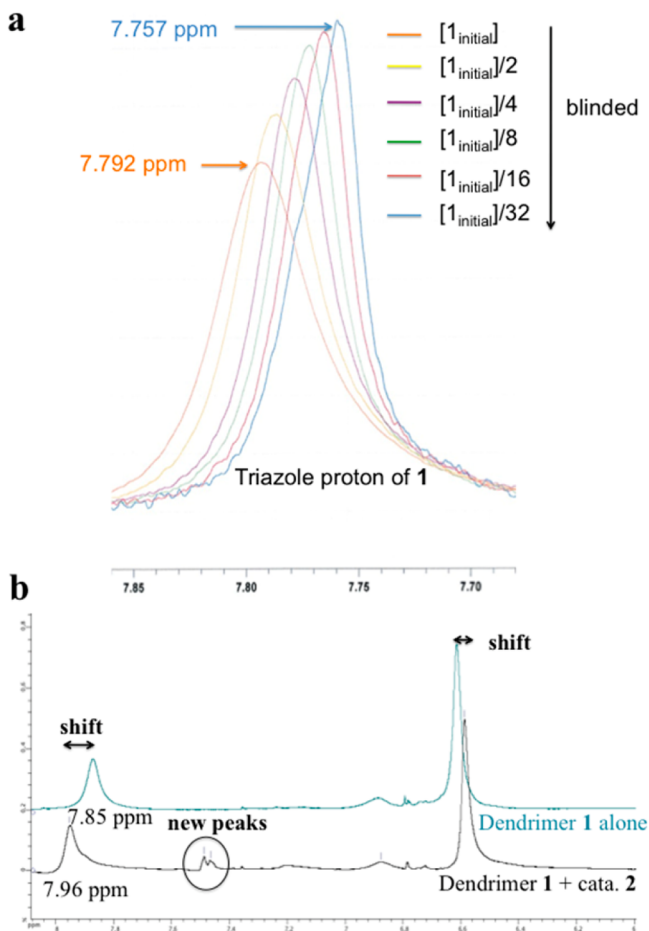


Figure 1. ¹H NMR characterization of the solubilization of the hydrophobic catalyst **2** in water and its encapsulation in the dendrimer **1**. (a) 600 MHz ¹H NMR in D₂O of **1** from concentrated solution [**1**] = 2.8×10^{-3} M (left) to diluted solution [**1**] = 8.7×10^{-5} M (right). (b) 600 MHz ¹H NMR of **1** + **2** in D₂O. New peaks appear around 7.5 ppm and shifts are observed, inter alia in the portion of the spectrum represented here, for two types of protons (triazole at 7.85 ppm and aromatic rings of the TEG dendron 6.62 ppm).

experiment suggests that, when **1** is concentrated, assemblies of dendrimers are formed with interdendritic interlocked TEG termini, whereas in diluted conditions, these assemblies are split. This observation is also confirmed by DOSY NMR experiments that show different diffusion coefficients when **1** is concentrated (2.8×10^{-3} M) or diluted (8.7×10^{-5} M). The hydrodynamic diameter of concentrated **1** calculated from the diffusion coefficient using the Stokes–Einstein law is 13.3 (± 0.2) nm, and 10.2 (± 0.2) nm when **1** is diluted (the calculated maximum diameter of **1** at full extension is approximately 6 nm).

The ¹H NMR spectrum of **1** + **2** in D₂O presents, compared to that of **1** alone, the appearance of new signals at 7.47–7.49 ppm (Figure 1b) corresponding to the protons of the phenyl groups of **2**, showing the solubilization in water of the hydrophobic complex **2**. It is also remarkable that in the presence of **2** the signals of the protons of the hydrophobic groups of the tethers of **1** (red and green regions of Scheme 1a) are slightly shifted (0.03 ppm in the red region, see Figure S2/ Table S1 of the Supporting Information), especially the triazole proton (around 0.1 ppm shift, see Figure 1b). This latter shift possibly results from interaction of this triazole with the Cu atom of **2** subsequent to reversible decoordination of a nitrogen ligand of **2**. This would eventually add to the driving force provided by the hydrophobic shelter for the encapsulation of **2** by **1**. NOESY NMR shows a weak interaction between the new peaks of **2** and the CH₃ substituents of the Si groups of **1**, which also confirms the presence of the catalyst **2** very close to the hydrophobic interior of **1** (see Figure S4 of the Supporting Information). The bulk of the core and the barrier of the methyl substituents of the Si atoms prevent significantly deeper interaction of **2** beyond the SiMe₂ groups near the dendrimer core.

Upon diluting the solution **1** + **2** from [**1**] = 2.8×10^{-3} M to [**1**] = 3.2×10^{-4} M (condition of the CuAAC reactions) the ratio of water-soluble **2** per mol **1** increases from 1/15 to 1/5 (Supporting Information, Figure S3), which is in agreement with the stoichiometry used during the catalytic CuAAC reaction with 1% dendrimer **1** and 0.1–0.2% catalyst **2** (Table 1, entries 1–3 and Table 2, entries 5–12).

Intradendritic Triazole Ligands of **1 As Additional Activators of Cu^I Catalysis.** The second strategy uses, in addition to and in synergy with the micellar effect of the amphiphilic dendrimer illustrated above, the intradendritic triazole activation of the Cu^I catalysis. In this case, it is not necessary to synthesize a Cu^I catalyst such as **2** with a nitrogen ligand because this role is played by the nine intradendritic triazole ligands of **1**. In precedent work on catalytically efficient dendrimer-encapsulated Pd nanoparticles, the role of the triazole ligands was the stabilization of the nanoparticles.^{18,39} On the other hand, here, the intradendritic triazole ligands activate Cu^I by increasing the electronic density for improved catalytic efficiency. Thus, the classic CuSO₄·5H₂O source can advantageously be used as precatalyst of the CuAAC reaction, and sodium ascorbate (NaAsc) as reducing agent of Cu^{II} to Cu^I, that is, the initially reported conditions.³¹ As **1** contains nine triazolyl rings, 9 equiv. Cu^{II} per dendrimer are used. After adding CuSO₄·5H₂O to an aqueous solution of **1**, Cu^{II} coordinates the intradendritic triazolyl ligands, then Cu^{II} is reduced in situ to Cu^I for intradendritic catalysis (Figure 2). The coordination of Cu^{II} to the triazole rings of **1** has been checked by ¹H NMR spectroscopy. After adding CuSO₄·5H₂O to a deuterium oxide solution of **1** (1 equiv per triazole), the NMR signal of the triazole proton of **1** at 7.90 ppm vanishes to

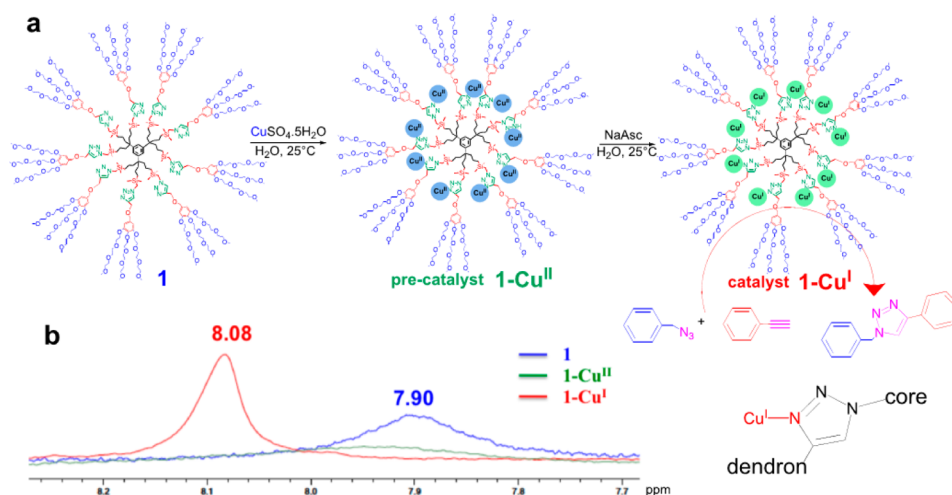


Figure 2. (a) Dendrimer **1** as nanoreactor/ligand for CuAAC catalysis. (b) Comparison of the NMR signals of the triazole proton of **1** alone (7.90 ppm), with Cu^{II} (very broad due to the paramagnetism) and Cu^I (shift to 8.08 ppm) showing the coordination of the intradendritic triazoles of **1** to the copper ions.

give a very broad signal due to the paramagnetic Cu^{II} species. When NaAsc is added to reduce Cu^{II} to Cu^I, the NMR signal of the triazole proton of **1** reappears but is shifted (8.08 ppm instead of 7.90 ppm when **1** is alone) showing the coordination of all the triazole rings to Cu^I (Figure 2b and Figure S8 of the Supporting Information).⁴⁰

The efficiency of the CuAAC catalyst involving this system has been tested again for the classic reaction between benzyl azide and phenyl acetylene with various amounts of catalyst, down to 1 ppm of copper. When the quantities of **1** and CuSO₄·5H₂O are 1%, the yield is 100% in 2.5 h of reaction against only 15% when the reaction is conducted without **1**. The reaction is quantitative with only 4 ppm of Cu^I in water at 30 °C during 24 h (entry 18) and reaches 50% of yield with 1 ppm of Cu^I (Table 3).

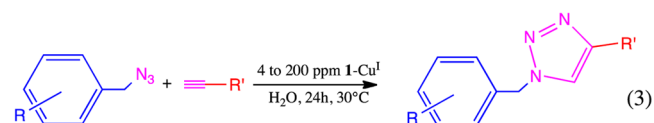
Table 3. CuAAC Reactions between Benzyl Azide and Phenyl Acetylene Using Various Amounts of 1–Cu^I^a

entry	Cu ^I ppm	time (h)	yield (%)	TON	TOF (h ⁻¹)
13 ^b	10000 (1 mol %)	2.5	99	99	39.6
14 ^b	2000	19	99	495	26.0
15	200	19	99	4 950	260
16	40	19	99	24 700	1 300
17	20	19	99	49 500	2 600
18	4	24	99	247 000	10 300
19	1	24	50	510 000	21 200
20	0	24	0	0	0

^aAll the reactions were carried out with 1 mmol of azide, 1.05 mmol of alkyne in 1 mL of H₂O. ^bThe reaction was carried out with 5 mL of water.

Such an extremely low quantity of copper has never been successfully used in only water at 30 °C for CuAAC reactions before the present study. At such extremely low catalyst amounts, the noncatalyzed Huisgen reaction is in competition with the CuAAC reaction at high temperature using the standard substrates.³⁷ At 30 °C, however, neither the Huisgen reaction in the absence of Cu^I catalyst nor the CuAAC reaction (entry 20) proceeds. In the case of very small amounts of copper, an excess of sodium ascorbate vs the low catalyst amount is added to the reaction in order to avoid oxidation of Cu^I that is air sensitive.

The CuAAC reaction is also carried out in water at 30 °C between various alkynes and azides (aromatic and aliphatic) with parts-per-million amounts of Cu^I (eq 3 and Table 4)



In order to check if the dendritic effect is positive and to distinguish between the micellar dendrimer effect and the Cu^I activation by coordination of a nitrogen atom of the “clicked” triazole in water, the results obtained in the presence of the Cu^I complex of dendrimer **1** were compared on one hand with those obtained with the Cu^I complex of the nondendritic molecule **4** (Scheme 2a), and on the other hand with those obtained with Cu^I in the presence of the water-soluble dendrimer **5**⁴¹ that does not contain triazole ligands (Scheme 2b).

With Cu^I stabilized by the nondendritic triazole ligand of **4**, the same conditions as in entry 15 (200 ppm of Cu^I) are followed, and the yield is also quantitative. When the amount of catalyst is reduced to 4 ppm as in entry 18, however, no reaction is observed upon several attempts, which emphasizes the key molecular micelle role of the dendritic nanostructure. With dendrimer **5** that does not contain triazole rings (Scheme 2b), Cu^I is introduced under the same conditions as with **1** and as in entry 17 (20 ppm of Cu^I). After 24 h, only 27% of isolated yield is obtained, whereas with **1**–Cu^I 99% is obtained in 19 h. This shows the crucial activation role of the triazole ring. When the reaction is performed without any dendrimer (using only the water solution of Cu^I), the isolated yield is 9%. These experiments show that both the micellar effect of the dendrimer **1** and the activation by coordination of Cu^I by the intradendritic triazole ligands have a very positive effect on the catalytic efficiency and that these two effects are cumulative, resulting in the considerable benefit of the dendritic nanoreactor **1** on the “click” reactions with the simple Sharpless-Fokin catalyst CuSO₄·5H₂O + sodium ascorbate in water.

These results advantageously compare with relatively recent ones (2008–2014) from the literature in Table 5, a large number of active catalysts for the CuAAC reactions being known.

Table 4. CuAAC Reactions between Various Azides and Alkynes with 1-Cu^I ^a (See eq 3)

Entry	Azide	Alkyne	Cu ^I	Yield (%) ^c
21			4 ppm	99
22			20 ppm	87
23 ^d			20 ppm	81
24			20 ppm	89
25			4 ppm	90
26			4 ppm	82
27			50 ppm	90
28 ^d			50 ppm	89
29			100 ppm	98
30			20 ppm	98
31			200 ppm	98

^aAll the reactions are carried out with 1-Cu^I at 30 °C during 24 h in 1 mL of H₂O. ^bPent-1-yne is hydrophobic and has a low boiling point, so that it is difficult to conduct experiments with a lower amount of catalyst. ^cIsolated yield. ^dReaction performed at 35 °C.

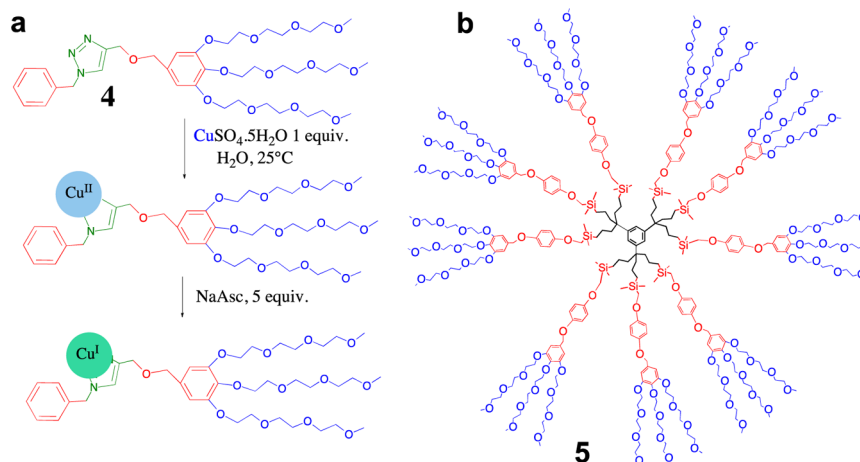
One of the best results has been recently reported by Yamada et al., who have described the synthesis of an amphiphilic self-assembled polymeric copper catalyst. This catalyst is active in the CuAAC reaction between benzyl azide and phenyl acetylene with 4.5 ppm of copper at 50 °C during 32 h in the mixed solvent *t*-BuOH/H₂O (1/3).⁴⁵ The presence of *t*-BuOH as cosolvent and 50 °C are necessary for a complete reaction. Another remarkable example was also recently reported by Shin et al. using β -cyclodextrin as nanoreactor for “click” reactions in water in the presence of CuSO₄ and sodium ascorbate at rt, but 5% mol of copper was needed in that case for a quantitative reaction in only water.⁴⁹ The catalysts Cu(PPh₃)NO₃⁵⁶ and

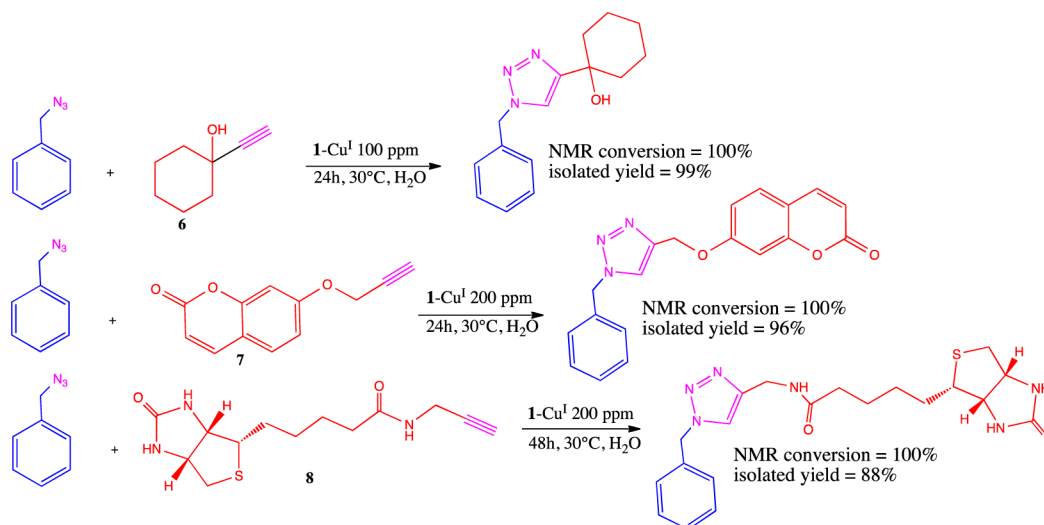
Table 5. Examples of Recent Efficient CuAAC Reactions in the Presence of Various Catalysts and Reaction Conditions^a

catalyst ^{ref}	Cu (% mol)	time (h)	solvent	temperature (°C)
Cu/Fe ⁴²	5 wt %	8	CH ₂ Cl ₂	30
Cu-NHC/Phen ⁴³	1	18	<i>t</i> -BuOH/ H ₂ O 2/1	20
Cu/AlO(OH) ⁴⁴	3	6	<i>n</i> -hexane	25
Cu ₂ O/benzoic acid ⁴⁵	1	0.13	H ₂ O	20
poly(imidazole-acrylamide)/ CuSO ₄ /NaAsc ⁴⁶	0.25	1.5	<i>t</i> -BuOH/ H ₂ O 1/3	50
poly(imidazole-acrylamide)/ CuSO ₄ /NaAsc ⁴⁶	0.00045	31	<i>t</i> -BuOH/ H ₂ O 1/3	50
bis-NHC-dicopper complex ⁴⁷	0.5	0.75	CH ₂ Cl ₂	20
TBTA-Cu ¹³³	0.25–1	24	<i>t</i> -BuOH/ H ₂ O 2/1	20
nano-FGT-Cu ⁴⁸	2.4	0.16	H ₂ O	Mw 120
Fe ₂ O ₃ -NHC-Cu ¹⁴⁹	0.25	18	H ₂ O	20
β -CD/CuSO ₄ /NaAsc ⁵⁰	5	0.25	H ₂ O	20
[Cu ₃ (14-H){S ₂ P(OEt) ₂ }] (PF ₆) ⁵¹	0.4	4	CH ₃ CN	20
CuSO ₄ /N ₂ H ₄ -H ₂ O ⁵²	0.0025	4	No	20
ammonium NHC-Cu ¹⁵³	5	3	H ₂ O	20
Fe ₂ O ₃ /SiO ₂ Tris(triazolyl) Cu ¹⁵⁴	0.5	20	H ₂ O	20
PS/SiO ₂ Tris(triazolyl) methane-Cu ¹⁵⁵	0.5	4	H ₂ O	20
SBA-15-imine/Cu ¹⁵⁶	0.1	6	H ₂ O	20
Cu(PPh ₃)NO ₃ ⁵⁷	0.5	0.66	H ₂ O	20
[(NHC _{Cy})Cu]PF ₆ ⁵⁸	2	1.5	H ₂ O	20
Catalyst 2 ³⁷	0.1	24	PhCH ₃	22

^aAll the above results correspond to the CuAAC reaction between benzyl azide and phenylacetylene. NHC: N-heterocyclic carbene, TBTA: tris(benzyltriazolylmethyl)amine, FGT: ferrite-glutathione, β -CD: β -cyclodextrin, SBA-15: mesoporous silica, NHC_{Cy}: NHC ligand with cyclohexyl substituents on the nitrogen atoms. Yields are between 90 to 100% except with Cu-NHPhen (78%) and CuSO₄/N₂H₄-Cu (82%).

[(NHC_{Cy})Cu]PF₆⁵⁷ are also active in water but 0.5% mol and 2% mol respectively are necessary for a complete reaction between benzyl azide and phenyl acetylene. Generally, the CuAAC “click” reaction is possible in water when the amount of liganded copper exceeds 0.1% mol (see Table 5); therefore, the activity of the present system is incomparable.

Scheme 2. (a) Complexation of the reference compound 4 by Cu^{II} followed by reduction to water-soluble, catalytically active Cu^I-triazole for CuAAC reactions. (b) Structure of dendrimer 5 that does not contain triazolyl groups.

Scheme 3. CuAAC Reactions with 1-Cu^I As Catalyst for Various Applications

To evaluate the scope and the applicability of the present system, the CuAAC reaction with 1-Cu^I was tested on hydrophobic biomolecules with medicinal, targeting, and labeling interests (Scheme 3). As a candidate, the 1-ethynylcyclohexanol **6** was chosen because of its simple structure and because it is an active metabolite of the old central nervous system depressant drug ethinamate. The 7-(propargyloxy)coumarin **7** belonging to the coumarin family was also tested in the CuAAC “click” reaction with 1-Cu^I. Coumarins are often used for their anti-oedematous properties, and their flavor properties have rendered this family famous in the perfume industry. Moreover coumarins are known as fluorescence dyes. The 3-(D-biotinylamido)-1-propyne **8** is an alkyne derivative of biotin that is known for instance for its role as a vitamin and coenzyme in the synthesis of fatty acids. Biotin is also known for its extremely high affinity with avidin. As exposed in Scheme 3, the catalyst 1-Cu^I is very active for the CuAAC “click” reaction even for these three biological molecules with only 100–200 ppm of Cu^I.

CONCLUDING REMARKS

The water-soluble dendrimer **1** acts as a molecular micelle nanoreactor in catalytic quantities (1% vs substrates or less) and is recycled and reused many times without any loss or decomposition. Under these conditions (water, 25 °C, 3 h), it considerably facilitates catalysis by [Cu(hexabenzyltren)]Br (0.1% vs substrate) of the CuAAC reactions that are nearly quantitative in the presence of this dendritic nanoreactor and do not work in its absence. Along this line, the “autocatalyzed” dendritic nanoreactor synthesis of **1** is remarkable.

This catalytic nanoreactor effect is confirmed by ¹H NMR evidence of the solubilization of the hydrophobic catalyst **2** in water in the presence of the dendrimer **1**, and the catalyst–dendrimer interaction is shown by the selective NMR shifts of intradendritic protons in the hydrophobic region, providing a proof for the solubilization role of **1**.

In addition to and in synergy with this effect, the presence of intradendritic triazole ligands allows catalyzing CuAAC reactions at 30 °C with down to 4 ppm of commercial CuSO₄·5H₂O and sodium ascorbate for quantitative yields and 1 ppm with 50% yield. The reaction with hydrophobic biomolecules has also been performed in only water at 30 °C, leading to quantitative yields. Comparisons of **1** with the nondendritic triazole ligand **4** and

with the water-soluble dendrimer **5** that has a hydrophobic core but does not contain triazole ligands show that both the micellar and intradendritic triazole coordination share key roles in the considerable catalyst activation in water. This opens the route to future biomedical and nanomaterials applications of the common CuAAC reaction with the cheap Sharpless–Fokin catalyst CuSO₄·5H₂O + sodium ascorbate, as already exemplified here in a few examples of biomedical or cosmetic interest.

ASSOCIATED CONTENT

Supporting Information

General data, syntheses of the catalysts **2** and 1-Cu^I, procedure and data for the encapsulation of catalyst **2** in **1**, complexation of Cu^I to the triazoles of **1**, syntheses and ¹H NMR spectra and data of the “click” reaction products, spectroscopic characterization of **3–5**, kinetic study of the autocatalytic synthesis of **1**, and characterization of **1** after reuse. This material is available free of charge via the Internet at <http://pubs.acs.org>.

AUTHOR INFORMATION

Corresponding Author

d.astruc@ism.u-bordeaux1.fr

Notes

The authors declare no competing financial interest.

ACKNOWLEDGMENTS

Helpful discussions with Dr Jaime Ruiz (Univ. Bordeaux) and financial support from the Université de Bordeaux, the CNRS, the Ministère de l'Enseignement Supérieur et de la Recherche (Ph.D. grant to C.D.) and L'Oréal are gratefully acknowledged.

REFERENCES

- (1) Breslow, R.; Overman, L. E. *J. Am. Chem. Soc.* **1970**, *92*, 1075–1077.
- (2) Yoshizawa, M.; Tamura, M.; Fujita, M. *Science* **2006**, *312*, 251–254.
- (3) Kang, J.; Rebek, J. *Nature* **1997**, *385*, 50–52.
- (4) Mock, W. L. *Top. Curr. Chem.* **1995**, *175*, 1–24.
- (5) Warmuth, R. *Angew. Chem., Int. Ed.* **1997**, *36*, 1347–1350.
- (6) Slagt, V. F.; van Leeuwen, P. W. N. M.; Reek, J. N. H. *Angew. Chem., Int. Ed.* **2003**, *42*, 5619–5623.

- (7) Walter, C. J.; Anderson, C. J.; Sanders, J. K. M. *J. Chem. Soc., Chem. Commun.* **1993**, 458–460.
- (8) Fiedler, D.; Leung, D. H.; Bergman, R. G.; Raymond, K. N. *Acc. Chem. Res.* **2005**, *38*, 351–360.
- (9) Wang, Z. J.; Clary, K. N.; Bergman, R. G.; Raymond, K. N.; Toste, F. D. *Nat. Chem.* **2013**, *5*, 100–103.
- (10) Yu, X.; Yue, K.; Hsieh, I.-F.; Li, Y.; Dong, X.-H.; Liu, C.; Xin, Y.; Wang, H.-F.; Shi, A.-C.; Newkome, G. R.; Ho, R.-M.; Chen, E.-Q.; Zhang, W.-B.; Cheng, S. Z. D. *Proc. Nat. Acad. Sci. U. S. A.* **2013**, *110*, 10078–10083.
- (11) Discher, D. E.; Eisenberg, A. *Science* **2002**, *297*, 967–973.
- (12) Crooks, R. M.; Zhao, M.; Sun, L.; Chechik, V.; Yeung, L. K. *Acc. Chem. Res.* **2001**, *34*, 181–190.
- (13) Scott, R. W. J.; Wilson, O. M.; Crooks, R. M. *Phys. Chem. B* **2005**, *109*, 692–704.
- (14) Myers, V. S.; Weier, M. G.; Carino, E. V.; Yancey, D. F.; Pande, S.; Crooks, R. M. *Chem. Sci.* **2011**, *2*, 1632–1646.
- (15) Bernechea, M.; de Jésus, E.; Lopez-Mardomingo, C. *Inorg. Chem.* **2009**, *48*, 4491–4496.
- (16) Astruc, D.; Boisselier, E.; Ornelas, C. *Chem. Rev.* **2010**, *110*, 1857–1959.
- (17) Astruc, D. *Nat. Chem.* **2012**, *4*, 255–267.
- (18) Deraedt, C.; Astruc, D. *Acc. Chem. Res.* **2014**, *46*, 494–503.
- (19) Newkome, G. R.; Yao, Z.; Baker, G. R.; Gupta, V. K. *J. Org. Chem.* **1985**, *50*, 2003–2004.
- (20) Newkome, G. R.; Moorefield, C. N.; Baker, G. R.; Saunders, M. J.; Grossman, S. H. *Angew. Chem., Int. Ed.* **1991**, *30*, 1178–1180.
- (21) Newkome, G. R.; Shreiner, C. *Chem. Rev.* **2010**, *110*, 6338–6442.
- (22) Jansen, J. F. G. A.; de Brabander-van den Berg, E. M. M.; Meijer, E. W. *Science* **1999**, *266*, 1226–1229.
- (23) Zimmerman, S. C.; Wendland, M. S.; Rakow, N. A.; Zharov, I.; Suslick, K. S. *Nature* **2002**, *418*, 399–403.
- (24) Ornelas, C.; Ruiz, J.; Belin, C.; Astruc, D. *J. Am. Chem. Soc.* **2009**, *131*, 590–601.
- (25) Ornelas, C.; Ruiz, J.; Cloutet, E.; Alves, S.; Astruc, D. *Angew. Chem., Int. Ed.* **2007**, *46*, 872–877.
- (26) Diallo, A. K.; Ornelas, C.; Salmon, L.; Ruiz, J.; Astruc, D. *Angew. Chem., Int. Ed. Engl.* **2007**, *46*, 8644–8648.
- (27) Astruc, D.; Liang, L.; Rapakousiou, A.; Ruiz, J. *Acc. Chem. Res.* **2012**, *45*, 630–640.
- (28) Helms, B.; Fréchet, J. M. J. *Adv. Synth. Catal.* **2006**, *348*, 1125–1148.
- (29) Fréchet, J. M. J. *J. Polym. Sci., Part A: Polym. Chem.* **2003**, *41*, 3713–3725.
- (30) Wu, P.; Feldman, A. K.; Nugent, A. K.; Hawker, C. J.; Scheel, A.; Voit, B.; Pyun, J.; Fréchet, J. M. J.; Sharpless, K. B.; Fokin, V. V. *Angew. Chem., Int. Ed.* **2004**, *43*, 3928–3932.
- (31) Rostovtsev, V. V.; Green, L. G.; Fokin, V. V.; Sharpless, K. B. *Angew. Chem., Int. Ed.* **2002**, *41*, 2596–2599.
- (32) Tornøe, C. W.; Christensen, C.; Meldal, M. *J. Org. Chem.* **2002**, *67*, 3057–3064.
- (33) Chan, T. R.; Hilgraf, R.; Sharpless, K. B.; Fokin, V. V. *Org. Lett.* **2004**, *6*, 2853–2855.
- (34) Hong, V.; Presolski, S. I.; Ma, C.; Finn, M. G. *Angew. Chem., Int. Ed.* **2009**, *48*, 9879–9883.
- (35) Golas, P. L.; Tsarevsky, N. V.; Sumerlin, B. S.; Matyjaszewski, K. *Macromolecules* **2006**, *39*, 6451–6457.
- (36) Golas, P. L.; Tsarevsky, N. V.; Matyjaszewski, K. *Macromol. Rapid Commun.* **2008**, *29*, 1167–1171.
- (37) Liang, L.; Ruiz, J.; Astruc, D. *Adv. Syn. Catal.* **2011**, *353*, 3434–3450.
- (38) Candelon, N.; Lastécouère, D.; Diallo, A. K.; Ruiz, J.; Astruc, D.; Vincent, J.-M. *Chem. Commun.* **2008**, 741–743.
- (39) Deraedt, C.; Salmon, L.; Etienne, L.; Ruiz, J.; Astruc, D. *Chem. Commun.* **2013**, *49*, 8169–8171.
- (40) For the complexation site of “clicked” 1,2,3-triazole ligands with various transition metals, see Badèche, S.; Daran, J.-C.; Ruiz, J.; Astruc, D. *Inorg. Chem.* **2008**, *47*, 4903–4908.
- (41) Boisselier, E.; Diallo, A. K.; Salmon, L.; Ornelas, C.; Ruiz, J.; Astruc, D. *J. Am. Chem. Soc.* **2010**, *132*, 2729–2742.
- (42) Kovacs, S.; Zih-Perényi, K.; Révész, A.; Novak, S. *Synthesis* **2012**, *44*, 3722–3730.
- (43) Teyssot, M.-L.; Chevry, A.; Traikia, M.; El-Ghozzi, M.; Avignant, D.; Gautier, A. *Chem.—Eur. J.* **2009**, *15*, 6322–6326.
- (44) Park, I. S.; Kwon, M. S.; Kim, Y.; Lee, J. S.; Park, J. *Org. Lett.* **2008**, *10*, 497–500.
- (45) Shao, C.; Zhu, R.; Luo, S.; Zhang, Q.; Wang, X.; Hu, Y. *Tetrahedron Lett.* **2011**, *52*, 3782–3785.
- (46) Yamada, Y. M. A.; Sarkar, S. M.; Uozumi, Y. *J. Am. Chem. Soc.* **2012**, *134*, 9285–9290.
- (47) Berg, R.; Straub, J.; Schreiner, E.; Mader, S.; Rominger, F.; Straub, B. F. *Adv. Synth. Catal.* **2012**, *354*, 3445–3450.
- (48) Baig, R. B. N.; Varma, R. S. *Green Chem.* **2012**, *14*, 625–632.
- (49) Collinson, J.-M.; Wilton-Ely, J. D. E. T.; Díez-González, S. *Chem. Commun.* **2013**, *49*, 11358–11360.
- (50) Shin, J.-A.; Lim, Y.-G.; Lee, K.-L. *J. Org. Chem.* **2012**, *77*, 4117–4122.
- (51) Lee, B.-H.; Wu, C.-C.; Fang, X.; Liu, C.-W.; Zhu, J.-L. *Catal. Lett.* **2013**, *143*, 572–577.
- (52) Pathigoolla, A.; Pola, R. P.; Sureshan, K. M. *Appl. Catal., A* **2013**, *453*, 151–158.
- (53) Wang, W.; Wu, J.; Xia, C.; Li, F. *Green Chem.* **2011**, *13*, 3440–3445.
- (54) Wang, D.; Etienne, L.; Echeverria, M.; Moya, S.; Astruc, D. *Chem.—Eur. J.* **2014**, *20*, 4047–4054.
- (55) Ozkal, E.; Llanes, P.; Bravo, F.; Ferrali, A.; Pericàs, M. A. *Adv. Synth. Catal.* **2014**, *356*, 857–869.
- (56) Roy, S.; Chatterjee, T.; Pramanik, M.; Singha Roy, A.; Bhaumik, A.; Islam, S. K. M. *J. Mol. Catal. A: Chem.* **2014**, *386*, 78–85.
- (57) Wang, D.; Li, N.; Zhao, M.; Shi, W.; Ma, C.; Chen, B. *Green Chem.* **2010**, *12*, 2120–2123.
- (58) Díez-González, S.; Nolan, S. P. *Angew. Chem., Int. Ed.* **2008**, *47*, 8881–8884.

Partie 5. Hétérogénéisation sur supports magnétiques de catalyseurs nanoparticulaires de palladium stabilisés par des dendrimères.

Partie 5. Hétérogénéisation sur supports magnétiques de catalyseurs nanoparticulaires de palladium stabilisés par des dendrimères.

L'un des inconvénients des PdPNs synthétisées tout au long de la thèse réside dans la nécessité de les garder en solution. Lorsqu'on utilise un dendrimère ou un polymère hydrophobe, les PdNPs se trouvent dans un milieu $\text{CHCl}_3/\text{MeOH}$ (2/1) et présentent une activité catalytique faible. En revanche, lorsqu'on utilise un dendrimère ou un polymère hydrosoluble, les PdNPs sont solubilisées dans l'eau et présentent une très grande activité en catalyse. Cependant, l'eau peut poser problème dans certaines réactions chimiques. L'idée à laquelle nous avons pensé a été d'hétérogénéiser ces PdNPs en partant de leur phase homogène. Pour cela, deux stratégies ont été employées. Dans ces deux stratégies, nous avons décidé d'utiliser des nanoparticules magnétiques (MNPs) comportant un cœur de Fe_2O_3 et une coquille de silice comme support étant donné la place importante que commençait à prendre ces support dans la chimie actuelle et surtout vu la simplicité de leur recyclabilité (aimant).⁽¹⁾ La première stratégie employée est très simple. Nous souhaitons garder l'efficacité de nos PdNPs stabilisées par G0 TEG tout en les rendant stables à l'état solide. Ainsi après avoir préparé notre solution de PdNPs, nous avons additionné le support magnétique à la solution et agité pendant 2 heures. Les analyses (ICP-OES, analyses élémentaires, ^1H RMN et XPS) ont révélées que 97% du Pd de départ ainsi que le dendrimère stabilisateur de PdNPs s'étaient imprégnés sur la surface des MNPs. Ce catalyseur présente une grande activité pour les réactions C-C bien que celle ci soit légèrement inférieure à celle des PdNPs non supportées en raison du passage de l'homogène à l'hétérogène. Ce catalyseur est recyclable au moins 5 fois sans trop de perte en activité (faible leaching) et est plus robuste. Sa robustesse a été testée lors de la réaction d'oxydation de l'alcool benzylique en présence de KOH et de O_2 . Les PdNPs non supportées précipitent instantanément en présence de KOH et de O_2 tandis que la réaction d'oxydation est quantitative avec le nouveau catalyseur supporté stable.

Au cours des 3 années de thèse, nous avons eu l'occasion de travailler avec le Dr. Wang Dong pour l'élaboration de la deuxième stratégie. L'idée principale était d'essayer de mimer le rôle des dendrimères lors de la stabilisation de PdNPs à la surface de MNPs. Pour commencer ce sujet, nous avons greffé par réaction "click" CuAAC un dendron tris-TEG à la surface de MNP. Ce nanomatériau a prouvé son efficacité dans la stabilisation de PdNPs, mais leur activité catalytique était un peu décevante, comparable à celle de nombreux catalyseurs. Mon collègue a donc par la suite synthétisé trois autres variétés de MNPs greffés par "click" CuAAC différemment. L'une de ces variétés contenait en surface des PEG₅₅₀, l'autre des PEG₂₀₀₀ et la dernière des dendrons nona-TEG. Ces quatre nanomatériaux ont été utilisés dans la stabilisation des PdNPs pour la catalyse, et un effet dendritique notable sur plusieurs points a été observé.

Références:

1) Wang, D.; Astruc, D. Fast-growing Field of Magnetically Recyclable Nanocatalysts, *Chem. Rev.* **2014**, *114*, 6949-6985.

DOI: 10.1002/cctc.201402775

Robust, Efficient, and Recyclable Catalysts from the Impregnation of Preformed Dendrimers Containing Palladium Nanoparticles on a Magnetic Support

Christophe Deraedt,^[a] Dong Wang,^[a] Lionel Salmon,^[b] Laetitia Etienne,^[c]
Christine Labrugère,^[c] Jaime Ruiz,^[a] and Didier Astruc*^[a]

The simple impregnation of γ -Fe₂O₃(core)/SiO₂(shell) magnetic nanoparticles with a dendrimer that contains stabilized Pd nanoparticles is presented as a new method to produce highly efficient heterogeneous catalysts. This technique provides

much better stability, recyclability, and activity in C–C cross-coupling reactions and selective oxidation of benzyl alcohol to benzaldehyde in water than unsupported Pd nanoparticles.

Introduction

■ ■ title changed for clarity, ok? ■ ■ The quest for improved catalysts and strategies for catalyst efficiency and recyclability is more challenging than ever to move toward better sustainability. Supported metal nanoparticles (NPs) are excellent catalysts for a variety of reactions because of their large surface-to-volume ratio, remarkable efficiency, topological properties, the interaction between NPs and the support, and their heterogenization on various oxide and carbon supports that allow their recovery.^[1] In particular, iron oxide magnetic nanoparticles (MNPs) have received considerable attention because they are biocompatible and can be recovered easily from reaction mixtures by using a simple external magnetic field.^[2]

Classically, the fixation of NPs on supports uses mostly the reduction of metal salts in the presence of the support followed by an adequate thermal treatment.^[3] Mesoporous supports (MCM-41, SBA) are frequently used supports of PdNPs-MNPs.^[4a–c] Other supports, such as polymer-coated MNPs,^[4d–g] ionic-liquid-modified MNPs,^[4h] sulfonated graphene-decorated MNPs,^[4i] are also employed for the stabilization of PdNPs. Phosphine and amine ligands grafted on MNPs are also common for this purpose.^[4j–o] Here we propose a new, very efficient method that involves PdNPs that are prestabilized by a water-soluble “clicked” dendrimer **1**^[5] then deposited on silica-coated maghemite γ -Fe₂O₃ MNPs **2** by simple mixing and stirring with the aqueous solution of PdNPs/**1**. This simple preparation pro-

vides the new heterogeneous PdNP/**1**/MNP catalyst **3** (Scheme 1). Quantitative or nearly quantitative yields of the desired products were obtained with relatively high turnover frequencies (TOFs) and unusually low amounts of Pd. The tested reactions were C–C cross-coupling reactions^[3,6] (Suzuki–Miyaura, Cu-free Sonogashira, and Heck reactions) and the selective aerobic oxidation of benzylic alcohol to benzaldehyde.^[7] Another crucial aspect of these new catalysts is their robustness and recyclability. The driving force for the strong PdNP fixation onto the silica shell is probably provided by multiple supramolecular H-bonding interactions between the triethylene glycol (TEG) termini of **1** and surface OH groups of the silica shell of **2** in synergy with the backfolding of intradendritic triazole groups of **1** that interact with the other side of the PdNP surface (Figure 1).

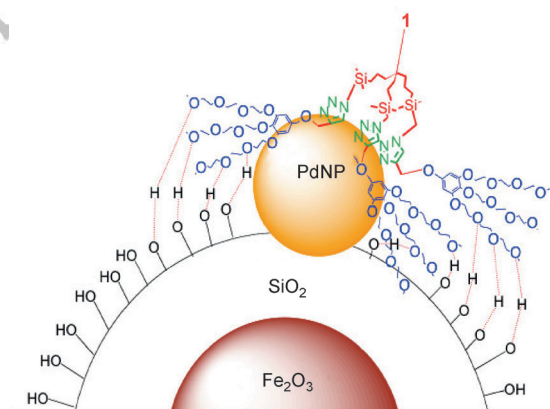


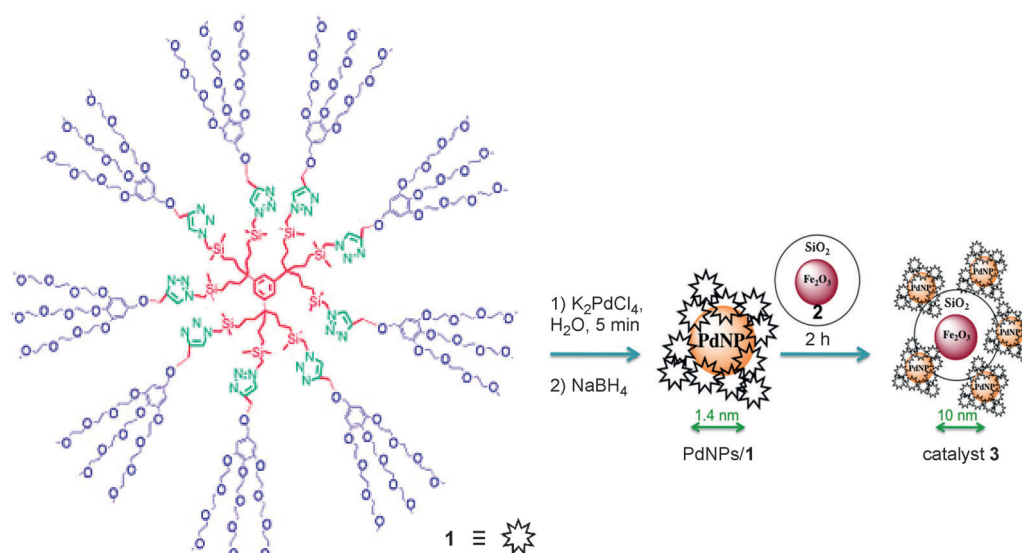
Figure 1. Schematic of the stabilization of dendrimer **1** on the silica surface and fixation of the PdNPs by supramolecular H-bonding interactions between the TEG termini of **1** and the OH groups at the surface of **2**.

[a] C. Deraedt, Dr. D. Wang, Dr. J. Ruiz, Prof. D. Astruc
ISM, UMR CNRS N°5255, Univ. Bordeaux
351, Cours de la Libération, 33405 Talence, Cedex (France)
E-mail: d.astruc@ism.u-bordeaux.fr

[b] Dr. L. Salmon
Laboratoire de Chimie de Coordination, CNRS UPR-8241
and Université de Toulouse
205 route de Narbonne, 31077 Toulouse, Cedex 04 (France)

[c] L. Etienne, C. Labrugère
PLACAMAT UMS CNRS 3626, Univ. Bordeaux
87 Avenue Albert Schweitzer, 33608 Pessac Cedex (France)

Supporting information for this article is available on the WWW under
<http://dx.doi.org/10.1002/cctc.201402775>.



Scheme 1. Preparation of **3** from the arene-cored dendrimer **1** that contains nine 1,2,3-triazolyl groups connected to nine Percec-type dendrons^[4a] terminated by 27 triethylene glycol groups.

Results and Discussion

The preparation of the nanomaterial **3** involves the synthesis of very small PdNPs that are stabilized by the nine 1,2,3-triazolyl ligands inside dendrimer **1**. Therefore, a stoichiometry of one equivalent of Pd^{II} per triazolyl group is employed, and the complexation is conducted in water. The reduction of Pd^{II} to PdNPs was achieved upon addition of an aqueous solution of NaBH₄ in large excess (10 equivalents of NaBH₄ per Pd atom), which provokes the fast formation of the PdNPs. The PdNPs were characterized by using TEM, which indicates a size of (1.4 ± 0.7) nm, whereas dynamic light scattering (DLS) measurements show that each PdNP is surrounded on average by approximately 10 dendrimers.^[5c] γ-Fe₂O₃ MNPs of approximately 10 nm diameter are synthesized by the coprecipitation method described by Shylesh et al.^[8a] Subsequently, these MNPs are coated with a dense silica layer to improve water solubility, biocompatibility, and to reduce Fe leaching from the core. Tetraethoxysilane (TEOS) is used as the silica source, and aqueous NH₃ is used as the hydrolyzing agent. To disperse **2** in the water solution of PdNPs/**1** well, the solution is plunged into an ultrasonic bath. Ultrasound also favors the ligation of PdNPs at the SiO₂ surface.^[8b] After 2 h of ultrasound treatment (entries 1 and 2 of Table 1), **3** is separated from the aqueous solution by using a simple magnet (Figure 2). The resulting aqueous solution was analyzed by inductively coupled plasma optical electron spectrometry (ICP-OES) and compared to initial aqueous solution of PdNPs/**1** to investigate the Pd loading. ICP-OES revealed that 94% of the starting Pd is loaded on the MNPs **2** (entry 2). With only 5 min of ultrasound treatment and 2 h of stirring, the Pd loading reached 97.5% (entry 3) and 99.9% with 16 h of stirring (entry 4). If the amount of **2** was reduced from 120 to 50 (entry 6) or 25 mg (entry 7), the Pd loading was lower at 60 and 40%, respectively. As expected, a larger amount of **2** (700 mg instead of 120 mg) led to a quantitative loading (entry 5).

Table 1. Impregnation of PdNPs/**1** onto **2** for the synthesis of catalyst **3**.

Entry ^[a]	2 [mg]	Ultrasound [h]	Stirring [h]	T [°C]	Pd loading on 3 [%] ^[b]
1	120	2	0	50	75.0
2	120	2	0	20	94.0
3	120	0.08	2	20	97.5
4	120	0.08	16	20	99.9
5	700	0.08	2	20	99.9
6	50	0.08	2	20	60.0
7	25	0.08	2	20	40.0

[a] Reactions were performed using 33 mL of an aqueous solution of PdNPs/**1** (2.6 mg of **1**+1.1 mg of K₂PdCl₄+1.1 mg of NaBH₄). [b] Pd loading was determined by ICP-OES.

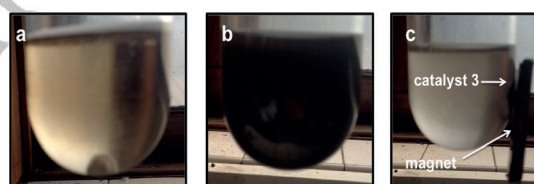


Figure 2. a) Brown aqueous solution of PdNPs/**1**. b) After addition of **2** to the aqueous solution of PdNPs/**1** (black color). c) After 2 h of stirring, the catalyst is separated with a magnet (disappearance of the brown color of the solution).

In conclusion, it is possible to obtain a quantitative loading of Pd upon mixing preformed PdNPs/**1** and MNPs coated with silica under optimized conditions. After the separation of the new magnetic catalyst **3** from the aqueous solution, the aqueous solution was evaporated, and the resulting residue was analyzed by ¹H NMR spectroscopy in CDCl₃ (or D₂O) to confirm if only PdNP or PdNP+**1** is loaded onto the MNPs **2**. In the case of entry 4 (quantitative impregnation), no trace of dendrimer **1** was observed in the ¹H NMR spectrum, which is not the case

for entry 6 (only 60% of Pd is loaded in this case). ^1H NMR spectroscopy indicates that PdNPs+dendrimer **1** are loaded completely onto the MNPs (in the case of entry 4). Elemental analysis shows that **3** is composed of an organic phase (by the presence of C, N, and O atoms), which supports the results of ^1H NMR spectroscopy. Moreover, **2** is used in a large amount (120 or 700 mg) in comparison with Pd (1.1 mg of K_2PdCl_4); thus given this low proportion of PdNPs compared to the $\gamma\text{-Fe}_2\text{O}_3$ MNPs **2**, it is possible that some PdNPs are trapped inside $\gamma\text{-Fe}_2\text{O}_3$ MNPs **2**.

Catalyst **3** was characterized by using high-resolution (HR)TEM, energy-dispersive X-ray (EDX) spectroscopy, and X-ray photoelectron spectroscopy. The size of the Fe core is between 5 and 10 nm as described in Ref. [8a], and small PdNPs are localized on the silica shell that have an average size of (2.0 ± 0.7) nm.

EDX spectroscopy was conducted in three independent zones (shown in Figure 3a) of an aggregate of **3** (Figure 4a). In all cases, the presence of Pd, Fe, and Si was evi-

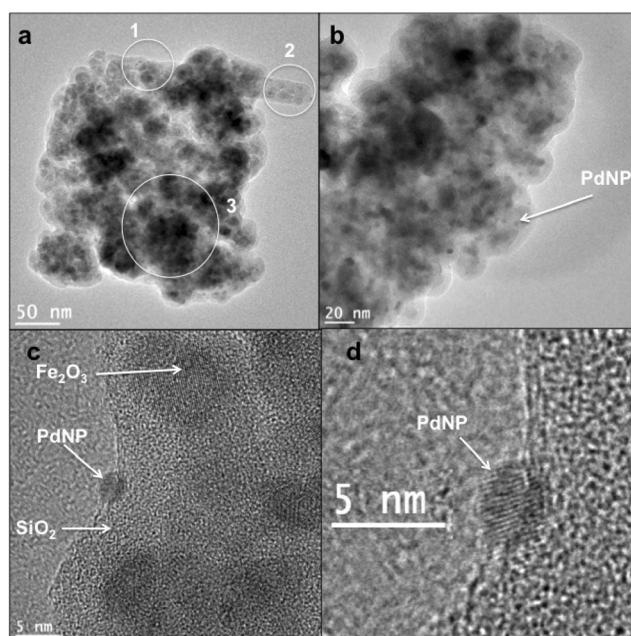


Figure 3. a) General view of an assembly of **3** by HRTEM microscopy. The three circled zones correspond to the zones of EDX spectroscopy. b) HRTEM of **3** at 20 nm scale. Small PdNPs are observed at the periphery of **3**. c) Distinction between Fe_2O_3 , SiO_2 , and PdNPs in the HRTEM picture (5 nm scale). d) Magnification of a PdNP.

denced. Zones 1 and 2 are localized at the periphery of the assembly and contain 2–3 wt% Pd (vs. 97–98% $\text{Fe}_2\text{O}_3\text{-SiO}_2$), whereas zone 3 is located more inside the assembly and contains only 0.5 wt% Pd. This is in agreement with the fact that supramolecular interactions allow the stabilization/impregnation of PdNPs/**1** on the silica shell surface of **2**.

X-ray photoelectron spectroscopy was conducted on **2** and **3**. As expected, the presence of organic atoms (peaks that correspond to the binding energies (BEs) of C 1s and N 1s) is more prominent in **3** than **2** (see Supporting Information). Moreover,

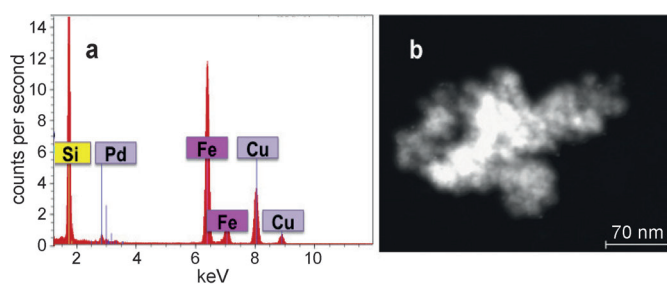
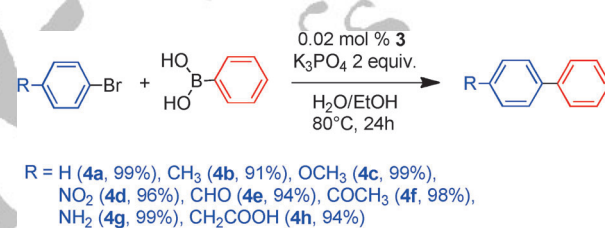


Figure 4. a) EDX spectrum showing the presence of Pd, Fe, and Si in the assembly of **3** (zone 1). b) High-angle annular dark-field scanning transmission electron microscopy image in which PdNPs at the periphery of the aggregate are better distinguished.

the photoelectron line at approximately $\text{BE} = 335.4$ eV indicates the presence of Pd^0 in **3**, which confirms the formation of PdNPs (see Supporting Information).

To confirm the applicability of the new catalyst, the Suzuki–Miyaura reaction was tested first. Catalytic Suzuki–Miyaura reactions were conducted in $\text{H}_2\text{O}/\text{EtOH}$ at 80°C within 24 h with 0.02 mol% of Pd from **3** in the presence of K_3PO_4 as a base (Scheme 2). Eight substrates were tested, and yields were ach-



Scheme 2. Suzuki–Miyaura reaction of various substrates with 200 ppm of Pd from **3** in $\text{H}_2\text{O}/\text{EtOH}$ at 80°C for 24 h performed with 1 mmol of bromoarene, 1.5 mmol of phenyl boronic acid, and 2 mmol of K_3PO_4 .

ieved from 91–99%. The results obtained are comparable to or even better than those achieved using the homogeneous catalyst PdNPs/**1** alone, which is remarkable. For instance, under the same conditions, **4f** is obtained with a yield $< 50\%$ with 0.02 mol% of PdNPs/**1**, whereas a yield of 98% is obtained with the same amount of Pd in **3**. Moreover, felbinac (**4h**) ($\text{R} = \text{CH}_2\text{CO}_2\text{H}$, Scheme 2), a nonsteroidal anti-inflammatory drug used to treat arthritis and inflammation is synthesized in this way, and the Suzuki–Miyaura reaction provides a 94% yield.

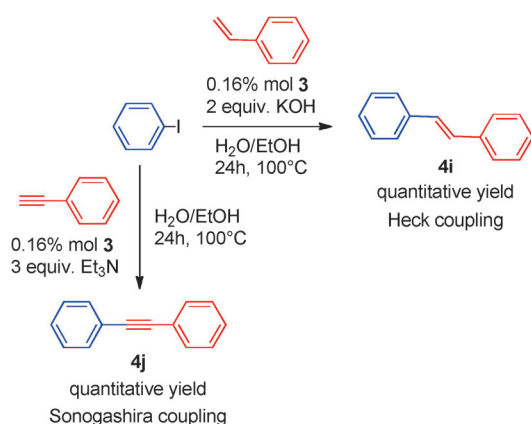
To determine the smallest amount of **3** necessary for the Suzuki–Miyaura reaction between bromobenzene and phenyl boronic acid, the yields, turnover numbers (TONs), and TOFs were measured in the presence of different amounts of **3**. With only 20 ppm of Pd after two days, the reaction yields 88% of coupled product, that is, a TON of 44 000 with a TOF of nearly 10^3 h^{-1} (Table 2).

Another major feature of this catalyst is that by applying a simple magnet, **3** is totally recovered. Catalyst **3** was used at least five times without much loss of activity. For instance, in the synthesis of **4a**, the yields decrease from 99% (first run) to 91% (fifth run). ICP-OES analysis shows that only 0.3% the Pd is lost from **3** after the first run.

Table 2. Suzuki–Miyaura reactions between bromobenzene and phenyl boronic acid with various amount of catalyst **3**.^[a]

Entry	3 [mol%Pd]	t [h]	Yield [%]	TON	TOF [h ⁻¹]
1	0.2	24	99	495	20.6
2	0.02	24	99	4950	206
3	0.005	24	60	12000	500
4	0.005	36	99	19000	550
5	0.003	48	91	30333	632
6	0.002	48	88	44000	917

[a] The reactions were performed with 1 mmol of bromobenzene, 1.5 mmol of phenyl boronic acid, 2 mmol of K₃PO₄ in H₂O/EtOH (10 mL/10 mL) at 80 °C. ■ column 3 heading ok, also in Table 3? ■



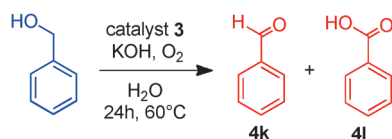
Scheme 3. Heck and Sonogashira coupling reactions.

The catalytic activity was also tested for the Heck and Cu-free Sonogashira reactions (Scheme 3).

The efficiency of **3** with only 0.16 mol% Pd for the Cu-free Sonogashira reaction was evaluated for the coupling between iodobenzene and phenylacetylene in the presence of Et₃N as a base. Within 24 h at 100 °C in a mixture of H₂O/EtOH as solvent, the desired product was isolated quantitatively.

The Heck reaction between iodobenzene and styrene was also performed under the same conditions as those of the Sonogashira reaction but with KOH as the base instead of Et₃N. Only the *E* isomer of stilbene was formed quantitatively in the reaction.

To evaluate the robustness, selectivity, and efficiency of **3**, the widely studied oxidation of benzyl alcohol by dioxygen to benzaldehyde **4k** was investigated (Scheme 4). This reaction was selected because the reaction does not proceed at all in the presence of only PdNPs/1, and PdNPs precipitate directly if O₂ is bubbled into the reaction medium; thus the reaction was executed as a “stability” test. With **3** instead of **1**,



Scheme 4. Selective benzyl alcohol oxidation with catalyst **3**.

the aerobic oxidation of benzyl alcohol in water with KOH as the base occurred very efficiently with only 0.09–0.20 mol% Pd from **3**. The reaction requires the presence of KOH as the base and 5 min of O₂ bubbling (an excess of O₂ leads to the formation of the byproduct **4l**). Moreover, the use of O₂ instead of a stoichiometric organic oxidant is highly valuable and much researched.^[9] The reaction performed in water at a relatively low temperature (60 °C) with only 0.2 mol% Pd (maximum) led to a quantitative conversion of the alcohol into the aldehyde (Table 3, entry 7).

Table 3. Investigation of the aerobic benzyl alcohol oxidation in water.

Entry ^[a]	3 [mol %Pd]	KOH [equiv.]	Byproduct	Conversion ^[d] [%]
1	0.09	2	–	74
2	0.09	0	–	0
3 ^[b]	0.09	2	–	33
4 ^[c]	0.09	2	4l	74
5	0.045	2	–	24
6	0.022	2	–	4
7	0.20	2	–	98

[a] The reactions were performed with 1 mmol of benzyl alcohol in H₂O (3 mL) over 24 h at 60 °C, and 5 min of O₂ was bubbled before starting the reaction. [b] The reaction was performed under air. [c] O₂ is present during the entire reaction. [d] Conversion of benzyl alcohol to benzaldehyde **4k**, measured by using NMR spectroscopy.

These results show that **3** is much more robust than PdNPs/1 and permits the use of the PdNPs as an efficient and reusable catalyst to be extended beyond C–C cross-coupling reactions.

Conclusions

The new concept of the impregnation of preformed dendrimers that contain Pd nanoparticles (NPs) on magnetic nanoparticles (MNPs) is highly productive for large improvements in terms of catalyst robustness, efficiency, and recyclability. The dendrimer-stabilized and encapsulated PdNPs/1 are impregnated quantitatively upon heterogenization on silica-coated maghemite γ-Fe₂O₃ MNPs **2** by simple mixing and stirring with the aqueous solution of PdNPs/1. This preparation produces a highly stabilized magnetic catalyst **3** that is active even with only 20 ppm of Pd for the Suzuki–Miyaura reaction of bromoarenes in the green mixture of solvent H₂O/EtOH and is reusable. This activity is among the highest ever reached for the Suzuki–Miyaura reaction with magnetic heterogeneous PdNPs. Actually, many magnetic PdNP systems have been used for the Suzuki–Miyaura coupling, but most of them require 0.054–3 mol% Pd^[4,10a–e] and only a few examples work with a lower amount of catalyst.^[10f] Moreover, the leaching amount of only 0.3% for a run leads to only 0.6 ppm Pd contamination of products, which is valuable for the synthesis of biological molecules such as felbinac (**4h**). This magnetic catalyst is so robust that the selective oxidation of benzyl alcohol by O₂ is quantitative at 60 °C in water with only 0.09–0.2 mol% Pd from **3**, which is not possible with nonimpregnated PdNPs/1 because

of the instantaneous aggregation of PdNPs in the presence of O₂. Finally, another advantage is that **3** is a solid, and the catalysis does not necessarily need to be conducted in water unlike that with PdNPs/**1**, which is a severe limitation. In summary, this method produced a stable, versatile, efficient, and recyclable magnetic catalyst for a variety of crucial reactions under sustainable conditions.

Experimental Section

Synthesis of PdNPs/**1**

Dendrimer **1** (2.59 mg, 3.6×10^{-4} mmol) was dissolved in water (1.1 mL) in a Schlenk flask, and an orange solution of K₂PdCl₄ (3.2×10^{-3} mmol in 1.1 mL water) was added to the solution of the dendrimer. Water (30 mL) was added, and the solution was stirred for 5 min. The concentration of Pd^{II} was 0.1 mM. An aqueous solution (1 mL) that contained NaBH₄ (3.2×10^{-2} mmol) was added dropwise to provoke the formation of a brown/black color (see below) that corresponds to the reduction of Pd^{II} to Pd⁰ and PdNP formation.

Two-step synthesis of MNPs **2**

1) Synthesis of the γ -Fe₂O₃ core protected by oleic acid

Ferrous chloride (0.25 g) and ferric chloride (0.5 g) were added under stirring to a nitrogen-purged 2-propanol solution (20 mL) to result in a yellowish orange reaction mixture. After 15 min of stirring, the temperature of the solution was increased to 80 °C, and aqueous NH₃ (10 mL) was added slowly. The color of the solution turned to dark brown, and the stirring was continued for another 2 h. The MNPs formed were protected by the addition of oleic acid (10 mM) in methanol (30 mL), removed from the solution by magnetic separation, washed with methanol, and then redispersed in ethanol.

2) Synthesis of the γ -Fe₂O₃ core and SiO₂ shell (MNPs **2**)

The suspension of γ -Fe₂O₃ core protected by oleic acid was diluted with deionized water (2 mL) and 2-propanol (10 mL), and the mixture was sonicated for approximately 5 min. NH₄OH (0.5 mL) and tetraethoxysilane (0.5 g) were added slowly to this well-dispersed MNP solution, and the reaction mixture was stirred for 4 h at RT. The material was then separated by centrifugation and redispersed in deionized water.

Synthesis of catalyst **3**

MNPs **2** (25, 50, 120 or 700 mg) were added to an aqueous solution of PdNPs/**1** (3.2×10^{-3} mmol of Pd). The mixture was treated ultrasonically for 5 min or 2 h. If only 5 min of ultrasound treatment was used, the mixture was stirred for 2 or 16 h (Table 1). Catalyst **3** was then separated from the water with a magnet. The water phase was kept, and **3** was dried overnight at 35–40 °C. To determine the Pd loading, the water phase was analyzed by ICP-OES and the value obtained was compared to the initial value determined for the solution of PdNPs/**1** (Table 1).

Catalysis of the Suzuki–Miyaura reaction

General procedure: Phenylboronic acid (1.5 mol, 1.5 equiv.), aryl halide (1 mmol, 1 equiv.), **3**, EtOH (10 mL), and H₂O (10 mL) were

successively added to a Schlenk flask containing tribasic potassium phosphate (2 mmol, 2 equiv.). The mixture was treated ultrasonically for 5 min to disperse the magnetic catalyst. The suspension was allowed to stir under N₂ or air (no difference in yield). After the reaction (24 or 48 h), the catalyst was separated from the reaction mixture with a magnet, and the aqueous phase was extracted twice with Et₂O (all the reactants and final products are soluble in Et₂O). The organic phase was dried over Na₂SO₄, and the solvent was removed in vacuo. In parallel, the reaction was checked using TLC with petroleum ether as the eluent in nearly all the cases and ¹H NMR spectroscopy. Purification by flash chromatography was conducted with silica gel as the stationary phase and petroleum ether as the mobile phase. The Schlenk flask that contained the catalyst was dried in vacuo to recover or reuse the catalyst.

If the catalyst was not recovered, the Schlenk flask was washed with a solution of aqua regia (HCl/HNO₃ 3:1 v/v) to remove traces of Pd or only with HCl (to remove traces of Fe).

Catalysis of the Sonogashira reaction

Alkyne (1.2 mmol, 1.2 equiv.), iodobenzene (1 mmol, 1 equiv.), **3**, EtOH (1 mL), and H₂O (1 mL) were added successively to a Schlenk flask containing triethylamine (3 mmol, 3 equiv.). The magnetic catalyst was dispersed by 5 min of ultrasonic activation. The suspension was allowed to stir under air. After 24 h, the catalyst was separated from the reaction mixture with a magnet, and the aqueous phase was extracted twice with Et₂O. The organic phase was dried over Na₂SO₄, and the solvent was removed in vacuo. In parallel, the reaction was checked using TLC with petroleum ether as the eluent and ¹H NMR spectroscopy. Purification by flash chromatography was conducted with silica gel as the stationary phase and petroleum ether as the mobile phase. The Schlenk flask that contained the catalyst was dried in vacuo to recover or reuse the catalyst. If the catalyst was not recovered, the Schlenk flask was washed with a solution of aqua regia (HCl/HNO₃ 3:1 v/v) to remove any traces of Pd or only with HCl (to remove the traces of Fe).

Catalysis of the Heck reaction

Styrene (1.2 mmol, 1.2 equiv.), iodobenzene (1 mmol, 1 equiv.), **3**, EtOH (10 mL), and H₂O (10 mL) were added successively to a Schlenk flask containing KOH (3 mmol, 3 equiv.). The magnetic catalyst was dispersed by 5 min of ultrasonic treatment. The suspension was allowed to stir under air. After 24 h, the catalyst was separated from the reaction mixture with a magnet, and the aqueous phase was extracted twice with Et₂O. The organic phase was dried over Na₂SO₄, and the solvent was removed in vacuo. In parallel, the reaction is checked using TLC with petroleum ether as the eluent and ¹H NMR spectroscopy. Purification by flash chromatography was conducted with silica gel as the stationary phase and petroleum ether as the mobile phase. The Schlenk flask containing the catalyst was dried in vacuo to recover or reuse the catalyst. If the catalyst was not recovered, the Schlenk flask was washed with a solution of aqua regia (HCl/HNO₃ 3:1 v/v) to remove any traces of Pd or only with HCl (to remove the traces of Fe).

Catalysis of benzyl alcohol oxidation

Benzyl alcohol (1.0 mmol, 1.0 equiv.), **3**, and H₂O (3 mL) were added successively to a Schlenk flask containing KOH (2 mmol, 2 equiv.). The magnetic catalyst was dispersed by 5 min of ultra-

sonic activation, and O₂ was bubbled inside the closed Schlenk flask for 5 min. The suspension was allowed to stir for 24 h. The catalyst was then separated from the reaction mixture with a magnet, and the water phase was extracted twice with Et₂O. The organic phase was dried over Na₂SO₄, and the solvent was removed in vacuo. The Schlenk flask containing the catalyst was dried in vacuo to recover or reuse the catalyst. If the catalyst was not recovered, the Schlenk flask was washed with a solution of aqua regia (HCl/HNO₃ 3:1 v/v) to remove any traces of Pd or only with HCl (to remove the traces of Fe).

Acknowledgements

Financial support from the Université de Bordeaux, the CNRS, the Ministère de l'Enseignement Supérieur et de la Recherche (PhD grant to C.D.), and L'Oréal are gratefully acknowledged.

Keywords: cross-coupling · dendrimers · nanoparticles · palladium · supported catalysts

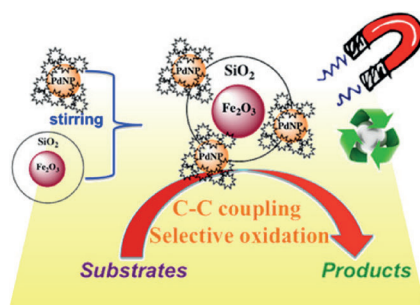
- [1] a) M. Haruta, M. Date, *Appl. Catal. A* **2001**, *222*, 427–437; b) *Nanotechnology in Catalysis, Vol. 1 and 2 (Nanostructure Science and Technology)* (Eds. B. Zhou, S. Hermans, G. A. Somorjai), **2003**; c) A. T. Bell, *Science* **2003**, *299*, 1688–1691; d) D. Astruc, F. Lu, J. Ruiz, *Angew. Chem. Int. Ed.* **2005**, *44*, 7852–7872; *Angew. Chem.* **2005**, *117*, 8062–8083; e) A. Corma, H. Garcia, *Chem. Soc. Rev.* **2008**, *37*, 2096–2126; f) J.-M. Basset, R. Psaro, D. Roberto, R. Ugo, Ed. *Modern Surface Organometallic Chemistry*, Wiley-VCH, Weinheim, **2009**; g) A. Corma, H. Garcia, F. X. Llambres i Xamena, *Chem. Rev.* **2010**, *110*, 4606–4655; h) L. M. Bronstein, Z. B. Shifrina, *Chem. Rev.* **2011**, *111*, 5301–5344; i) *Nanomaterials in Catalysis* (Eds.: P. Serp, K. Philippot), Wiley-VCH, Weinheim, **2013**; j) M. Haruta, *Angew. Chem. Int. Ed.* **2014**, *53*, 52–56; *Angew. Chem.* **2014**, *126*, 54–58.
- [2] a) A. H. Lu, E. L. Salabas, F. Schüth, *Angew. Chem. Int. Ed.* **2007**, *46*, 1222–1244; *Angew. Chem.* **2007**, *119*, 1242–1266; b) S. Roy, M. A. Pericas, *Org. Biomol. Chem.* **2009**, *7*, 2669–2677; c) S. Shylesh, V. Schünnemann, W. R. Thiel, *Angew. Chem. Int. Ed.* **2010**, *49*, 3428–3459; *Angew. Chem.* **2010**, *122*, 3504–3537; d) Y. Zhu, L. P. Stubbs, F. Ho, R. Liu, C. P. Ship, J. A. Maguire, N. S. Hosmane, *ChemCatChem* **2010**, *2*, 365–374; e) C. W. Lim, I. S. Lee, *Nano Today* **2010**, *5*, 412–434; f) V. Polshettiwar, R. Luque, A. Fihri, H. Zhu, M. Bouhrara, J.-M. Basset, *Chem. Rev.* **2011**, *111*, 3036–3075; g) L. M. Rossi, A. S. Garcia, L. L. R. Vono, *J. Braz. Chem. Soc.* **2012**, *23*, 1959–1971; h) P. Li, L. Wang, L. Zhang, G.-W. Wang, *Adv. Synth. Catal.* **2012**, *354*, 1307–1318; i) M. B. Gawande, P. S. Branco, R. S. Varma, *Chem. Soc. Rev.* **2013**, *42*, 3371–3393; j) D. Wang, D. Astruc, *Chem. Rev.* **2014**, *114*, 6949–6985.
- [3] a) M. T. Reetz, W. Helbig, S. A. Quaiser in *Active Metals: Preparation, Characterizations, Applications* (Ed.: A. Fürstner), Wiley-VCH, Weinheim, **1996**, p. 279; b) H. Bönemann, R. Richards, *Eur. J. Inorg. Chem.* **2001**, 2455–2480; c) T. Yonezawa, N. Toshima, *Polymer-Stabilized Metal Nanoparticles: Preparation, Characterization and Applications, in Advanced Functional Molecules and Polymers, Vol. 2* (Ed.: H. S. Nalwa), OPA N.V. ■■■ please add publisher and city of publication ■■■, **2001**, Chap. 3, pp. 65–86; d) *Nanoparticles and Catalysis* (Ed.: D. Astruc), Wiley-VCH, Weinheim, **2008**.
- [4] a) W. Li, B. Zhang, X. Li, H. Zhang, Q. Zhang, *Appl. Catal. A* **2013**, *459*, 65–72; b) P. Wang, F. Zhang, Y. Long, M. Xie, R. Li, J. Ma, *Catal. Sci. Technol.* **2013**, *3*, 1618–1624; c) J. Sun, Z. Dong, X. Sun, P. Li, F. Zhang, W. Hu, H. Yang, H. Wang, R. Li, *J. Mol. Catal. A* **2013**, *367*, 46–51; d) A. Alonso, A. Shafir, J. Macanás, A. Vallribera, M. Muñoz, D. N. Muraviev, *Catal. Today* **2012**, *193*, 200–206; e) S. Li, W. Zhang, M.-H. Sob, C.-M. Che, R. Wang, R. Chen, *J. Mol. Catal. A* **2012**, *359*, 81–87; f) A. Schätz, T. R. Long, R. N. Grass, W. J. Stark, P. R. Hanson, O. Reiser, *Adv. Funct. Mater.* **2010**, *20*, 4323–4328; g) M. Zeltner, A. Schätz, M. L. Hefti, W. J. Stark, *J. Mater. Chem.* **2011**, *21*, 2991–2996; h) J. Wang, B. Xu, H. Sun, G. Song, *Tetrahedron Lett.* **2013**, *54*, 238–241; i) J. Hu, Y. Wang, M. Han, Y. Zhou, X. Jiang, P. Sun, *Catal. Sci. Technol.* **2012**, *2*, 2332–2340; j) K.-H. Choi, M. Shokouhimehr, Y.-E. Sung, *Bull. Korean Chem. Soc.* **2013**, *34*, 1477–1480; k) Q. Zhang, H. Su, J. Luo, Y. Wei, *Catal. Sci. Technol.* **2013**, *3*, 235–243; l) Z. Yinghuai, S. C. Peng, A. Emi, S. Zhenshun, Monalisa, R. A. Kemp, *Adv. Synth. Catal.* **2007**, *349*, 1917–1922; m) A. Khalafi-Nezhad, F. Panahi, *J. Organomet. Chem.* **2013**, *741–742*, 7–14; n) Q. Du, W. Zhang, H. Ma, J. Zheng, B. Zhou, Y. Li, *Tetrahedron* **2012**, *68*, 3577–3584; o) N. T. S. Phan, H. V. Le, *J. Mol. Catal. A* **2011**, *334*, 130–138.
- [5] a) V. Percec, C. Mitchell, W.-D. Cho, S. Uchida, M. Glodde, G. Ungar, X. Zeng, Y. Liu, V. S. K. Balagurusamy, *J. Am. Chem. Soc.* **2004**, *126*, 6078–6094; b) E. Boisselier, A. K. Diallo, L. Salmon, C. Ornelas, J. Ruiz, D. Astruc, *J. Am. Chem. Soc.* **2010**, *132*, 2729–2742; c) C. Deraedt, L. Salmon, J. Ruiz, D. Astruc, *Chem. Commun.* **2013**, *49*, 8169–8171; d) C. Deraedt, D. Astruc, *Acc. Chem. Res.* **2014**, *47*, 494–503.
- [6] a) N. Miyaoura, A. Suzuki, *Chem. Rev.* **1995**, *95*, 2457–2483; b) I. P. Beletskaya, A. V. Cheprakov, *Chem. Rev.* **2000**, *100*, 3009–3066; c) R. M. Crooks, M. Zhao, L. Sun, V. Chechik, L. K. Yeung, *Acc. Chem. Res.* **2001**, *34*, 181–190; d) J. Hassan, M. Sévignon, C. Gozzi, E. Schulz, M. Lemaire, *Chem. Rev.* **2002**, *102*, 1359–1469; e) T. Imaoka, H. Horiguchi, K. Yamamoto, *J. Am. Chem. Soc.* **2003**, *125*, 340–341; f) F. Lu, J. Ruiz, D. Astruc, *Tetrahedron Lett.* **2004**, *45*, 9443–9445; g) R. W. J. Scott, O. M. Wilson, R. M. Crooks, *J. Phys. Chem. B* **2005**, *109*, 692–704; h) J. G. de Vries, *Dalton Trans.* **2006**, 421–429; i) V. S. Myers, M. W. Weier, E. V. Carino, D. F. Yancey, S. Pande, R. M. Crooks, *Chem. Sci.* **2011**, *2*, 1632–1646; j) R. Chinchilla, C. Najera, *Chem. Soc. Rev.* **2011**, *40*, 5084–5121; k) I. Favier, D. Maded, E. Teuma, M. Gomez, *Curr. Org. Chem.* **2011**, *15*, 3127–3174.
- [7] a) M. I. Fernandez, G. Tojo, *Oxidation of Alcohols to Aldehydes and Ketones: A Guide to Current Common Practice*, Springer, New York, **2006**; b) M. J. Schultz, M. S. Sigman, *Tetrahedron* **2006**, *62*, 8227–8241; c) N. Dimitratos, J. A. Lopez-Sanchez, G. J. Hutchings, *Chem. Sci.* **2012**, *3*, 20–44; d) Z. Shi, C. Tang, N. Jiao, *Chem. Soc. Rev.* **2012**, *41*, 3381–3430; e) C. Parmeggiani, F. Cardona, *Green Chem.* **2012**, *14*, 547–564.
- [8] a) S. Shylesh, L. Wang, W. R. Thiel, *Adv. Synth. Catal.* **2010**, *352*, 425–432; b) Ultrasonication is an efficient method for the impregnation of Pd ions on a magnetic support: U. Laska, C. G. Frost, G. J. Price, P. K. Plucinski, *J. Catal.* **2009**, *268*, 318–328.
- [9] a) K. Yamaguchi, N. Mizumo, *Angew. Chem. Int. Ed.* **2002**, *41*, 4538–4542; *Angew. Chem.* **2002**, *114*, 4720–4724; b) A. Tashiro, A. Mitsuishi, R. Irie, T. Katsuki, *Synlett* **2003**, *12*, 1868–1870.
- [10] a) W. Tang, J. Li, X. Jin, J. Sun, J. Huang, R. Li, *Catal. Commun.* **2014**, *43*, 75–78; b) J. Sun, Z. Dong, X. Sun, P. Li, F. Zhang, W. Hu, H. Yang, H. Wang, R. Li, *J. Mol. Catal. A* **2013**, *367*, 46–51 ■■■ duplicate of ref. 4, which one would you like to delete? ■■■; c) M. Shokouhimehr, J. E. Lee, S. I. Han, T. Hyeon, *Chem. Commun.* **2013**, *49*, 4779–4781; d) A. S. Singh, U. B. Patil, J. M. Nagarkar, *Catal. Commun.* **2013**, *35*, 11–16; e) M. Shokouhimehr, T. Kim, S. W. Jun, K. Shin, Y. Jang, B. H. Kim, J. Kim, T. Hyeon, *Appl. Catal. A* **2014**, *476*, 133–139; f) B. Karimi, F. Mansouri, H. Vali, *Green Chem.* **2014**, *16*, 2587–2596.

Received: September 26, 2014

Published online on ■■■ ■■■, 0000

FULL PAPERS

All dendrimers on deck: The simple impregnation of $\gamma\text{-Fe}_2\text{O}_3$ (core)/ SiO_2 (shell) magnetic nanoparticles with a dendrimer that contains stabilized Pd nanoparticles is a new method to produce a highly efficient heterogeneous catalyst, which provides much better stability, recyclability, and activity in C–C cross-coupling reactions and selective oxidation of benzyl alcohol to benzaldehyde in water than unsupported Pd nanoparticles.



C. Deraedt, D. Wang, L. Salmon,
L. Etienne, C. Labrugère, J. Ruiz,
D. Astruc*

■ ■ - ■ ■

**Robust, Efficient, and Recyclable
Catalysts from the Impregnation of
Preformed Dendrimers Containing
Palladium Nanoparticles on
a Magnetic Support**



Magnetic dendritic palladium nanoparticles @CNRS @univbordeaux @Univ_Toulouse #catalyst [SPACE RE-](#)
[SERVED FOR IMAGE AND LINK](#)

ChemCatChem is piloting a social networking feature involving Twitter, an online microblogging service that enables its users to send and read text-based messages of up to 140 characters, known as “tweets”. Please check the pre-written tweet in the galley proofs for accuracy. Should you or your institute have a Twitter account, please let us know the appropriate username (e.g., @ChemCatChem), and we will do our best to include this information in the tweet. This tweet will be posted to the journal’s Twitter account upon online publication of your article.



WILEY-VCH
Galley Proofs

Heterogeneous Catalysis | Hot Paper |

Efficient and Magnetically Recoverable “Click” PEGylated γ -Fe₂O₃-Pd Nanoparticle Catalysts for Suzuki–Miyaura, Sonogashira, and Heck Reactions with Positive Dendritic EffectsDong Wang,^[a] Christophe Deraedt,^[a] Lionel Salmon,^[b] Christine Labrugère,^[c] Laetitia Etienne,^[d] Jaime Ruiz,^[a] and Didier Astruc^{*[a]}

Abstract: The engineering of novel catalytic nanomaterials that are highly active for crucial carbon–carbon bond formations, easily recoverable many times, and biocompatible is highly desirable in terms of sustainable and green chemistry. To this end, catalysts comprising dendritic “click” ligands that are immobilized on a magnetic nanoparticle (MNP) core, terminated by triethylene glycol (TEG) groups, and incorporate Pd nanoparticles (PdNPs) have been prepared. These nanomaterials are characterized by transmission electron microscopy (TEM), high-resolution TEM, inductively coupled plasma analysis, Fourier transform infrared spectroscopy, X-ray photoelectron spectra and energy-dispersive X-ray

spectroscopy. They are shown to be highly active, dispersible, and magnetically recoverable many times in Suzuki, Sonogashira, and Heck reactions. In addition, a series of pharmacologically relevant or natural products were successfully synthesized using these magnetic PdNPs as catalyst. For comparison, related PdNP catalysts deposited on MNPs bearing linear “click” PEGylated ligands are also prepared. Strong positive dendritic effects concerning ligand loading, catalyst loading, catalytic activity, and recyclability are observed, that is, the dendritic catalysts are much more efficient than non-dendritic analogues.

Introduction

With the rapid development of modern industry, environmental concerns are increasing every day. The maximization of synthetic efficiency and minimization of waste generation are basic constraints that need be addressed in order to solve the environmental problems.^[1] In a related context, the use of heterogeneous catalysts appears to be one of the promising methodologies for the development of environmentally friendly organic transformation process, because of their separability, reusability, and unique activity that are provided through the interaction between the catalytic species and supports.^[2] Among transition metal nanoparticle (NP) catalysts,^[3] magnetic nanoparticles (MNPs) have recently received a lot of attention

as excellent supports.^[4] MNP catalysis is nowadays undergoing an explosive development, because MNP-immobilized catalysts perfectly combine the advantages of catalytically active NPs and magnetic NPs. NP catalysts benefit from activity, selectivity, and stability, resulting from the large surface-to-volume ratio, tunable size, shape, composition, electronic structure, and solubility, whereas MNPs are easily assembled, accessible, and recoverable with an external magnetic field for reuse. Therefore MNP catalysts fully embody the principles of green chemistry and sustainability.

Dendrimers, dendrons, and dendronized and dendritic polymers, a family of nanosized three-dimensional well-defined highly branched molecular frameworks, have been demonstrated to have essential and promising applications in catalysis.^[5–9] In particular, dendrimer-encapsulated metal nanoparticles (DENs) and dendrimer-stabilized NPs (DSNs) have proved to be efficient catalysts for a variety of reactions^[10] since Crooks and co-workers pioneered catalysis by polyamidoamine (PAMAM)-encapsulated Pd nanoparticles (PdNPs).^[11] The DENs and DSNs possess a variety of key properties including tunable size due to the predictable number of metal atoms in the pre-catalyst, solubility and stability caused by the functional groups and steric embedding effects, loose binding to the NP surface, and the possibility of heterogenization by fixation on a solid support. PAMAM dendrimers,^[12] polypropyleneimine (PPI) dendrimers,^[13] and phenylazomethine dendrimers^[14] are the most-used dendrimers for the stabilization of metal NPs. It was recently reported that triethylene glycol (TEG)-terminated

[a] Dr. D. Wang, C. Deraedt, Dr. J. Ruiz, Prof. D. Astruc
ISM, Univ. Bordeaux, 351 Cours de la Libération
33405 Talence Cedex (France)
E-mail: d.astruc@ism.u-bordeaux1.fr

[b] Dr. L. Salmon
LCC, CNRS, 205 Route de Narbonne
31077 Toulouse Cedex (France)

[c] C. Labrugère
PLACAMAT UMS CNRS 3626, Univ. Bordeaux
87 Avenue Albert Schweitzer, 33608 Pessac Cedex (France)

[d] L. Etienne
ICMCB, UPR CNRS No. 9048, Univ. Bordeaux
87 Avenue Albert Schweitzer, 33608 Pessac Cedex (France)

Supporting information for this article is available on the WWW under <http://dx.doi.org/10.1002/chem.201404590>.

"click" dendrimers containing Percec-type dendrons,^[15] constructed using Newkome-type 1→3 connectivity,^[16] were remarkably powerful for assembling DENs and DSNs involving AuNPs and PdNPs.^[17] The latter exhibited unprecedented catalytic performance in C–C cross-coupling reactions and reduction of 4-nitrophenol, owing to smooth complexation of triazole to Pd atoms, water solubility provided by TEG termini, and the formation of dendritic nanoreactors containing hydrophilic periphery and hydrophobic interior.^[17a,b] Likewise, molecular and ionic catalysts are also activated as, for instance, in "click" CuAAC reactions.^[17c]

The introduction of dendritic fragments into MNPs has been utilized during the past few years, and this engineering considerably increased the number of functional groups on the surface of MNPs and strongly improved the dispersion of MNPs in organic or aqueous solvent.^[4e,18] These MNP-immobilized dendritic fragments are promising catalysts,^[18] reusable adsorbents of metal ions,^[18c] and potential drug carriers.^[18d] In the field of catalysis, most of these MNPs catalysts bearing dendritic frameworks were MNP-anchored metal complexes, organocatalysts, and biocatalysts. To the best of our knowledge, the only example on magnetic DENs or DSNs has been reported by Bronstein's group.^[18g] These authors used poly(phenylenepridyl) dendrons as capping molecules to successively stabilize iron oxide NPs and PdNPs. The magnetically recoverable Pd catalysts that were obtained in this way afforded excellent catalytic performance in the selective hydrogenation of dimethylethylcarbinol to dimethylvinylcarbinol.

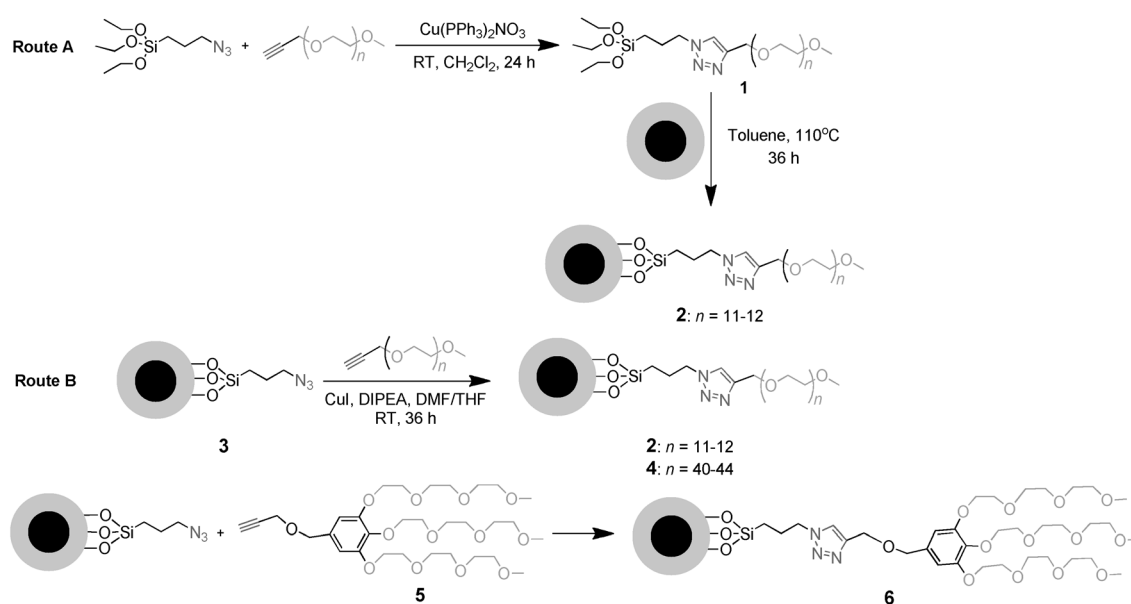
Herein, we report the engineering, synthesis, characterization, and catalytic efficiency and recyclability of PdNPs that are supported on new MNPs containing dendritic "click" PEGylated ligands. High efficiency of these PdNP catalysts is found in Suzuki–Miyaura, Sonogashira, and Heck reactions, and positive dendritic effects are demonstrated in terms of loading amount of catalyst, catalytic activity, and, in particular, recyclability.

Results and Discussion

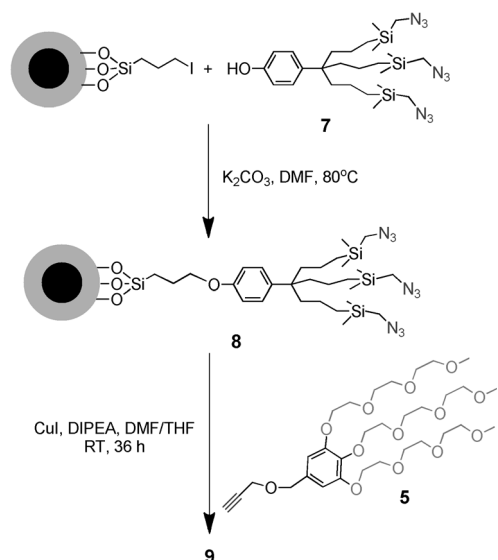
Syntheses of MNP-immobilized PEGylated triazolyl ligands

The syntheses of MNP-immobilized linear and dendritic PEGylated triazolyl ligands were the primary steps of this project. Magnetic linear PEG550-triazole **2** was prepared through two strategies (Scheme 1); grafting pre-synthesized Si(OEt)₃-functionalized PEG–triazole on the surface of iron oxide MNPs (route A), or direct "click" synthesis of PEG–triazole on the surface of iron oxide MNPs after the introduction of azido groups (route B). In route A, the "click" reaction of (3-azidopropyl)triethoxysilane with PEG550 alkyne was readily conducted in the presence of [Cu(PPh₃)₂NO₃] in anhydrous CH₂Cl₂ at room temperature (RT) giving Si(OEt)₃-functionalized PEG–triazole **1** that was further immobilized on the surface of MNPs via heterogenization with the Si–OH binding sites of SiO₂/γ-Fe₂O₃ NPs. In route B, the "click" reaction was successfully carried out between PEG550 alkyne and azido-modified iron oxide NPs. The loading of the ligands in **2** was calculated by determination of the nitrogen content (CHN elemental analysis), and the result revealed that the loadings were 0.17 mmol g⁻¹ and 0.26 mmol g⁻¹ for routes A and B, respectively. The lower ligand loading of route A seems to be attributable to the low efficiency of the heterogenization process that is caused by the bulky chain of compound **1**. To obtain higher ligand loading, route B was used in the preparations of the MNP-immobilized linear PEG2000-triazole ligand **4** and Percec-type dendron–triazole ligand **6** (Scheme 1). The former contains a longer hydrophilic PEG chain than **2**, and the latter possesses a TEG-terminated dendritic framework.

There are two strategies for the modification of MNPs with dendritic fragments:^[4e] i) divergent synthesis of dendritic fragments on the surface of MNPs after the introduction of a linker, and ii) grafting of pre-synthesized dendritic fragments.



Scheme 1. Syntheses of MNP-immobilized linear and dendritic PEGylated triazolyl ligands **2**, **4**, and **6**.

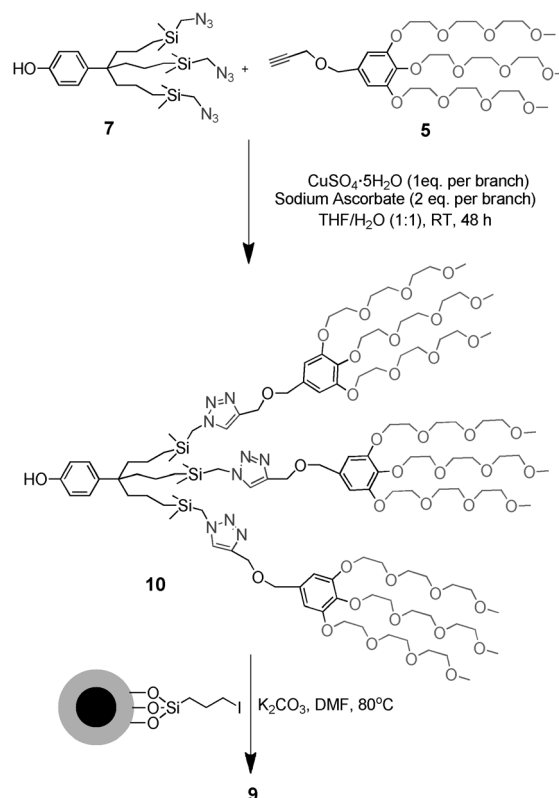


Scheme 2. Divergent synthesis of MNP-immobilized dendritic tris-triazole ligand with triethylene glycol (TEG) tethers.

The synthesis of MNP-immobilized dendritic tris-triazole ligand **9** was achieved through both strategies. The divergent synthesis approach is shown in Scheme 2. Iodo-functionalized MNPs were derived by coupling $SiO_2/\gamma\text{-Fe}_2O_3$ NPs with pre-synthesized (3-iodopropyl)triethoxysilane.^[19] The dendritic precursor **7** bearing a phenol and three azido groups has been reported previously.^[20] Newkome-type 1 \rightarrow 3 connectivity^[16] was then applied using nucleophilic substitution of the terminal iodine by the phenolate group of **7** in the presence of K_2CO_3 in DMF.^[20] This reaction provided dendritic azide-functionalized MNPs **8** in which the presence of azido groups was verified by the appearance of the N_3 band at 2102 cm^{-1} in the Fourier transform infrared (FT-IR) spectra. The loading amount of the azido groups was 0.86 mmol g^{-1} , as measured by elemental analysis (EA). Finally, the “click” reaction of **8** with the Percec-type dendron **5** efficiently proceeded to afford the MNP-anchored dendritic TEG-triazole ligand **9** (Figure 1). In the process, the reaction was monitored by FT-IR as indicated by the almost complete disappearance of the IR signal of 2102 cm^{-1} that characterizes the azido group.

Scheme 3 depicts the other synthetic method for grafting the pre-synthesized dendritic fragments. The “click” reaction of dendritic azide **7** with Percec-type^[15] dendron **5** was successfully performed using the “Sharpless–Fokin catalyst”^[21] in a mixture of THF and H_2O , providing the phenolic hydroxy group-functionalized tris-triazole dendron **10**. Thereafter, the desired MNP-immobilized dendritic tris-triazole ligand **9** was constructed via the Williamson reaction between **10** and iodo-modified MNPs.^[20]

EA showed that the triazole loading amounts of **9** were 0.63 and 0.42 mmol g^{-1} , for the divergent synthesis and the grafting of pre-synthesized unit method, respectively. It was thus clear that the divergent synthesis was more efficient than the grafting of pre-synthesized units, considering that the amount of loaded functional groups is a very key issue for the evaluation of loading protocols. In addition, the obtained MNPs **9** pos-



Scheme 3. Synthesis of the MNP-immobilized dendritic tris-triazole ligand with TEG tethers through the grafting of pre-synthesized dendrons.

Table 1. Loading amounts of triazolyl ligand in MNPs **2**, **4**, **6**, and **9**, and loading amounts of PdNP in MNP **2**-PdNPs, MNP **4**-PdNPs, MNP **6**-PdNPs, and MNP **9**-PdNPs.

MNPs	Triazole loading [mmol g ⁻¹]	Pd loading [mmol g ⁻¹]
MNP 2 ^[a]	0.26	
MNP 4 ^[a]	0.14	
MNP 6 ^[a]	0.27	
MNP 9 ^[b]	0.63	
MNP 2 -PdNPs		0.072
MNP 4 -PdNPs		0.048
MNP 6 -PdNPs		0.082
MNP 9 -PdNPs		0.210

[a] The MNPs were prepared through route B; [b] The MNPs were prepared through the divergent method.

sessed much higher ligand loading than that of MNP-immobilized linear ligands **2** and **4** (Table 1). This result shows that the introduction of a dendritic structure remarkably increases the density of functional groups around the MNPs, which is the indication of a positive dendritic effect.

Transmission electron microscopy (TEM) images revealed that all of MNPs **2**, **4**, **6**, and **9** exhibited core-shell morphology with an average particle size of about 25 nm, ranging from 10 to 40 nm (see the Supporting Information, Figures S2, S3 a).

Note that in the synthetic processes of these magnetic PE-Gylated triazolyl ligands, magnetic separation was repeatedly

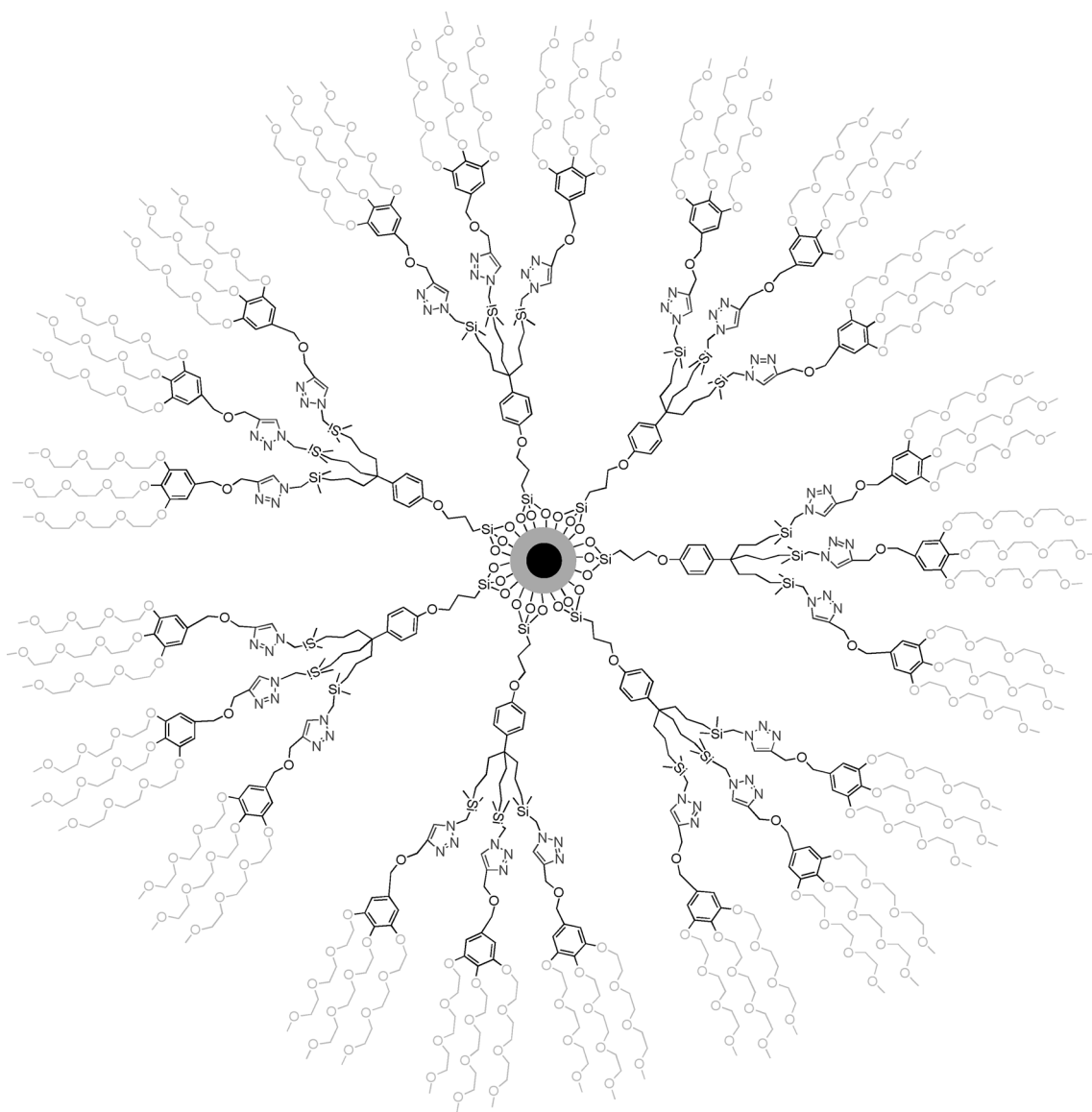
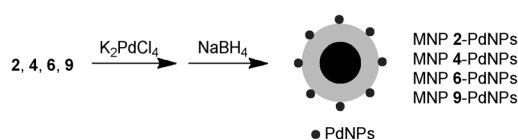


Figure 1. Structure of MNP 9.

used in purifying operations as an efficient, time saving, "green", and easy-to-operate protocol.

Preparation and characterization of iron oxide NP-immobilized PdNP catalysts

MNPs 2, 4, 6, and 9 are highly dispersible and even partially soluble in water owing to the presence of PEG or TEG, providing the possibility that MNPs 2, 4, 6, and 9 are used as supports for efficient immobilization of PdNPs in water. First, the coordination of Pd^{II} with a triazolyl fragment was achieved by adding 2 equivalents of K₂PdCl₄ per triazolyl group into a suspension of MNP-immobilized PEGylated triazolyl ligands in water. The complexation of triazole to Pd^{II} has been established in earlier reports.^[10o,17a,b] PdNPs were then loaded onto the MNP supports following by the reduction of Pd^{II} to Pd⁰ using 10 equivalents of NaBH₄ per triazole group (Scheme 4).



Scheme 4. Syntheses of MNP-PdNPs.

These MNP-PdNPs were characterized by TEM, high-resolution TEM (HRTEM), energy-dispersive X-ray spectroscopy (EDX), FT-IR, and inductively coupled plasma optical emission spectrometry (ICP-OES).

Taking MNP9-PdNPs as an example, the production was performed utilizing as support the MNP 9 that had been prepared by the divergent synthesis method. The TEM image of MNP9-PdNPs revealed the core-shell structure and the almost unchanged size compared to unloaded MNP 9 (Figure 2b).

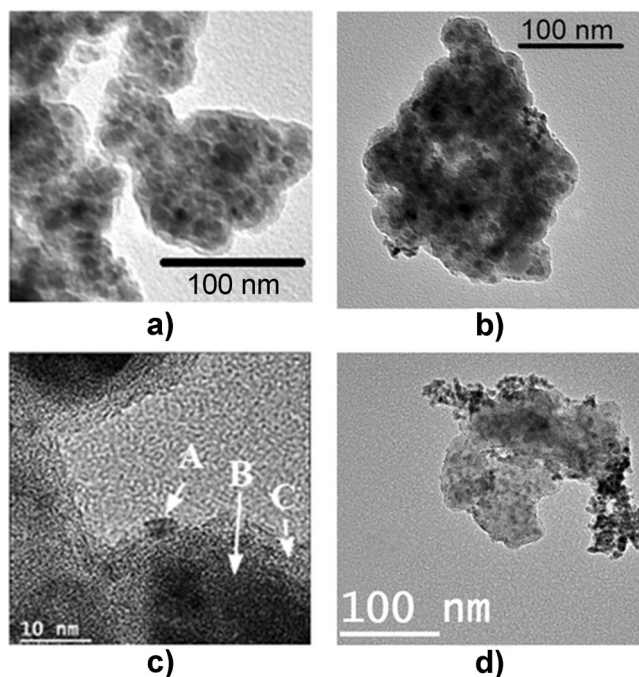


Figure 2. a) TEM image of MNP 9; b) TEM image of MNP 9–PdNPs; c) HRTEM image of MNP 9–PdNPs (A: PdNP; B: γ -Fe₂O₃ core; C: SiO₂ shell); d) TEM image of MNP 9–PdNPs after 8 reaction cycles in the Suzuki–Miyaura reaction.

Moreover, the HRTEM pictures showed that the sizes of formed PdNPs were smaller than 5 nm, with an average size of approximately 3.0 nm (see the Supporting Information, Figures S2, S3 c).

The elemental composition was determined by EDX analysis and the results, shown in Figure 3, indicate Si, O, Fe and Pd signals that are provided by MNP 9–PdNPs. For further characterization of the sample, high-resolution scanning transmission

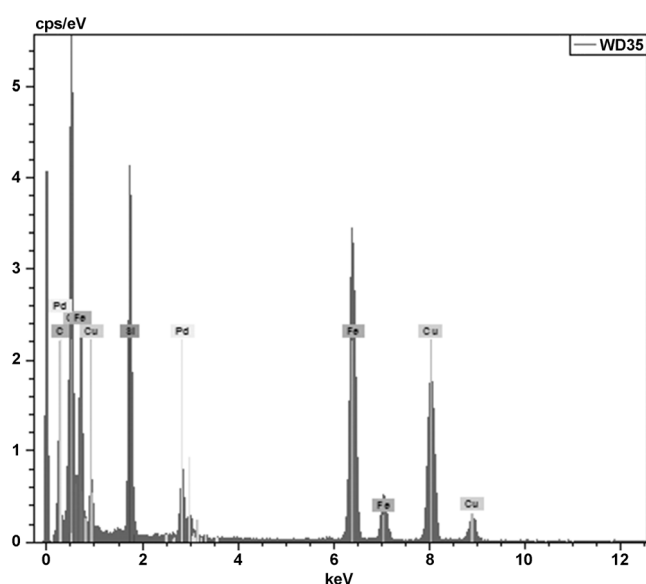


Figure 3. EDX spectrum of MNP 9–PdNPs.

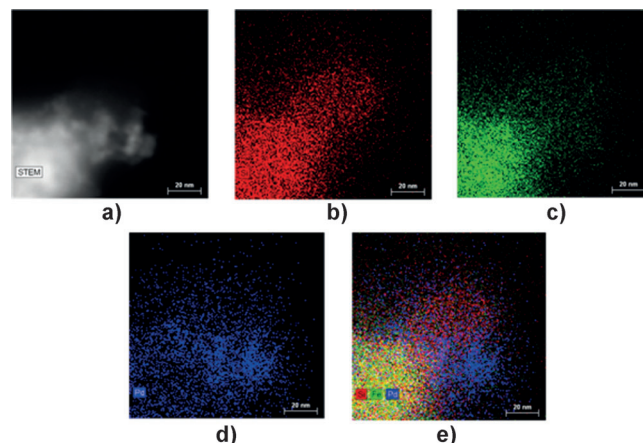


Figure 4. STEM dark-field image (a) and elemental maps of MNP 9–PdNPs for Si (b), Fe (c), Pd (d), and mixture of Si, Fe, Pd (e) obtained by EDX.

electron microscopy-coupled quantified energy-dispersive X-ray spectroscopy (HRSTEM-EDX) mapping of the sample was also investigated (Figure 4, S2). Looking at the compositional maps of Si, Fe, Pd, and mainly the combined composition image, the presence of the iron oxide nanoparticles is clearly distinguished in the core of the MNP that is encapsulated by the silicon oxide shell, while the palladium nanoparticles are localized at the border.

Thanks to the HRTEM images, it was also possible to observe the atomic arrangements in several Pd and Fe₂O₃ particles. Figure 5 b shows the atomic planes for a γ -Fe₂O₃ nanoparticle and the corresponding selected-area electron diffraction (SAED) pattern showing a [111] orientation of a face-centered cubic

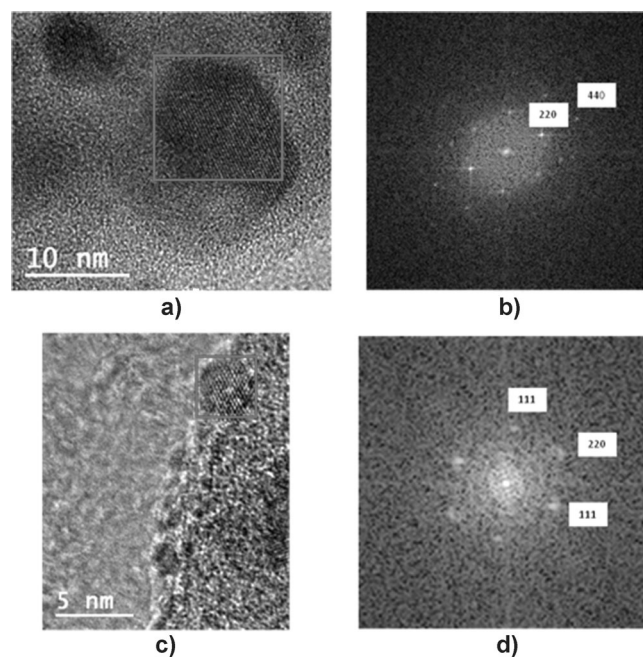


Figure 5. a) HRTEM image of the Fe₂O₃ nanoparticles; b) the corresponding SAED of Fe₂O₃ nanoparticles; c) HRTEM image of the Pd nanoparticles; d) the corresponding SAED of Pd nanoparticles.

(fcc) structure. Similar treatment for a selected Pd nanoparticle revealed a [011] orientation of a face-centered cubic (fcc) structure (Figure 5 d).

ICP-OES analysis showed that the Pd loading of MNP9–PdNPs is 0.21 mmol g⁻¹, which is approximately 3 times larger than that of MNP2–PdNPs and 4 times larger than that of MNP4–PdNPs (Table 1) and signifies a positive dendritic effect regarding catalyst loading. In addition, the amount of the Cu residual in MNP9–PdNPs was measured using ICP analysis, showing that this amount in MNP9–PdNPs is 3.15 × 10⁻⁶ mmol g⁻¹, which is negligible compared to the Pd loading.

Insight into the chemical composition and oxidation state of MNP9–PdNPs has been provided by X-ray photoelectron spec-

troscopy (XPS) analysis and, for comparison, MNP9 has also been investigated. From Figure 6, the characteristic signals for Fe, O, N, C, and Si are clearly observed in the XPS spectra of both MNP9 and MNP9–PdNPs (Figure 6a,6b). In the XPS spectrum of MNP9–PdNPs, the photoelectron line at a binding energy of approximately 335.3 eV indicates the presence of the Pd element in the metallic state, confirming the formation of PdNPs (Figure 6c). The very small shoulder at a binding energy of 337.3 eV reveals the existence of only a small trace of Pd oxide. These results demonstrate that the catalyst MNP9–PdNPs is composed of iron oxide, SiO₃X bonds, organic fragment (ligand), and PdNPs (see the atomic percentage of each element in Tables S1 and S2 in the Supporting Information). To investigate the sitting position of the PdNPs in

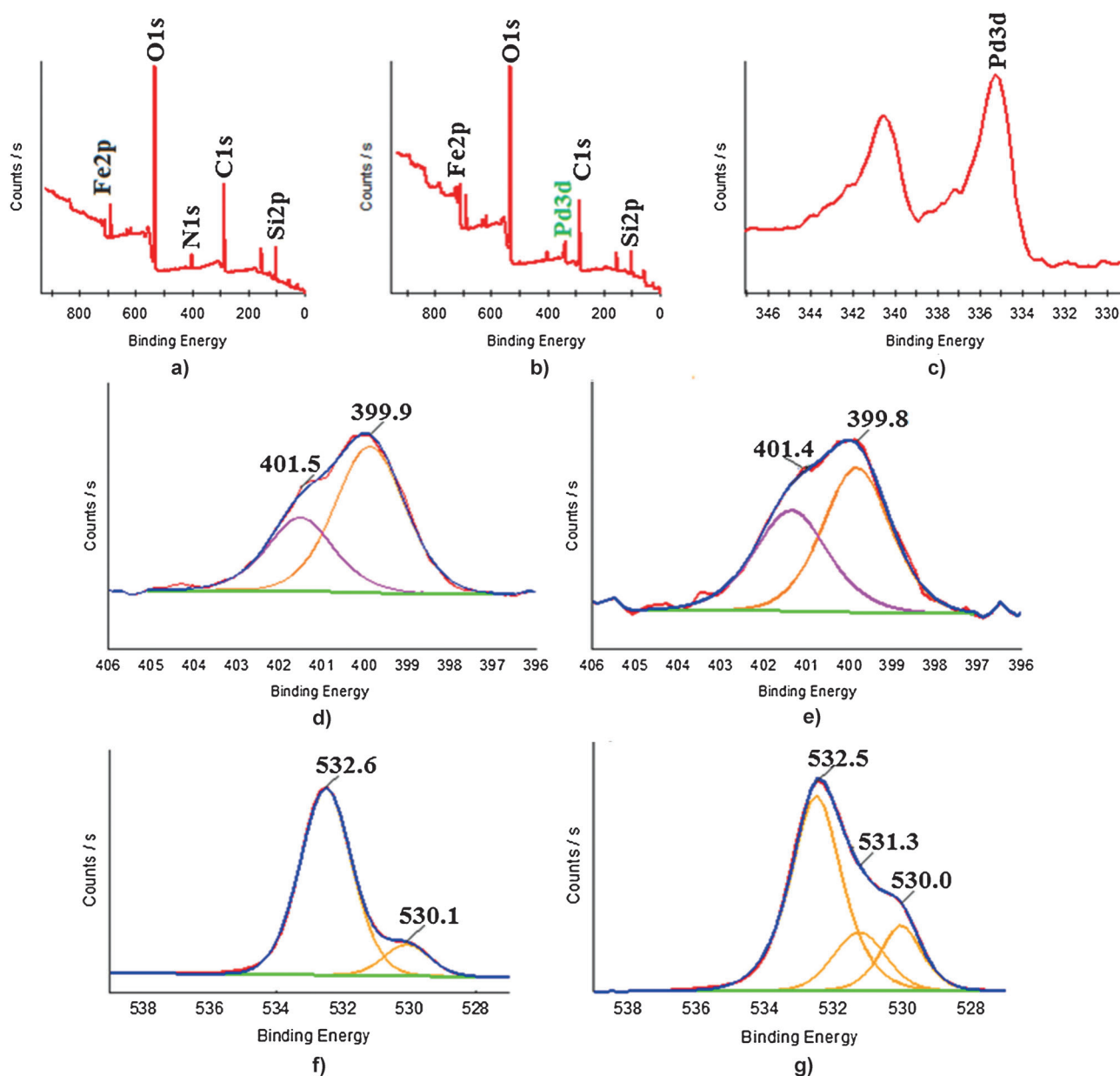


Figure 6. XPS spectra of a) full spectrum of MNP9, b) full spectrum of MNP9–PdNPs, and c) Pd3d in MNP9–PdNPs; d) curve fitting of N1s region in the XPS spectrum of MNP9; e) curve fitting of N1s region in the XPS spectrum of MNP9–PdNPs; f) curve fitting of O1s region in the XPS spectrum of MNP9; g) curve fitting of O1s region in the XPS spectrum of MNP9–PdNPs.

MNP9–PdNPs, curve fittings of N1s and O1s regions in the XPS spectra of MNP9 and MNP9–PdNPs are produced. Two binding energies of N1s at approximately 410.4 and 399.9 eV are observed in both cases of MNP9 and MNP9–PdNPs (Figure 6d,e). The binding energy at 410.4 eV belongs to more “electron-poor” nitrogen atoms. The comparison shows that there is no real shift of binding energy of N1s with or without PdNPs, and the proportion of binding energy at 410.4 eV increases from 33% to 45% after the deposition of PdNPs. Comparing the curve fitting of O1s region in MNP9 to that in MNP9–PdNPs, a new component at 531.3 eV binding energy appears in MNP9–PdNPs (Figure 6f,g). These changes in N1s and O1s spectra confirm the interaction or proximity between the Pd atoms and the N and O atoms.

We know that in dendrimers containing triazole ligands, these ligands quantitatively coordinate to Pd^{II} according to a 1:1 stoichiometry, which was demonstrated by cyclic voltammetry with ferrocenyltriazole-terminated dendrimers.^[20a] In the case of MNP9–PdNPs the approximate average number of ligands around one iron oxide NP is of the order of 10000. The average number of PdNPs loaded on one iron oxide NP is approximately 3.6 (see calculations in the Supporting Information).

In arene-cored dendrimers, PdNPs are trapped inside dendrimers upon weak interaction with the triazole ligand. We also know that this interaction is weak, because these nitrogen ligands are not π -acceptors for metal(0), and indeed triazole ligands are very easily displaced from the PdNP surface, for instance in metal-surface catalysis of nitrophenol reduction. In the present case, the SiOH groups of the silica core are a dense assembly of ligands for PdNP stabilization, which has already been suggested. The HRTEM pictures (Figures 2c and 5c) clearly show PdNPs sitting on the silica surface. Thus it is believed that the PdNPs are stabilized on the silica surface on one (inner) side and by back-folding triazole ligands on the other (outer) side (Figure 7),^[22] and the above-mentioned results of XPS analysis also provide evidence for this hypothesis. Indeed the silica core–triazole ligand distance is adequate for

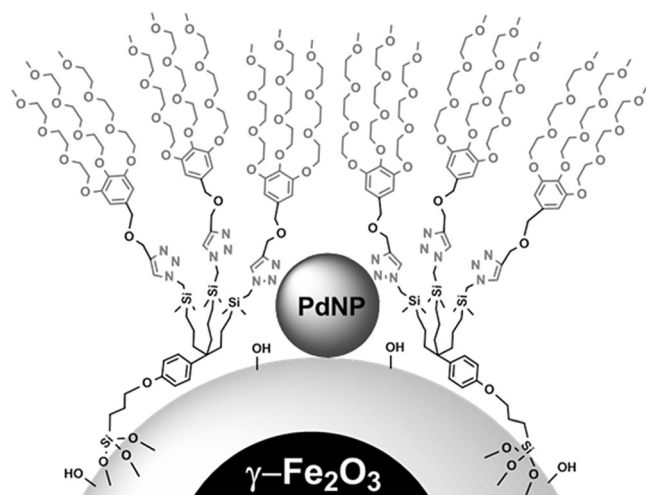


Figure 7. Proposed structure of MNP9–PdNPs.

such stabilization. In this way, the stabilization of the PdNPs is strengthened, but it also leaves the outer surface available for easy triazole displacement by substrates in catalysis experiments.

Investigation of the activities, recyclabilities, and substrate scope of MNP–PdNPs in the Suzuki–Miyaura reaction

The Pd-catalyzed Suzuki–Miyaura reactions for the construction of C–C bonds are crucial in modern chemical transformations involving the syntheses of pharmaceuticals, functional materials, and natural compounds. The catalytic activities of these MNP–PdNPs were evaluated in Suzuki–Miyaura reactions using bromobenzene and phenylboronic acid as model substrates. In these preliminary experiments, MNP9–PdNPs was chosen as the catalyst for optimizing investigations that were first conducted in aqueous media (mixture of EtOH and H₂O) with various catalytic amount of [Pd], using K₂CO₃ as a base at 80 °C under nitrogen atmosphere (Table 2). Increasing yields of the desired biphenyl product were observed with increasing catalytic amounts, in the range of 0.063–0.315 mol%. The reaction reached a yield of 91%, using 0.315 mol% of [Pd] (corresponding to 15 mg of MNP9–PdNPs), within 24 h. Attempts involving the replacement of K₂CO₃ by others bases including Na₂CO₃, KOH, and K₃PO₄, decrease of the reaction temperature, or reduction the reaction time caused lower yields (Table 2).

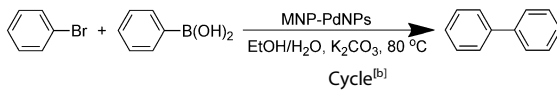
The recyclability, a key issue of heterogeneous catalysts from both the practical and environment points of view, was tested

Table 2. Optimization of the Suzuki–Miyaura reaction between bromobenzene and phenylboronic acid using MNP9–PdNPs as catalyst.^[a]

Entry	Amount [mol %]	Solvent (mL)	Base	Temperature [°C]	Time [h]	Yield ^[c] [%]
1	0.063	EtOH/H ₂ O (10:10)	K ₂ CO ₃	80	24	31
2	0.189	EtOH/H ₂ O (10:10)	K ₂ CO ₃	80	24	63
3	0.315 ^[b]	EtOH/H ₂ O (10:10)	K ₂ CO ₃	80	24	91
4	0.625	EtOH/H ₂ O (10:10)	K ₂ CO ₃	80	24	93
5	0.315	EtOH/H ₂ O (10:10)	K ₂ CO ₃	45	24	45
6	0.315	EtOH/H ₂ O (10:10)	K ₂ CO ₃	80	2	34
7	0.315	EtOH/H ₂ O (10:10)	K ₂ CO ₃	80	10	66
8	0.315	EtOH/H ₂ O (3:3)	K ₂ CO ₃	80	24	80
9	0.315	EtOH/H ₂ O (10:10)	Na ₂ CO ₃	80	24	79
10	0.315	EtOH/H ₂ O (10:10)	KOH	80	24	64
11	0.315	EtOH/H ₂ O (10:10)	K ₃ PO ₄	80	24	72

[a] The reaction was carried out with bromobenzene (1 mmol) and phenylboronic acid (1.5 mmol) in the presence of the catalyst MNP9–PdNPs and base (2 equiv) in EtOH/H₂O under a nitrogen atmosphere; [b] 15 mg of MNP9–PdNPs; [c] yields of product isolated by column chromatography.

Table 3. Investigation of the recyclabilities of MNP–PdNPs in the Suzuki–Miyaura reaction between bromobenzene and phenylboronic acid.^[a]

										
	1	2	3	4	5	6	7	8	9	10
MNP 2–PdNPs	80	62	25							
MNP 4–PdNPs	82	82	66	35						
MNP 6–PdNPs	87	87	83	83	40					
MNP 9–PdNPs	91	91	89	89	88	87	87	87	80	69

[a] The reaction was carried out with bromobenzene (1 mmol) and phenylboronic acid (1.5 mmol) in the presence of the catalyst MNP–PdNPs (0.315 mol %) and K₂CO₃ (2 equiv) under a nitrogen atmosphere for 24 h; [b] yields [% ± 2%] of isolated product for each cycle.

for all MNP–PdNPs under optimized conditions. As shown in Table 3, the reactions catalyzed by MNP 2–PdNPs and MNP 4–PdNPs containing linear ligands were smoothly performed with 0.315 mol % of [Pd], and the biphenyl product was isolated in 80% and 82% yields, respectively. Then, these two catalysts were readily separated from the reaction medium using an external magnet and reused for the next cycles (see the Supporting Information, Figure S4c). An obvious decrease in activity was found in the second and third reaction cycles (Table 3). MNP 6–PdNPs bearing monotriazole Percec-type dendron, however, showed a good catalytic performance in terms of activity and recyclability. The magnetically recoverable catalyst produced a yield of 87% in the first run and maintained a similar activity in the next three cycles. Interestingly, MNP 9–PdNPs containing tris-triazole dendrons were a superior catalyst. Remarkably, its catalytic activity did not deteriorate during 8 successive runs affording yields of 87–91%, a steady loss of activity only being detected from the ninth cycle (Table 3). The TEM analysis of the recovered catalyst revealed that the size and morphology of both MNP 9–PdNPs and the corresponding PdNPs after 8 cycles did not change (Figure 2d). ICP analysis indicated that only 0.24 and 0.95 ppm Pd leached out from the initial MNP 9–PdNPs catalyst after the first and the eighth cycles respectively, which implied that MNP 9–PdNPs was highly stable. In addition, MNP 9–PdNPs maintained the same catalytic activity for months following storage at RT in air.

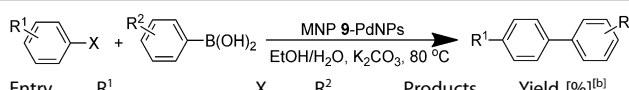
In the case of the Suzuki–Miyaura reactions, the comparison among these MNP–PdNPs catalysts clearly indicated positive dendritic effects regarding both activity and recyclability, in particular regarding recyclability issue. The improved catalytic performance seemingly benefited from the presence of the dendritic framework that efficiently stabilized the PdNP and played a crucial role as a barrier to inhibit the release of the PdNP or part of it from the MNP support.

To check whether the catalytic activity originated from the immobilized PdNPs or from leached Pd, a control experiment was performed. Therefore the Suzuki–Miyaura reaction between bromobenzene and phenylboronic acid in the presence of MNP 9–PdNPs was allowed to proceed for 2 h under the optimized conditions providing the desired cross-coupling product in 34% yield. Subsequently, the catalyst was magnetically

separated at 80 °C; the remaining reaction solution was transferred to another Schlenk flask and was stirred again for another 22 h. Then the biphenyl product was isolated in 36% yield, which showed that almost no yield increase had occurred after removing the immobilized PdNP catalyst. The result of the hot magnetic separation experiment^[23] confirms the heterogeneous nature of the catalyst.

Encouraged by the efficiency of the reaction protocol described above, the scope of the Suzuki–Miyaura reaction was examined with MNP 9–PdNPs (0.315 mol % of [Pd]) in the mixture of EtOH and H₂O under nitrogen atmosphere at 80 °C (Table 4). A series of bromobenzenes bearing various substitu-

Table 4. Investigation of the substrate scope in the presence of MNP–PdNPs in the Suzuki–Miyaura reaction.^[a]

						
Entry	R ¹	X	R ²	Products	Yield [%] ^[b]	
1	H	Br	H	11 a	91	
2	4-NO ₂	Br	H	11 b	92	
3	4-CHO	Br	H	11 c	94	
4	4-CH ₃ CO	Br	H	11 d	94	
5	4-CH ₃ CH ₂ OCO	Br	H	11 e	83	
6	4-NH ₂	Br	H	11 f	89	
7	4-CH ₃ O	Br	H	11 g	92	
8	4-CH ₃	Br	H	11 h	90	
9	2,4,6-TrisCH ₃	Br	H	11 i	91 ^[c]	
10	H	Br	4-CH ₃	11 j	89	
11	H	Br	2-CH ₃	11 k	74	
12	4-NO ₂	Cl	H	11 b	88 ^[d]	
13	H	Cl	H	11 a	49 ^[e]	

[a] The reaction was carried out with bromobenzene (1 mmol) and phenylboronic acid (1.5 mmol) in the presence of catalyst MNP 9–PdNPs (0.315 mol %) and K₂CO₃ (2 equiv) in EtOH/H₂O (10 mL/10 mL) under a nitrogen atmosphere for 24 h; [b] yields of isolated product; [c] the reaction time is 86 h; [d] the reaction was carried out in the presence of 1 mol % of [Pd] for 72 h; [e] the reaction was carried out in the presence of 1.5 mol % of [Pd] for 72 h.

ents were tested in reactions with phenylboronic acid. Bromobenzenes containing electron-withdrawing (NO₂, CHO, CH₃CO, CH₃CH₂OCO) and electron-donating (NH₂, CHO, CH₃) groups in the *para* position were suitable coupling partners, and the corresponding coupling products (**11 b–h**) were efficiently synthesized in 83–94% yields. No direct correlation could be drawn between the outcome and the electronic nature of bromobenzene substituents. The challenging reaction with 2,4,6-trimethyl bromobenzene generated the corresponding product in 91% yield (Table 4, entry 9). Substituted arylboronic acids were also investigated, and they all reacted smoothly with bromobenzene to provide the desired products in good yields (Table 4, entries 10, 11). Moreover, the reaction of 4-nitrochlorobenzene smoothly proceeded with 1 mol % of MNP 9–PdNPs, producing the corresponding coupling product in 88% yield (Table 4, entry 12); when the unactivated chlorobenzene was employed in the reaction, in the presence of 2 mol % of [Pd], within 72 h the corresponding product biphenyl was obtained in 49% yield (Table 4, entry 13).

Investigation of the activities and recyclabilities of MNP-PdNPs in the Sonogashira and Heck reactions

The Sonogashira and Heck coupling reactions are also two common strategies of C–C bonds construction, respectively forming conjugated compounds and arylated olefins. MNP 2-PdNPs, MNP 6-PdNPs and MNP 9-PdNPs were all used as catalysts in both Sonogashira and Heck reactions.

The Sonogashira reaction of iodobenzene and phenylacetylene was chosen to test the recyclability of the MNP-PdNPs bearing linear or dendritic PEGylated triazolyl ligands. The reactions were performed with 1.5 mol% of [Pd] using Et₃N as base in THF at 65 °C for 24 h. After each reaction cycle, the catalyst was separated from the reaction mixture using a magnet and successively washed with CH₂Cl₂ and acetone and then re-used in a subsequent run. The yields of the first reaction cycle catalyzed by MNP 2-PdNPs, MNP 6-PdNPs, and MNP 9-PdNPs were 78%, 82%, and 85%, respectively (Table 5). The recyclability re-

Table 5. Investigation of the recyclabilities of MNP-PdNPs in the Sonogashira reaction between iodobenzene and phenylacetylene.^[a]

	Cycle ^[b]						
	1	2	3	4	5	6	7
MNP 2-PdNPs	78	65					
MNP 6-PdNPs	82	80	79	63			
MNP 9-PdNPs	85	83	83	81	80	80	75

[a] The reaction was carried out with iodobenzene (1 mmol), phenylacetylene (1.2 mmol) in the presence of catalysts MNP-PdNPs (1.5 mol%) and Et₃N (2 equiv) in THF (5 mL) at 65 °C under a nitrogen atmosphere for 24 h; [b] yields [% ± 2%] of isolated product for each cycle.

sults showed that an obvious loss in activity of MNP 2-PdNPs bearing linear PEG550-triazole ligand occurred in the second run; MNP 6-PdNPs with the small dendron could be easily recycled three times with slight loss of catalytic activity. It is particularly gratifying, however, that MNP 9-PdNPs containing dendritic tris-triazole ligands maintained almost the same catalytic activity from the first to the sixth cycle. The results in Table 5 show that the catalytic recyclability was significantly influenced by the structure of PEGylated triazolyl ligands, the dendritic frame greatly improving the recyclability.

The recyclability test of MNP 2-PdNPs, MNP 6-PdNPs, and MNP 9-PdNPs was also carried out for the Heck cross-coupling reaction of iodobenzene with styrene utilizing 1.5 mol% of [Pd] and 2 equiv of K₂CO₃ at 120 °C in DMF (Table 6). The desired (*E*)-1,2-diphenylethene was isolated in good yields and 100% selectivity in the first run in all cases with these MNP-PdNPs. A superior activity and recyclability were also found with increase of the dendritic grade of ligands around the MNPs (Table 6). The recycling performances of these MNP-PdNPs in the Heck reaction were generally not as good as those obtained for both Suzuki and Sonogashira reactions, which was caused by the harsher conditions of the Heck reac-

Table 6. Investigation of the recyclabilities of MNP-PdNPs in the Heck reaction between iodobenzene and styrene.^[a]

	Cycle ^[b]				
	1	2	3	4	5
MNP 2-PdNPs	73	36			
MNP 6-PdNPs	81	77	57		
MNP 9-PdNPs	85	84	84	82	74

[a] The reaction was carried out with iodobenzene (0.6 mmol), styrene (0.5 mmol) in the presence of the catalyst MNP-PdNPs (1.5 mol%) and K₂CO₃ (2 equiv) in DMF (5 mL) at 120 °C under a nitrogen atmosphere for 24 h; [b] yields [% ± 2%] of isolated product for each cycle.

tion. Nevertheless, the recyclability was good again with MNP 9-PdNPs and much superior to those of the other catalysts, showing another dramatically positive dendritic effect.

Syntheses of pharmacologically relevant or natural products based on Suzuki–Miyaura, Sonogashira, and Heck reactions

The synthesis of pharmacologically interesting or natural products is one of the most important applications of C–C coupling reactions. The impressive ability of Pd catalysts to create C–C bonds provides many new avenues for designing medicinal candidates.

Inspired by its high efficiency, excellent recyclability, negligible Pd leaching, and the biocompatibility of iron, MNP 9-PdNPs was utilized in the syntheses of pharmacologically important or natural products through Suzuki–Miyaura, Sonogashira, and Heck reactions (Figure 8).

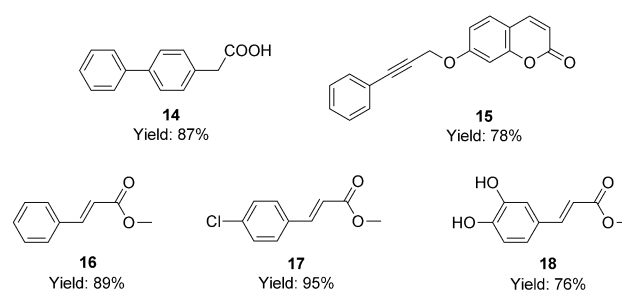


Figure 8. Pharmacologically relevant or natural products synthesized by using MNP 9-PdNPs as catalyst.

Felbinac **14**, a commercial nonsteroidal anti-inflammatory drug, is used to treat arthritis and inflammation.^[24] The Suzuki reaction of 4-bromophenylacetic acid with phenylboronic acid was smoothly conducted, using MNP 9-PdNPs as catalyst under the optimized conditions, providing Felbinac in 87% yield. Coumarin (*2H*-chromen-2-one) is a naturally occurring constituent of many plants and essential oils. Coumarin and its derivatives have been proved to be useful for treating various ailments, including cancer, spasms, brucellosis, burns, and rheumatic disease.^[25] The internal alkyne **15**, containing cou-

marin fragment, was synthesized with 78% yield through Sonogashira reaction between ethyne-functionalized coumarin and iodobenzene in the presence of 1.5 mol% of [Pd] and 1 equivalent of Et₃N at 40 °C. Diverse derivatives of cinnamic acid possess various pharmacological activities.^[26] For example, methyl cinnamate **16** is used as a flavoring agent and a composition of soap; methyl 4-chlorocinnamate **17** has antifungal activity; methyl caffeate **18** exhibits antitumor activity against Sarcoma 180, as well as antimicrobial activity. Heck reactions involving these corresponding aromatic iodides and methyl acrylate were carried out under optimal conditions. Compounds **16**, **17**, and **18** were successfully isolated with 76–95% yield and almost 100% selectivity.

Conclusion

The investigation of catalyst engineering around a MNP has led to disclose favorable dendritic loading according to a divergent synthesis compared to that by grafting of pre-synthesized units, which represents a new kind of positive dendritic effect. Other design features that have involved TEG termini and click syntheses were also favorable because of the advantageous NP dispersity and Pd^{II} binding, respectively, leading upon reduction to efficient 3 nm-sized PdNPs in the γ -Fe₂O₃-Pd catalysts. MNP **6**-PdNPs and MNP **9**-PdNPs containing dendritic frames provided impressive and superior performances concerning both activity and recyclability in Suzuki–Miyaura, Sonogashira, and Heck reactions compared to the linear counterparts in star-shaped MNP catalysts. In particular, MNP **9**-PdNPs, decorated with larger dendrons containing tris-triazole groups, showed the best catalytic results among these catalysts. In addition, in the case of MNP **9**-PdNPs-catalyzed Suzuki–Miyaura reactions, ICP analysis revealed that the amount of Pd leached from the initial catalyst is negligible after 8 cycles. Finally, the morphology and size of MNP **9**-PdNPs did not significantly vary over time.

A new lesson regarding the design and engineering of catalysts deposited on MNPs is that MNPs decorated with dendritic frame are clearly favorable concerning the goal of efficiency for practical and environmentally friendly reactions. Indeed, it is impressive that MNP **9**-PdNPs remains stable for months in air and is recyclable many times without significant yield decrease or morphology/size change, which is attributed to the barrier formed by the dendritic frame at the dendrimer periphery that protects the intradendritic PdNP catalyst. The principles and results presented here should thus open a gate for more applications of MNPs–Den–NPs catalysts in “green” chemistry.

Experimental Section

Synthesis of γ -Fe₂O₃@SiO₂ nanoparticles:^[27] Nitrogen-purged 2-propanol (20 mL) was added into a dried Schlenk tube containing ferric chloride (0.5 g, 3.08 mmol) and ferrous chloride (0.25 g, 1.97 mmol). After 15 min of stirring, the temperature of the solution was raised to 80 °C, and aqueous NH₃ (10 mL) was slowly added. The stirring was continued for another 2 h. The γ -Fe₂O₃

nanoparticles formed were protected by the addition of 10 mM oleic acid in methanol (30 mL), removed from the solution using an external magnet, washed with methanol (20 mL), and then re-dispersed in ethanol (20 mL). 2 g of a suspension of γ -Fe₂O₃ in ethanol was diluted with deionized water (4 mL) and 2-propanol (20 mL), and the mixture was sonicated for approximately 15 min. To this well-dispersed solution, aqueous NH₃ (1 mL) followed by tetraethoxysilane (1 g) were slowly added and stirred for further 4 h at RT. The obtained γ -Fe₂O₃@SiO₂ NPs were then separated by centrifugation and redispersed in deionized water.

Synthesis of iron oxide nanoparticle-immobilized PEGylated triazolyl ligand **2**.

Route A: Under an atmosphere of nitrogen, **1** (0.3 g, 0.36 mmol) in anhydrous CH₂Cl₂ (2 mL) was added to a suspension of MNPs SiO₂/ γ -Fe₂O₃ (0.3 g) in anhydrous toluene (30 mL). The mixture was then stirred at 110 °C under nitrogen atmosphere for 36 h. The dark brown solid material obtained was magnetically separated, washed repeatedly with toluene (2 × 10 mL), CH₂Cl₂ (10 mL), diluted aqueous solution of ammonia (until there is no blue color in the solution),^[17b] H₂O (2 × 20 mL), and acetone (2 × 10 mL) to remove any unanchored species and then dried in vacuo.

Route B: Compound PEG550 alkyne (0.64 g, 1.12 mmol) and 3-azidopropyltriethoxysilane-functionalized MNP **3** (1 g) were mixed with CuI (8 mg, 4.17 × 10⁻² mmol), in DMF/THF (1:1, 40 mL) under nitrogen. *N,N*-Diisopropylethylamine (2 mL) was injected into the mixture that was then stirred at RT for 36 h. The reaction was monitored by FT-IR for the almost complete disappearance of the IR signal of 2104 cm⁻¹ corresponding to the azide group. Then the mixture was submitted to magnetic separation, and the MNPs were washed sequentially with DMF (20 mL), THF (20 mL), CH₂Cl₂ (20 mL), diluted aqueous solution of ammonia (until there is no blue color in the solution),^[17b] H₂O (2 × 20 mL), and acetone (20 mL), and finally dried in vacuo.

Synthesis of iron oxide nanoparticle-immobilized PEGylated triazolyl ligand **4:** The synthesis was conducted as for the ligand **2** following route B, except that PEG550 alkyne was replaced by PEG2000 alkyne.

Synthesis of iron oxide nanoparticle-immobilized dendritic mono-triazole ligand **6:** The synthesis was carried out as for the ligand **2** following route B, except that PEG550 alkyne was replaced by Percec-type dendron **5**.

Synthesis of iron oxide nanoparticles-immobilized dendritic azide **8:** In a dried Schlenk tube, a mixture of 3-iodopropyltriethoxysilane-functionalized MNP (0.5 g), dendron **7** (350 mg, 0.61 mmol), and K₂CO₃ (0.8 g) in anhydrous DMF (40 mL) was sonicated for approximately 15 min and stirred at 80 °C under nitrogen for 48 h. Then, the mixture was submitted to magnetic separation, and the MNPs were washed sequentially with DMF (20 mL), CH₂Cl₂ (20 mL), saturated aqueous solution of Na₂S₂O₃ (2 × 20 mL), H₂O (3 × 20 mL), and acetone (2 × 20 mL), and finally dried in vacuo.

Synthesis of iron oxide nanoparticle-immobilized dendritic tris-triazole ligand **9 through the divergent synthesis method:** MNP **8** (0.5 g) and Percec-type dendron **5** (455 mg, 0.72 mmol) were mixed with CuI (8 mg, 4.17 × 10⁻² mmol) in DMF/THF (1:1, 20 mL) under nitrogen. *N,N*-Diisopropylethylamine (2 mL) was injected into the mixture, which was then sonicated for approximately 15 min and stirred at RT for 36 h. The reaction was monitored by FT-IR for the almost complete disappearance of the IR signal of 2102 cm⁻¹ corresponding to the azide group. Then the mixture was submitted to magnetic separation, and the MNPs were washed sequentially with DMF (10 mL), THF (10 mL), CH₂Cl₂

(10 mL), H₂O (2 × 10 mL), and acetone (10 mL), and finally dried in vacuo.

Synthesis of iron oxide nanoparticle-immobilized dendritic triazole ligand 9 by grafting of pre-synthesized dendron: The synthesis was carried out as for the synthesis of MNPs 8 except that dendron 7 was replaced by dendron 10.

Synthesis of iron oxide nanoparticle-immobilized PdNPs (taking MNP9–PdNPs as an example): In a Schlenk flask, the suspension of MNP 9 (200 mg, 0.126 mmol triazole) in H₂O (15 mL) was sonicated for approximately 10 min under nitrogen. Then, an orange solution of K₂PdCl₄ (82 mg, 0.252 mmol, 2 equiv per triazole) in Milli-Q H₂O (15 mL) was added to the Schlenk flask. The mixture was stirred at RT for 2 h, then submitted to magnetic separation, and the MNPs were washed with Milli-Q H₂O (10 mL) under nitrogen. After the addition of Milli-Q H₂O (20 mL), 10 mL a solution of NaBH₄ (1.26 mmol) in water (10 mL) was injected. The mixture was stirred at RT for 2 h and the color of the mixture changed to black from brown, which indicated the reduction of Pd²⁺ to Pd⁰ and PdNP formation. The mixture was submitted to magnetic separation, and the MNPs were washed with Milli-Q H₂O (2 × 10 mL) and acetone (10 mL) under nitrogen, and the catalyst was dried at 45 °C for at least 4 h in vacuo and stored under nitrogen before use.

Acknowledgements

Financial support from the China Scholarship Council (CSC) of the People's Republic of China (Ph. D. grant to D.W.), the MRT (PhD grant to C.D.), the Universities of Bordeaux and Toulouse 3, the Centre National de la Recherche Scientifique (CNRS), and L'Oréal are gratefully acknowledged.

Keywords: C–C coupling · dendrimers · heterogeneous catalysis · magnetic nanoparticles · palladium

- [1] a) P. T. Anastas, J. C. Warner, *Green Chemistry: Theory and Practice*, Oxford University Press, New York, **1998**; b) M. Doble, A. K. Kruthivent, *Green Chemistry and Engineering*, Academic Press, London, **2007**; c) S. K. Sharma, A. Mudhoo, *Green Chemistry for Environmental Sustainability*, CRC Press, Boca Raton, FL, USA, **2010**.
- [2] a) G. A. Somorjai, *Introduction to Surface Chemistry and Catalysis*, Wiley, New York, **1994**; b) A. Corma, *Chem. Rev.* **1995**, *95*, 559–614; c) M. Haruta, *Catal. Today* **1997**, *36*, 153–166; d) *Handbook of Heterogeneous Catalysis* (Eds.: G. Ertl, H. Knozinger, J. Weitkamp), Wiley-VCH, Weinheim, Germany, **1997**; e) A. Corma, *Chem. Rev.* **1997**, *97*, 2373–2419; f) M. Haruta, M. Date, *Appl. Catal. A* **2001**, *222*, 427–437; g) *Modern Surface Organometallic Chemistry* (Eds.: J.-M. Basset, R. Psaro, D. Roberto, R. Ugo), Wiley-VCH, Weinheim, **2009**; h) A. Corma, H. García, F. X. Llabrés i Xamena, *Chem. Rev.* **2010**, *110*, 4606–4655.
- [3] a) I. P. Beletskaya, A. V. Cheprakov, *Chem. Rev.* **2000**, *100*, 3009–3066; b) F. Lu, J. Ruiz, D. Astruc, *Tetrahedron Lett.* **2004**, *45*, 9443–9445; c) C. Burda, X. Chen, R. Narayanan, M. A. El-Sayed, *Chem. Rev.* **2005**, *105*, 1025–1102; d) D. Astruc, F. Lu, J. Ruiz, *Angew. Chem. Int. Ed.* **2005**, *44*, 7852–7872; *Angew. Chem.* **2005**, *117*, 8062–8083; e) *Nanoparticles and Catalysis* (Ed.: D. Astruc), Wiley-VCH, Weinheim, **2008**; f) P. Chen, X. Zhou, H. Shen, N. M. Andoy, E. Choudhary, K.-S. Han, G. Liu, W. Meng, *Chem. Soc. Rev.* **2010**, *39*, 4560–4570; g) A. Molnár, *Chem. Rev.* **2011**, *111*, 2251–2320; h) J. E. Mondloch, E. Bayram, R. G. Finke, *J. Mol. Catal. A* **2012**, *355*, 1–38; i) L. M. Bronstein, Z. B. Shifrina, *Chem. Rev.* **2011**, *111*, 5301–5344; j) C. Bai, M. Liu, *Nano Today* **2012**, *7*, 258–281; k) *Nanomaterials and Catalysis* (Eds.: P. Serp, K. Philippot), Wiley-VCH, Weinheim, **2013**.
- [4] a) A. H. Lu, E. L. Salabas, F. Schüth, *Angew. Chem. Int. Ed.* **2007**, *46*, 1222–1244; *Angew. Chem.* **2007**, *119*, 1242–1266; b) S. Shylesh, V. Schü-
- nemann, W. R. Thiel, *Angew. Chem. Int. Ed.* **2010**, *49*, 3428–3459; *Angew. Chem.* **2010**, *122*, 3504–3537; c) Y. Zhu, L. P. Stubbs, F. Ho, R. Liu, C. P. Ship, J. A. Maguire, N. S. Hosmane, *ChemCatChem* **2010**, *2*, 365–374; d) V. Polshettiwar, R. Luque, A. Fihri, H. Zhu, M. Bouhrara, J. M. Basset, *Chem. Rev.* **2011**, *111*, 3036–3075; e) Q. M. Kainz, O. Reiser, *Acc. Chem. Res.* **2014**, *47*, 667–677; f) D. Wang, D. Astruc, *Molecules* **2014**, *19*, 4635–4653; g) D. Wang, D. Astruc, *Chem. Rev.* **2014**, *114*, 6949–6985.
- [5] a) G. R. Newkome, E. He, C. N. Moorefield, *Chem. Rev.* **1999**, *99*, 1689–1746; b) D. Astruc, F. Chardac, *Chem. Rev.* **2001**, *101*, 2991–3023; c) R. van Heerbeek, P. C. J. Kamer, P. W. N. M. van Leeuwen, J. N. H. Reek, *Chem. Rev.* **2002**, *102*, 3717–3756; d) L. J. Twyman, A. S. H. King, I. K. Martin, *Chem. Soc. Rev.* **2002**, *31*, 69–82; e) B. Helms, J. M. J. Fréchet, *Adv. Synth. Catal.* **2006**, *348*, 1125–1148; f) E. de Jesús, J. C. Flores, *Ind. Eng. Chem. Res.* **2008**, *47*, 7968–7981; g) D. Astruc, E. Boisselier, C. Ornelas, *Chem. Rev.* **2010**, *110*, 1857–1959; h) D. Astruc, *Nat. Chem.* **2012**, *4*, 255–267; i) A. M. Caminade, A. Ouali, M. Keller, J. P. Majoral, *Chem. Soc. Rev.* **2012**, *41*, 4113–4125; j) D. Wang, D. Astruc, *Coord. Chem. Rev.* **2013**, *257*, 2317–2334.
- [6] M. E. Piotti, F. Rivero, R. Bond, C. J. Hawker, J. M. J. Fréchet, *J. Am. Chem. Soc.* **1999**, *121*, 9471–9472.
- [7] J. M. J. Fréchet, *J. Polym. Sci. Part A* **2003**, *41*, 3713–3725.
- [8] B. Helms, C. O. Liang, C. J. Hawker, J. M. J. Fréchet, *Macromolecules* **2005**, *38*, 5411–5415.
- [9] M. Sowinska, Z. Urbanczyk-Lipkowska, *New J. Chem.* **2014**, *38*, 2168–2203.
- [10] a) L. Balogh, D. A. Tomalia, *J. Am. Chem. Soc.* **1998**, *120*, 7355–7356; b) R. M. Crooks, M. Zhao, L. Sun, V. Chechik, L. K. Yeung, *Acc. Chem. Res.* **2001**, *34*, 181–190; c) L. K. Yeung, R. M. Crooks, *Nano Lett.* **2001**, *1*, 14–17; d) E. H. Rahim, F. S. Kamounah, J. Frederiksen, J. B. Christensen, *Nano Lett.* **2001**, *1*, 499–503; e) N. Satoh, J. S. Cho, M. Higushi, K. Yamamoto, *J. Am. Chem. Soc.* **2003**, *125*, 8104–8105; f) R. W. J. Scott, A. K. Datye, R. M. Crooks, *J. Am. Chem. Soc.* **2003**, *125*, 3708–3709; g) R. W. Scott, O. M. Wilson, S.-K. Oh, E. A. Kenik, R. M. Crooks, *J. Am. Chem. Soc.* **2004**, *126*, 15583–15591; h) M. Ooe, M. Murata, T. Mizugaki, K. Ebitani, *J. Am. Chem. Soc.* **2004**, *126*, 1604–1608; i) O. M. Wilson, R. W. J. Scott, J. C. Garcia-Martinez, R. M. Crooks, *J. Am. Chem. Soc.* **2005**, *127*, 1015–1024; j) R. W. J. Scott, C. Sivadirananarayana, O. M. Wilson, Z. Yan, D. W. Goodman, R. M. Crooks, *J. Am. Chem. Soc.* **2005**, *127*, 1380–1381; k) M. V. Gómez, J. Guerra, A. H. Velders, R. M. Crooks, *J. Am. Chem. Soc.* **2008**, *130*, 341–350; l) C. Deraedt, D. Astruc, *Acc. Chem. Res.* **2014**, *47*, 494–503.
- [11] a) M. Zhao, L. Sun, R. M. Crooks, *J. Am. Chem. Soc.* **1998**, *120*, 4877–4878; b) M. Zhao, R. M. Crooks, *Angew. Chem. Int. Ed.* **1999**, *38*, 364–366; *Angew. Chem.* **1999**, *111*, 375–377; c) V. S. Myers, M. W. Weier, E. V. Carino, D. F. Yancey, S. Pande, R. M. Crooks, *Chem. Sci.* **2011**, *2*, 1632–1646.
- [12] a) D. A. Tomalia, H. Baker, J. Dewald, M. Hall, G. Kallos, S. Martin, J. Roeck, J. Ryder, P. Smith, *Polym. J.* **1985**, *17*, 117–132; b) D. A. Tomalia, A. M. Naylor, W. Goddard III, *Angew. Chem. Int. Ed. Engl.* **1990**, *29*, 138–175; *Angew. Chem.* **1990**, *102*, 119–157.
- [13] a) E. M. M. de Brabander-van den Berg, E. W. Meijer, *Angew. Chem. Int. Ed. Engl.* **1993**, *32*, 1308–1311; *Angew. Chem.* **1993**, *105*, 1370–1372; b) A. W. Bosman, H. M. Janssen, E. W. Meijer, *Chem. Rev.* **1999**, *99*, 1665–1688.
- [14] a) M. Higuchi, S. Shiki, S. Ariga, K. Yamamoto, *J. Am. Chem. Soc.* **2001**, *123*, 4414–4420; b) K. Yamamoto, M. Higushi, S. Shiki, M. Tsuruta, H. Chiba, *Nature* **2002**, *415*, 509–511; c) N. Satoh, T. Nakashima, K. Kamikura, K. Yamamoto, *Nat. Nanotechnol.* **2008**, *3*, 106–111.
- [15] a) V. Percec, G. Johansson, G. Ungar, J. Zhou, *J. Am. Chem. Soc.* **1996**, *118*, 9855–9866; b) V. S. K. Balagurusamy, G. Ungar, V. Percec, G. Johansson, *J. Am. Chem. Soc.* **1997**, *119*, 1539–1555; c) V. Percec, M. Peterca, A. E. Dulcey, M. R. Imam, S. D. Hudson, S. Nummelin, P. Adelman, P. A. Heiney, *J. Am. Chem. Soc.* **2008**, *130*, 13079–13094.
- [16] a) G. R. Newkome, Z. Yao, G. R. Baker, V. K. Gupta, *J. Org. Chem.* **1985**, *50*, 2003–2004; b) G. R. Newkome, C. N. Moorefield, *Aldrichimica Acta* **1992**, *25*, 31–38; c) G. R. Newkome, *Pure Appl. Chem.* **1998**, *70*, 2337–2343; d) G. R. Newkome, C. Shreiner, *Chem. Rev.* **2010**, *110*, 6338–6442; e) F. Moulines, D. Astruc, *Angew. Chem. Int. Ed. Engl.* **1988**, *27*, 1347–1349; *Angew. Chem.* **1988**, *100*, 1394–1396; f) F. Moulines, L. Djakovitch, R. Boese, B. Gloaguen, W. Thiel, J.-L. Fillaut, M.-H. Delville, D. Astruc,

- Angew. Chem. Int. Ed. Engl.* **1993**, *32*, 1075–1077; *Angew. Chem.* **1993**, *105*, 1132–1134.
- [17] a) E. Boisselier, A. K. Diallo, L. Salmon, C. Ornelas, J. Ruiz, D. Astruc, *J. Am. Chem. Soc.* **2010**, *132*, 2729–2742; b) C. Deraedt, L. Salmon, D. Astruc, *Adv. Synth. Catal.* **2014**, *356*, 2525–2536; c) C. Deraedt, N. Pinaud, D. Astruc, *J. Am. Chem. Soc.* **2014**, *136*, 12092–12098.
- [18] a) R. Abu-Reziq, H. Alper, D. Wang, M. L. Post, *J. Am. Chem. Soc.* **2006**, *128*, 5279–5282; b) K. Uzun, E. Çevik, M. Şenel, H. Sözeri, A. Baykal, M. F. Abasiyanik, M. S. Toprak, *J. Nanopart. Res.* **2010**, *12*, 3057–3067; c) C. M. Chou, H. L. Lien, *J. Nanopart. Res.* **2011**, *13*, 2099–2107; d) Q. M. Kainz, A. Schätz, A. Zöpfl, W. J. Stark, O. Reiser, *Chem. Mater.* **2011**, *23*, 3606–3613; e) A. Pourjavadi, S. H. Hosseini, S. T. Hosseini, S. A. Aghayeeimbody, *Catal. Commun.* **2012**, *28*, 86–89; f) H. Wang, B. Shentu, W. Zhang, C. Gu, Z. Weng, *Eur. Polym. J.* **2012**, *48*, 1205–1211; g) N. V. Kuchkina, E. Y. Yuzik-Klimova, S. A. Sorokina, A. S. Peregudov, D. Y. Antonov, S. H. Gage, B. S. Boris, L. Z. Nikoshvili, E. M. Sulman, D. G. Morgan, W. E. Mahmoud, A. A. Al-Ghamdi, L. M. Bronstein, Z. B. Shifrina, *Macromolecules* **2013**, *46*, 5890–5898.
- [19] W. Guo, A. Monge-Marcet, X. Cattoën, A. Shafir, R. Pleixats, *React. Funct. Polym.* **2013**, *73*, 192–199.
- [20] a) C. Ornelas, J. Ruiz, E. Cloutet, S. Alves, D. Astruc, *Angew. Chem. Int. Ed.* **2007**, *46*, 872–877; b) R. Djeda, A. Rapakousiou, L. Liang, N. Guidolin, J. Ruiz, D. Astruc, *Angew. Chem. Int. Ed.* **2010**, *49*, 8152–8156; c) A. Rapakousiou, Y. Wang, C. Belin, N. Pinaud, J. Ruiz, D. Astruc, *Inorg. Chem.* **2013**, *52*, 6685–6693.
- [21] V. V. Rostovtsev, L. G. Green, V. V. Fokin, K. B. Sharpless, *Angew. Chem. Int. Ed.* **2002**, *41*, 2596–2599; *Angew. Chem.* **2002**, *114*, 2708–2711.
- [22] N. J. S. Costa, P. K. Kiyohara, A. L. Monteiro, Y. Coppel, K. Philippot, L. M. Rossi, *J. Catal.* **2010**, *276*, 382–389; b) M. Zhu, G. Diao, *J. Phys. Chem. C* **2011**, *115*, 24743–24749; c) W. Li, B. Zhang, X. Li, H. Zhang, Q. Zhang, *Appl. Catal. A* **2013**, *459*, 65–72; d) J. Wang, B. Xu, H. Sun, G. Song, *Tetrahedron Lett.* **2013**, *54*, 238–241; e) F. González de Rivera, I. Angurell, M. D. Rossell, R. Erni, J. Llorca, N. J. Divins, G. Muller, M. Seco, O. Rossell, *Chem. Eur. J.* **2013**, *19*, 11963–11974; f) M. Beygzadeh, A. Alizadeh, M. M. Khodaei, D. Kordestani, *Catal. Commun.* **2013**, *32*, 86–91.
- [23] a) A. Schätz, T. R. Long, R. N. Grass, W. J. Stark, P. R. Hanson, O. Reiser, *Adv. Funct. Mater.* **2010**, *20*, 4323–4328; b) J. Hu, Y. Wang, M. Han, Y. Zhou, X. Jiang, P. Sun, *Catal. Sci. Technol.* **2012**, *2*, 2332–2340; c) F. González de Rivera, I. Angurell, M. D. Rossell, R. Erni, J. Llorca, N. J. Divins, G. Muller, M. Seco, O. Rossell, *Chem. Eur. J.* **2013**, *19*, 11963–11974; d) Q. Zhang, H. Su, J. Luo, Y. Wei, *Catal. Sci. Technol.* **2013**, *3*, 235–243.
- [24] C. Kohler, E. Tolman, W. Wooding, L. Ellenbogen, *Arzneim.-Forsch.* **1980**, *30*, 702–707.
- [25] D. Egan, R. O’Kennedy, E. Moran, D. Cox, E. Prosser, R. D. Thornes, *Drug. Metab. Rev.* **1990**, *22*, 503–529.
- [26] P. Sharma, *J. Chem. Pharm. Res.* **2011**, *3* (2), 403–423.
- [27] S. Shylesh, L. Wang, W. R. Thiel, *Adv. Synth. Catal.* **2010**, *352*, 425–432.

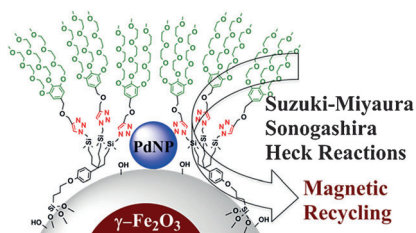
Received: July 25, 2014

Published online on ■ ■ ■ ■, 0000

FULL PAPER

Magnetically recoverable catalysts:

Catalysts comprising dendritic “click” ligands that are immobilized on a magnetic nanoparticle core, terminated by triethylene glycol groups, and incorporate Pd nanoparticles have been prepared and characterized. They are shown to be highly active, dispersible, and magnetically recoverable many times in Suzuki, Sonogashira, and Heck reactions.



Heterogeneous Catalysis

*D. Wang, C. Deraedt, L. Salmon,
C. Labrugère, L. Etienne, J. Ruiz,
D. Astruc**



Efficient and Magnetically Recoverable
“Click” PEGylated $\gamma\text{-Fe}_2\text{O}_3\text{-Pd}$
Nanoparticle Catalysts for Suzuki-
Miyaura, Sonogashira, and Heck
Reactions with Positive Dendritic
Effects

**Partie 6. NaBH₄ réducteur de
précurseurs Pd^{II} et Au^{III} et
stabilisateur de nanoparticules
extrêmement actives en catalyse.**

Partie 6. NaBH₄ réducteur de précurseurs Pd^{II} et Au^{III} et stabilisateur de nanoparticules extrêmement actives en catalyse.

L'utilisation d'un stabilisateur lors de la synthèse de nanoparticules est essentielle. Peu d'exemples dans la littérature décrivent l'utilisation d'une molécule simple jouant le rôle à la fois de réducteur d'ions métallique en nanoparticule et de stabilisateur. L'exemple le plus connu est celui des citrates utilisés lors de la synthèse de AuNPs proposé par Turkevich.⁽¹⁾ Le borohydrure de sodium NaBH₄ est le réducteur le plus utilisé au cours de la synthèse de nanoparticules, mais il est toujours accompagné d'un stabilisateur. On pouvait se demander si NaBH₄ peut aussi jouer un rôle dans la stabilisation ? Au cours de la thèse nous nous sommes rendu compte à plusieurs reprises que certaines de nos nanoparticules (Pd et Au) étaient stables sans rien d'autre que le réducteur NaBH₄. Nous nous sommes alors penché sur le sujet à la fin de la 3^{ème} année de thèse. Nous avons démontré qu'en présence d'une quantité suffisante de NaBH₄ et pour une concentration spécifique de Au(III) (ou Pd(II)) les AuNPs (ou PdNPs) étaient stables dans l'eau pendant plus d'un mois. Ces nanoparticules ont été utilisées en catalyse de réduction du 4-NP et ont présenté une activité inégalée. Ceci a été rationalisé par le fait que cette réaction catalytique a lieu en surface de la nanoparticule et que nos nanoparticules ne présentent aucun encombrement pouvant freiner l'approche du substrat à la surface. Concernant la stabilisation des nanoparticules, il est probable que les ions BH₄⁻ (ou H⁻) accompagnés des ions Cl⁻ viennent se ligander en surface de la nanoparticule.⁽²⁾ La présence d'excès d'eau entraîne l'hydrolyse lente de BH₄⁻ en B(OH)₄⁻ dont la couverture supramoléculaire en surface est responsable de la stabilisation par les ions B(OH)₄⁻ et Cl⁻ par la suite.

Références:

- 1) Turkevich, J.; Stevenson, P. C.; Hillier, J. A study of the nucleation and growth processes in the synthesis of colloidal gold, *Discuss. Faraday. Soc.*, **1951**, *11*, 55–75.
- 2) Deng, Z.; Irish, D. E. SERS Investigation of the adsorption and decomposition of tetramethylammonium ions on silver electrode surfaces in aqueous media, *J. Phys. Chem.* **1994**, *98*, 11169–11177.



Cite this: *Chem. Commun.*, 2014, 50, 14194

Received 30th July 2014,
Accepted 22nd September 2014

DOI: 10.1039/c4cc05946h

www.rsc.org/chemcomm

Sodium borohydride stabilizes very active gold nanoparticle catalysts†

Christophe Deraedt,^a Lionel Salmon,^b Sylvain Gatard,^a Roberto Ciganda,^{a,c} Ricardo Hernandez,^c Jaime Ruiz^a and Didier Astruc^{*a}

Long-term stable 3 nm gold nanoparticles are prepared by a simple reaction between HAuCl₄ and sodium borohydride in water under ambient conditions which very efficiently catalyze 4-nitrophenol reduction to 4-nitroaniline.

Gold nanoparticles (AuNPs) have attracted much attention owing to their unique properties and applications in optics, electronics, sensing, biomedicine and catalysis.¹ Among AuNP stabilizers, thiolate² (Brust–Schiffrin method) and citrate³ (Turkevich–Frens method) are the most efficient ones for solution chemistry, whereas various oxides provide excellent solid supports for catalysis.^{1,4} Quite surprisingly, we found that the reaction of HAuCl₄ with NaBH₄ in water under ambient conditions provides small AuNPs (3 nm) that are stable for at least a month and are the fastest known catalysts for 4-nitrophenol reduction in water, retaining the same catalytic activity with time.

NaBH₄ is one of the most classic reductants in organic and inorganic chemistry,⁵ and it is used to reduce transition metal salts to metal(0) NPs in the presence of a stabilizer,² such as in the Brust–Schiffrin procedure. NaBH₄ reduces substrates by hydride transfer,⁵ but single-electron transfer is also possible given the electron-rich nature of borohydride anion characterized by a cathodic oxidation potential.⁶ Borohydrides also act as bi- or tridentate ligands.⁷ Finally, in the presence of metal catalysts NaBH₄ reacts with water to produce hydrogen and borate, a reaction that is exploited in “direct” borohydride fuel cells.⁸ Thus, in AuNP synthesis from HAuCl₄ and NaBH₄, the latter plays these multiple roles *inter alia* recalling those of citrate in the Turkevich–Frens method.³ It has already been reported that thiols on AuNPs can be reductively desorbed in the presence of

NaBH₄, which allows for the growth of AuNPs,⁹ and that AuNPs can be synthesized in water by adding an equimolar amount of NaBH₄ and NaOH to an equimolar mixture of HAuCl₄ and HCl.¹⁰ A large variety of reductants to reduce Au^{III} to AuNPs are known,¹¹ but in our approach the AuNP synthesis and long-term stabilization is simple, because only NaBH₄ addition to HAuCl₄ in water is involved overall under ambient conditions.

HAuCl₄ (1.5 mg) was solubilized in water (33 mL) to obtain a concentration of [Au] = 1.3 × 10⁻¹ mM. In order to optimize the HAuCl₄/NaBH₄ ratio, various amounts of NaBH₄ were added under N₂ (2, 10, 50 or 100 equivalents per Au atom in the preparation of solutions A, B, C and D, respectively).‡ With 10 equiv. of NaBH₄ (solution B), AuNPs were found to be stable for at least a month without any additive. The four solutions are of different colors (Fig. 1a). The pink-red solution A shows a surface plasmon band (SPB)^{1b,c} at 515 nm (Fig. 1b), and some precipitate appeared after a few days, although the color remained the same. Transmission electron microscopy (TEM) revealed that the average size of these NPs was 5.5 ± 0.2 nm. The orange solution B shows a SPB at 505 nm and turns pink-red after several tens of minutes under N₂ or air, with a SPB at 514 nm, probably due to sintering, but no aggregation was observed at least up to 1 month.¹² TEM of B indicated an average size of 3.2 ± 0.8 nm of these AuNPs (Fig. 2), which remained the same after 1 month (see ESI†). Solutions C and D are purple and grey, respectively, without

^a ISM, UMR CNRS No. 5255, Univ. Bordeaux, 33405 Talence Cedex, France.
E-mail: d.astruc@ism.u-bordeaux.fr; Fax: +33-5-4000-2994

^b Laboratoire de Chimie de Coordination, CNRS UPR-8241 and Université de Toulouse, UPS, INP, F-31077 Toulouse, France

^c Facultad de Química de San Sebastian, Universidad del País Vasco, Apdo. 1072, 20080 San Sebastian, Spain

† Electronic supplementary information (ESI) available: Synthesis and kinetics data and comparative catalysis table. See DOI: 10.1039/c4cc05946h

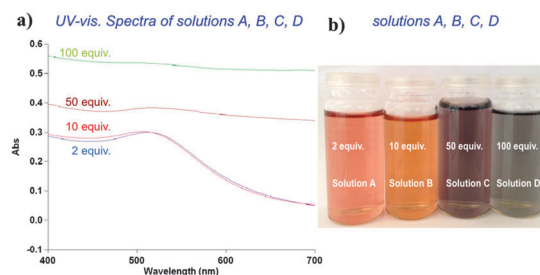


Fig. 1 (a) UV-vis spectra of the AuNP solutions A–D. (b) Various colours of the AuNP solutions A–D.

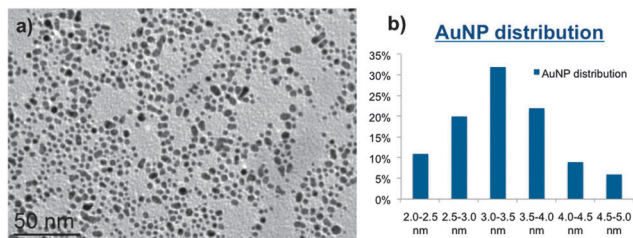


Fig. 2 (a) TEM pictures of AuNPs solution B, and (b) size distribution. The average measured size is 3.2 ± 0.8 nm (245 AuNPs).

any SPB, which indicates agglomeration¹² that is confirmed by a higher absorbance intensity around 700 nm compared to those for A or B, and precipitation was observed after 60 min and 10 min, respectively. The aggregation of AuNPs can be attributed to the decrease of surface potential that results from the electron injection into the AuNPs upon adding excess NaBH_4 .¹³ Some AuNPs were observed by TEM in solution C (see ESI†) in addition to the precipitate, and AuNPs in solution D fully aggregated after 1 hour.

Stabilization in solution B involves (i) slow hydrolysis of a large excess of NaBH_4 to NaB(OH)_4 (a few % per hour) that is only very weakly catalyzed by AuNPs at 25 °C,^{8b,c} (ii) strong covalent Au–H and/or Au– BH_4 bond formation with the AuNP core¹⁴ and (iii) the presence of Cl^- near the AuNP core.¹⁵ Thus after a short time, AuNP cores are surrounded by stabilizing H and/or BH_4 ligands and a smaller proportion of Cl^- . After a long time, the hydridic ligands are slowly but irreversibly hydrolyzed to H_2 , OH^- and NaB(OH)_4 as a result of slow AuNP catalysis of this hydrolysis,^{8b} so that the only remaining stabilizers after, e.g., a month are electrostatic: Cl^- and mostly B(OH)_4^- (incorporating water in a weak supramolecular hydrogen-bonded network) with Na^+ cations in a second layer.

Such AuNPs prepared and stabilized using only HAuCl_4 and NaBH_4 in water might be ideally suitable for AuNP-catalyzed reduction of 4-nitrophenol (4-NP) to 4-aminophenol (4-AP) by NaBH_4 (ref. 16) that would play roles of both the AuNP ligand and substrate. Indeed, the reaction mechanism is still unknown, although strong evidence has been provided by Ballauff's group for a process fitting the Langmuir–Hinshelwood (LH) model that assumes the adsorption of both reactants on the surface of the catalyst for AuNPs.^{16d,g,h} Thus we investigated the reduction of 4-NP in the presence of 100 equiv. of NaBH_4 .

This reaction was monitored by UV-vis spectroscopy, the intensity of the band at 400 nm that corresponds to the nitrophenolate anion decreases with time along with the growth of a weak 4-AP band at 300 nm. The reaction is fitted with a pseudo-first-order kinetics with respect to 4-NP in the presence of excess NaBH_4 , leading to the determination of the rate constant k_{app} (eqn (1)):

$$-\ln(C_t/C_0) = k_{\text{app}}t \quad (1)$$

(C_t is the concentration of 4-NP at a time t and C_0 is the concentration of 4-NP at time $t = 0$). The four solutions A, B, C and D were used in the reduction of 4-NP one hour after their synthesis, and the results are summarized in Table 1. A new

Table 1 Catalysis of 4-NP reduction with various AuNP solutions

Solution	AuNPs (%)	Reaction time (s)	k_{app} (s^{-1})	TOF (h^{-1})
B	1	120	2×10^{-2}	3000
B	0.2	200	9×10^{-3}	9000
B	0.05	1320	1×10^{-3}	5455
A	0.2	240	9×10^{-3}	7500
C	0.2	2400	1×10^{-3}	750
D	0.2	—	—	—
E	0.2	540	7×10^{-3}	3333

All the reactions were carried out with 0.05 mmol of 4-NP and 5 mmol of NaBH_4 in 100 mL of water ($[4\text{-NP}] = 5 \times 10^{-1}$ mM).

solution E composed of only Au^{III} ($[\text{HAuCl}_4] = 1.3 \times 10^{-1}$ mM) was prepared in order to compare it with pre-formed AuNPs. The results show that the activity of the AuNPs is linked to their stability. The stability order of the solutions is $\text{B} > \text{A} > \text{E} > \text{C} > \text{D}$, and the order of the k_{app} values is the same (Table 1).

The complete precipitation of AuNPs in solution D after one hour prevents any catalysis. The reduction of 4-NP in the presence of 0.2% mol Au^{III} (solution E) leads to complete conversion after 540 seconds, i.e. $k_{\text{app}} = 7 \times 10^{-3} \text{ s}^{-1}$ which is also high, but lower than the rate constant observed with the same amount of gold coming from pre-formed AuNPs of solution B (Fig. 3). This may be explained by the fact that upon introducing Au^{III} in the water solution of 4-NP + NaBH_4 , Au^{III} is very rapidly reduced without size control leading to some catalytically inactive precipitate due to the large excess of NaBH_4 . Upon decreasing the AuNP concentration of solution B from 1% mol to 0.05% mol, this catalyst is still very active, and the reaction is completed in 1320 seconds with a $k_{\text{app}} = 1 \times 10^{-3} \text{ s}^{-1}$ (instead of 120 seconds and $k_{\text{app}} = 2 \times 10^{-2} \text{ s}^{-1}$). Remarkably, using solution B at a concentration of 0.2% mol, the TOF reaches 9000 s^{-1} , which is very impressive for this reaction. Ten days after the synthesis of AuNPs (solution B), the reduction of 4-NP was tested again. No real change in the catalytic activity was observed (reaction completed in 280 seconds with 0.2% mol of AuNPs, and $k_{\text{app}} = 9 \times 10^{-3} \text{ s}^{-1}$), which shows the stability of these catalytically very reactive AuNPs.

In conclusion, one of the simplest syntheses of long-term stable AuNPs has been disclosed using only HAuCl_4 and NaBH_4 in water at room temperature. Moreover, these AuNPs are impressively

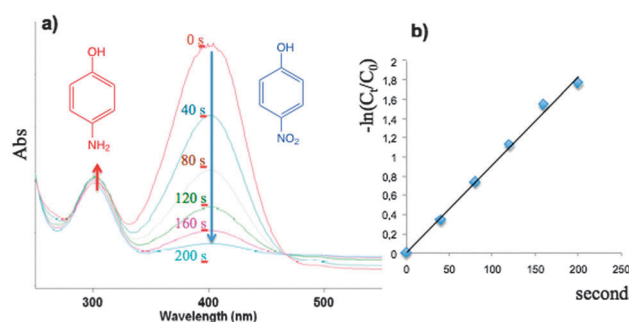


Fig. 3 Kinetic study at 20 °C of 4-NP reduction by NaBH_4 with 0.2% mol AuNPs (solution B) using UV-vis spectroscopy at 400 nm (a) and the plot of $-\ln(C_t/C_0)$ vs. time (s) for its decrease (b). No isosbestic point is observed by UV-vis spectroscopy due to H_2 bubbling during the reaction.¹⁷

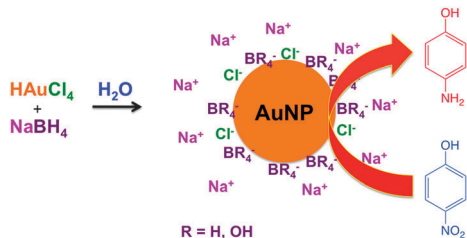


Fig. 4 Schematic representation of the properties of stabilization and efficient catalytic reactivity at the surface of AuNPs.

efficient catalysts for the reduction of 4-nitrophenol by NaBH_4 even with a low amount of Au (0.05% mol), providing one of the highest rate constants and TOFs ever recorded at 20 °C (see the comparative table in the ESI†).

In summary, the remarkable properties of these AuNPs are that they are stable for more than a month and, at the same time, remain extremely catalytically active for a long time. This dual property might be explained by AuNP stabilization by BH_4^- and/or H^- that have been shown to form strong bonds with the AuNP core¹⁴ and by Cl^- resulting from HAuCl_4 reduction. In the long term, the hydridic bonds with AuNPs are slowly hydrolyzed leaving only electrostatic stabilization by B(OH)_4^- and Cl^- near the AuNP core with their Na^+ cations standing behind (as shown in Fig. 4). In both cases, catalysis of 4-NP reduction by NaBH_4 is fast, because the latter is either already present on the AuNP surface or rapidly introduced through the permeable electrostatic anion layer.

It is probable that in the near future a variety of other AuNP-catalyzed reactions could also be further improved using this strategy.

Notes and references

‡ Preparation of solution B: 1.5 mg of HAuCl_4 ($M_w = 339.7 \text{ g mol}^{-1}$, $n = 4.4 \times 10^{-3} \text{ mmol}$) is dissolved in 32 mL of water to obtain $[\text{Au}] = 1.38 \times 10^{-1} \text{ mM}$. After stirring for 15 min 1 mL of a NaBH_4 solution (1.5 mg of NaBH_4 dissolved in 1 mL of water; 10 equiv. per Au atom) is added quickly. This solution is directly used in UV-vis spectroscopy to register the SPB band of the AuNPs.

- (a) M. Haruta, *Catal. Today*, 1997, **36**, 153–166; (b) Y. W. C. Cao, R. Jin and C. A. Mirkin, *Science*, 2002, **297**, 1536–1540; (c) L. R. Hirsch, R. J. Stafford, J. A. Bankson, S. R. Sershen, B. Rivera, R. E. Price, J. D. Hazle, N. J. Halas and J. L. West, *Proc. Natl. Acad. Sci. U. S. A.*, 2003, **100**, 13549–13554; (d) M.-C. Daniel and D. Astruc, *Chem. Rev.*, 2004, **104**, 293–346; (e) J. Perez-Juste, I. Pastoriza-Santos, L. M. Liz-Marzan and P. Mulvaney, *Coord. Chem. Rev.*, 2005, **249**, 1870–1901; (f) A. Corma and H. Garcia, *Chem. Rev.*, 2007, **107**, 2096–2126; (g) Y. Xia, Y. Xiong, B. Lim and S. E. Skrabalak, *Angew. Chem., Int. Ed.*, 2009, **48**, 60–103; (h) A. Corma, A. Leyva-Perez and J. Maria Sabater, *Chem. Rev.*, 2011, **111**, 1657–1712; (i) *Gold Nanoparticles for Physics, Chemistry, Biology*, ed. C. Louis and O. Pluchery, Imperial College Press, 2012; (j) N. Dimitratos, J. A. Lopez-Sanchez and G. J. Hutchings, *Chem. Sci.*, 2012, **3**, 20–44; (k) N. Li, P. Zhao and

- D. Astruc, *Angew. Chem., Int. Ed.*, 2014, **52**, 1756–1789; (l) M. Haruta, *Angew. Chem., Int. Ed.*, 2014, **53**, 52–56.
- (a) M. Brust, M. Walker, D. Bethell, D. J. Schiffrin and R. J. Whyman, *J. Chem. Soc., Chem. Commun.*, 1994, 801–802; (b) P. Mulvaney, *Langmuir*, 1996, **12**, 788–800; (c) M. Brust and C. Kiely, *Colloids Surf., A*, 2002, **202**, 175–186.
- (a) J. Turkevich, P. C. Stevenson and J. Hillier, *Discuss. Faraday Soc.*, 1951, **11**, 55–75; (b) G. Frens, *Colloid Polym. Sci.*, 1972, **250**, 736–774.
- (a) M. Haruta and M. Date, *Appl. Catal., A*, 2001, **222**, 427–437; (b) P. McMorn and G. J. Hutchings, *Chem. Soc. Rev.*, 2004, **33**, 108–122; (c) A. Corma and H. Garcia, *Chem. Soc. Rev.*, 2008, **37**, 2096–2126.
- (a) H. C. Brown, *Organic Syntheses via Boranes*, John Wiley & Sons, Inc., New York, 1975; (b) J. Seyden-Penne, *Reductions by the Alumino- and Borohydrides in Organic Synthesis*, VCH-Lavoisier, Paris, 1991.
- P. Michaud, D. Astruc and J. H. Ammeter, *J. Am. Chem. Soc.*, 1982, **104**, 3755–3757.
- (a) C. R. Lucas and C. R. Lucas, *Inorg. Synth.*, 1977, **17**, 93–95; (b) M. Ephritikhine, *Chem. Rev.*, 1997, **97**, 2193–2242; (c) M. Besora and A. Lledós, *Struct. Bonding*, 2008, **130**, 149–202.
- (a) N. A. Choudhury, R. K. Raman, S. Sampath and A. K. Shukla, *J. Power Sources*, 2005, **143**, 1–8; (b) U. B. Demirci, O. Akdim, J. Andrieu, J. Annaouer, R. Chamoun and P. Miele, *Fuel Cells*, 2010, **10**, 335–350; (c) L. Yu and M. A. Matthews, *Int. J. Hydrogen Energy*, 2011, **36**, 7416–7422.
- M. Dasog, W. Hou and R. W. J. Scott, *Chem. Commun.*, 2011, **47**, 8569–8571.
- M. N. Martin, J. I. Basham, P. Chando and S.-K. Eah, *Langmuir*, 2010, **26**, 7410–7417.
- (a) W. Ostwald, *Z. Phys. Chem.*, 1897, **22**, 289–330; (b) N. G. Bastus, J. Comenge and V. Puntès, *Langmuir*, 2011, **27**, 11098–11105.
- (a) P. Zhao, N. Li and D. Astruc, *Coord. Chem. Rev.*, 2013, **257**, 638–665; (b) Y. Wang, L. Salmon, J. Ruiz and D. Astruc, *Nat. Commun.*, 2014, **5**, 3489, DOI: 10.1038/ncomms4489.
- (a) E. J. W. Verwey and J. Th. G. Overbeek, *Theory of the Stability of Lyophobic Colloids*, Elsevier, New York, 1948; (b) J. N. Israelachvili, *Intermolecular and Surface Forces*, Academic Press, London, 1992; (c) U. Kreibig and M. Vollmer, *Optical Properties of Metal Clusters*, Springer, Berlin, 1995; (d) B. M. Quinn, P. Lijeroth, V. Ruiz, T. Laaksonen and K. Kontturi, *J. Am. Chem. Soc.*, 2003, **125**, 6644–6645; (e) K. B. Male, J. Li, C. Chi Bun, S.-C. Ng and J. H. T. Luong, *J. Phys. Chem. C*, 2008, **112**, 443–451; (f) R. Ciganda, N. Li, C. Deraedt, S. Gatard, P. Zhao, L. Salmon, R. Hernandez, J. Ruiz and D. Astruc, *Chem. Commun.*, 2014, **50**, 10126–10129.
- S. M. Ansar, F. S. Ameer, W. Hu, S. Zou, C. U. Pittman Jr. and D. Zhang, *Nano Lett.*, 2013, **13**, 1226–1229.
- Z. Deng and D. E. Irish, *J. Phys. Chem.*, 1994, **98**, 11169–11177.
- (a) T. K. Sau, A. Pal and T. Pal, *J. Phys. Chem. B*, 2001, **105**, 9266–9272; (b) K. Esumi, R. Isono and T. Yoshimura, *Langmuir*, 2004, **20**, 237–243; (c) K. Kuroda, T. Ishida and M. Haruta, *J. Mol. Catal. A: Chem.*, 2009, **298**, 7–11; (d) S. Wunder, F. Polzer, Y. Lu and M. Ballauff, *J. Phys. Chem. C*, 2010, **114**, 8814–8820; (e) S. Saha, A. Pal, S. Kundu, S. Basu and T. Pal, *Langmuir*, 2010, **26**, 2885–2893; (f) S.-N. Wang, M.-C. Zhang and W. Q. Zhang, *ACS Catal.*, 2011, **1**, 207–211; (g) S. Wunder, Y. Lu, M. Albrecht and M. Ballauff, *ACS Catal.*, 2011, **1**, 908–916; (h) P. Herves, M. Perez-Lorenzo, L. M. Liz-Marzan, J. Dzubielia, Y. Lu and M. Ballauff, *Chem. Soc. Rev.*, 2012, **41**, 5577–5587; (i) J. Li, C.-Y. Liu and Y. Liu, *J. Mater. Chem.*, 2012, **22**, 8426–8430; (j) J. Zhang, D. Han, H. Zhang, M. Chaker, Y. Zhao and D. Ma, *Chem. Commun.*, 2012, **48**, 11510–11512; (k) A. Shivhare, S. J. Ambrose, H. Zhang, R. W. Purves and R. W. J. Scott, *Chem. Commun.*, 2013, **49**, 276–278; (l) P. Pachfule, S. Kandambeth, D. Diaz and R. Banerjee, *Chem. Commun.*, 2014, **50**, 3169–3171.
- Z. V. Feng, J. L. Lyon, J. S. Croley, R. M. Crooks, D. A. Vanden Bout and K. J. Stevenson, *J. Chem. Educ.*, 2009, **86**, 368–372.

Annexes

Annexes

En annexes, se trouvent les travaux effectués en collaboration avec différentes personnes du groupe Nanosciences et Catalyse, sortant de l'axe principal de la thèse.

Tout d'abord figure une revue sur la catalyse de métathèse rédigée avec Martin d'Halluin, encadré lors de son stage de Master 2. Vient ensuite un travail élaboré également en collaboration avec Martin d'Halluin sur la synthèse d'un nouvel alcyne-imidazolium pour une possible fonctionnalisation de nanomatériaux par CuAAC ou réaction de Sonogashira avec l'exemple d'un dendrimère. A l'origine, ce travail devait conduire à la synthèse des catalyseurs au ruthénium de type Grubbs de 2^{ème} génération supportés, mais nous avons échoué à plusieurs reprises lors de la synthèse du carbène à partir de l'alcyne-imidazolium suivi de l'échange avec la tri-cyclohexyl phosphine du catalyseur de Grubbs de 1^{ère} génération.

Cette partie d'annexes se termine par la comparaison entre les activités catalytiques observées lors de la réduction du 4-NP pour des catalyseurs AuNPs stabilisés par différents ligands mono- ou macromoléculaires et synthétisés au sein du groupe, étude à laquelle une contribution secondaire a été apportée lors de cette thèse. Nous y démontrons l'impact de l'encombrement électronique et stérique des ligands lors d'une catalyse s'effectuant en surface d'une nanoparticule et soulignons le caractère de réservoir d'électrons des nanoparticules métalliques, essentiel en catalyse impliquant un transfert polyélectronique comme c'est le cas pour la réduction du 4-NP.

DOI:10.1002/ejic.201300682

Metathesis Reactions: Recent Trends and Challenges

Christophe Deraedt,^[a] Martin d'Halluin,^[a] and Didier Astruc*^[a]

Keywords: Metathesis / Supported catalysts / Z-selectivity / Alkynes

Metathesis reactions are now essential for the synthesis of complex organic molecules; a large variety of useful materials are available, and progress in this field is growing rapidly. Emphasis in this review on metathesis is placed on the recent developments of stereoselectivity aspects by using new families of molybdenum (Schrock type) and ruthenium (Grubbs type) catalysts for olefin metathesis. Recent progress in alkyne metathesis catalysts (Fürstner type) and their properties and impressive synthetic applications are highlighted as well as new terminal alkyne metathesis catalysts (Tamm type). The various strategies involved in recovering the catalyst and

removing metal impurities from products towards "green chemistry" are briefly reviewed. The relationship of olefin metathesis is shown with the alkyne metathesis reaction that was exploited by Fürstner, with alkane metathesis that was achieved by using surface organometallic chemistry and highlighted by Basset, and with the use of classic organometallic catalysts by the Goldman and Brookhart groups. Finally, recent developments in polymer chemistry that involve stereochemical control, low polydispersities, and applications are summarized.

Contents

1. Introduction
2. Classic Alkene Metathesis Catalysts and Reaction Types

3. Enantioselectivity and Stereoselectivity in Alkene Metathesis
4. Catalyst Recovery and Methods To Avoid Metal Contamination
5. Alkyne Metathesis
6. Alkane Metathesis
7. Polymer Chemistry
8. Conclusion and Outlook

[a] ISM, UMR CNRS 5255, Univ. Bordeaux,
33405 Talence Cedex, France
E-mail: d.astruc@ism.u-bordeaux1.fr
Homepage: astruc.didier.free.fr



Christophe Deraedt received his Master's degree in nanosciences and life chemistry in 2011 at the University of Bordeaux I. He is presently in his second year of his PhD work in the research group "Nanosciences and Catalysis" working with Prof. Didier Astruc on the synthesis and uses of "green" nanoreactors for the catalysis of reactions including carbon-carbon bond formation and transformation.



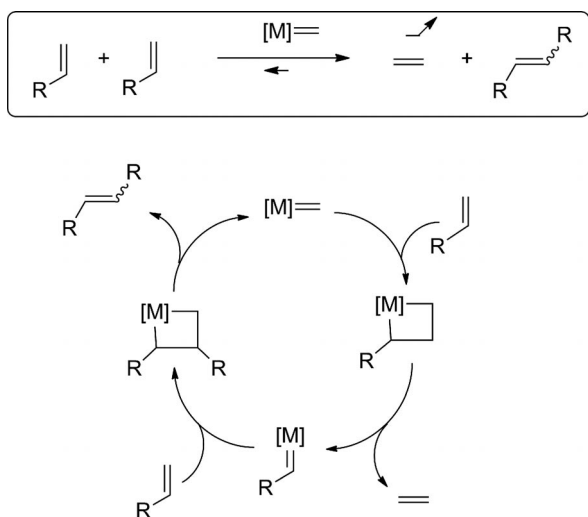
Martin d'Halluin studied at the University of Bordeaux I and received his Master's degree in molecular and macromolecular chemistry. He is currently pursuing an internship in the laboratory of Prof. Didier Astruc and is working on the synthesis of supported metathesis catalysts. His interests are in the area of catalysis.



Didier Astruc is a Professor of Chemistry at the University of Bordeaux and a Member of the Institut Universitaire de France. He obtained his PhD in Rennes under the supervision of R. Dabard and pursued postdoctoral work at MIT with R. R. Schrock. His present interests are in dendrimers and nanoparticles and their applications in catalysis, molecular materials science, and nanomedicine.

1. Introduction

Metathesis reactions, that is, the reorganization (transposition) of multiple carbon–carbon bonds, have appeared as an essential method to construct molecules, including natural and new complex organic molecules and polymers, in an efficient and green way.^[1–22] As such, their contribution to medicine, biochemistry, and materials science is essential and is growing rapidly. The most important metathesis reaction is olefin metathesis (Scheme 1), because olefins are common molecules, and terminal and disubstituted olefins are easily available, but alkyne metathesis has also recently been considerably developed.



Scheme 1. General Chauvin mechanism of olefin metathesis.

From these simple olefins, the challenging synthesis of tri- and tetrasubstituted olefins with well-defined stereochemistry becomes possible through a stereoselective olefin metathesis reaction, and decisive progress in this area is very recent with new Schrock-type and Grubbs-type catalysts.

Alkyne metathesis is less common but is, nonetheless, all the more useful, because various natural molecules contain alkynyl groups and because alkyne metathesis does not involve stereochemical problems, which is in contrast to alkene metathesis. The recent development of new alkyne metathesis catalysts and their application to organic synthesis by Fürstner and his group is considerable. Metathesis reac-

tions of alkenes and alkynes are very similar and involve the coordination of the alkene or alkyne to the electronically deficient metal center of a metal–alkylidene or metal–alkylidyne metathesis catalyst, respectively.^[6] According to the well-established Chauvin mechanism,^[2,21] the mechanism then includes the formation of a metallocyclobutane or metallocyclobutadiene intermediate that produces a new metal–alkylidene–olefin or a new metal–alkylidyne–alkyne that yields a metathesized unsaturated hydrocarbon and the new catalytic species containing a metal–carbon multiple bond (Scheme 1). Alkyne metathesis is not only useful per se, but it is also useful to solve stereochemical problems in alkene metathesis, because alkyne reduction can be stereoselective.^[5]

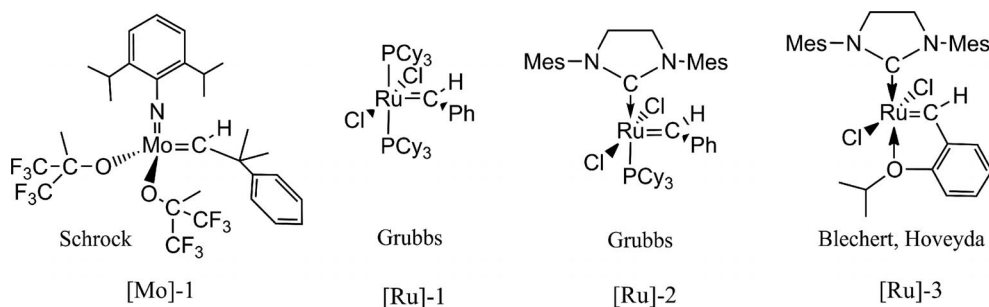
Alkane metathesis proceeds by dehydrogenation to the alkene followed by alkene metathesis and hydrogenation of the metathesized alkene, and this development has been pioneered by the Basset group.^[22] Recent progress of this old reaction has also emerged from classic organometallic chemistry. Thus, it appears that alkene metathesis is central, because as indicated above, it bears connections to alkyne and alkane metatheses.

Another challenging problem is that of the recovery of the catalyst and the leaching of metals into the reaction medium, because industrial requirements do not tolerate more than 5 ppm of a metal contaminant. This crucial problem has been recently intensively searched, and valuable methods have started to appear.^[15]

In this review, we will thus focus on the recent trends of the metathesis reactions indicated above including stereoselectivity in olefin metathesis, recent improvements in alkyne metathesis, metal catalysts recovery, and increased efficiency in the synthesis of polymer materials by metathesis.

2. Classic Alkene Metathesis Catalysts and Reaction Types

Presently, the most used olefin metathesis catalysts are the Schrock catalyst, [Mo]-1;^[4] the first- and second-generation Grubbs catalysts, [Ru]-1^[23] (Cy = cyclohexyl) and [Ru]-2 (Mes = mesityl),^[24] respectively; and the chelated Blechert–Hoveyda catalyst, [Ru]-3 (Scheme 2).^[6,7] [Mo]-1 is more reactive than the ruthenium catalyst, but it is also air and moisture sensitive and thus more difficult to use. The use

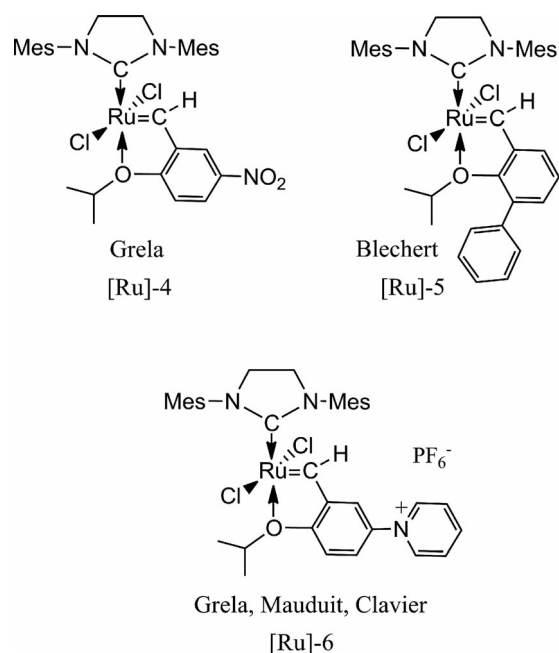


Scheme 2.

of the ruthenium catalysts is advantageous, as they are air and water stable. Thus, the most frequently used catalysts are the commercial compounds [Ru]-1 and [Ru]-2; the latter is more reactive and more stable than the former. [Ru]-3 is particularly robust. The ruthenium catalysts are not compatible with amine and phosphane groups, whereas [Mo]-1 is. In contrast, the Ru catalysts are compatible with alcohols, carboxylic acids, aldehydes, which is not the case for the Mo catalysts.

The N-heterocyclic carbene (NHC) ligands shown in Scheme 2 for [Ru]-2 and [Ru]-3 were introduced in metathesis reactions and in catalysis in general by Herrmann.^[25] There are many structural variations that are helpful in catalyst design, in particular with regard to the N substituent, although the Mes substituent is the most frequently used.^[25,26] NHC ligands are strong σ -donor ligands that largely contribute to the stability of the complex and the efficiency of the catalytic cycles, as in many other catalytic reactions.^[25–28]

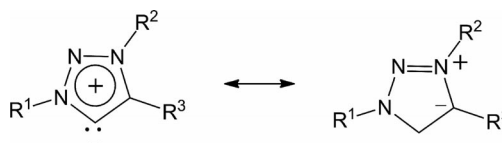
The catalytic activity of the robust [Ru]-3 catalyst was improved by Grella's group who introduced the strongly electron-withdrawing nitro substituent in the isopropoxybenzylidene ligand, that is, [Ru]-4 (Scheme 3), to destabilize the Ru–ether ligand bond.^[29,30] A similar result was obtained by Blechert's group upon introducing a phenyl substituent in [Ru]-5 that sterically destabilizes this metal–ligand bond.^[6,31,32] A very large number of variations of this type of catalyst have been reported.^[13,15] For instance, a water-solubilizing ammonium group such as that in [Ru]-6 allows easy removal of the catalyst in the aqueous phase from the organic products by liquid–liquid extraction after the metathesis reaction (Scheme 3). Analogous results were obtained with ether and polyethylene glycol (PEG) substituents. This strategy was extended to the anchoring of one of



Scheme 3.

the ligands to organic (PEG, Merrifield resin) and inorganic (silica, metal oxide) polymer supports.^[8]

Myriads of structural variations of NHC ligands in Ru metathesis catalysts have been reported and reviewed. Buchmeiser examined the metathesis activities of complexes containing ligands derived from 1,3-diazepin-2-ylidene that showed good activities for ring-opening metathesis polymerization (ROMP) reactions. Of particular interest are the ruthenium complexes of the so-called mesoionic carbene (MIC) ligands developed by the groups of Bertrand and Grubbs (Scheme 4), because of the remarkable donicity properties of this new class of ligand and their excellent performances in various types of olefin metathesis reactions. For instance, cycloaddition between 1,3-diaza-2-azoniallene salts and alkynes provides 1,3-diaryl-1*H*-1,2,3-triazolium salts that are precursors of the highly stable 1,2,3-triazolyl-5-ylidene MICs and the corresponding Ru metathesis catalysts.^[33,34]

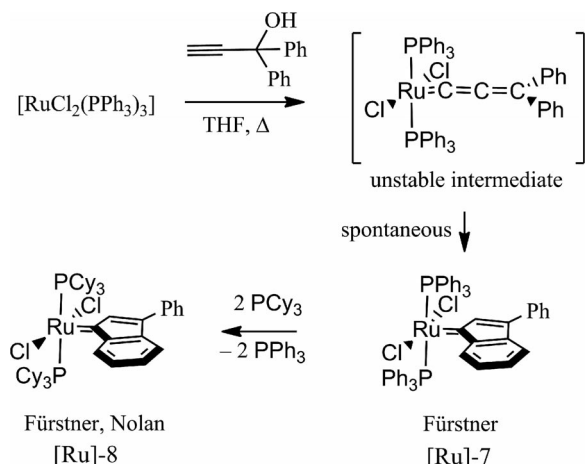


Scheme 4. Bertrand's mesoionic ligands for Ru metathesis catalysts.

In the case of a Ru–benzylidene complex bearing both a classic bis(mesityl) NHC ligand and a MIC ligand, protonolysis of the Ru–MIC bond upon reaction with a Brønsted acid generated an extremely active metathesis catalyst. The protonation step was shown to be rate determining in the generation of the MIC-free 14-electron metathesis-active species $[\text{Ru}(\text{NHC})(=\text{CHPh})\text{Cl}_2]$.^[35]

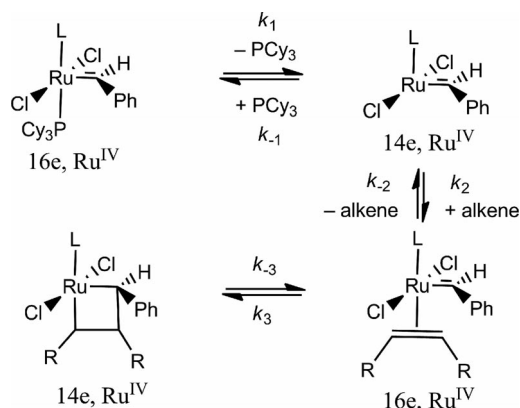
Other structural variations of metathesis catalysts that has been recently conducted mostly by the Buchmeiser, Fogg, and Grubbs groups (see above) involve pseudohalide derivatives that are obtained by substitution of the chloride ligands of the ruthenium and molybdenum complexes by pseudohalides X (X = halide, alkoxide, aryloxy, mono- or bidentate carboxylate, nitrate, trifluoromethanesulfonate, isocyanate, isothiocyanate) upon reaction with AgX. The best results with these catalysts are eventually obtained for ROMP reactions (see Section 6), whereas the efficiency of the catalysts are lower than those of the chloro precursors in ring-closing metathesis (RCM) and cross metathesis (CM).^[36–44]

Readily accessible indenylidene complexes [Ru]-7 and [Ru]-8^[5,45–51] that are robust and efficient olefin metathesis catalysts have been reported by the groups of Fürstner^[45–47,51] and Nolan.^[48,49] These complexes were shown to be in many cases fully equivalent to [Ru]-2 and [Ru]-3, although their activities under ambient conditions were lower.^[13] Great interest in these catalysts lies in their practical and easy synthesis subsequent to the serendipitous discovery of the spontaneous formation of [Ru]-7 by Fürstner's group (Scheme 5).^[5,45]



Scheme 5. Synthesis of the indenylidene Ru metathesis catalysts.

The reason for the enhanced catalytic activity obtained by destabilization of the ether–ruthenium bond in the 16-electron precatalysts [Ru]-3–6 is the generation of the catalytically active 14-electron ruthenium species resulting from ether ligand decooordination as well as from phosphane decooordination in the 16-electron precatalysts [Ru]-1 and [Ru]-2 (Scheme 6). Remarkably, Piers' group isolated 14-electron ruthenium phosphonium–alkylidene complexes that are better metathesis catalysts, as they do not require ligand decooordination before olefin binding, which results in very low olefin binding energy, high catalytic activity in model RCM reactions,^[52–55] and the direct relevant observation of ruthenacyclobutane intermediates resulting from olefin coordination.^[53–55] Grubbs' group also observed ruthenacyclobutane intermediates.^[56]

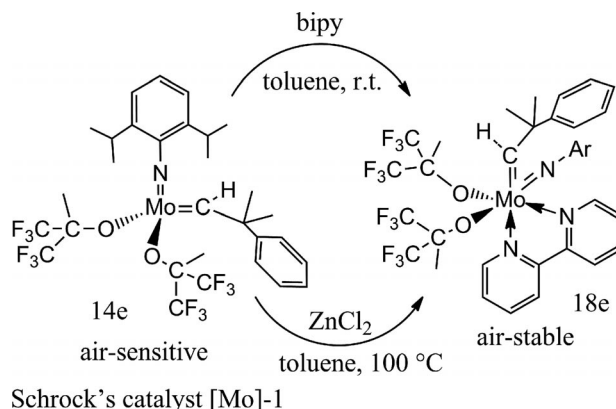


Scheme 6. Mechanism of olefin metathesis reactions with Ru catalysts. With L = PCy₃ (complex [Ru]-1), $k_1 = 10^2$; $k_2/k_{-1} = 10^{-4}$; with L = saturated NHC (complex [Ru]-2), $k_1 = 1$; $k_2/k_{-1} = 1$. It is the faster complexation of the olefins by the 14e intermediate that makes the [Ru]-2 catalyst more active than the [Ru]-1 catalyst (not the phosphane decooordination step).^[57]

Whatever the type of olefin metathesis and the structure of the ruthenium precatalyst, the general Chauvin mechanism applies, as exemplified in Scheme 1 for CM.

The Schrock family of catalysts derived from [Mo]-1 are 14-electron complexes, and olefin coordination to form active 14-electron metallacyclobutanes proceeds directly

without ligand decooordination.^[4,7,58] Although Schrock's catalysts are air and moisture sensitive, Füstner's group discovered that their reaction with 2,2'-bipyridine (bipy) makes them air stable and even storable in air for long periods of time. The bipyridine complexes are not themselves catalytically active, but catalytic activity can be restored anytime upon addition of ZnCl₂ to the pyridine adduct in the metathesis reaction medium (Scheme 7).

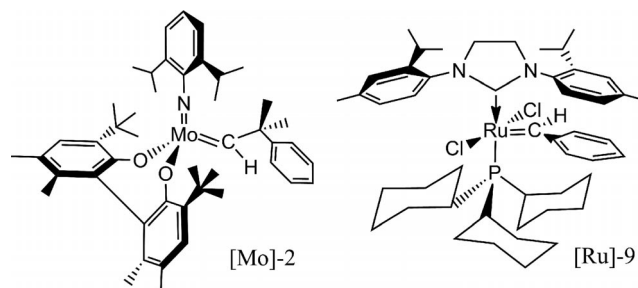


Scheme 7. How to protect Schrock's olefin metathesis catalysts from air and moisture according to Füstner.^[59]

Specialized olefin metathesis catalysts for stereoselective and/or polymerization will be introduced in the corresponding sections. The most common modes of olefin metathesis that are catalyzed by Schrock-type and Grubb-type complexes are RCM, CM, and ROMP.

3. Enantioselectivity and Stereoselectivity in Alkene Metathesis

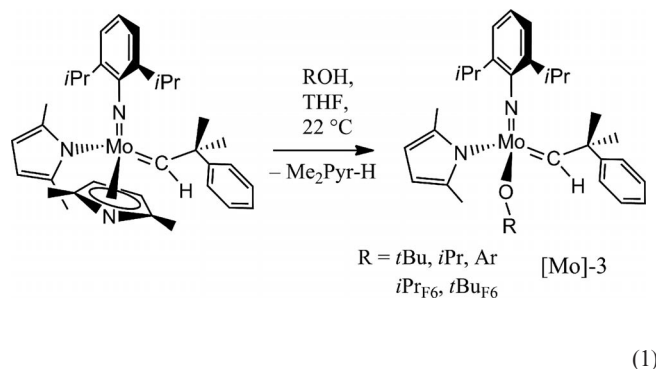
Chiral molybdenum and ruthenium catalysts such as [Mo]-2^[58] and [Ru]-9^[59] (Scheme 8) are known to favor high enantioselectivity for ring-closing and ring-opening/cross metathesis, although enantioselective CM still remains a challenge.



Scheme 8.

The Schrock group created a new generation of Mo and W alkene metathesis catalysts containing a pyrrolide ligand (or a methylated derivative).^[58] The pyrrolide ligand is comparable to the cyclopentadienyl ligand and can be bonded to the metal in a monohapto (η^1) or pentahapto (η^5) fashion depending on the bulk requirement of the metal center in the complex. The mono(pyrrolide) complexes of Schrock's

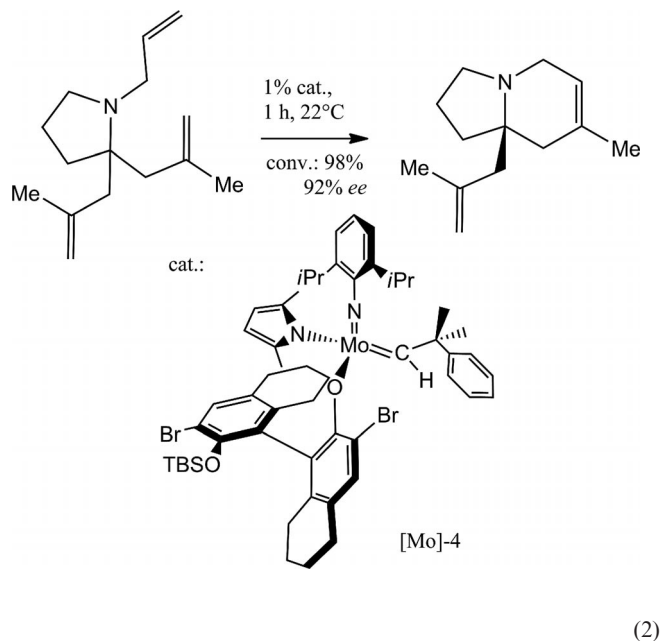
family are accessible by reaction of an alcohol or phenol with a bis(pyrrolide) precursor [Equation (1); Me₂Pyr-H = 1,4-dimethylpyrrole, Ar = arene, *i*Pr_{F6} = perfluoroisopropyl, *i*Bu_{F6} = perfluoroisobutyl].



The Mo complexes are more active metathesis catalysts than the W complexes, and interestingly, mono(pyrrolide) Mo complexes such as [Mo]-3 are also more active in RCM, ring-opening cross metathesis (ROCM), and ROMP reactions than the related bis(alkoxide), bis(aryloxo), and bis-(pyrrolide) Mo complexes.^[60,61] Moreover, the reaction of chiral phenoxide with the bis(pyrrolide) complex yields two diastereoisomers (the Mo center itself is chiral); the *S*_{Mo} (i.e., chiral Mo center with the *S* configuration) form of [Mo]-4 is largely preferred and can be separated by crystallization. An example of a very efficient desymmetrization reaction by using chiral mono(pyrrolide) Mo catalyst [Mo]-4 is shown in Equation (2) (TBSO = *tert*-butylsilyl ether).^[62]

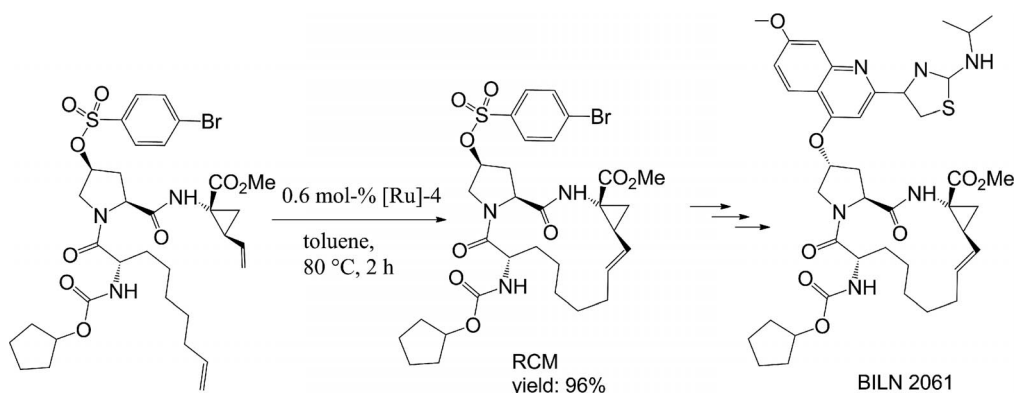
The regioselectivity issue has long been recognized as a major problem in olefin metathesis. RCM for small-ring formation, typically five-membered carbon rings, leads to *Z* cycloolefins for clear steric reasons, but the regioselectivity is lost in the formation of large rings that are of higher biosynthetic interest.

There are favorable examples, however. For instance, the macrocyclic hepatitis C virus (HCV) S3 protease inhibitor labeled BILN 2061 (CiluprevirTM) was synthesized by RCM. The best results were obtained with Grela's catalyst [Ru]-4 to yield the precursor macrocycle of BILN 2061 (Scheme 9) with the desired *Z* selectivity^[63–65] by using a RCM reaction that was scaled up to 400 kg.^[66]



In cross olefin metathesis, the regioselectivity is, in general, also weak. An elegant way to overcome this regioselectivity problem was first disclosed by Fürstner by using alkyne metathesis followed by regioselective reduction to the *Z* olefin by using the Lindlar catalyst, and the *E* olefin could be obtained by Birch reduction. This strategy was exemplified for the total synthesis of epothilone C, for which nonselective RCM had been less attractive than conventional methods. The total synthesis of epothilone C was indeed subsequently achieved by Fürstner's group through alkyne metathesis followed by stereospecific reduction with the Lindlar catalyst to give the precursor that yielded the final product in only one more step.^[67]

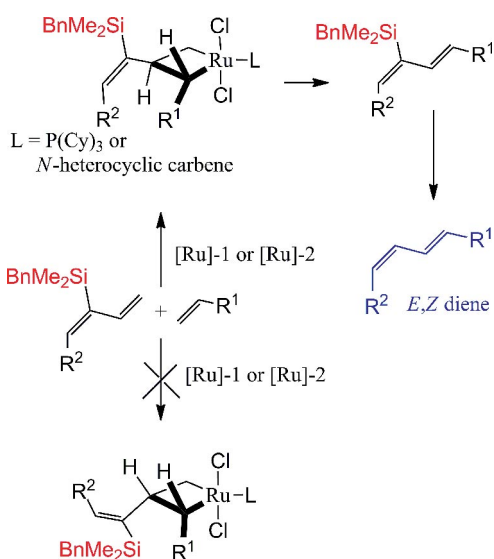
The problem of *E* selectivity in CM reactions was further initially examined by the groups of Grubbs and Blechert.^[19] On the basis of the fact that thermodynamic control favors the *E* olefin over the *Z* isomer, these groups disclosed that the *E* selectivity could be improved if the metathesis reactions were conducted with an olefin bearing a bulky or electron-withdrawing substituent. For instance, with an ester or nitrile substituent, formation of the *E* product was completely stereoselective with the use of standard catalysts.



Scheme 9. Synthesis of BILN 2061 involving a stereospecific RCM step most efficiently catalyzed by Grela's complex [Ru]-4.^[65]

This principle was, for instance, successfully applied to the metathesis functionalization of olefin-terminated dendrimers.^[68]

Given that *Z* olefins are less thermodynamically stable than their *E* isomers, direct access to *Z* olefins suffered from the classic thermodynamic control of olefin metathesis reactions. For CM reactions, *Z* selectivity is thus difficult to induce, and there are only a few examples involving substrates with an sp-hybridized substituent such as acrylonitrile or enynes for which the *Z* selectivity of the CM was between 65 and 90%.^[69] Fürstner and Gallenkamp proposed a strategy for the stereoselective synthesis of *E,Z*-configured 1,3-dienes by RCM catalyzed by [Ru]-3. This strategy consisted of positioning a bulky R₃Si group on the diene-ene substrate to stereodirect the reaction and to protect the internal alkene. This procedure was applied to the synthesis of various macrocyclic *E,Z*-configured 1,3-dienes including lactimidomycin,^[70] a potent translation and cell-migration inhibitor (Scheme 10).

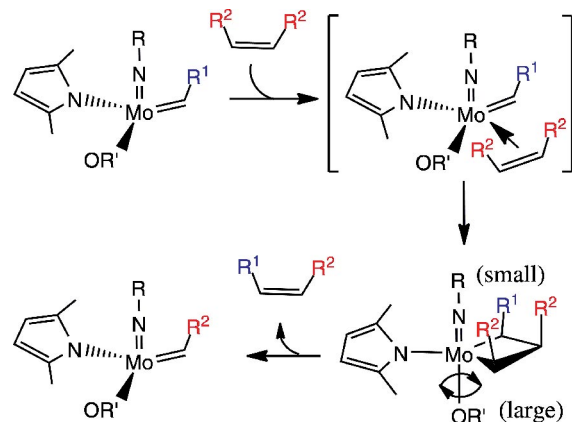


Scheme 10. Fürstner's strategy leading to a selective *E,Z* diene.^[70] BnMe₂Si = dimethylbenzylsilyl.

During the recent years, the groups of Schrock and Grubbs have disclosed new classes of Mo and Ru catalysts, respectively, that provoke kinetic control of *Z* olefin formation in CM, homocoupling metathesis, and RCM. In all cases, the principle consists of designing new catalysts with a bulky ligand that forces the substituent of the incoming olefin to be on the opposite side to the bulky ligand of the catalyst.

To induce kinetic control of *Z* selectivity in CM, the Schrock and Hoveyda groups used efficient mono(aryloxidepyrrolide) (MAP) complexes (Mo and W).^[71–74] The aryloxide ligand is especially bulky, as in [Mo]-4, whereas the imido ligand bears an adamantyl substituent that is not bulky, unlike in [Mo]-4. The mechanism explaining the *Z*-selective metathesis with MAP complexes is the following:

The situation allows coordination of the olefin *trans* to the pyrrolide ligand so that the substituent of the olefin points away from the flexible bulky aryloxide and it is also on the side of the imido group; this leads to the formation of a metallacyclobutane in which the two substituents are *cis*, the precursor of the *Z* olefin (Schemes 11 and 12). In this way, the *Z* selectivities that were obtained with the Mo and W catalysts were attributed to the differences in the sizes of the two apical ligands of the incipient metallacyclobutane complex.

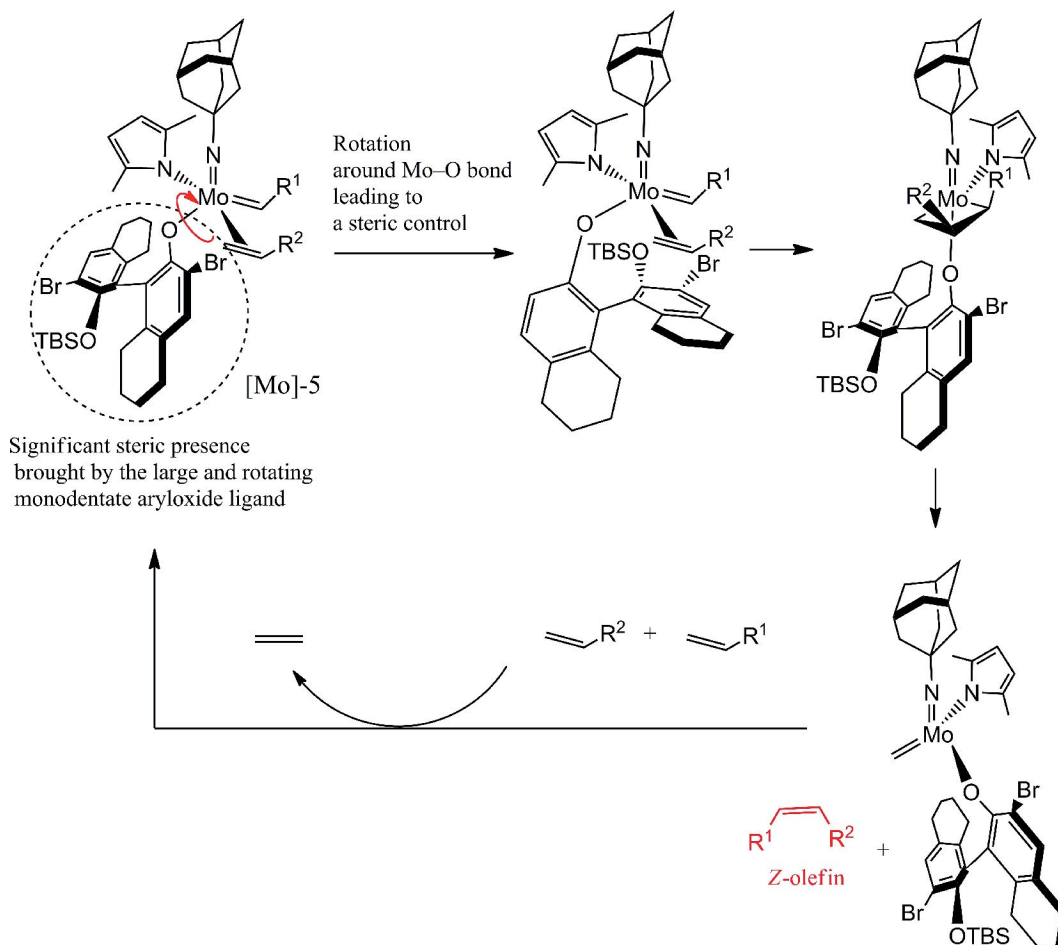


Scheme 11. General mechanism of *Z*-selective metathesis with Schrock's molybdenum catalyst.

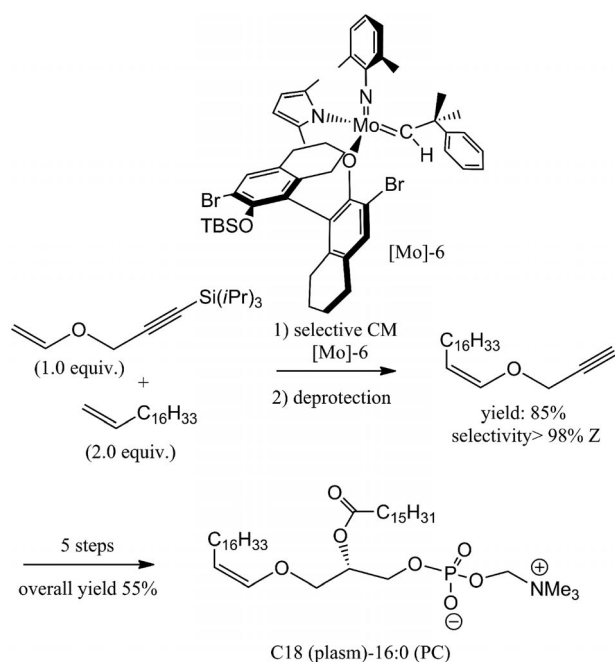
The presence of the *E* olefin in the catalysis with this complex is, according to the authors, possibly due to the isomerization of the *Z* olefin. Moreover, the inherent reversibility of olefin metathesis and the higher reactivity of *Z* alkenes (vs. *E* isomers) further exacerbate the problem for *Z* selectivity. The production of six different products in the case of CM versus the production of only two products in homocoupling metathesis is also a problem to note. The CM between enol (and allylic amides) and alkenes with the same Mo catalyst was studied for natural product synthesis applications, for instance, the antioxidant plasmalogen phospholipid and a potent immunostimulant KRN7000 (Scheme 13).

An excess amount of cheap enol is important for the *Z* selectivity of the reaction (up to 98% and 97% yield), and the establishment of a reduce pressure system has been proven to be very efficient to avoid the reversibility of the reaction induced by the production of ethylene.^[75] This finding implies that the *Z* olefin can be easily converted into the *E* olefin with the same catalyst in the presence of a huge amount of ethylene through ethenolysis.^[76] Mo and W MAP catalysts were also used recently in RCM for natural products synthesis.^[77] The synthesis of nakadomarin A (anticancer, antifungal, and antibacterial first isolated from the sea sponge Amphimedon) was conducted in seven steps, and the first step corresponds to *Z*-selective RCM (97% *Z* and 90% yield) catalyzed by [Mo]-7 (Scheme 14).

In parallel, the group of Grubbs developed a new series of ruthenium metathesis catalyst that provides *Z* selectivity.



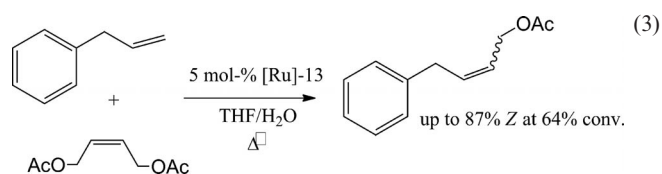
Scheme 12. Steric control by the large and rotating monodentate aryloxide ligand of [Mo]-5 leading to *Z*-selective metathesis.^[71,75]

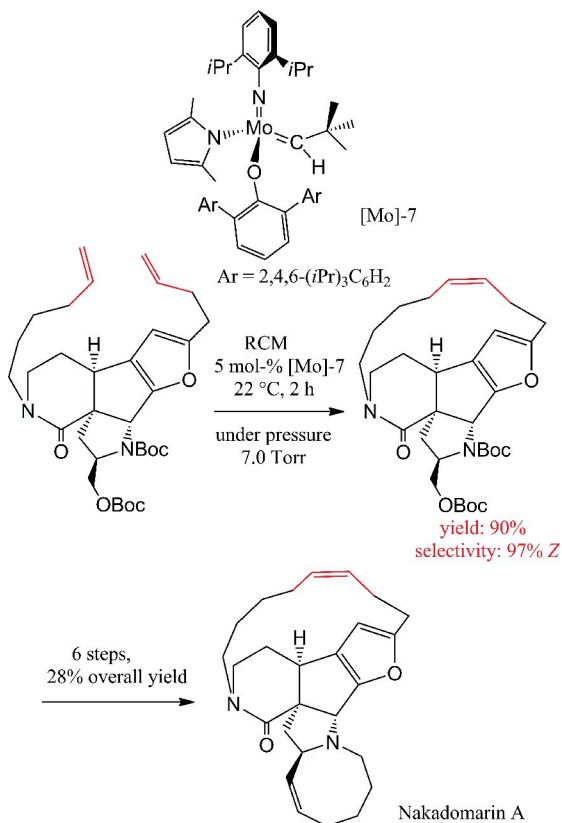


Scheme 13. Synthesis of C18 (plasm)-16:0 (PC) through *Z*-selective CM catalyzed by [Mo]-6.^[75]

According to Scheme 15 and starting from [Ru]-10 and NHCs, the complexes [Ru]-3 and [Ru]-11 were produced. They underwent chloride abstraction upon reaction with silver pivalate, but the electron-deficient ruthenium center then activated a C–H bond from a methyl group of the Mes substituent of the NHC ligand or from the adamantly substituent to give the new ruthenium–alkyl complexes [Ru]-12 and [Ru]-13, respectively, in which the pivalate ligand is chelated to the Ru center.^[78–80] These complexes provide *Z*-selective CM,^[78,79] and the selectivity and efficiency are improved upon replacing the pivalate ligand in [Ru]-13 by a nitrate ligand in [Ru]-15 via [Ru]-14, as indicated in Scheme 15.^[80]

Complex [Ru]-13 was the first Ru complex to catalyze the CM of two different olefins with 90% *Z* isomer and 64% yield [Equation (3)].^[79]

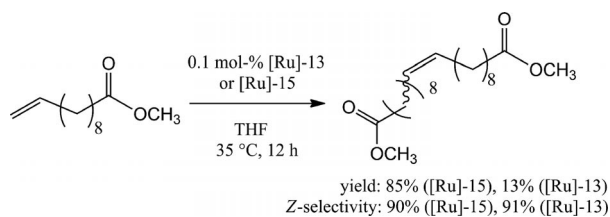




Scheme 14. Synthesis of nakadomarin A through Z-selective RCM catalyzed by [Mo]-7.^[77] Boc = *tert*-butoxycarbonyl.

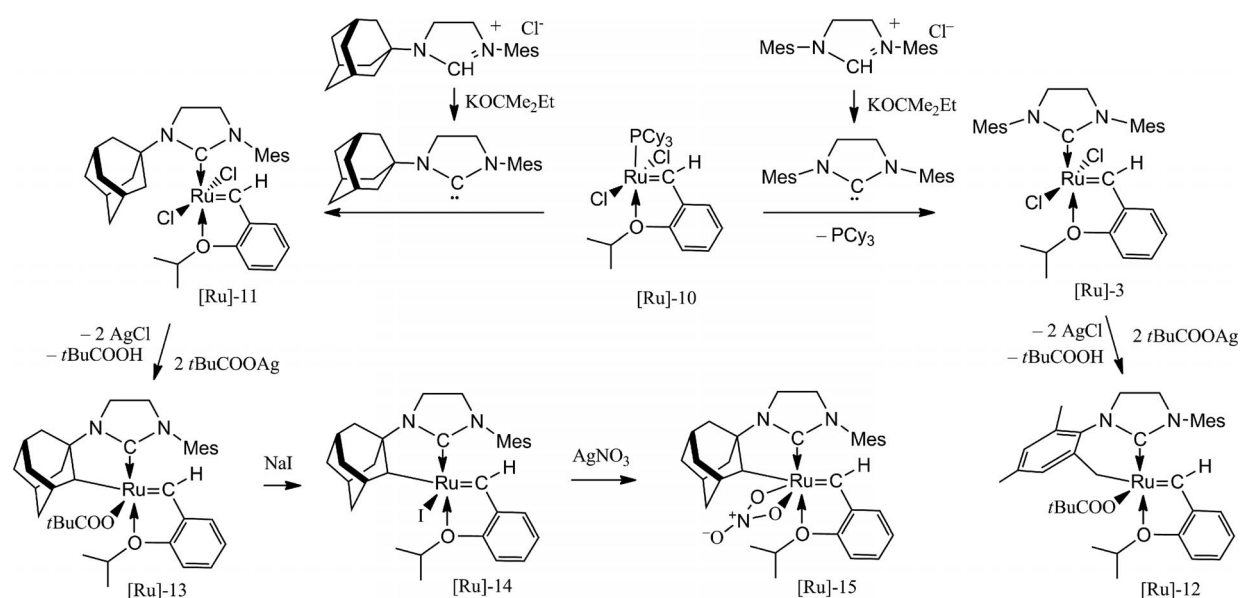
The Z-selective homocoupling of various functional terminal olefins (such as olefinic alcohol, allylsilane, allyl acetate, allyl borane, etc.) was investigated with [Ru]-13. The reaction works very well in protic solvents (e.g., MeOH, EtOH) at 35 °C (with a vent of the inert atmosphere to remove the ethylene that deactivates the catalyst) leading to

a conversion >95% and a Z selectivity >95%. This catalyst is air sensitive but not water sensitive.^[79] A screening of various closely related catalysts of this family led to the conclusion that the adamantyl part was essential for the selectivity of the reaction, that the *ortho* substitution of the aryl group on the NHC ligand was important for stabilization and avoiding undesirable C–H activation, and finally that the bidentate ligand played a key role. Indeed, if this bidentate ligand was replaced by a monodentate ligand, the activity decreased markedly. With the nitrate ligand in [Ru]-15, an increase in the activity [Equation (4)] with a turnover number (TON) up to 1000 was achieved, and the Z selectivity was >95%. Furthermore, the nitrate catalyst [Ru]-15 is more stable in air than the carboxylate catalyst [Ru]-13, and it is easier to purify.^[80]



(4)

These observations were confirmed by DFT calculations. The mechanism of olefin metathesis employing previous unchelated Ru (without pivalate or nitrate ligand) catalysts with phosphane or NHC ligands such as [Ru]-1 and [Ru]-2 was investigated extensively by computational studies by various research groups.^[81] The generally accepted mechanism involves a 14-electron Ru–alkylidene species that binds to an olefin molecule from the bottom position (i.e., *trans* to the NHC ligand) or the side position (i.e., *cis* to the NHC ligand). Low-temperature studies of metallacycles formed from Ru catalysts with NHC ligands are most consistent



Scheme 15. Synthesis route of [Ru] catalysts that are useful in classic metathesis and in Z-selective metathesis.^[78–80]

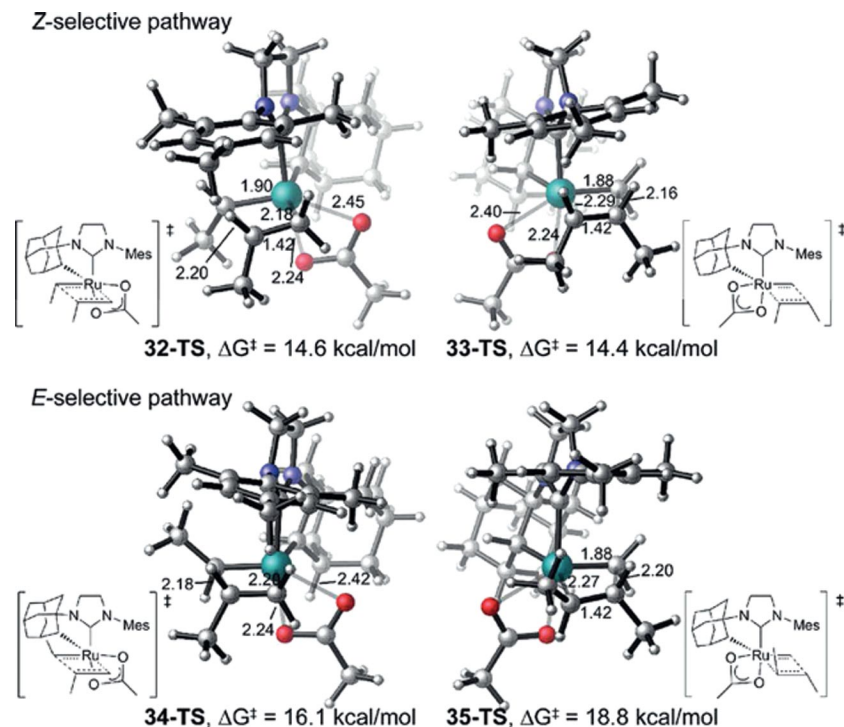


Figure 1. Transition state (TS) structures for the side- and bottom-bound pathways with Z-selective catalyst. Reprinted with permission from ref.^[81] Copyright © 2012 American Chemical Society.

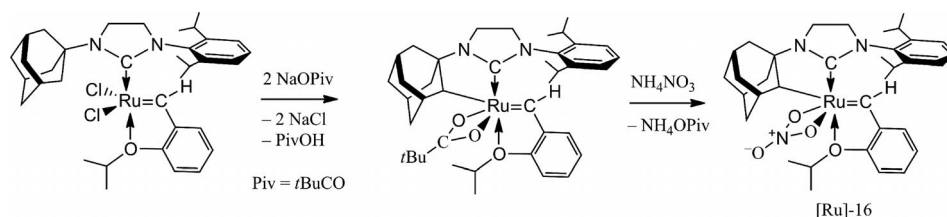
with a bottom-bound metallacycle.^[53–56] Previous DFT studies suggested that the bottom-bound pathway was more favorable with unchelated Ru catalysts^[82–84] and that the formation of the *E* products was favored both kinetically and thermodynamically.^[84,85] In contrast, if chelated catalyst (i.e., Z-selective catalyst) are used, the DFT calculations showed that the side-bound pathway requires less energy than the bottom-bound pathway. The strong preference for the side-bound mechanism with the chelated catalysts is due to a combination of steric and electronic effects of the chelating NHC ligand. The side-bound pathway implies the *cis* attack of the olefin to the NHC and a *trans* attack to the adamantyl group (Figure 1), which leads to the *Z* olefin.^[81,86]

Given that the steric bulk of the NHC ligand controls the *Z* selectivity of the metathesis reactions, the Grubbs group engaged the synthesis of a catalyst related to [Ru]-15 and containing a NHC ligand with the very bulky 2,6-di-(isopropyl)phenyl (DIPP) substituent. The synthetic route initially used for [Ru]-15 employing silver pivalate (Scheme 15) failed, but the targeted catalyst was successfully obtained by using the new route shown in Scheme 16.

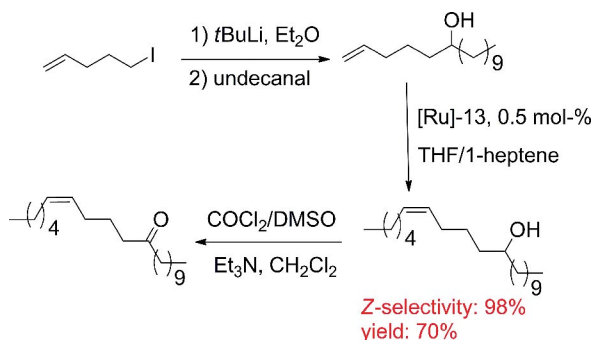
This bulkier [Ru]-16 catalyst exhibits higher *Z* selectivity than the previously reported [Ru]-15 catalyst. For example, with the homodimerization of methyl 10-undecenoate [Equation (4)], [Ru]-16 provided both yield and *Z* selectivity >95%.^[87] Grubbs' group also spread the *Z*-selectivity of RCM and CM to the synthesis of interesting biological molecules by using [Ru]-16. Thus, the synthesis of macrocycles containing 13 to 20 carbon atoms was achieved with a *Z* selectivity up to 94% (74% yield),^[88] and in 2013, the total synthesis of insect pheromones in a few steps was reported with a *Z* selectivity of 80% and a yield of 70% (Scheme 17).^[89]

4. Catalyst Recovery and Methods to Avoid Metal Contamination

Industrial applications require the improvement of two main aspects in catalysis. First, the leaching of metal from the catalyst in the solution containing the reaction product must be avoided. To face this problem, two main strategies can be used. The first one is the treatment of the product



Scheme 16. Grubbs' synthetic route to the highly Z-selective metathesis catalyst [Ru]-16.

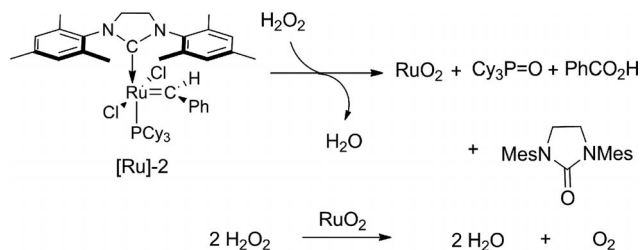


Scheme 17. Synthesis of an insect pheromone through Z-selective CM catalyzed by [Ru]-13.^[88]

by using a metal scavenger to eliminate the trace amounts of metal. The second one is the design of a catalyst that does not leach during the reaction. The second strategy consists of recovering and recycling the catalyst. To easily recover and recycle the catalyst, various methods can be envisaged. One way is to immobilize the catalyst on a surface to avoid metal leaching into the reaction mixture. A second way is to design a catalyst containing a functional group that will be used in the purification steps. For this purpose, ruthenium catalysts have been the most currently investigated among metathesis catalysts owing to their stability towards air and moisture. Some examples of Ru-based catalysts are introduced and discussed below.

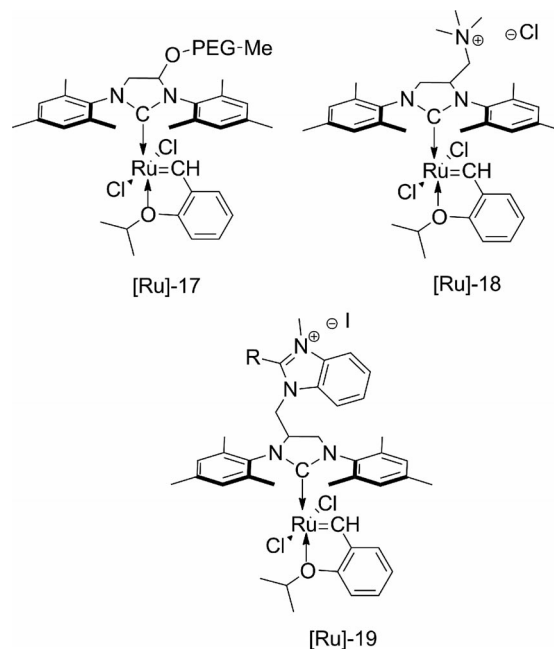
An early catalyst was described by Grubbs et al.^[90] that contained a water-soluble phosphane, tris(hydroxymethyl)phosphane, to remove the water-soluble catalyst from the products. A contamination level of 206 ppm was reached after adding 86 equivalents of this phosphane and conducting silica gel filtration. Paquette et al.^[91] then reported the use of $\text{Pb}(\text{OAc})_4$ and reached a Ru level around 300 ppm and a Pb level around 5 ppm. The method developed by Grubbs was then improved by Georg et al.^[92] by using triphenylphosphane oxide ($\text{Ph}_3\text{P}=\text{O}$) or DMSO as a metal scavenger (50 equiv.), which led to a Ru level of 240 ppm after silica gel filtration. These methods are simple and cheap, especially the one involving the use of DMSO, but the Ru level was still too high to allow industrial applications. For pharmaceutical use in particular, the authorized Ru level is 5 ppm for oral drugs and 0.5 ppm for parenteral drugs. More recently, Knight et al. reported the use of hydrogen peroxide (H_2O_2) as a metal scavenger.^[93] H_2O_2 plays the role of an oxidant and decomposes the Ru catalyst into various byproducts that are easy to separate from the crude reaction product (Scheme 18). A Ru level below 5 ppm was reached in the case of Grubbs second-generation catalyst [Ru]-2.

To reach a Ru contamination level of <5 ppm, new homogeneous catalysts and supported catalysts have been introduced. Grubbs et al. reported a PEG-tagged Grubbs second-generation catalyst, [Ru]-17, that exhibited good solubility in both organic solvents and water.^[94] Upon treating the crude product of the metathesis reaction with water extraction and activated carbon, a Ru level as low as 0.04 ppm was reached.



Scheme 18. Oxidative decomposition pathway for the Grubbs second-generation catalyst [Ru]-2 by using H_2O_2 .^[93]

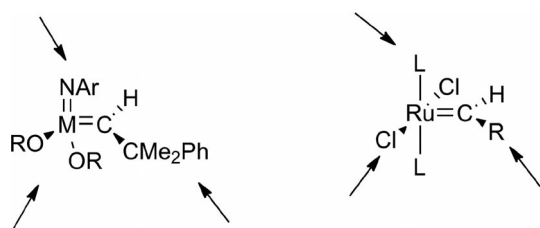
This strategy of designing catalysts bearing a tagged NHC ligand was also very recently used by Grela et al.^[95,96] This group reported catalysts containing a NHC ligand tagged with an ammonium or a benzimidazolium moiety in [Ru]-18 and [Ru]-19 that presented very good solubility in water, which allowed easy purification upon water extraction and very low Ru contamination of the metathesis product, below 1 ppm (Scheme 19).



Scheme 19. [Ru]-17,^[94] [Ru]-18,^[95] and [Ru]-19.^[96]

Polymer-supported metathesis catalysts were reviewed by Buchmeiser in 2009.^[97] The polymeric support can be connected to various ligands of the catalyst (Scheme 20), which usually affords a very low level of metal contamination in the product of the metathesis reaction. In principle, Grubbs-type catalysts can be immobilized by (1) one of the neutral, 2-electron donor ligands, that is, the phosphane, the (substituted) pyridine, or the NHC; (2) the alkylidene ligand; (3) halogen exchange; and (4) noncovalent interactions. In the case of derivatives of Grubbs second-generation catalysts, anchoring through the NHC ligand might be the most appropriate method. The synthesis of the NHCs is simple and involves functionalization by a support. This NHC moiety is moreover well fixed on the catalyst in com-

parison to the alkylidene part, in the case of the Blechert and Hoveyda catalyst [Ru]-3 and derivatives. The boomerang effect claimed earlier and defined as the release–return mechanism was shown to be unreliable. Indeed, Plenio et al. investigated the recoordination of the alkylidene part at the end of the reaction by fluorescence. The functionalization of this part with a dansyl fluorophore allowed a fluorescence signal corresponding to the decooordination of this moiety from the metal to be monitored, because this signal would be quenched if the fluorophore was close to the metal.^[98] The fluorescence signal increased to a maximum until the end of the reaction and then remained at this maximum intensity, which showed that there was no recoordination of the fluorophore to the metal. The recovery of the initial precatalyst in some cases could be due to an excess amount of the precatalyst, as not all of the precatalyst had undergone initiation of the reaction.



Scheme 20. Indication of the possibilities of support anchorage positions on catalyst ligands.

The use of the alkylidene anchor was described by Yinghuai et al. in which the catalyst was supported on magnetic nanoparticles (Scheme 21).^[99]

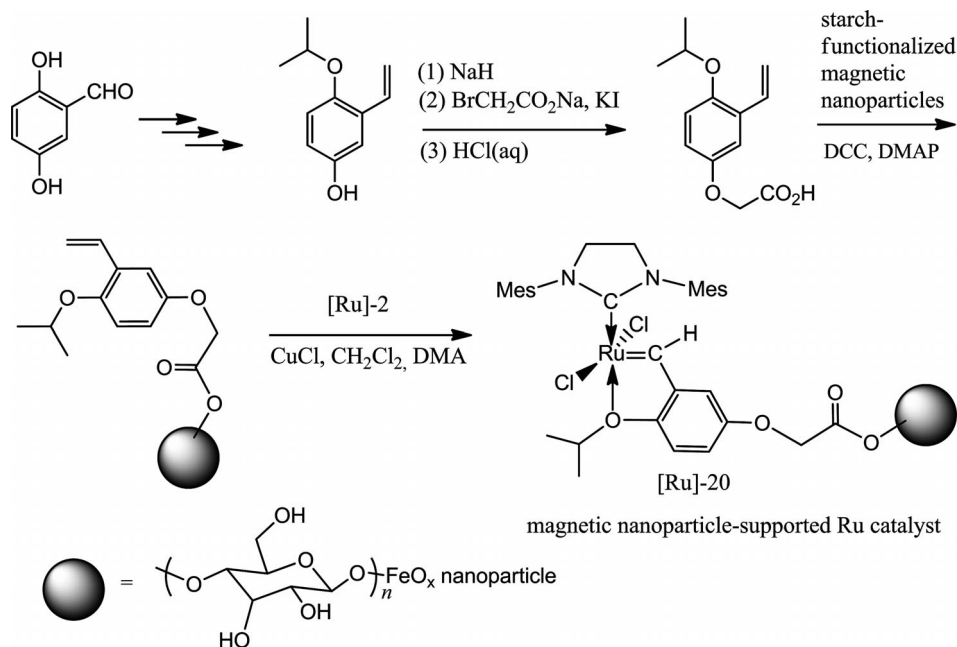
This [Ru]-20 catalyst derived from [Ru]-3 was tested in various metathesis reactions; it was recovered by magnetic

attraction and reused over at least five runs (possibly because of the lack of the boomerang effect, which implies the non-recoordination of the alkylidene at the end of the reaction and consequently the loss of the Ru moiety). The Ru contamination of the crude product was less than 4 ppm [detected by inductively coupled plasma mass spectrometry (ICP-MS)]. This anchoring position could be used especially in the case of ROMP (Scheme 22), in which the alkylidene part becomes the terminal part of the polymer, and this is of interest for easy purification of the targeted compound.^[97]

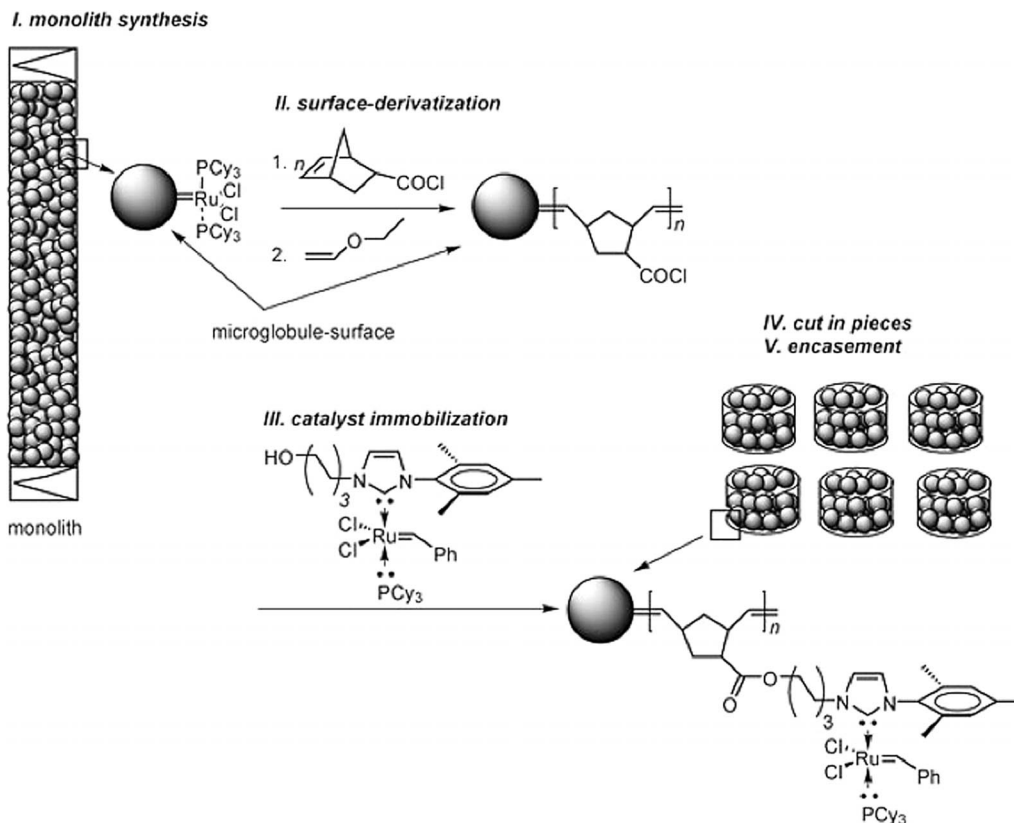
For example, Buchmeiser and Fürstner et al. reported the immobilization of a Grubbs-type catalyst on a ROMP-derived monolith.^[100] The synthetic concept entailed the manufacture of the monolithic structure by ROMP, its in situ functionalization with norborn-2-ene carboxylic chloride, and reaction with [RuCl₂(PCy₃)(NHC)(CHPh)] {NHC = 1-(2,4,5-trimethylphenyl)-3-(6-hydroxyhexyl)imidazol-2-ylidene}.^[101] The monolithic disk-immobilized catalyst was used in various metathesis-based reactions including RCM, ring-opening CM (ROCM), and enyne metathesis (EYM). Using 0.23–0.59 mol-% of the supported catalyst, TONs up to 330 were achieved, and the metal leaching was reported to be <3%.

In the case of Grubbs third-generation catalysts, two pyridine ligands or two 3-bromopyridine ligands are added to Grubbs second-generation catalyst (see Section 7). Functionalization of third-generation catalysts was also performed by exchange of pyridine or 3-pyridine with a functional pyridine.^[102]

Silica is also a valuable support for metathesis catalysts, and there are indeed many examples of metathesis catalysts that are immobilized on silica gel.^[102–104] A most recent one

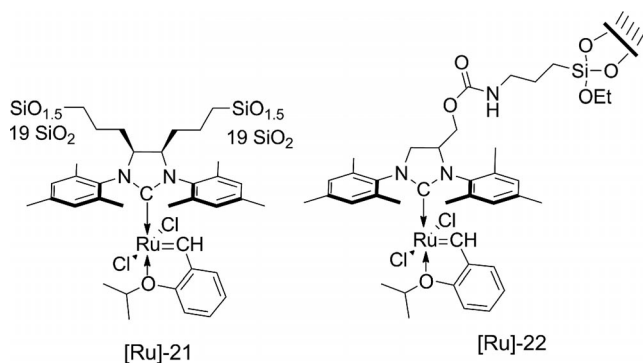


Scheme 21. Synthesis of catalyst [Ru]-20 supported on magnetic nanoparticles, a derivative of [Ru]-3. DCC = dicyclohexylcarbodiimide; DMAP = *p*-dimethylaminopyridine, DMA = dimethylacetamide.



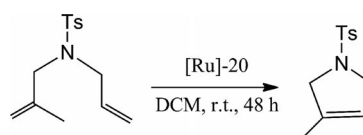
Scheme 22. Immobilization of a second-generation Grubbs-type catalyst through a NHC on a monolithic support. Reprinted with permission from ref.^[100] Copyright © 2009 American Chemical Society.

reported by Monge-Marcet et al. showed the synthesis of [Ru]-21, a catalysts derived from [Ru]-3, that was immobilized through a bis(silylated) NHC (Scheme 23).^[105]



Scheme 23. [Ru]-21 and [Ru]-22.^[105]

This catalyst was then used for the RCM of various substrates that delivered products in very good yields. The study of the recyclability of this catalyst indicated that it could be reused over at least five runs without a significant loss in activity over the first three runs. The recyclability test (four successive runs) for the RCM of **A** provided the product in 99, 93, 76, and 21% yield over the four runs, respectively [Equation (5), Ts = *para*-tolylsulfonyl]. In 2013, the same team reported related catalyst [Ru]-22 that showed high activity and good recyclability (Scheme 23).^[106]



(5)

To promote the use of such supported catalysts in industrial processes, investigations were conducted in continuous flow reactors.^[107,108] Ying et al. reported the immobilization of a [Ru]-3-type catalyst on nanoporous silica. This catalyst was then used in a circulating flow reactor (Figure 2, a).^[107] The recyclability of this catalyst and the amount of Ru leached were examined in RCM (Figure 2, b). The catalyst was reused over at least eight runs with an overall conversion yield of 90% and a Ru leaching content of around 1.6 ppm after a reaction time of 180 min.

Very recently, Kirschring et al. reported the use of two [Ru]-3-type derivatives, [Ru]-23 and [Ru]-24 (Scheme 24, Figure 3), supported on silica through polar interactions and adsorption.^[108]

The catalyst was used in RCM over four runs and the amount of ruthenium leached was evaluated by ICP-MS at several reaction time intervals. The data showed that the Ru contamination of the crude product was very low (less than 1 ppm after 20 min of reaction). This technique seems to be very valuable toward industrial applications, but the problem of catalyst deactivation remains.

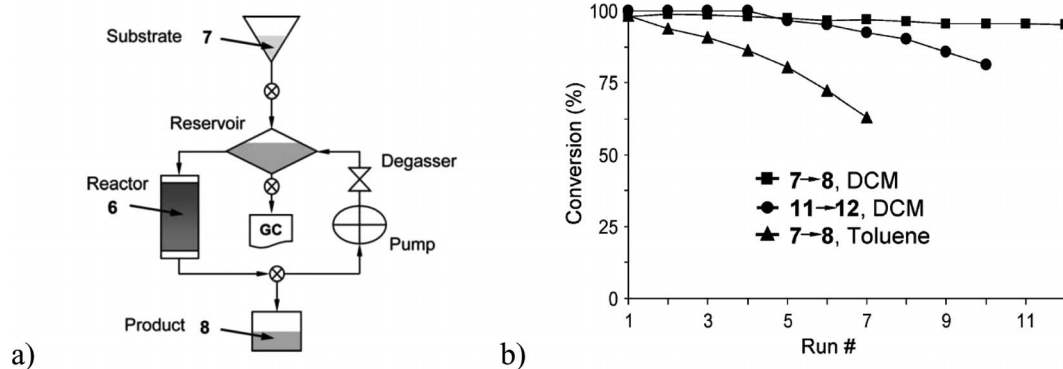
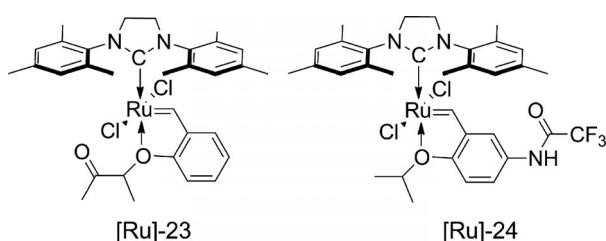


Figure 2. (a) Scheme of the circulating flow reactor. (b) Recyclability study. Reproduced from ref.^[107] with permission of The Royal Society of Chemistry.



Scheme 24. Silica-supported catalysts [Ru]-23 and [Ru]-24 that were used in circulating and continuous flow reactors (see Figure 3).^[108]

The use of a supporting ionic liquid phase (SILP) also represents a recycling strategy and an environmentally benign concept for continuous flow reactions. Wasserscheid et al. immobilized Grubbs catalyst in the form of SILP materials and used them in the gas-phase CM of various substrates under very mild conditions.^[109] Buchmeiser et al. also used the SILP technology for metathesis under continuous flow. These groups prepared ROMP-derived monoliths^[110] with norborn-2-ene, tris(norborn-5-ene-2-ylmethyl-oxy)methylsilane, and [Ru]-1 in the presence of 2-propanol and toluene and surface-grafted them with norborn-5-en-2-

ylmethyl-*N,N,N*-trimethylammonium tetrafluoroborate ([NBE-CH₂-NMe₃][BF₄]). Subsequent immobilization of the ionic liquid (IL) 1-butyl-2,3-dimethylimidazolium tetrafluoroborate ([BDMIM][BF₄]) containing a new dicationic ruthenium alkylidene catalyst created the SILP catalyst. The use of a second liquid transport phase that contained the substrate and that was immiscible with the IL allowed continuous metathesis reactions to be achieved (Figure 4). TONs up to 3700 were obtained for the RCM of various substrates; under continuous flow, TONs up to 900 were recorded, and catalyst leaching less than 0.1% was noted.^[111]

In 2013, Tabari et al. proposed a method to reactivate Ru catalysts after deactivation through a one-pot reactivation procedure by using 1-(3,5-dialkoxyphenyl)-1-phenylprop-2-yn-1-ol (Scheme 25).^[112]

The authors were able to reactivate 43% of the decomposed catalyst (based on Ru content). The in situ reactivated catalyst [Ru]-25 was then reused in the RCM of diethyl diallylmalonate. The catalyst showed a lower activity than that of the original catalyst possibly as a result of the presence of a catalyst inhibitor in the un-reactivated Ru species.

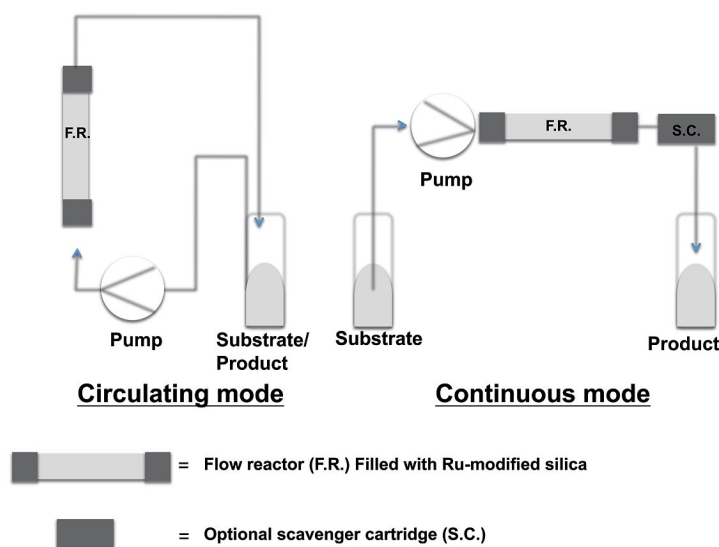


Figure 3. Circulating (left) and continuous (right) flow reactors.^[108]

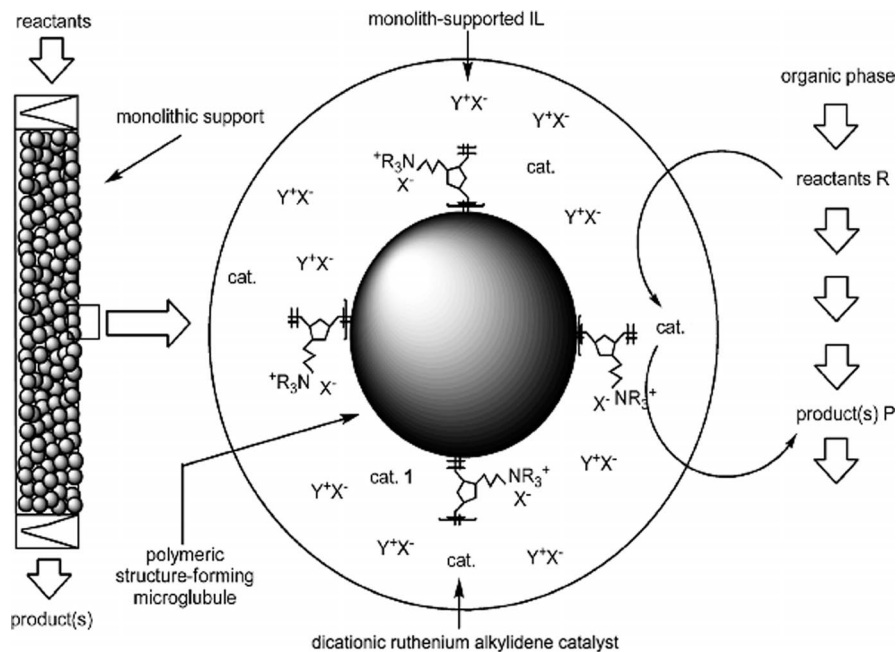
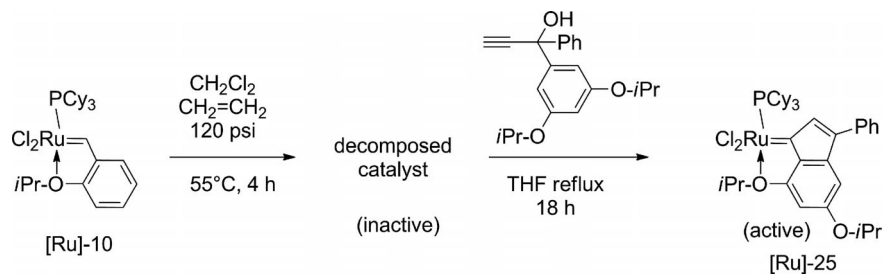


Figure 4. Continuous metathesis under biphasic conditions upon using monolith-supported ILs. $Y^+X^- = [BDMIM][BF_4]$. Reprinted with permission from ref.^[111] Copyright © 2012 Wiley-VCH Verlag GmbH & Co. KGaA.



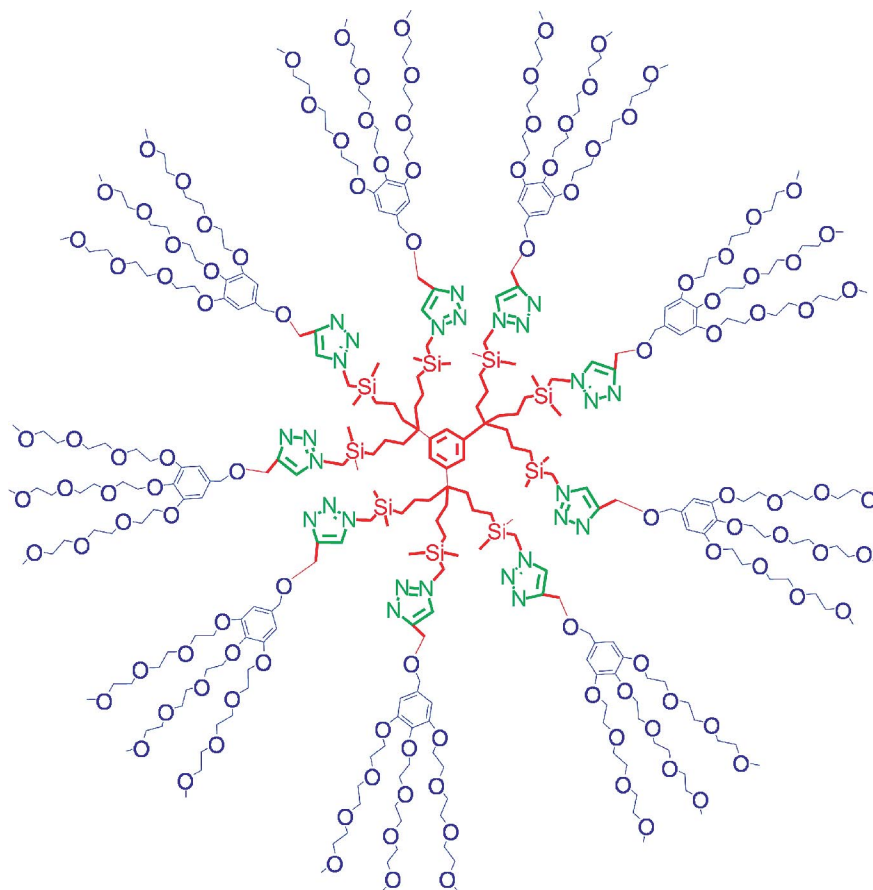
Scheme 25. Reactivation of a decomposed Ru metathesis catalyst.^[112]

Another strategy consisted of using a dendritic nanoreactor (Scheme 26) in water acting as a unimolecular micelle to metathesize water-insoluble organic substrates by using various ruthenium metathesis catalysts. This allowed the amount of olefin metathesis catalyst [Ru]-2 to be lowered to 0.06% for RCM reactions with recycling of the dendrimer. It is probable that the dendritic nanoreactor inhibits the decomposition of the ruthenium–methylene intermediate by encapsulation, which results in a TON that is approximately 50 times the TON obtained in the same reaction in the absence of the dendrimer.^[113]

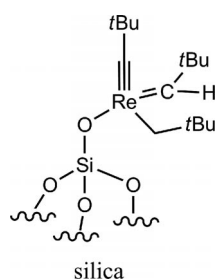
Schrock's Mo and W catalysts were also made insoluble and were thus easy to eliminate from the products, although only a few authors have addressed this problem owing to the air and moisture sensitivity of the catalyst. An elegant, general, and in-depth strategy was developed by Basset's group. They used silica as a ligand to anchor early transition-metal catalysts on solid supports by exploiting the robustness of early-transition-metal–oxygen bonds. This group has indeed provided well-defined heterogeneous catalysts for olefin metathesis upon coordinating active metal

centers (Mo, W, Re) to silica, for which the metal bears ligands that have already proved useful in homogeneous catalysis in addition to silica as an additional ligand.^[75] Given that Schrock had turned metathesis-inactive alkylidene early-transition-metal complexes into active catalysts by the introduction of alkoxy groups, Basset used the beneficial role of the related siloxide ligand from silica for his catalysts. The $[(SiO)M(=CH*t*Bu)(CH_2*t*Bu)_2]$ ($M = Mo$ or W) and $[(SiO)Mo(=NH)(=CH*t*Bu)(CH_2*t*Bu)]$ ^[114] catalysts were active at 25 °C, unlike previously reported ill-defined heterogeneous catalysts and the early Mo and W oxides on silica or alumina. The only oxide that had catalyzed olefin metathesis at 25 °C was Re_2O_7/Al_2O_3 , but it suffered from a low number of active sites, side reactions caused by the acid support, and deactivation of the catalyst.^[115] In contrast, Basset's silica-supported rhenium catalyst $[(SiO)-Re(C*t*Bu)(=CH*t*Bu)(CH_2*t*Bu)]$ (Scheme 27) catalyzed the metathesis of propene at 25 °C with an initial rate of $0.25 \text{ mol mol}^{-1} (\text{Re}) \text{ s}^{-1}$.

The formation of 3,3-dimethylbutene and 4,4-dimethylpentene in a 3:1 ratio resulted from CM between propene



Scheme 26. Dendrimer terminated by tetraethyleneglycol groups acting as a nanoreactor for the metathesis of water-insoluble organic substrates.^[113]



Scheme 27. Example of Basset's highly active silica-supported alkyne metathesis catalysts.^[22]

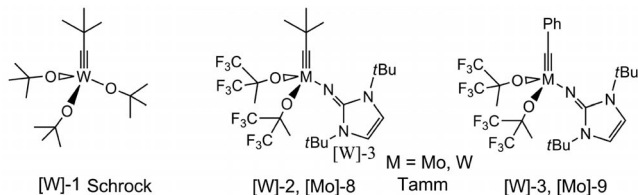
and the neopentylidene ligand, and the ratio of CM products matched the relative stability of the metallacyclobutane intermediates. CM of propene and isobutene and self-metathesis of methyl oleate were also achieved, and the TON reached 900 for the latter reaction, which was unprecedented for heterogeneous and most homogeneous catalysts.^[116,117] In addition to the advantage of separating the solid catalyst from the products, Schrock emphasized that another advantage of the support is to minimize bimolecular alkylidene coupling by retaining the metal centers far apart on the solid support. Finally, Basset's work produced silica-supported Schrock-type metathesis catalysts that are sometimes, as for $[\text{Mo}(\text{NAr})(\text{CHCMe}_2\text{R})(\text{O}i\text{Bu})$

$(\text{OSi}700)]$,^[118] dramatically more active in metathesis with their siloxide ligand than their soluble version with the *t*BuO ligand, although it is difficult to deconvolute the various reasons for increased catalytic activity.

5. Alkyne Metathesis

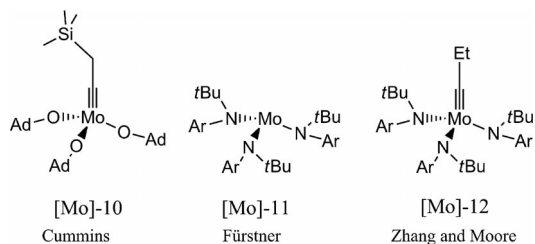
In 1974, Mortreux and Blanchard discovered that alkyne metathesis could be catalyzed by $\text{Mo}(\text{CO})_6$ and resorcinol^[119] and that it proceeds according to the Chauvin mechanism^[21] via a metallacyclobutadiene intermediate.^[120] One category of alkyne metathesis catalyst rapidly appeared from Schrock's research, and that is, the high-valent $[\text{X}_3\text{W}\equiv\text{CR}]$ species in which R does not play an important role in catalysis itself but instead controls the stability of the complex, the initiation rate of the reaction, and the way in which the catalyst is synthesized, but the anionic ancillary ligands X play a decisive role. Schrock and co-workers pioneered the development of 12-electron metal-alkylidyne complexes, such as the commercial prototype neopentylidene complex $[\text{Me}_3\text{CC}\equiv\text{W}(\text{OCCMe}_3)_3]$, $[\text{W}]-1$,^[1,4,121-134] that catalyzes ring-closing alkyne metathesis (RCAM) reactions^[135] and CM, and this catalysis has also been successfully employed in natural product syntheses (Scheme 28).^[136-139] Although this catalyst tolerates many

functional groups, the metathesis becomes problematic if the substrates contain thio ethers, amines, or crown ether segments.^[136] It is suggested that these donor sites might deactivate the catalyst by coordination to its high-oxidation-state tungsten center.^[140,141]



Scheme 28.

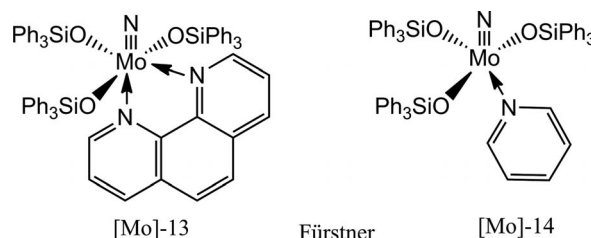
Recently, Tamm and co-workers synthesized variants of Schrock-type alkylidyne complexes, that is, imidazolin-2-iminatotungsten-neopentylidyne complexes such as [W]-2, [Mo]-8, [W]-3, and [Mo]-9 (Scheme 28), in which the imidazolin-2-imide ligands have a strong electron-donating capacity towards the metal center. These complexes display high catalytic activity in a variety of metathesis reactions at ambient temperature with a low catalyst loading. The combination of an electron-donating imido ligand with two electron-withdrawing alkoxide ligands seems to be crucial for creating highly efficient catalyst systems.^[142–147] Tungsten-based catalysts are more active in this case than molybdenum ones, which can be rationalized by the higher Lewis acidity of the tungsten catalysts. Several other molybdenum complexes are active in alkyne metathesis, such as $[\text{Me}_3\text{SiCH}_2\text{C}\equiv\text{Mo}(\text{OAd})_3]$ (Ad = adamantyl), [Mo]-10,^[148] developed by Cummins and co-workers; Fürstner's catalyst $[\text{Mo}\{\text{N}(\text{tBu})\text{Ar}\}_3]$, [Mo]-11 (activated with CH_2Cl_2 in toluene),^[149–151] and $[\text{EtC}\equiv\text{Mo}\{\text{N}(\text{tBu})\text{Ar}\}_3] + p\text{-nitrophenol}$, [Mo]-12, developed by Zhang and Moore^[152–155] (Scheme 29).



Scheme 29.

The [Mo]-12 catalyst requires careful handling under rigorously inert conditions under an argon atmosphere, as this complex is capable of activating many small molecules, including N_2 .^[156] {Note that, remarkably, only Mortreux's catalytic system $[\text{Mo}(\text{CO})_6 + p\text{-chlorophenol}]$ is robust enough to air/moisture but is applicable almost exclusively to hydrocarbon molecules}.^[157] The required absence of N_2 in alkyne metathesis with the use of [Mo]-12 is related to the thermodynamic stability of nitride complexes that are generated from such a metal-alkylidyne complex.^[158] The

more polarized $\text{M}\equiv\text{N}$ bond gives a more positive charge density at the metal center, but poorly donating ancillary ligands destabilize the nitride relative to the alkylidyne ligand in Fürstner's Mo-nitride alkyne metathesis precatalysts [Mo]-13 and [Mo]-14 (Scheme 30), which are isolobal to Mo-alkylidyne analogues.



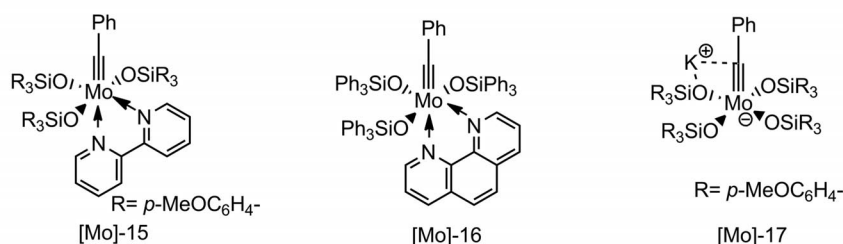
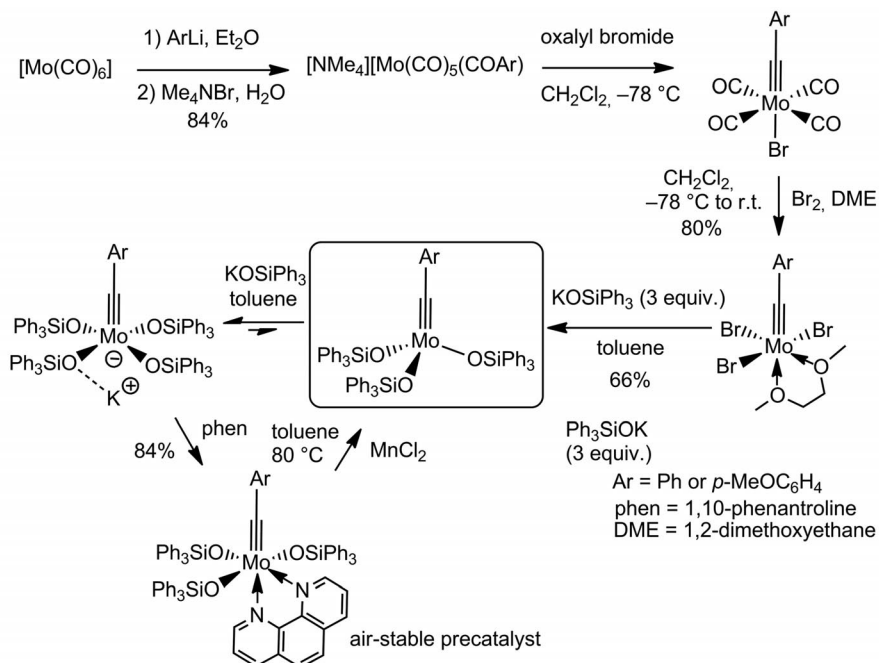
Scheme 30.

This was confirmed by the slow conversion of a nitride complex bearing fluorinated alkoxides into the corresponding propylidyne complex, a nitrile/alkyne cross-metathesis (NACM) reaction, upon heating the nitride complex in the presence of 3-hexyne.^[158–161] Recall that, analogously, at the time of the discovery of olefin metathesis by American industrial chemists, oxygen from air was found to favor olefin metathesis initiated by tungsten inorganic precatalysts, which was much later taken into account by the favorable formation of $\text{W}=\text{O}$ species (by double oxidative addition of O_2) that were converted into $\text{W}=\text{CH}_2$ species upon reaction with olefins. Thus, alkylidyne triarylsilanolate molybdenum complexes developed by Fürstner's group (see the synthesis in Scheme 31) are excellent catalysts for various metathesis reactions and, moreover, are tolerant to polar and/or sensitive groups. The silanolates that leave the Mo^{VI} center are sufficiently Lewis acidic, which favors substrate binding and ensures low barriers to metallacycle formation.^[162] As was the case for alkene catalysts,^[59] these alkyne metathesis catalysts are air stable subsequent to protection by 1,10-phenanthroline or 2,2'-bipyridine.^[163,164]

The intermolecular metathesis reaction of alkynes of the general type $\text{RC}\equiv\text{CMe}$ leads to very good results with the precatalysts shown in Schemes 30 and 31 (less than 10 mol-% of catalyst was used). Precatalysts such as [Mo]-13, [Mo]-15, and [Mo]-16 are activated with MnCl_2 , and during the metathesis reaction, the use of 5 Å molecular sieves^[165,166] is necessary to trap butyne that is formed during the metathesis reaction to displace the equilibrium towards the product.

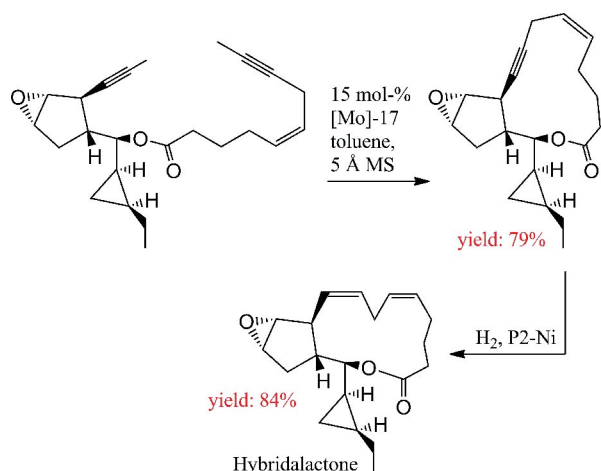
These catalysts are useful in metathesis reactions including alkyne cross-metathesis (ACM), RCAM, acyclic diyne metathesis (ADIMET), and alkyne metathesis polymerization (AMP) and are used in total synthesis. Recent reviews by Fürstner,^[167] Tamm and Xu,^[144] and Moore and Zhang^[168] have focused on alkyne metathesis and applications. These catalysts are used in several total syntheses, and only a few examples are shown below.

The total synthesis of hybridalactone was investigated by Fürstner et al., and the two last steps correspond to RCAM with [Mo]-17 (15 mol-%) before hydrogenation of the triple



Scheme 31. Synthesis of alkylidyne triarylsilanolate molybdenum complexes developed by Fürstner's group.

bond (Scheme 32).^[169,170] The alkyne metathesis step during the total synthesis of cruentaren A was investigated by three



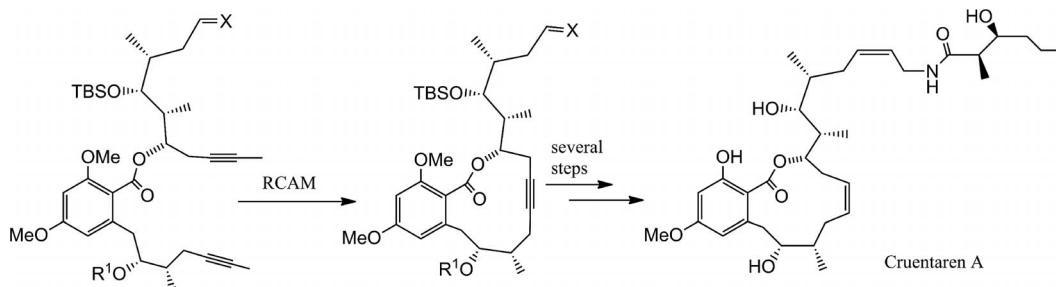
Scheme 32. Two last steps in the total synthesis of hybridalactone.

research groups. The RCAM was conducted with four common catalysts and good results were obtained (Table 1).

Several drawbacks appear even if the complexes are now less sensitive to special groups or are stable in air: (1) The use of anhydrous solvents is imperative because hydrolysis^[175,176] is the most serious problem. (2) Dimerization of the complex can occur if the ligands are too small. (3) The use of terminal alkynes can be a limitation in the absence of specific conditions (see below), which leads to deactivation of the catalyst with the formation of deprotonated metallocyclobutadienes (DCMs; Scheme 33).^[177–184]

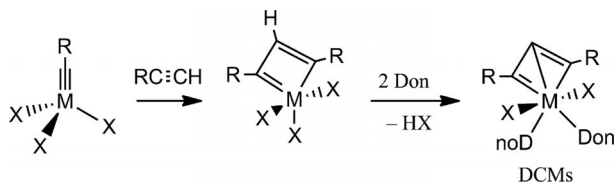
There are a few examples of terminal alkyne metathesis (TAM) reactions, however. TAM was first reported by Mortreux et al. with the neopentylidyne complex $[\text{Me}_3\text{CC}\equiv\text{W}(\text{O}i\text{Bu})_3]$, [W]-2, which is able to catalyze TAM of various aliphatic alkynes such as 1-pentyne, 1-hexyne, and 1-heptyne in diethyl ether.^[185,186] The reaction is favored by the addition of quinuclidine as an external ligand, and its use leads to 80% conversion to 6-dodecyne in the case of the TAM of 1-heptyne within 1 min at 80 °C with the catalyst (4 mol-%).^[187]

Table 1. End of the synthesis path to cruentaren A. Alkyne metathesis step: comparison of various Mo and W catalysts.



R ^[a]	X ^[b]	Catalyst (mol-%)	T [°C]	Yield [%]	Ref.
TIPS	H, ODMB	[W]-2 (10)	85	91	[171]
TBDPS	=CHCH ₂ OTHP	[W]-2 (10)	80	— ^[c]	[172]
TBDPS	=CHCH ₂ OTHP	[Mo]-11 (10) ^[d]	80	87	[172]
TBDPS	=CHCH ₂ OTHP	[Mo]-17 (2)	80	82	[173]
TIPS	=CHCH ₂ OPMB	[Mo]-14 (40)	110	75	[174]

[a] TIPS = triisopropylsilyl, TBDPS = *tert*-butyldiphenylsilyl. [b] DMB = 3,4-dimethoxybenzyl, THP = tetrahydropyranyl, PMB = *p*-methoxybenzyl. [c] Only the THP group in the substrate was cleaved. [d] Activated CH₂Cl₂.



Scheme 33. Formation of DCMs with terminal alkynes in the presence of a donor ligand (Don).

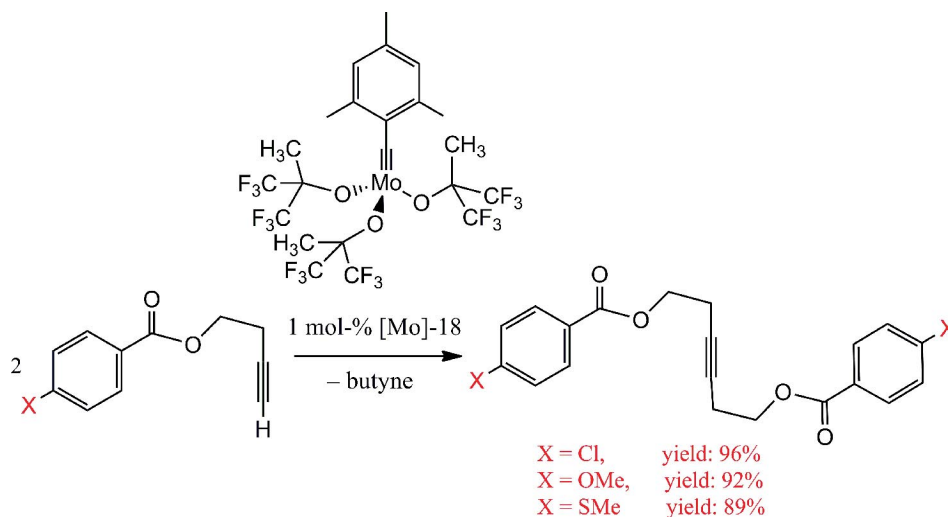
Tamm and co-workers very recently reported the synthesis of the new catalyst [Mo]-19, which permits alkyne metathesis of internal and terminal alkynes. TAM works very well at room temperature in toluene in 1 h with [Mo]-18 (1 mol-%). The reaction was conducted with several terminal alkynes; moreover, RCM of terminal alkynes also works (Scheme 34).

The improved catalytic activity of [Mo]-19 for TAM relative to other alkyne metathesis catalysts was taken into ac-

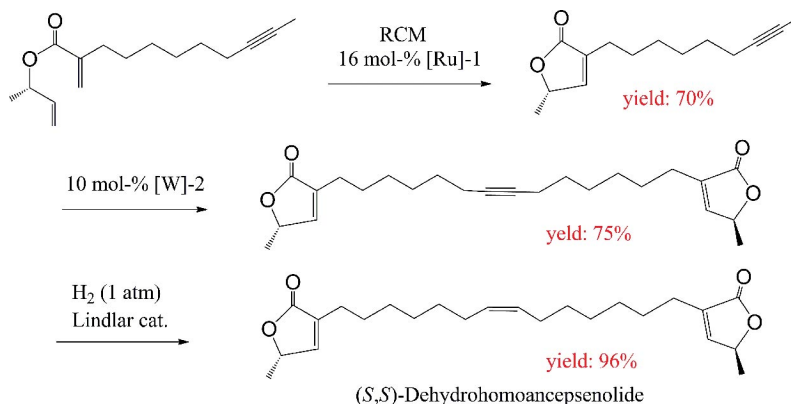
count by (1) the reduced formation of deprotonated metallacyclobutadiene complexes as a result of the low basicity of the hexafluoro-*tert*-butanolato ligand in comparison with the alkoxy or silanolate ligand of classic catalysts; (2) the absence of a donor ligand and coordinating solvent to stabilize the deprotonated metallacyclobutadiene, which leads to a highly active catalyst; and (3) high dilution that is highly favorable in suppressing polymerization and/or intermolecular deactivation processes.^[188]

Alkyne metathesis is strictly orthogonal to alkene metathesis, because none of the commonly used metal alkylidyne catalysts are capable of activating olefins of any kind. The total synthesis of (*S,S*)-dehydrohomoancepsenolide confirms this orthogonality. Indeed, the first step in the RCM in the presence of [Ru]-1 is compatible with the alkyne group in the molecule (Scheme 35).^[189]

The other way round, however, the orthogonal character is less strict: alkene metathesis catalysts of the Grubbs and



Scheme 34. Homocoupling of various terminal alkynes.



Scheme 35. Combined alkene and alkyne metathesis steps as part of the total synthesis of (S,S)-dehydrohomoancepsenolide.

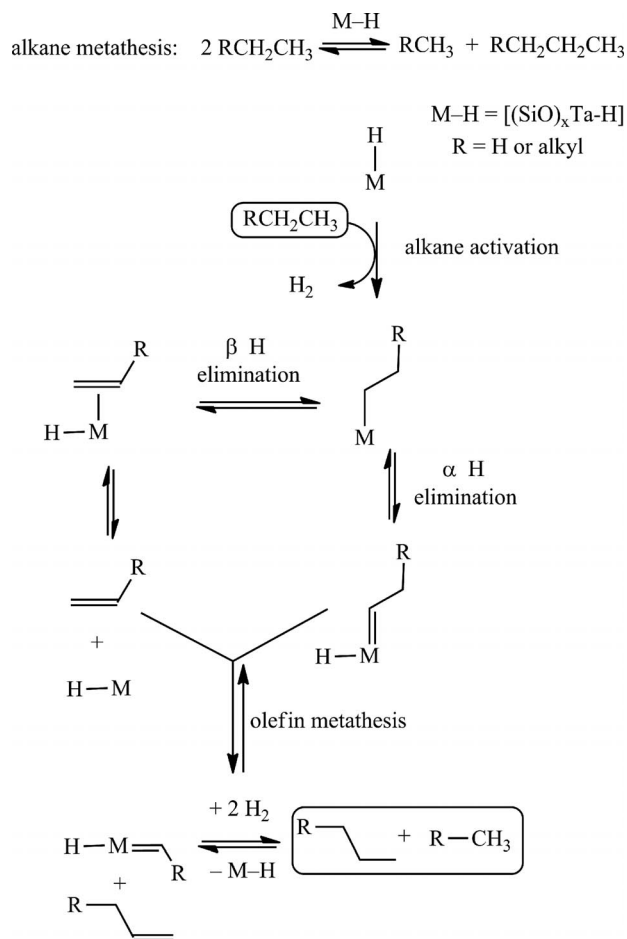
Schrock types can react with alkynes, as evidenced from a large body of EYM and polymerization chemistry.^[190–193]

Finally, as for alkene metathesis (see below), the fixation of alkyne metathesis catalysts was developed by Basset and co-workers by using the concept of surface organometallic chemistry (SOMC), whereby an oxide support such as silica serves as an efficient ancillary ligand set for recoverable alkyne metathesis catalysts. Thus, Basset's group designed *inter alia* the very efficient catalyst [(Silica-O)Re(C-*t*Bu)(=CH-*t*Bu)(CH₂*t*Bu)], a rhenium–silica complex containing both alkylidene and alkylidyne ligands, for the fast metathesis of 2-pentyne. Note that the silyloxy ligands from silica in Basset's catalysts serve as the triarylsilanolate ligands in Fürstner's complexes to increase the favorable Lewis acidity of the catalytically active metal center discussed above.^[22,117]

6. Alkane Metathesis

A family of well-defined single-site heterogeneous Ta- and W-alkylidene catalysts containing siloxy ligands that metathesize alkanes were also reported by Basset's group.^[22,194] Butane metathesis was achieved by the Chevron company in the 1970s with the use of the heterogeneous catalyst Pt–Al₂O₃ at 400 °C.^[195] In contrast, Basset's catalysts resulted from the reactions of silica with Schrock's high-oxidation-state olefin metathesis catalysts. The siloxy ligand brought by silica played the role of the alkoxy ligands and favored metathesis activity; improved reactivity of the catalyst with the siloxy ligand resulted from the increased metal electrophilic properties relative to those of the alkoxy complexes. In these systems, the metathesis of olefins follows *in situ* alkane dehydrogenation.^[196–203] In particular, Basset et al. noticed that propane and propene gave similar C_{*n*+1}/C_{*n*+2} ratios of CM products on silica-supported Ta–neopentylidene catalysts at 150 °C. The complexes [(SiO)_{*x*}Ta(=CH*t*Bu)(CH₂*t*Bu)_{3–*x*}] (*x* = 1 or 2) catalyzed the metathesis of alkanes into a mixture of higher and lower alkanes at 150 °C, as did the hydride complex [(SiO)_{*x*}TaH]. For instance, ethane reversibly yielded methane and propane. The mechanism was suggested to proceed by a composite series of σ -bond metathesis reactions of the C–H

bonds and α - and β -eliminations (rather than direct σ -bond metathesis of the C–C bonds). The α -elimination from d² metal–methyl or metal–alkyl species formed HTa=CH₂ or HTa=CHR, respectively, and the mechanism was proposed to then follow an alkene metathesis pathway with olefins generated by β -elimination (including metallacyclobutane intermediates as in the Chauvin mechanism, see Scheme 36).^[22,194,203]



Scheme 36. Alkane metathesis at 150 °C with Basset's single-site early-transition-metal catalysts containing siloxy ligands and its mechanism. The alkane activation step involves σ -bond metathesis between the M–H bond and an alkane C–H bond.^[194]

Multiple activation by a single site and in-depth characterization techniques of surface organometallic species resulted in very efficient, well-controlled, and robust heterogeneous metathesis catalysts for alkanes, alkenes, and alkynes.

Goldman and Brookhart also recently directly mimicked the system of the Chevron company^[195] by using well-defined homogeneous catalysts for alkane metathesis. The challenge was the compatibility between the alkane dehydrogenation catalyst and the olefin metathesis catalyst operating separately in solution. Successful “tandem” catalytic activation by using homogeneous catalysts for both alkane dehydrogenation and olefin metathesis was thus reported in 2006. The dehydrogenation catalysts are Ir pincer complexes nicely designed and improved by Goldman and further optimized by both research groups, and the olefin metathesis catalyst is a Schrock-type complex such as $[\text{Mo}(\text{N-Ar})(=\text{CHCMe}_2\text{Ph})(\text{OR}_{\text{F}_6})_2]$ (OR_{F_6} = perfluoroalkoxy group) or a heterogeneous catalyst, Re_2O_7 on Al_2O_3 . Reactions in neat octane or decane require heating over several days at more than 125 °C to approach alkane metathesis equilibrium, but the reaction is limited by the decomposition of the Mo-alkylidene catalyst.^[204–207] More than 40 Mo and W alkylidene catalysts were tested, and the W catalysts outperformed Mo ones; the greatest activity was obtained with the use of $[\text{W}(\text{NAr})(=\text{CHCMe}_2\text{Ph})(\text{OSiPh}_3)_2]$ (Scheme 37). Indeed, as in Basset’s catalyst (see above), the siloxy ligand brings an advantage over the alkoxy ligand, because it presumably reduces the donation of the p electron density to the metal.^[58]

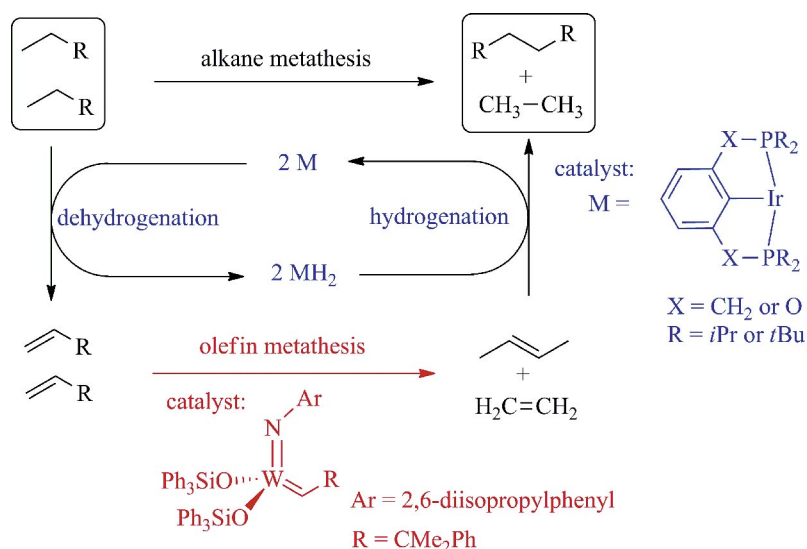
7. Polymer Chemistry

ROMP is one of the most important olefin metathesis reactions. It is mostly used for norbornene derivatives (high strain cycle: 27.2 kcal mol⁻¹). Other cycloolefins that undergo ROMP are those that are also subjected to release of

ring strain upon opening, which provides the driving force for the reaction, that is, in particular cyclobutene, cyclopentene, cyclooctene (high strain cycle: 7.4 kcal mol⁻¹), and dicyclopentadiene. Cyclopentene was polymerized by ROMP to *trans*- and *cis*-cyclopentenamers for the rubber industry soon after the discovery of olefin metathesis.^[208] The ROMP reaction of 2-norbornene catalyzed by RuCl_3/HCl in butanol operates in air and gives a *trans* polymer of molecular weight $>3 \times 10^6$ g mol⁻¹ in 90% yield (Norsorex). The ROMP reaction of *endo*-dicyclopentadiene (obtained from naphtha crackers) leads to opening of the strained norbornene ring to yield linear polymers. Under certain conditions, however, the cyclopentene double bond also opens to give cross-linking with simple tungsten chloride catalysts, but Grubbs-type ruthenium catalysts allow undesirable odors to be avoided. These polymers are largely used for heavy-vehicle applications. Degussa has been producing Vestenamer 8012 by ROMP of cyclooctene since 1980, a polymer that is useful in blends.^[209,210]

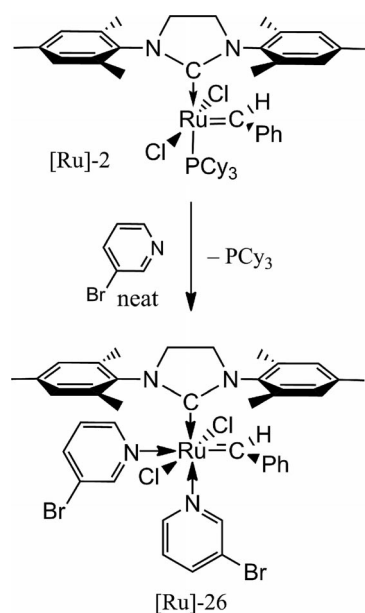
In recent years, stereocontrol of the monomer units introduced by ROMP with regard to the *cis/trans* configuration of the exocyclic double bond, the configuration of the allylic bridgehead carbon atoms, and the linkage of unsymmetrically substituted monomers has been addressed.^[211,212] For instance, a Schrock-type Mo initiator with hexa(isopropyl)terphenoxide and mono(pyrrolide) ligands allowed *cis* selectivity in the ROMP of norbornadiene and cyclooctene derivatives, although this initiator suffered from high sensitivity towards moisture and oxygen.^[213] Another example is the alternative polymerization of cyclooctene and norbornene that was achieved with Ru initiators on the basis of the different insertion rates of norbornene and cyclooctene that depend on the monomer inserted just before.^[214–219]

Most advances in polymer materials synthesized by ROMP have involved Ru benzylidene and indenylidene catalysts.^[219,220] These ruthenium-based initiators are usually



Scheme 37. Alkane metathesis system designed by the Goldman and Brookhart groups by using compatible Ir dehydrogenation/hydrogenation catalyst together and Schrock’s W olefin metathesis catalyst.

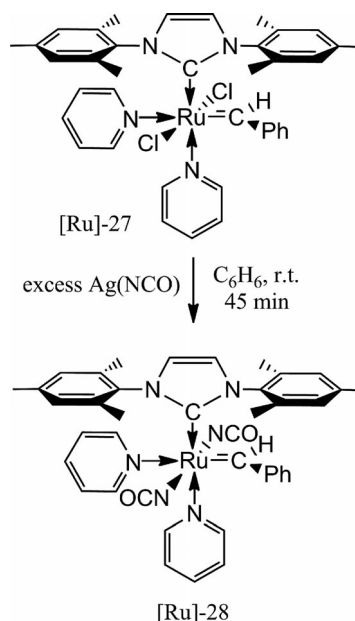
chosen for ROMP because of their functional group tolerance and their ability to achieve copolymer syntheses.^[221,222] For instance, the third-generation Grubbs catalyst [Ru]-26, synthesized from [Ru]-2 and 3-bromopyridine [Equation (6)], and other analogous bis(pyridine) complexes are among the fastest-initiating Ru systems. This fast initiation of [Ru]-26 has proven to be useful in the production of polymers with narrow polydispersity and for the synthesis of block copolymers.^[223] Since the discovery of this catalyst, research on ROMP has increased markedly (more than 200 publications in 2009), and thus, only some examples will be described below.



The problem of competing interchain metathesis and backbiting can be circumvented with by performing the ROMP reactions at -20 to -30 °C. Alternatively, the possibility of conducting ROMP reactions more conveniently for both bulky and unencumbered norbornene monomers at room temperature was disclosed by Fogg's group by using the Ru–isocyanate initiator [Ru]-28 obtained upon reaction of [Ru]-27 with AgNCO [Equation (7)].^[224]

Highly functionalized polynorbornene homopolymers were synthesized by ROMP, for instance, with radical moieties [2,2,6,6-tetramethylpiperidin-1-yloxy] (TEMPO) for applications as cathode active materials in organic radical batteries.^[225] Random copolymer synthesis allows, for instance, optical sensors to be incorporated.^[220] Well-defined block copolymers with narrow size distributions have been reported.^[217] End-group functionalization can be implemented by using a carbene-functionalized initiator, a chain-transfer agent during polymerization, or a terminating agent and is a valuable means for combining different polymerization techniques [reversible addition–fragmentation chain transfer (RAFT), atom-transfer radical polymerization (ATRP), etc.].^[226] Materials applications include resistant plastics, antifouling coating, thermoplastic elasto-

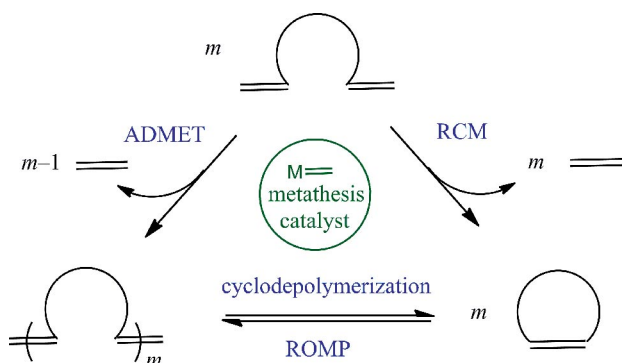
mers, and emulsifiers,^[227] liquid crystals,^[228] porous polymers,^[229] and self-healing materials.^[230]



New-generation olefin-metathesis catalysis opens new avenues for future design of sophisticated well-defined block copolymers with specific physical properties. For instance, General Electric developed poly(norbornene-decaborane) copolymers that act as single sources of carbon nitride and boron carbonitride ceramics. The ROMP reaction was also used to synthesize nanomaterials of biological interest. Recently, Grubbs et al. reported the preparation of drug-loaded bivalent-bottle-brush polymers by ROMP.^[231] In this work, they used ROMP to assemble a norbornene macromonomer containing two different branches, a PEG chain (for water solubility), and a drug attached to the monomer through a photocleavable linker. The drug was released unmodified, and the release could be controlled. In 2011, the same group developed a different approach for the synthesis of a similar polymer.^[232] They first polymerized by ROMP a norbornene containing a PEG chain and a chloride function. After replacing the chloride by azide they used the Sharpless click reaction to attach a doxorubicin moiety containing the same photodegradable linker. The size of the macromonomer is a very important factor in the polymerization process.^[233,234] Indeed, in some cases the steric bulk could provoke high polydispersity index values and incomplete polymerization reactions.^[235] Recently, functionalizable and biodegradable polymers were synthesized by ROMP, which could also be applied for releasing applications.^[236] ROMP has been used for functionalized supports^[237] in some cases, as shown in the above example of the ROMP-derived monoliths synthesized by Buchmeiser et al. The latter allows continuous metathesis of various substrates^[111] and also the separation of biomolecules.^[238,239] Recent reviews on ROMP chemistry have been published by Slugovc et al.,^[240] Abdellatif^[241] et al., and

Kilbinger et al.^[242] Besides ROMP, polymer materials chemistry has also been developed by using acyclic diene metathesis (ADMET) polymerization that proceeds if the RCM of the terminal diene is sterically inhibited.

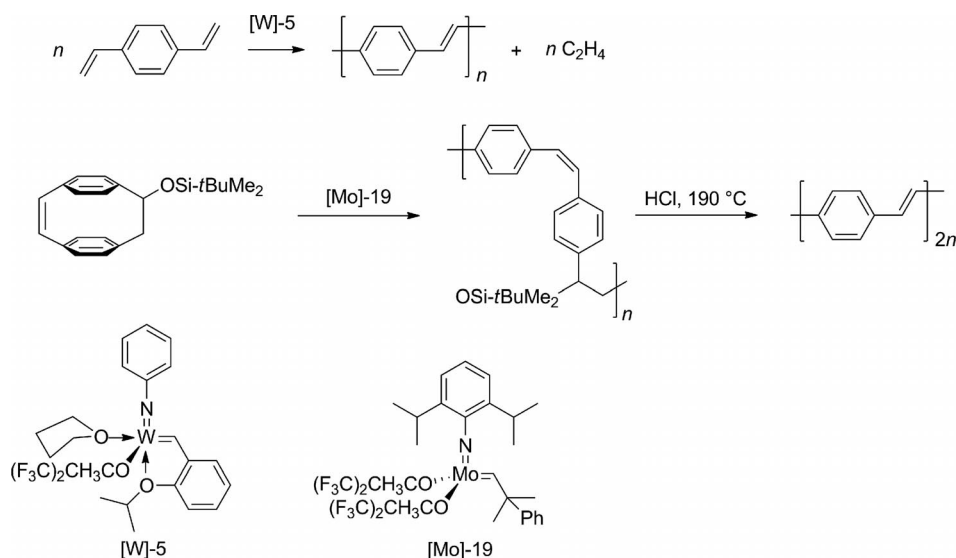
A unifying view should be highlighted by recalling that the ROMP and ADMET reactions are also connected to RCM and that the reverse reaction of ROMP, cyclodepolymerization, is also known (Scheme 38). The equilibrium between RCM and its reverse reaction, which leads to oligomerization, and the ring-chain equilibria in ROMP were emphasized and analyzed in depth by Monfette and Fogg.^[243]



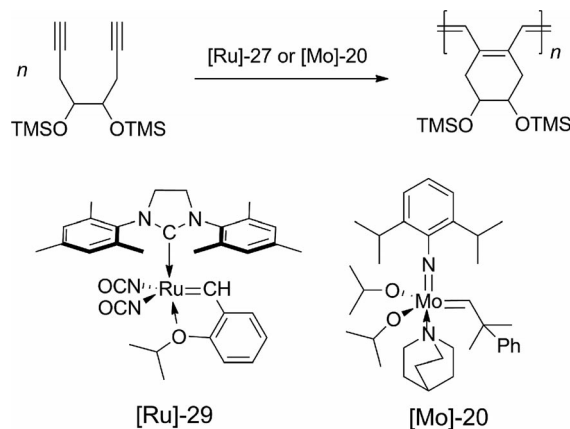
Scheme 38. Monfette and Fogg's scheme of the relationships between ring-closing, ring-opening, and polymerization/depolymerization processes in metathesis reactions initiated by metal-carbene complexes.^[243]

Recently, Bunz et al. reviewed the use of both ROMP and ADMET in the synthesis of conjugated polymers^[244] that are of great interest for organic electronics. For example, poly(*p*-phenylene vinylene) (PPV) was synthesized by both ROMP and ADMET (Scheme 39).

The synthesis of conjugated polymers was also performed by the reaction of diyne cyclopolymerization (Scheme 40).^[245]

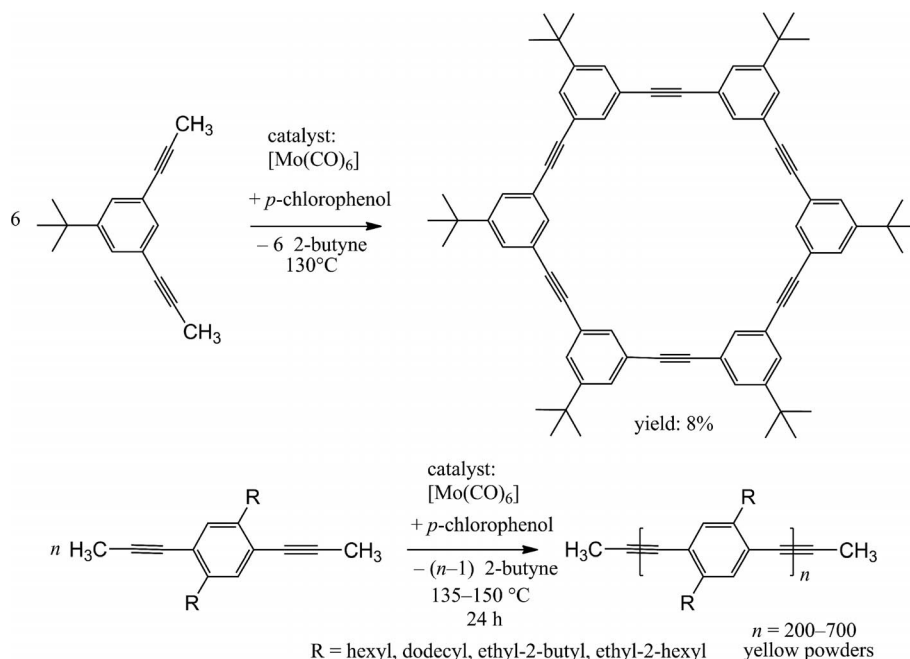


Scheme 39. Synthesis of PPV by two different paths: ADMET and ROMP.



Scheme 40. Example of diyne cyclopolymerization.

The polymerization of alkenes by ADMET^[246,247] (Scheme 38) occupies a less important place in current polymer chemistry than the ROMP process, but variations in the monomer structure provide access to a broad range of precisely defined polymers that allows direct correlation of structure–property relationships.^[248] The efficiency of this metathesis polymerization was enhanced by the works of Wagener and co-workers. Thus, polyolefins with a perfectly controlled lamellar thickness and thick distribution were synthesized,^[249] as were precisely defined primary structures of olefins containing halogens.^[250] The ADMET polymerization is a valuable technique for the preparation of sophisticated end-group functionalized polymers in a straightforward fashion. For example, Barner-Kowollik and Meier's group reported highly orthogonal functionalization of ADMET polymers through photoinduced Diels–Alder reactions for the synthesis of triblock copolymers.^[251] The synthesis of defined macromolecular architectures such as diblock copolymers and star-shaped structures by ADMET is also known.^[252]

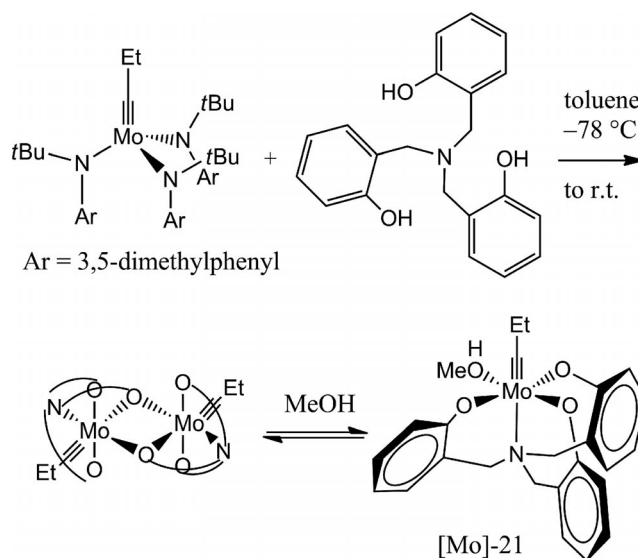


Scheme 41. Examples of ADIMET cyclooligomerization developed by Bunz's group.

Concerning metathesis polymerization of alkynes, ring-opening alkyne metathesis polymerization (ROAMP) and acyclic diene metathesis polymerization (ADIMET) have also been used.

ADIMET has been widely employed for the synthesis of poly(aryleneethynylene)s (PAEs) that are remarkable for their electronic and optical properties.^[244,253–255] [W]-2 or Mortreux's catalyst are used for this polymerization, which leads to molecules with higher molecular weights and fewer defects than polymers obtained by Sonogashira C–C coupling.^[256,257] Cyclooligomerization^[258–266] of dipropynylated arenes has been studied by several groups. Bunz pioneered this chemistry and synthesized several oligomers including a hexagonal cyclooligomer upon linking six 1,3-dipropynylated arenes and polymers by ADIMET (Scheme 41).^[264,265]

For ROAMP, very few examples have been reported because of the lack of catalysts that can initiate controlled metathesis polymerization and also because of the shortage of useful substrates for this reaction. The first example of an effective well-characterized catalytic system for ROAMP was described recently by Nuckolls's group.^[267] The bench-stable molybdenum alkylidyne complex was generated in situ according to Jyothish and Zhang's report^[268] and was subsequently isolated and well characterized. The system of Jyothish and Zhang proved to be very efficient for alkyne homodimerization, RCAM and ACM and avoids undesired polymerization (coming from an associative pathway). After isolation, Nuckoll's group observed a dimeric complex, catalyst [Mo]-21 (Scheme 42), that is not sensitive to water and is active for ROAMP in the presence of MeOH.



Scheme 42. Synthesis of the catalyst [Mo]-21, active in ROAMP.

8. Conclusion and Outlook

Over the last decade, tremendous progress has been made in the efficiency and recyclability of metathesis reactions. In this microreview, we have emphasized recent trends and challenges concerning catalyst selectivity and metal recovery. The new generations of metathesis catalysts have not only improved the robustness of olefin and alkyne metathesis catalysts, but also provided stereo- and enantioselectivity for olefin metathesis that were not accessible earlier. In the molybdenum-alkylidene catalyst family, this im-

provement is related to the discovery of the mono(pyrrolide) complexes, whereas in the ruthenium–benzylidene catalyst family, this improvement is due to the introduction of catalysts containing metal–alkyl bonds with a chelating oxoanionic ligand. A strategy to direct *E* selective CM was based on thermodynamic control, that is, on the choice of substrates, but it is the design of the relative bulk of the catalyst ligands that dictates kinetic control of *Z* selectivity. The continuous design of new stereochemical subtleties of ligands will be needed for further improvement in this direction, towards the enantioselective syntheses of chiral organic molecules. Considerable recent improvement in the efficiency and stability of alkyne metathesis catalysts on the basis of fundamental discoveries of a new family of molybdenum–alkylidyne catalysts has already produced an impressive body of applications in the synthesis of complex organic molecules. Finally, alkane metathesis is not only dependent on alkene metathesis catalysts, but also on the delicate compatibility between olefin metathesis and hydrogenation/dehydrogenation catalysts either on the same metal center or different ones.

The availability of highly selective catalysts now produces many developments in organic synthesis toward applications in oleochemistry, agrochemicals (insect pheromones, etc.), fragrances, drugs, and pharmacy. Although this microreview has only included key representative examples of applications to organic synthesis, recent reviews have presented more comprehensive treatments in this area.^[269–273] The challenge now also involves transfer of the metathesis procedures to industry, which requires the scale-up of the production of pure chemicals at low costs without contamination by metals.

Acknowledgments

Financial support from Université Bordeaux 1, the Centre National de la Recherche Scientifique, and the Agence Nationale pour la Recherche is gratefully acknowledged.

- [1] a) R. H. Grubbs (Ed.), *Handbook of Metathesis*, vol. 1: *Catalyst Development*, Wiley-VCH, Weinheim, Germany, **2003**; b) R. H. Grubbs (Ed.), *Handbook of Metathesis*, vol. 2: *Applications in Organic Synthesis*, Wiley-VCH, Weinheim, Germany, **2003**; c) R. H. Grubbs (Ed.), *Handbook of Metathesis*, vol. 3: *Applications in Polymer Synthesis*, Wiley-VCH, Weinheim, Germany, **2003**.
- [2] Y. Chauvin, *Angew. Chem.* **2006**, *118*, 3824–3831; *Angew. Chem. Int. Ed.* **2006**, *45*, 3740–3747 (Nobel Lecture).
- [3] R. H. Grubbs, *Angew. Chem.* **2006**, *118*, 3845–3850; *Angew. Chem. Int. Ed.* **2006**, *45*, 3760–3765 (Nobel Lecture).
- [4] R. R. Schrock, *Angew. Chem.* **2006**, *118*, 3832–3844; *Angew. Chem. Int. Ed.* **2006**, *45*, 3748–3759 (Nobel Lecture).
- [5] A. Fürstner, *Angew. Chem.* **2000**, *112*, 3140–3172; *Angew. Chem. Int. Ed.* **2000**, *39*, 3012–3043.
- [6] S. J. Connon, S. Blechert, *Angew. Chem.* **2003**, *115*, 1944–1968; *Angew. Chem. Int. Ed.* **2003**, *42*, 1900–1923.
- [7] R. R. Schrock, A. H. Hoveyda, *Angew. Chem.* **2003**, *115*, 4740–4782; *Angew. Chem. Int. Ed.* **2003**, *42*, 4592–4633.
- [8] H. Clavier, K. Grela, A. Kirschning, M. Mauduit, S. P. Nolan, *Angew. Chem.* **2007**, *119*, 6906–6922; *Angew. Chem. Int. Ed.* **2007**, *46*, 6786–6801.
- [9] L. Delaude, A. F. Noël, *Metathesis*, in: *Kirk-Othmer Encyclopedia of Chemical Technology* (Ed.: A. Seidel), Wiley, New York, **2007**, vol. 26, p. 920–958.
- [10] A. M. Thayer, *Chem. Eng. News* **2007**, *85*, 37–47.
- [11] V. Dragutan, I. Dragutan, A. Demonceau, *Coord. Chem. Rev.* **2007**, *251*, 765–794.
- [12] P. Sledz, M. Mauduit, K. Grela, *Chem. Soc. Rev.* **2008**, *37*, 2433–2442.
- [13] M. Bieniek, A. Michowska, D. L. Usanov, K. Grela, *Chem. Eur. J.* **2008**, *14*, 806–818.
- [14] C. Samojłowicz, M. Bieniek, K. Grela, *Chem. Rev.* **2009**, *109*, 3708–3742.
- [15] C. E. Diesendruck, E. Tzur, N. G. Lemcoff, *Eur. J. Inorg. Chem.* **2009**, 4185–4203.
- [16] G. C. Vougioukalakis, R. H. Grubbs, *Chem. Rev.* **2010**, *110*, 1746–1787.
- [17] Y. Imamoglu, V. Dragutan (Eds.), *Metathesis Chemistry*, Springer, Dordrecht, **2007**.
- [18] V. Dragutan, A. Demonceau, I. Dragutan, E. Sh. Finkelshtein (Eds.), *Green Metathesis Chemistry*, Springer, Dordrecht, **2010**.
- [19] S. Kress, S. Blechert, *Chem. Soc. Rev.* **2012**, *41*, 4389–4408.
- [20] D. Astruc, *New J. Chem.* **2006**, *30*, 1848–1852.
- [21] Y. Chauvin, J. L. Hérisson, *Makromol. Chem.* **1971**, *141*, 161–176.
- [22] J.-M. Basset, C. Copéret, D. Soulivong, M. Taoufik, J. T. Cazat, *Acc. Chem. Res.* **2010**, *43*, 323–334.
- [23] P. Schwab, M. B. France, J. W. Ziller, R. H. Grubbs, *Angew. Chem.* **1995**, *107*, 2179–2181; *Angew. Chem. Int. Ed. Engl.* **1995**, *34*, 2039–2041.
- [24] M. Scholl, S. Ding, C. W. Lee, R. H. Grubbs, *Org. Lett.* **1999**, *1*, 953–956.
- [25] W. A. Herrmann, *Angew. Chem.* **2002**, *114*, 1342–1363; *Angew. Chem. Int. Ed.* **2002**, *41*, 1290–1309.
- [26] S. Díez-González, N. Marion, S. P. Nolan, *Chem. Rev.* **2009**, *109*, 3612–3676.
- [27] D. Bourissou, O. Guerret, F. P. Gabbaï, G. Bertrand, *Chem. Rev.* **2000**, *100*, 39–92.
- [28] D. Astruc, *Organometallic Chemistry and Catalysis*, Springer, Heidelberg, **2008**, ch. 9, 15, and 21.
- [29] K. Grela, S. Harutyunyan, A. Michrowska, *Angew. Chem.* **2002**, *114*, 4210–4212; *Angew. Chem. Int. Ed.* **2002**, *41*, 4038–4040.
- [30] A. Michrowska, R. Bujok, S. Harutyunyan, V. Sashuk, G. Dolgonos, K. Grela, *J. Am. Chem. Soc.* **2004**, *126*, 9318–9325.
- [31] S. J. Connon, A. M. Dunne, S. Blechert, *Angew. Chem.* **2002**, *114*, 3989–3993; *Angew. Chem. Int. Ed.* **2002**, *41*, 3835–3838.
- [32] H. Wakamatsu, S. Blechert, *Angew. Chem.* **2002**, *114*, 2509–2511; *Angew. Chem. Int. Ed.* **2002**, *41*, 2403–2405.
- [33] P. S. Kumar, K. Wurst, M. R. Buchmeiser, *Organometallics* **2009**, *28*, 1785–1790.
- [34] J. Bouffard, B. K. Keitz, R. Tonner, G. Guisado-Barrios, G. Frenking, R. H. Grubbs, G. Bertrand, *Organometallics* **2011**, *30*, 2617–2627.
- [35] B. K. Keitz, J. Bouffard, G. Bertrand, R. H. Grubbs, *J. Am. Chem. Soc.* **2011**, *133*, 8498–8501.
- [36] Review: E. B. Anderson, M. R. Buchmeiser, *Synlett* **2012**, *23*, 185–207.
- [37] T. S. Albach, S. Mix, D. Fischer, S. Maechling, J. O. Krause, C. Sievers, S. Blechert, O. Nuyken, M. R. Buchmeiser, *J. Org. Chem.* **2005**, *70*, 4687–4694.
- [38] P. S. Kumar, K. Wurst, M. R. Buchmeiser, *Chem. Asian J.* **2009**, *4*, 1275–1983.
- [39] M. R. Buchmeiser, I. Ahmad, V. Gurrarn, P. S. Kumar, *Macromolecules* **2011**, *44*, 4098–4106.
- [40] J. C. Conrad, D. Amoroso, P. Czechura, G. P. A. Yap, D. E. Fogg, *Organometallics* **2003**, *22*, 3634–3636.
- [41] S. D. Drouin, H. M. Foucault, G. P. A. Yap, D. E. Fogg, *Can. J. Chem.* **2005**, *83*, 748–754.
- [42] J. C. Conrad, H. H. Parnas, J. L. Snelgrove, D. E. Fogg, *J. Am. Chem. Soc.* **2005**, *127*, 11882–11883.

- [43] J. C. Conrad, K. D. Camm, D. E. Fogg, *Inorg. Chim. Acta* **2006**, 359, 1967–1973.
- [44] S. Monfette, D. E. Fogg, *Organometallics* **2006**, 25, 1940–1944.
- [45] A. Fürstner, A. F. Hill, M. Liebl, J. D. E. T. Wilton-Ely, *Chem. Commun.* **1999**, 601–602.
- [46] A. Fürstner, K. Radkowski, C. Wirtz, R. Goddard, C. W. Lehmann, R. Mynott, *J. Am. Chem. Soc.* **2002**, 124, 7061–7069.
- [47] B. Scheiper, F. Glorius, A. Leitner, A. Fürstner, *Proc. Natl. Acad. Sci. USA* **2004**, 101, 11960–11965.
- [48] L. Jafarpour, H.-J. Schane, E. D. Stevens, S. P. J. Nolan, *Organometallics* **1999**, 18, 5416–5419.
- [49] H. Clavier, J. L. Petersen, S. P. Nolan, *J. Organomet. Chem.* **2006**, 691, 5444–5447.
- [50] For a review of indenylideneruthenium metathesis catalyst, see: V. Dragutan, I. Dragutan, F. Verpoort, *Platinum Met. Rev.* **2005**, 49, 33–40.
- [51] A. Fürstner, O. Guth, A. Düffels, G. Seidel, M. Liebl, B. Gabor, R. Mynott, *Chem. Eur. J.* **2001**, 7, 4811–4820.
- [52] P. E. Romero, W. E. Piers, R. McDonald, *Angew. Chem.* **2004**, 116, 6287–6291; *Angew. Chem. Int. Ed.* **2004**, 43, 6161–6165.
- [53] P. E. Romero, W. E. Piers, *J. Am. Chem. Soc.* **2005**, 127, 5032–5033.
- [54] P. E. Romero, W. E. Piers, *J. Am. Chem. Soc.* **2007**, 129, 1698–1704.
- [55] E. F. Van der Eide, P. E. Romero, W. E. Piers, *J. Am. Chem. Soc.* **2008**, 130, 4485–4491.
- [56] G. A. Wenzel, R. H. Grubbs, *J. Am. Chem. Soc.* **2006**, 128, 16048–16049.
- [57] T. M. Trnka, R. H. Grubbs, *Acc. Chem. Res.* **2001**, 34, 18–29.
- [58] R. R. Schrock, *Chem. Rev.* **2009**, 109, 3211–3226.
- [59] J. Heppekausen, A. Fürstner, *Angew. Chem.* **2011**, 123, 7975–7978; *Angew. Chem. Int. Ed.* **2011**, 50, 7829–7832.
- [60] T. W. Funk, J. M. Berlin, R. H. Grubbs, *J. Am. Chem. Soc.* **2006**, 128, 1840–1846.
- [61] A. Poater, X. Solans-Monfort, E. Clot, C. Copéret, O. Eisenstein, *J. Am. Chem. Soc.* **2007**, 129, 8207–8216.
- [62] S. J. Malcolmson, S. Meek, E. S. Sattely, R. R. Schrock, A. H. Hoveyda, *Nature* **2008**, 456, 933–937.
- [63] A. Fürstner, C. Mathes, K. Grela, *Chem. Commun.* **2001**, 1057–1059.
- [64] Y. S. Tسانtrizos, J.-M. Ferland, A. McClory, M. Poirier, V. Farina, N. K. Yee, X.-J. Wang, N. Haddad, X. Wei, L. Zhang, *J. Organomet. Chem.* **2006**, 691, 5163–5171.
- [65] M. Bienek, R. Bujok, H. Stepowska, A. Jacobi, R. Hagenkötter, D. Arlt, K. Jarzemska, K. Wozniak, K. Grela, *J. Organomet. Chem.* **2006**, 691, 5289–5297.
- [66] T. Nicola, M. Brenner, K. Donsbach, P. Kreye, *Org. Process Res. Dev.* **2005**, 9, 513–515.
- [67] A. Fürstner, T. Dierkes, *Org. Lett.* **2000**, 2, 2463–2465; A. Fürstner, C. Mathes, K. Grela, *Chem. Commun.* **2001**, 1057–1059.
- [68] C. Ornelas, D. Méry, E. Cloutet, J. Ruiz, D. Astruc, *J. Am. Chem. Soc.* **2008**, 130, 1495–1506.
- [69] a) W. E. Crowe, D. R. Goldberg, *J. Am. Chem. Soc.* **1995**, 117, 5162–5163; b) E. C. Hansen, D. Lee, *Org. Lett.* **2004**, 6, 2035–2038.
- [70] D. Gallenkamp, A. Fürstner, *J. Am. Chem. Soc.* **2011**, 133, 9232–9235.
- [71] R. R. Schrock, *Chem. Rev.* **2009**, 109, 3211–3226.
- [72] I. Ibrahim, M. Yu, R. R. Schrock, A. H. Hoveyda, *J. Am. Chem. Soc.* **2009**, 131, 3844–3845.
- [73] M. M. Flook, A. J. Jiang, R. R. Schrock, P. Müller, A. H. Hoveyda, *J. Am. Chem. Soc.* **2009**, 131, 7962–7963.
- [74] S. C. Marinescu, R. R. Schrock, P. Müller, M. K. Takase, A. H. Hoveyda, *Organometallics* **2011**, 30, 1780–1782.
- [75] S. J. Meek, R. V. O'Brien, J. Llaveria, R. R. Schrock, A. H. Hoveyda, *Nature* **2011**, 471, 461–466.
- [76] S. C. Marinescu, D. S. Levine, Y. Zhao, R. R. Schrock, A. H. Hoveyda, *J. Am. Chem. Soc.* **2011**, 133, 11512–11514.
- [77] M. Yu, C. Wang, A. F. Kyle, P. Jakubec, D. J. Dixon, R. R. Schrock, A. H. Hoveyda, *Nature* **2011**, 479, 88–93.
- [78] K. Endo, R. H. Grubbs, *J. Am. Chem. Soc.* **2011**, 133, 8525–8527.
- [79] B. K. Keitz, K. Endo, M. B. Herbert, R. H. Grubbs, *J. Am. Chem. Soc.* **2011**, 133, 9686–9688.
- [80] B. K. Keitz, K. Endo, P. R. Patel, M. B. Herbert, R. H. Grubbs, *J. Am. Chem. Soc.* **2012**, 134, 693–699.
- [81] P. Liu, X. Xu, X. Dong, B. K. Keitz, M. B. Herbert, R. H. Grubbs, K. N. Houk, *J. Am. Chem. Soc.* **2012**, 134, 1464–1467.
- [82] L. Cavallo, A. Correa, *J. Am. Chem. Soc.* **2006**, 128, 13352–13353.
- [83] C. Adlhart, P. J. Chen, *J. Am. Chem. Soc.* **2004**, 126, 3496–3510.
- [84] D. Benitez, E. Tkatchouk, W. A. Goddard, *Chem. Commun.* **2008**, 6194.
- [85] L. Cavallo, N. Bahri-Laleh, R. Credendino, J. Beilstein, *Org. Chem.* **2011**, 7, 40–45.
- [86] Y. Dang, Z.-X. Wang, X. Wang, *Organometallics* **2012**, 31, 8654–8657.
- [87] L. E. Rosebrugh, M. B. Herbert, V. M. Marx, B. K. Keitz, R. H. Grubbs, *J. Am. Chem. Soc.* **2013**, 135, 1276–1279.
- [88] V. M. Marx, M. B. Herbert, B. K. Keitz, R. H. Grubbs, *J. Am. Chem. Soc.* **2013**, 135, 94–97.
- [89] M. B. Herbert, V. M. Marx, R. L. Pederson, R. H. Grubbs, *Angew. Chem.* **2013**, 125, 328–332; *Angew. Chem. Int. Ed.* **2013**, 52, 310–314.
- [90] H. D. Maynard, R. H. Grubbs, *Tetrahedron Lett.* **1999**, 40, 4137–4140.
- [91] L. A. Paquette, J. D. Schloss, I. Efremov, F. Fabris, F. Gallou, J. Méndez-Andino, J. Yang, *Org. Lett.* **2000**, 2, 1259–1261.
- [92] Y. M. Ahn, K. Yang, G. I. Georg, *Org. Lett.* **2001**, 3, 1411–1413.
- [93] D. W. Knight, I. R. Morgan, A. J. Proctor, *Tetrahedron Lett.* **2010**, 51, 638–640.
- [94] S. H. Hong, R. H. Grubbs, *Org. Lett.* **2007**, 9, 1955–1957.
- [95] K. Skowerski, C. Wierzbicka, G. Szczepaniak, Ł. Gułajski, M. Bieniek, K. Grela, *Green Chem.* **2012**, 14, 3264–3268.
- [96] M. Klučiar, K. Grela, M. Mauduit, *Dalton Trans.* **2013**, 42, 7354–7358.
- [97] M. R. Buchmeiser, *Chem. Rev.* **2009**, 109, 303–321.
- [98] T. Vorfalt, K. J. Wannowius, V. Thiel, H. Plenio, *Chem. Eur. J.* **2010**, 16, 12312–12315.
- [99] Z. Yinghuai, L. Kuijin, N. Huimin, L. Chuanyao, L. P. Stubbs, C. F. Siong, T. Muihua, S. C. Peng, *Adv. Synth. Catal.* **2009**, 351, 2650–2656.
- [100] M. Mayr, D. Wang, R. Kröll, N. Schuler, S. Prühs, A. Fürstner, M. R. Buchmeiser, *Adv. Synth. Catal.* **2005**, 347, 484–492.
- [101] S. Prühs, C. W. Lehmann, A. Fürstner, *Organometallics* **2004**, 23, 280–287.
- [102] K. Mennecke, K. Grela, U. Kunz, A. Kirschning, *Synlett* **2005**, 2948.
- [103] M. Mayr, M. R. Buchmeiser, K. Wurst, *Adv. Synth. Catal.* **2002**, 344, 712–719.
- [104] D. P. Allen, M. M. Van Wingerden, R. H. Grubbs, *Org. Lett.* **2009**, 11, 1261–1264.
- [105] A. Monge-Marcet, R. Pleixats, X. Cattoën, M. Wong Chi Man, *J. Mol. Catal. A* **2012**, 357, 59–66.
- [106] A. Monge-Marcet, R. Pleixats, X. Cattoën, M. Wong Chi Man, *Tetrahedron* **2013**, 69, 341–348.
- [107] J. Lim, S. Seong Lee, J. Y. Ying, *Chem. Commun.* **2010**, 46, 806–808.
- [108] W. Solodenko, A. Doppiu, R. Frankfurter, C. Vogt, A. Kirschning, *Aust. J. Chem.* **2013**, 66, 183–191.
- [109] J. Scholz, S. Loekman, N. Szesni, W. Hieringer, A. Görling, M. Haumann, P. Wasserscheid, *Adv. Synth. Catal.* **2011**, 353, 2701–2707.
- [110] E. Baird Anderson, M. R. Buchmeiser, *ChemCatChem* **2012**, 4, 30–44.

- [111] B. Autenrieth, W. Frey, M. R. Buchmeiser, *Chem. Eur. J.* **2012**, *18*, 14069–14078.
- [112] D. S. Tabari, D. R. Tolentino, Y. Schrodi, *Organometallics* **2013**, *32*, 5–8.
- [113] A. K. Diallo, E. Boisselier, L. Liang, J. Ruiz, D. Astruc, *Chem. Eur. J.* **2010**, *16*, 11832–11835.
- [114] M. Chabanas, A. Baudouin, C. Copéret, J.-M. Basset, W. Lukens, A. Lesage, S. Hediger, L. Emsley, *J. Am. Chem. Soc.* **2003**, *125*, 492–504.
- [115] J. M. Basset, C. Copéret, L. Lefort, B. M. Maunders, O. Maury, E. Le Roux, G. Saggio, S. Soignier, D. Soulivong, G. J. Sunley, M. Taoufik, J. Thivolle-Cazat, *J. Am. Chem. Soc.* **2005**, *127*, 8604–8605.
- [116] W. A. Herrmann, A. W. Stumpf, T. Priermeier, S. Bogdanović, V. Dufaud, J.-M. Basset, *Angew. Chem.* **1996**, *108*, 2978–2980; *Angew. Chem. Int. Ed. Engl.* **1996**, *35*, 2803–2805.
- [117] R. P. Saint-Arroman, M. Chabanas, A. Baudouin, C. Copéret, J. M. Basset, A. Lesage, L. Emsley, *J. Am. Chem. Soc.* **2001**, *123*, 3820–3821.
- [118] F. Blanc, N. Rendón, R. Berthoud, J.-M. Basset, C. Copéret, Z. J. Tonzetich, R. R. Schrock, *Dalton Trans.* **2008**, 3156–3158.
- [119] A. Mortreux, M. Blanchard, *J. Chem. Soc., Chem. Commun.* **1974**, 786–787.
- [120] T. J. Katz, J. McGinnis, *J. Am. Chem. Soc.* **1975**, *97*, 1592–1594.
- [121] J. H. Wengrovius, J. Sancho, R. R. Schrock, *J. Am. Chem. Soc.* **1981**, *103*, 3932–3934.
- [122] S. F. Pedersen, R. R. Schrock, M. R. Churchill, H. J. Wasserman, *J. Am. Chem. Soc.* **1982**, *104*, 6808–6809.
- [123] R. R. Schrock, *Angew. Chem.* **2006**, *118*, 3832–3844; *Angew. Chem. Int. Ed.* **2006**, *45*, 3748–3759.
- [124] R. R. Schrock, C. Czekelius, *Adv. Synth. Catal.* **2007**, *349*, 55–77.
- [125] A. Fürstner, P. W. Davies, *Chem. Commun.* **2005**, 2307.
- [126] W. Zhang, J. S. Moore, *Adv. Synth. Catal.* **2007**, *349*, 93–120.
- [127] M. Mori, *Adv. Synth. Catal.* **2007**, *349*, 121–135.
- [128] R. R. Schrock, *Angew. Chem.* **2006**, *118*, 3832–3844; *Angew. Chem. Int. Ed.* **2006**, *45*, 3748–3759.
- [129] M. H. Chisholm, K. Folting, D. M. Hoffman, J. C. Huffman, *J. Am. Chem. Soc.* **1984**, *106*, 6794–6805.
- [130] M. H. Chisholm, B. K. Conroy, B. W. Eichhorn, K. Folting, D. M. Hoffman, J. C. Huffman, N. S. Marchant, *Polyhedron* **1987**, *6*, 783–792.
- [131] R. R. Schrock, D. N. Clark, J. Sancho, J. H. Wengrovius, S. M. Rocklage, S. F. Pedersen, *Organometallics* **1982**, *1*, 1645–1651.
- [132] M. L. Listemann, R. R. Schrock, *Organometallics* **1985**, *4*, 74–83.
- [133] J. Sancho, R. R. Schrock, *J. Mol. Catal. A* **1982**, *15*, 75–79.
- [134] R. R. Schrock, *Chem. Commun.* **2013**, *49*, 5529–5531.
- [135] A. Fürstner, G. Seidel, *Angew. Chem.* **1998**, *110*, 1758–1760; *Angew. Chem. Int. Ed.* **1998**, *37*, 1734–1736.
- [136] A. Fürstner, O. Guth, A. Rumbo, G. Seidel, *J. Am. Chem. Soc.* **1999**, *121*, 11108–11113.
- [137] A. Fürstner, A. Rumbo, *J. Org. Chem.* **2000**, *65*, 2608–2611.
- [138] A. Fürstner, T. Dierkes, *Org. Lett.* **2000**, *2*, 2463–2464.
- [139] A. Fürstner, G. Seidel, *J. Organomet. Chem.* **2000**, *606*, 75–78.
- [140] A. Fürstner, C. Mathes, C. W. Lehmann, *Chem. Eur. J.* **2001**, *7*, 5299–5317.
- [141] T. Masuda, F. Sanda, *Handbook of Metathesis* (Ed.: R. H. Grubbs), Wiley-VCH, Weinheim, Germany, **2003**, vol. 3, p. 375–406.
- [142] B. Haberlag, X. Wu, K. Brandhorst, J. Grunenberg, C. G. Daniliuc, P. G. Jones, M. Tamm, *Chem. Eur. J.* **2010**, *16*, 8868–8877.
- [143] S. Beer, C. G. Hrib, P. G. Jones, K. Brandhorst, J. Grunenberg, M. Tamm, *Angew. Chem.* **2007**, *119*, 9047–9051; *Angew. Chem. Int. Ed.* **2007**, *46*, 8890–8894.
- [144] X. Wu, M. Tamm, *Beilstein J. Org. Chem.* **2011**, *7*, 82–93.
- [145] A. Poater, X. Solans-Monfort, E. Clot, C. Copéret, O. Eisenstein, *J. Am. Chem. Soc.* **2007**, *129*, 8207–8216.
- [146] S. Lysenko, B. Haberlag, C. G. Daniliuc, P. G. Jones, M. Tamm, *ChemCatChem* **2011**, 115–118.
- [147] S. Beer, K. Brandhorst, C. G. H. Xian Wu, B. Haberlag, J. Grunenberg, P. G. Jones, M. Tamm, *Organometallics* **2009**, *28*, 1534–1545.
- [148] Y.-C. Tsai, P. L. Diaconescu, C. C. Cummins, *Organometallics* **2000**, *19*, 5260–5262.
- [149] A. Fürstner, C. Mathes, C. W. Lehmann, *J. Am. Chem. Soc.* **1999**, *121*, 9453–9454.
- [150] a) C. C. Cummins, *Chem. Commun.* **1998**, 1777–1786; b) C. C. Cummins, *Chem. Commun.* **1999**, *121*, 9453–9454.
- [151] A. Fürstner, C. Mathes, C. W. Lehmann, *Chem. Eur. J.* **2001**, *7*, 5299–5317.
- [152] W. Zhang, S. Kraft, J. S. Moore, *J. Am. Chem. Soc.* **2004**, *126*, 329–335.
- [153] W. Zhang, S. Kraft, J. S. Moore, *Chem. Commun.* **2003**, 832–833.
- [154] W. Zhang, Y. Lu, J. S. Moore, *Org. Synth.* **2007**, *84*, 163–176.
- [155] W. Zhang, H. M. Cho, J. S. Moore, *Org. Synth.* **2007**, *84*, 177–191.
- [156] For a review, see: C. C. Cummins, *Chem. Commun.* **1998**, 1777–1786.
- [157] The catalytic active species of the Mortreux system are probably trisphenoxide alkylidyne molybdenum species in low concentration. Under the reaction conditions employed for the metathesis (130–150 °C), the apparent higher stability of this system to air could be (partially) due to the fact that reactions between trisphenoxides and oxygen/moisture are slow. Upon preactivation with heptyne, the Mortreux catalyst works at temperatures that are only 40–50 °C higher than those required for [W]-1.^[216] Upon addition of diphenoxyethane and a bed of molecular sieves, phenylpropene was metathesized at only 50 °C by the [Mo(CO)₆] + *p*-chlorophenol system; see: V. Huc, R. Weihofen, I. Martin-Jimenez, P. Oulié, C. Lepetit, G. Lavigne, R. Chauvin, *New J. Chem.* **2003**, *27*, 1412–1414.
- [158] M. Bindl, R. Stade, E. K. Heilmann, A. Picot, R. Goddard, A. Fürstner, *J. Am. Chem. Soc.* **2009**, *131*, 9468–9470.
- [159] A. M. Geyer, E. S. Wiedner, J. B. Gary, R. L. Gdula, N. C. Kuhlmann, M. J. A. Johnson, B. D. Dunietz, J. W. Kampf, *J. Am. Chem. Soc.* **2008**, *130*, 8984–8999.
- [160] R. L. Gdula, M. J. A. Johnson, *J. Am. Chem. Soc.* **2006**, *128*, 9614–9615.
- [161] A. M. Geyer, M. J. Holland, R. L. Gdula, J. E. Goodman, M. J. A. Johnson, J. W. Kampf, *J. Organomet. Chem.* **2012**, *708–709*, 1–9.
- [162] For theoretical studies, see: a) J. Zhu, G. Jia, Z. Lin, *Organometallics* **2006**, *25*, 1812–1819; b) T. Woo, E. Folga, T. Ziegler, *Organometallics* **1993**, *12*, 1289–1298. According to these studies, molybdenum complexes have higher barriers to metallacycle formation than the analogous tungsten complexes; the barriers can be lowered by decreasing the electron-donor abilities of the ancillary ligands.
- [163] J. Heppekausen, R. Stade, R. Goddard, A. Fürstner, *J. Am. Chem. Soc.* **2010**, *132*, 11045–11057.
- [164] J. Heppekausen, R. Stade, A. Kondoh, G. Seidel, R. Goddard, A. Fürstner, *Chem. Eur. J.* **2012**, *18*, 10281–10299.
- [165] J. Heppekausen, R. Stade, R. Goddard, A. Fürstner, *J. Am. Chem. Soc.* **2010**, *132*, 11045–11057.
- [166] The possibility of conducting catalytic alkyne metathesis in the presence of 4 Å molecular sieves has also been addressed; see ref.^[129]
- [167] A. Fürstner, *Angew. Chem.* **2013**, *125*, 2860–2887; *Angew. Chem. Int. Ed.* **2013**, *52*, 2794–2819.
- [168] X. Wu, M. Tamm, *Beilstein J. Org. Chem.* **2011**, *7*, 82–93.
- [169] V. Hickmann, A. Kondoh, B. Gabor, M. Alcarazo, A. Fürstner, *J. Am. Chem. Soc.* **2011**, *133*, 13471–3480.

- [170] V. Hickmann, M. Alcarazo, A. Fürstner, *J. Am. Chem. Soc.* **2010**, *132*, 11042–11044.
- [171] a) V. V. Vintonyak, M. E. Maier, *Angew. Chem.* **2007**, *119*, 5301–5303; *Angew. Chem. Int. Ed.* **2007**, *46*, 5209–5211; b) V. V. Vintonyak, M. E. Maier, *Org. Lett.* **2007**, *9*, 655–658.
- [172] A. Fürstner, M. Bindl, L. Jean, *Angew. Chem.* **2007**, *119*, 9435–9438; *Angew. Chem. Int. Ed.* **2007**, *46*, 9275–9278.
- [173] J. Heppekausen, R. Stade, R. Goddard, A. Fürstner, *J. Am. Chem. Soc.* **2010**, *132*, 11045–11057.
- [174] M. Fouché, L. Rooney, A. G. M. Barrett, *J. Org. Chem.* **2012**, *77*, 3060–3070.
- [175] I. Feinstein-Jaffe, S. F. Pedersen, R. R. Schrock, *J. Am. Chem. Soc.* **1983**, *105*, 7176–7177.
- [176] I. Feinstein-Jaffe, J. C. Dewan, R. R. Schrock, *Organometallics* **1985**, *4*, 1189–1193.
- [177] J. H. Freudenberger, R. R. Schrock, *Organometallics* **1986**, *5*, 1411–1417.
- [178] L. G. McCullough, R. R. Schrock, J. C. Dewan, J. C. Murdzek, *J. Am. Chem. Soc.* **1985**, *107*, 5987–5998.
- [179] H. Strutz, J. C. Dewan, R. R. Schrock, *J. Am. Chem. Soc.* **1985**, *107*, 5999–6005.
- [180] M. R. Churchill, J. W. Ziller, *J. Organomet. Chem.* **1985**, *281*, 237–248.
- [181] L. G. McCullough, M. L. Listemann, R. R. Schrock, M. R. Churchill, J. W. Ziller, *J. Am. Chem. Soc.* **1983**, *105*, 6729–6730.
- [182] A. Mortreux, F. Petit, M. Petit, T. Szymanska-Buzar, *J. Mol. Catal. A* **1995**, *96*, 95–105.
- [183] A. Bray, A. Mortreux, F. Petit, M. Petit, T. Szymanska-Buzar, *J. Chem. Soc., Chem. Commun.* **1993**, 197–199.
- [184] J. Heppekausen, R. Stade, A. Kondoh, G. Seidel, R. Goddard, A. Fürstner, *Chem. Eur. J.* **2012**, *18*, 10281–10299.
- [185] A. Mortreux, O. Coutelier, *J. Mol. Catal. A* **2006**, *254*, 96–104.
- [186] M. Sauthier, P. Zinck, A. Mortreux, *C. R. Chim.* **2010**, *13*, 304–314.
- [187] O. Coutelier, A. Mortreux, *Adv. Synth. Catal.* **2006**, *348*, 2038–2042.
- [188] B. Haberlag, M. Freytag, C. G. Daniliuc, P. G. Jones, M. Tamm, *Angew. Chem.* **2012**, *124*, 13195–13199; *Angew. Chem. Int. Ed.* **2012**, *51*, 13019–13022.
- [189] A. Fürstner, T. Dierkes, *Org. Lett.* **2000**, *2*, 2463–2465.
- [190] S. T. Diver, A. J. Giessert, *Chem. Rev.* **2004**, *104*, 1317–1382.
- [191] E. C. Hansen, D. Lee, *Acc. Chem. Res.* **2006**, *39*, 509–519.
- [192] M. Mori, *Top. Organomet. Chem.* **1999**, *1*, 133–154.
- [193] C. Fischmeister, C. Bruneau, *Beilstein J. Org. Chem.* **2011**, *7*, 156–166.
- [194] C. Copéret, M. Chabanas, R. P. Saint-Arroman, J.-M. Basset, *Angew. Chem.* **2003**, *115*, 164–191; *Angew. Chem. Int. Ed.* **2003**, *42*, 156–181.
- [195] R. L. Burnett, T. R. Hughes, *J. Catal.* **1973**, *31*, 55–64.
- [196] V. Vidal, A. Theolier, J. Thivole-Cazat, J.-M. Basset, *Science* **1997**, *276*, 99–102.
- [197] C. Copéret, O. Maury, J. Thivolle-Cazat, J.-M. Basset, *Angew. Chem.* **2001**, *113*, 2393–2396; *Angew. Chem. Int. Ed.* **2001**, *40*, 2331–2334.
- [198] J.-M. Basset, C. Copéret, D. Soulivong, M. Taoufik, J. Thivole-Cazat, *Angew. Chem.* **2006**, *118*, 6228–6231; *Angew. Chem. Int. Ed.* **2006**, *45*, 6082–6085.
- [199] F. Blanc, C. Copéret, J. Thivole-Cazat, J.-M. Basset, *Angew. Chem.* **2006**, *118*, 6347–6349; *Angew. Chem. Int. Ed.* **2006**, *45*, 6201–6203.
- [200] S. Schinzel, H. Chermette, C. Copéret, J.-M. Basset, *J. Am. Chem. Soc.* **2008**, *130*, 7984–7987.
- [201] F. Blanc, J. Thivole-Cazat, J.-M. Basset, C. Copéret, *Chem. Eur. J.* **2008**, *14*, 9030–9037.
- [202] O. Maury, L. Lefort, V. Vidal, J. Thivolle-Cazat, J.-M. Basset, *Organometallics* **2010**, *29*, 6612–6614.
- [203] C. Copéret, J.-M. Basset, *Adv. Synth. Catal.* **2007**, *349*, 78–92.
- [204] A. S. Goldman, A. H. Roy, Z. Huang, R. Ahuja, W. Schinski, M. Brookhart, *Science* **2006**, *312*, 257–261.
- [205] R. Ahuja, S. Kundu, A. S. Goldman, M. Brookhart, B. C. Vicente, S. L. Scott, *Chem. Commun.* **2008**, 253–255.
- [206] Z. Huang, E. Rolfe, E. C. Carson, M. Brookhart, A. S. Goldman, S. H. El-Khalafi, A. H. R. MacArthur, *Adv. Synth. Catal.* **2010**, *352*, 125–135.
- [207] M. C. Halbach, S. Kundu, M. Brookhart, A. S. Goldman, *Acc. Chem. Res.* **2012**, *45*, 947–958.
- [208] V. Dragutan, R. Streck, *Catalytic Polymerization of Cycloolefins*, Elsevier, Amsterdam, **2000**.
- [209] J. C. Mol, *J. Mol. Catal. A* **2004**, *213*, 39–45.
- [210] O. M. Singh, *J. Sci. Ind. Res.* **2006**, *65*, 957–965.
- [211] L. Delaude, A. Demonceau, A. F. Noels, *Macromolecules* **2003**, *36*, 1446–1456.
- [212] T. Y. Tsunogae, I. Igarashi, *Macromolecules* **2006**, *39*, 4663–4670.
- [213] M. M. Flook, A. J. Jiang, R. R. Schrock, P. Müller, A. H. Hoveyda, *J. Am. Chem. Soc.* **2009**, *131*, 7962–7963.
- [214] M. Bornand, P. Chen, *Angew. Chem.* **2005**, *117*, 8123–8125; *Angew. Chem. Int. Ed.* **2005**, *44*, 7909–7911.
- [215] M. Bornand, S. Tocker, P. Chen, *Organometallics* **2007**, *26*, 3585–3596.
- [216] K. Vehlow, D. Wang, M. R. Buchmeiser, S. Blechert, *Angew. Chem.* **2008**, *120*, 2655–2658; *Angew. Chem. Int. Ed.* **2008**, *47*, 2615–2618.
- [217] M. Lichtenheldt, D. Wang, K. Vehlow, I. Reinhardt, C. Kühnel, U. Decker, M. R. Buchmeiser, S. Blechert, *Chem. Eur. J.* **2009**, *15*, 9451–9457.
- [218] S. Sutthasupa, M. Shiotsuki, T. Masuda, F. Sanda, *J. Am. Chem. Soc.* **2009**, *131*, 10546–10551.
- [219] A. Leitgeb, J. Wappel, C. Slugovc, *Polymer* **2010**, *51*, 2927–2946.
- [220] C. W. Bielawski, R. H. Grubbs, *Prog. Polym. Sci.* **2007**, *32*, 1–29.
- [221] C. W. Bielawski, R. H. Grubbs, *Controlled and Living Polymerizations*, Wiley-VCH, Weinheim, Germany, **2009**, p. 297.
- [222] J. Qu, T. Katsumata, M. Satoh, J. Wada, T. Matsuda, *Polymer* **2009**, *50*, 391–396.
- [223] T. L. Choi, R. H. Grubbs, *Angew. Chem.* **2003**, *115*, 1785–1788; *Angew. Chem. Int. Ed.* **2003**, *42*, 1743–1746.
- [224] S. Monfette, J. Marleau-Gillette, J. C. Conrad, R. McDonald, D. E. Fogg, *Dalton Trans.* **2012**, *41*, 14476–14479.
- [225] N. Noormofidi, C. Slugovc, *Eur. Polym. J.* **2010**, *46*, 694–701.
- [226] S. Hilf, A. F. M. Kilbinger, *Nat. Chem.* **2009**, *1*, 537–546.
- [227] N. Hadjichristidis, S. Pispas, M. Pitsikalis, H. Iatrou, D. J. Lohse, *Graft Copolymers, Encyclopedia of Polymer Science and Technology*, 3rd ed. Wiley, Hoboken, NJ, **2004**.
- [228] G. Trimmel, S. Riegler, G. Fuchs, C. Slugovc, F. Stelzer, *Adv. Polym. Sci.* **2005**, *176*, 43–87.
- [229] M. R. Buchmeiser, *J. Sep. Sci.* **2008**, *31*, 1907–1922.
- [230] P. H. Ge, W. Fu, C. Campana, E. Hertweck, W. A. Herman, R. D. Adams, U. H. F. Bunz, *Angew. Chem.* **2000**, *112*, 3753–3756; *Angew. Chem. Int. Ed.* **2000**, *39*, 3607–3610.
- [231] J. A. Johnson, Y. Y. Lu, A. O. Burts, Y. Xia, A. C. Durrell, D. A. Tirrell, R. H. Grubbs, *Macromolecules* **2010**, *43*, 10326–10335.
- [232] J. A. Johnson, Y. Y. Lu, A. O. Burts, Y.-H. Lim, M. G. Finn, J. T. Koberstein, N. J. Turro, D. A. Tirrell, R. H. Grubbs, *J. Am. Chem. Soc.* **2011**, *133*, 559–566.
- [233] B. Helms, J. L. Mynar, C. J. Hawker, J. M. J. Fréchet, *J. Am. Chem. Soc.* **2004**, *126*, 15020–15021.
- [234] C. J. Hawker, J. M. J. Fréchet, *Polymer* **1992**, *33*, 1507–1511.
- [235] H. Jung, T. P. Carberry, M. Weck, *Macromolecules* **2011**, *44*, 9075–9083.
- [236] J. M. Fishman, L. L. Kiessling, *Angew. Chem.* **2013**, *125*, 5165–5168; *Angew. Chem. Int. Ed.* **2013**, *52*, 5061–5064.
- [237] M. R. Buchmeiser, F. Sinner, M. Mupa, K. Wurs, *Macromolecules* **2000**, *33*, 32–39.

- [238] R. Bandari, J. Kuballa, M. R. Buchmeiser, *J. Sep. Sci.* **2013**, *36*, 1169–1175.
- [239] R. Bandari, M. R. Buchmeiser, *Analyst* **2012**, *137*, 3271–3277.
- [240] A. Leitgeb, J. Wappel, C. Slugovc, *Polymer* **2010**, *51*, 2927–2946.
- [241] K. Nomura, M. M. Abdellatif, *Polymer* **2010**, *51*, 1861–1881.
- [242] S. Hilf, A. F. M. Kilbinger, *Nat. Chem.* **2009**, *1*, 537–546.
- [243] S. Monfette, D. E. Fogg, *Chem. Rev.* **2009**, *109*, 3783–3816.
- [244] U. H. F. Bunz, D. Mäker, M. Porz, *Macromol. Rapid Commun.* **2012**, *33*, 886–910.
- [245] S. Naumann, J. Unold, W. Frey, M. R. Buchmeiser, *Macromolecules* **2011**, *44*, 8380–8387.
- [246] T. W. Baughman, K. B. Wagener, *Adv. Polym. Sci.* **2005**, *176*, 1–42.
- [247] P. P. Matloka, K. B. Wagener, *J. Mol. Catal. A* **2006**, *257*, 89–98.
- [248] T. W. Baughman, K. B. Wagener, *Adv. Polym. Sci.* **2005**, *176*, 1–42.
- [249] S. Hosoda, Y. Nozue, Y. Kawashima, S. Utsumi, T. Nagamatsu, K. Wagener, E. Berda, G. Rojas, T. Baughman, J. Leonard, *Macromol. Symp.* **2009**, *282*, 50–64.
- [250] E. Boz, K. B. Wagener, *Macromolecules* **2006**, *39*, 4437–4447.
- [251] M. Winkler, J. O. Mueller, K. K. Oehlenschlaeger, L. Montero de Espinosa, M. A. R. Meier, C. Barner-Kowollik, *Macromolecules* **2012**, *45*, 5012–5019.
- [252] L. Montero de Espinosa, M. A. R. Meier, *Chem. Commun.* **2011**, *47*, 1908–1910.
- [253] K. Weiss, A. Michel, E.-M. Auth, U. H. F. Bunz, T. Mangel, K. Müllen, *Angew. Chem.* **1997**, *109*, 522–525.
- [254] L. Kloppenburg, D. Jones, U. H. F. Bunz, *Macromolecules* **1999**, *32*, 4194.
- [255] U. H. F. Bunz, *Modern Arene Chemistry* (Ed.: D. Astruc), Wiley-VCH, Weinheim, Germany, **2002**, ch. 7, p. 217.
- [256] U. H. F. Bunz, *Acc. Chem. Res.* **2001**, *34*, 998–1010.
- [257] U. H. F. Bunz, *Handbook of Metathesis* (Ed.: R. H. Grubbs), Wiley-VCH, Weinheim, Germany, **2003**, vol. 3, p. 354–374.
- [258] N. G. Pschirer, W. Fu, R. D. Adams, U. H. F. Bunz, *Chem. Commun.* **2000**, 87–88.
- [259] W. Zhang, S. M. Brombosz, J. L. Mendoza, J. S. Moore, *J. Org. Chem.* **2005**, *70*, 10198–10201.
- [260] A. D. Finke, D. E. Gross, A. Han, J. S. Moore, *J. Am. Chem. Soc.* **2011**, *133*, 14063–14070.
- [261] W. Zhang, J. S. Moore, *Angew. Chem.* **2006**, *118*, 4524–4548; *Angew. Chem. Int. Ed.* **2006**, *45*, 4416–4439.
- [262] C. A. Johnson, Y. Lu, M. M. Haley, *Org. Lett.* **2007**, *9*, 3725–3728.
- [263] J. Jiang, G. N. Tew, *Org. Lett.* **2008**, *10*, 4393–4396.
- [264] P.-H. Ge, W. Fu, W. A. Herrmann, E. Herdtweck, C. Campana, R. D. Adams, U. H. F. Bunz, *Angew. Chem.* **2000**, *112*, 3753–3756.
- [265] W. Steffen, B. Köhler, M. Altmann, U. Scherf, K. Stitzer, H.-C. zur Loye, U. H. F. Bunz, *Chem. Eur. J.* **2001**, *7*, 117.
- [266] S. W. Sisco, J. S. Moore, *J. Am. Chem. Soc.* **2012**, *134*, 9114–9117.
- [267] D. W. Paley, D. F. Sedbrook, J. Decatur, F. R. Fischer, M. L. Steigerwald, C. Nuckolls, *Angew. Chem.* **2013**, *125*, 4689–4692; *Angew. Chem. Int. Ed.* **2013**, *52*, 4591–4594.
- [268] K. Jyothish, W. Zhang, *Angew. Chem.* **2011**, *123*, 3497–3500; *Angew. Chem. Int. Ed.* **2011**, *50*, 3435–3438.
- [269] K. C. Nicolaou, P. G. Bulger, D. Sarlah, *Angew. Chem.* **2005**, *117*, 4564–4601; *Angew. Chem. Int. Ed.* **2005**, *44*, 4490–4527.
- [270] A. M. Hoveyda, S. J. Malcolmson, S. J. Meek, A. R. Zhugralin, *Angew. Chem.* **2010**, *122*, 38–49; *Angew. Chem. Int. Ed.* **2010**, *49*, 34–44.
- [271] J. Cossy, S. Arseniyadis, C. Meyer, *Metathesis in Natural Product Synthesis* Wiley-VCH, Weinheim, Germany, **2010**.
- [272] J.-A. Richard, S. Y. Ng, D. Y.-K. Chen, *Modern Tools for the Synthesis of Complex Bioactive Molecules* (Eds.: J. Cossy, S. Arseniyadis), Wiley-VCH, Weinheim, Germany, **2012**, p. 155–188.
- [273] A book on metathesis edited by Prof. Karol Grela is scheduled to appear in 2014: K. Grela (Ed.), *Olefin Metathesis—Theory and Practice*, John Wiley & Sons, Hoboken, in press.

Received: May 29, 2013
Published Online: August 27, 2013

Alkynyl-functionalized imidazolium, “click” dendrimer functionalisation and palladium nanoparticle stabilization

Christophe Deraedt,^a Martin d'Halluin,^a Stephanie Lesturgez,^b Lionel Salmon, Graziella Goglio,^b Jaime Ruiz,^a Didier Astruc^{*a}

^aISM, UMR CNRS 5255, Univ. Bordeaux, 351 Cours de la Libération, 33405 Talence Cedex, France.

^bICMCB, UPR CNRS N°9048, 87 avenue, Pey-Berland, 33608 Pessac Cedex, France.

^cLCC, CNRS, 205 Route de Narbonne, 31077 Toulouse Cedex, France.

Abstract

Functionalization of imidazolium salts (IMs) that allow easy derivation of molecular or solid supports are called for towards various applications. Here the synthesis of an alkyne-containing IM is achieved in three steps from 2,4,6-trimethylaniline, and this IM is further successfully functionalized using either Sonogashira or “click” CuAAC reaction that was applied to dendritic IM synthesis in high yield. Applications are illustrated by Pd nanoparticle stabilization by the IM dendrimer for Suzuki-Miyaura catalysis.

Keywords: imidazolium. click reaction. dendrimer. palladium nanoparticle. catalysis

Introduction

Imidazolium salts (IMs) that are derived from imidazole via alkylation of both nitrogen atoms, leading to ion pairs, are widely used in the chemical and biological fields, for instance as anti-cancer and anti-microbial drugs^[1] They are also well-known for their ionic liquid properties and are used as electrolytes or green solvents because of their low vapor pressure and high chemical stability.^[2] Another key property is their deprotonation to *N*-heterocyclic carbenes (NHCs) such as **1** or bisimidazolines that have many applications in organic synthesis.^[3] NHCs are been widely used as strong σ -donor ligands in metal complexes such as the Ru metathesis catalysts,^[4,5] for which functionalizable versions are useful for recycling purposes. Thus the synthesis of various NHCs is of interest, especially NHCs that are modified

with “clickable” termini for easy functionalization of materials. Along this line, we targeted the synthesis of the new IMS **2** containing an alkyne termini that is easily “clickable” using a copper (I) alkyne-azide cycloaddition (CuAAC) reaction^[6] or involved in Sonogashira C-C cross coupling^[7] for example. Materials with azido termini, easily accessible from halogeno derivatives, are readily available, thus azido-terminated dendrimers, azido-polymers, azido-nanoparticles (silica, iron oxide) are often functionalized by CuAAC reaction.

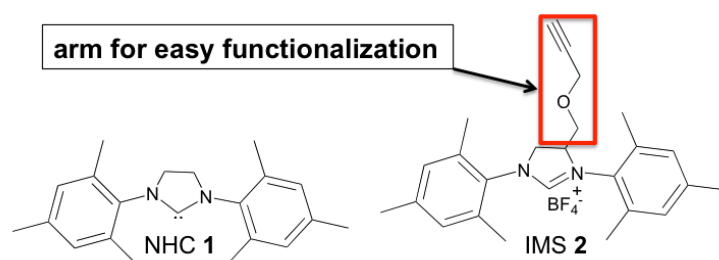


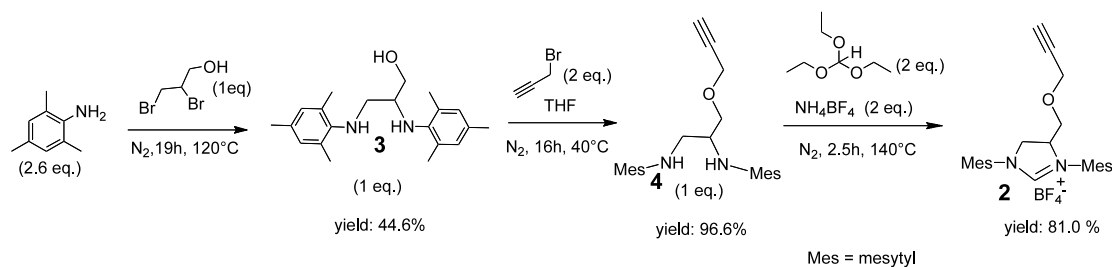
Figure 1. NHC **1** used in Ru metathesis catalysts and the targeted IMS **2**.

Dendrimers^[8] that correspond to molecular micelles,^[9] occupy a privileged place among branched macromolecules, because they are multifaceted monodisperse macromolecules, and their supramolecular properties have potential applications in medicinal chemistry^[10] and nanoscience. In this later area, they are often used as sensors,^[11] green catalysts^[12] or stabilizer of nanoparticles (NP).^[13] We^[11b,c,14] and others^[15] have experimented the useful functionalization of azido-terminated dendrimers for various syntheses and applications including PdNPs stabilization for catalysis,^[16] and this method is now also applied here to functionalize dendrimers with IMS termini.

Results and discussion

Synthesis of the propargyl IMS **2**

The synthesis of **2** has been successfully achieved in only three steps from commercial products with an over yield of 35% (Scheme 1).



Scheme 1. Synthesis of the alkyne-containing imidazolium **2**

This rather modest yield is related to the known first step involving the reaction on a relatively large scale between 2,4,6-trimethylaniline and 2,3-dibromopropanol during 19 hours at 120°C under nitrogen to form *N,N*-dimesityl-2,3-diamino-1-propanol **3** in only 44.6 % yield.^[17] The hydroxyl group of **3** is then functionalized upon reaction with propargyl bromide in THF (16 h at 40°C) in order to introduce the alkyne terminal group in the IMS, leading to the desired *N,N*-dimesityl-2,3-diamino-1-propoxypropargyl **4** in 96.6% yield. The appearance of two new signals at 2.41 ppm (triplet) and at 4.10 ppm (dd) in the ¹H NMR spectrum of the final product shows the success of the reaction and the presence of the alkyne moiety (Figure 2).

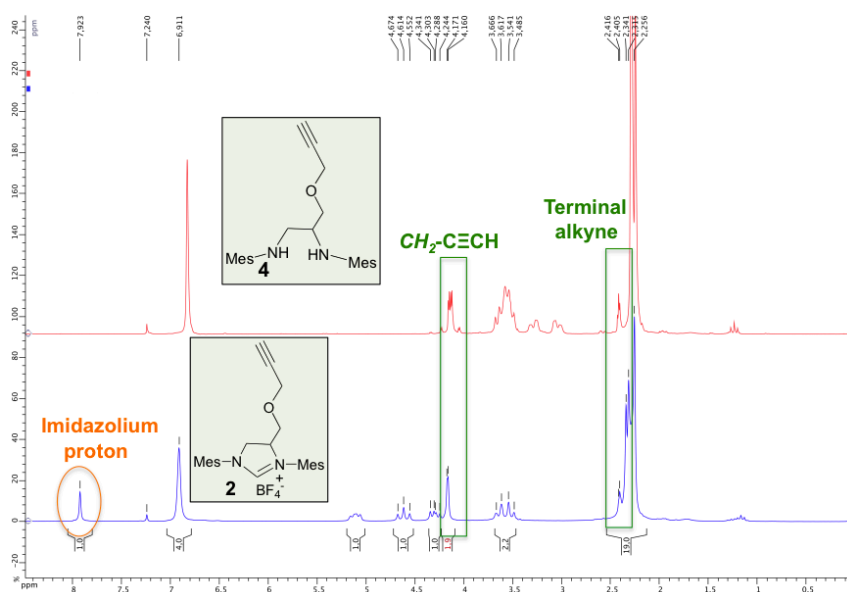


Figure 2. ¹H NMR spectra of **4** (up) and **2** (down).

The infrared spectrum reveals the presence of the alkyne with the absorption bands at $\nu_{\text{C}\equiv\text{C}} = 2113 \text{ cm}^{-1}$ and $\nu_{\text{C}\equiv\text{N}} = 3268 \text{ cm}^{-1}$ (Figure 3). The last step of the synthesis of the propargyl IMS **2** involves the reaction of **4** with triethylorthoformate and NaBF₄ in 2.5 hours at 140°C yielding **2** in 81.0 % yield (Scheme 1). The compound **2** is

obtained as a brown solid and fully characterized by ^1H and ^{13}C NMR, mass spectrometry and infrared spectroscopy. The ^1H NMR spectrum of **2** indicates the presence of a new deshielded proton at 7.92 ppm (Figure 2). This new signal corresponds to the imidazolium proton localized between the two nitrogen atoms. The signals of the protons of the mesityl and the terminal alkyne remain unchanged. Moreover the infrared spectra of **4** and **2** are a little bit different. The appearance of two new intense peaks at 1631 cm^{-1} and 1059 cm^{-1} in the infrared spectrum of **2** are characteristic of $\text{C}=\text{N}$ and BF_4^- groups respectively (Figure 3).

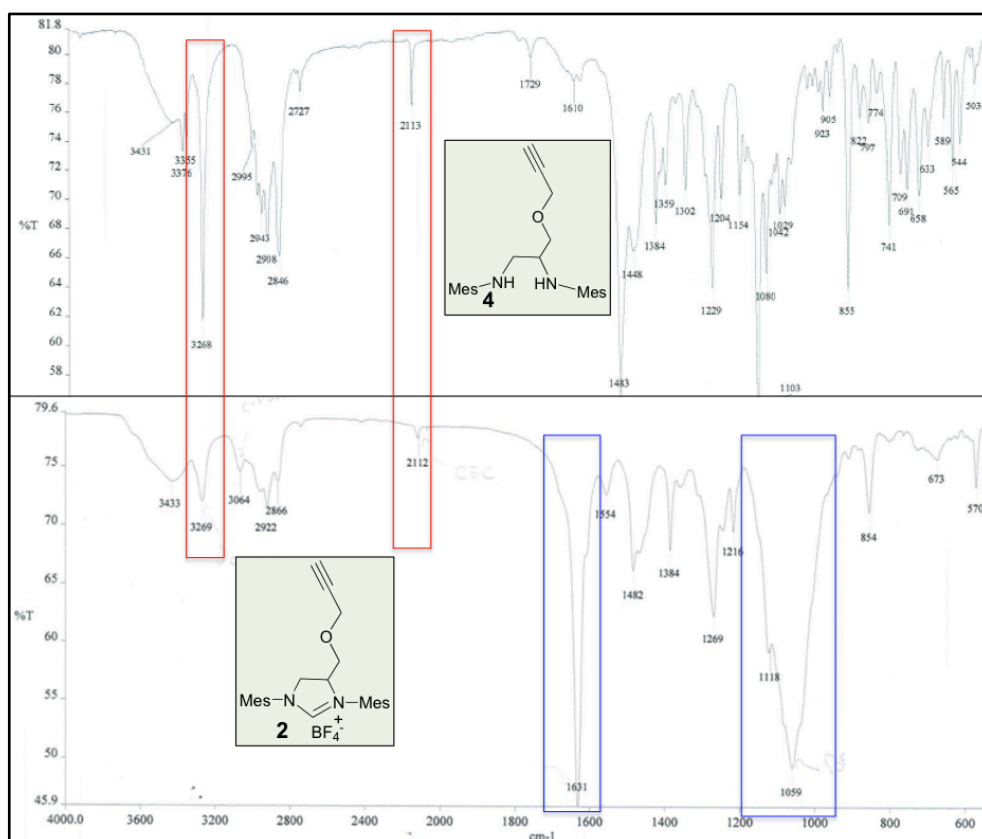
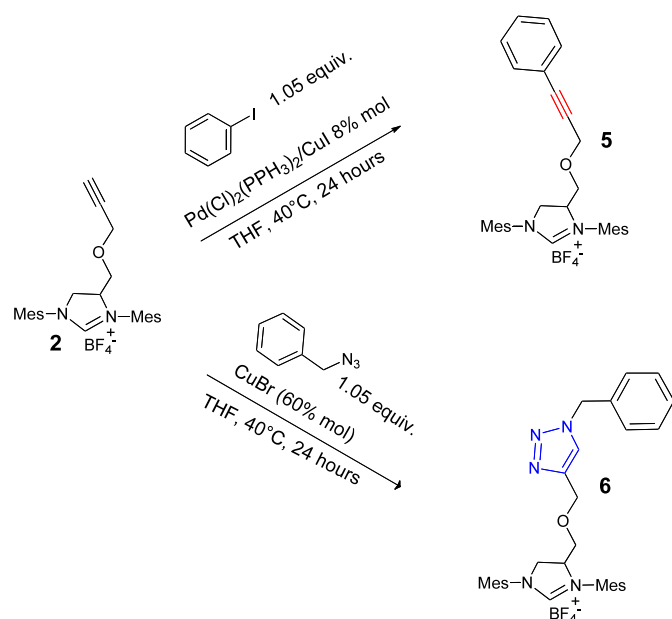


Figure 3. Infrared spectra of **4** (up) and **2** (down).

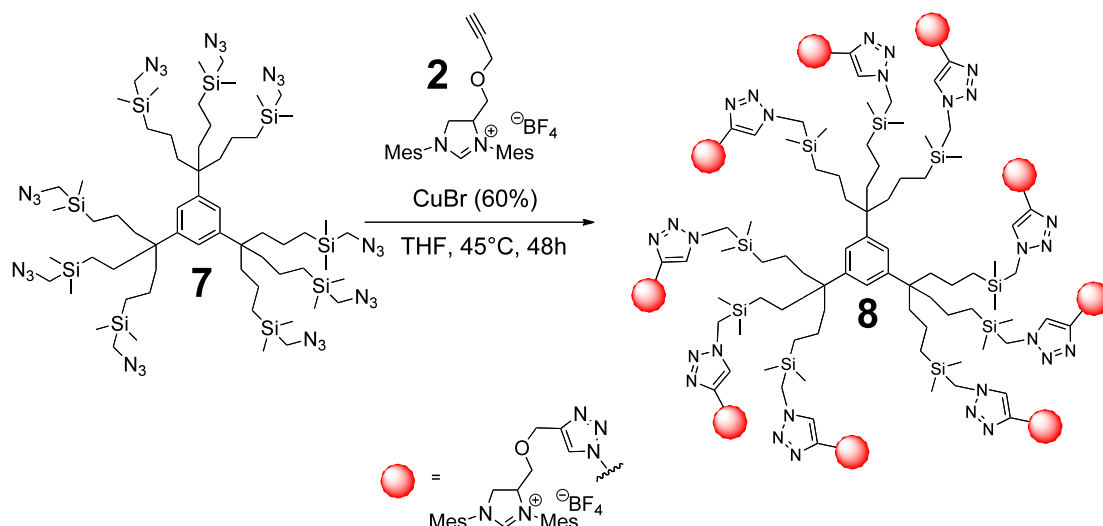
After obtaining **2**, two different reactions were tested: the Sonogashira C-C cross coupling and the CuAAC “click” reaction. The Sonogashira reaction between **2** and iodobenzene was carried out in THF in presence of DIPA as a base and $[\text{Pd}(\text{Cl})_2(\text{PPH}_3)_2]$ (8% mol) + CuI (8% mol) as co-catalysts during 1 day at 40°C . The final product **5** was purified by precipitation in ether and recovered only 71% yield, mainly due to the formation of side products (Scheme 2). The compound **2** also reacts with benzyl azide in THF in the presence of CuBr (60% mol) as catalyst during two days at 40°C . The desired product **6** was recovered after precipitation in ether in

90.5% yield (Scheme 2). Since the CuAAC reaction leads to a better yield than the Sonogashira reaction and is more convenient, the “click” reaction was selected to functionalize a dendritic core.



Scheme 2. IMS **2** involving in both the Sonogashira and CuAAC reactions.

The “click” reaction between **2** and the 1,3 nona azido core **7** was performed in THF at 45°C (Scheme 3). An amount of 60% CuBr per branch is necessary to complete the “click” reaction between **2** and **7**, probably because of more or less stoichiometric coordination of the copper ions of the catalyst by the 1,2,3-triazole ligand and trapping inside the dendrimer. This inhibition effect has already been noted in “click” dendrimer construction when the CuAAC “click” reaction is conducted in the presence of a simple copper salt as catalyst rather than a copper (I) catalyst^[11b] containing a polydentate nitrogen ligand.^[14,18] The end of the reaction is monitored by infrared spectroscopy, the disappearance of the ν_{N_3} band at 2097 cm^{-1} being observed after two days.



Scheme 3. Synthesis of the imidazolium dendrimer **8** by CuAAC “click” chemistry.

The imidazolium dendrimer **8** is obtained as a brown shining powder in 85% yield, which indicates the easy use and highly reactivity of **2** in CuAAC catalysis. The dendrimer **8** is characterized by ^1H and ^{13}C NMR and infrared spectroscopy and by mass spectrometry. Surprisingly, **8** is neither soluble in water nor in alcoholic solvents; on the other hand, it is well soluble in acetonitrile, acetone, dimethyl formamide.

As an application, the stabilization of palladium nanoparticles (PdNPs) with **8** using its intradendritic triazolyl rings was probed. In previous examples, PdNPs stabilized by dendrimers were synthesized in water solution when the dendrimer is water soluble, and this solution was directly used as catalyst for C-C coupling.^[13c] Given the insolubility of **8** in water, the stabilization of PdNPs with **8** is probed here in acetonitrile for further isolation of the dendrimer-stabilized PdNPs in the solid state. Indeed an acetonitrile solution of a stoichiometric amount of 9 equiv. $[\text{Pd}(\text{OAc})_2]$ per dendrimer is added to the acetonitrile solution of **8**, provoking an instantaneous color change from brown/orange to intense green. Then, reduction of triazole-coordinated Pd(II) to Pd(0) is conducted upon addition of NaBH_4 as a solid (6 equivalents per Pd atom) to the **8**/ $\text{Pd}(\text{OAc})_2$ solution leading to a direct change of color from green to brown/black that is characteristic of PdNPs followed by isolation at the solid state

after removing the solvent. These PdNPs are analyzed by TEM microscopy and the images reveal that most of the PdNPs have a size between 2.0 nm and 6.0 nm (average size = 4 ± 1.2 nm), but another population with size in small quantity around 16 nm is also observed (Figure 4).

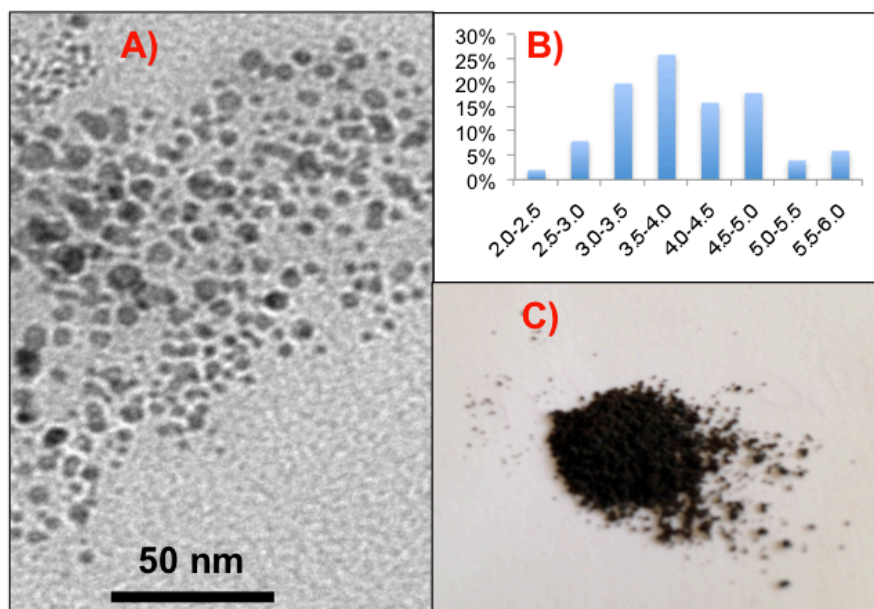
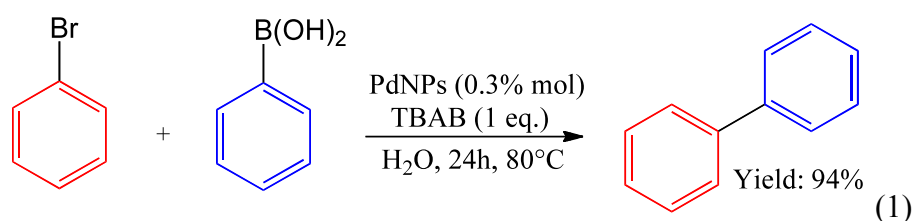


Figure 4. PdNPs stabilized by dendrimer **8** and analyzed by TEM (A), their distribution histogram (B) and isolation at the solid state (C).

The formation of these PdNPs is due to the evaporation of the solvent, leading to nano-scale aggregations. X-ray diffraction (XRD) analysis reveals that the catalyst contains only Pd⁰ indicating complete reduction of Pd^{II} by the excess of NaBH₄. The new catalyst is tested for the Suzuki-Miyaura C-C cross-coupling reaction that has become one of the most known and powerful Pd⁰ reaction allowing the synthesis of biaryl compounds, such as natural products, pharmaceuticals, polymers, etc.^[19]



Thus coupling between bromobenzene and phenyl boronic acid is carried out in water at 80°C during 24h with 0.3% mol of the Pd catalyst. The presence of TBAB as phase transfer agent is mandatory for total conversion (isolated yield: 94%).

Conclusion

The successful synthesis of a new alkyne-containing IMS **2** has been achieved, and this IMS has been easily functionalized using both the Sonogashira and the “click” CuAAC reactions. Easy functionalization by CuAAC reaction has been conducted with a nona-branched dendritic core **7** in high yield, showing that the functional IMS allows easy derivatization of supports. This dendrimer **8** is potentially usable as ionic liquid; moreover in the presence of a base such as tBuOK or KHMDS **2**, **5**, **6** or **8** are sources of carbenic species for metal coordination.^[20] Finally, the IMS **2** has been shown to be a good precursor of catalytically active PdNPs.

Experimental section

Synthesis of *N,N'*-dimesityl-2,3-diamino-1-propanol, **3**

In a Schlenk tube, 10g of 2,3-dibromopropanol (45.9 mmol, 1 eq.) and 16 g of 2,4,6-trimethylaniline (118 mmol, 2.6 eq.) were introduced. The reaction medium was stirred at 120°C during 20 hours. The temperature was decreased to room temperature and 50 mL of a water solution of NaOH (15% mol) were added. Then, 50 mL of CH₂Cl₂ was added, the organic phase was collected, and the water phase was extracted twice with 2x50 mL of CH₂Cl₂. The organic phases were gathered, dried on Na₂SO₄, and the solvent was evaporated under reduced pressure. The crude product was purified by silica chromatography column with Et₂O: pentane (1:1), and 6.7 g of **3** was obtained (44.6% of yield).

Synthesis of *N1,N2*-dimesityl-3-(prop-2-yn-1-yloxy)propane-1,2-diamine, **4**.

In a Schlenk tube, 3.1 g of **3** (9.48 mmol, 1 eq.), 2.1 mL of propargyl bromide (19 mmol, 2 eq.) and 40 mL of distilled THF were introduced. Then NaH (28.5 mmol, 3

eq.) was slowly added. The reaction was stirred at 40°C during 16 hours. At the end of the reaction and when the temperature decreases to room temperature, 20 mL of water was added. The THF solvent was evaporated under reduced pressure, and the water phase was extracted 3 times with 50 mL of CH₂Cl₂. The organic phases were gathered, dried on Na₂SO₄, the solvent was evaporated under reduced pressure, and 3.3 g of the desired product **4** was obtained as a brown solid (96.6% of yield).

¹H NMR (200 MHz; CDCl₃) δ (ppm): Ar-CH₃ 2.24-2.37 (m, 18H); C≡CH 2.41 (t, 1H, ²J = 2.4 Hz); CH₂ 3.08 (dd, 1H, ²J = 12 Hz, ³J = 5.7 Hz); CH₂ 3.33 (dd, 1H, ²J = 12 Hz, ³J = 5.6 Hz); CH+ CH₂ +2xNH 3.5-3.75 (m, 5H); CH₂ 4.18 (dd, 1H, ²J = 15.7 Hz, ³J = 2.5 Hz); CH₂ 4.23 (dd, 1H, ²J = 15.7 Hz, ³J = 2.5 Hz); H aromatic 6.87 (s, 4H)

¹³C NMR (50.33 MHz; CDCl₃) δ (ppm): 18.52; 19.00; 20.74 (CH₃ Ar); 50.75; 56.68; 58.66; 70.50 (3xCH₂ + 1xCH); 74.91; 79.62 (C ethylenic); 129.45; 129.60; 129.79; 130.09; 131.02; 131.46; 141.75; 143.77 (C Aromatic).

Synthesis of 1,3-dimesityl-4-((prop-2-yn-1-yloxy)methyl)-4,5-dihydro-1H-imidazol-3-ium tetrafluoroborate, **2**

In a Schlenk tube, 2.7 g of **4** (7.4 mmol, 1 eq) and 2.5 mL trimethyl orthoformate (15 mmol, 2 eq) and 770 mg of NH₄BF₄ (7.4 mmol, 1 eq.) were introduced. The reaction was stirred at 140°C during 2.5 hours under N₂. At the end of the reaction the temperature was decreased to 50°C, and the liquid was evaporated under reduced pressure. The resulting brown solid was washed several times with pentane and Et₂O and then was dried under reduced pressure for a few hours, and 2.77 g of **2** was obtained (81 % yield).

¹H NMR (200 MHz; CDCl₃) δ (ppm): Ar-CH₃ 2.24-2.39 (m, 18H); C≡CH 2.43 (m, 1H); CH₂ 3.5-3.7 (m, 2H); CH₂ 4.19 (d, 2H); CH₂ 4.25-4.38 (m, 1H); CH₂ 4.63 (m, 1H); CH 5.12 (m, 1H); H aromatic 6.93 (s, 4H); H imidazolium 7.92 (s, 1H)

¹³C NMR (50.33 MHz; CDCl₃) δ (ppm): 17.70; 18.28; 21.14 (CH₃ Ar); 52.82; 58.62; 63.83; 66.28 (3xCH₂, 1xCH); 76.02; 78.2 (C ethylenic); 128.39; 130.15; 130.35; 130.64; 135.46; 135.59; 136.10; 140.50; 140.76 (C aromatic); 158.53 (C imidazolium).

Synthesis of 4-(((1-benzyl-1H-1,2,3-triazol-4-yl)methoxy)methyl)-1,3-dimesityl-4,5-dihydro-1H-imidazol-3-ium tetrafluoroborate (test for the CuAAC “click” reaction).

In a Schlenk flask, benzyl azide (0.75 mmol, 1 eq.) and 470 mg of **2** (0.78 mmol, 1.05 eq.) were solubilized in 5 mL of distilled THF, then 48 mg of CuBr (60% mol) were added, and the reaction was conducted at 40°C during 36 hours. At the end of the reaction, 20 mL of water and 1 mL of an ammonia solution (37%) were added, and the media was stirred during 10 min. The aqueous phase was extracted 3 times with 20 mL of CH₂Cl₂. The organic phases are gathered and washed 3 times with 20 mL of water, dried on Na₂SO₄, the solvent was evaporated, and 230 mg of the desired “click” product was obtained (90.5 % of yield).

¹H NMR (200 MHz; CDCl₃) δ (ppm): Ar-CH₃ 2.18-2.32 (m, 18H); CH₂ 3.52 (d, 1H); CH₂ 3.73 (dd, 1H, ²J = 11.4 Hz, ³J = 2 Hz); CH₂ 4.34 (dd, 1H, ²J = 12 Hz ³J = 7.3 Hz); CH₂ 4.46-4.66 (m, 3H); CH 5.04 (m, 1H); CH₂-triazole 5.48 (s, 2H); H benzyl 6.7-7 (m, 5H); H aromatic 7.32 (s, 4H); H-triazole 7.71 (s, 1H); H imidazolium 7.85 (s, 1H)
¹³C NMR (50.33 MHz; CDCl₃), δ (ppm): 17.62; 18.40; 21.21 (CH₃ Ar); 52.93; 54.35; 64.25; 66.49 (3xCH₂, 1xCH); 123.95; 128.38; 128.60; 128.90; 129.29; 130.19; 130.52; 135.02; 135.43; 136.18; 140.80; 140.93 (C Aromatic + 2 C triazole); 158.01 (C imidazolium).

Synthesis of the imidazolium dendrimer, 8

In a Schlenk flask, 100 mg of the azido-core **7** (0.066 mmol, 1 eq.) and 305 mg of **2** (0.66 mmol, 1.1 eq.) were solubilized in 5 mL of distilled THF, then 60 mg of CuBr (60% mol) were added, and the reaction was conducted at 40°C during 48 hours. At the end of the reaction, a precipitate on the wall of the Schlenk flask was observed. The product was filtered and washed with THF several times. Acetone or acetonitrile was used to solubilize the product, then filtration on celite was performed. The solvent was evaporated, and 320 mg of the desired “click” product was obtained (85 % yield).

¹H NMR of **8** in CD₃CN (200 MHz, ppm): 8.70 (9H imidazolium), 8.20 (9H, trz), 7.07-6.94 (37H, Ar + 3H core), 5.24-3.58 (81H), 2.43-2.23 (162 H, CH₃ mesityl), 1.81-0.68 (54H, CH₂CH₂CH₂Si); 0.05 (54H, Si(CH₃)₂)

¹³C NMR of **8** in CD₃CN (50 MHz, ppm): 160.45 (CH, imidazolim), 147.94 (Cq trz), 141.65-129.82 (aromatics + CH trz), 67.72-53.82 (3CH₂, CH), 45.02 (CH₂CH₂CH₂Si), 42.54 (SiCH₂trz), 21.39-15.83 (CH₃ mesityl + CH₂Si + CH₂CH₂Si).

Acknowledgement

Financial support from the Univ. Bordeaux and Toulouse III, the CNRS and the Ministère de l'Enseignement Supérieur et de la Recherche (PhD grant to CD) are gratefully acknowledged.

References

- [1] S. N. Riduan, Y. Zhang, *Chem. Soc. Rev.* **2013**, *42*, 9055—9070
- [2] Y. G. Zhang, J. Y. G. Chan, *Energy Environ. Sci.* **2010**, *3*, 408–417.
- [3] E. B. Anderson, T. E. Long, *Polymer* **2010**, *51*, 2447–2454.
- [4] T. M. Trnka, R. H. Grubbs, *Acc. Chem. Res.* **2001**, *34*, 18-29.
- [5] a) C. Deraedt, M. d'Halluin, D. Astruc, *Eur. J. Inorg. Chem.* **2013**, *28*, 4881-4908; b) Olefin Metathesis. Theory and Practice (Ed: K. Grela) Wiley, Hoboken, New Jersey **2014**.
- [6] a) V. V. Rostovtsev, L. G. Green, V. V. Fokin, K. B. Sharpless, *Angew. Chem., Int. Ed.* **2002**, *41*, 2596–2599; b) C. W. Tornøe, C. Christensen, M. Meldal, *J. Org. Chem.* **2002**, *67*, 3057–3064.
- [7] a) P. D. Stevens, F. G. Li, J. D. Fan, M. Yen, Y. Gao, *Chem. Commun.* **2005**, 4435-4437; b) R. Chinchilla, C. Najera, *Chem. Soc. Rev.* **2011**, *40*, 5084-5121.
- [8] D. Astruc, E. Boisselier, C. Ornelas, *Chem. Rev.* **2010**, *110*, 1857-1959; b) A.-M. Caminade, C.-O. Turin, R. Laurent, A. Ouali, B. Delavaux-Nicot, *Dendrimers*, Wiley Chichester, UK., **2011**; c) *Designing Dendrimers* (Eds: S. Campagna, P. Ceroni, F. Puntoriero) Wiley, Hoboken, NJ, **2012**.
- [9] G. R. Newkome, Z. Yao, G. R. Baker, V. K. Gupta, *J. Org. Chem.* **1985**, *50*, 2003-2004; b) G. R. Newkome, *Pure Appl. Chem.* **1998**, *70*, 2337-2343.
- [10] C. C. Lee, J. A. MacKay, J. M. J. Fréchet, F. C. Szoka, *Nat. Biotechnol.* **2005**, *23*, 1517-1526.

- [11] a) G. R. Newkome, E. He, C. N. Moorefield, *Chem. Rev.* **1999**, *99*, 1689-1746; b) C. Ornelas, J. Ruiz, E. Cloutet, S. Alves, D. Astruc, *Angew. Chem. Int. Ed.* **2007**, *46*, 872–877; c) R. Djeda, A. Rapakousiou, L. Liang, N. Guidolin, J. Ruiz, D. Astruc, *Angew. Chem. Int. Ed.* **2010**, *49*, 8152–8156; d) C. M. Casado, B. Alonso, J. Losada, M. P. Garcia-Armada In *Designing Dendrimers* (Eds: S. Campagna, P. Ceroni, F. Puntoriero) Wiley, Hoboken, NJ, **2012**, 219-262.
- [12] D. Wang, D. Astruc, *Coord. Chem. Rev.* **2013**, *257*, 2317-2334.
- [13] a) R. M. Crooks, M. Zhao, L. Sun, V. Chechik, L. K. Yeung, *Acc. Chem. Res.* **2001**, *34*, 181-190; b) V. S. Myers, M. G. Weier, E. V. Carino, D. F. Yancey, S. Pande, R. M. Crooks, *Chem. Sci.* **2011**, *2*, 1632-1646; c) C. Deraedt, D. Astruc, *Acc. Chem. Res.* **2014**, *47*, 494-503.
- [14] D. Astruc, L. Liang, A. Rapakousiou, J. Ruiz *Acc. Chem. Res.* **2012**, *45*, 630-640.
- [15] a) P. Wu, M. Malkoch, J. N. Hunt, R. Vestberg, E. Kaltgrad, M. G. Finn, V. V. Fokin, K. B. Sharpless, C. J. Hawker, *Chem. Commun* **2005**, 5775-5777; b) G. Franc, A. K. Kakkar, *Chem. Commun.* **2008**, 5267-5276; c) X. Q. Xiong, *Aust. J. Chem.* **2009**, *62*, 1371-1377; d) G. Franc, A. K. Kakkar, *Chem. Soc. Rev.* **2010**, *39*, 1536-1544.
- [16] a) I. P. Beletskaya, A. V. Cheprakov, A. V. *Chem.Rev.* **2000**, *100*, 3009-3066; b) F. Lu, J. Ruiz, D. Astruc, *Tetrahedron Lett.* **2004**, 9443-9445; c) D. Astruc, J. Ruiz, F. Lu, *Angew. Chem. Int. Ed.*, **2005**, *44*, 7852-7872; d) J. G. de Vries, *Dalton Trans.* **2006**, 421-429. *Modern Surface Organometallic Chemistry*, (Eds.: J.-M. Basset, R. Psaro, D. Roberto, R. Ugo), Wiley-VCH, Weinheim, **2009**; e) L. M. Bronstein, Z. B. Shifrina, *Chem. Rev.* **2011**, *111*, 5301-5344; f) *Nanomaterials in Catalysis*; (Eds.: P. Serp, K. Philippot), Wiley-VCH, Weinheim, **2013**.
- [17] M. Mayr, M. R. Buchmeiser, K. Wurst, *Adv. Synth. Catal.* **2002**, *344*, 712-719.
- [18] a) L. Liang, J. Ruiz, D. Astruc, *Adv. Syn. Catal.* **2011**, *353*, 3434-3450; b) C. Deraedt, N. Pinaud, D. Astruc, *J. Am. Chem. Soc.* **2014**, *136*, 12092–12098.

- [19] a) N. Miyaura, A. Suzuki, *Chem. Rev.* **1995**, *95*, 2457-2483; b) J. Hassan, M. Sévignon, C. Gozzi, E. Schulz, M. Lemaire, *Chem. Rev.* **2002**, *12*, 1359-1469.
- [20] a) A. J. Arduengo, R. L. Harlow, M. Kline, *J. Am. Chem. Soc.* **1991**, *113*, 361-363; b) D. Bourissou, O. Guerret, F. P. Gabbaï, G. Bertrand, *Chem. Rev.* **2000**, *100*, 39-92; c) B. K. Keitz, J. Bouffard, G. Bertrand, R. H. Grubbs, *J. Am. Chem. Soc.* **2011**, *133*, 8498-8501.



Cite this: *Chem. Commun.*, 2014, 50, 10126

Received 11th June 2014,
Accepted 14th July 2014

DOI: 10.1039/c4cc04454a

www.rsc.org/chemcomm

Gold nanoparticles as electron reservoir redox catalysts for 4-nitrophenol reduction: a strong stereoelectronic ligand influence†

Roberto Ciganda,^{ab} Na Li,^a Christophe Deraedt,^a Sylvain Gatard,^a Pengxiang Zhao,^{ac} Lionel Salmon,^d Ricardo Hernández,^b Jaime Ruiz^a and Didier Astruc^{*a}

The stereoelectronic properties of the stabilizing ligands of gold nanoparticles (AuNPs) are shown to play a considerable role in their catalytic efficiency for 4-nitrophenol reduction by NaBH₄, consistent with a mechanism involving restructuring of the AuNP surface that behaves as an “electron reservoir”.

Gold nanoparticles (AuNPs) have recently received considerable interest for a variety of applications owing to their unique physical and chemical properties.¹ In particular, their extensive use in catalysis² has followed the seminal discovery of low-temperature CO oxidation by small AuNPs by Haruta.³ Among the transition metal-catalyzed redox reactions, the reduction of nitroaromatics is one of the most crucial ones.⁴ Indeed, 4-nitrophenol (4-NP) is anthropogenic, toxic and inhibitory in nature. Its reduction product, 4-aminophenol (4-AP), finds applications as a photographic developer of black and white films, a corrosion inhibitor, a dyeing agent, a precursor for the manufacture of analgesic and antipyretic drugs, and in particular, as an intermediate for the synthesis of paracetamol.⁵ Noble metal nanoparticle catalysts are widely employed for the reduction of 4-NP to 4-AP,^{6–8} and this reaction, with an excess amount of NaBH₄, has often been used as a model reaction to examine the catalytic performance of metal NPs,^{6,7} as first shown by Pal *et al.*⁸ AuNP catalysts that have been examined so far are solid-supported AuNPs⁷ or various thiolate-AuNPs. The reaction mechanism is still unknown, although Ballauff's group provided strong evidence for a process fitting the Langmuir–Hinshelwood

(LH) model. This mechanism involves adsorption of both reactants on the surface of the catalyst for AuNPs or PdNPs that are immobilized on the surface of spherical polyelectrolyte brushes with an induction time caused by dynamic restructuring of the nanoparticle surface.^{6c,7b,d,9} For other AuNPs, Pal's group also showed that the catalytic reaction took place at the AuNP surface.¹⁰ Ghosh's group showed that the rate constant increased with a decrease in the size of AuNPs and was proportional to the total surface area of AuNPs,⁹ as reported by Ballauff's group;¹¹ and Liu *et al.* reported that surface functional groups influenced the catalytic behavior.¹² Katz suggested a completely different mechanism in which the active site was a leached gold species that was present in exceedingly small concentrations.¹³ Zhang *et al.* suggested that the borohydride salt transferred a hydride to the AgNPs in the case of TiO₂-supported AgNPs.¹⁴ Scott's group showed that in the presence of excess borohydride salts, thiolate-AuNPs that catalyze 4-NP reduction grew to larger sizes.¹⁵

Here we show the dramatic influence of the stereoelectronic effects of the ligand on the reaction rate, and we emphasize the electron reservoir behavior of the gold nanoparticle catalysts. Therefore, we compare, under identical conditions, the rates of the homogeneous 4-NP reduction by excess NaBH₄ catalyzed in water by water-soluble AuNPs stabilized by citrate, polyethylene glycol (PEG) thiolate of different lengths, and mono, bifunctional, polymeric and dendritic 1,2,3-triazoles terminated with PEG 400 or 2000 (Fig. 1). The catalytic 4-NP reduction is easily monitored *via* UV-vis spectroscopy by the decrease of the strong adsorption of the 4-nitrophenolate anion at 400 nm, directly leading to the rate constant.⁸ Isosbestic points in the spectra of the reacting mixtures demonstrate that no side reaction occurs.^{6c} The various stable AuNPs that are studied have sizes around 3 nm, but larger AuNPs have also been examined for comparison (Table 1). The reduction rate has been observed, as in many preceding cases, to be pseudo-first order in the presence of a large molar excess of NaBH₄ (here 81 equiv. NaBH₄ per mol 4-NP). All the apparent kinetic constants are summarized in Table 1. In order to obtain data that are independent of the surface, the rate constant ($k_1 = k_{app}/S$) was also estimated

^a Univ. Bordeaux, ISM, UMR 5515, 33405 Talence Cedex, France.

E-mail: d.astruc@ism.u-bordeaux.fr

^b Facultad de Química de San Sebastian, Universidad del País Vasco, Apdo. 1072, 20080 San Sebastian, Spain

^c Science and Technology on Surface Physics and Chemistry Laboratory, PO Box 718-35, Miayang 621907, Sichuan, China

^d LCC UPR 241, 205 Route de Narbonne, 31077 Toulouse Cedex, France

† Electronic supplementary information (ESI) available: UV-vis spectra of the reduction of 4-NP by AuNPs, the corresponding plots of $-\ln(C_t/C_0)$ as a function of time and $\ln k_{app}$ vs. $1/T$ and AuNP synthesis and characterization. See DOI: 10.1039/c4cc04454a

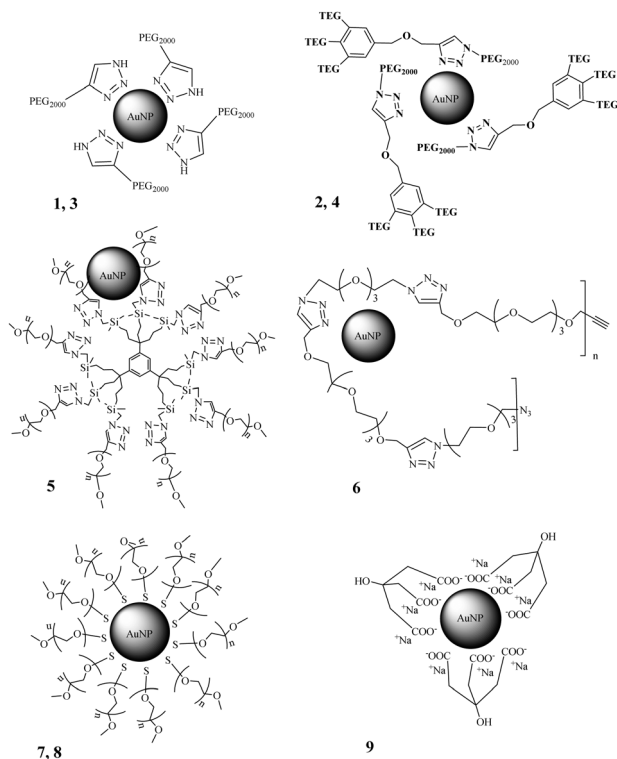


Fig. 1 Various AuNPs under study. See the diameters (D) in Table 1. The ligands of **7** and **8** are respectively HS-PEG400 and HS-PEG2000.

Table 1 Catalytic AuNP activity in the reduction of 4-NP at 20 °C

AuNPs stabilized	D (nm)	k_{app} (s ⁻¹)	t_0 (s)	k_1 (L s ⁻¹ m ⁻²)	E_a (kJ mol ⁻¹)
1	3	Fast ^a	0	—	24
2	3	Fast ^b	0	—	29
3	6	1.4×10^{-2}	0	4.3×10^{-2}	37
4	6	6.7×10^{-3}	0	2×10^{-2}	40
5	3.5	7.5×10^{-3}	0	1.2×10^{-2}	—
6	3.6	1.1×10^{-2}	0	1.9×10^{-2}	—
7	3.5	7×10^{-4}	900	1×10^{-3}	132
8	13.5	4×10^{-4}	2100	3×10^{-3}	—
9	13.5	6×10^{-4}	1200	4×10^{-4}	—

^a At 13 °C: $k_{app} = 1.2 \times 10^{-2}$ s⁻¹, $k_1 = 1.7 \times 10^{-2}$ L s⁻¹ m⁻². ^b At 13 °C: $k_{app} = 9.6 \times 10^{-3}$ s⁻¹, $k_1 = 1.4 \times 10^{-2}$ L s⁻¹ m⁻².

normalized to the surface (S) with the assumption of the LH mechanistic model^{7b,16} (see Table 1). The results clearly show that the best stabilizers, thiolates, provide the slowest AuNP catalysts, followed by the citrate. Citrate-AuNPs are large, but the comparison between thiolate-AuNPs and citrate-AuNPs of the same size (diameter: 13.5 nm) shows that the citrate-AuNPs are slightly less slow catalysts than the thiolate-AuNPs. The similarity of results with these two types of ligands, however, reveals a similarity of bonding to the AuNP, *i.e.* the citrate-AuNP bond should reflect the coordination of citrate to the AuNP surface, as the thiolate-AuNP bond, in spite of the difference in electronegativity and polarizability between these two chalcogen atoms.

All the 1,2,3-triazole (trz)-stabilized AuNPs¹⁷ that are examined here are much more efficient catalysts than the AuNPs that are

stabilized by the formally anionic thiolate and citrate ligands. This reveals the considerable advantage, in terms of catalytic reaction rates, of neutral ligands such as triazoles that form only weak coordination bonds with the AuNP surface given the impossibility of back bonding due to high-lying nitrogen π^* orbitals. This weak bonding of the trz ligands, compared to the stronger bonding of thiolate and citrate ligands, is responsible for their easy displacement from the AuNP surface by substrates. It is also striking that the induction time (t_0), which is usually directly connected to the surface rearrangement on the AuNP surface,^{7b,d} is found only with the thiolate-AuNPs and citrate-AuNPs.

With these ligands, they are rather long, and by contrast, under these conditions, no induction times are found for all the trz-AuNPs, confirming the very facile trz displacement by the substrates. Among the trz-AuNPs, the dendrimer-stabilized trz-AuNPs are the less efficient catalysts. The polymer-stabilized trz-AuNPs are more efficient than the related dendrimer-stabilized trzAuNPs, but less so than the non-dendritic mono- and disubstituted trz ligands. Thus, it appears that this order of catalytic efficiency of the trz-AuNPs is related to their steric effects, the largest steric bulk being provided by the dendrimer framework that is bulkier than that of the polymer, whereas the less bulky non-macromolecular trz ligands provide by far the most efficient AuNP catalysts. These two AuNPs catalyze reactions that are so fast, under the same conditions as the other liganded AuNP catalysts, that they are too fast to observe a measurable rate at 25 °C. It is possible to compare these two AuNP catalysts, however, at lower temperatures. Then the mono-substituted trz-AuNPs appear to be more efficient than the bulkier disubstituted trz-AuNPs, as expected.

These results confirm that ligand displacement by substrates on the AuNP surfaces is the dominant feature of the mechanism that involves restructuring of the surface. This is in accord with the mechanism proposed by Ballauff and others following the LH kinetic model, which in particular also discards a leaching mechanism. With the series of trz-AuNPs, it also appears that diffusion of substrates towards the trz-AuNPs shows the filtration effect of the dendrimer and polymer frameworks, because the order of reaction rates follows the order of steric bulk of the trz-containing frameworks.

These data also confirm that the AuNPs play the role of an inner-sphere redox catalyst,¹⁸ because BH_4^- transfers a hydride to the AuNP surface, resulting in the formation of a covalent Au-H bond.^{7d} This means that the negative charge is transferred to the AuNP, as already suggested,^{7d,19} charge delocalization being largely facilitated by the low-lying conduction band of the AuNPs. Indeed, addition of $NaBH_4$ to the trz-AuNPs leads to a color change corresponding to a blue shift of the surface plasmon band (SPB) that indicates the accumulation of several negative charges at the AuNP surface. Such a shift that has been already observed in particular for thiolate-AuNPs is shown here for trz-AuNPs (Fig. 2).

This effect is accompanied by another effect, AuNP aggregation, *i.e.* AuNP size increase (Ostwald ripening),²⁰ upon $NaBH_4$ addition, that is characterized by a red shift of the SPB.

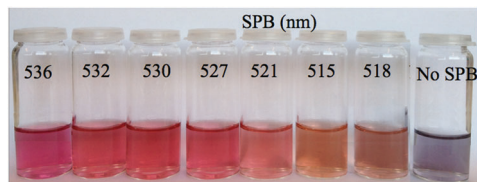


Fig. 2 Trz-AuNPs **3** after addition from left to right of 0, 0.1, 0.2, 0.3, 0.4, 0.5, 1, 1.5 and 2 equiv. of NaBH_4 per gold atom. The blue shift upon NaBH_4 addition is emphasized by values of λ_{max} (SPB).

After observation of the blue shift upon NaBH_4 addition, this red shift appears upon addition of more NaBH_4 . Gold precipitation then occurs when the amount of added NaBH_4 becomes too high (Fig. 2).

The accumulation of negative charges at the AuNP surface proceeds along with the Au–H bond formation until the resulting electrostatic effect becomes too important. Along this line, electrochemical experiments conducted by Quinn's group by differential pulse voltammetry using well-defined thiolate– Au_{147} NPs showed a series of 15 electrochemically and chemically reversible single electron transfer steps with Coulomb blockades (only limited by the electrochemical window) leading to stable multiply charged AuNPs.²¹ In the presence of nitrophenolate anions on the AuNP surface, the electrochemical peak spacing that corresponds to the quantized capacitance charging was found to be decreased compared to that obtained in its absence, which corresponds to a small decrease of the AuNP capacitance.²² This shows that the AuNPs behave as “electron reservoirs”.²³ This role is efficiently fulfilled by the AuNP redox catalysts for 4-NP reduction in the transformation of inner-sphere single electron transfers from borohydride ions to the surface into a multi-electron transfer. A multi-electron transfer is necessary for each 4-NP reduction to 4-AP. The citrate anions, as hydrides, form coordination bonds with the AuNP surface involving partial charge transfer from the ligand to the AuNP surface. Such a coordination with a tripod of dihapto carboxylates that are coordinated to Au(111) is known,²⁴ although the degree of AuNP–O covalency and charge transfer has not been addressed.

In conclusion, the role of the stabilizing ligands in the AuNP catalyzed 4-NP reduction has been shown here to be crucial. It is involved both in the restructuring at the AuNP surface following the LH kinetic model with considerable variation of efficiency from “anionic” thiolate or citrate ligands to neutral trz ligands and the steric or filtering effect²⁵ of the substrate through the bulk of the trz ligand framework. The difficulty in exchanging the thiolate ligands does not inhibit Suzuki–Miyaura cross carbon–carbon coupling reactions with analogous PdNPs,^{26a} because a leaching mechanism is involved.^{26b} On the other hand, it considerably slows down AuNP-catalyzed 4-NP reduction in contrast to the situation involving easily exchanged trz ligands.¹⁷ The data and apparent accumulation of several negative charges in the AuNPs that occurs while the Au–H bonds form upon NaBH_4 reaction emphasize the role of “electron reservoirs” of these redox catalysts. Well-known precedents are found for instance in the role of PtNPs as redox catalysts

in water photosplitting.²⁷ These findings should significantly contribute to shed light on the surface mechanism and optimize the design of effective catalysts for this intensively searched “green” aqueous reaction.

Financial support from Gobierno Vasco (R. C., post-doctoral scholarship), Universidad del País Vasco, Chinese Scholarship Council (N. L., PhD grant), Ministère de la Recherche et de la Technologie (C. D., PhD grant), the CNRS (S. G. delegation), and the University of Bordeaux is gratefully acknowledged.

Notes and references

- (a) M.-C. Daniel and D. Astruc, *Chem. Rev.*, 2004, **104**, 293; (b) X. Chen and S. S. Mao, *Chem. Rev.*, 2007, **107**, 2891; (c) Y. Xia, Y. Xiong, B. Lim and S. E. Skrabalak, *Angew. Chem., Int. Ed.*, 2009, **48**, 60; (d) *Gold Nanoparticles for Physics, Chemistry, Biology*, ed. C. Louis and O. Pluchery, Imperial College Press, 2012.
- (a) M. Haruta and M. Date, *Appl. Catal., A*, 2001, **222**, 227; (b) F. Porta, L. Prati, M. Rossi and G. Scari, *J. Catal.*, 2002, **210**, 464; (c) M. Haruta, *Nature*, 2005, **437**, 1098; (d) D. I. Enache, J. K. Edwards, P. Landon, B. Solsona-Espriu, A. F. Carley, A. A. Herzing, M. Watanabe, C. J. Kiely, D. W. Knight and G. J. Hutchings, *Science*, 2006, **311**, 362; (e) C. D. Pina, E. Falletta, L. Prati and M. Rossi, *Chem. Soc. Rev.*, 2008, **37**, 2077; (f) A. Corma and H. Hermenegildo, *Chem. Soc. Rev.*, 2008, **37**, 2096; (g) A. Corma, A. Leyva-Perez and J. Maria Sabater, *Chem. Rev.*, 2011, **111**, 1657; (h) N. Dimitratos, J. A. Lopez-Sanchez and G. J. Hutchings, *Chem. Sci.*, 2012, **3**, 20.
- (a) M. Haruta, T. Kobayashi, H. Sano and N. Yamada, *Chem. Lett.*, 1987, 405; (b) M. Haruta, N. Yamada, T. Kobayashi and S. Iijima, *J. Catal.*, 1989, **115**, 301; (c) M. Haruta, *Catal. Today*, 1997, **36**, 153; (d) M. Haruta, *Angew. Chem., Int. Ed.*, 2014, **53**, 52.
- A. Corma and P. Serna, *Science*, 2006, **313**, 332.
- (a) Y.-T. Woo and D. Y. Lai, *Aromatic Amino and Nitro-Amino Compounds and Their Halogenated Derivatives. Paty's Toxicology*, Wiley, New York, 2001, pp. 1–96; (b) S. C. Mitchell and R. H. Waring, Aminophenols, in *Ullmann's Encyclopedia of Industrial Chemistry*, Wiley-VCH, 2002.
- (a) A. Gangula, R. Podila, R. M. L. Karanam, C. Janardhana and A. M. Rao, *Langmuir*, 2011, **27**, 15268–15274; (b) Y. Zhang, X. Cui, F. Shi and Y. Deng, *Chem. Rev.*, 2012, **112**, 2467–2505; (c) P. Herves, M. Perez-Lorenzo, L. M. Liz-Marzán, J. Dzubielia, Y. Lu and M. Ballauff, *Chem. Soc. Rev.*, 2012, **41**, 5577–5587; (d) N. C. Antonels and R. Meijboom, *Langmuir*, 2013, **29**, 13433–13442.
- (a) K. Kuroda, T. Ishida and M. Haruta, *J. Mol. Catal. A: Chem.*, 2009, **298**, 7–11; (b) S. Wunder, F. Polzer, Y. Lu and M. Ballauff, *J. Phys. Chem. C*, 2010, **114**, 8814–8820; (c) S.-N. Wang, M.-C. Zhang and W. Q. Zhang, *ACS Catal.*, 2011, **1**, 207–211; (d) S. Wunder, Y. Lu, M. Albrecht and M. Ballauff, *ACS Catal.*, 2011, **1**, 908–916; (e) J. Li, C.-Y. Liu and Y. Liu, *J. Mater. Chem.*, 2012, **22**, 8426–8430; (f) J. Zhang, D. Han, H. Zhang, M. Chaker, Y. Zhao and D. Ma, *Chem. Commun.*, 2012, **48**, 11510–11512; (g) A. Shivhare, S. J. Ambrose, H. Zhang, R. W. Purves and R. W. J. Scott, *Chem. Commun.*, 2013, **49**, 276–278; (h) P. Pachfule, S. Kandambeth, D. Diaz and R. Banerjee, *Chem. Commun.*, 2014, **50**, 3169.
- N. Pradhan, A. Pal and T. Pal, *Colloids Surf., A*, 2002, **196**, 247–257.
- S. Panigrahi, S. Basu, S. Praharaj, S. Pande, S. Jana, A. Pal, S. K. Ghosh and T. Pal, *J. Phys. Chem. C*, 2007, **111**, 4596.
- S. Saha, A. Pal, S. Kundu, S. Basu and T. Pal, *Langmuir*, 2010, **26**, 2885–2893.
- Y. Mei, G. Sharma, Y. Lu, M. Drechsler, T. Irgang, R. Kempe and M. Ballauff, *Langmuir*, 2005, **21**, 12229–12234.
- (a) W. Liu, X. Yang and W. Huang, *J. Colloid Interface Sci.*, 2006, **304**, 160; (b) W. Liu, X. Yang and L. Xie, *J. Colloid Interface Sci.*, 2007, **313**, 494.
- M. M. Nigra, J.-M. Ha and A. Katz, *Catal. Sci. Technol.*, 2013, **3**, 2976–2983.
- H. Zhang, X. Li and G. Chen, *J. Mater. Chem.*, 2009, **19**, 8223–8231.
- M. Dasog, W. Hou and R. W. J. Scott, *Chem. Commun.*, 2011, **47**, 8569–8571.
- S. Panigrahi, S. Basu, S. Praharaj, S. Pande, S. Jana and A. Pal, *J. Phys. Chem. C*, 2007, **111**, 4596–4605.
- (a) D. Astruc, L. Liang, A. Rapakousiou and J. Ruiz, *Acc. Chem. Res.*, 2012, **45**, 630–640; (b) D. Astruc, *Nat. Chem.*, 2012, **4**, 255–267.

- 18 (a) H. Taube, H. Myers and R. L. Rich, *J. Am. Chem. Soc.*, 1953, **75**, 4118; (b) J.-M. Savéant, *Acc. Chem. Res.*, 1980, **13**, 25; (c) J.-M. Lehn, *Science*, 1985, **227**, 849; (d) D. Astruc, *Electron Transfer and Radical Processes in Transition-Metal Chemistry*, VCH, New York, 1995, ch. 7, pp. 479–506.
- 19 (a) P. Mulvaney, *Langmuir*, 1996, **12**, 788–800; (b) M. Brust and C. Kiely, *Colloids Surf., A*, 2002, **202**, 175–186.
- 20 (a) W. Ostwald, *Z. Phys. Chem.*, 1897, **22**, 289–330; (b) N. G. Bastus, J. Comenge and V. Puentes, *Langmuir*, 2011, **27**, 11098–11105.
- 21 B. M. Quinn, P. Lijeroth, V. Ruiz, T. Laaksonen and K. Kontturi, *J. Am. Chem. Soc.*, 2003, **125**, 6644–6645.
- 22 S. Chen and K. Huang, *Langmuir*, 2000, **16**, 2014–2018.
- 23 (a) J.-R. Hamon, D. Astruc and P. Michaud, *J. Am. Chem. Soc.*, 1981, **103**, 758–766; (b) C. Ornelas, J. Ruiz, C. Belin and D. Astruc, *J. Am. Chem. Soc.*, 2009, **131**, 590–601.
- 24 (a) S. Floate, M. Hosseini, M. R. Arshadi, D. Ritson, K. L. Young and R. J. Nichols, *J. Electroanal. Chem.*, 2003, **542**, 67–71; (b) Y. Lin, G.-B. Pan, G.-J. Su, X.-H. Fang, L.-J. Wan and C.-L. Bai, *Langmuir*, 2003, **19**, 10000–10003.
- 25 (a) R. M. Crooks, M. Zhao, L. Sun, V. Chechik and L. K. Yeung, *Acc. Chem. Res.*, 2001, **34**, 181–190; (b) V. S. Myers, M. W. Weier, E. V. Carino, D. F. Yancey and R. M. Crooks, *Chem. Sci.*, 2011, **2**, 1632–1646.
- 26 (a) F. Lu, J. Ruiz and D. Astruc, *Tetrahedron Lett.*, 2004, 9443–9445; (b) A. Diallo, C. Ornelas, L. Salmon, J. Ruiz and D. Astruc, *Angew. Chem., Int. Ed.*, 2007, **46**, 8644–8648.
- 27 (a) J.-M. Lehn and J.-P. Sauvage, *Nouv. J. Chim.*, 1977, **1**, 449–451; (b) A. Hagfeldt and M. Grätzel, *Chem. Rev.*, 1995, **95**, 49–68.

Liste de publications

1) Deraedt, C.; D'Halluin, M.; Astruc, D. **Metathesis reactions: recent trends and challenges.** *Eur. J. Inorg. Chem.*, 4881-4908, **08/2013**

2) Deraedt, C.; Salmon, L.; Etienne, L.; Ruiz, J.; Astruc, D. **“Click” dendrimers as efficient nanoreactors in aqueous solvent: Pd nanoparticle stabilization for sub-ppm Pd catalysis of Suzuki–Miyaura reactions of aryl bromides.** *Chem. Commun.*, 49, 8169-8171, **09/2013**

3) Deraedt, C.; Salmon, L.; Ruiz, J.; Astruc, D. **Efficient Click-Polymer-Stabilized Palladium Nanoparticle Catalysts for Suzuki–Miyaura Reactions of Bromoarenes and Reduction of 4-Nitrophenol in Aqueous Solvents.** *Adv. Synth. Catal.*, 355, 2992-3001, **10/2013** (highlights in current synthetic organic chemistry, **Suzuki-Miyaura coupling using polymer-stabilized Pd nanoparticles.** *SYNFACTS.*, **2014**, 10(1): 0101 and *ChemInform.*, **2014**, 45(15))

4) Deraedt, C.; Astruc, D. **“Homeopathic” Palladium Nanoparticle Catalysis of Cross Carbon-Carbon Coupling Reactions.** *Acc. Chem. Res.*, 47, 494-503, **02/2014**

5) Gatard, S.; Salmon L.; **Deraedt, C.;** Ruiz, J.; Astruc, D.; Bouquillon, S. **Gold Nanoparticles Stabilized by Glycodendrimers: Synthesis and Application to the Catalytic Reduction of 4-Nitrophenol.** *Eur. J. Inorg. Chem.*, 2014, 2671-2677, **05/2014**

6) Deraedt, C.; Wang, Y.; Rapakousiou, A.; Salmon, L.; Bousquet, M.; Astruc, D. **Multi-function Redox Polymers: Electrochrome, Polyelectrolyte, Sensor, Electrode Modifier, Nanoparticle Stabilizer and Catalyst Template.** *Angew. Chem.*, 53, 8445-8449, **05/2014**

7) Deraedt, C.; Salmon, L.; Astruc, D. **“Click” Dendrimer-stabilized Pd Nanoparticles as a Green Catalyst for Efficient C-C Cross-coupling Reactions and Reduction of 4-Nitrophenol.** *Adv. Synth. Catal.*, 356, 2525-2538, **06/2014**

8) Gatard, S.; Salmon L.; **Deraedt, C.;** Ruiz, J.; Astruc, D.; Bouquillon, S. **Palladium Nanoparticles Stabilized by Glycodendrimers and their Application in Catalysis,** *Eur. J. Inorg. Chem.*, 26, 4369-4375, **07/2014**

9) Ciganda, R.; Li, Na.; **Deraedt, C.;** Gatard, S.; Zhao, P.; Salmon, L.; Hernandez, R.; Ruiz, J.; Astruc, D. **Gold nanoparticles as electron reservoir redox catalysts for 4-nitrophenol reduction: a strong stereoelectronic ligand influence,** *Chem. Commun.*, 50, 10126—10129, **07/2014**

10) Deraedt, C.; Pinaud, N.; Astruc, D.; **A Recyclable Catalytic Dendrimer Nanoreactor for Part-Per-Million Cu^I Catalysis of “Click” Chemistry in Water.** *J. Am. Chem. Soc.*, 136, 12092-12098, **08/2014**

Deraedt, C.; Salmon, L.; Gatard, S.; Ciganda, R.; Hernandez, R.; Ruiz, J.; Astruc, D.; **Sodium borohydride stabilizes very efficient gold nanoparticle catalyst.** *Chem. Commun.*, 50, 14194-14196, **09/2014**

11) Rapakousiou, A.; **Deraedt, C.**; Gu, A.; Salmon, L.; Belin, C.; Ruiz, J.; Astruc, D.; **Mixed-Valent Intertwined Polymer Units Containing Biferrocenium Chloride Side Chains Form Nanosnakes that Encapsulate Gold Nanoparticles**, *J. Am. Chem. Soc.*, 136, 13995-13998, **09/2014**

12) Wang, D.; **Deraedt, C.**; Salmon, L.; Labrugère, C.; Etienne, L.; Ruiz, J.; Astruc, D.; **Efficient and Magnetically Recoverable “Click” PEGylated γ -Fe₂O₃-Pd Nanoparticle Catalysts for Suzuki-Miyaura, Sonogashira, and Heck Reactions with Positive Dendritic Effects**, *Chem. Eur. J.*, DOI:10.1002/chem.201404590, **11/2014**

13) Deraedt, C.; Wang, D.; Salmon, L.; Etienne, L.; Labrugère, C.; Ruiz, J.; Astruc, D.; **Robust, efficient and recyclable catalyst by impregnation of dendritically preformed Pd nanoparticles on magnetic support**, *ChemCatChem*, DOI: 10.1002/cctc.201402775, **11/2014**

14) Deraedt, C.; Rapakousiou, A., Gu, H.; Salmon, L.; Ruiz, J.; Astruc, D.; **Catalytically-active Palladium Nanoparticles Stabilized by Triazolylbiferrocenyl-containing Polymers**, *J. Inorg. Organomet. Polym.*, DOI: 10.1007/s10904-014-0161-6, **01/2015**

15) Deraedt, C.; d’Halluin, M.; Lesturgez, S.; Salmon, L.; Goglio, G.; Ruiz, J.; Astruc, D.; **Alkynyl-functionalized imidazolium for “click” dendrimer functionalisation and palladium nanoparticle stabilization**, *Eur. J. Inorg. Chem.*, 1345-1350, **02/2015**

16) Rapakousiou, A.; **Deraedt, C.**; Irigoyen, J.; Wang, Y.; Pinaud, N.; Salmon, L.; Ruiz, J.; Astruc, D.; **Synthesis and redox activity of “clicked” triazolylbiferrocenyl polymers, network encapsulation of gold and silver nanoparticles and anion sensing**, *Inorg. Chem.*, DOI: 10.1021/ic5028916, **02/2015**

17) Wang, D.; **Deraedt, C.**; Salmon, L.; Labrugère, C.; Etienne, L.; Ruiz, J.; Astruc, D.; **A tris(triazolate) ligand for a highly active and magnetic recoverable palladium catalyst of selective alcohol oxidation using air at atmospheric pressure**, *Chem. Eur. J.*, DOI: 10.1002/chem.201500122, **03/2015**

18) Wang, D.; **Deraedt, C.**; Ruiz, J.; Astruc, D.; **Sodium hydroxide-catalyzed transfer hydrogenation of carbonyl compounds and nitroarenes using ethanol or isopropanol of both solvent and hydrogen donor**, *J. Mol. Catal.; A Chem.*, 400, DOI: 10.1016/j.molcata.2015.01.024, **05/2015**

19) Wang, D.; **Deraedt, C.**; Ruiz, J.; Astruc, D.; **Magnetic and dendritic catalyst**, *Acc. Chem. Res.*, just accepted **2015**

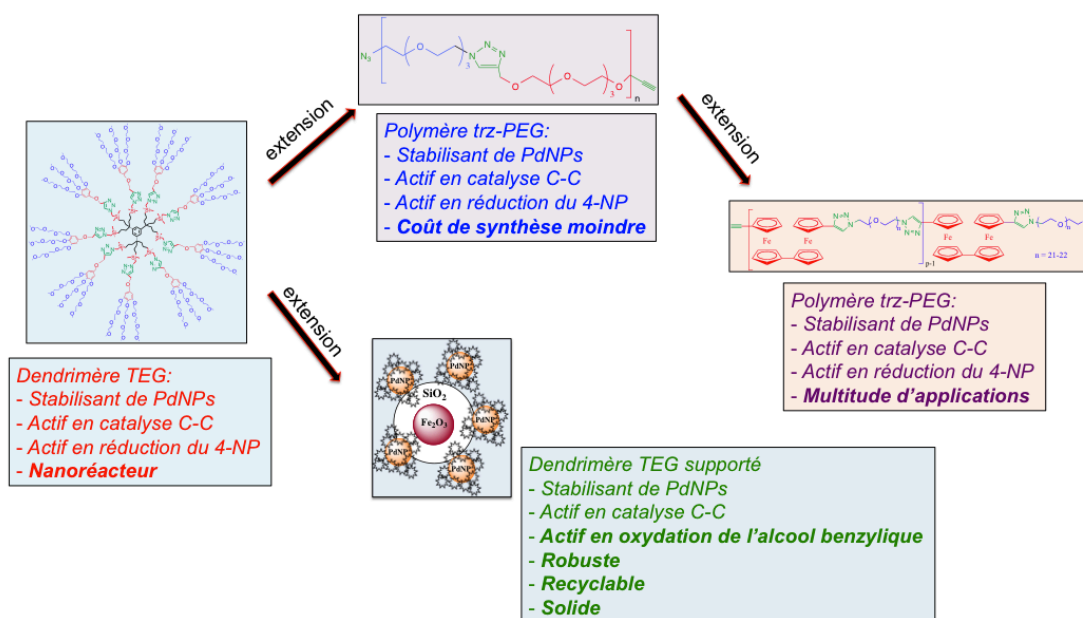
Conclusions et perspectives

Conclusions et perspectives

Durant ces travaux de thèse, nous avons élaboré diverses nanoparticules de palladium (PdNPs) stabilisées par des dendrimères ou des polymères. Ces solutions de PdNPs se sont avérées très actives en catalyse (couplage C-C et réductions du 4-nitrophenol), allant même jusqu'à une catalyse homéopathique ne nécessitant que $3 \cdot 10^{-5}$ % de palladium (Suzuki-Miyaura), c'est-à-dire 0,3 ppm. L'inconvénient majeur de ces PdNPs, la présence obligatoire d'une quantité notable de solvant, a pu être surmonté grâce à l'imprégnation des PdNPs sur des supports magnétiques entraînant une robustesse accrue du catalyseur. L'objectif annoncé au début de la thèse de contribuer à une chimie verte a pu être réalisé grâce à l'infime quantité de nos catalyseurs au Pd utilisés lors de ces réactions catalytiques.

L'idée d'essayer d'améliorer les caractéristiques des catalyseurs a constitué à chaque fois un défi. L'utilisation, dans un premier temps, du dendrimère TEG pour stabiliser des PdNPs a été d'une très grande efficacité, mais le coût de synthèse de ce dendrimère pouvait représenter une limitation. C'est pourquoi, après avoir déterminé les parties essentielles du dendrimère jouant un rôle lors de la stabilisation des PdNPs actives, nous avons développé la synthèse d'un polymère comparable par réaction CuAAC en une étape. La synthèse d'un second type de co-polymère comportant une unité triazolylbiférocénique a permis d'étendre le champ d'application.

Parallèlement à ce sujet, et tout en respectant l'objectif de la chimie "verte", nous avons montré que le dendrimère amphiphile composé de 27 terminaisons TEG pouvait aussi servir de nanoréacteur lors de la réaction "click" CuAAC dans l'eau. Ce nanoréacteur permet de solubiliser des substrats hydrophobes et le catalyseur et de les confiner dans son cœur hydrophobe, favorisant la réaction catalytique dans ce milieu de micelle moléculaire dendritique. La présence du catalyseur moléculaire hydrophobe dans le dendrimère a pu être démontrée, de même que la complexation des ions cuivre (I) aux 1,2,3-triazoles.



Nous remercions encore une fois le Dr. Abdou Diallo qui a synthétisé pour la première fois le dendrimère TEG procurant ainsi un point de départ pour la thèse, ainsi qu' Amalia Rapakousiou, Yanlan Wang, Na Li, Dong Wang et Sylvain Gatard pour les fructueuses collaborations à l'occasion de cette thèse au sein de notre groupe.

Concernant les perspectives, une multitude d'entre elles sont envisageables et présentent des possibilités. Différents types de nanoparticules pourraient être stabilisées par ces macromolécules et ainsi d'autres réactions catalytiques pourraient être testées. L'utilisation du nanoréacteur dans d'autres réactions catalytiques serait aussi réalisable y compris l'utilisation de celui-ci dans le domaine biomédical du fait de sa biocompatibilité. L'imprégnation sur support magnétique permettrait d'éliminer la présence d'eau dans les PdNPs et d'augmenter la robustesse du catalyseur et d'autres réactions catalytiques plus complexes et plus sensibles devraient être testées. L'imprégnation sur d'autres types de support de type semi-conducteur tels que TiO_2 , ZnO , CeO_2 pourrait aussi être envisagé pour des applications en photo-catalyse par exemple. Enfin l'élaboration des co-polymères PEG-trz-biFc à multiples applications ouvre la voie à la création de nouveaux nanomatériaux utiles. La synthèse de dendrimères solubles dans l'eau comportant des 1,2,3-triazoles et des groupements biferrocéniques pourrait être appliquée. De plus, d'autres types d'unités (fluorochrome, chromophore, molécule à intérêt biologique...) pourraient être greffées dans ces macromolécules.